PATHOGENESIS OF DIMORPHIC FUNGAL INFECTIONS

EDITED BY: Angel Gonzalez and Carlos Pelleschi Taborda
PUBLISHED IN: Frontiers in Cellular and Infection Microbiology

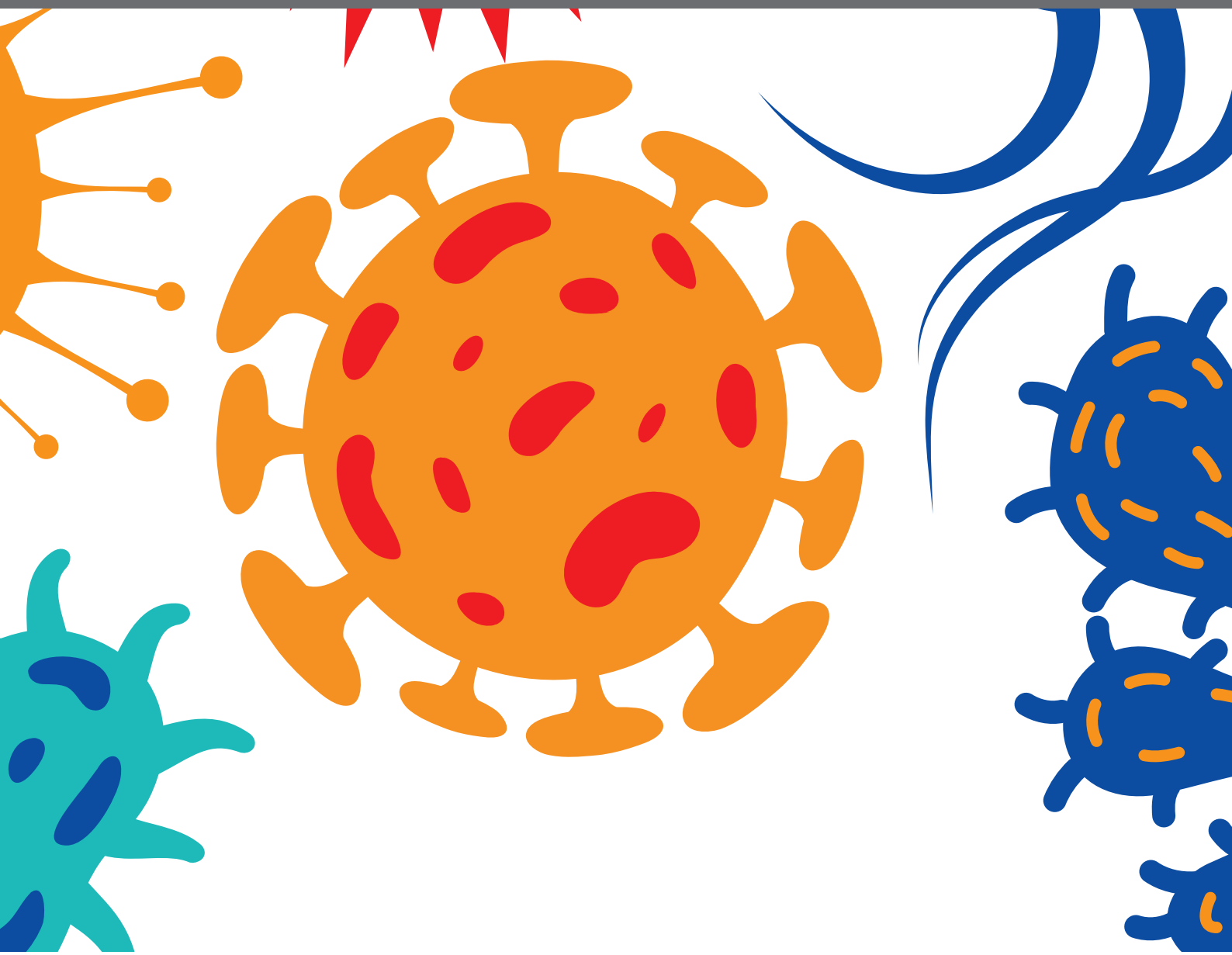

frontiers Research Topics

frontiers

ISSN 1664-8714
ISBN 978-2-88971-970-9
DOI 10.3389/978-2-88971-970-9

About Frontiers

Frontiers is more than just an open-access publisher of scholarly articles: it is a pioneering approach to the world of academia, radically improving the way scholarly research is managed. The grand vision of Frontiers is a world where all people have an equal opportunity to seek, share and generate knowledge. Frontiers provides immediate and permanent online open access to all its publications, but this alone is not enough to realize our grand goals.

Frontiers Journal Series

The Frontiers Journal Series is a multi-tier and interdisciplinary set of open-access, online journals, promising a paradigm shift from the current review, selection and dissemination processes in academic publishing. All Frontiers journals are driven by researchers for researchers; therefore, they constitute a service to the scholarly community. At the same time, the Frontiers Journal Series operates on a revolutionary invention, the tiered publishing system, initially addressing specific communities of scholars, and gradually climbing up to broader public understanding, thus serving the interests of the lay society, too.

Dedication to Quality

Each Frontiers article is a landmark of the highest quality, thanks to genuinely collaborative interactions between authors and review editors, who include some of the world's best academicians. Research must be certified by peers before entering a stream of knowledge that may eventually reach the public - and shape society; therefore, Frontiers only applies the most rigorous and unbiased reviews.
Frontiers revolutionizes research publishing by freely delivering the most outstanding research, evaluated with no bias from both the academic and social point of view. By applying the most advanced information technologies, Frontiers is catapulting scholarly publishing into a new generation.

What are Frontiers Research Topics?

Frontiers Research Topics are very popular trademarks of the Frontiers Journals Series: they are collections of at least ten articles, all centered on a particular subject. With their unique mix of varied contributions from Original Research to Review Articles, Frontiers Research Topics unify the most influential researchers, the latest key findings and historical advances in a hot research area! Find out more on how to host your own Frontiers Research Topic or contribute to one as an author by contacting the Frontiers Editorial Office: frontiersin.org/about/contact

PATHOGENESIS OF DIMORPHIC FUNGAL INFECTIONS

Topic Editors:
Angel Gonzalez, University of Antioquia, Colombia
Carlos Pelleschi Taborda, University of São Paulo, Brazil

Citation: Gonzalez, A., Taborda, C. P., eds. (2021). Pathogenesis of Dimorphic Fungal Infections. Lausanne: Frontiers Media SA. doi: 10.3389/978-2-88971-970-9

Table of Contents

frontiers in Cellular and Infection Microbiology

EDITORIAL
published: 11 November 2021
doi: 10.3389/fcimb.2021.793245

Editorial: Pathogenesis of Dimorphic Fungal Infections

Angel Gonzalez[1*] *and Carlos P. Taborda*[2]

[1] School of Microbiology, Universidad de Antioquia, Medellín, Colombia, [2] Institute of Biomedical Sciences, Department of Microbiology and Institute of Tropical Medicine, Laboratory of Medical Mycology (LIM53), University of São Paulo, São Paulo, Brazil

Keywords: fungal pathogenesis, dimorphic fungi, Histoplasma, Paracoccidioides, Coccidioides, Blastomyces, Talaromyces, Emergomyces

Editorial on the Research Topic

Pathogenesis of Dimorphic Fungal Infections

PATHOGENESIS OF DIMORPHIC FUNGAL INFECTIONS

Dimorphic fungal infections are responsible for the development of life-threatening diseases, especially in patients with a compromised immune system that include those infected with the human immunodeficiency virus (HIV) or those receiving antineoplastic agents, immunosuppressive agents used in solid organ receptors, immunomodulatory therapies, and other biological products. Also, the progressive devastation of tropical forests changing the entire balance of nature is responsible for increase of endemic mycoses. These infections are caused by dimorphic fungi belonging to species of the genus *Histoplasma*, *Paracoccidioides*, *Coccidioides*, *Blastomyces*, *Talaromyces*, and *Emergomyces*, which are distributed in defined geographical areas. The mortality and morbidity caused by these mycoses have increased rapidly during the last decades, especially in countries where infections, by these fungi, are endemic. In this Research Topic you will find a number of reports aiming at a better understanding of the pathogenesis of dimorphic fungal infections and all the factors involved in both the host and the causative agent. Contributions focus mainly on virulence factors of fungal agents, host-pathogen interactions, risk factors in the host, immune response, and diagnosis.

The study conducted by Assunção et al. describes some aspects of the nutritional immunity and how the response is of *Histoplasma capsulatum* under zinc (Zn) deprivation through genomic and proteomic analysis. These authors report that this fungus harbor eight genes related to Zn homeostasis, and the expression of ZAP1, ZRT1, and ZRT2 is induced under zinc-limiting conditions; moreover, during zinc deprivation, proteins related to energy production pathways, oxidative stress, and cell wall remodeling were regulated, as well, increase in chitin and glycan content in fungal cell wall was observed.

Among the different virulence factors in *H. capsulatum*, Fregonezi et al. describe that blocking a heat shock protein of 60 kilodaltons (Hsp60) with a monoclonal antibody reduces the metabolic activity and biomass of this pathogen, and in addition, this blockage increases the survival of the larvae *Galleria mellonella* after infection, thus indicating that this Hsp60 participates in both the biofilm formation and pathogenesis. Furthermore, Gonçalves et al. describe that *H. capsulatum* produce cellular-attached (C-gly-*Hc*) and secreted (E-gly) glycans with reactivity to glucuronoxylomannan (GXM) monoclonal antibodies developed against GXM from *Cryptococcus neoformans*; noteworthy, this GXM-like *Hc* glycans also react with sera of cryptococcosis patients,

OPEN ACCESS

Edited and reviewed by:
Anuradha Chowdhary, University of Delhi, India

***Correspondence:**
Angel Gonzalez
angel.gonzalez@udea.edu.co

Specialty section:
This article was submitted to Fungal Pathogenesis, a section of the journal Frontiers in Cellular and Infection Microbiology

Received: *11 October 2021*
Accepted: *21 October 2021*
Published: *11 November 2021*

Citation:
Gonzalez A and Taborda CP (2021) Editorial: Pathogenesis of Dimorphic Fungal Infections. Front. Cell. Infect. Microbiol. 11:793245. doi: 10.3389/fcimb.2021.793245

and additionally, acapsular *C. neoformans* (cap59 strain) covered with this GXM-like *Hc* glycans were more resistant to phagocytosis and macrophage killing and increase death rates of *G. mellonella* larvae, suggesting that these molecules are important during host-fungal interactions.

In *Paracoccidioides brasiliensis*, a study addressed by Zonta et al. reported that this pathogen releases a DNase-like protein that degrades neutrophil extracellular traps (NETs) that allows its fungal escape. On these lines, Longo et al. also demonstrated that *P. brasiliensis* produces a unique 1-Cys peroxiredoxin, which is localized both in the cytoplasm and cell wall, which confer it the capability to decompose hydrogen peroxide, one of the most abundant and antioxidant compounds produced by the host in response to infection. Furthermore, Almeida Donanzam et al. inform that exoantigens from *P. brasiliensis* and *P. lutzii* strains induce significant proliferation of both human and murine pulmonary fibroblast and increased levels of the pro-fibrotic cytokine TGF-β1 and pro-collagen type I, suggesting that these fungal components participate in the fibrogenesis process induced by these fungal pathogens.

In *Coccidioides*, Peláez-Jaramillo et al. conducted an elegant lipidomic work; in this study, the authors demonstrated that this fungal pathogen secrets a lipid-rich, membranous cell surface layer, *in vivo* and *in vitro*, composed mainly by phospholipids [acylglycerols and sphingolipids (sphingosine and ceramide)] and saturated fatty acids (myristic, palmitic, elaidic, oleic, and stearic acid), which contribute to the suppression of inflammatory response and the subsequent dissemination of the fungal infection.

Danchik and Casadevall describe that cell surface hydrophobicity (CSH) is an important cellular and biophysical parameter that affects both cell-cell and cell-surface interactions; and in dimorphic fungal pathogens, this parameter can be affected by multiple variables including altered cell wall composition, genetic modification, changes in temperature, and altered nutrient availability that in turn could affect, indirectly, several biological process such as biofilm formation, virulence, and response to antifungal treatments.

Other important aspect that allows dimorphic fungal pathogens to survive inside macrophages is their intracellular metabolism; thus, the fungal growth, proliferation, and survival within macrophages require strategies for acquisition of sufficient nutrients from the nutrient-depleted phagosomal environment. On these lines, Shen and Rappleye, after a rigorous review of transcriptomic and functional genetic studies in *Histoplasma* and *Paracoccidioides*, describe how these fungal dimorphic pathogens activate their metabolism to the resources available in the macrophage phagosome. Noteworthy, Giusiano G. describes an interesting mechanism called the "Trojan horse model" in which *Paracoccidioides* persists, as a facultative intracellular pathogen, within phagocytes, and allows it to transmigrate and disseminate to other tissues; thus, this mechanism, also reported for other fungi, is considered a factor of pathogenicity.

Regarding the immune response developed by the host against these fungal pathogens, Diep and Hoyer compilate several studies and resume the innate and adaptive immune response against *Coccidioides* infection. Of note, Jannuzzi et al. contribute with an interesting review highlighting the role played by intracellular pattern recognition receptors [(PRRs)—TLR3, TLR7, TLR8, and TLR9—which recognize mainly genetic material] both in controlling the infection and in the host's susceptibility against important fungal infections, including paracoccidioidomycosis. Interestingly, de Oliveira et al., using an experimental model of PCM, observed that β2 integrin appears to play an important role in fungal survival inside macrophages, which serve as a protective environment for this fungal pathogen. Additionally, Puerta-Arias et al., after an exhaustive review of several studies, also describe that T-cell-mediated immunity, mainly T helper (Th)1 and Th17 responses, is essential for protection against the majority of the dimorphic fungi; thus, IL-17 production is associated with neutrophil and macrophage recruitment at the site of infection accompanied by chemokine and pro-inflammatory cytokines, a mechanism mediated by some PRRs and adaptor molecules, which in turn play distinctly different roles for each pathogen, being beneficial mediating fungal controls or detrimental promoting disease pathologies.

Kischkel et al. contribute with an important review concerning the use of nanoparticles to develop new therapeutic options, including vaccination against systemic mycosis including those caused by *Candida* spp., *Cryptococcus* spp., *Histoplasma* spp., *Paracoccidioides* spp., *Coccidioides* spp., and *Aspergillus* spp.; these authors provide important information about the use of different types of nanoparticles, nanocarriers, and their corresponding mechanism of action.

With respect to the diagnosis of dimorphic fungal infections, Almeida et al. inform the development of a co-immunoprecipitation assay using a protein extract from the yeast morphotype of *H. capsulatum* and pooled sera from patients with proven histoplasmosis, followed by a shotgun mass spectrometry identification of antigenic targets; the authors found three antigens as potential antigenic targets (M antigen, catalase P, and YPS-3), and 16 regions from these three proteins were proposed as putative B-cell epitopes exclusive to *H. capsulatum*; they indicate their possible use in new methods for the diagnosis of histoplasmosis.

Noteworthy, Nacher et al. contribute with two reports; in the first one, they describe three cases of HIV patients with disseminated histoplasmosis who had adrenal insufficiency, a presentation that is not common in these types of immunosuppressed patients. In the second contribution, Nacher et al. described a series of cases of patients with advanced HIV and disseminated histoplasmosis with superficial and deep lymphadenopathies; of interest, the presence of deep lymphadenopathies was associated with fewer biomarkers of severity and a lower risk of death.

Finally, Drak Alsibai et al. contribute with a report of 15 years of experience of a Pathology Center of French Guiana; the authors made a cytological and histopathological analysis of samples from patients with disseminated histoplasmosis, the largest series to date, and described that digestive involvement was the most frequent, usually with tuberculoid form a greater load of fungal cells, and concluded that cytology and pathology are widely available methods that can give life-saving results in a short time to help orient clinicians facing a potentially fatal infection requiring prompt treatment.

The above contributions to this Research Topic highlight recent advances and increase our knowledge about the complex host-fungal interactions and how through several virulence attributes, dimorphic fungal pathogens are able to survive in different environments, especially into the mammalian host, and how they overcome the immune response. Understanding these mechanisms could provide novel targets for implementing new therapeutic strategies or intervention.

AUTHOR CONTRIBUTIONS

AG and CT edited the topic and wrote the manuscript. All authors contributed to the article and approved the submitted version.

Conflict of Interest: The authors declare that the research was conducted in the absence of any commercial or financial relationships that could be construed as a potential conflict of interest.

frontiers in Cellular and Infection Microbiology

ORIGINAL RESEARCH
published: 04 August 2020
doi: 10.3389/fcimb.2020.00394

The Human Pathogen *Paracoccidioides brasiliensis* Has a Unique 1-Cys Peroxiredoxin That Localizes Both Intracellularly and at the Cell Surface

Larissa Valle Guilhen Longo[1†], Carlos Alexandre Breyer[2†], Gabriela Machado Novaes[2], Gregory Gegembauer[1], Natanael Pinheiro Leitão Jr.[1], Carla Elizabete Octaviano[1], Marcos Hikari Toyama[2], Marcos Antonio de Oliveira[2] and Rosana Puccia[1*]*

[1] Departamento de Microbiologia, Imunologia e Parasitologia, Escola Paulista de Medicina—Universidade Federal de São Paulo, São Paulo, Brazil, [2] Instituto de Biociências, Universidade Estadual Paulista Júlio de Mesquita Filho, São Paulo, Brazil

OPEN ACCESS

Edited by:
Carlos Pelleschi Taborda, University of São Paulo, Brazil

Reviewed by:
Célia Maria de Almeida Soares, Universidade Federal de Goiás, Brazil
Juan G. McEwen, University of Antioquia, Colombia

***Correspondence:**
Marcos Antonio de Oliveira
scaffix@gmail.com
Rosana Puccia
ropuccia@gmail.com

[†] These authors have contributed equally to this work

Specialty section:
This article was submitted to Fungal Pathogenesis, a section of the journal Frontiers in Cellular and Infection Microbiology

Received: *24 April 2020*
Accepted: *26 June 2020*
Published: *04 August 2020*

Citation:
Longo LVG, Breyer CA, Novaes GM, Gegembauer G, Leitão NP Jr, Octaviano CE, Toyama MH, de Oliveira MA and Puccia R (2020) The Human Pathogen Paracoccidioides brasiliensis Has a Unique 1-Cys Peroxiredoxin That Localizes Both Intracellularly and at the Cell Surface. Front. Cell. Infect. Microbiol. 10:394. doi: 10.3389/fcimb.2020.00394

Paracoccidioides brasiliensis is a temperature-dependent dimorphic fungus that causes systemic paracoccidioidomycosis, a granulomatous disease. The massive production of reactive oxygen species (ROS) by the host's cellular immune response is an essential strategy to restrain the fungal growth. Among the ROS, the hydroperoxides are very toxic antimicrobial compounds and fungal peroxidases are part of the pathogen neutralizing antioxidant arsenal against the host's defense. Among them, the peroxiredoxins are highlighted, since some estimates suggest that they are capable of decomposing most of the hydroperoxides generated in the host's mitochondria and cytosol. We presently characterized a unique *P. brasiliensis* 1-Cys peroxiredoxin (PbPrx1). Our results reveal that it can decompose hydrogen peroxide and organic hydroperoxides very efficiently. We showed that dithiolic, but not monothiolic compounds or heterologous thioredoxin reductant systems, were able to retain the enzyme activity. Structural analysis revealed that PbPrx1 has an α/β structure that is similar to the 1-Cys secondary structures described to date and that the quaternary conformation is represented by a dimer, independently of the redox state. We investigated the PbPrx1 localization using confocal microscopy, fluorescence-activated cell sorter, and immunoblot, and the results suggested that it localizes both in the cytoplasm and at the cell wall of the yeast and mycelial forms of *P. brasiliensis,* as well as in the yeast mitochondria. Our present results point to a possible role of this unique *P. brasiliensis* 1-Cys Prx1 in the fungal antioxidant defense mechanisms.

Keywords: *Paracoccidioides brasiliensis*, 1-Cys Prx, hydroperoxides, peroxiredoxin, dimorphic fungi, ROS

INTRODUCTION

Paracoccidioidomycosis (PCM) is a systemic mycosis endemic in Latin America. Lethality rates range from 3 to 5% and about 80% of the PCM cases are reported in Brazilian patients (Martinez, 2017). The thermal dimorphic fungus *Paracoccidioides brasiliensis* is one of the PCM etiologic agents and the infection occurs by inhalation of fungal conidia from the environment mycelial

form. The active disease, which depends on the transition to the yeast phase to occur in the lungs alveolar space, is mostly characterized by damage of the lungs and upper airways, but also of the oral mucosa and skin (Bocca et al., 2013; Martinez, 2017).

The pathogen survival depends on its mechanisms of escaping the host's immune response. An essential host defense strategy comprises the production of reactive oxygen and nitrogen species (ROS and RNS) by the immune cells, the so called respiratory burst (Campos et al., 2005; Halliwell and Gutteridge, 2015). Among the several species generated by the respiratory burst, hydrogen peroxide (H_2O_2), and peroxynitrite (NOO^-) are able to generate secondary reactive species, such as organic hydroperoxides (OHPs), especially lipid hydroperoxides and other reactive species. These compounds can cause protein dysfunction and damage of biomolecules, therefore negatively affecting the pathogen homeostasis (Halliwell and Gutteridge, 2015; El-Benna et al., 2016). Several fungicides are also able to promote the ROS increase, including OHPs, which are related to fungi annihilation (Edlich and Lyr, 1992; Belenky et al., 2013; Shekhova et al., 2017). On the other hand, some fungal pathogens are able to produce OHPs to protect themselves against invasion and host tissue destruction by other microorganisms (Deighton et al., 1999).

The main enzymes involved in the pathogen antioxidant defense mechanisms against hydroperoxides are the catalase, glutathione peroxidase, and peroxiredoxins (Nevalainen, 2010). Among them, the peroxiredoxins (Prx) are noteworthy due to their high abundance in living organisms and their exceptional ability to reduce several kinds of hydroperoxides at high efficiency (10^4-10^8 $M^{-1}s^{-1}$) (Netto et al., 2016). In fact, some works reveal that Prxs are able to decompose most of the hydroperoxides generated in the cell (Winterbourn, 2008; Cox et al., 2009). Despite the high enzymatic efficiency, members of the Prx family differ in substrate preference between H_2O_2 and organic hydroperoxides (Peskin et al., 2007; Parsonage et al., 2008).

Peroxiredoxins utilize a highly reactive cysteine residue (peroxidatic cysteine—C_P) for hydroperoxide decomposition, being classified into 1-Cys Prx and 2-Cys Prx according to the number of cysteines involved in the catalytic cycle (Rhee and Kil, 2017). The Prx catalytic triad is represented by the C_P, a Thr/Ser, and an Arg. While C_P and Thr/Ser are embedded in the universal Prx motif PXXXT/SXXC_P, the Arg residue is distant in the sequence, but it is brought closer to the Thr/Ser as a consequence of protein folding (Tairum et al., 2012, 2016).

However, specific motif signatures can be found within different classes of Prx. In the 1-Cys Prx from some fungal species, a highly conserved PV/TC_PTTE motif is found (Nevalainen, 2010; Rocha et al., 2018). The most studied member of the 1-Cys Prx is the mammalian Prdx6, which is a dual-function enzyme with both peroxidase and acidic Ca^{2+}-independent phospholipase A2 activities (Nevalainen, 2010; Zhou et al., 2018). This additional function seems to protect cell membrane phospholipids against oxidative damage (peroxidation) and hydrolysis. Remarkably, some 1-Cys Prx from pathogens have distinguished features in comparison with the corresponding host enzymes, placing them as promising targets for the development of specific drugs (Wen et al., 2007; Rocha et al., 2018).

Previous work from our group revealed the presence of an ortholog of a mitochondrial peroxiredoxin (PbPrx1) in the cell wall proteome from both the yeast and the mycelial forms of *P. brasiliensis* (Longo et al., 2014). Importantly, this protein has also been described in the proteome of extracellular vesicle (EV) of this and other human fungal pathogens (Vallejo et al., 2012). More recently, we have observed by quantitative proteome that PbPrx1 is 2–3-fold more abundant in EVs isolated from *P. brasiliensis* cell supernatants after nitrosative and oxidative stress (Leitão et al., unpublished).

Considering the possible role of peroxiredoxins in the fungal defense mechanisms against the host immune system, we presently aimed at characterizing PbPrx1. We initially found that it corresponds to a unique 1-Cys Prx sequence in the *P. brasiliensis* genome. The corresponding protein was recombinantly expressed, purified, and the enzymatic activity was characterized. Our results point to a possible role of this unique *P. brasiliensis* 1-Cys Prx1 in the fungal antioxidant defense mechanisms.

MATERIALS AND METHODS

Fungal Strains and Culture Conditions

P. brasiliensis (isolate Pb18) was cultivated as previously described (Vallejo et al., 2011). Overall, yeast cells were maintained in modified YPD (0.5% yeast extract, 0.5% casein peptone, 1.5% glucose, pH 6.5) slants at 4°C. For the experiments, yeasts were recovered by seeding into fresh slants for growth for 7 days at 36°C. Actively growing yeasts were inoculated into liquid Ham's F12 medium (Life Technologies, Grand Island, NY, USA) supplemented with 1.5% glucose (F12/glc) for pre-growth under shaking for 4 days at 36°C. The cells were then transferred to fresh F12/glc and cultivated for 2 extra days. Viability (>95%) was estimated by trypan blue staining.

RNA Extraction and cDNA Cloning

For RNA extraction, freshly grown cells suspended in TRIzol reagent (Thermo Fisher Scientific, Waltham, MA, USA) were mechanically disrupted by vortexing with glass beads for 10 min or submitted to a Precellys 24 high-throughput homogenizer (Bertin Technologies, Rockville, Washington, DC, USA). Total RNA was then isolated following chloroform extraction and isopropanol precipitation. Genomic DNA was removed with RNase-free DNase I (Promega Corp., Madison, WI, USA), as previously described (Goldman et al., 2003). The efficiency of hydrolysis was tested by PCR amplification of the Pb*GP43* gene using primers that included (or not) the introns (Cisalpino et al., 1996). Three micrograms of total RNA were reverse transcribed using SuperScript III reverse transcriptase (Thermo Fisher Scientific, Waltham, MA, USA) and oligo$(dT)_{12-18}$ primers. Using the cDNA as template, a 680-bp fragment was amplified by PCR using the PbPrx1-F and PbPrx1-R primers (**Table 1**) and Taq Platinum High Fidelity enzyme. The Pb*PRX1* amplified fragment was cloned into pGEM-T easy (Promega Corp., Madison, WI, USA) at the *Bam* HI/*Hind* III sites and

TABLE 1 | Primers used in PCR and sequencing during this study.

Name	Application	Sequence
Prx1-F	Cloning	5′-AGGATCCAATGGCTGAAGAACATCGT-3′
Prx1-R	Cloning	5′-TAAGCTTTTAGTTCTTGATGGTAGTA-3′
Gp43-F	DNAse control	5′-GGGACACCTTTATCACT-3′
Gp43-R	DNAse control	5′-CCAAGACATACAAGAACGTC-3′
$T7_{pHIS1}$	Sequencing	5′-TAATACCACTCACTATAGGG-3′
T7 terminator	Sequencing	5′-GCTAGTTATTGCTCAGCGG-3′
$T7_{pGEM}$	Sequencing	5′-TAATACGACTCACTATAGGG-3′
SP6	Sequencing	5′-ATTTAGGTGACACTATAGAA-3′
Prx1-F	qPCR	5′-ATTTCACTCCTACCTGCAC-3′
Prx1-R	qPCR	5′-CGTTGATGTCGTTGATCCAG-3′
TUB-1	qPCR	5′-CGGCTAATGGAAAATACATGGC-3′
TUB-2	qPCR	5′-GTCTTGGCCTTGAGAGATGCAA-3′

BamHI and HindIII restriction sites are highlighted in gray.

a recombinant plasmid was selected in *Escherichia coli* DH5α resistant to the ampicillin marker. Correct in-frame ligation was checked by endonuclease restriction and sequencing. The insert was excised from pGEM-T easy using *Bam* HI/*Hind* III (New England Biolabs, Ipswich, MA, USA) and subcloned into the same sites of both the pHIS1 (pHIS1-*pbPRX1*) or the pET28PP (pET28PP-*pbPRX1*) expression vectors (Novagen, WI, USA). The resulting plasmids were used for expression of the recombinant protein, respectively in *E. coli* BL21(DE3) pLys-S (Novagen, Madison, WI, USA), to be used in antibody production, or *E. coli* BL21 Tuner (DE3) (Novagen, Madison, WI, USA), for biochemical analysis. The recombinant protein pHIS1-*pbPRX1* was not soluble and yielded only 2 mg/ml, but that was enough to immunize mice for antibody production. The recombinant protein pET28PP-*pbPRX1*, on the other hand, was produced in a later phase of the work specifically to perform complete biochemical analysis, which demands high amounts of enzyme. It was soluble and yielded 20 mg/mL.

Protein Expression and Purification for Biochemical Analysis

Single colonies of *E. coli* BL21 Tuner (DE3) harboring the pET28PP-*pbPRX1* vector were cultured overnight at 37°C in 2XYT medium containing ampicillin (100 μg mL^{-1}), diluted in fresh medium and grown to an OD_{600} = 0.6–0.8. IPTG (0.5 mM final concentration) was added and the cells were incubated for 16 h at 30°C, at 250 rpm. The cells were harvested by centrifugation and the pellet was washed, suspended in start buffer (10 mM Tris-Cl pH 8.0, 1% Triton), and sonicated (three cycles of 30 s, 30% amplitude, 60 s in ice). Cell extracts were treated for 15 min with 1% streptomycin sulfate in ice and the suspensions were centrifuged (12,000 rpm, 60 min) to remove nucleic acid precipitates and insoluble components. Cell extracts were purified by IMAC using His-Trap columns (GE Healthcare, Piscataway, USA) eluted with an imidazole gradient. Imidazole was removed by gel filtration using a PD10 column (GE Healthcare, Piscataway, USA), the His-tag was excised using HRV3C protease (Novagen, Madison, WI, USA) and the reaction was performed overnight in 10 mM Tris-Cl (pH 8.0). His-Tag and HRV3C protease were separated from recombinant rPbPrx1 by IMAC (**Supplementary Figure 1A**). The thioredoxin 1 (Trx1), thioredoxin reductase 1 (TrxR1), and thiol specific antioxidant 1 (Tsa1) from *Saccharomyces cerevisiae* were expressed and purified as previously described (Oliveira et al., 2010). Briefly, *E. coli* BL21 (DE3) cultures containing the pET15b/*tsa1*, the pPROEX/*trxr1*, and the pET17/*trx1* vectors were stimulated with 1 mM IPTG for 3 h. The cells were lysed and centrifuged to remove the precipitate. The Tsa1 and TrxR1 recombinant proteins (**Supplementary Figures 1B,C**) were purified by imidazole gradient (0–0.5 M imidazole) using a Hi-Trap column (GE Healthcare, Piscataway, USA). Trx1 purification was carried out by size exclusion chromatography (**Supplementary Figure 1D**) using a HiLoad 16/600 Superdex 75 column (GE Healthcare, Piscataway, USA). The enzyme concentration was determined spectrophotometrically by molar extinction coefficient (rPbPrx1 ε_{280} = 22,920 M^{-1} cm^{-1}; Tsa1ε280 = 23,950; Trx1ε_{280} = 9,970 M^{-1} cm^{-1}, and TrxR1 ε_{280} = 24,410 M^{-1} cm^{-1}). The recombinant protein samples were stored at −20°C.

Mice Immunization

Recombinant PbPrx1 (rPbPrx1) expressed from the pHIS1-*pbPRX1* vector was purified in Ni-NTA agarose (Qiagen, Germantown, MD, USA). Purified rPbPrx1 (100 μg) was emulsified in incomplete Freund's adjuvant and inoculated subcutaneously in Balb/C mice at days 0, 15, and 30, when the sera were collected, tested, and aliquoted at −20°C. Control pre immune serum was obtained before immunization. Monospecific affinity-purified pre-immune and immune anti-rPbPrx1 mouse sera were prepared as previously described (Batista et al., 2006). Briefly, the purified rPbPrx1 was immobilized onto nitrocellulose membranes and incubated with pre-immune and immune anti-rPbPrx1 mouse sera. The affinity-purified antibodies were eluted and stored at −20°C until use. The use of animals in this work was reviewed and approved by the Ethics Committee for Research (UNIFESP) numbers CEP 0366/07 and CEP 6379211014.

Confocal Microscopy and Immunoblotting

For confocal microscopy, fungal cells were fixed in 4% paraformaldehyde for 20 min at room temperature, washed twice in PBS and permeabilized in Triton X-100 0.5% for 15 min. Fixed cells were washed three times in PBS and quenched with 3% bovine serum albumin (Sigma-Aldrich, St. Louis, MO, USA) in PBS (blocking buffer) for 16 h at 4°C. Quenched cells were incubated with primary antibodies at 1:50 (monospecific pre-immune and anti-rPbPrx1 mouse serum) in blocking buffer for 2 h at 37°C, washed three times in PBS and incubated for 1 h at 37°C in the dark with secondary anti-mouse-IgG (1:100) labeled with both Alexa (Alexa FluorR 488, Invitrogen) and 25 μM Calcofluor White. Microscopy slides were mounted with anti-fading Vectashield (Vector Laboratories, Burlingame, CA, USA) and sealed. Images were analyzed by confocal microscopy (Carl Zeiss LSM-510 NLO, Oberkochen, BadenWurttemberg, Germany).

Western immunoblot reactions were performed with immune and pre immune anti-rPbPrx1 sera against cell wall and mitochondrial extracts. Incubation was carried out overnight at 4°C under shaking. The membranes were washed three times in 0.1% Tween 20 diluted in PBS and incubated for 1 h at 37°C with goat anti-rabbit conjugated to peroxidase (Sigma). The reactions were developed using an enhanced chemiluminescence kit (ECL reagent, Pierce, Rockford, IL, USA). Cell wall and mitochondrial extracts were produced as described elsewhere (Batista et al., 2006; Longo et al., 2014). Briefly, for extraction of cell wall proteins, *P. brasiliensis* yeast and mycelial cells were washed three times in ice-cold 25 mM Tris–HCl, pH 8.5, and incubated with 2 mM DTT in the same buffer supplemented with 1 mM phenylmethylsulfonyl fluoride (PMSF) and 5 mM ethylenediaminetetraacetic acid (EDTA) to inhibit the action of proteases. For isolation of mitochondria, nitrogen-frozen yeast cells were mechanically disrupted in a mortar, thawed in 0.6 M sorbitol, 20 mM Hepes, pH 7.4, and sonicated for 5 min. Cell debris were pelleted (1,500 × g, 5 min) and the mitochondrial fraction was precipitated from the supernatant (1,200 × g, 10 min).

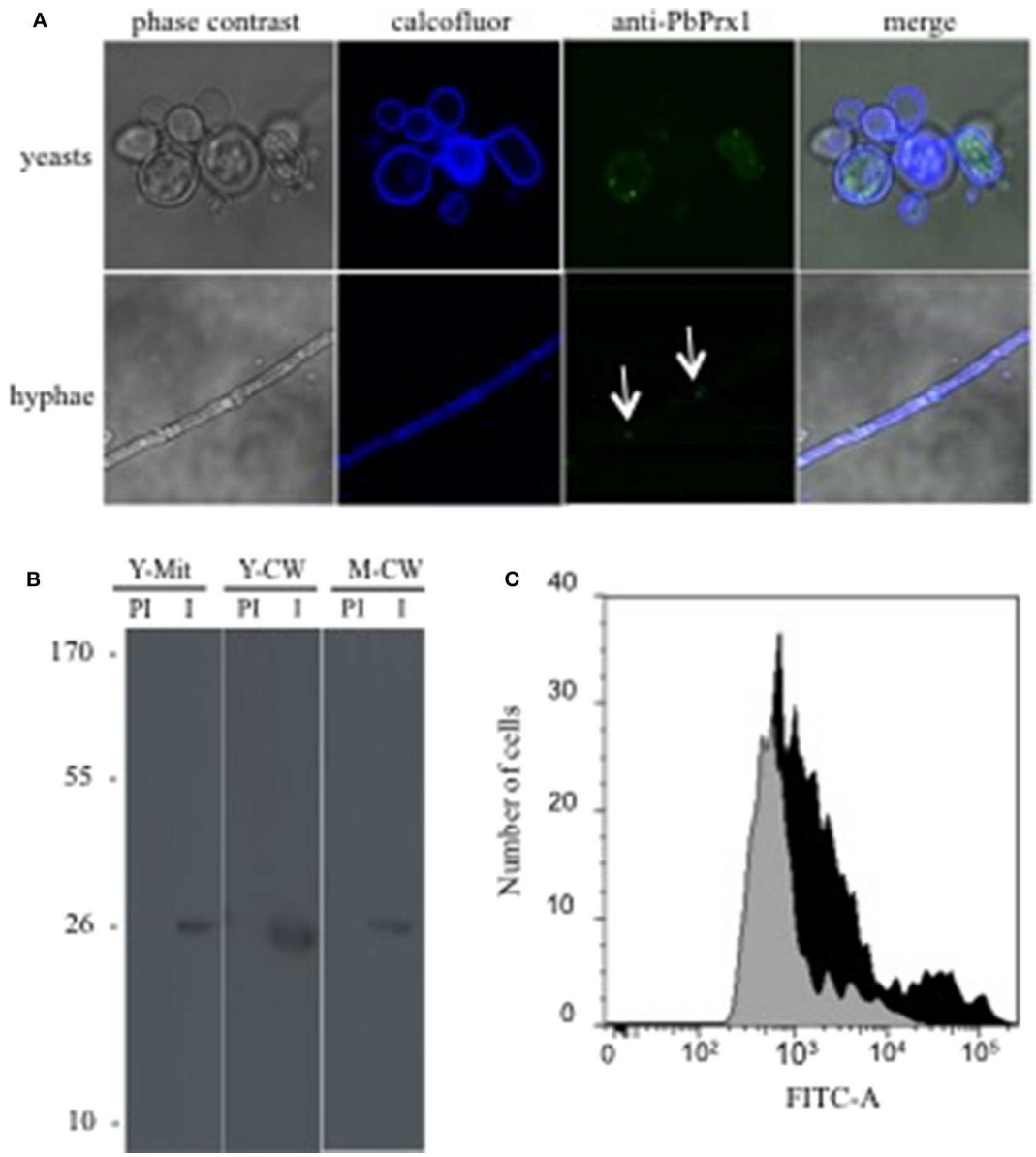

FIGURE 1 | *P. brasiliensis* PbPrx1 localizes both in the cytoplasm and at the cell wall. **(A)** Confocal microscopy of yeast and mycelial cells. In blue, Calcofluor White staining of the cell wall. In green, reactivity with anti-rPbPrx1 monospecific antibodies (1:50). **(B)** Western blot reaction of cell wall (CW) and mitochondrial (Mit) extracts from the yeast (Y) and mycelial (M) fungal phases with anti-rPbPrx1 (I) and preimmune monospecific antibodies (PI, 1:100). The molecular mass is indicated on the left in kilodaltons (kDa). **(C)** FACS analysis of *P. brasiliensis* non-permeabilized yeast cells incubated with either anti-rPbPrx1 (black) or preimmune (gray) antibodies (1:100).

Flow Cytometry Analysis

For fluorescence-activated cell sorter (FACS) analysis, *P. brasiliensis* yeast cells were prepared as previously described (Soares et al., 1998), with modifications. Fungal cells were fixed for 1 h at room temperature in 4% (vol/vol) paraformaldehyde in PBS, pH 7.2. Fixed cells were precipitated by centrifugation (1 min at 5,600 × g), washed three times in PBS and quenched for 1 h at room temperature in PBS containing 1% BSA (blocking buffer). The cells were incubated overnight at 4°C with monospecific anti-rPbPrx1 or pre-immune control (1:100 in blocking buffer). After five washes in PBS, the cells were incubated in the dark for 1 h at 37°C with Alexa-488-anti-rabbit IgG (Sigma-Aldrich) at 1:300 in blocking buffer. Labeled cells were rinsed five times, resuspended in PBS, and analyzed in a FACS Canto II (BD Biosciences, San Jose, CA, USA). A total of 10,000 cells were analyzed for fluorescence at 492 to 520 nm. Unlabeled control cells were previously analyzed for autofluorescence, relative cell size, and granularity.

qPCR Analysis

For evaluation of the Pb*PRX1* expression in *P. brasiliensis* undergoing oxidative stress, logarithmic yeast cells growing in F12/glc were subdivided into aliquots and centrifuged. Cell pellets were resuspended in 5 mL PBS containing or not (control) 5 mM H_2O_2, cumene hydroperoxide (CHP), or tert-butyl peroxide (*t*-BOOH), and incubated for 15, 30, and 60 min. Cell pellets were collected by centrifugation, washed in PBS, frozen in liquid N_2 and kept at −80°C until RNA extraction. Quantitative PCR (qPCR) was performed in triplicate using a SYBR-green-based PCR master mix (Applied Biosystems, Foster City, CA, USA) with reverse-transcribed RNA template and 0.5 M of each primer (**Table 1**). Cycling was carried out in triplicate in a Real-Time 7500 thermocycler (StepOnePlus™ Real-Time PCR System—Applied Biosystems™) starting with a holding stage at 95°C (10 min), followed by 40 cycles at 95°C (15 s) and 60°C (60 s). The dissociation curve was determined with an additional cycle of 95°C (15 s), 60°C (60 s), and 95°C (15 s). Changes in the transcript levels were determined using the threshold cycle (ΔΔCT) method (Schmittgen and Livak, 2008) after normalization of cycle thresholds based on the expression of the alpha-tubulin gene (XM_010765319.1). The alpha-tubulin gene is a standard normalizing gene for qPCR in *P. brasiliensis,* considering that its expression is stable and does not tend to fluctuate even under oxidative stress (Grossklaus et al., 2013). Statistical significance was determined by the Student's *t*-test.

Characterization of the rPbPrx1 Thiol-Dependent Peroxidase Activity by the DTT Oxidation Assay

rPbPrx1 (12.5 μM) expressed in pET28PP—*pbPRX1* was incubated for 10 min in a solution containing 10 mM 1,4-dithiothreitol (DTT), 5 mM H_2O_2 or *t*-BOOH, 100 μM diethylenetriaminepentaacetic acid (DTPA), and 1 mM sodium azide in 10 mM Hepes-NaOH, pH 7.4. The rate of DTT oxidation was measured spectrophotometrically at 310 nm (ε_{280} = 110 M^{-1} cm^{-1}) at 30°C, as previously described (Tairum et al., 2012).

rPbPrx1 Peroxidase Inactivation by NEM Alkylation

To determine whether the peroxidase activity is cysteine-dependent, rPbPrx1 (2 mg mL^{-1}) was treated with DTT for 1 h at room temperature. The excess DTT was removed by gel filtration using a PD-10 desalting column (GE Healthcare, Piscataway, USA). The reduced protein was incubated in 1 mM N-ethylmaleimide (NEM) (Sigma, München, Germany) overnight at 4°C. The excess NEM was removed by gel filtration using a PD-10 desalting column (GE Healthcare, Piscataway, USA). N-Ethylmaleimide (NEM) is an alkylating reagent that reacts with sulfhydryl groups, thus blocking the Prx activity. The reactions were performed at 30°C in a solution containing 50 mM Hepes-NaOH (pH 7.4), 100 μM DTPA, 1 mM

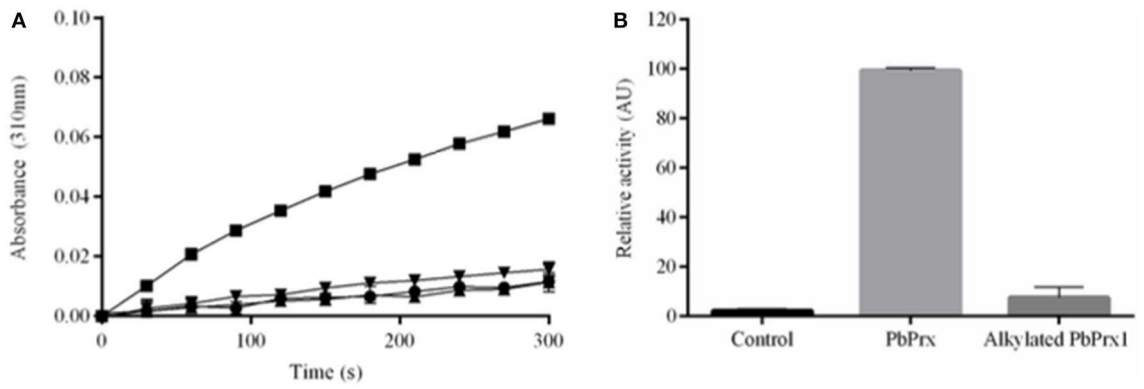

FIGURE 2 | The rPbPrx1 peroxidase activity is thiol-dependent. **(A)** The rPbPrx1 peroxidase activity was monitored by the DTT oxidation assay (λ = 310 nm). The reactions were performed with 12.5 μM rPbPrx1 at 30°C with either 5 mM H_2O_2 (▼) or *t*-BOOH (■). Control reactions were performed in triplicate, at least three times, with either *t*-BOOH (•) or H_2O_2 (▲) in the absence of enzyme. **(B)** To determine the peroxidase cysteine-dependent activity, rPbPrx1 was reduced by treatment with DTT for 1 h at room temperature. The reactions were performed as described above for (■). The peroxidase activity was monitored by the DTT oxidation assay (λ = 310 nm) and the results are shown as relative activity in graphic bars. All experiments were performed at least three times and yielded similar results.

sodium azide, 12.5 μM rPbPrx1, 10 mM DTT, and 5 mM *t*-BOOH. The peroxidase activity was monitored by the DTT oxidation ($\lambda = 310$ nm).

Ferrous Oxidation Xylenol Orange (FOX) Assay

rPbPrx1 hydroperoxide activity was determined using the FOX assay (Nelson and Parsonage, 2011). Reactions were prepared to a final volume of 50 μL in 50 mM Hepes-NaOH (pH 7.4), 5 μM rPbPrx1, 100 μM sodium azide, 100 μM DTPA, 1 mM DTT, and 150 μM hydroperoxide [H_2O_2, *t*-BOOH, CHP, and linoleic acid hydroperoxide (L-OOH)] and incubated at room temperature. To investigate additional electron donors of rPbPrx1, decomposition of *t*-BOOH was monitored using 1 mM DTT, 3 mM GSH, 3 mM β-mercaptoethanol, or 300 μM DHLA as reducing agents.

Thioredoxin-Dependent Peroxidase Activity Using the *S. cerevisiae* Trx System

Thioredoxin peroxidase activity was evaluated using the heterologous cytosolic thioredoxin system from *S. cerevisiae* by monitoring the NADPH oxidation. The reaction was carried out at 30°C in a final 100 μL volume containing 50 mM Hepes-NaOH, pH 7.4, 150 μM NADPH, either 200 μM *t*-BOOH or H_2O_2, 1 μM rPbPrx1, 1 μM *S. cerevisiae* Trx1, and 0.3 μM *S. cerevisiae* TrxR1. Positive control was performed using 1 μM Tsa1. The reaction was initiated by the addition of hydroperoxide and NADPH oxidation was monitored at 340 nm ($\varepsilon_{340} = 6220\ M^{-1}\ cm^{-1}$). Negative control was performed without the addition of peroxidases.

Evaluation of the rPbPrx1 Phospholipase Activity

The rPbPrx1 phospholipase activity was evaluated using an adaptation of the method described by Petrovic et al. (2001). Reaction mixtures (250 μL) containing 40 μM rPbPrx1 in 10 mM Tris-Cl pH 8.0 were started with 25 μL 4-nitro-3-octanoyloxy benzoic acid (NOBA) solubilized in acetonitrile 100% to a final concentration of 3 mg mL^{-1}. Reactions were maintained at 25°C for 60 min and absorbance (A_{425nm}) was recorded. The *Rattus norvegicus* Prx6 was used as a positive control of the phospholipase activity.

Determination of Thermal Stability

Thermal shift assays for rPbPrx1 were performed by circular dichroism (CD). CD spectra of rPbPrx1 were obtained using a

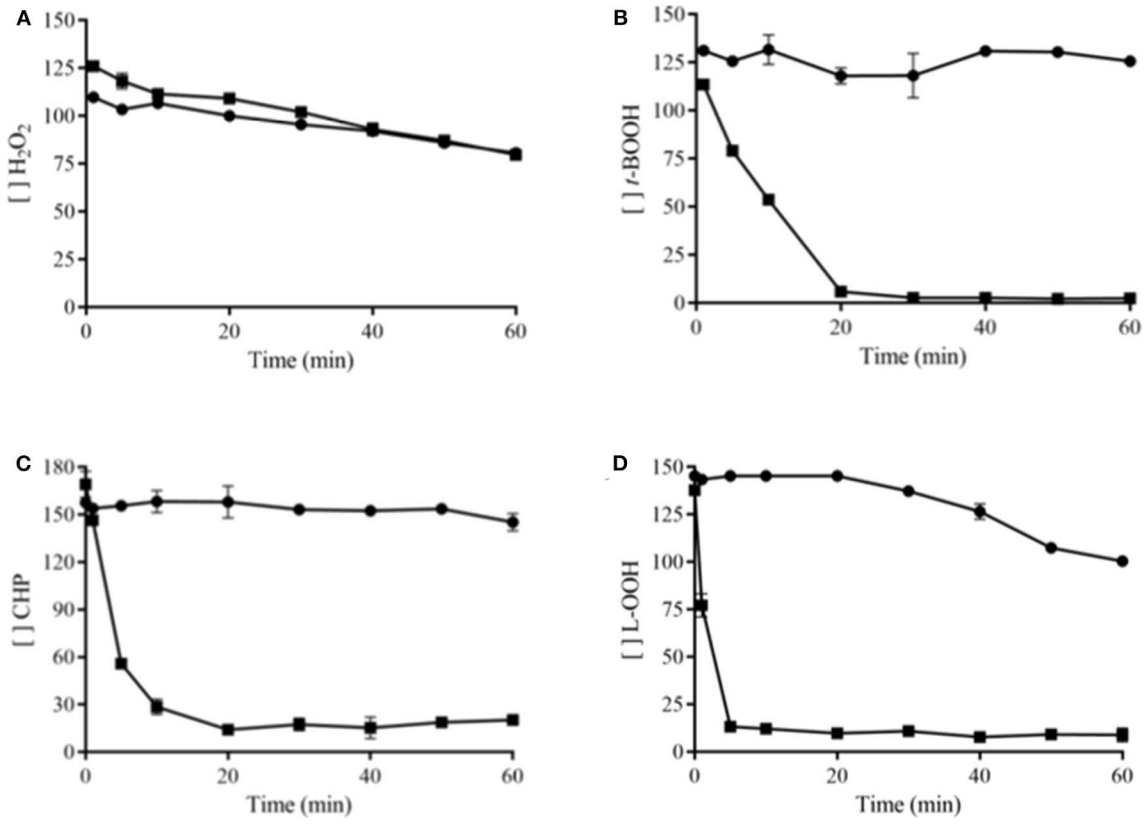

FIGURE 3 | rPbPrx1 and hydroperoxide specificity. The FOX assay was performed at room temperature with 5 μM rPbPrx1 (■) or without protein (•, negative control), using 150 μM of H_2O_2 **(A)**, *t*-BOOH **(B)**, CHP **(C)**, or L-OOH **(D)** as substrate. The absorbance was monitored at 560 nm. The graphics were generated using GraphPad Prism and show the remaining concentration of hydroperoxides during a 60-min reaction time. All experiments were performed in triplicate and repeated at least three times yielding consistent results.

0.1-cm path length cuvette containing 5 μM of protein sample in 10 mM Tris buffer, pH 8.0. Assays were carried out in a Jasco J-810 spectropolarimeter (Jasco Inc., Tokyo, Japan) at temperatures varying from 20 to 80°C, at an increment of 2°C min^{-1}. Melting temperatures (T_m) were calculated by fitting the sigmoidal melting curve to the Boltzmann equation using GraphPad Prism version 5.01 (GraphPad Prism Software, San Diego, USA), with R2 values of >0.98. The spectra are shown as an average of eight scans recorded from 190 to 260 nm. The content of secondary structures was estimated using the CDNN 2.1 software (Bohm et al., 1992).

Analysis of the rPbPrx1 Quaternary Structure by Size-Exclusion Chromatography

Size-exclusion chromatography experiments were performed by analytical HPLC equipped with a PU 2880 Plus injector and a PDA MD 2018 detector (LC-2000 series; Jasco, Tokyo, Japan). The samples (50 μM in 100 mM Tris-HCl, pH 7.4) were separated by a system containing a Phenomenex BioSep-SEC-S3000 column (7.8 × 300 mm, 5 μm, resolution range of 1–300 kDa, Phenomenex, Inc., Torrance, California, USA) at a flow rate of 1.0 mL min^{-1} in 100 mM Tris-HCl, pH 7.4, containing 50 mM NaCl. The elution profile was monitored by absorbance at λ = 280 nm. Bovine thyroglobulin (670 kDa), bovine gamma globulin (158 kDa), ovalbumin (44 kDa), myoglobin (17 kDa), and vitamin B_{12} (1.35 kDa) were used as molecular standards (Bio-Rad Laboratories, Richmond, USA). Chromatograms were analyzed using Jasco BORWIN, version 1.50, software (Jasco, Tokyo, Japan). The redox treatments for rPbPrx1 were either 5 mM TCEP (reductant) or 1.2 molar equivalent of hydrogen peroxide (oxidant) for 30 min, at 25°C prior to the chromatographic runs.

RESULTS

The *P. brasiliensis* Genome Bears a Single 1-Cys Prx-like Gene

Database search (https://www.ncbi.nlm.nih.gov) showed that *P. brasiliensis* has a single Prx1 ortholog (PbPrx1) that is 222-amino-acid long and has a deduced molecular mass of 24.7 kDa. Amino acid sequence alignments of PbPrx1 with 1-Cys Prx1 from other species shows that PbPrx1 has only one conserved cysteine (Cys51; **Supplementary Figure 2**, red asterisk), which corresponds to the Cys91 from *S. cerevisiae* ScPrx1. The signature sequence PVC_PTTE, characteristic to the 1-Cys Prx1 group, carries a point substitution of the second residue (V→T) resulting in the PTC_PTTE sequence, which is also observed in other phylogenetically-related temperature-dependent dimorphic species such as *P. lutzii*, *H. capsulatum*, and *Blastomyces dermatitidis* (**Supplementary Figure 2**). Overall, the PbPrx1 sequence showed 57% identity and 72% similarity to the 1-Cys Prx1 isoform from ScPrx1. As expected, we observed higher homology with the isoforms from *H. capsulatum* (HcPrx1; 89% identity) and *B. dermatitidis* (BdPrx1; 87% identity), while the identity between PbPrx1 and PlPrx1 is 98%. In **Supplementary Figure 2**, the green box shows a Ca^{2+}-independent phospholipase A2 (PLA2) motif GDSWG (Nevalainen, 2010) that is not conserved in PbPrx1, PlPrx1, HcPrx1, or BdPrx1. In these sequences, the Ser residue involved in catalysis is substituted for Lys/His (GDK/HYV). Importantly, PbPrx1 does not have an *N*-terminal mitochondrial signal peptide, which can be seen in the Prx1 isoforms from *S. cerevisiae*, *Aspergillus nidulans*, and *Candida albicans*, thus suggesting a cytosolic localization of the protein (**Supplementary Figure 2**).

PbPrx1 Cellular Location

In order to study the PbPrx1 cell localization, we produced mice anti-rPbPrx1 immune sera, using a recombinant rPbPrx1 protein as immunogen, and monospecific anti-PbPrx1 antibodies. Confocal microscopy images seen in **Figure 1A** show fluorescence label in the cytoplasm, in a punctuated pattern, in both the yeast and mycelial phases of *P. brasiliensis*. Interestingly, PbPrx1 seems to accumulate close to hyphal septa (white arrows). Cell wall and mitochondrial localization were further investigated by immunoblot (**Figure 1B**), which revealed a 25-kDa protein band reacting with anti-rPbPrx1 antibodies in the yeast mitochondrial extracts, even though the PbPrx1 sequence lacks an *N*-terminal mitochondrial signal peptide (**Supplementary Figure 2**). Similarly, anti-rPbPrx1 antibodies specifically reacted with a single protein band of approximately 25 kDa in cell wall extracts from *P. brasiliensis* yeasts and mycelia, suggesting that PbPrx1 colocalizes at the *P. brasiliensis* yeast cell wall. Although cell wall localization was not clear in confocal images, PbPrx1 surface labeling has also been suggested by FACS analysis of non-permeabilized *P. brasiliensis* yeast cells

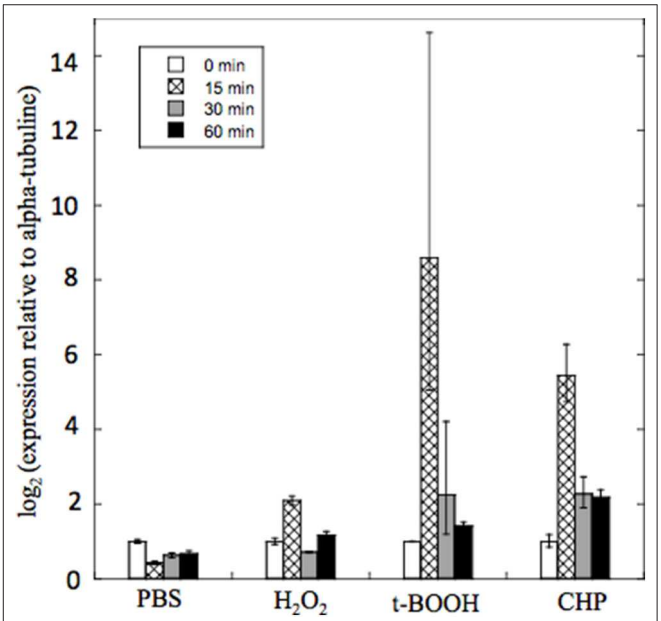

FIGURE 4 | Quantitative real time RT-PCR of Pb*PRX1* from Pb18 yeast cells after oxidative stress. The cells were incubated for 60 min in PBS containing 5 mM H_2O_2, *t*-BOOH, or CHP (cumene hydroperoxide). Changes in transcript levels were determined in comparison to incubation with PBS alone. The cycle thresholds were normalized with the expression of the alpha-tubulin gene.

labeled with anti-rPbPrx1 antibodies (**Figure 1C**). Anti-rPbPrx1 immune serum reacted with yeast cells with higher fluorescence intensity than pre-immune serum (5-fold increase), suggesting that the reaction was specific. The number of positive cells was also 50% higher in the reaction with anti-rPbPrx1 immune serum than with pre-immune serum. Taken together, our results suggest that PbPrx1 localizes to the cytoplasm and cell wall of the yeast and mycelial forms of *P. brasiliensis,* as well as in the yeast mitochondria.

Biochemical Characterization of rPbPrx1

To determine whether *P. brasiliensis* PbPrx1 is a thiol-dependent peroxidase, the activity for both H_2O_2 and *t*-BOOH consumption was monitored by DTT oxidation. As indicated in **Figure 2**, both hydroperoxides were reduced, although the enzyme exhibited higher affinity for *t*-BOOH than for H_2O_2 (v_0 = 0.89 and 2.73 μM s^{-1}, respectively). Peroxidatic cysteine-dependent activity was confirmed by NEM alkylation, corroborating with the evidence that the PbPrx1 is a peroxiredoxin (**Figure 2B**). To evaluate the rPbPrx1 phospholipase activity, we performed a phospholipase assay using 4-Nitro-3-(octanoyloxy) benzoic acid (NOBA). As predicted by structural analysis, the PbPrx1 does not have phospholipase activity (**Supplementary Figure 2**). Together, our results show that PbPrx1 is a thiol-dependent peroxidase that has higher affinity for organic hydroperoxides, but that lacks phospholipase activity.

In order to confirm that organic substrates are decomposed more efficiently by PbPrx1, we also performed a FOX assay with both H_2O_2 and different organic hydroperoxides

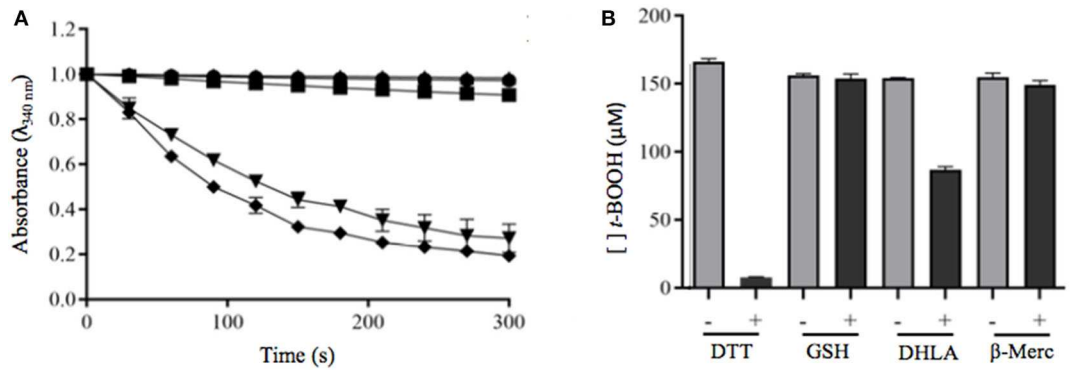

FIGURE 5 | Evaluation of dithiolic and monothiolic compounds as electron donors to rPbPrx1. **(A)** Trx-linked rPbPrx1 peroxidase activity was evaluated using the *S. cerevisiae* heterologous Trx system and rPbPrx1 by monitoring the NADPH oxidation (λ = 340 nm) at 30°C in the presence of either *t*-BOOH (•) or H_2O_2 (■). Reactions without rPbPrx1 were used as negative controls (▲). As positive controls, we used samples containing *S. cerevisiae* Tsa1 (*t*-BOOH, ▼; H_2O_2, ♦). **(B)** FOX assay evaluation of rPbPrx1 thiol-dependent peroxidase activity using different reductant thiolic compounds. The peroxidase activity was evaluated from the amount of remaining hydroperoxide (λ = 560 nm). The reactions were performed using different reducing agents: GSH (3 mM), β-mercaptoetanol (3 mM), and DHLA (300 μM). The bars represent the final concentration of *t*-BOOH after 15 min. All experiments were performed at least three times and yielded similar results.

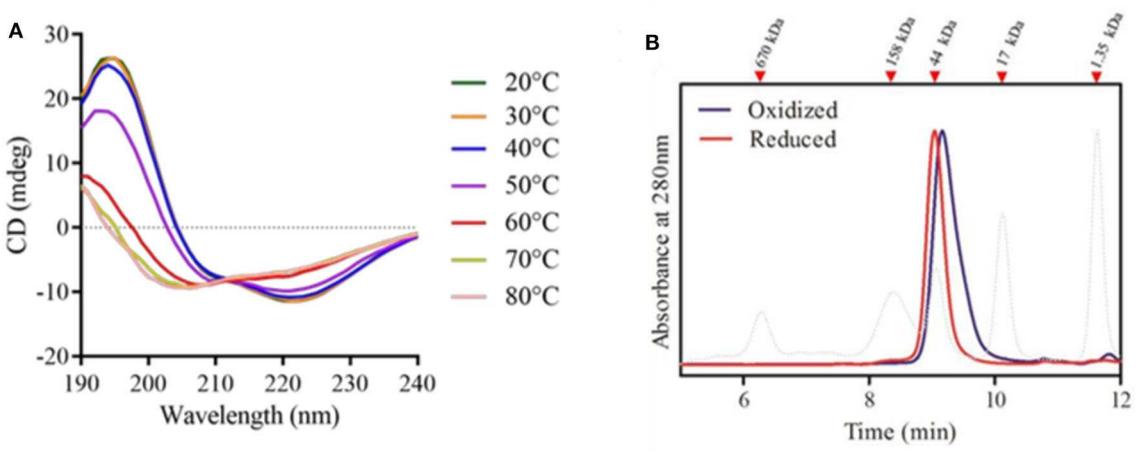

FIGURE 6 | rPbPrx1 structural analysis by circular dichroism (CD). **(A)** rPbPrx1 thermal shift assay. rPBPrx1 (5 μM) was evaluated at different temperatures (20–80°C) in 10 mM Tris buffer (pH 8.0) and the results are presented as an average of eight scans recorded from 190 to 260 nm. All spectra were corrected against the buffer. The table showing the percentage of secondary structures in accordance with the temperature profile is available as **Supplementary Table 1**. **(B)** Size-exclusion chromatography of rPpPrx1 in reduced (red line) and oxidized (blue line) forms was performed in a BioSep-SEC-S2000 column and monitored by absorbance at 280 nm. The elution profile of molecular standards is represented by dotted lines. All experiments were performed at least three times with similar results.

such as tert-butyl (*t*-BOOH), cumene (CHP), and linoleic hydroperoxides (L-OOH). The enzyme catalytic efficiency was significantly higher for L-OOH (**Figure 3D**), with initial velocity (V_0) of 12.12 ± 1.2 μM min^{-1}, which is ∼2.7-fold higher than that for CHP (4.52 ± 0.06 μM min^{-1}) and ∼8.8-fold higher than that stimated for *t*-BOOH (1.37 ± 0.02 μM min^{-1}) (**Figures 3B–D**). On the other hand, the enzyme did not show significant decomposition rate for hydrogen peroxide (0.024 μM min^{-1}) (**Figure 3A**). Thus, our results confirm that rPbPrx1 has pronounced affinity for organic peroxides, particularly for more hydrophobic OHPs (CHP and LOOH). That may indicate the presence of a hydrophobic microenvironment in the active site of the enzyme, as observed for some Prx (Hall et al., 2009, 2011).

Pb*PRX1* Gene Expression

To gain insight into the physiological roles of PbPrx1 during oxidative stress, its expression pattern was characterized when yeast cells were exposed to both inorganic (H_2O_2) and organic (*t*-BOOH and CHP) peroxides for 15, 30, and 60 min (**Figure 4**). As a general trend, the Pb*PRX1* gene was regulated in a time-dependent manner, with higher expression levels at 15 min, followed by decreased expression in the following timepoints. Pb*PRX1* gene expression was induced by the three hydroperoxides, but a more pronounced upregulation was seen with organic peroxides. Pb*PRX1* gene expression increased 8.5- and 5.4-fold, respectively for *t*-BOOH and CHP, in comparison to only 2-fold for H_2O_2. These results infer that PbPrx1 might have a more important physiological role during oxidative stress caused by organic hydroperoxides, which is consistent with the higher affinity of PbPrx1 for these molecules (**Figure 3**).

Analysis of rPbPrx1 Reductants

To investigate the possible PbPrx1 reductants, the following reducing agents were tested: DTT and DHLA (dithiolic), GSH and β-ME (monothiolic), and the heterologous *S. cerevisiae* Trx system, which is responsible for Prx reduction in this organism. It can be inferred from the results seen in **Figure 5B** that rPbPrx1 only receives electrons from dithiolic compounds of low molecular weight (DTT and DHLA), but not from monothiolic compounds (GSH and β-ME) or from the heterologous *S. cerevisiae* Txr reducing system compounds (**Figure 5A**), although they have been described as possible reducing agents to other 1-Cys Prx (Pedrajas et al., 2000; Monteiro et al., 2007; Rocha et al., 2018).

Evaluation of the rPbPrx1 Secondary and Quaternary Structure

Recombinant rPbPrx1 samples were analyzed by CD to assess the structural content and conformational changes related to temperature. Our results indicate the presence of an α/β protein with secondary structure composed of ∼36% α-helices, ∼27% β structures, and ∼37% unstructured regions (**Figure 6A**, **Supplementary Table 1**), similar to what has been observed for 1-Cys Prx from other organisms (Choi et al., 1998; Sarma et al., 2005). The enzyme has poor thermal stability, maintaining its native conformation only at temperatures up to 40°C (**Figure 6A**), which, on the other hand, is compatible with its activity in the human host.

Size exclusion chromatography was performed to analyze rPbPrx1 quaternary structure. The elution pattern shows single peaks compatible with molecules of ∼45 kDa, suggesting that the enzyme is mainly found in a dimeric form. rPbPrx1 analysis in different redox states indicates that the oxidized structure elutes more compactly than that observed in the reduced state (**Figure 6B**), however maintaining the dimeric structure.

DISCUSSION

In the present work, we characterized a single Prx1 ortholog found in the genome of the dimorphic fungus *P. brasiliensis* (PbPrx1). The PbPrx1 protein analysis showed that the universal motif PVC_PTTE of the 1-Cys Prx sequences contains a substitution of the second aminoacidic residue (Val), a hydrophobic residue, to a polar Thr (PTC_PTTE). This substitution is shared by other dimorphic fungi, which may suggest a characteristic signature for this group of fungal species. In another related group of fungal species, specifically, *A. niger, A. oryzae,* and *C. tropicalis,* the Val residue is substituted by Ile (PIC_PTTE). Since this amino acid is in the vicinity to the catalytic cysteine (C_P), the mentioned substitutions may affect both the catalytic activity of the Prx and its substrate preference. On the other hand, the sequence analysis revealed the inexistence of a phospholipase C-terminal motif, which is in agreement with our experimental results indicating that PbPrx1 does not show phospholipase activity. So far, there are only two fungal 1-Cys Prx1 bearing phospholipase activity, namely the AfPrx1 and AfPrxC isoforms from *A. fumigatus* (Bannitz-Fernandes et al., 2019). Concerning the secondary and quaternary structures, the PbPrx1 does not differ significantly from that of other organisms in the secondary structure content (Gretes et al., 2012). As to the PbPrx1 quaternary structure, we found a dimer, while both dimers and monomers have been observed in the human Prx6 by SEC (Wu et al., 2006).

We also demonstrated that the thiol peroxidase activity is dependent on a Cys residue and that the enzyme has higher affinity for *t*-BOOH than for H_2O_2. The fact that PbPrx1 can decompose organic hydroperoxides more efficiently than hydrogen peroxide is not an exclusive characteristic of PbPrx1. Other thiol peroxidases, such as the human PrxV, *E. coli* thiol peroxidase (EcTpx), and the organic hydroperoxide resistance protein (Ohr) from *Xylella fastidiosa* are 100–1000-fold more reactive with organic peroxides, as a consequence of a hydrophobic active site microenvironment, which enables interactions with hydrophobic oxidizing substrates (Cussiol et al., 2003; Perkins et al., 2014; Alegria et al., 2017; Piccirillo et al., 2018). In this context, our data suggest that the active site microenvironment of PbPrx1 is also highly hydrophobic, suggesting that PbPrx1 may act as a strong scavenger of organic peroxides in *P. brasiliensis* cells. Regarding the reductant substrates, we showed that PbPrx1 is not able to receive electrons from a heterologous *S. cerevisiae* thioredoxin reducing system or from monothiolic compounds (GSH and β-ME). The

recombinant PbPrx1 was only reduced by dithiolic compounds of low molecular weight (DTT and DHLA).

We have previously found the PbPrx1 protein in the cell wall proteome from both the yeast and mycelial forms of *P. brasiliensis*, isolates Pb18 and Pb3, and in the extracellular vesicle (EV) proteome from *P. brasiliensis* Pb18 (Longo et al., 2014). In Pb18, PbPrx1 was 2–3-fold more abundant upon nitrosative and oxidative stress (Leitão et al., unpublished), suggesting a role for the enzyme during stress. We have presently shown predominant cytoplasmic localization of PbPrx1 in *P. brasiliensis* by confocal microscopy, but the protein was additionally labeled in cell wall extracts and in the surface of non-permeabilized yeast cells by FACS analysis. Surprisingly, the PbPrx1 was also identified in mitochondrial protein extracts from yeast cells by Western blot, despite the fact that the predicted sequence lacks an *N*-terminal mitochondrial signal peptide. Although we cannot discard that the mitochondrial extract may be contaminated with small amounts of cytoplasmic PbPrx1, it is more likely to assume that PbPrx1 is not directed to the mitochondria through the classical import pathway guided by amino-terminal presequences, but instead through internal targeting signals, as seen for more than 50% of mitochondrial proteins (Bolender et al., 2008). In the mitochondria, PbPrx1 might play a role in protecting against ROS that is generated as a result of protein misfolding and aggregate formation (Weids and Grant, 2014).

To gain insights into the physiological roles of PbPrx1, its gene expression pattern was characterized when yeast cultures were exposed to organic and inorganic hydroperoxides. Our data showed a consistent time-dependent induction in the Pb*PRX1* gene expression when *P. brasiliensis* yeasts were exposed to the organic hydroperoxides *t*-BOOH and CHP, with peaks by 15 min of exposure of 8.5-fold and 5.45-fold increase, respectively. For *t*-BOOH, for instance, this value was 2–4-fold the induction caused by H_2O_2 (2-fold), which is in agreement with the fact that PbPrx1 showed higher affinity for organic hydroperoxides. Similarly, the *C. albicans* Prx1 (CaPrx1) peroxidase activity is able to reduce both *t*-BOOH and H_2O_2, but intracellular reactive oxygen species accumulate only when *prx1*Δ is treated with *t*-BOOH, indicating that its cellular function is more specific to organic hydroperoxides (Srinivasa et al., 2012). The increase in the expression of 1-Cys Prx1 upon oxidative stress was also described in *A. fumigatus*. The three 1-Cys Prx genes *PRX1, PRXB, and PRXC*, which show high activity against H_2O_2, were induced in a time-dependent manner when Paraquat was used as the oxidant molecule (Rocha et al., 2018).

The importance to study pathogen enzymes with antioxidant properties comes from the fact that tolerance to oxidative stress is an important trait of virulence in several microorganisms (Banin et al., 2003; Piacenza et al., 2013; Kaihami et al., 2014; Rocha et al., 2018). For that reason, they could also be targets for antifungal agents. In *C. albicans,* the Prx1 ortholog (Tsa1) is found in the cell wall specifically in the pathogenic hyphal phase, while the protein localizes in the cytosol and nucleus of yeast cells, pointing to a role in pathogenicity (Urban et al., 2003). In *P. brasiliensis*, attenuated yeast cells recovered their virulence after serial passages in mice and this process positively modulated the fungal antioxidant repertoire (Castilho et al., 2018). Additionally, proteins involved in the oxidative stress response in *P. brasiliensis* yeast cells were up-regulated during macrophage infection (Parente-Rocha et al., 2015).

Together, our results reveal that PbPrx1 is a peroxidase widely distributed inside (cytosol and mitochondria) and outside (cell wall and extracellular vesicles) *P. brasiliensis* cells. It is highly reactive with organic hydroperoxides (OHPs) and strongly induced by these oxidants, thus suggesting a role of importance in protecting *P. brasiliensis* against insults caused by organic hydroperoxides.

DATA AVAILABILITY STATEMENT

All datasets presented in this study are included in the article/**Supplementary Material**.

ETHICS STATEMENT

The animal study was reviewed and approved by the Ethics Committtee for Research (UNIFESP) numbers: CEP 0366/07 and CEP 6379211014.

AUTHOR CONTRIBUTIONS

LL, GG, NL, and CO performed the cloning, antibody production, localization, and qRT-PCR experiments. CB, GN, and MT performed the biochemical characterization experiments. LL, CB, MO, and RP drafted the manuscript. All authors critically reviewed and approved the final manuscript.

FUNDING

We thank CAPES, CNPq, and Fundação de Amparo à Pesquisa do Estado de São Paulo (FAPESP Grants 06/05095-6, 07/50930-3, 11/13500-6, 13/07937-8, 13/25950-1, 17/19942-7, and 17/20291-0) for financial support.

ACKNOWLEDGMENTS

We thank Luiz Severino da Silva and Filipe Menegatti de Melo for technical assistance.

SUPPLEMENTARY MATERIAL

The Supplementary Material for this article can be found online at: https://www.frontiersin.org/articles/10.3389/fcimb.2020.00394/full#supplementary-material

Supplementary Figure 1 | Recombinant protein purification by IMAC. **(A)** rPbPrx1 expression was performed using *E. coli* Tuner (DE3) containing the pET28PP-*pbPRX1* vector. The protein purification was performed using IMAC: lanes 2–6 represent imidazol gradient progressive elution fractions; lane 6 shows the purified protein used in the experiments. The expressed protein in pHIS1–*pbPRX1* was purified in a Ni-NTA column and the profile of the purified protein was similar to that in lane 6. **(B)** *S. cerevisiae* Trx1 was expressed in *E. coli* BL 21 (DE3), purified by the boiling method and size exclusion chromatography using a HiLoad 16/600 Superdex 75 (GE Healthcare, Piscataway, USA). The elution fractions are shown; fractions 11-14 were pooled for use in the experiments. **(C)** *S. cerevisiae* Tsa1 was expressed in *E. coli* BL 21 (DE3) e

purified by IMAC HiPrep IMAC FF Column (GE Healthcare). The elution fractions are shown; fractions 5-8 were pooled for use in the experiments. **(D)** Baker yeast TrxR1 was expressed in *E. coli* BL 21 (DE3) e purified by IMAC HiPrep IMAC FF Column (GE Healthcare). The elution fractions are shown; fractions 6–8 were pooled for use in the experiments. Lane 1 of each gel: unstained Protein MW Marker (Thermo Fisher Scientific).

Supplementary Figure 2 | Amino acid alignment of 1-Cys Prx1 deduced sequences from pathogenic fungi and other species reveal conserved structural elements with *P. brasiliensis* Prx1. Amino acid sequence alignment was performed using ClustalΩ and graphic representation was generated using Jalview. Identical residues are shaded in blue and sequence similarity is indicated by a blue gradient based on the physicochemical characteristic conservation of the amino acid. The sequences correspond to the following species: Prx1_Pb = *P. brasiliensis* (NCBI accession number: XP_010758730.1); Prx1_Pl = *P. lutzii* (XP_002794671.1); Prx1_Hc = *Histoplasma capsulatum* (EEH07081.1); Prx1_Bd = *Blastomyces dermatitidis* (EEQ85711.1); Prx1_An = *Aspergillus niger* (XP_001401704.2); Prx1_Ao = *A. oryzae* (XP_001821217.1); Px1_Af = *A. fumigatus* (XP_747511.1); Prx1_Ca = *Candida albicans* (XP_717002.1); Prx1_Ct = *C. tropicalis* (XP_002550813.1); Prx1_Sc = *Saccharomyces cerevisiae* (NP_009489.1); Prx1_Pp = *Picchia pastoris* (XP_002490091); Prdx6_Hs = *Homo sapiens* (P30041.3); Prdx6_Rn = *Rattus novergicus* (O35244.3); Pdrx6_Mm = *Mus musculus* (O08709.3). The red line denotes the *N*-terminal mitochondrial signal peptide. The green box highlights the phospholipase A2 (PLA2) motif and the green asterisk the catalytic Ser residue. The red box denotes the conserved P-V/I-C-T-T/S-E signature (catalytic cysteine marked by a red asterisk) of the 1-Cys Prx1 sequences.

Supplementary Figure 3 | PLA2 activity evaluation using NOBA. The assay was performed at 25°C in reaction mixtures containing 20 mM Tris, pH 7.8, 0.001 mg rPbPrx1, 150 mM NaCl, 10 mM CaCl, 0.1 mg/ml 3-(octanoyloxy) benzoic acid (NOBA). The absorbance was monitored at 425 nm for 60 min.

Supplementary Table 1 | PbPrx1 thermal shift analysis by circular dichroism.

REFERENCES

Alegria, T. G., Meireles, D. A., Cussiol, J. R., Hugo, M., Trujillo, M., De Oliveira, M. A., et al. (2017). Ohr plays a central role in bacterial responses against fatty acid hydroperoxides and peroxynitrite. *Proc. Natl. Acad. Sci. U.S.A.* 114, E132–E141. doi: 10.1073/pnas.1619659114

Banin, E., Vassilakos, D., Orr, E., Martinez, R. J., and Rosenberg, E. (2003). Superoxide dismutase is a virulence factor produced by the coral bleaching pathogen *Vibrio shiloi*. *Curr. Microbiol.* 46, 418–422. doi: 10.1007/s00284-002-3912-5

Bannitz-Fernandes, R., Aleixo-Silva, R., Silva, J. P., Dodia, C., Vazquez-Medina, J. P., Tao, J. Q., et al. (2019). Non-mammalian Prdx6 enzymes (proteins with 1-Cys Prdx mechanism) display PLA(2) activity similar to the human orthologue. *Antioxidants* 8:52. doi: 10.3390/antiox8030052

Batista, W. L., Matsuo, A. L., Ganiko, L., Barros, T. F., Veiga, T. R., Freymuller, E., et al. (2006). The PbMDJ1 gene belongs to a conserved MDJ1/LON locus in thermodimorphic pathogenic fungi and encodes a heat shock protein that localizes to both the mitochondria and cell wall of *Paracoccidioides brasiliensis*. *Eukaryot Cell* 5, 379–390. doi: 10.1128/EC.5.2.379-390.2006

Belenky, P., Camacho, D., and Collins, J. J. (2013). Fungicidal drugs induce a common oxidative-damage cellular death pathway. *Cell Rep.* 3, 350–358. doi: 10.1016/j.celrep.2012.12.021

Bocca, A. L., Amaral, A. C., Teixeira, M. M., Sato, P. K., Shikanai-Yasuda, M. A., and Soares Felipe, M. S. (2013). Paracoccidioidomycosis: eco-epidemiology, taxonomy and clinical and therapeutic issues. *Future Microbiol.* 8, 1177–1191. doi: 10.2217/fmb.13.68

Bohm, G., Muhr, R., and Jaenicke, R. (1992). Quantitative analysis of protein far UV circular dichroism spectra by neural networks. *Protein Eng.* 5, 191–195. doi: 10.1093/protein/5.3.191

Bolender, N., Sickmann, A., Wagner, R., Meisinger, C., and Pfanner, N. (2008). Multiple pathways for sorting mitochondrial precursor proteins. *EMBO Rep.* 9, 42–49. doi: 10.1038/sj.embor.7401126

Campos, E. G., Jesuino, R. S., Dantas Ada, S., Brigido Mde, M., and Felipe, M. S. (2005). Oxidative stress response in *Paracoccidioides brasiliensis*. *Genet. Mol. Res.* 4, 409–429.

Castilho, D. G., Navarro, M. V., Chaves, A. F. A., Xander, P., and Batista, W. L. (2018). Recovery of the *Paracoccidioides brasiliensis* virulence after animal passage promotes changes in the antioxidant repertoire of the fungus. *FEMS Yeast Res.* 18:foy007. doi: 10.1093/femsyr/foy007

Choi, H. J., Kang, S. W., Yang, C. H., Rhee, S. G., and Ryu, S. E. (1998). Crystal structure of a novel human peroxidase enzyme at 2.0 A resolution. *Nat. Struct. Biol.* 5, 400–406. doi: 10.1038/nsb0598-400

Cisalpino, P. S., Puccia, R., Yamauchi, L. M., Cano, M. I., Da Silveira, J. F., and Travassos, L. R. (1996). Cloning, characterization, and epitope expression of the major diagnostic antigen of *Paracoccidioides brasiliensis*. *J. Biol. Chem.* 271, 4553–4560. doi: 10.1074/jbc.271.8.4553

Cox, A. G., Winterbourn, C. C., and Hampton, M. B. (2009). Mitochondrial peroxiredoxin involvement in antioxidant defence and redox signalling. *Biochem. J.* 425, 313–325. doi: 10.1042/BJ20091541

Cussiol, J. R., Alves, S. V., De Oliveira, M. A., and Netto, L. E. (2003). Organic hydroperoxide resistance gene encodes a thiol-dependent peroxidase. *J. Biol. Chem.* 278, 11570–11578. doi: 10.1074/jbc.M300252200

Deighton, N., Muckenschnabel, I. I., Goodman, B. A., and Williamson, B. (1999). Lipid peroxidation and the oxidative burst associated with infection of *Capsicum annuum* by *Botrytis cinerea*. *Plant J.* 20, 485–492. doi: 10.1046/j.1365-313x.1999.00622.x

Edlich, W., and Lyr, H. (1992). *Target Sites of Fungicides With Primary Effects on Lipid Peroxidation.* Boca Raton, FL: CRC Press Inc.

El-Benna, J., Hurtado-Nedelec, M., Marzaioli, V., Marie, J. C., Gougerot-Pocidalo, M. A., and Dang, P. M. (2016). Priming of the neutrophil respiratory burst: role in host defense and inflammation. *Immunol. Rev.* 273, 180–193. doi: 10.1111/imr.12447

Goldman, G. H., Dos Reis Marques, E., Duarte Ribeiro, D. C., De Souza Bernardes, L. A., Quiapin, A. C., Vitorelli, P. M., et al. (2003). Expressed sequence tag analysis of the human pathogen *Paracoccidioides brasiliensis* yeast phase: identification of putative homologues of *Candida albicans* virulence and pathogenicity genes. *Eukaryot Cell* 2, 34–48. doi: 10.1128/EC.2.1.34-48.2003

Gretes, M. C., Poole, L. B., and Karplus, P. A. (2012). Peroxiredoxins in parasites. *Antioxid. Redox Signal.* 17, 608–633. doi: 10.1089/ars.2011.4404

Grossklaus, D. A., Bailão, A. M., Rezende, T. C. V., Borges, C. L., Oliveira, M. A. P., Parente, J. A., et al. (2013). Response to oxidative stress in *Paracoccidioides* yeast cells as determined by proteomic analysis. *Microbes. Infect.* 15, 347–364. doi: 10.1016/j.micinf.2012.12.002

Hall, A., Nelson, K., Poole, L. B., and Karplus, P. A. (2011). Structure-based insights into the catalytic power and conformational dexterity of peroxiredoxins. *Antioxid. Redox Signal.* 15, 795–815. doi: 10.1089/ars.2010.3624

Hall, A., Sankaran, B., Poole, L. B., and Karplus, P. A. (2009). Structural changes common to catalysis in the Tpx peroxiredoxin subfamily. *J. Mol. Biol.* 393, 867–881. doi: 10.1016/j.jmb.2009.08.040

Halliwell, B., and Gutteridge, J. M. (2015). *Free Radicals in Biology and Medicine.* Oxford:Oxford University Press. doi: 10.1093/acprof:oso/9780198717478.001.0001

Kaihami, G. H., Almeida, J. R., Santos, S. S., Netto, L. E., Almeida, S. R., and Baldini, R. L. (2014). Involvement of a 1-Cys peroxiredoxin in bacterial virulence. *PLoS Pathog.* 10:e1004442. doi: 10.1371/journal.ppat.1004442

Longo, L. V., da Cunha, J. P. C., Sobreira, T. J. P., and Puccia, R. (2014). Proteome of cell wall extracts from pathogenic *Paracoccidioides brasiliensis*: comparison among morphological phases, isolates, and reported fungal extracellular vesicle proteins. *EuPA Open Proteomics* 3, 216–228. doi: 10.1016/j.euprot.2014.03.003

Martinez, R. (2017). New trends in paracoccidioidomycosis epidemiology. *J. Fungi* 3:1. doi: 10.3390/jof3010001

Monteiro, G., Horta, B. B., Pimenta, D. C., Augusto, O., and Netto, L. E. (2007). Reduction of 1-Cys peroxiredoxins by ascorbate changes the thiol-specific antioxidant paradigm, revealing another function of vitamin C. *Proc. Natl. Acad. Sci. U.S.A.* 104, 4886–4891. doi: 10.1073/pnas.0700481104

Nelson, K. J., and Parsonage, D. (2011). Measurement of peroxiredoxin activity. *Curr. Protoc. Toxicol.* 49, 7.10.1–7.10.28. doi: 10.1002/0471140856.tx0710s49

Netto, L. E., De Oliveira, M. A., Tairum, C. A., and Da Silva Neto, J. F. (2016). Conferring specificity in redox pathways by enzymatic thiol/disulfide exchange reactions. *Free Radic. Res.* 50, 206–245. doi: 10.3109/10715762.2015.1120864

Nevalainen, T. J. (2010). 1-Cysteine peroxiredoxin: a dual-function enzyme with peroxidase and acidic Ca^{2+}-independent phospholipase A_2 activities. *Biochimie* 92, 638–644. doi: 10.1016/j.biochi.2010.01.019

Oliveira, M. A., Discola, K. F., Alves, S. V., Medrano, F. J., Guimaraes, B. G., and Netto, L. E. (2010). Insights into the specificity of thioredoxin reductase-thioredoxin interactions. A structural and functional investigation of the yeast thioredoxin system. *Biochemistry* 49, 3317–3326. doi: 10.1021/bi901962p

Parente-Rocha, J. A., Parente, A. F., Baeza, L. C., Bonfim, S. M., Hernandez, O., Mcewen, J. G., et al. (2015). Macrophage interaction with *Paracoccidioides brasiliensis* yeast cells modulates fungal metabolism and generates a response to oxidative stress. *PLoS ONE* 10:e0137619. doi: 10.1371/journal.pone.0137619

Parsonage, D., Karplus, P. A., and Poole, L. B. (2008). Substrate specificity and redox potential of AhpC, a bacterial peroxiredoxin. *Proc. Natl. Acad. Sci. U.S.A.* 105, 8209–8214. doi: 10.1073/pnas.0708308105

Pedrajas, J. R., Miranda-Vizuete, A., Javanmardy, N., Gustafsson, J. A., and Spyrou, G. (2000). Mitochondria of *Saccharomyces cerevisiae* contain one-conserved cysteine type peroxiredoxin with thioredoxin peroxidase activity. *J. Biol. Chem.* 275, 16296–16301. doi: 10.1074/jbc.275.21.16296

Perkins, A., Poole, L. B., and Karplus, P. A. (2014). Tuning of peroxiredoxin catalysis for various physiological roles. *Biochemistry* 53, 7693–7705. doi: 10.1021/bi5013222

Peskin, A. V., Low, F. M., Paton, L. N., Maghzal, G. J., Hampton, M. B., and Winterbourn, C. C. (2007). The high reactivity of peroxiredoxin 2 with H(2)O(2) is not reflected in its reaction with other oxidants and thiol reagents. *J. Biol. Chem.* 282, 11885–11892. doi: 10.1074/jbc.M700339200

Petrovic, N., Grove, C., Langton, P. E., Misso, N. L., and Thompson, P. J. (2001). A simple assay for a human serum phospholipase A_2 that is associated with high-density lipoproteins. *J. Lipid Res.* 42, 1706–1713.

Piacenza, L., Peluffo, G., Alvarez, M. N., Martinez, A., and Radi, R. (2013). *Trypanosoma cruzi* antioxidant enzymes as virulence factors in Chagas disease. *Antioxid. Redox Signal.* 19, 723–734. doi: 10.1089/ars.2012.4618

Piccirillo, E., Alegria, T. G. P., Discola, K. F., Cussiol, J. R. R., Domingos, R. M., De Oliveira, M. A., et al. (2018). Structural insights on the efficient catalysis of hydroperoxide reduction by Ohr: crystallographic and molecular dynamics approaches. *PLoS ONE* 13:e0196918. doi: 10.1371/journal.pone.0196918

Rhee, S. G., and Kil, I. S. (2017). Multiple functions and regulation of mammalian peroxiredoxins. *Annu. Rev. Biochem.* 86, 749–775. doi: 10.1146/annurev-biochem-060815-014431

Rocha, M. C., de Godoy, K. F., Bannitz-Fernandes, R., Fabri, J., Barbosa, M. M. F., De Castro, P. A., et al. (2018). Analyses of the three 1-Cys peroxiredoxins from *Aspergillus fumigatus* reveal that cytosolic Prx1 is central to H_2O_2 metabolism and virulence. *Sci. Rep.* 8:12314. doi: 10.1038/s41598-018-30108-2

Sarma, G. N., Nickel, C., Rahlfs, S., Fischer, M., Becker, K., and Karplus, P. A. (2005). Crystal structure of a novel *Plasmodium falciparum* 1-Cys peroxiredoxin. *J. Mol. Biol.* 346, 1021–1034. doi: 10.1016/j.jmb.2004.12.022

Schmittgen, T. D., and Livak, K. J. (2008). Analyzing real-time PCR data by the comparative C(T) method. *Nat. Protoc.* 3, 1101–1108. doi: 10.1038/nprot.2008.73

Shekhova, E., Kniemeyer, O., and Brakhage, A. A. (2017). Induction of mitochondrial reactive oxygen species production by itraconazole, terbinafine, and amphotericin B as a mode of action against *Aspergillus fumigatus*. *Antimicrob. Agents Chemother.* 61, e00978–e00917. doi: 10.1128/AAC.00978-17

Soares, R. M., Costa e Silva-Filho, F., Rozental, S., Angluster, J., De Souza, W., Alviano, C. S., et al. (1998). Anionogenic groups and surface sialoglycoconjugate structures of yeast forms of the human pathogen *Paracoccidioides brasiliensis*. *Microbiology* 144(Pt 2), 309–314. doi: 10.1099/00221287-144-2-309

Srinivasa, K., Kim, N. R., Kim, J., Kim, M., Bae, J. Y., Jeong, W., et al. (2012). Characterization of a putative thioredoxin peroxidase prx1 of *Candida albicans*. *Mol. Cells* 33, 301–307. doi: 10.1007/s10059-012-2260-y

Tairum, C. A., Santos, M. C., Breyer, C. A., Geyer, R. R., Nieves, C. J., Portillo-Ledesma, S., et al. (2016). Catalytic Thr or Ser residue modulates structural switches in 2-Cys peroxiredoxin by distinct mechanisms. *Sci. Rep.* 6:33133. doi: 10.1038/srep33133

Tairum, C. A. Jr., de Oliveira, M. A., Horta, B. B., Zara, F. J., and Netto, L. E. (2012). Disulfide biochemistry in 2-cys peroxiredoxin: requirement of Glu50 and Arg146 for the reduction of yeast Tsa1 by thioredoxin. *J. Mol. Biol.* 424, 28–41. doi: 10.1016/j.jmb.2012.09.008

Urban, C., Sohn, K., Lottspeich, F., Brunner, H., and Rupp, S. (2003). Identification of cell surface determinants in *Candida albicans* reveals Tsa1p, a protein differentially localized in the cell. *FEBS Lett.* 544, 228–235. doi: 10.1016/S0014-5793(03)00455-1

Vallejo, M. C., Matsuo, A. L., Ganiko, L., Medeiros, L. C., Miranda, K., Silva, L. S., et al. (2011). The pathogenic fungus *Paracoccidioides brasiliensis* exports extracellular vesicles containing highly immunogenic alpha-galactosyl epitopes. *Eukaryot Cell* 10, 343–351. doi: 10.1128/EC.00227-10

Vallejo, M. C., Nakayasu, E. S., Matsuo, A. L., Sobreira, T. J., Longo, L. V., Ganiko, L., et al. (2012). Vesicle and vesicle-free extracellular proteome of *Paracoccidioides brasiliensis*: comparative analysis with other pathogenic fungi. *J. Proteome Res.* 11, 1676–1685. doi: 10.1021/pr200872s

Weids, A. J., and Grant, C. M. (2014). The yeast peroxiredoxin Tsa1 protects against protein-aggregate-induced oxidative stress. *J. Cell Sci.* 127, 1327–1335. doi: 10.1242/jcs.144022

Wen, L., Huang, H. M., Juang, R. H., and Lin, C. T. (2007). Biochemical characterization of 1-Cys peroxiredoxin from *Antrodia camphorata*. *Appl. Microbiol. Biotechnol.* 73, 1314–1322. doi: 10.1007/s00253-006-0608-y

Winterbourn, C. C. (2008). Reconciling the chemistry and biology of reactive oxygen species. *Nat. Chem. Biol.* 4, 278-286. doi: 10.1038/nchembio.85

Wu, Y. Z., Manevich, Y., Baldwin, J. L., Dodia, C., Yu, K., Feinstein, S. I., et al. (2006). Interaction of surfactant protein A with peroxiredoxin 6 regulates phospholipase A_2 activity. *J. Biol. Chem.* 281, 7515–7525. doi: 10.1074/jbc.M504525200

Zhou, S., Dodia, C., Feinstein, S. I., Harper, S., Forman, H. J., Speicher, D. W., et al. (2018). Oxidation of peroxiredoxin 6 in the presence of GSH increases its phospholipase A(2) activity at cytoplasmic pH. *Antioxidants* 8:4. doi: 10.3390/antiox8010004

Conflict of Interest: The authors declare that the research was conducted in the absence of any commercial or financial relationships that could be construed as a potential conflict of interest.

frontiers in Cellular and Infection Microbiology

REVIEW
published: 03 September 2020
doi: 10.3389/fcimb.2020.00463

Therapies and Vaccines Based on Nanoparticles for the Treatment of Systemic Fungal Infections

Brenda Kischkel[1,2]*, *Suélen A. Rossi*[1,2], *Samuel R. Santos Junior*[1,2], *Joshua D. Nosanchuk*[3], *Luiz R. Travassos*[4] *and Carlos P. Taborda*[1,2]*

[1] Department of Microbiology, Institute of Biomedical Sciences, University of São Paulo, São Paulo, Brazil, [2] Laboratory of Medical Mycology-Institute of Tropical Medicine of São Paulo/LIM53/Medical School, University of São Paulo, São Paulo, Brazil, [3] Departments of Medicine [Division of Infectious Diseases], Microbiology and Immunology, Albert Einstein College of Medicine and Montefiore Medical Center, Bronx, NY, United States, [4] Department of Microbiology, Immunology and Parasitology, Federal University of São Paulo, São Paulo, Brazil

OPEN ACCESS

Edited by:
James Bernard Konopka,
Stony Brook University, United States

Reviewed by:
Jose L. Lopez-Ribot,
University of Texas at San Antonio, United States
Amir M. Farnoud,
Ohio University, United States

***Correspondence:**
Brenda Kischkel
brendakischkel@usp.br
Carlos P. Taborda
taborda@usp.br

Specialty section:
This article was submitted to Fungal Pathogenesis, a section of the journal Frontiers in Cellular and Infection Microbiology

Received: 24 June 2020
Accepted: 28 July 2020
Published: 03 September 2020

Citation:
Kischkel B, Rossi SA, Santos Junior SR, Nosanchuk JD, Travassos LR and Taborda CP (2020) Therapies and Vaccines Based on Nanoparticles for the Treatment of Systemic Fungal Infections. Front. Cell. Infect. Microbiol. 10:463. doi: 10.3389/fcimb.2020.00463

Treatment modalities for systemic mycoses are still limited. Currently, the main antifungal therapeutics include polyenes, azoles, and echinocandins. However, even in the setting of appropriate administration of antifungals, mortality rates remain unacceptably high. Moreover, antifungal therapy is expensive, treatment periods can range from weeks to years, and toxicity is also a serious concern. In recent years, the increased number of immunocompromised individuals has contributed to the high global incidence of systemic fungal infections. Given the high morbidity and mortality rates, the complexity of treatment strategies, drug toxicity, and the worldwide burden of disease, there is a need for new and efficient therapeutic means to combat invasive mycoses. One promising avenue that is actively being pursued is nanotechnology, to develop new antifungal therapies and efficient vaccines, since it allows for a targeted delivery of drugs and antigens, which can reduce toxicity and treatment costs. The goal of this review is to discuss studies using nanoparticles to develop new therapeutic options, including vaccination methods, to combat systemic mycoses caused by *Candida* sp., *Cryptococcus* sp., *Paracoccidioides* sp., *Histoplasma* sp., *Coccidioides* sp., and *Aspergillus* sp., in addition to providing important information on the use of different types of nanoparticles, nanocarriers and their corresponding mechanisms of action.

Keywords: drug delivery systems, vaccine adjuvant, antifungal therapy, mycosis, *Candida albicans*, *Cryptococcus* sp., *Histoplasma capsulatum*

INTRODUCTION

Fungal diseases are broadly classified according to the degree of interactions between the pathogen and the host tissue in superficial, subcutaneous, and systemic infections (Tiew et al., 2020). Superficial mycoses, which are estimated to occur in 25% of the world population, are the most common form of fungal infection. Systemic mycosis, however, is most severe since it is associated to a high mortality rate, significant morbidity, limited chemotherapeutic options, and the diagnosis is frequently difficult and complex (Kauffman, 2007; Brunet et al., 2018).

Opportunistic fungal infections usually occur in immunocompromised individuals as a result of subjacent infection or the treatment itself. Infections of endogenous origin caused by pathogens such as *Candida albicans* can also occur (Colombo et al., 2017; Rautemaa-Richardson and Richardson, 2017). Species of *Aspergillus*, *Candida, Cryptococcus*, and *Trichosporon* are the main agents of opportunistic mycoses. Endemic fungal infections are usually caused by dimorphic fungi, found in the soil or in animal feces. Host acquisition occurs by inhalation of infectious spores/infective propagules (Rodríguez-Cerdeira et al., 2014). In the case of endemic mycoses, immunocompetent individuals dwelling in endemic areas may develop severe disease following inhalation of fungal particles, associated or not to a competent immune response (Edwards et al., 2013). The main species that cause endemic mycoses are *Blastomyces dermatitidis, Coccidioides immitis* and *Coccidioides posadasii, Histoplasma capsulatum, Paracoccidioides,* particularly *P. brasiliensis* and *P. lutzii, Sporothrix*, primarily *S. brasiliensis* and *S. schenckii,* and *Talaromyces marneffei* (Brown et al., 2012; Limper et al., 2017).

In the second half of the 20th century, a worldwide, progressive increase in the number of immunocompromised individuals took place, paralleling the outcome of HIV epidemics as well as the expanded use of immunosuppressive drugs in cancer, autoimmune disease, and transplant patients (Coelho and Casadevall, 2016; Armstrong-James et al., 2017). As a consequence, systemic mycoses have been considered an emergent threat, because immunocompromised individuals are more susceptible to fungal infection (Lockhart, 2019). Cryptococcosis is an excellent example of the profound impact of fungal infections over time, in humans. The number of infections caused by *Cryptococcus* has increased from 300 cases in 1,950 to ∼1 million cases in 2008 causing ∼600,000 deaths per year in patients with HIV (Park et al., 2009; Del Poeta and Casadevall, 2012). Currently this number is closer to ∼180,000 deaths annually (Rajasingham et al., 2017). Globally, the estimated number of deaths per year has been 6 million among invasive fungal infections (Stop neglecting fungi, 2017). In the case of invasive *Candida* and *Aspergillus* infections, the mortality rate could reach 60–80%, respectively (Perlroth et al., 2007; Moriyama et al., 2014). Bongomin et al. (2017) estimated the number of mycoses in the Leading International Fungal Education (LIFE) portal, which covers 80% of the world's population (5.7 billion people), and estimated that there occurred annually ∼3,000,000 cases of pulmonary aspergillosis, ∼250,000 of invasive aspergillosis, ∼700,000 of invasive candidiasis, and ∼500,000 of histoplasmosis of which ∼100,000 were disseminated cases. The global estimate of *Paracoccidioides* and *Coccidioides* cases is 4,000 and 25,000, respectively. It must be emphasized that these are considered neglected diseases, therefore the number of reported cases can be an underestimate of the actual burden of the disease. In Brazil, paracoccidioidomycosis (PCM) ranks as the 8th death causing infectious disease in patients without immunosuppression, surpassing histoplasmosis, or cryptococcosis in this group of patients. In fact, there is no compulsory notification of fungal infections in Brazil and the disease frequently occurs in rural and poor farmer populations. They frequently lack access to medical care, therefore the presumed incidence of the mycoses that differ from the real one (Shikanai-Yasuda and Mendes, 2007; Giacomazzi et al., 2016).

Fungal infections are often defined as difficult to treat, including the toxicity of antifungals and their interaction with other drugs (Westerberg and Voyack, 2013; Bicanic, 2014; Brunet et al., 2018). There is broad consensus that currently available antifungal therapy is limited and far from ideal (LaSenna and Tosti, 2015; Armstrong-James et al., 2017; Brunet et al., 2018). In the USA, fungal diseases may cost more than 7.0 billion dollars a year (Benedict et al., 2019), and the treatment of invasive fungal infections 70,000 dollars per patient (Ashley et al., 2012). Particularly in under resourced populations, the long periods and high costs of treatment contribute to patients abandoning their chemotherapy, when clinical symptoms may disappear, but are frequently followed by disease recurrences.

Systemic fungal infections are largely treated with polyenes, azoles or echinocandins, depending on the fungal pathogen and the clinical condition of the patient (Polvi et al., 2015; Souza and Amaral, 2017). The traditional antifungal agent is amphotericin B (AmB), a polyene with a broad spectrum of action, involving interaction with fungal ergosterol, destabilization of the cell membrane and, consequently, the death of the pathogen (Palacios et al., 2011). The drug interacts also with mammalian sterols, such as cholesterol, which can lead to treated patient collateral effects (Carmona and Limper, 2017). Azoles are widely prescribed against invasive fungal infections, mainly represented by fluconazole, voriconazole, itraconazole (ITZ), posaconazole, and isavuconazole (Gintjee et al., 2020). Azoles act by inhibiting lanosterol 14α-demethylase (Erg11), which converts lanosterol into ergosterol (Di Mambro et al., 2019). Its activity is also associated to inhibition of cytochrome P450 with undesired side effects. Echinocandins, micafungin, caspofungin, and anidulafungin target, on the other hand, receptors that do not exist in human cells such as β(1,3)-D-glucan synthase, an enzyme responsible for the synthesis of β-1,3 glucan, a structural component of the fungal cell wall (Di Mambro et al., 2019). Such reactivity makes echinocandins more tolerable, with limited toxicity and drug interaction. However, a limited spectrum of action is exhibited toward certain yeasts and molds, with no activity against important opportunistic yeasts such as *Cryptococcus* sp. and dimorphic fungi (Lewis, 2011; Gintjee et al., 2020).

Azole resistance is well-recognized in *Aspergillus fumigatus, Cryptococcus neoformans, Coccidioides* spp., *H. capsulatum*, and *Candida* sp. (Wheat et al., 2001; Kriesel et al., 2008; Snelders et al., 2011; Vincent et al., 2013; Fontes et al., 2017). The resistance to azoles is mainly due to mutations in fungal DNA, which reduce the interactions between the drug and the cell target (Hagiwara et al., 2016). As examples, in *A. fumigatus* azole resistance mechanisms include the insertion of repeated

Abbreviations: AmB, Amphotericin B; ITZ, Itraconazole; NPs, nanoparticles; PLGA, Poly (lactic-co-glycolic acid); PEG, polyethylene glycol; NLCs, Nanostructured lipid carriers; SLNs, solid lipid Nanoparticles; PAMAM, poly (amidoamine); AgNPs, Silver nanoparticles; AuNPs, gold nanoparticles.

sequences in tandem into the *cyp51A* promoter, amino acid substitutions in the structure of the target Cyp51A protein, and overexpression of the ABC transporter Cdr1B (Hagiwara et al., 2016). Although rare, resistance to AmB can occur intrinsically or it may be induced. *Candida tropicalis* resists the action of AmB by reducing mitochondrial production of reactive oxygen species (ROS) (Vincent et al., 2013). In *Aspergillus terreus* the genes encoding catalase (CAT) and superoxide dismutase (SOD) are essential for intrinsic resistance, since the inhibition of these enzymes makes the isolates susceptible to treatment by the drug (Jukic et al., 2017). Low levels of β-1,3 glucan lead to the lack of efficacy of echinocandins against certain species, but resistance can also develop, primarily through hotspot mutations, such as changes in glucan synthase genes (Huang et al., 2016).

An intact immune system prevents the development of most invasive fungal infections. Hence, there is significant interest in stimulating the immune system to get a more effective response against pathogenic fungi primary or during treatment of the installed disease. Studies supported that therapeutic or prophylactic vaccines can stimulate the immune system in experimental mycosis models, even in immunosuppressed mice (Silva et al., 2017). The combination of vaccination and antifungal chemotherapy leads to improved treatment efficacy and reduction of treatment period, which would also potentially prevent relapses (Travassos and Taborda, 2017). Currently there is no licensed vaccine, prophylactic or therapeutic, to treat human systemic mycoses (Travassos and Taborda, 2017). Experimental vaccines have been developed for histoplasmosis, aspergillosis, candidiasis, cryptococcosis, coccidioidomycosis, and PCM (Brown et al., 2012), but none have progressed to market. Such delay is linked to a myriad of obstacles, which include lack of adequate formulation, high development costs, and lack of market interest (Cassone and Casadevall, 2012). In addition, the fact that some fungal diseases mainly affect immunocompromised individuals is an obstacle to the generation of an effective vaccine for this population. Currently, different research groups have focused on the development of a vaccine that can be used both in healthy patients and in immunodeficient ones or otherwise high-risk patients, providing protection without aggravating the patient's clinical condition (Spellberg, 2011; Cassone and Casadevall, 2012; Medici et al., 2015; Travassos and Taborda, 2017). Additionally, the identification of appropriate adjuvants has been a major obstacle for fungal vaccine development.

Nanotechnology is a field that has been widely explored as an innovative and low-cost strategy for the development of new antifungals and more efficient vaccines (Souza and Amaral, 2017). This application of nanotechnology in vaccine development has attracted the attention of researchers since nanotherapeutics can utilize low toxicity materials that allow for the slow and direct delivery of drugs and antigens to specific targets (Zhao et al., 2014). In relation to antifungal chemotherapy, nanoparticles (NPs) have been used due to their intrinsic antifungal activity or as a drug delivery vehicle with a focus on reducing the concentration of drug required for treatment (Zhao et al., 2014). In the formulation of vaccines, NPs can act as a delivery tool capable of improving the stability of antigens such as peptides and the immunogenicity of the antigen, as well as possible immunostimulant adjuvants (Zhao et al., 2014).

In this review, we discuss the use of NPs in the development of new therapeutic approaches and vaccines against systemic mycoses, briefly commenting on the types of NPs used for this purpose and their mechanism of action. Finally, we present the current state of art of NPs for the development of new antifungal agents and vaccines aiming at systemic mycoses with a focus on *Candida* sp., *Cryptococcus* sp., *Paracoccidioides* sp., *Histoplasma* sp., *Coccidioides* sp., and *Aspergillus* sp..

NPs AND THE DEVELOPMENT OF A NEW THERAPEUTIC APPROACH AND VACCINATION ALTERNATIVE

The treatment of systemic fungal infections has limitations since currently available antifungals exhibit low biodistribution and treatment effectiveness, with lack of selectivity, and serious side effects (Voltan et al., 2016). Nanotechnology appears as an alternative to these problems since NPs can function as a controlled and specific drug delivery system, which can improve mycosis treatment without impairing the patient's quality of life.

NPs can be obtained by physical, chemical, or biological methods. The synthetic process should consider constraints of large-scale production, stability, cost, and toxicity. Methodologies involving physical synthesis can be expensive, particularly due to the equipment used for electronic excitation (Haroon Anwar, 2018). Inorganic solvents used in the chemical reduction are highly toxic, including citrate, borohydride, thioglycerol, and 2-mercaptoethanol (Zhang X.-F. et al., 2016). The biological synthesis of NPs can significantly reduce the risk of producing toxic compounds by employing plant extracts, or bacterial and fungal metabolites with antimicrobial potential, acting as reducing agents, and/or stabilizers of NPs (Ahmed et al., 2018; Lakshmeesha et al., 2019). In addition to developing NPs appropriate for medical application, the nanoformulation is also essential since the efficacy of biological activity and cytotoxicity depends on the physicochemical properties exhibited by NPs, such as size, shape, surface area, solubility, aggregation, composition with coating reactivity of particles in solution, ion release efficiency, and type of the reducing agent used in the synthetic process (Carlson et al., 2008; Murdock et al., 2008; Lin et al., 2014).

NPs exhibit antimicrobial activity through different mechanisms. Nanometric particles can cross the cell interstitium and release metal ions from the surface of the NPs inside the cell, increasing the antimicrobial activity, due to their interaction with proteins, inhibiting their activity or causing damage to the cell wall, leading to pathogen death (Oberdörster et al., 2005; Reddy et al., 2012). Another mechanism of action is through oxidative stress, which can vary based on the specific chemical properties of the materials, such as the formation of surface groups that act as reactive sites. Active sites reacting with O_2 lead to the formation of ROS that increase tissue damage (Nel et al., 2006). Oxidation of fatty acid double bonds in cell membranes, may alter membrane permeability and increase the osmotic

stress resulting in cell death. In addition, ROS can damage the DNA, RNA, and proteins of the pathogen (Reddy et al., 2012; Huang et al., 2014; Rónavári et al., 2018; Rodrigues et al., 2019). Increased toxicity is inversely proportional to NPs size. Specifically, small NPs have a larger gravimetric specific surface area, which allows more molecules to be exposed for interaction and raising damage (Nel et al., 2006).

The antimicrobial activity of NPs against pathogens *in vitro* and *in vivo* has been extensively reported in the literature (Ambrosio et al., 2019; Lakshmeesha et al., 2019; Xue et al., 2019). Nanoformulations showing a broad spectrum of action by inhibiting the growth of different pathogens such as fungi, bacteria or viruses, such as silver NPs (AgNPs), have been described (Yah and Simate, 2015). Mohammed Fayaz et al. (2012) developed a method for coating polyurethane condoms with Ag and demonstrated that the product was able to inactivate HIV-1/2 and significantly inhibit the growth of bacteria (*Escherichia coli, Staphylococcus aureus, Micrococcus luteus*, and *Klebsiella pneumoniae)* and *Candida* (*C. tropicalis, C. krusei, C. glabrata*, and *C. albicans*). In addition, chitosan-carbon nanotube (Chitosan-CNT) hydrogels, exploited in medicine for dressing and drug administration applications, inhibited the growth of *S. aureus*, *E. coli*, and *C. tropicalis* (Venkatesan et al., 2014).

The ability to form a biofilm is an important virulence mechanism that microorganisms such as bacteria and fungi are able to build during infection, which is also associated with disease persistence as well as relapses (Wojtyczka et al., 2013; Sav et al., 2018). The antibiofilm activity of NPs has been studied and the potential of nanoformulations to disrupt these complex matrices have been reported (Khan et al., 2012; Gondim et al., 2018; Yang et al., 2019).

Nanotechnology effectively combat both extracellular and intracellular pathogens. In the case of extracellular pathogens, biocompatibility and the time spent in the bloodstream in adequate concentrations is essential for the successful treatment of systemic infections. Therapy for intracellular pathogens requires a more nuanced approach that includes the proper targeting of nanocarriers to infected cells through different ligands. In general, drugs targeting intracellular pathogens have to disrupt or transit the cell membrane and release and maintain the drug at the therapeutic level for the desired time inside the target cell. Certain nanocarriers enter the cell through endocytic mechanisms and remain stable within the endolysosomes until they gain access to the cytosol to release the drug. Otherwise, the release of the drug into the endolysosome could render it ineffective (Armstead and Li, 2011). The nanometric scale of particles allows for drug delivery into specific locations of the body, entering living cells to deliver drug or antigen payloads into macrophages and dendritic cells, which is particularly useful in the treatment of intracellular pathogens such as *H. capsulatum* (Couvreur, 2013; Dube et al., 2014). Dendritic cells are capable of absorbing particles of 20–200 nm, whereas particles of 0.5–5 μm are taken up by macrophages (Xiang et al., 2006). Receptors on these cells act, thus, to improve antigen processing and activate pathways that will enhance the immune response (Zhao et al., 2014). An example is β-1,3-glucan, a polysaccharide found in the cell wall of most fungi that interacts directly with the Dectin-1 receptor present on the surface of macrophages (Brown et al., 2002). Activation of Dectin-1 enhances phagocytosis and consequently promote a greater absorption of NPs into macrophages (Goodridge et al., 2009). Several studies have validated that nanoparticles can target intracellular pathogens; however, most of these studies have targeted the bacterium *Mycobacterium tuberculosis* or the parasite *Leishmania brasiliensis* (Dube et al., 2014; Tukulula et al., 2015, 2018). Poly (lactic-co-glycolic acid) (PLGA) NPs made functional by β-1,3-glucan and carrying rifampin have shown promise for the treatment of tuberculosis, and these particles were not cytotoxic and were quickly recognized by macrophages (Tukulula et al., 2015, 2018). Chitosan—PLGA core-shell NPs with β-1,3 glucan and rifampin, increased the intracellular concentration of rifampin and showed an enhanced ability to modulate immune responses of human alveolar macrophages (Dube et al., 2014). In addition to β-glucan, other types of ligands such as antibodies can be incorporated on the surface of nanocarriers to target specific compartments of the target cell to act against intracellular pathogens. The use of pH-responsive polymers, which specifically release drugs in the presence of defined pHs, also represents an attractive alternative that can be explored against fungal pathogens (Armstead and Li, 2011). Interestingly, Mehta et al. (1997) suggested that the liposomal AmB synthesized by the authors in the 7:3 ratio of DMPC: DMPG (similar to Abelcet) is captured and retained by macrophages. These macrophages demonstrated enhanced killing of yeast cells, in this case *C. albicans*. However, this was not due to differential activation of the macrophages. The authors proposed that the candidicidal activity of the formulation occurred due to the macrophages retaining the liposomal AmB and releasing the drug to kill the yeast (i.e., drug delivery via macrophages).

Nanotechnology has advanced in recent decades with the development of innovative nanoscale products for various applications. **Figure 1** illustrates the main advantages of using NPs in the medical field. Currently, the nanomedicine market includes new approaches in the diagnosis, prevention, and therapy of diverse diseases. In 2006, these innovations sustained a market of US $6.8 billion (Wagner et al., 2006). A recent study predicted an annual growth of 12.6% such that the market can reach up to US $261 billion in 2023 (reviewed by Marques et al., 2019).

TYPES OF NANOCARRIERS

Several types of nanostructures are currently being investigated for the delivery of antifungal drugs and improve their ability to serve as adjuvants for vaccine delivery (Ribeiro et al., 2013; Souza and Amaral, 2017). These nanostructures can be classified according to their composition into (Soliman, 2017): polymeric NPs, phospholipid-based vesicles, nanostructured lipid carriers (NLCs), dendrimers, nano-emulsions (NE), and metallic and magnetic NPs. Below, we briefly present the types of nanocarriers that can be used in formulations for systemic administration of antifungals and antigen delivery.

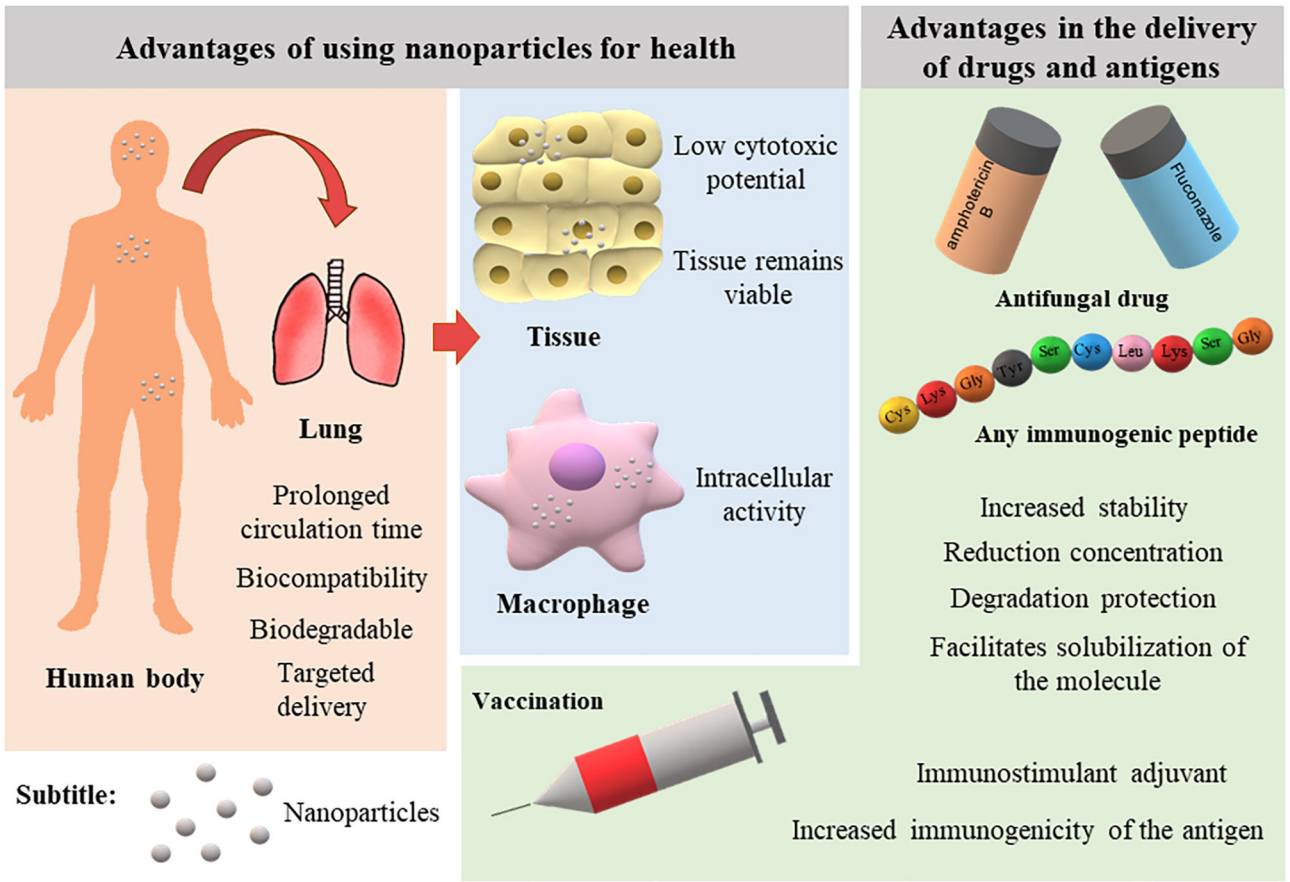

FIGURE 1 | Advantages of nanoparticles for therapy and vaccination of infectious diseases.

Polymeric Nanoparticles

The most common materials used for nano-carrier development are polymers (Bolhassani et al., 2014). Polymeric NPs are formed by chains of identical chemical structures, called monomers. Polymers are generated by the union of several monomers (Sahoo et al., 2007). Polymers and monomers may be extracted from nature or chemically synthesized. The main polymers used in the production of NPs for mycosis treatment are alginate, chitosan, and PLGA (Italia et al., 2011; Yang et al., 2011; Spadari et al., 2017; Fernandes Costa et al., 2019).

Alginate is a natural polymer found mainly in the cell wall of algae of the Phylum *Phaeophyta*, and it is formed by the junction of two monomers, α-L-guluronic acid (G block), and β-D-mannuronic acid (M block) (Jain and Bar-Shalom, 2014). The difference in concentrations between the monomers and the variations in their arrangement defines how rigid the polymer structure will be, and consequently the NPs (Jain and Bar-Shalom, 2014). Alginate NPs can be obtained through different techniques that work in basically the same way, with alginate interacting with calcium salts and promoting polymer folding to form NPs (Jain and Bar-Shalom, 2014; Lopes et al., 2017). Alginate is a water-soluble polymer, and alginate-based NPs have biocompatible mucoadhesive characteristics and are non-cytotoxic (Yehia et al., 2009).

Chitosan is a polymer obtained from the deacetylation of chitin, which is widely distributed in nature, particularly in the animal and fungal kingdoms. In the animal kingdom, chitin is present in insect, arachnid, and crustacean exoskeletons, whereas fungal chitin is a cell wall component in most fungi (Frank et al., 2020). Chitosan may be used for the production of nanogels, nano-emulsions, and NPs. Among the different applications of chitosan are food supplementation, wound healing, and immunomodulation (Dai et al., 2011; Ahmed and Aljaeid, 2016). Due to its hydrophobic character and positive charge, chitosan is ideal for the production of NPs and delivery of different types of molecules in mucous membranes (Frank et al., 2020). DNA/RNA, peptides, proteins, and drugs (Illum, 2003; Riteau and Sher, 2016) are effectively delivered by chitosan NPs. Since chitosan is biocompatible, biodegradable, and non-cytotoxic, it is one of the most promising polymers for the development of vaccines or parenteral treatment in different types of systemic infections (Sharma et al., 2015; Frank et al., 2020).

PLGA is a synthetic co-polymer produced from the linkage of glycolic acid (GA) and lactic acid (LA) monomers, the

same molecules produced by PLGA biodegradation (Amaral et al., 2009; Souza et al., 2015). The properties of PLGA are directly related to the molecular weight and proportions of the monomers. Therefore, the mechanical resistance, biodegradation rate, and the hydrolysis of the nanocarrier are influenced by the degree of crystallinity of the PLGA, which depends on the molar ratio between GA and LA. The most commonly used concentration being 50% poly lactic acid (PLA) and 50% poly glycolic acid (PGA) (Danhier et al., 2012). In addition, alkaline or strongly acidic pHs can accelerate the biodegradation of the polymer. Due to its biocompatibility, low cytotoxicity, and biodegradability, PLGA is one of the few Food and Drug Administration (FDA) approved polymers for use in complexing drugs or immunogenic molecules (Danhier et al., 2012). The production of PLGA NPs requires different techniques depending on the polarity of the molecules to be complexed (Amaral et al., 2010). PLGA NPs can be used for delivery of molecules via the enteral and parenteral routes, both followed by rapid body clearance (Semete et al., 2010). Pegylation, or the incorporation of polyethylene glycol (PEG) molecules on the NP surface, can make the NPs "invisible" to phagocytic cells and extend their half-life (Semete et al., 2010).

Amphiphilic block-copolymers, with hydrophilic shell and hydrophobic core, are used to form polymeric micelles, and these micelles can successfully deliver hydrophobic compounds. Polymeric micelles can improve drug administration and penetration, promoting drug accumulation in the target tissue. For these reasons, this type of nanocarrier has been explored to target drugs to the central nervous system, which is further discussed below in the topic on *Cryptoccocus* sp. (Shao et al., 2012).

Phospholipid-Based Vesicles: Liposomes

Liposomes are lipid particles formed in a bilayer with a hydrophobic interior layer and a hydrophilic exterior, similar to the structure of a cellular plasma membrane (Nisini et al., 2018). Liposomes can be unilamellar (one bilayer) or multilamellar (several bilayers separated by some hydrophilic fluid), The feature of hydrophilic, hydrophobic, and hydrophilic spaces makes liposomes the most versatile particles for transporting molecules, which can be dispersed inside the lipid bilayer to interact with hydrophobic molecules or dispersed in the aqueous nucleus thus interacting with hydrophilic molecules. These features allow liposomes to carry large amounts of molecules and permits improved control over the release of these payload molecules (Lila and Ishida, 2017; Nisini et al., 2018).

Their similarity to plasma membranes provides another interesting facet of liposomes in that sterols can be added to modify the stiffness of the bilayer and liposomes can be used to anchor molecules that can direct and facilitate delivery of charged payloads. Liposomes can also be functionalized to simulate an infection; thereby an immune-like response can be stimulated reducing the need for adjuvants (Rukavina and Vanić, 2016; Kube et al., 2017; Lila and Ishida, 2017).

Several drugs have been incorporated into liposomes. Currently, formulations carrying AmB are commercially available as AmBisome® and Abelcet®. Ambisome® is a liposomal formulation of unicellular vesicles, formed from hydrogenated phosphatidylcholine from soy, cholesterol, distestylphosphatidylglycerol (DMPG) and AmB in the ratio 2:1:0.8:0.4. Abelcet® is a lipid complex with a multilamellar structure, formed of diesteroylphosphatidylcholine (DMPC) and DMPG in a 7:3 ratio, carrying 36 mol% of AmB. These formulations are adminstered worldwide to treat fungal infections (Newton et al., 2016; Godet et al., 2017).

Nanostructured Lipid Carriers (NLCs)

NLCs are a mixture of solid lipid and a fraction of liquid lipid from natural sources, which make them biodegradable and biocompatible particles (Gartziandia et al., 2015; Khan et al., 2015). NLCs are second generation carriers that may overcome the disadvantages of solid lipid NPs (SLNs), which present low drug loading capacity and drug loss due to reorganization and formation of highly ordered crystalline arrangements during storage (Soliman, 2017). Thus, NLCs have improved characteristics due to the incorporation of a liquid lipid fraction that offers greater drug retention capacity and long-term stability, making this type of system more effective in drug delivery since most drugs are lipophilic in nature (Salvi and Pawar, 2019). ITZ incorporated into NLCs has shown more than 98% encapsulation efficiency in different studies and remained stable after 6-month storage (Pardeike et al., 2016; El-Sheridy et al., 2019). Beloqui et al. (2013) evaluated the tissue distribution of NLCs after intravenous administration in rats and confirmed that radiolabeled NLCs remain in circulation up to 24 h after administration. In addition, nanocarrier biodistribution is influenced by the particle size and charge. Large particles are captured by the lung and small particles by the liver and bone marrow, whereas positive NPs are observed in the kidney and negative NPs home to the liver. Therefore, NLCs have become valuable alternatives in drug delivery studies.

Dendrimers

Dendrimers are highly branched polymeric NPs consisting of a multifunctional central core, branches, and end groups that allow functionalization (Sherje et al., 2018). Dendrimers can be constructed convergently (from edges to center) or divergently (from center to edges), and the form of construction is made in stages (generations) where each stage promotes uniform growth in size and shape because binding of branches is mirrored (Ahmed et al., 2016). Dendrimers are widely studied for the transport of drugs active against infections, inflammation, and cancer, or for the transport of genetic material such as DNA, RNA, or plasmids (Mendes et al., 2017). The main chemical components used for core construction are poly (amidoamine) (PAMAM), poly (propylene imine) (DAB or PPI), and poly (ether hydroxylamine) (PEHAM) (Voltan et al., 2016; Sherje et al., 2018).

Despite their wide range of applications, dendrimers may cause relevant cytotoxicity due to their composition, because the vast majority of dendrimers have a strong cationic characteristic that can cause membrane destabilization (Ghaffari et al., 2018; Sherje et al., 2018). However, various additions to these dendrimers have been introduced, which reduce the cytotoxic

effects and prolong the body circulation time (Ghaffari et al., 2018).

Nano-Emulsions (NE)

NE consist of isotropic mixtures of drugs, lipids, hydrophilic surfactants, and co-solvents, with droplet sizes ranging from 10 to 500 nm (Mundada et al., 2016). In general, they are kinetically stable and can replace less stable nanocarriers such as liposomes (Mahtab et al., 2016; Hussain et al., 2017). NE are of great interest as antifungal drug-delivery vehicles, since the lipophilic nature of the formulation permits the solubilization of drugs, which, coupled to the small size of the droplets, make them easily absorbed through biological membranes such as the intranasal mucosa (Thakkar et al., 2015; Hussain et al., 2016). Other authors have discussed intranasally administered NE as an efficient alternative for brain targeting drugs (Kumar et al., 2016; Chatterjee et al., 2019; Iqbal et al., 2019), including the analgesic Tramadol (Lalani et al., 2015) and the anti-depressive Paroxetine (Pandey et al., 2016). This approach is potentially relevant for the treatment of meningitis caused by *Cryptococcus* spp. Due to the versatility of NE in formulating gels, creams and foams, this approach has become widely explored in topical mycosis therapy (Jaiswal et al., 2015; Mahtab et al., 2016).

Metallic and Magnetic Nanoparticles

Metallic NPs are extremely interesting, since, apart from acting as drug carriers, they represent an alternative to the treatment of infectious diseases via their intrinsic antimicrobial activity, which is well described for metals such as zinc, silver (Ag), and copper (Seil and Webster, 2012). Several studies have validated the intrinsic potential of metallic NPs in antimicrobial therapy (Franci et al., 2015; Malekkhaiat Häffner and Malmsten, 2017; Majid et al., 2018) and demonstrated their biocompatibility (Zhao et al., 2018). Silver is one of the noble metals most commonly used to generate NPs due to its unique properties such as chemical stability, good conductivity, and antimicrobial, antiviral, and antifungal potential as well as displaying anti-inflammatory activity (Ahmad et al., 2003). Metallic NPs have been widely explored in the literature for their synthesis from biological sources (Dipankar and Murugan, 2012; Thangamani and Bhuvaneshwari, 2019; Kischkel et al., 2020). The synthesis of NPs from plants or microorganisms is possible based on metabolites and proteins present in the extracts. These metabolites are essential for green synthetic pathways as they act to reduce metal and stabilize NPs (Khanna et al., 2019). Flavonoids, phenolic compounds, terpenoids, heterocyclic compounds, enzymes, and tannic acid are among the most commonly used compounds (Akhtar et al., 2013). Therefore, biologically synthesized NPs have the advantage of bringing together properties of the metal and the molecules used for synthesis (Dipankar and Murugan, 2012). Magnetic NPs can be formed from other metals such as iron, gold (Au), nickel, cobalt, and metal oxides (Huang et al., 2014). An advantage of using magnetic NPs is the ability to target their accumulation in the body, as magnetic NPs can be directed through a magnetic field generated by an external magnet to the specific site of drug delivery (Hussein-Al-Ali et al., 2014). This approach theoretically decreases the amount of drug needed for treatment and reduces drug concentration in non-target organs, which minimizes the incidence of serious side effects (Chomoucka et al., 2010; Rózalska et al., 2018; Rodrigues et al., 2019). In particular, superparamagnetic iron oxide NPs are a promising alternative for antifungal delivery, since they are highly responsive to external magnetic fields (Souza and Amaral, 2017).

A schematic representation of the nanocarrier types described above can be seen in **Figure 2**.

CURRENT SCENARIO OF NANOTECHNOLOGY IN THE TREATMENT AND VACCINATION OF FUNGAL INFECTIONS

Candidiasis

Species of the genus *Candida* are part of the human microbiota. However, under conditions of immunosuppression or lowering biological barriers, these microorganisms cause serious infections. Among *Candida* species, *C. albicans* is the species most associated with superficial and systemic infections (Pfaller and Diekema, 2010). Among the other species, *C. auris*, has emerged as a major threat due to its remarkable tendency for intrinsic multidrug-resistance (Kordalewska and Perlin, 2019). Treatment of invasive candidiasis is based on three classes of antifungals: polyenes, azoles and echinocandins. However, these drugs have variable effectiveness in the setting of biofilms (Tumbarello et al., 2007; Sawant and Khan, 2017).

Diverse NPs have been studied for their activity against *Candida.* For example, gold NPs (AuNPs) have been studied aiming at their antifungal activity in *C. albicans* biofilms, since in conjunction with photosensitizer, AuNPs can increase the effectiveness of photodynamic therapy (Khan et al., 2012; Sherwani et al., 2015; Maliszewska et al., 2017). AuNPs can destabilize the cell membrane of the pathogen through direct interaction with proteins and lipids. In addition, the association of photosensitizers with metallic nanoparticles can reduce the risk of pathogens developing resistance to photodynamic therapy (Maliszewska et al., 2017).

The effect of AgNPs against *Candida* spp. have also been widely studied, both against planktonic cells and biofilms (Monteiro et al., 2011; Lara et al., 2015). Kischkel et al. (2020) evaluated the efficacy of AgNPs carried with propolis extract (PE) against mature biofilms of *Candida* species and other fungi and observed that the concentration required for the fungicidal activity of the formulation was below the cytotoxic concentration.

Curcumin has broad antimicrobial activity and it is nontoxic. However, due to several factors, such as degradation and rapid systemic elimination, curcumin has had limited applications as a therapeutic due to its low bioavailability in the blood (Anand et al., 2007). AgNPs have been created to enhance curcumin delivery. The Curcumin—AgNPs significantly inhibit fluconazole resistant *C. albicans* and *C. glabrata,* and the inhibition depended on the concentration of curcumin used (Paul et al., 2018).

Rózalska et al. (2018) studied biogenic AgNPs against reference strains of *C. albicans*, *C. glabrata*, and *C. parapsilosis*

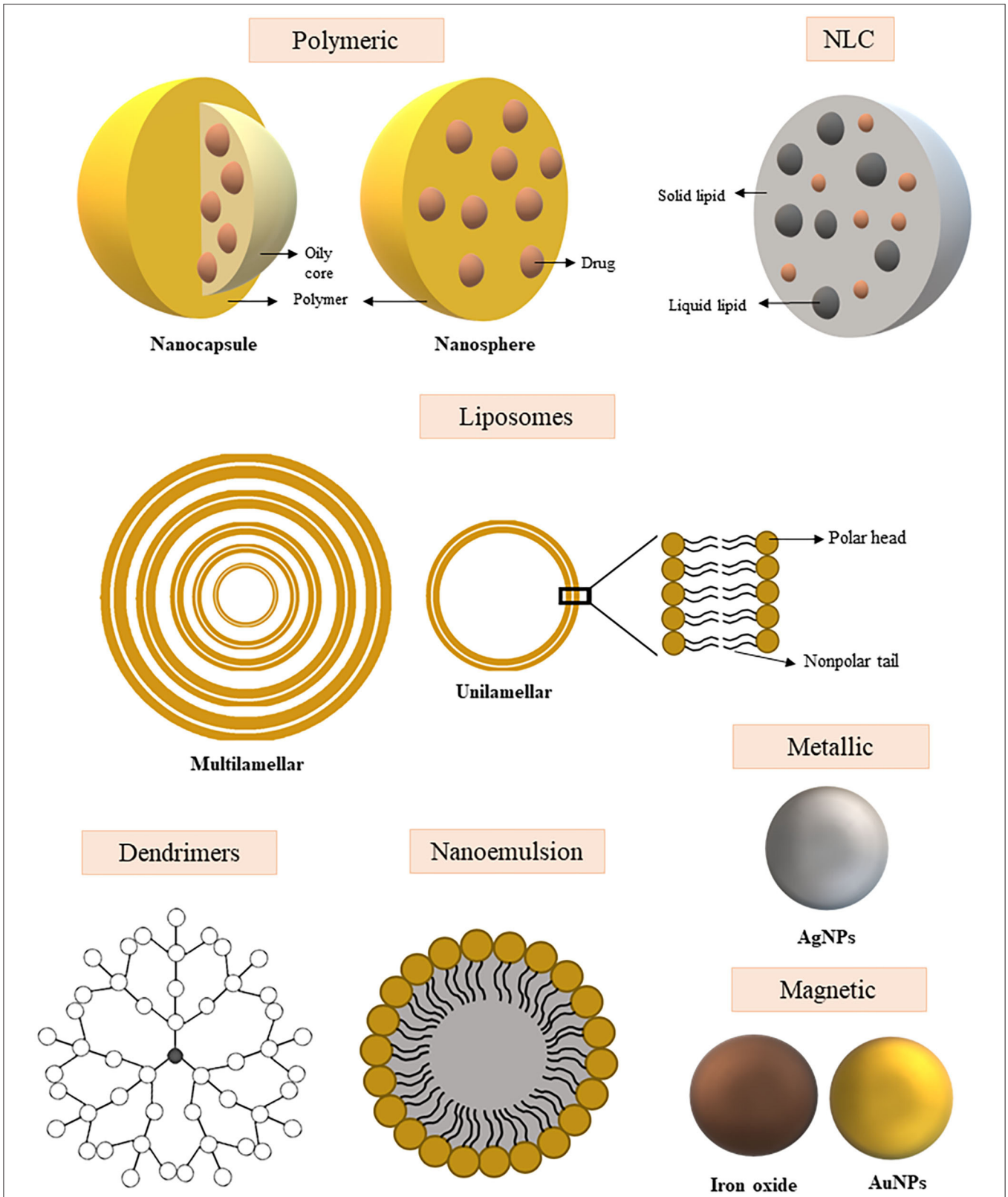

FIGURE 2 | Schematic representation of the different types of nanoparticles used for the development of new therapeutic approaches and vaccination of systemic fungal infections. Polymeric nanoparticles: Nanocapsules contain an open core with drug space, surrounded by a polymeric membrane. The nanospheres carry the

(Continued)

FIGURE 2 | drugs evenly distributed over a polymeric matrix. NLC (Nanostructured lipid carriers): Structure composed of a solid lipid and liquid lipid fraction into which the drug may be incorporated within the structure. Liposomes: Nanoparticle with unilamellar or multilamellar structure with space for drug transport between layers and/or core. Dendrimers: Complex structure branched and highly organized around the nucleus, the drug can be incorporated between the layers or on the surface of the structure. Nanoemulsion: Colloidal dispersion composed of an oil and water phase that promotes drug encapsulation. Metallic nanoparticle: Nanoparticle of metal core and intrinsic antimicrobial activity. Magnetic nanoparticle: Nanoparticle of metal core with magnetic properties.

and found that the particles were effective at a low minimum inhibitory concentration (MIC) range (1.56–6.25 μg/mL), which did not concomitantly show cytotoxicity. Notably, the biogenic AgNPs were stable *in vitro* for long periods. In addition, AgNPs used in combination with fluconazole were able to decrease the biological activity of *C. albicans* biofilms, which was attributed to the ability of the NPs to enhance the penetration of the azole disturbing the cell membrane, while Ag destabilized efflux transporter efficacy. However, despite the advantages of biomolecule synthesis, AgNPs have a tendency to aggregate and this effect impairs their antimicrobial activity (Rózalska et al., 2018).

Vazquez-Muñoz et al. (2014) observed that AgNPs did not penetrate the intracellular environment and that fungal cell death may have occurred due to the release of silver ions from AgNPs accumulated outside the cells, resulting in smaller NPs located throughout the cytoplasm. In another publication, ROS production, changes in ergosterol levels, and other effects acted together to enhance the effect of AgNPs against *C. albicans* (Radhakrishnan et al., 2018b). In addition, intracellular ROS levels could be reversed by ascorbic acid antioxidant without altering the effectiveness of AgNPs against *C. albicans* (Radhakrishnan et al., 2018a).

The antifungal effects of AmB and nystatin coupled to magnetic NPs (MNP-AmB and MNP- Nystatin) have been studied against clinical isolates of *C. albicans*. Niemirowicz et al. (2016) observed that MNP-AmB and MNP-Nystatin showed significant fungicidal effect and prevented biofilm formation. The observed effect could be due to catalase inactivation (Cat1) in cells exposed to nanosystem treatment, since disturbance of the redox balance could lead to inhibition of *C. albicans* growth. Subsequently, magnetic NPs coated with peptide LL-37 and ceragenin CSA-13 also showed fungicidal effects against *Candida* sp. due to increased ROS production associated to pore formation in the cell membrane, thus assisting NPs penetration into the yeast cells (Niemirowicz et al., 2017b).

Using encapsulated AmB in PLGA-PEG NPs (PLGA-PEG-AmB), the efficacy, toxicity, and oral bioavailability of these formulations were evaluated, *in vivo* and *in vitro*. Compared to free AmB, the PLGA-PEG-AmB NPs decreased MIC against *C. albicans* cells. Using a hemolysis assay, NP formulations had lower toxicities compared with Fungizone®. *In vivo*, blood urea nitrogen, and plasma creatinine measurements remained normal after a week of oral administration of PLGA-PEG-AmB NPs in rats. Finally, bioavailability of the PLGA-PEG-AmB NPs was further enhanced with the addition of glycyrrhizin acid (GA) (Radwan et al., 2017).

NPs of PLGA with chitosan containing AmB (PLGA-CHI-AmB) were synthesized and the derived NPs achieved nanometer size, low polydispersity, positive surface charge, and good encapsulation capacity for AmB. Notably, chitosan, in addition to having mucoadhesive properties, helps maintain the stability of nanoparticles and increases their biocompatibility. However, the PLGA-CHI-AmB showed variable MICs against with different *Candida* sp.. This result can be explained by the prolonged release of AmB, resulting in less activity *in vitro*. Although AmB is available to act on the target, the release kinetics of the NPs of PLGA with chitosan needs to be more controlled to achieve efficacy (Ludwig et al., 2018).

Among the virulence factors of *C. albicans*, the transition from yeast to hyphae represents an important factor in its pathogenicity. Farnesol is a molecule produced by *C. albicans* and it is an important quorum-sensing molecule that inhibits the growth of hyphae (Kruppa, 2009). Chitosan NPs were formulated to encapsulate farnesol and miconazole, which were then evaluated in a murine model of vulvovaginal candidiasis. Interestingly, no *in vitro* synergism between miconazole and farnesol was found. Farnesol-containing chitosan NPs, however, were effective in reducing the pathogenicity in mice, and farnesol-containing NPs inhibited hyphal growth in *C. albicans.* Additionally, the NPs tested showed no toxicity in cultured fibroblasts (Fernandes Costa et al., 2019).

SLNs and NLCs were created that were easily loaded with AmB and the NPs displayed lower hemolytic activity compared with Fungizone®. The AmB SLNs and NLCs were also more effective than free AmB or Fungizone® against *C. albicans*. The data suggest that these formulations may increase antifungal activity, increase AmB solubility, and decrease the toxic effect of treatment. This effect may be due to by the sustained release of AmB in the formulations and by its monomeric state, since AmB with a low degree of aggregation is more selective and binds mainly to ergosterol (Jansook et al., 2018).

Antifungal SLNs have been studied with drug resistant *Candida.* Fluconazole loaded SLNs (FLZ-SLNs) were more effective than free fluconazole against the species tested. The FLZ-SLNs displayed fast drug release in the first 30 min followed by sustained release over 24 h (Moazeni et al., 2016; Kelidari et al., 2017). One of the main resistance mechanisms in yeasts is the overexpression of efflux pumps, reducing the levels of azoles within the cell. The increased susceptibility to antifungals, in this case, may be related to the protection that NLCs provided to FLZ, protecting the drug from being discharged from the cell. In addition, the hydrophobic surface of FLZ-NLCs can increase the penetration of the drug into yeast (Kelidari et al., 2017).

Lipid core NPs and fluconazole containing NLCs were evaluated in fluconazole resistant *Candida*. Although the NLCs were not effective, the lipid nucleus NPs were active at reduced fluconazole concentrations. Additionally, the lipid nucleus-fluconazole NPs prevented fluconazole recognition by efflux pumps in fungal cells (Domingues Bianchin et al., 2019).

To reduce the toxicity reported for miltefosine and maintain its antifungal effect, Spadari et al. (2019) evaluated the activity of miltefosine-loaded alginate NPs against *Candida* and *Cryptococcus* species. Miltefosine encapsulation in 80% alginate NPs significantly reduced the toxic effects compared to free miltefosine in an *in vitro* system as well as in *Galleria mellonella.* Moreover, the treatment of *G. mellonella* infected with *C. albicans* with miltefosine -alginate NPs significantly extended larval survival time. The effect obtained may be associated with the controlled release of the drug, since alginate-based nanocarriers allow for the constant release of the drug, which can maintain its bioavailability and reduce potential adverse effects. Another advantage described is the size of the nanoparticles obtained in this study (average size of 279.1 ± 56.7 nm), which are favorable for mucosal and oral administration (Spadari et al., 2019).

The first study involving NPs as a *C. albicans* vaccine was published by Han and Cutler (1995), in which they used phosphatidylcholine and cholesterol liposomes to carry manganese extracted from *C. albicans*. Vaccination provided protection against widespread infection and the antiserum from infected animals was able to protect BALB/cByJ and SCID mice against *C. albicans* and *C. tropicalis*. Also, in this study, a specific monoclonal antibody was obtained, MAb B6.1, which protected against widespread infection. Subsequently, the vaccine potential of this mAb against vaginal candidiasis was evaluated (Han et al., 1998). Concurrently, another study evaluated vaccine potential of *C. albicans* ribosomes incorporated into liposomes composed of dimyristoyl phosphatidyl choline (DMPC) and dimyristoyl phosphatidyl glycerol (DMPG). Immunization of mice with these liposomes resulted in 60% survival rate of animals with disseminated candidiasis (Eckstein et al., 1997).

Heat shock protein 90 represents a highly conserved *C. albicans* chaperone that is also an immunogenic protein abundantly present in the fungal cell wall, which has been studied as a potential vaccine candidate (Matthews et al., 1987). Mašek et al. (2011), incorporated rHSP90 into the surface of nickel chelating liposomes associated with norAbuMDP pyrogen adjuvant, a compound of lipophilic derivatives of muramyl dipeptide (MDP), for intradermal vaccination of BALB/c mice and observed comparable Th1 and Th2 response to Freund's complete adjuvant vaccine. Later, Knotigová et al. (2015), evaluated the vaccine efficacy of rHSP90 in nickel-chelating liposomes associated with two pyrogen-free adjuvants (norAbuMDP and norAbuGMDPs) in ICR mice and rabbits, and showed stimulation of innate and adaptive immune response against the rHSP90-containing nano formulation.

More recently, Carneiro et al. (2015, 2016) employed dimethyldioctadecylammonium bromide (DODAB) monoolein-based liposomes for delivery of *C. albicans* wall proteins. In the first study, prophylactic vaccination using the NPs in BALB/c mice stimulated humoral and cellular immune response with production of IgG antibodies against two specific proteins found in the cell wall, Cht3p and Xog1p. Additionally, there was no apparent toxicity of the NPs. In a second study, two formulations with different lipid concentrations for protein loading, called ADS1 and ADS2, each containing a total lipid concentration of 1,774 and 266 μg/ml, respectively, were evaluated. The results showed that only the administration of ADS1 was able to confer protection against infection in mice, with a high production of specific antibodies that increased fungal phagocytosis. There was also an increased production of IL-4, IL-17, and IL-10 cytokines, demonstrating a mixed Th1, Th2, and anti-inflammatory response.

Studies involving NPs for treatment of candidiasis are shown in **Table 1** and for vaccination in **Table 4**.

Cryptococcosis

Cryptococcosis is a systemic mycosis caused by *C. neoformans*/*C. gattii* species complexes (Hagen et al., 2015), associated with high morbidity and mortality rates, especially in immunocompromised individuals and low-income countries (reviewed in Mourad and Perfect, 2018). The infection begins with inhalation of fungal propagules and in healthy individuals can be eliminated without significant symptoms. Asymptomatic spread frequently occurs, which can also lead to disease relapse in immunosuppressed infected individuals. Immunocompromised hosts can develop the primary infection. In either situation, the mycosis frequently affects the central nervous system as a meningoencephalitis (Kwon-Chung et al., 2014). Although individuals infected with human immunodeficiency virus (HIV) are the main risk group affected by *C. neoformans*, patients receiving immunosuppressive drugs and chemotherapy are also at risk (Sloan and Parris, 2014). Notably, *C. gattii* is mostly associated with immunocompetent individuals, although some other risk factors may contribute to the development of the disease (Marr et al., 2012; Chen et al., 2014; Saijo et al., 2014).

The choice treatment of cryptococcosis presented as cryptococcal meningitis or severe pulmonary cryptococcosis, is based on the administration of AmB in combination with 5-fluorocytosine, followed by fluconazole as a maintenance drug, for weeks to lifetime (Perfect et al., 2010). In countries where 5-fluorocytosine is not available fluconazole can be used as a replacement in conjunction with AmB (Perfect et al., 2010). In little resourced areas, high doses fluconazole may be used as primary therapy.

AmB deoxycholate remains an important drug for the treatment of deep fungal infections. However, its use for the treatment of cryptococcal meningitis is limited due to the inability of the drug to cross the blood-brain barrier (Xu et al., 2011). Searching for a brain drug delivery system, some nanocarriers have been studied and interesting results against *Cryptococcus* sp. have been reported (Ren et al., 2009; Xu et al., 2011; Pedroso et al., 2018). Early nannocarrier studies used polysorbate 80, a surfactant and emulsifier that improves NP uptake by human and bovine primary brain capillary endothelial cells. Polysorbate 80 coated particles can increase the concentration of drug in the brain by up to 20 times 1 hour after the injection and are therefore considered an efficient

TABLE 1 | Nanoformulations studied for the treatment of fungal infections caused by *Candida* and *Cryptococcus* yeasts.

Nanoparticle	Drug (*)	Fungi	*In vitro/in vivo*	References
AuNP	–	*C. albicans*	*in vitro* and *in vivo* (mice)	Khan et al., 2012; Sherwani et al., 2015; Maliszewska et al., 2017
AgNP	FLZ	*C. albicans* *C. glabrata* *C. parapsilosis* *C. tropicalis* *Candida kefyr*	*In vitro*	Monteiro et al., 2011; Vazquez-Muñoz et al., 2014; Lara et al., 2015; Paul et al., 2018; Radhakrishnan et al., 2018a,b; Rózalska et al., 2018
	Propolis	*C. albicans* *C. glabrata* *C. parapsilosis* *C. tropicalis* *C. krusei* *F. oxysporum* *T. interdigitale* *T. rubrum* *M. canis*	*In vitro*	Kischkel et al., 2020.
Magnetic	AmB/NYS	*C. albicans*	*In vitro*	Niemirowicz et al., 2016, 2017b.
PLGA-PEG PLGA-CHI	AmB	*C. albicans* *C.glabrata* *C. tropicalis* *Trichosporon asahii* *C. guilhermondii*	*In vitro* and *in vivo* (rats)	Radwan et al., 2017; Ludwig et al., 2018
Chitosan	farnesol/miconazole	*C. albicans*	*In vitro* and *in vivo* (mice)	Fernandes Costa et al., 2019
Solid lipid	AmB/FLZ	*C. albicans* *C. glabrata* *C. parapsilosis* *C. neoformans* *fumigatus* *Penicillium marneffei*	*In vitro*	Moazeni et al., 2016; Jansook et al., 2018
Nanostructured lipid carrier	AmB/FLZ	*C. neoformans* *C. tropicalis* *C. krusei* *C. paraposilosis* *C. glabrata* *C. kefyre* *fumigatus* *Penicillium marneffei*	*In vitro*	Kelidari et al., 2017; Jansook et al., 2018; Domingues Bianchin et al., 2019
Core-shell architecture of silver nanostructure (Pd@AgNSs)	AmB	*Cryptococcus spp.*	*In vitro*	Zhang C. et al., 2016
AgNPs and AuNPs	–	*C. neoformans* *C. gattii* *Candida* spp. *Dermatophytes*	*In vitro*	Ishida et al., 2014; Rónavári et al., 2018
Chloroaluminum phthalocyanine nanoemulsion (ClAlP/NE)	–	*C. neoformans*	*In vitro* photodynamic antimicrobial chemotherapy (PACT)	Rodrigues et al., 2012
PLA-b-PEG coated with polysorbate 80 (Tween-80)	AmB	*C. neoformans*	*In vivo*	Ren et al., 2009
Polybutylcyanoacrylate (PBCA)	AmB	*C. neoformans*	*In vivo* (mice)	Xu et al., 2011
Angiopep-PEG-PE polymeric micelles	AmB	*C. neoformans*	*In vitro* and *in vivo* (mice)	Shao et al., 2012
BSA nanoparticles coated with polysorbate- 80	AmB	*C. neoformans*	*In vitro*	Pedroso et al., 2018
Nanoparticle crystal encapsulated (encochleated)	AmB/5FC	*C. neoformans*	*In vivo* (mice)	Lu et al., 2019
PLGA/PLGA-PEG	ITZ/AmB	*C. neoformans* *C. albicans*	*In vitro* and *in vivo* (mice)	Moraes Moreira Carraro et al., 2017; Tang et al., 2018
SDCS nanomicelles	AmB	*C. neoformans*, *C. albicans*	*In vitro*	Usman et al., 2018
PAMAM-sulfonamide dendrimers	-	*C. neoformans* *C. glabrata*	*In vitro*	Carta et al., 2015

(*) Drugs: AmB, Amphotericin B; ITZ, Itraconazole; NYS, Nystatin; FLZ, Fluconazole; 5FC, 5 fluorocytosine.

brain "driver" (Ramge et al., 2000). Xu et al. (2011) developed AmB-polybutylcyanoacrylate NPs and polysorbate coated (AmB-PBCA-NPs) for systemic administration in a mouse model. According to the authors, NPs of ∼69 nm were detected in the brain 30 min after injection and in a higher concentration than liposomal AmB. Interestingly, AmB deoxycholate was not detected in the brain; however, survival rates were 80, 60, and 0% for AmB-PBCA-NPs, Liposomal AmB, and AmB deoxycholate, respectively. According to Ren et al. (2009), polysorbate 80 also improves the trapping effectiveness of AmB in the polymeric system as PLA-b-PEG. In *in vitro* tests, 100% of the AmB was released between 35 and 40 h. In NPs containing the polysorbate, almost 100% of AmB was released between 60 and 70 h.

Lipid based AmB cochleates (CAMB) is a new type of AmB nanocarrier with potential for oral administration, showing greater stability and resistance to gastrointestinal degradation (Santangelo et al., 2000). Lu et al. (2019) recently studied the administration of CAMB in combination with 5-fluorocytosine and found it to be highly effective in a murine model of cryptococcal meningoencephalitis. *In vivo* data also showed that CAMB doses up to 90 mg/kg/day appeared to be non-toxic. A particular benefit of the CAMB formulation is that the release of the drug is calcium dependent and can thus maintain its stability until reaching the intracellular environment. This provides a mechanism for controlling drug release as well as enhancing CNS drug levels (Lu et al., 2019).

Several studies, therefore, have focused on the development of safe, effective, and less expensive alternatives for the use of AmB. Liposomal, colloidal dispersion, and lipid complexes are examples of nano formulations that have been shown to attenuate toxic effects in therapy (Reviewed in Spadari et al., 2017).

Formulations with nanomicelles of AmB using sodium deoxycholate sulfate (SDCS) have been developed for targeted pulmonary delivery through inhalation of nanoformulation. According to Usman et al. (2018), the AmB-SDCS is equivalent in efficacy to Fungizone®, but the NPs does not cause toxic effects in respiratory and kidney cell lines. AmB-SDCS formulations showed activity against *C. neoformans*, *C. albicans*, and *S. cerevisiae*. A phagocytosis assay using NR8383 cells revealed that AmB-SDCS accumulated within the host effector cells without evidence of phagocytic cell damage. As we have already discussed, macrophages internalize particles of 0.5–5 μm. AmB-SDCS have a diameter of 0.9–1.6 μm. In addition to size, the surface chemistry of NPs can also influence uptake by macrophages as hydrophobic particles can stick to the cell surface (Xiang et al., 2006; Usman et al., 2018). This study demonstrated the effectiveness of an aerosolized lipid formulation in the delivery of AmB to alveolar macrophages *in vitro*, one of the main reservoirs of fungi such as *Cryptococcus* and *Aspergillus*. However, further studies are needed to validate the method *in vivo*.

Nanotechnology can overcome certain limitations of current antifungal drugs (Niemirowicz et al., 2017a). Similar to AmB, the hydrophobic character of ITZ causes the drug to have poor tissue penetration. Nanocarriers used for controlled drug release could help increase ITZ levels. Curić et al. (2017) incorporated ITZ into poly (butyl cyanoacrylate) nanocapsules, helping the drug stability and targeting. Aiming at oral administration, a system using PLGA and chitosan NPs was developed and analyzed for efficacy against *C. neoformans* pulmonary infection. A chitosan-binding peptide, screened by phage display, was conjugated to PLGA NPs (CP-NPs) with or without free chitosan (C-CP-NPs) and ITZ was incorporated in the NP. Notably, free chitosan (C-CP-NPs/ITZ) did not influence the efficiency of drug incorporation and it did not impact drug release. Both CP-NPs/ITZ and C-CP-NPs/ITZ prolonged the survival of mice with pulmonary cryptococcosis, although C-CP-NPs/ITZ was more effective (Tang et al., 2018).

Antimicrobial activity of some nanomaterials, such as Ag and Au, is commonly reported, inhibiting or killing both eukaryotic and prokaryotic pathogens (Musarrat et al., 2010; Yu et al., 2016). Although safety uncertainty of AgNPs causes conflicting information, the therapeutic effect against some pathogens is unquestionable (Vazquez-Muñoz et al., 2017).

Zhang C. et al. (2016) conducted a study using core-shell architecture of Ag nanostructure (Pd@AgNSs), to evaluate the antifungal activity against invasive fungi. This nanostructured Ag was obtained through deposition techniques based on palladium seeds that generated NPs with a high degree of biocompatibility due to the uniform size and shape. Pd@AgNSs displayed broad activity against ascomycetes and basidiomycetes, including strains considered resistant to fluconazole. The antifungal effect of the Pd@AgNSs was independent on the size of the nanoparticles. The authors speculate that the hexagonal shape of the NPs had a greater influence on antifungal properties and that this potent activity masked the expected size effects. Pd@AgNSs were cidal to fungi through mechanisms that included alterations in protein synthesis and energy metabolism. In addition, Pd@AgNSs induced increased numbers of vacuoles, which may be associated with survival strategies of the fungus itself to improve protein transport, since cell stress can increase energy demand and therefore result in increased numbers of mitochondria. Pd@AgNSs also acted synergistically with AmB, reducing the effective AmB concentration to 0.125 μg/mL.

NPs synthesized by biological routes have been explored for efficacy against cryptococcosis. In this type of synthesis, we emphasize that it is necessary to take into account the source of obtaining secondary metabolites. The source must offer a toxin-free extract that is rich in substances such as flavonoids, terpenoids, among others, which are mainly responsible for the synthesis and stabilization of metal ions that influence the final cytoxicity of the nanoformulation (Ahmed et al., 2018; Lakshmeesha et al., 2019).

Ag and Au NPs were synthesized using cell-free extract of *Phaffia rhodozyma*, the red yeast containing astaxanthin, a type of natural antioxidant that aids in the formation of metallic NPs. These biologically synthesized AgNPs and AuNPs showed no toxicity to human HaCat keratinocytes. Although the AgNPs were broadly effective against basidiomyces and ascomyces, the AuNPs were also able to inhibit *C. neoformans* (Rónavári et al., 2018). Ishida et al. (2014) created Ag nanostructures using an aqueous extract of *Fusarium oxysporum* that was effective against *Candida* and *Cryptococcus* species, particularly *C. gatti*. The AgNPs induced changes in the cytoplasmic membrane and wall of *Cryptococcus* spp. strains, but not of *Candida* spp..

Photodynamic antimicrobial chemotherapy is a method that can be combined with nanocarriers (Rodrigues et al., 2012). In this case, the nanocarrier is called a photosensitizer and can be applied to the skin lesion caused by the fungus where it can bind fungal cells and accumulate at the infection site. The photosensitizer is then exposed to visible light at appropriate wavelengths to induce the production of ROS resulting in the death of the fungus (Donnelly et al., 2008). Therefore, the photosensitizer must be an agent that is directed at the fungal cell while the light focuses on the lesion. Photodynamic antimicrobial therapy was evaluated in melanized *C. neoformans* cells using chloroaluminum phthalocyanine incorporated into NE (ClAlP/NE). ClAlP/NE effected the viability of *C. neoformans* cells in a dose depenent manner according to both the amount of the particle and the intensity of the light applied. The use of this alternative was helpful in the treatment of skin lesions caused by *C. neoformans* and other fungi (Rodrigues et al., 2012).

The studies involving NPs for cryptococcosis treatment are summarized in **Table 1**.

Aspergillosis

The members of the genus *Aspergillus* are described as opportunistic pathogens capable of inducing allergic reactions to systemic infections in humans. *A. fumigatus* is the most predominant species, responsible for 90% of invasive infections (Paulussen et al., 2017). It is a globally ubiquitous organism and dominant in different habitats due to various morphological and physiological factors (Cray et al., 2013). Importantly, azole resistance is an emerging problem in *A. fumigatus*, which has resulted in treatment failures (Seyedmousavi et al., 2014).

Different types of polymeric NPs have been explored as carriers of AmB for the treatment of experimental aspergillosis (Shirkhani et al., 2015; Salama et al., 2016; Yang et al., 2018). Among them, Italia et al. (2011) reported the efficacy of PLGA NPs for oral administration of AmB, The oral administration of PLGA NPs was superior to parenteral Ambisome® and Fungizone® in neutropenic murine models of disseminated and invasive aspergillosis. Notably, conventional AmB (Fungizone®) is ineffective in this model. The AmB PLGA NPs promoted greater oral absorption of AmB compared to AmB alone. The NPs were able to protect the drug from degradation by pH and gastrointestinal enzymes, thereby overcoming incoming metabolism and allowing more NPs to be captured by lymph nodes (Italia et al., 2011). Therefore, oral administration of AmB may represent a promising strategy for the treatment of disseminated fungal infections, or at least azole refractory oral thrush. Similarly, Van de Ven et al. (2012) found that a PLGA and nanosuspension NPs containing AmB administered by intraperitoneal route in mice were two and four times more effective in reducing fungal load, respectively, than Ambisome® and Fungizone® in disseminated aspergillosis models. In this case, the authors hypothesized that the state of aggregation of AmB in the delivery system may influence the interaction of NPs with ergosterol present in fungal membranes. These differences in the aggregation states of the particles in solution were confirmed by analyzing the UV/VIS spectra of the evaluated formulations. In addition, the authors speculated that PLGA and nanosuspension NPs may have transported the drug directly to the tissue compartment, since the nanoformulation has an ideal size for blood circulation (≤100 nm) and may promote rapid uptake by the reticuloendothelial system, as is the case of formulations like Abelcet® and Amphocil® (Van de Ven et al., 2012).

Some nanoformulations, besides being effective in the treatment of aspergillosis *in vitro* and *in vivo*, may have reduced side effects in relation to some commercially available formulations. mPEG-b-P(Glu-co-Phe) carrying AmB is stable in plasma and has lower nephrotoxicity than free AmB (Yang et al., 2018). A PEG-Lipid NPS carrying AmB showed low cytotoxicity against human kidney cells than Fungizone® and AmBisome®, in addition to lower hematotoxicity compared to Fungizone® (Jung et al., 2009). PEG/PLA with ITZ caused moderate hemolysis, although it showed superior *in vitro* antifungal activity compared to free ITZ (Essa et al., 2013). The increased toxicity of Fungizone® or free ITZ can be explained by the faster release of the drug compared to studied NP and/or Ambisome® formulations. The strong interactions between AmB and the lipids, phospholipids or polymers present in the these formulations can delay the release of the drug, and, consequently, reduce the cytotoxic effects. On the other hand, a lower toxicity of PEG-LNPs compared to AmBisome® suggests that nanoformulation may be more efficient (Jung et al., 2009).

Some studies have considered evaluating the efficacy of inhaled formulations in the prophylaxis of aspergillosis, since infection by Aspergillus sp. starts from inhalation of infectious spores (Rodríguez-Cerdeira et al., 2014). A lipid complex of AmB (Abelcet®) was administered as an aerosol for prophylaxis for pulmonary aspergillosis model in rats. Through this technique it was possible to observe higher and prolonged levels of the compound in the lungs, and higher survival rates after 2 and 10 days of infection compared to aero-AmB (Fungizone®) (Cicogna et al., 1997). In 12 human lung transplant recipients, the nebulized Abelcet® was well distributed in the lungs, but the deposition rate was below expectations (Corcoran et al., 2006). Shirkhani et al. (2015) explored the efficacy of PMA, delivered via nebulizer to prevent *Aspergillus* infection in a mouse transplant immunosuppression model, in which 3 days of prophylactic treatment were sufficient to deposit the AmB NPs in the lung and prevent fungal growth. In this case, a polymethacrylic acid was used to transform the insoluble AmB into a 78–9 nm particle of water-soluble AmB-PMA and with a UV/VIS spectrum identical to the liposomal AmB. PMA does not have immunomodulatory properties, so the administration of AmB-PMA by nebulization would constitute a pre-transplant prophylactic therapy approach capable of effectively delivering the drug to the lung and protecting against the development of fungal infections that initially come into contact with the lung.

Different AmB formulations have been tested to treat eye complications caused by *A. fumigatus* (Zhao et al., 2015; Khames et al., 2019). The development of nanostructured systems for delivering medication to the cornea consists of advantages such as improving the penetration of the drug into the cornea, improving mucoadhesive properties and prolonged residence time. SLNs represent an efficient delivery system for this purpose

due to the lipophilic nature and the small size that allows the penetration of physiological barriers and the sustained release of drugs without impairing vision. In order to improve the penetration of natamycin (NAT) into the cornea, Khames et al. (2019) incorporated the drug into SLNs. The NAT-SLNs effectively released NAT for 10-h and improved the corneal permeation compared to a free drug. The NAT-SLNs were more potent than free NAT *in vitro*. Furthermore, the NAT-SLNs showed no cytotoxic effect in corneal tissues obtained from goats.

On the other hand, Zhao et al. (2015) compared voriconazole and liposomal AmB in guinea pig endophthalmitis model. Both drugs were able to treat endophthalmitis. However, voriconazole was more effective than liposomal AmB using a similar dose (20 μg) in the initial treatment period, since the group treated with voriconazole after induction of endophthalmitis, showed lower inflammation in the early and middle stages. The retinal histopathology was normal after administration of both drugs. A lower performance of liposomal AmB in the initial stage of treatment can be explained due to the presence of cholesterol, acting as a stabilizer in NPs, as well as the controlled release of the drug that occurs when the fungus comes into contact with liposomal AmB and the drug is released liposome. Thus, resulting in a delayed efficacy compared to free voriconazole.

Nanoformulations for AmB delivery are the most studied, considering that it is a first line antifungal in the treatment of fungal infections. Side effects of AmB deoxycholate have been reduced with the development of several liposomal formulations. However, these formulations are not produced under the same conditions and/or in the same concentration of lipids and drugs, for example, as mentioned in topic 2.2 on the composition of Abelcet® and Ambisome®. On the other hand, two formulations with similar chemical composition can result in particles of different sizes, such as AmBisome® (77.8 nm) and Lambin® (122.2 nm). These differences can influence the physical-chemical properties as well as the biological activity of these formulations (Olson et al., 2015). AmBisome®, for example, is one of the most commonly reported AmB formulations referenced in articles to compare the efficiency of other nanoformulations (Clemons et al., 2005; Jung et al., 2009; Sheikh et al., 2010; Italia et al., 2011). Below, we cite some articles that show some differences in the biological activity of these commercial liposomal formulations that can be explained by differences in the synthesis and composition of the final formulation.

A study compared the toxicity and efficacy of two AmB lipid formulations, AmBisome® and Lambin®, in mice. The application of a single dose of 50 mg/kg of the drugs led to 80% mortality with Lambin® and 0% with AmBisome®. After daily intravenous administration of 5 mg/kg of the drugs, tubular renal changes were observed in mice that received Lambin®. Although both drugs significantly decreased fungal burden in the lungs of mice treated after *A. fumigatus* infection, survival rates were 30% with Lambin® and 60% with AmBisome®. The histopathology showed that treated animals with AmBisome® presented fewer fungal elements and less tissue damage (Olson et al., 2015).

Olson et al. (2006) established the ideal concentration for treatment of pulmonary aspergillosis taking into consideration the toxicity and efficacy of AmBisome® and Abelcet® formulations in a murine model. Both formulations showed prolonged survival at 12 mg/kg. Due to the reduced nephrotoxicity of AmBisome®, increased doses of 15 or 20 mg/kg can be used safely. Seyedmousavi et al. (2013) demonstrated that AmBisome® is able to prolong the survival of the mouse regardless of the mechanism of azole resistance displayed in isolates used for infection.

Lewis et al. (2007) compared the accumulation kinetics of AmBisome® and Abelcet in the lungs of immunosuppressed mice and with invasive pulmonary aspergillosis. In conclusion, Abelcet® at 5 mg/kg/day conveys active AmB in the lung faster than AmBisome®, leading to a more rapid reduction in fungal burden. At concentrations higher than 10 mg/kg/day there was no pharmacodynamic difference between the formulations. Regarding neutropenia, Siopi et al. (2019), demonstrated in mice that the appropriate doses of AmBisome® range 1–3 mg/kg for non-neutropenic patients and 7.5–10 mg/kg for neutropenic patients with isolates of *A. fumigatus* with MIC from 0.5 to 1 mg/L.

Patients were evaluated for responsiveness to AmBisome® in chronic pulmonary aspergillosis therapy. Seventy-one patients were included in the study, in which all responded to long-term therapy; however, 25% patients developed acute kidney injury, indicating that these drugs should be used with caution (Newton et al., 2016).

Combination therapy for the treatment of invasive fungal infections can be explored in an attempt to lessen the side effects of more potent drugs like AmB by combining it with other less toxic antifungals. Thus, promoting the reduction of the concentration of AmB used in a monotherapy. In addition, some studies based on the combination of antifungals aim to assess whether there is synergistic or additive potential between specific antifungals (Olson et al., 2010). In murine models of disseminated aspergillosis, combined therapy of AmBisome® prior to echinocandin or both drugs administered together were as effective as AmBisome® alone. Both classes of drugs target the cell membrane, as we mentioned earlier. The authors support the use of AmBisome® before echinocandins due to the greater reduction in fungal burden observed in the study (Olson et al., 2010). The combination of AmBisome® with voriconazole was effective for treatment of CNS aspergillosis, while the combination of AmBisome® with micafungin or caspofungin did not show much benefit in CNS disease treatment (Clemons et al., 2005).

The oligosaccharide OligoG, an alginate derived from seaweed, inhibited the growth of *Candida* and *Aspergillus* strains *in vitro*, in a dose dependent manner. In addition, it inhibited hyphal growth depending on the strain and disrupted biofilm formation. OligoG was also associated with other antifungals such as nystatin, AmB, fluconazole, miconazole, voriconazole and terbinafine, which potentiated their inhibitory effects *in vitro*. The combination of drugs led to a decrease of up to 4 times in MIC, with nystatin being the best association, promoting a reduction of up to 16 times in MIC (Tøndervik et al., 2014).

Salama et al. (2016) evaluated the activity of cross-linked chitosan biguanidine (CChG) loaded with AgNPs. The thermal

TABLE 2 | Nanoformulations studied for the treatment of fungal infections caused by the *Aspergillus* sp..

Nanoparticle	Drug (*)	Fungi	*In vitro/in vivo*	References
PLGAvv	AmB	*A. fumigatus*	*In vivo* (mice)	Italia et al., 2011; Van de Ven et al., 2012
	VOR		*In vivo* (rabbits)	Yang et al., 2011
Chitosan biguanidine	Silver	*A. fumigatus* *G. candidum* *S. recemosum*	*In vitro*	Salama et al., 2016
PMA	AmB	*A. fumigatus*	*In vitro/in vivo* (mice)	Shirkhani et al., 2015
PEG/PLA	ITZ	*A. fumigatus* *C. albicans*	*In vitro*	Essa et al., 2013
PEG-LNPs	AmB		*In vitro/in vivo* (rats and mice)	Jung et al., 2009
Alginate oligosaccharides (OligoG)	–	*C. albicans* *C. parapsilosis C. Krusei* *C. lusitaniae* *C. tropicalis* *C. glabrata* *niger* *A. fumigatus* *A. flavus*	*In vitro*	Tøndervik et al., 2014
mPEG-*b*-P-(Glu-*co*-Phe))	AmB	*A. fumigatus*	*in vivo* (mice)	Yang et al., 2018
Nanossuspension	AmB	*C. albicans* *A. fumigatus* *T. rubrum*	*In vitro/in vivo* (mice)	Van de Ven et al., 2012
	ITZ	*A. fumigatus*	*In vivo* (quails)	Wlaz et al., 2015
Liposomal (AmBisome®)	AmB	*A. fumigatus*	*In vivo* (mice)	Clemons et al., 2005; Olson et al., 2006, 2010, 2015; Lewis et al., 2007; Jung et al., 2009; Italia et al., 2011; Seyedmousavi et al., 2013; Siopi et al., 2019
			In vivo (rabbits and mice)	Sheikh et al., 2010.
			In vivo (human)	Newton et al., 2016; Godet et al., 2017
Lipossomal	AmB	*A. fumigatus*	*In vitro/in vivo* (guinea pig)	Zhao et al., 2015
Liposomal—Lambin® (Lbn)	AmB	*A. fumigatus*	*In vivo* (mice)	Olson et al., 2015
Lipossomal (Abelcet®)	AmB	*A. fumigatus*	*In vivo* (mice)	Olson et al., 2006; Lewis et al., 2007
			In vivo (rats)	Cicogna et al., 1997
SLNs	NAT	*A. fumigatus* and *C. albicans*	*In vitro/ex vivo* (goat corneas)	Khames et al., 2019

(*) Drugs: AmB, Amphotericin B; VOR, voriconazole; ITZ, Itraconazole; NYS, Nystatin.

stability of the polymer was improved due to silver incorporation, resulting in NPs with lower cytotoxicity for MCF-7 cells (human breast adenocarcinoma cell line) and improved antimicrobial activity against bacteria and fungi compared to chitosan or CChG. In this case, the association of polymers with AgNPs is mainly aimed at improving antimicrobial activity due to the intrinsic properties of Ag in association with sustained delivery through polymers. The degradation of the nanocomposite at higher temperatures after the association of CChG and AgNPs, is due to the interaction of these compounds that promoted an enhanced stabilization of the structure.

The studies involving NPs in aspergillosis treatment are summarized in **Table 2**.

PCM

PCM is a systemic mycosis caused by thermo-dimorphic fungi of the genus *Paracoccidioides* (Taborda et al., 2015). PCM has two clinical forms, acute/subacute form (juvenile) and chronic form (adult) (Shikanai-Yasuda and Mendes, 2007). PCM treatment is based on chemotherapy, the chief ones being azole agents such as fluconazole, polyenes such as AmB and sulfonamides such as Bactrim® (Shikanai-Yasuda and Mendes, 2007; Amaral et al., 2009; Souza and Amaral, 2017).

The targeting of NPs commonly can be achieved by adding antibodies to the surface of the particle. However, additional molecules also have this potential to target NPs to specific tissues. Just as polysorbate 80 assists in targeting drugs to the brain, the incorporation of dimercaptosuccinic acid (DMSA) in nanocarrier systems directs NPs mainly to the lung. However, the mechanisms by which this tropism occurs has not been well-established (Amaral et al., 2009). PLGA and DMSA NPs carrying AmB (Nano-D-AMB) were evaluated for treatment efficacy of chronic PCM caused by *P. brasiliensis*. After 30 days of infection, BALB/c mice were treated with 6 mg/kg Nano-D-AMB at 72 h intervals. Treated mice had reduced body weight loss, absence of stress (piloerection and hypotrichosis) and renal or hepatic

TABLE 3 | Nanoformulations studied for the treatment of fungal infections caused by dimorphic fungi *Coccidiodes* sp., *Paracoccidiodes* sp. and *Histoplasma* spp..

Nanoparticle	Drug (*)	Fungi	*In vitro/in vivo*	References
Lipid complex; colloidal dispersion and liposomal	AmB and NYS	*C. immitis*	*In vitro*	González et al., 2002
Liposomal (AmBisome)	AmB	*C. immitis*	*In vivo* (human)	Antony et al., 2003; Rangel et al., 2010; Nakhla, 2018; Sidhu et al., 2018
			In vivo (rabbits)	Clemons et al., 2002
		C. posadasii	*In vivo* (rabbits)	Clemons et al., 2009
		Coccidiodes spp.	*In vivo* (human)	Stewart et al., 2018
		H. capsulatum	*In vivo* (human)	Johnson et al., 2002
Lipid complex (Abelcet)	AmB	*C. immitis*	*In vivo* (human)	Koehler et al., 1998; Sidhu et al., 2018
		C. posadasii	*In vivo* (rabbits)	Capilla et al., 2007; Clemons et al., 2009
PLGA-DMSA	AmB	*P. brasiliensis*	*In vivo* (mice)	Amaral et al., 2009; Souza et al., 2015
	ITZ		*In vitro*	Cunha-Azevedo et al., 2011
Nanostructured lipid system (NLS)	Dodecyl gallate (DOD)	*P. brasiliensis* and *P. lutzii*	*In vitro/in vivo*	Singulani et al., 2018

(*) Drugs: AmB, Amphotericin B; ITZ, Itraconazole; NYS, Nystatin.

abnormalities compared to the AmB deoxycholate treated group. In addition, the formulation raised no genotoxic and cytotoxic effects (Amaral et al., 2009). A subsequent study showed that the nano-D-AMB is highly captured in the lungs, liver, and spleen of mice (Souza et al., 2015). DMSA-PLGA NPs loaded with ITZ have also been studied against *P. brasiliensis* and the PLGA-ITZ had lower MICs compared to ITZ alone with less cytotoxicity compared to the free drug (Cunha-Azevedo et al., 2011).

Gallic acid is a secondary metabolite derived from plants such as *Paeonia rockii*, *Astronium* sp., and *Syzygium cumini*, among others. Interestingly, reversed gallic acid, or dodecyl gallate (DOD) has antifungal activity (Singulani et al., 2018). A recent study evaluated the antifungal efficacy of DOD associated with NLS (DOD + NLS) *in vitro* and *in vivo*. The results showed that the formulation exhibited good *in vitro* activity against *P. brasiliensis* and *P. lutzii* (0.24 and 0.49 mg/L, respectively), low toxicity in pulmonary fibroblasts (>250 mg/L) and zebrafish embryos (>125 mg/L). In addition, DOD + NLS reduced the fungal load in mouse lungs at a concentration of 10 mg/kg (Singulani et al., 2018).

Although promising, vaccines that have been studied against PCM have shown a rapid degradation of the immunogen (Travassos and Taborda, 2012). The most efficient way to protect the immunogenic molecule, reduce its concentration and reduce the number of doses was achieved by complexing it into NPs, as shown by Amaral et al. (2010), Jannuzzi et al. (2018), and Ribeiro et al. (2013). For example, the immunomodulatory peptide P10 trapped in PLGA NPs was effective in treating chronic murine PCM after 90 days of treatment with 5 or 10 50 μL^{-1}, and the P10-PLGA NPs induced a robust, protective Th1 immune response (Amaral et al., 2010).

Variable single-chain fragments (scFv) obtained from the monoclonal antibody (mAb) 7.B12 that mimics gp43, the main *P. brasiliensis* antigen was incorporated into PLGA. After scFv-PLGA treatment of infected mice, a reduction in fungal load and increased production of IFN-γ and IL-12 cytokines was observed, as well as an abundance of macrophages and dendritic cells was seen in the lung tissue (Jannuzzi et al., 2018).

Ribeiro et al. (2013) used liposomes and PLGA to deliver plasmids containing the genetic information necessary for the expression of *Mycobacterium leprae* heat shock proteins (DNAhsp65). Both formulations were able to promote immune response modulation and fungal load reduction with the advantage of nasal administration of the liposomal formulation that could be more easily accepted by patients.

The studies involving NPs for PCM treatment are summarized in **Table 3** and for vaccination in **Table 4**.

Histoplasmosis

Histoplasmosis is an invasive endemic mycosis caused by the thermo dimorphic fungus *H. capsulatum* (Kauffman, 2007). Histoplasmosis is considered the most common respiratory fungal infection with a worldwide distribution of an asymptomatic infection to deep pulmonary mycosis and/or systemic disease, depending on the infectious inoculum and the immunologic condition of the host (Sepúlveda et al., 2017). The yeast form of *H. capsulatum* has mechanisms to prevent intracellular death by phagocytes. In addition, the intracellular localization of the fungus makes it difficult to treat the infection, as macrophages can act as a barrier, preventing the antifungal drug from interacting with its target in the cell (Edwards et al., 2013).

Currently, only AmBisome® has been evaluated in the treatment of histoplasmosis. A study compared the efficacy of AmB deoxycholate and AmBisome® in the treatment of 81 patients with moderate and severe histoplasmosis associated with AIDS. The AmB deoxycholate achieved clinical success in 14 of 22 patients (64%), with death of 3. Side effects developed in 63%, with nephrotoxicity in 37%. AmBisome® was effective in 45 of 51

TABLE 4 | Studies reporting the use of nanoformulations as an antigen delivery vehicle for *Candida albicans* and *Paracoccidioides brasiliensis* vaccine.

Fungi	Nanoformulation + adjuvant	Antigen	Animal model	Route of administration	References
Candida albicans and *C. tropicalis*	PC/Chol liposomes	Fraction of *C. albicans* mannan	BALB/cByJ mice	Intravenous	Han and Cutler, 1995
Candida albicans	DMPC/DMPGLiposomes + LA	Ribosomes of *C. albicans*	ICR mice	Subcutaneous	Eckstein et al., 1997
	Metallochelating liposomes + MDP	rHSP90	BALB/c mice	Intradermal	Mašek et al., 2011
	Metallochelating liposomes + MDP and GMDP	rHSP90	ICR mice	Intradermal	Knotigová et al., 2015
	MO liposomes + DODAB	*C. albicans* wall proteins	BALB/c mice	Subcutaneous	Carneiro et al., 2015, 2016
Paracoccidiodes brasiliensis	PLGA	P10 peptide	BALB/c mice	–	Amaral et al., 2010
		Single-chain Variable fragments (scFv)	BALB/c mice	Intramuscular	Jannuzzi et al., 2018
	PLGA e Liposomes	DNAhsp65	BALB/c mice	Intramuscular or intranasally	Ribeiro et al., 2013

patients (88%), although one patient died, 25% experienced drug-related side effects with 9% developing nephrotoxicity (Johnson et al., 2002) (**Table 3**).

Although the design of nanoparticles for delivery to specific cells is critical (as mentioned in topic 1), we believe that it is only a matter of time before these strategies are more deeply explored and improved upon in relation to fungal infections caused by pathogens such as *H. capsulatum*. These strategies can enhance the efficacy of treatment and, potentially, reduce occurrences of the disease.

There is no NP-based strategy for vaccination against *H. capsulatum*, although there are studies based on glucan particles extracted from *S. cerevisiae* (Wüthrich et al., 2015; Deepe et al., 2018).

Coccidioidomycosis

Coccidioidomycosis is caused by inhalation of infectious propagules of the dimorphic fungus *C. immitis* or *C. posadasii*. It is an endemic mycosis in the southwestern USA, Mexico, and some regions of South America (Stockamp and Thompson, 2016). Studies indicated that 17–29% cases of pneumonia acquired in highly endemic areas were caused by *Coccidioides* spp. (Thompson, 2011). Patients may have varying complications of the disease, from pulmonary to widespread infections reaching bones, joints, meninges, and skin (Thompson, 2011; McConnell et al., 2017).

Prior to nanoformulations, it was believed that the use of AmB to treat meningitis was not possible due to the low concentration of drugs reaching the brain. However, AmBisome®, was effective in animal models (Clemons et al., 2002). The increased ability of liposomal AmB to reach the disease site is due to the transport by infiltrating monocytic cells (Clemons et al., 2009). The authors compared the efficacy of liposomal AmB formulation of Abelcet® and AmBisome® in the treatment of meningitis caused by *C. posadasii* in New Zealand white rabbits. The treated animals showed a reduction in fungal burden on the brain and spinal cord, 100–10,000 times lower than the untreated group. Statistically, both formulations were considered equally efficient. However, as we described, a formulation with higher liposomal effects has been described for drug delivery to the brain for the treatment of cryptococcoccal meningitis (Xu et al., 2011).

To evaluate the efficacy and toxicity of Abelcet® and AmBisome® in the treatment of severe coccidioidomycosis in human patients, a retrospective review was conducted in patients between 2005 and 2014. Both formulations were equally effective in the treatment without significant difference, however, due to acute kidney injury, the treatment had to be discontinued in 10 patients treated with Abelcet® and in only one with AmBisome® (Sidhu et al., 2018). The toxicity of the Abelcet® has previously been discussed (Koehler et al., 1998).

AmBisome® is effective in treating coccidioidomycosis in human patients (Stewart et al., 2018). During treatment of coccidioidal meningitis for a period of 9 months, AmBisome® did not present clinical or laboratory data suggestive of toxicity (Rangel et al., 2010). In addition, AmBisome® has been successful in treating disseminated coccidioidomycosis in patients undergoing steroid therapy (Antony et al., 2003). It was employed in case of rare dissemination to the spine that required surgical intervention, being associated with continuous therapy with other azoles (Nakhla, 2018).

The studies involving NPs in the treatment of coccidioidomycosis are summarized in **Table 3**.

Blastomyces sp. and *Pneumocystis* sp. are important pathogens that cause systemic infections. The effectiveness of nanoformulations against these genera has not yet been discussed in the literature.

CONCLUDING REMARKS

The search for new and more effective therapeutic options for the treatment of fungal infections has advanced continuously

with the use of new technologies such as the development of NPs. Different types of nanoformulations have been studied and greater efficacy and less toxicity have been achieved in the administration of conventional antifungal drugs, such as AmB, compared to the free drug available in today's market. In this way, nanotechnology allows for the development of formulations that can improve not only the effectiveness of the treatment, but also the quality of life of the patient by reducing side effects, especially during prolonged therapies. In addition, we emphasize here the importance of developing new drugs that can overcome resistance and that can be combined with NPs in the development of improved therapies. Nanotechnology is still an expanding field in vaccinology and pharmacology. The application of NPs for antigen delivery is at an early stage of development, but the first studies already show the advantages of this system, as described in this review. In addition, NPs can be obtained by different synthetic methods that allow for the adaptation of production according to the needs of the manufacturer. Obstacles, however, such as the standardization of NPs still need to make progress in this field.

AUTHOR CONTRIBUTIONS

BK conceived, designed, did the literature review, provided, and wrote the manuscript. SR and SS did the literature review, provided, and wrote the manuscript. JN, LT, and CT assisted in the preparation, final review, and co-wrote the manuscript. All authors listed approved it for publication.

FUNDING

This research was funded by São Paulo Research Foundation (FAPESP) grants 2016/08730-6, 2018/26402-1, and 2017/25780-0. CNPq (grant 420480/2018-8) and CAPES-Education Ministry, Brazil. CT and LT are research fellows of the CNPq.

REFERENCES

Ahmad, A., Mukherjee, P., Senapati, S., Mandal, D., Khan, M. I., Kumar, R., et al. (2003). Extracellular biosynthesis of silver nanoparticles using the fungus Fusarium oxysporum. *Colloids Surf. B Biointerfaces* 28, 313–318. doi: 10.1016/S0927-7765(02)00174-1

Ahmed, A.-A., Hamzah, H., and Maaroof, M. (2018). Analyzing formation of silver nanoparticles from the filamentous fungus Fusarium oxysporum and their antimicrobial activity. *Turk. J. Biol.* 42, 54–62. doi: 10.3906/biy-1710-2

Ahmed, S., Vepuri, S. B., Kalhapure, R. S., and Govender, T. (2016). Interactions of dendrimers with biological drug targets: reality or mystery - a gap in drug delivery and development research. *Biomater. Sci.* 4, 1032–1050. doi: 10.1039/C6BM00090H

Ahmed, T. A., and Aljaeid, B. M. (2016). Preparation, characterization, and potential application of chitosan, chitosan derivatives, and chitosan metal nanoparticles in pharmaceutical drug delivery. *Drug Des. Devel. Ther.* 10, 483–507. doi: 10.2147/DDDT.S99651

Akhtar, M. S., Panwar, J., and Yun, Y. S. (2013). Biogenic synthesis of metallic nanoparticles by plant extracts. *ACS Sustain. Chem. Eng.* 1, 591–602. doi: 10.1021/sc300118u

Amaral, A. C., Bocca, A. L., Ribeiro, A. M., Nunes, J., Peixoto, D. L. G., Simioni, A. R., et al. (2009). Amphotericin B in poly(lactic-co-glycolic acid) (PLGA) and dimercaptosuccinic acid (DMSA) nanoparticles against paracoccidioidomycosis. *J. Antimicrob. Chemother.* 63, 526–533. doi: 10.1093/jac/dkn539

Amaral, A. C., Marques, A. F., Muñoz, J. E., Bocca, A. L., Simioni, A. R., Tedesco, A. C., et al. (2010). Poly(lactic acid-glycolic acid) nanoparticles markedly improve immunological protection provided by peptide P10 against murine paracoccidioidomycosis. *Br. J. Pharmacol.* 159, 1126–1132. doi: 10.1111/j.1476-5381.2009.00617.x

Ambrosio, J. A. R., Pinto, B. C. D. S., da Silva, B. G. M., Passos, J. C. D. S., Beltrame Junior, M., Costa, M. S., et al. (2019). Gelatin nanoparticles loaded methylene blue as a candidate for photodynamic antimicrobial chemotherapy applications in *Candida albicans* growth. *J. Biomater. Sci. Polym. Ed.* 30, 1356–1373. doi: 10.1080/09205063.2019.1632615

Anand, P., Kunnumakkara, A. B., Newman, R. A., and Aggarwal, B. B. (2007). Bioavailability of curcumin: problems and promises. *Mol. Pharm.* 4, 807–818. doi: 10.1021/mp700113r

Antony, S., Dominguez, D. C., and Sotelo, E. (2003). Use of liposomal amphotericin B in the treatment of disseminated coccidioidomycosis. *J. Natl. Med. Assoc.* 95, 982–5.

Armstead, A. L., and Li, B. (2011). Nanomedicine as an emerging approach against intracellular pathogens. *Int. J. Nanomed.* 6, 3281–3293. doi: 10.2147/IJN.S27285

Armstrong-James, D., Brown, G. D., Netea, M. G., Zelante, T., Gresnigt, M. S., van de Veerdonk, F. L., et al. (2017). Immunotherapeutic approaches to treatment of fungal diseases. *Lancet Infect. Dis.* 17, e393–e402. doi: 10.1016/S1473-3099(17)30442-5

Ashley, E. D., Drew, R., Johnson, M., Danna, R., Dabrowski, D., Walker, V., et al. (2012). Cost of invasive fungal infections in the era of new diagnostics and expanded treatment options. *Pharmacother. J. Hum. Pharmacol. Drug Ther.* 32, 890–901. doi: 10.1002/j.1875-9114.2012.01124

Beloqui, A., Solinís, M. A., Delgado, A., Évora, C., del Pozo-Rodríguez, A., and Rodríguez-Gascón, A. (2013). Biodistribution of Nanostructured Lipid Carriers (NLCs) after intravenous administration to rats: influence of technological factors. *Eur. J. Pharm. Biopharm.* 84, 309–314. doi: 10.1016/j.ejpb.2013.01.029

Benedict, K., Jackson, B. R., Chiller, T., and Beer, K. D. (2019). Estimation of direct healthcare costs of fungal diseases in the United States. *Clin. Infect. Dis.* 68, 1791–1797. doi: 10.1093/cid/ciy776

Bicanic, T. A. (2014). Systemic fungal infections. *Medicine* 42, 26–30. doi: 10.1016/j.mpmed.2013.10.006

Bolhassani, A., Javanzad, S., Saleh, T., Hashemi, M., Aghasadeghi, M. R., and Sadat, S. M. (2014). Polymeric nanoparticles: potent vectors for vaccine delivery targeting cancer and infectious diseases. *Hum. Vaccin. Immunother.* 10, 321–332. doi: 10.4161/hv.26796

Bongomin, F., Gago, S., Oladele, R. O., and Denning, D. W. (2017). Global and multi-national prevalence of fungal diseases-estimate precision. *J. Fungi* 3:57. doi: 10.3390/jof3040057

Brown, G. D., Denning, D. W., Gow, N. A. R., Levitz, S. M., Netea, M. G., and White, T. C. (2012). Hidden killers: human fungal infections. *Sci. Transl. Med.* 4:165rv13. doi: 10.1126/science.1222236

Brown, G. D., Taylor, P. R., Reid, D. M., Willment, J. A., Williams, D. L., Martinez-Pomares, L., et al. (2002). Dectin-1 is a major β-Glucan receptor on macrophages. *J. Exp. Med.* 196, 407–412. doi: 10.1084/jem.20020470

Brunet, K., Alanio, A., Lortholary, O., and Rammaert, B. (2018). Reactivation of dormant/latent fungal infection. *J. Infect.* 77, 463–468. doi: 10.1016/j.jinf.2018.06.016

Capilla, J., Clemons, K. V., Sobel, R. A., and Stevens, D. A. (2007). Efficacy of amphotericin B lipid complex in a rabbit model of coccidioidal meningitis. *J. Antimicrob. Chemother.* 60, 673–676. doi: 10.1093/jac/dkm264

Carlson, C., Hussain, S. M., Schrand, A. M., K., Braydich-Stolle, L. K., Hess, K. L., Jones, R. L., et al. (2008). Unique cellular interaction of silver nanoparticles: size-dependent generation of reactive oxygen species. *J. Phys. Chem. B* 112, 13608–13619. doi: 10.1021/jp712087m

Carmona, E. M., and Limper, A. H. (2017). Overview of treatment approaches for fungal infections. *Clin. Chest Med.* 38, 393–402. doi: 10.1016/j.ccm.2017.04.003

Carneiro, C., Correia, A., Collins, T., Vilanova, M., Pais, C., Gomes, A. C., et al. (2015). DODAB:monoolein liposomes containing *Candida albicans* cell wall surface proteins: a novel adjuvant and delivery system. *Eur. J. Pharm. Biopharm.* 89, 190–200. doi: 10.1016/j.ejpb.2014.11.028

Carneiro, C., Correia, A., Lima, T., Vilanova, M., Pais, C., Gomes, A. C., et al. (2016). Protective effect of antigen delivery using monoolein-based liposomes in experimental hematogenously disseminated candidiasis. *Acta Biomater.* 39, 133–145. doi: 10.1016/j.actbio.2016.05.001

Carta, F., Osman, S. M., Vullo, D., AlOthman, Z., Del Prete, S., Capasso, C., et al. (2015). Poly(amidoamine) dendrimers show carbonic anhydrase inhibitory activity against α-, β-, γ- and η-class enzymes. *Bioorg. Med. Chem.* 23, 6794–6798. doi: 10.1016/j.bmc.2015.10.006

Cassone, A., and Casadevall, A. (2012). Recent progress in vaccines against fungal diseases. *Curr. Opin. Microbiol.* 15, 427–433. doi: 10.1016/j.mib.2012.04.004

Chatterjee, B., Gorain, B., Mohananaidu, K., Sengupta, P., Mandal, U. K., and Choudhury, H. (2019). Targeted drug delivery to the brain via intranasal nanoemulsion: Available proof of concept and existing challenges. *Int. J. Pharm.* 565, 258–268. doi: 10.1016/j.ijpharm.2019.05.032

Chen, S. C.-A., Meyer, W., and Sorrell, T. C. (2014). *Cryptococcus gattii* infections. *Clin. Microbiol. Rev.* 27, 980–1024. doi: 10.1128/CMR.00126-13

Chomoucka, J., Drbohlavova, J., Huska, D., Adam, V., Kizek, R., and Hubalek, J. (2010). Magnetic nanoparticles and targeted drug delivering. *Pharmacol. Res.* 62, 144–149. doi: 10.1016/j.phrs.2010.01.014

Cicogna, C. E., White, M. H., Bernard, E. M., Ishimura, T., Sun, M., Tong, W. P., et al. (1997). Efficacy of prophylactic aerosol amphotericin B lipid complex in a rat model of pulmonary aspergillosis. *Antimicrob. Agents Chemother.* 41, 259–61. doi: 10.1128/AAC.41.2.259

Clemons, K. V., Capilla, J., Sobel, R. A., Martinez, M., Tong, A.-J., and Stevens, D. A. (2009). Comparative efficacies of lipid-complexed amphotericin B and liposomal amphotericin B against coccidioidal meningitis in rabbits. *Antimicrob. Agents Chemother.* 53, 1858–1862. doi: 10.1128/AAC.01538-08

Clemons, K. V., Espiritu, M., Parmar, R., and Stevens, D. A. (2005). Comparative efficacies of conventional amphotericin b, liposomal amphotericin B (AmBisome), caspofungin, micafungin, and voriconazole alone and in combination against experimental murine central nervous system aspergillosis. *Antimicrob. Agents Chemother.* 49, 4867–4875. doi: 10.1128/AAC.49.12.4867-4875.2005

Clemons, K. V., Sobel, R. A., Williams, P. L., Pappagianis, D., and Stevens, D. A. (2002). Efficacy of intravenous liposomal amphotericin B (AmBisome) against coccidioidal meningitis in rabbits. *Antimicrob. Agents Chemother.* 46, 2420–2426. doi: 10.1128/AAC.46.8.2420-2426.2002

Coelho, C., and Casadevall, A. (2016). Cryptococcal therapies and drug targets: the old, the new and the promising. *Cell. Microbiol.* 18, 792–799. doi: 10.1111/cmi.12590

Colombo, A. L., de Almeida Júnior, J. N., Slavin, M. A., Chen, S. C.-A., and Sorrell, T. C. (2017). Candida and invasive mould diseases in non-neutropenic critically ill patients and patients with haematological cancer. *Lancet Infect. Dis.* 17, e344–e356. doi: 10.1016/S1473-3099(17)30304-3

Corcoran, T. E., Venkataramanan, R., Mihelc, K. M., Marcinkowski, A. L., Ou, J., McCook, B. M., et al. (2006). Aerosol deposition of lipid complex amphotericin-B (Abelcet) in lung transplant recipients. *Am. J. Transplant.* 6, 2765–2773. doi: 10.1111/j.1600-6143.2006.01529.x

Couvreur, P. (2013). Nanoparticles in drug delivery: past, present and future. *Adv. Drug Deliv. Rev.* 65, 21–23. doi: 10.1016/j.addr.2012.04.010

Cray, J. A., Bell, A. N. W., Bhaganna, P., Mswaka, A. Y., Timson, D. J., and Hallsworth, J. E. (2013). The biology of habitat dominance; can microbes behave as weeds? *Microb. Biotechnol.* 6, 453–492. doi: 10.1111/1751-7915.12027

Cunha-Azevedo, E. P., Silva, J. R., Martins, O. P., Siqueira-Moura, M. P., Bocca, A. L., Felipe, M. S. S., et al. (2011). *In vitro* antifungal activity and toxicity of itraconazole in DMSA-PLGA nanoparticles. *J. Nanosci. Nanotechnol.* 11, 2308–2314. doi: 10.1166/jnn.2011.3576

Curić, A., Möschwitzer, J. P., and Fricker, G. (2017). Development and characterization of novel highly-loaded itraconazole poly(butyl cyanoacrylate) polymeric nanoparticles. *Eur. J. Pharm. Biopharm.* 114, 175–185. doi: 10.1016/j.ejpb.2017.01.014

Dai, T., Tanaka, M., Huang, Y. Y., and Hamblin, M. R. (2011). Chitosan preparations for wounds and burns: antimicrobial and wound-healing effects. *Expert Rev. Anti. Infect. Ther.* 9, 857–879. doi: 10.1586/eri.11.59

Danhier, F., Ansorena, E., Silva, J. M., Coco, R., Le Breton, A., and Préat, V. (2012). PLGA-based nanoparticles: an overview of biomedical applications. *J. Control. Release* 161, 505–522. doi: 10.1016/j.jconrel.2012.01.043

Deepe, G. S., Buesing, W. R., Ostroff, G. R., Abraham, A., Specht, C. A., Huang, H., et al. (2018). Vaccination with an alkaline extract of Histoplasma capsulatum packaged in glucan particles confers protective immunity in mice. *Vaccine* 36, 3359–3367. doi: 10.1016/j.vaccine.2018.04.047

Del Poeta, M., and Casadevall, A. (2012). Ten Challenges on Cryptococcus and Cryptococcosis. *Mycopathologia* 173, 303–310. doi: 10.1007/s11046-011-9473-z

Di Mambro, T., Guerriero, I., Aurisicchio, L., Magnani, M., and Marra, E. (2019). The yin and yang of current antifungal therapeutic strategies: how can we harness our natural defenses? *Front. Pharmacol.* 10:80. doi: 10.3389/fphar.2019.00080

Dipankar, C., and Murugan, S. (2012). The green synthesis, characterization and evaluation of the biological activities of silver nanoparticles synthesized from Iresine herbstii leaf aqueous extracts. *Colloids Surf. B. Biointerfaces* 98, 112–119. doi: 10.1016/j.colsurfb.2012.04.006

Domingues Bianchin, M., Borowicz, S. M., da Rosa Monte Machado, G., Pippi, B., Stanisçuaski Guterres, S., Raffin Pohlmann, A., et al. (2019). Lipid core nanoparticles as a broad strategy to reverse fluconazole resistance in multiple Candida species. *Colloids Surf. B Biointerfaces* 175, 523–529. doi: 10.1016/j.colsurfb.2018.12.011

Donnelly, R. F., McCarron, P. A., and Tunney, M. M. (2008). Antifungal photodynamic therapy. *Microbiol. res.* 163, 1–12. doi: 10.1016/j.micres.2007.08.001

Dube, A., Reynolds, J. L., Law, W.-C., Maponga, C. C., Prasad, P. N., and Morse, G. D. (2014). Multimodal nanoparticles that provide immunomodulation and intracellular drug delivery for infectious diseases. *Nanomed. Nanotechnol. Biol. Med.* 10, 831–838. doi: 10.1016/j.nano.2013.11.012

Eckstein, M., Barenholz, Y., Bar, L. K., and Segal, E. (1997). Liposomes containing *Candida albicans* ribosomes as a prophylactic vaccine against disseminated candidiasis in mice. *Vaccine* 15, 220–224. doi: 10.1016/S0264-410X(96)00137-5

Edwards, J. A., Kemski, M. M., and Rappleye, C. A. (2013). Identification of an aminothiazole with antifungal activity against intracellular Histoplasma capsulatum. *Antimicrob. Agents Chemother.* 57, 4349–4359. doi: 10.1128/AAC.00459-13

El-Sheridy, N. A., Ramadan, A. A., Eid, A. A., and El-Khordagui, L. K. (2019). Itraconazole lipid nanocapsules gel for dermatological applications: *in vitro* characteristics and treatment of induced cutaneous candidiasis. *Colloids Surf. B Biointerfaces* 181, 623–631. doi: 10.1016/j.colsurfb.2019.05.057

Essa, S., Louhichi, F., Raymond, M., and Hildgen, P. (2013). Improved antifungal activity of itraconazole-loaded PEG/PLA nanoparticles. *J. Microencapsul.* 30, 205–217. doi: 10.3109/02652048.2012.714410

Fernandes Costa, A., Evangelista Araujo, D., Santos Cabral, M., Teles Brito, I., Borges de Menezes Leite, L., Pereira, M., et al. (2019). Development, characterization, and *in vitro-in vivo* evaluation of polymeric nanoparticles containing miconazole and farnesol for treatment of vulvovaginal candidiasis. *Med. Mycol.* 57, 52–62. doi: 10.1093/mmy/myx155

Fontes, A. C., Bretas Oliveira, D., Santos, J. R., Carneiro, H. C., Ribeiro, NQ., Oliveira, L. V., et al. (2017). A subdose of fluconazole alters the virulence of *Cryptococcus gattii* during murine cryptococcosis and modulates type I interferon expression. *Med. Mycol.* 55, 203–212. doi: 10.1093/mmy/myw056

Franci, G., Falanga, A., Galdiero, S., Palomba, L., Rai, M., Morelli, G., et al. (2015). Silver nanoparticles as potential antibacterial agents. *Molecules* 20, 8856–8874. doi: 10.3390/molecules20058856

Frank, L. A., Onzi, G. R., Morawski, A. S., Pohlmann, A. R., Guterres, S. S., and Contri, R. V. (2020). Chitosan as a coating material for nanoparticles intended for biomedical applications. *React. Funct. Polym.* 147:104459. doi: 10.1016/j.reactfunctpolym.2019.104459

Gartziandia, O., Herran, E., Pedraz, J. L., Carro, E., Igartua, M., and Hernandez, R. M. (2015). Chitosan coated nanostructured lipid carriers for brain delivery of proteins by intranasal administration. *Colloids Surf. B Biointerfaces* 134, 304–313. doi: 10.1016/j.colsurfb.2015.06.054

Ghaffari, M., Dehghan, G., Abedi-Gaballu, F., Kashanian, S., Baradaran, B., Ezzati Nazhad Dolatabadi, J., et al. (2018). Surface functionalized dendrimers as controlled-release delivery nanosystems for tumor targeting. *Eur. J. Pharm. Sci.* 122, 311–330. doi: 10.1016/j.ejps.2018.07.020

Giacomazzi, J., Baethgen, L., Carneiro, L. C., Millington, M. A., Denning, D. W., Colombo, A. L., et al. (2016). The burden of serious human fungal infections in Brazil. *Mycoses* 59, 145–150. doi: 10.1111/myc.12427

Gintjee, T. J., Donnelley, M. A., and Thompson, G. R. (2020). Aspiring antifungals: review of current antifungal pipeline developments. *J. Fungi* 6:28. doi: 10.3390/jof6010028

Godet, C., Couturaud, F., Ragot, S., Laurent, F., Brun, A. L., Bergeron, A., et al. (2017). Aspergillose bronchopulmonaire allergique: évaluation d'un traitement d'entretien par Ambisome® nébulisé [Allergic bronchopulmonary aspergillosis: evaluation of a maintenance therapy with nebulized Ambisome®]. *Rer. Mal. Respire.* 34, 581–587. doi: 10.1016/j.rmr.2017.04.001

Gondim, B. L. C., Castellano, L. R. C., de Castro, R. D., Machado, G., Carlo, H. L., Valença, A. M. G., et al. (2018). Effect of chitosan nanoparticles on the inhibition of Candida spp. biofilm on denture base surface. *Arch. Oral Biol.* 94, 99–107. doi: 10.1016/j.archoralbio.2018.07.004

González, G. M., Tijerina, R., Sutton, D. A., Graybill, J. R., and Rinaldi, M. G. (2002). *In vitro* activities of free and lipid formulations of amphotericin B and nystatin against clinical isolates of Coccidioides immitis at various saprobic stages. *Antimicrob. Agents Chemother.* 46, 1583–1585. doi: 10.1128/AAC.46.5.1583-1585.2002

Goodridge, H. S., Wolf, A. J., and Underhill, D. M. (2009). β-glucan recognition by the innate immune system. *Immunol. Rev.* 230, 38–50. doi: 10.1111/j.1600-065X.2009.00793.x

Hagen, F., Khayhan, K., Theelen, B., Kolecka, A., Polacheck, I., Sionov, E., et al. (2015). Recognition of seven species in the Cryptococcus gattii/*Cryptococcus neoformans* species complex. *Fungal Genet. Biol.* 78, 16–48. doi: 10.1016/j.fgb.2015.02.009

Hagiwara, D., Watanabe, A., Kamei, K., and Goldman, G. H. (2016). Epidemiological and genomic landscape of azole resistance mechanisms in Aspergillus fungi. *Front. Microbiol.* 7:1382. doi: 10.3389/fmicb.2016.01382

Han, Y., and Cutler, J. E. (1995). Antibody response that protects against disseminated candidiasis. *Infect. Immun.* 63, 2714–2719. doi: 10.1128/IAI.63.7.2714-2719.1995

Han, Y., Morrison, R. P., and Cutler, J. E. (1998). A vaccine and monoclonal antibodies that enhance mouse resistance to *Candida albicans* vaginal infection. *Infect Immun.* 66, 5771–5776. doi: 10.1128/IAI.66.12.5771-5776.1998

Haroon Anwar, S. (2018). A brief review on nanoparticles: types of platforms, biological synthesis and applications. *Res. Rev. J. Mater. Sci.* 6, 109–116. doi: 10.4172/2321-6212.1000222

Huang, K.-S., Shieh, D.-B., Yeh, C.-S., Wu, P.-C., and Cheng, F.-Y. (2014). Antimicrobial applications of water-dispersible magnetic nanoparticles in biomedicine. *Curr. Med. Chem.* 21, 3312–3122. doi: 10.2174/0929867321666140304101752

Huang, W., Liao, G., Baker, G. M., Wang, Y., Lau, R., Paderu, P., et al. (2016). Lipid flippase subunit Cdc50 mediates drug resistance and virulence in *Cryptococcus neoformans*. *mBio* 7, e00478–e00416. doi: 10.1128/mBio.00478-16

Hussain, A., Samad, A., Singh, S. K., Ahsan, M. N., Haque, M. W., Faruk, A., et al. (2016). Nanoemulsion gel-based topical delivery of an antifungal drug: *in vitro* activity and *in vivo* evaluation. *Drug Deliv.* 23, 642–657. doi: 10.3109/10717544.2014.933284

Hussain, A., Singh, S., Webster, T. J., and Ahmad, F. J. (2017). New perspectives in the topical delivery of optimized amphotericin B loaded nanoemulsions using excipients with innate anti-fungal activities: a mechanistic and histopathological investigation. *Nanomed. Nanotechnol. Biol. Med.* 13, 1117–1126. doi: 10.1016/j.nano.2016.12.002

Hussein-Al-Ali, S. H., El Zowalaty, M. E., Hussein, M. Z., Geilich, B. M., and Webster, T. J. (2014). Synthesis, characterization, and antimicrobial activity of an ampicillin-conjugated magnetic nanoantibiotic for medical applications. *Int. J. Nanomed.* 9, 3801–3814. doi: 10.2147/IJN.S61143

Illum, L. (2003). Nasal drug delivery - possibilities, problems and solutions. *J. Controlled Release* 87, 187–198. doi: 10.1016/S0168-3659(02)00363-2

Iqbal, R., Ahmed, S., Jain, G. K., and Vohora, D. (2019). Design and development of letrozole nanoemulsion: a comparative evaluation of brain targeted nanoemulsion with free letrozole against status epilepticus and neurodegeneration in mice. *Int. J. Pharm.* 565, 20–32. doi: 10.1016/j.ijpharm.2019.04.076

Ishida, K., Cipriano, T. F., Rocha, G. M., Weissmüller, G., Gomes, F., Miranda, K., et al. (2014). Silver nanoparticle production by the fungus Fusarium oxysporum: nanoparticle characterisation and analysis of antifungal activity against pathogenic yeasts. *Mem. Inst. Oswaldo Cruz* 109, 220–228. doi: 10.1590/0074-0276130269

Italia, J. L., Sharp, A., Carter, K. C., Warn, P., and Kumar, M. N. V. R. (2011). Peroral amphotericin B polymer nanoparticles lead to comparable or superior *in vivo* antifungal activity to that of intravenous Ambisome® or Fungizone™. *PLoS ONE* 6:e25744. doi: 10.1371/journal.pone.0025744

Jain, D., and Bar-Shalom, D. (2014). Alginate drug delivery systems: Application in context of pharmaceutical and biomedical research. *Drug Dev. Ind. Pharm.* 40, 1576–1584. doi: 10.3109/03639045.2014.917657

Jaiswal, M., Dudhe, R., and Sharma, P. K. (2015). Nanoemulsion: an advanced mode of drug delivery system. *3 Biotech* 5, 123–127. doi: 10.1007/s13205-014-0214-0

Jannuzzi, G. P., Souza, N., Françoso, K. S., Pereira, R. H., Santos, R. P., Kaihami, G. H., et al. (2018). Therapeutic treatment with scFv–PLGA nanoparticles decreases pulmonary fungal load in a murine model of paracoccidioidomycosis. *Microb. Infect.* 20, 48–56. doi: 10.1016/j.micinf.2017.09.003

Jansook, P., Pichayakorn, W., and Ritthidej, G. C. (2018). Amphotericin B-loaded solid lipid nanoparticles (SLNs) and nanostructured lipid carrier (NLCs): effect of drug loading and biopharmaceutical characterizations. *Drug Dev. Ind. Pharm.* 44, 1693–1700. doi: 10.1080/03639045.2018.1492606

Johnson, P. C., Wheat, L. J., Cloud, G. A., Goldman, M., Lancaster, D., Bamberger, D. M., et al. (2002). Safety and efficacy of liposomal amphotericin B compared with conventional amphotericin B for induction therapy of histoplasmosis in patients with AIDS. *Ann. Intern. Med.* 137, 105–109. doi: 10.7326/0003-4819-137-2-200207160-00008

Jukic, E., Blatzer, M., Posch, W., Steger, M., Binder, U., Lass-Flörl, C., et al. (2017). Oxidative stress response tips the balance in *Aspergillus terreus* Amphotericin B Resistance. *Antimicrob. Agents Chemother.* 61:AAC.00670-17. doi: 10.1128/AAC.00670-17

Jung, S. H., Lim, D. H., Jung, S. H., Lee, J. E., Jeong, K. S., Seong, H., et al. (2009). Amphotericin B-entrapping lipid nanoparticles and their *in vitro* and *in vivo* characteristics. *Eur. J. Pharm. Sci.* 37, 313–320. doi: 10.1016/j.ejps.2009.02.021

Kauffman, C. A. (2007). Histoplasmosis: a clinical and laboratory update. *Clin. Microbiol. Rev.* 20, 115–132. doi: 10.1128/CMR.00027-06

Kelidari, H. R., Moazeni, M., Babaei, R., Saeedi, M., Akbari, J., Parkoohi, P. I., et al. (2017). Improved yeast delivery of fluconazole with a nanostructured lipid carrier system. *Biomed. Pharmacother.* 89, 83–88. doi: 10.1016/j.biopha.2017.02.008

Khames, A., Khaleel, M. A., El-Badawy, M. F., and El-Nezhawy, A. O. H. (2019). Natamycin solid lipid nanoparticles - sustained ocular delivery system of higher corneal penetration against deep fungal keratitis: preparation and optimization. *Int. J. Nanomed.* 14, 2515–2531. doi: 10.2147/IJN.S190502

Khan, S., Alam, F., Azam, A., and Khan, A. U. (2012). Gold nanoparticles enhance methylene blue-induced photodynamic therapy: a novel therapeutic approach to inhibit *Candida albicans* biofilm. *Int. J. Nanomed.* 7, 3245–3257. doi: 10.2147/IJN.S31219

Khan, S., Baboota, S., Ali, J., Khan, S., Narang, R. S., and Narang, J. K. (2015). Nanostructured lipid carriers: an emerging platform for improving oral bioavailability of lipophilic drugs. *Int. J. Pharm. Invest.* 5, 182–191. doi: 10.4103/2230-973X.167661

Khanna, P., Kaur, A., and Goyal, D. (2019). Algae-based metallic nanoparticles: synthesis, characterization and applications. *J. Microbiol. Methods* 163:105656. doi: 10.1016/j.mimet.2019.105656

Kischkel, B., Castilho, P. F., de, Oliveira, K. M. P., de, Bruschi, M. L., Svidzinski, T. I. E., et al. (2020). Silver nanoparticles stabilized with propolis shows reduced toxicity and potential activity against fungal infections. *Future Microbiol.* 15, 521–539. doi: 10.2217/fmb-2019-0173

Knotigová, P. T., Zyka, D., Mašek, J., Kovalová, A., Krupka, M., Bartheldyová, E., et al. (2015). Molecular adjuvants based on nonpyrogenic lipophilic derivatives of norAbuMDP/GMDP formulated in nanoliposomes: stimulation of innate and adaptive immunity. *Pharm. Res.* 32, 1186–1199. doi: 10.1007/s11095-014-1516-y

Koehler, A. P., Cheng, A. F., Chu, K. C., Chan, C. H., Ho, A. S., and Lyon, D. J. (1998). Successful treatment of disseminated

coccidioidomycosis with amphotericin B lipid complex. *J. Infect.* 36, 113–115. doi: 10.1016/S0163-4453(98)93522-8

Kordalewska, M., and Perlin, D. S. (2019). Identification of drug resistant *Candida auris*. *Front. Microbial.* 10:1918. doi: 10.3389/fmicb.2019.01918

Kriesel, J. D., Sutton, D. A., Schulman, S., Fothergill, A. W., and Rinaldi, M. G. (2008). Persistent pulmonary infection with an azole-resistant *Coccidioides* species. *Med. Mycol.* 46, 607–610. doi: 10.1080/13693780802140923

Kruppa, M. (2009). Quorum sensing and *Candida albicans*. *Mycoses* 52, 1–10. doi: 10.1111/j.1439-0507.2008.01626.x

Kube, S., Hersch, N., Naumovska, E., Gensch, T., Hendriks, J., Franzen, A., et al. (2017). Fusogenic liposomes as nanocarriers for the delivery of intracellular proteins. *Langmuir* 33, 1051–1059. doi: 10.1021/acs.langmuir.6b04304

Kumar, A., Pandey, A. N., and Jain, S. K. (2016). Nasal-nanotechnology: revolution for efficient therapeutics delivery. *Drug Deliv.* 23, 671–683. doi: 10.3109/10717544.2014.920431

Kwon-Chung, K. J., Fraser, J. A., Doering, T. L., Wang, Z., Janbon, G., Idnurm, A., et al. (2014). *Cryptococcus neoformans* and *Cryptococcus gattii*, the etiologic agents of cryptococcosis. *Cold Spring Harb. Perspect. Med.* 4:a019760. doi: 10.1101/cshperspect.a019760

Lakshmeesha, T. R., Kalagatur, N. K., Mudili, V., Mohan, C. D., Rangappa, S., Prasad, B. D., et al. (2019). Biofabrication of zinc oxide nanoparticles with syzygium aromaticum flower buds extract and finding its novel application in controlling the growth and mycotoxins of Fusarium graminearum. *Front. Microbiol.* 10:1244. doi: 10.3389/fmicb.2019.01244

Lalani, J., Baradia, D., Lalani, R., and Misra, A. (2015). Brain targeted intranasal delivery of tramadol: comparative study of microemulsion and nanoemulsion. *Pharm. Dev. Technol.* 20, 992–1001. doi: 10.3109/10837450.2014.959177

Lara, H. H., Romero-Urbina, D. G., Pierce, C., Lopez-Ribot, J. L., Arellano-Jiménez, M. J., and Jose-Yacaman, M. (2015). Effect of silver nanoparticles on *Candida albicans* biofilms: an ultrastructural study. *J. Nanobiotechnol.* 13:91. doi: 10.1186/s12951-015-0147-8

LaSenna, C. E., and Tosti, A. (2015). Patient considerations in the management of toe onychomycosis - role of efinaconazole. *Patient Prefer. Adherence* 9, 887–891. doi: 10.2147/PPA.S72701

Lewis, R. E. (2011). Current concepts in antifungal pharmacology. *Mayo Clin. Proc.* 86, 805–817. doi: 10.4065/mcp.2011.0247

Lewis, R. E., Liao, G., Hou, J., Chamilos, G., Prince, R. A., and Kontoyiannis, D. P. (2007). Comparative analysis of amphotericin B lipid complex and liposomal amphotericin B kinetics of lung accumulation and fungal clearance in a murine model of acute invasive pulmonary aspergillosis. *Antimicrob. Agents Chemother.* 51, 1253–1258. doi: 10.1128/AAC.01449-06

Lila, A. S. A., and Ishida, T. (2017). Liposomal delivery systems: design optimization and current applications. *Biol. Pharm. Bull.* 40, 1–10. doi: 10.1248/bpb.b16-00624

Limper, A. H., Adenis, A., Le, T., and Harrison, T. S. (2017). Fungal infections in HIV/AIDS. *Lancet Infect. Dis.* 17, e334–e343. doi: 10.1016/S1473-3099(17)30303-1

Lin, P.-C., Lin, S., Wang, P. C., and Sridhar, R. (2014). Techniques for physicochemical characterization of nanomaterials. *Biotechnol. Adv.* 32, 711–726. doi: 10.1016/j.biotechadv.2013.11.006

Lockhart, S. R. (2019). Emerging and reemerging fungal infections. *Semin. Diagn. Pathol.* 36, 177–181. doi: 10.1053/j.semdp.2019.04.010

Lopes, M., Abrahim, B., Veiga, F., Seiça, R., Cabral, L. M., Arnaud, P., et al. (2017). Preparation methods and applications behind alginate-based particles. *Expert Opin. Drug Deliv.* 14, 769–782. doi: 10.1080/17425247.2016.1214564

Lu, R., Hollingsworth, C., Qiu, J., Wang, A., Hughes, E., Xin, X., et al. (2019). Efficacy of oral encochleated amphotericin b in a mouse model of cryptococcal meningoencephalitis. *MBio* 10:e00724-19. doi: 10.1128/mBio.00724-19

Ludwig, D. B., de Camargo, L. E. A., Khalil, N. M., Auler, M. E., and Mainardes, R. M. (2018). Antifungal Activity of Chitosan-Coated Poly(lactic-co-glycolic) Acid Nanoparticles Containing Amphotericin B. *Mycopathologia* 183, 659–668. doi: 10.1007/s11046-018-0253-x

Mahtab, A., Anwar, M., Mallick, N., Naz, Z., Jain, G. K., and Ahmad, F. J. (2016). Transungual delivery of ketoconazole nanoemulgel for the effective management of onychomycosis. *AAPS PharmSciTech.* 17, 1477–1490. doi: 10.1208/s12249-016-0488-0

Majid, A., Ahmed, W., Patil-Sen, Y., and Sen, T. (2018). "Synthesis and characterisation of magnetic nanoparticles in medicine," in *Micro and Nanomanufacturing*. Vol. II (Cham: Springer International Publishing), 413–442. doi: 10.1007/978-3-319-67132-1_14

Malekkhaiat Häffner, S., and Malmsten, M. (2017). Membrane interactions and antimicrobial effects of inorganic nanoparticles. *Adv. Colloid Interface Sci.* 248, 105–128. doi: 10.1016/j.cis.2017.07.029

Maliszewska, I., Lisiak, B., Popko, K., and Matczyszyn, K. (2017). Enhancement of the efficacy of photodynamic inactivation of *Candida albicans* with the use of biogenic gold nanoparticles. *Photochem. Photobiol.* 93, 1081–1090. doi: 10.1111/php.12733

Marques, M. R. C., Choo, Q., Ashtikar, M., Rocha, T. C., Bremer-Hoffmann, S., and Wacker, M. G. (2019). Nanomedicines - tiny particles and big challenges. *Adv. Drug Deliv. Rev.* 151–152, 23–43. doi: 10.1016/j.addr.2019.06.003

Marr, K. A., Datta, K., Pirofski, L., and Barnes, R. (2012). *Cryptococcus gattii* infection in healthy hosts: a sentinel for subclinical immunodeficiency? *Clin. Infect. Dis.* 54, 153–154. doi: 10.1093/cid/cir756

Mašek, J., Bartheldyová, E., Turánek-Knotigová, P., Skrabalová, M., Korvasová, Z., Plocková, J., et al. (2011). Metallochelating liposomes with associated lipophilised norAbuMDP as biocompatible platform for construction of vaccines with recombinant His-tagged antigens: preparation, structural study and immune response towards rHsp90. *J. Control. Release* 151, 193–201. doi: 10.1016/j.jconrel.2011.01.016

Matthews, R. C., Burnie, J. P., and Tabaqchali, S. (1987). Isolation of immunodominant antigens from sera of patients with systemic candidiasis and characterization of serological response to *Candida albicans*. *J. Clin. Microbiol.* 25, 230–237. doi: 10.1128/JCM.25.2.230-237.1987

McConnell, M. F., Shi, A., Lasco, T. M., and Yoon, L. (2017). Disseminated coccidioidomycosis with multifocal musculoskeletal disease involvement. *Radiol. Case Rep.* 12, 141–145. doi: 10.1016/j.radcr.2016.11.017

Medici, N. P., Del Poeta, M., Medici, N. P., and Del Poeta, M. (2015). New insights on the development of fungal vaccines: from immunity to recent challenges. *Mem. Inst. Oswaldo Cruz* 110, 966–973. doi: 10.1590/0074-02760150335

Mehta, R. T., Poddar, S., Kalidas, M., Gomez-Flores, R., and Dulski, K. (1997). Role of macrophages in the candidacidal activity of liposomal amphotericin B. *J Infect. Dis.* 175, 214–217. doi: 10.1093/infdis/175.1.214

Mendes, L. P., Pan, J., and Torchilin, V. P. (2017). Dendrimers as nanocarriers for nucleic acid and drug delivery in cancer therapy. *Molecules* 22:1401. doi: 10.3390/molecules22091401

Moazeni, M., Kelidari, H. R., Saeedi, M., Morteza-Semnani, K., Nabili, M., Gohar, A. A., et al. (2016). Time to overcome fluconazole resistant Candida isolates: solid lipid nanoparticles as a novel antifungal drug delivery system. *Colloids Surf. B. Biointerfaces* 142, 400–407. doi: 10.1016/j.colsurfb.2016.03.013

Mohammed Fayaz, A., Ao, Z., Girilal, M., Chen, L., Xiao, X., Kalaichelvan, P., et al. (2012). Inactivation of microbial infectiousness by silver nanoparticles-coated condom: a new approach to inhibit HIV- and HSV-transmitted infection. *Int. J. Nanomed.* 7, 5007–5018. doi: 10.2147/IJN.S34973

Monteiro, D. R., Gorup, L. F., Silva, S., Negri, M., de Camargo, E. R., Oliveira, R., et al. (2011). Silver colloidal nanoparticles: antifungal effect against adhered cells and biofilms of *Candida albicans* and *Candida glabrata*. *Biofouling* 27, 711–719. doi: 10.1080/08927014.2011.599101

Moraes Moreira Carraro, T. C., Altmeyer, C., Maissar Khalil, N., and Mara Mainardes, R. (2017). Assessment of *in vitro* antifungal efficacy and *in vivo* toxicity of Amphotericin B-loaded PLGA and PLGA-PEG blend nanoparticles. *J. Mycol. Med.* 27, 519–529. doi: 10.1016/j.mycmed.2017.07.004

Moriyama, B., Gordon, L. A., McCarthy, M., Henning, S. A., Walsh, T. J., and Penzak, S. R. (2014). Emerging drugs and vaccines for Candidemia. *Mycoses* 57, 718–733. doi: 10.1111/myc.12265

Mourad, A., and Perfect, J. R. (2018). The war on cryptococcosis: a review of the antifungal arsenal. *Mem. Inst. Oswaldo Cruz* 113:e170391. doi: 10.1590/0074-02760170391

Mundada, V., Patel, M., and Sawant, K. (2016). Submicron emulsions and their applications in oral delivery. *Crit. Rev. Ther. Drug Carr. Syst.* 33, 265–308. doi: 10.1615/CritRevTherDrugCarrierSyst.2016017218

Murdock, R. C., Braydich-Stolle, L., Schrand, A. M., Schlager, J. J., and Hussain, S. M. (2008). Characterization of nanomaterial dispersion in solution prior to *in vitro* exposure using dynamic light scattering technique. *Toxicol. Sci.* 101, 239–253. doi: 10.1093/toxsci/kfm240

Musarrat, J., Dwivedi, S., Singh, B. R., Al-Khedhairy, A. A., Azam, A., and Naqvi, A. (2010). Production of antimicrobial silver nanoparticles in water extracts of the

fungus Amylomyces rouxii strain KSU-09. *Bioresour. Technol.* 101, 8772–8776. doi: 10.1016/j.biortech.2010.06.065

Nakhla, S. G. (2018). Complications and management of a rare case of disseminated coccidioidomycosis to the vertebral spine. *Case Rep. Infect. Dis.* 2018, 1–3. doi: 10.1155/2018/8954016

Nel, A., Xia, T., Mädler, L., and Li, N. (2006). Toxic potential of materials at the nanolevel. *Science* 311, 622–627. doi: 10.1126/science.1114397

Newton, P. J., Harris, C., Morris, J., and Denning, D. W. (2016). Impact of liposomal amphotericin B therapy on chronic pulmonary aspergillosis. *J. Infect.* 73, 485–495. doi: 10.1016/j.jinf.2016.06.001

Niemirowicz, K., Durnaś, B., Piktel, E., and Bucki, R. (2017a). Development of antifungal therapies using nanomaterials. *Nanomedicine* 12, 1891–1905. doi: 10.2217/nnm-2017-0052

Niemirowicz, K., Durnaś, B., Tokajuk, G., Głuszek, K., Wilczewska, A. Z., Misztalewska, I., et al. (2016). Magnetic nanoparticles as a drug delivery system that enhance fungicidal activity of polyene antibiotics. *Nanomed. Nanotechnol. Biol. Med.* 12, 2395–2404. doi: 10.1016/j.nano.2016.07.006

Niemirowicz, K., Durnaś, B., Tokajuk, G., Piktel, E., Michalak, G., Gu, X., et al. (2017b). Formulation and candidacidal activity of magnetic nanoparticles coated with cathelicidin LL-37 and ceragenin CSA-13. *Sci. Rep.* 7:4610. doi: 10.1038/s41598-017-04653-1

Nisini, R., Poerio, N., Mariotti, S., De Santis, F., and Fraziano, M. (2018). The multirole of liposomes in therapy and prevention of infectious diseases. *Front. Immunol.* 9:155. doi: 10.3389/fimmu.2018.00155

Oberdörster, G., Oberdörster, E., and Oberdörster, J. (2005). Nanotoxicology: an emerging discipline evolving from studies of ultrafine particles. *Environ. Health Perspect.* 113, 823–839. doi: 10.1289/ehp.7339

Olson, J. A., Adler-Moore, J. P., Schwartz, J., Jensen, G. M., and Proffitt, R. T. (2006). Comparative efficacies, toxicities, and tissue concentrations of amphotericin B lipid formulations in a murine pulmonary aspergillosis model. *Antimicrob. Agents Chemother.* 50, 2122–2131. doi: 10.1128/AAC.00315-06

Olson, J. A., George, A., Constable, D., Smith, P., Proffitt, R. T., and Adler-Moore, J. P. (2010). Liposomal amphotericin B and echinocandins as monotherapy or sequential or concomitant therapy in murine disseminated and pulmonary Aspergillus fumigatus infections. *Antimicrob. Agents Chemother.* 54, 3884–3894. doi: 10.1128/AAC.01554-09

Olson, J. A., Schwartz, J. A., Hahka, D., Nguyen, N., Bunch, T., Jensen, G. M., et al. (2015). Toxicity and efficacy differences between liposomal amphotericin B formulations in uninfected and Aspergillus fumigatus infected mice. *Med. Mycol.* 53, 107–118. doi: 10.1093/mmy/myu070

Palacios, D. S., Dailey, I., Siebert, D. M., Wilcock, B. C., and Burke, M. D. (2011). Synthesis-enabled functional group deletions reveal key underpinnings of amphotericin B ion channel and antifungal activities. *Proc. Natl. Acad. Sci. U.S.A.* 108, 6733–6738. doi: 10.1073/pnas.1015023108

Pandey, Y. R., Kumar, S., Gupta, B. K., Ali, J., and Baboota, S. (2016). Intranasal delivery of paroxetine nanoemulsion via the olfactory region for the management of depression: formulation, behavioural and biochemical estimation. *Nanotechnology* 27:025102. doi: 10.1088/0957-4484/27/2/025102

Pardeike, J., Weber, S., Zarfl, H. P., Pagitz, M., and Zimmer, A. (2016). Itraconazole-loaded nanostructured lipid carriers (NLC) for pulmonary treatment of aspergillosis in falcons. *Eur. J. Pharm. Biopharm.* 108, 269–276. doi: 10.1016/j.ejpb.2016.07.018

Park, B. J., Wannemuehler, K. A., Marston, B. J., Govender, N., Pappas, P. G., and Chiller, T. M. (2009). Estimation of the current global burden of cryptococcal meningitis among persons living with HIV/AIDS. *AIDS* 23, 525–530. doi: 10.1097/QAD.0b013e328322ffac

Paul, S., Mohanram, K., and Kannan, I. (2018). Antifungal activity of curcumin-silver nanoparticles against fluconazole-resistant clinical isolates of Candida species. *AYU* 39:182. doi: 10.4103/ayu.AYU_24_18

Paulussen, C., Hallsworth, J. E., Álvarez-Pérez, S., Nierman, W. C., Hamill, P. G., Blain, D., et al. (2017). Ecology of aspergillosis: insights into the pathogenic potency of Aspergillus fumigatus and some other Aspergillus species. *Microb. Biotechnol.* 10, 296–322. doi: 10.1111/1751-7915.12367

Pedroso, L. S., Khalil, N. M., and Mainardes, R. M. (2018). Preparation and *in vitro* evaluation of efficacy and toxicity of Polysorbate 80-coated bovine serum albumin nanoparticles containing Amphotericin B. *Curr. Drug Deliv.* 15, 1055–1063. doi: 10.2174/1567201815666180409103028

Perfect, J. R., Dismukes, W. E., Dromer, F., Goldman, D. L., Graybill, J. R., Hamill, R. J., et al. (2010). Clinical practice guidelines for the management of cryptococcal disease: 2010 update by the infectious diseases society of America. *Clin. Infect. Dis.* 50, 291–322. doi: 10.1086/649858

Perlroth, J., Choi, B., and Spellberg, B. (2007). Nosocomial fungal infections: epidemiology, diagnosis, and treatment. *Med. Mycol.* 45, 321–346. doi: 10.1080/13693780701218689

Pfaller, M. A., and Diekema, D. J. (2010). Epidemiology of invasive mycoses in North America. *Crit. Rev. Microbiol.* 36, 1–53. doi: 10.3109/10408410903241444

Polvi, E. J., Li, X., O'Meara, T. R., Leach, M. D., and Cowen, L. E. (2015). Opportunistic yeast pathogens: reservoirs, virulence mechanisms, and therapeutic strategies. *Cell. Mol. Life Sci.* 72, 2261–2287. doi: 10.1007/s00018-015-1860-z

Radhakrishnan, V. S., Dwivedi, S. P., Siddiqui, M. H., and Prasad, T. (2018a). *In vitro* studies on oxidative stress-independent, Ag nanoparticles-induced cell toxicity of *Candida albicans*, an opportunistic pathogen. *Int. J. Nanomed.* 13, 91–96. doi: 10.2147/IJN.S125010

Radhakrishnan, V. S., Reddy Mudiam, M. K., Kumar, M., Dwivedi, S. P., Singh, S. P., and e Prasad, T. (2018b). Silver nanoparticles induced alterations in multiple cellular targets, which are critical for drug susceptibilities and pathogenicity in fungal pathogen (*Candida albicans*). *Int. J. Nanomed.* 13, 2647–2663. doi: 10.2147/IJN.S150648

Radwan, M. A., AlQuadeib, B. T., Šiller, L., Wright, M. C., and Horrocks, B. (2017). Oral administration of amphotericin B nanoparticles: antifungal activity, bioavailability and toxicity in rats. *Drug Deliv.* 24, 40–50. doi: 10.1080/10717544.2016.1228715

Rajasingham, R., Smith, R. M., Park, B. J., Jarvis, J. N., Govender, N. P., Chiller, T. M., et al. (2017). Global burden of disease of HIV-associated cryptococcal meningitis: an updated analysis. *Lancet Infect. Dis.* 17, 873–881. doi: 10.1016/S1473-3099(17)30243-8

Ramge, P., Unger, R. E., Oltrogge, J. B., Zenker, D., Begley, D., Kreuter, J., et al. (2000). Polysorbate-80 coating enhances uptake of polybutylcyanoacrylate (PBCA)-nanoparticles by human and bovine primary brain capillary endothelial cells. *Eur. J. Neurosci.* 12, 1931–1940. doi: 10.1046/j.1460-9568.2000.00078.x

Rangel, M. A. C., Rivera, N. G., Castillo, R. D., Soto, J. C., and Talamante, S. (2010). Tratamiento de coccidioidomicosis meníngea con anfotericina liposomal: presentación de un caso. *Boletín Médico del Hospital Infantil de México*. 67, 142–146. Available online at: http://www.scielo.org.mx/scielo.php?script=sci_arttext&pid=S1665-11462010000200008&lng=es&tlng=es

Rautemaa-Richardson, R., and Richardson, M. D. (2017). Systemic fungal infections. *Medicine* 45, 757–762. doi: 10.1016/j.mpmed.2017.09.007

Reddy, L. H., Arias, J. L., Nicolas, J., and Couvreur, P. (2012). Magnetic nanoparticles: design and characterization, toxicity and biocompatibility, pharmaceutical and biomedical applications. *Chem. Rev.* 112, 5818–5878. doi: 10.1021/cr300068p

Ren, T., Xu, N., Cao, C., Yuan, W., Yu, X., Chen, J., et al. (2009). Preparation and therapeutic efficacy of polysorbate-80-coated amphotericin B/PLA-b-PEG nanoparticles. *J. Biomater. Sci. Polym. Ed.* 20, 1369–1380. doi: 10.1163/092050609X12457418779185

Ribeiro, A. M., Souza, A. C. O., Amaral, A. C., Vasconcelos, N. M., Jerônimo, M. S., Carneiro, F. P., et al. (2013). Nanobiotechnological approaches to delivery of DNA vaccine against fungal infection. *J. Biomed. Nanotechnol.* 9, 221–230. doi: 10.1166/jbn.2013.1491

Riteau, N., and Sher, A. (2016). Chitosan: an adjuvant with an unanticipated STING. *Immunity* 44, 522–524. doi: 10.1016/j.immuni.2016.03.002

Rodrigues, G. B., Primo, F. L., Tedesco, A. C., and Braga, G. U. L. (2012). *In vitro* photodynamic inactivation of *Cryptococcus neoformans* melanized cells with chloroaluminum phthalocyanine nanoemulsion. *Photochem. Photobiol.* 88, 440–447. doi: 10.1111/j.1751-1097.2011.01055.x

Rodrigues, G. R., López-Abarrategui, C., de la Serna Gómez, I., Dias, S. C., Otero-González, A. J., and Franco, O. L. (2019). Antimicrobial magnetic nanoparticles based-therapies for controlling infectious diseases. *Int. J. Pharm.* 555, 356–367. doi: 10.1016/j.ijpharm.2018.11.043

Rodríguez-Cerdeira, C., Arenas, R., Moreno-Coutiño, G., Vásquez, E., Fernández, R., and e Chang, P. (2014). Systemic fungal infections in patients

with human inmunodeficiency virus. *Actas Dermo-Sifiliográfica*. 105, 5–17. doi: 10.1016/j.adengl.2012.06.032

Rónavári, A., Igaz, N., Gopisetty, M. K., Szerencsés, B., Kovács, D., Papp, C., et al. (2018). Biosynthesized silver and gold nanoparticles are potent antimycotics against opportunistic pathogenic yeasts and dermatophytes. *Int. J. Nanomed.* 13, 695–703. doi: 10.2147/IJN.S152010

Rózalska, B., Sadowska, B., Budzyńska, A., Bernat, P., and Rózalska, S. (2018). Biogenic nanosilver synthesized in Metarhizium robertsii waste mycelium extract - as a modulator of *Candida albicans* morphogenesis, membrane lipidome and biofilm. *PLoS ONE* 13:e0194254. doi: 10.1371/journal.pone.0194254

Rukavina, Z., and Vanić, Ž. (2016). Current trends in development of liposomes for targeting bacterial biofilms. *Pharmaceutics* 8:18. doi: 10.3390/pharmaceutics8020018

Sahoo, S. K., Parveen, S., and Panda, J. J. (2007). The present and future of nanotechnology in human health care. *Nanomedicine* 3, 20–31. doi: 10.1016/j.nano.2006.11.008

Saijo, T., Chen, J., Chen, S. C.-A., Rosen, L. B., Yi, J., Sorrell, T. C., et al. (2014). Anti-granulocyte-macrophage colony-stimulating factor autoantibodies are a risk factor for central nervous system infection by *Cryptococcus gattii* in otherwise immunocompetent patients. *MBio* 5, e00912–e00914. doi: 10.1128/mBio.00912-14

Salama, H. E., Saad, G. R., and Sabaa, M. W. (2016). Synthesis, characterization, and biological activity of cross-linked chitosan biguanidine loaded with silver nanoparticles. *J. Biomater. Sci. Polym. Ed.* 27, 1880–1898. doi: 10.1080/09205063.2016.1239950

Salvi, V. R., and Pawar, P. (2019). Nanostructured lipid carriers (NLC) system: A novel drug targeting carrier. *J. Drug Deliv. Sci. Technol.* 51, 255–267. doi: 10.1016/j.jddst.2019.02.017

Santangelo, R., Paderu, P., Delmas, G., Chen, Z. W., Mannino, R., Zarif, L., et al. (2000). Efficacy of oral cochleate-amphotericin B in a mouse model of systemic candidiasis. *Antimicrob. Agents Chemother.* 44, 2356–2360. doi: 10.1128/AAC.44.9.2356-2360.2000

Sav, H., Rafati, H., Öz, Y., Dalyan-Cilo, B., Ener, B., Mohammadi, F., et al. (2018). Biofilm formation and resistance to fungicides in clinically relevant members of the fungal genus Fusarium. *J. Fungi* 4:16. doi: 10.3390/jof4010016

Sawant, B., and Khan, T. (2017). Recent advances in delivery of antifungal agents for therapeutic management of candidiasis. *Biomed. Pharmacother.* 96, 1478–1490. doi: 10.1016/j.biopha.2017.11.127

Seil, J. T., and Webster, T. J. (2012). Antimicrobial applications of nanotechnology: methods and literature. *Int. J. Nanomed.* 7, 2767–2781. doi: 10.2147/IJN.S24805

Semete, B., Booysen, L. I. J., Kalombo, L., Venter, J. D., Katata, L., Ramalapa, B., et al. (2010). *In vivo* uptake and acute immune response to orally administered chitosan and PEG coated PLGA nanoparticles. *Toxicol. Appl. Pharmacol.* 249, 158–165. doi: 10.1016/j.taap.2010.09.002

Sepúlveda, V. E., Márquez, R., Turissini, D. A., Goldman, W. E., and Matute, D. R. (2017). Genome sequences reveal cryptic speciation in the human pathogen Histoplasma capsulatum. *MBio* 8:e01339-17. doi: 10.1128/mBio.01339-17

Seyedmousavi, S., Melchers, W. J. G., Mouton, J. W., and Verweij, P. E. (2013). Pharmacodynamics and dose-response relationships of liposomal amphotericin B against different azole-resistant Aspergillus fumigatus isolates in a murine model of disseminated aspergillosis. *Antimicrob. Agents Chemother.* 57, 1866–1871. doi: 10.1128/AAC.02226-12

Seyedmousavi, S., Mouton, J. W., Melchers, W. J. G., Brüggemann, R. J. M., and Verweij, P. E. (2014). The role of azoles in the management of azole-resistant aspergillosis: From the bench to the bedside. *Drug Resist. Updat.* 17, 37–50. doi: 10.1016/j.drup.2014.06.001

Shao, K., Wu, J., Chen, Z., Huang, S., Li, J., Ye, L., et al. (2012). A brain-vectored angiopep-2 based polymeric micelles for the treatment of intracranial fungal infection. *Biomaterials* 33, 6898–6907. doi: 10.1016/j.biomaterials.2012.06.050

Sharma, R., Agrawal, U., Mody, N., and Vyas, S. P. (2015). Polymer nanotechnology based approaches in mucosal vaccine delivery: challenges and opportunities. *Biotechnol. Adv.* 33, 64–79. doi: 10.1016/j.biotechadv.2014.12.004

Sheikh, S., Ali, S. M., Ahmad, M. U., Ahmad, A., Mushtaq, M., Paithankar, M., et al. (2010). Nanosomal Amphotericin B is an efficacious alternative to Ambisome® for fungal therapy. *Int. J. Pharm.* 397, 103–108. doi: 10.1016/j.ijpharm.2010.07.003

Sherje, A. P., Jadhav, M., Dravyakar, B. R., and Kadam, D. (2018). Dendrimers: a versatile nanocarrier for drug delivery and targeting. *Int. J. Pharm.* 548, 707–720. doi: 10.1016/j.ijpharm.2018.07.030

Sherwani, M. A., Tufail, S., Khan, A. A., and Owais, M. (2015). Gold nanoparticle-photosensitizer conjugate based photodynamic inactivation of biofilm producing cells: potential for treatment of C. *albicans Infection in BALB/c Mice. PLoS ONE* 10:e0131684. doi: 10.1371/journal.pone.0131684

Shikanai-Yasuda, M. A., and Mendes, R. P. (2007). Consensus Brazilian guidelines for the clinical management of paracoccidioidomycosis. *Rev. Soc. Bras. Med. Trop.* 50, 715–740. doi: 10.1590/0037-8682-0230-2017

Shirkhani, K., Teo, I., Armstrong-James, D., and Shaunak, S. (2015). Nebulised amphotericin B-polymethacrylic acid nanoparticle prophylaxis prevents invasive aspergillosis. *Nanomedicine* 11, 1217–1226. doi: 10.1016/j.nano.2015.02.012

Sidhu, R., Lash, D. B., Heidari, A., Natarajan, P., and Johnson, R. H. (2018). Evaluation of amphotericin B lipid formulations for treatment of severe coccidioidomycosis. *Antimicrob. Agents Chemother.* 62:e02293-17. doi: 10.1128/AAC.02293-17

Silva, L., Dias, L. S., Rittner, G., Muñoz, J. E., Souza, A., Nosanchuk, J. D., et al. (2017). Dendritic cells primed with *Paracoccidioides brasiliensis* Peptide P10 are therapeutic in immunosuppressed mice with paracoccidioidomycosis. *Front. Microbiol.* 8:1057. doi: 10.3389/fmicb.2017.01057

Singulani, J., Scorzoni, L., Lourencetti, N. M. S., Oliveira, L. R., Conçolaro, R. S., da Silva, P. B., et al. (2018). Potential of the association of dodecyl gallate with nanostructured lipid system as a treatment for paracoccidioidomycosis: *in vitro* and *in vivo* efficacy and toxicity. *Int. J. Pharm.* 547, 630–636. doi: 10.1016/j.ijpharm.2018.06.013

Siopi, M., Mouton, J. W., Pournaras, S., and Meletiadis, J. (2019). *In vitro* and *in vivo* exposure-effect relationship of liposomal amphotericin b against aspergillus fumigatus. *Antimicrob. Agents Chemother.* 63:e02673–18. doi: 10.1128/AAC.02673-18

Sloan, D. J., and Parris, V. (2014). Cryptococcal meningitis: epidemiology and therapeutic options. *Clin. Epidemiol.* 6, 169–182. doi: 10.2147/CLEP.S38850

Snelders, E., Karawajczyk, A., Verhoeven, R. J. A., Venselaar, H., Schaftenaar, G., Verweij, P. E., et al. (2011). The structure–function relationship of the Aspergillus fumigatus cyp51A L98H conversion by site-directed mutagenesis: the mechanism of L98H azole resistance. *Fungal Genet. Biol.* 48, 1062–1070. doi: 10.1016/j.fgb.2011.08.002

Soliman, G. M. (2017). Nanoparticles as safe and effective delivery systems of antifungal agents: Achievements and challenges. *Int. J. Pharm.* 523, 15–32. doi: 10.1016/j.ijpharm.2017.03.019

Souza, A. C. O., and Amaral, A. C. (2017). antifungal therapy for systemic mycosis and the nanobiotechnology era: improving efficacy, biodistribution and toxicity. *Front. Microbiol.* 8:336. doi: 10.3389/fmicb.2017.00336

Souza, A. C. O., Nascimento, A. L., De Vasconcelos, N. M., Jerônimo, M. S., Siqueira, I. M., R-Santos, L., et al. (2015). Activity and *in vivo* tracking of Amphotericin B loaded PLGA nanoparticles. *Eur. J. Med. Chem.* 95, 267–276. doi: 10.1016/j.ejmech.2015.03.022

Spadari, C., de, C., Lopes, L. B., and Ishida, K. (2017). Potential use of alginate-based carriers as antifungal delivery system. *Front. Microbiol.* 8:97. doi: 10.3389/fmicb.2017.00097

Spadari, C. C., de Bastiani, F. W. M., S., Lopes, L. B., and Ishida, K. (2019). Alginate nanoparticles as non-toxic delivery system for miltefosine in the treatment of candidiasis and cryptococcosis. *Int. J. Nanomed.* 14, 5187–5199. doi: 10.2147/IJN.S205350

Spellberg, B. (2011). Vaccines for invasive fungal infections. *F1000 Med. Rep.* 3:13. doi: 10.3410/M3-13

Stewart, E. R., Eldridge, M. L., McHardy, I., Cohen, S. H., and Thompson, G. R. (2018). Liposomal amphotericin B as monotherapy in relapsed coccidioidal meningitis. *Mycopathologia* 183, 619–622. doi: 10.1007/s11046-017-0240-7

Stockamp, N. W., and Thompson, G. R. (2016). Coccidioidomycosis. *Infect. Dis. Clin. North Am.* 30, 229–246. doi: 10.1016/j.idc.2015.10.008

Stop neglecting fungi (2017). *Nat. Microbiol.* 2:17120. doi: 10.1038/nmicrobiol.2017.120

Taborda, C. P., Urán, M. E., Nosanchuk, J. D., and Travassos, L. R. (2015). Paracoccidioidomycosis: challenges in the development of a vaccine against an

endemic mycosis in the Americas. *Rev. Inst. Med. Trop. São Paulo* 57, 21–24. doi: 10.1590/S0036-46652015000700005

Tang, Y., Wu, S., Lin, J., Cheng, L., Zhou, J., Xie, J., et al. (2018). Nanoparticles targeted against cryptococcal pneumonia by interactions between chitosan and its peptide ligand. *Nano Lett.* 18, 6207–6213. doi: 10.1021/acs.nanolett.8b02229

Thakkar, H. P., Khunt, A., Dhande, R. D., and Patel, A. A. (2015). Formulation and evaluation of Itraconazole nanoemulsion for enhanced oral bioavailability. *J. Microencapsul.* 32, 559–569. doi: 10.3109/02652048.2015.1065917

Thangamani, N., and Bhuvaneshwari, N. (2019). Green synthesis of gold nanoparticles using Simarouba glauca leaf extract and their biological activity of micro-organism. *Chem. Phys. Lett.* 732:136587. doi: 10.1016/j.cplett.2019.07.015

Thompson, G. R. (2011). Pulmonary coccidioidomycosis. *Semin. Respir. Crit. Care Med.* 32, 754–763. doi: 10.1055/s-0031-1295723

Tiew, P. Y., Mac Aogain, M., Ali, N. A. B. M., Thng, K. X., Goh, K., Lau, K. J. L., et al. (2020). The mycobiome in health and disease: Emerging concepts, methodologies and challenges. *Mycopathologia* 185, 207–231. doi: 10.1007/s11046-019-00413-z

Tøndervik, A., Sletta, H., Klinkenberg, G., Emanuel, C., Powell, L. C., Pritchard, M. F., et al. (2014). Alginate oligosaccharides inhibit fungal cell growth and potentiate the activity of antifungals against Candida and Aspergillus spp. *PLoS ONE* 9:e112518. doi: 10.1371/journal.pone.0112518

Travassos, L. R., and Taborda, C. P. (2012). Paracoccidioidomycosis vaccine. *Hum. Vaccines Immunother.* 8, 1450–1453. doi: 10.4161/hv.21283

Travassos, L. R., and Taborda, C. P. (2017). Linear epitopes of paracoccidioides brasiliensis and other fungal agents of human systemic mycoses as vaccine candidates. *Front. Immunol.* 8:224. doi: 10.3389/fimmu.2017.00224

Tukulula, M., Gouveia, L., Paixao, P., Hayeshi, R., Naicker, B., and Dube, A. (2018). Functionalization of PLGA Nanoparticles with 1,3-β-glucan Enhances the Intracellular Pharmacokinetics of Rifampicin in Macrophages. *Pharm. Res.* 35:111. doi: 10.1007/s11095-018-2391-8

Tukulula, M., Hayeshi, R., Fonteh, P., Meyer, D., Ndamase, A., Madziva, M. T., et al. (2015). Curdlan-conjugated PLGA nanoparticles possess macrophage stimulant activity and drug delivery capabilities. *Pharm. Res.* 32, 2713–2726 doi: 10.1007/s11095-015-1655-9

Tumbarello, M., Posteraro, B., Trecarichi, E. M., Fiori, B., Rossi, M., Porta, R., et al. (2007). Biofilm production by Candida species and inadequate antifungal therapy as predictors of mortality for patients with candidemia. *J. Clin. Microbiol.* 45, 1843–1850. doi: 10.1128/JCM.00131-07

Usman, F., Khalil, R., Ul-Haq, Z., Nakpheng, T., and Srichana, T. (2018). Bioactivity, safety, and efficacy of Amphotericin B Nanomicellar aerosols using sodium deoxycholate sulfate as the lipid carrier. *AAPS PharmSciTech.* 19, 2077–2086. doi: 10.1208/s12249-018-1013-4

Van de Ven, H., Paulussen, C., Feijens, P. B., Matheeussen, A., Rombaut, P., Kayaert, P., et al. (2012). PLGA nanoparticles and nanosuspensions with amphotericin B: potent *in vitro* and *in vivo* alternatives to Fungizone and AmBisome. *J. Control Release* 161, 795–803. doi: 10.1016/j.jconrel.2012.05.037

Vazquez-Muñoz, R., Avalos-Borja, M., and Castro-Longoria, E. (2014). Ultrastructural analysis of *Candida albicans* when exposed to silver nanoparticles. *PLoS ONE* 9:e108876. doi: 10.1371/journal.pone.0108876

Vazquez-Muñoz, R., Borrego, B., Juárez-Moreno, K., García-García, M., Mota Morales, J. D., Bogdanchikova, N., et al. (2017). Toxicity of silver nanoparticles in biological systems: does the complexity of biological systems matter? *Toxicol. Lett.* 276, 11–20. doi: 10.1016/j.toxlet.2017.05.007

Venkatesan, J., Jayakumar, R., Mohandas, A., Bhatnagar, I., and Kim, S.-K. (2014). Antimicrobial activity of chitosan-carbon nanotube hydrogels. *Materials* 7, 3946–3955. doi: 10.3390/ma7053946

Vincent, B. M., Lancaster, A. K., Scherz-Shouval, R., Whitesell, L., and Lindquist, S. (2013). Fitness trade-offs restrict the evolution of resistance to amphotericin B. *PLoS Biol.* 11:e1001692. doi: 10.1371/journal.pbio.1001692

Voltan, A. R., Quindós, G., Alarcón, K. P. M., Fusco-Almeida, A. M., Mendes-Giannini, M. J. S., and Chorilli, M. (2016). Fungal diseases: could nanostructured drug delivery systems be a novel paradigm for therapy? *Int. J. Nanomed.* 11, 3715–3730. doi: 10.2147/IJN.S93105

Wagner, V., Dullaart, A., Bock, A.-K., and Zweck, A. (2006). The emerging nanomedicine landscape. *Nat. Biotechnol.* 24, 1211–1217. doi: 10.1038/nbt1006-1211

Westerberg, D. P., and Voyack, M. J. (2013). Onychomycosis: current trends in diagnosis and treatment. *Am. Fam. Phys.* 88, 762–770.

Wheat, L. J., Connolly, P., Smedema, M., Brizendine, E., Hafner, R., AIDS Clinical Trials Group, and the Mycoses Study Group of the National Institute of Allergy and Infectious Diseases (2001). Emergence of resistance to fluconazole as a cause of failure during treatment of histoplasmosis in patients with acquired immunodeficiency disease syndrome. *Clin. Infect. Dis.* 33, 1910–1913. doi: 10.1086/323781

Wlaz, P., Knaga, S., Kasperek, K., Wlaz, A., Poleszak, E., Jezewska-Witkowska, G., et al. (2015). Activity and safety of inhaled itraconazole nanosuspension in a model pulmonary aspergillus fumigatus infection in inoculated young quails. *Mycopathologia* 180, 35–42. doi: 10.1007/s11046-015-9885-2

Wojtyczka, R., Dziedzic, A., Idzik, D., Kepa, M., Kubina, R., Kabała-Dzik, A., et al. (2013). susceptibility of staphylococcus aureus clinical isolates to propolis extract alone or in combination with antimicrobial drugs. *Molecules* 18, 9623–9640. doi: 10.3390/molecules18089623

Wüthrich, M., Brandhorst, T. T., Sullivan, T. D., Filutowicz, H., Sterkel, A., Stewart, D., et al. (2015). Calnexin induces expansion of antigen-specific CD4(+) T cells that confer immunity to fungal ascomycetes via conserved epitopes. *Cell Host Microbe.* 17, 452–465. doi: 10.1016/j.chom.2015.02.009

Xiang, S. D., Scholzen, A., Minigo, G., David, C., Apostolopoulos, V., Mottram, P. L., et al. (2006). Pathogen recognition and development of particulate vaccines: does size matter? *Methods* 40, 1–9. doi: 10.1016/j.ymeth.2006.05.016

Xu, N., Gu, J., Zhu, Y., Wen, H., Ren, Q., and Chen, J. (2011). Efficacy of intravenous amphotericin B-polybutylcyanoacrylate nanoparticles against cryptococcal meningitis in mice. *Int. J. Nanomed.* 6, 905–913. doi: 10.2147/IJN.S17503

Xue, B., Zhang, Y., Xu, M., Wang, C., Huang, J., Zhang, H., et al. (2019). Curcumin-silk fibroin nanoparticles for enhanced anti- *Candida albicans* Activity *in vitro* and *in vivo*. *J. Biomed. Nanotechnol.* 15, 769–778. doi: 10.1166/jbn.2019.2722

Yah, C. S., and Simate, G. S. (2015). Nanoparticles as potential new generation broad spectrum antimicrobial agents. *Daru* 23:43. doi: 10.1186/s40199-015-0125-6

Yang, C., Xue, B., Song, W., Kan, B., Zhang, D., Yu, H., et al. (2018). Reducing the toxicity of amphotericin B by encapsulation using methoxy poly(ethylene glycol)-b-poly(l-glutamic acid-co-l-phenylalanine). *Biomater. Sci.* 6, 2189–2196. doi: 10.1039/C8BM00506K

Yang, L., Dong, X., Wu, X., Xie, L., and Min, X. (2011). Intravitreally implantable voriconazole delivery system for experimental fungal endophthalmitis. *Retina* 31, 1791–1800. doi: 10.1097/IAE.0b013e31820d3cd2

Yang, M., Du, K., Hou, Y., Xie, S., Dong, Y., Li, D., et al. (2019). Synergistic antifungal effect of Amphotericin B-Loaded Poly(Lactic-Co-Glycolic Acid) nanoparticles and ultrasound against *Candida albicans* biofilms. *Antimicrob. Agents Chemother.* 63:e02022-18. doi: 10.1128/AAC.02022-18

Yehia, S., El-Gazayerly, O., and Basalious, E. (2009). Fluconazole mucoadhesive buccal films: *in vitro/in vivo* performance. *Curr. Drug Deliv.* 6, 17–27. doi: 10.2174/156720109787048195

Yu, Q., Li, J., Zhang, Y., Wang, Y., Liu, L., and Li, M. (2016). Inhibition of gold nanoparticles (AuNPs) on pathogenic biofilm formation and invasion to host cells. *Sci. Rep.* 6:26667. doi: 10.1038/srep26667

Zhang, C., Chen, M., Wang, G., Fang, W., Ye, C., Hu, H., et al. (2016). Pd@Ag nanosheets in combination with Amphotericin B exert a potent anti-cryptococcal fungicidal effect. *PLoS ONE* 11:e0157000. doi: 10.1371/journal.pone.0157000

Zhang, X.-F., Liu, Z.-G., Shen, W., and Gurunathan, S. (2016). Silver nanoparticles: synthesis, characterization, properties, applications, and therapeutic approaches. *Int. J. Mol. Sci.* 17, 1534. doi: 10.3390/ijms17091534

Zhao, J., Cheng, Y., Song, X., Wang, C., Su, G., and Liu, Z. (2015). A comparative treatment study of intravitreal voriconazole and liposomal Amphotericin B in an aspergillus fumigatus endophthalmitis model. *Invest. Ophthalmol. Vis. Sci.* 56, 7369–7376. doi: 10.1167/iovs.15-17266

Zhao, L., Seth, A., Wibowo, N., Zhao, C.-X., Mitter, N., Yu, C., et al. (2014). Nanoparticle vaccines. *Vaccine* 32, 327–337. doi: 10.1016/j.vaccine.2013.11.069

Zhao, W., Liu, Q., Zhang, X., Su, B., and Zhao, C. (2018). Rationally designed magnetic nanoparticles as anticoagulants for blood purification. *Colloids Surf B Biointerfaces* 164, 316–323. doi: 10.1016/j.colsurfb.2018.01.050

Conflict of Interest: The authors declare that the research was conducted in the absence of any commercial or financial relationships that could be construed as a potential conflict of interest.

frontiers in Cellular and Infection Microbiology

REVIEW
published: 16 October 2020
doi: 10.3389/fcimb.2020.592259

Living Within the Macrophage: Dimorphic Fungal Pathogen Intracellular Metabolism

Qian Shen[1] *and Chad A. Rappleye*[2]*

[1] Department of Biology, Rhodes College, Memphis, TN, United States, [2] Department of Microbiology, Ohio State University, Columbus, OH, United States

Histoplasma and *Paracoccidioides* are related thermally dimorphic fungal pathogens that cause deadly mycoses (i.e., histoplasmosis and paracoccidioidomycosis, respectively) primarily in North, Central, and South America. Mammalian infection results from inhalation of conidia and their subsequent conversion into pathogenic yeasts. Macrophages in the lung are the first line of defense, but are generally unable to clear these fungi. Instead, *Histoplasma* and *Paracoccidioides* yeasts survive and proliferate within the phagosomal compartment of host macrophages. Growth within macrophages requires strategies for acquisition of sufficient nutrients (e.g., carbon, nitrogen, and essential trace elements and co-factors) from the nutrient-depleted phagosomal environment. We review the transcriptomic and recent functional genetic studies that are defining how these intracellular fungal pathogens tune their metabolism to the resources available in the macrophage phagosome. In addition, recent studies have shown that the nutritional state of the macrophage phagosome is not static, but changes upon activation of adaptive immune responses. Understanding the metabolic requirements of these dimorphic pathogens as they thrive within host cells can provide novel targets for therapeutic intervention.

Keywords: *Histoplasma*, *Paracoccidioides*, macrophage, phagosome, metabolism, fungal pathogen, gluconeogenesis, nutritional immunity

OPEN ACCESS

Edited by:
Angel Gonzalez,
University of Antioquia, Colombia

Reviewed by:
Flavio Vieira Loures,
Federal University of São Paulo, Brazil
Julhiany De Fátima Da Silva,
Universidade Estadual Paulista, Brazil

***Correspondence:**
Chad A. Rappleye
rappleye.1@osu.edu

Specialty section:
This article was submitted to Fungal Pathogenesis, a section of the journal Frontiers in Cellular and Infection Microbiology

Received: *06 August 2020*
Accepted: *15 September 2020*
Published: *16 October 2020*

Citation:
Shen Q and Rappleye CA (2020) Living Within the Macrophage: Dimorphic Fungal Pathogen Intracellular Metabolism. Front. Cell. Infect. Microbiol. 10:592259. doi: 10.3389/fcimb.2020.592259

INTRODUCTION

Histoplasma and *Paracoccidioides* species cause respiratory and systemic disease in mammals (histoplasmosis and paracoccidioidomycosis, respectively). Disease results from inhalation of aerosolized fungal conidia from the environmental mold form. Severity of disease ranges from subclinical to acute, and is largely a function of the dose inhaled and the immunological defenses of the host (Kauffman, 2009; Queiroz-Telles and Escuissato, 2011; Salzer et al., 2018). In immunocompromised individuals (e.g., HIV patients), infection can result in life-threatening disseminated disease. Recent phylogenetic analyses based on genome sequencing efforts have split the original *Histoplasma capsulatum* and *Paracoccidiodies brasiliensis* designations into additional species (Van Dyke et al., 2019). Although some physical and biochemical differences exist among these species groups, in this review we will refer to studies in each fungus by the respective genus name unless necessary to specifically highlight findings unique to a species.

The *Histoplasma* and *Paracoccidiodies* genera comprise closely related fungi which are characterized by thermal dimorphism. Conidia, produced by the environmental mycelial forms,

convert into pathogenic yeast forms in response to the elevated temperature following inhalation by a mammalian host. The yeasts are budding yeasts, with *Paracoccidioides* yeasts typically characterized by multiple budding daughter cells around a central yeast body. A hallmark of these dimorphic fungal pathogens is the link between pathogenesis and conversion into yeasts (Medoff et al., 1987; Maresca and Kobayashi, 1989; Aristizabal et al., 1998; Borges-Walmsley et al., 2002).

During infection, *Histoplasma* and *Paracoccidioides* yeast cells are phagocytosed by cells of the innate immune system. Studies with cultured phagocytes (i.e., macrophages) show roughly 10%-30% of *Paracoccidioides* yeasts are taken up by macrophages (Soares et al., 2010; da Silva et al., 2016) while up to 60% of *Histoplasma* yeasts are phagocytosed (Newman et al., 1990; Garfoot et al., 2016) within 60–90 min in tissue culture conditions. Studies of respiratory infection in mice show that nearly all *Histoplasma* yeasts are found within $CD45^+$ phagocytes (Deepe et al., 2008). Thus, *Histoplasma* yeasts reside almost exclusively within phagocytes during infection *in vivo*, and many, but not all *Paracoccidioides* yeasts are intracellular. Non-activated host phagocytes are relatively ineffective in killing and controlling *Histoplasma* and *Paracoccidioides* yeasts. Activation of phagocytes during adaptive immunity by T helper cell type 1 (Th1) is typically required for host control of these fungi (Allendoerfer and Deepe, 1997, 1998; Souto et al., 2000; Calich et al., 2008; de Castro et al., 2013) thereby distinguishing *Histoplasma* and *Paracoccidioides* from opportunistic fungal pathogens, which are readily controlled without T-cell activation. Recently, IL-17 signaling was shown to also contribute to the control of *Paracoccidioides* (Tristão et al., 2017).

To effectively use phagocytes as host cells, *Histoplasma* and *Paracoccidioides* yeasts express mechanisms that facilitate binding to host phagocytes and survival of macrophage defenses. Although the fungal cell wall contains β-glucans which can alert the immune system to the presence of a fungal invader, *Histoplasma* yeasts effectively hide this β-glucan signature by overlaying the immunostimulatory β-glucans with α-glucan polysaccharides (Rappleye et al., 2004, 2007). In addition, *Histoplasma* yeasts secrete an endoglucanase (Eng1) that trims away remaining exposed β-glucans (Garfoot et al., 2016). Although a similar mechanism has not been shown for *Paracoccidioides*, the cell wall of *Paracoccidioides* yeasts also has a high content of α-glucan (Kanetsuna et al., 1972) and decreased α-glucan is associated with decreased virulence (San-Blas et al., 1977). *Histoplasma* expresses two extracellular antioxidant enzymes, Sod3 and CatB, which together effectively eliminate phagocyte-derived reactive oxygen (Youseff et al., 2012; Holbrook et al., 2013) and facilitate *Histoplasma* survival during uptake by macrophages. Consistent with the pathogenesis-enabling role of these mechanisms, α-glucan production and secretion of Eng1, Sod3, and CatB characterize the virulent yeasts, but not the avirulent mycelial cells.

Pathogenic yeast not only survive the encounter with phagocytes, but also use the phagocyte as a permissive niche during infection. As long-term intracellular residents of the macrophage, *Histoplasma* and *Paracoccidioides* yeasts must adapt their metabolism to nutrients available in the phagosome. The phagosome environment is generally assumed to be nutrient poor, yet these fungi are able to scavenge sufficient carbon, nitrogen, sulfur, and micronutrients from the host cell to support fungal growth and replication. Many studies have used gene expression profiling to infer which metabolic pathways are active during residence within the phagosome. Interpretation of differentially expressed genes, however, is complicated by the *in vitro* growth condition used as the comparison. Furthermore, a large number of genes that characterize the pathogenic yeast phase of the dimorphic fungi are controlled by phase-differentiation factors such as the Ryp proteins (Shen and Rappleye, 2017; Beyhan and Sil, 2019) suggesting that some metabolic genes may not be regulated by the nutritional environment, but instead their expression is set by the differentiation state (i.e., yeasts vs. mycelia). Genetic studies, and the functional tests it facilitates, are a means to more conclusively determine the metabolism used by intracellular yeasts to parasitize the macrophage. Recent studies highlighted below integrate key findings that define the metabolic pathways required for intracellular yeast proliferation, and by extension, the host substrates that are consumed by these fungal pathogens during infection.

INTRAPHAGOSOMAL CARBON METABOLISM

Glycolysis

Most *in vitro* fungal growth media is based on glucose as the primary carbon source since glucose affords rapid fungal growth. Although this rich carbon source may reflect some host environments (e.g., the bloodstream), other host niches, including the macrophage phagosome are characterized by alternative carbon sources. Gene expression studies in which specific metabolic pathways are up-regulated in specific host environments can reveal the presence of different carbon sources. Bailão et al. (2006) conducted the first study with *Paracoccidioides* yeasts to determine which genes are up-regulated during infection. Comparing the gene expression profile of yeasts grown in human blood to yeasts grown *in vitro*, Bailão et al. (2006) found that glyceraldehyde 3-phosphate dehydrogenase (GAPDH) was up-regulated in blood. Since GAPDH is involved in both glycolysis and gluconeogenesis, it remains unclear if glucose catabolism contributes to *Paracoccidioides* infection of host cells. While some *Paracoccidioides* cells may be taken up by phagocytes in blood (e.g., neutrophils), significant numbers may remain extracellular. Thus, the results might reflect the transcriptional responses of a mixed population consisting of both extracellular yeasts and intracellular yeasts from different types of phagocytes. Thus, the high concentration of extracellular glucose in the blood, not the intracellular phagosome environment, may be the primary driver of GAPDH up-regulation.

Profiling of yeasts resident within macrophages offers a more direct assessment of the transcriptional profiles supporting intraphagosomal growth. Tavares et al. (2007) conducted a differential expression study comparing the

gene expression profile of *Paracoccidioides* yeasts grown in murine peritoneal macrophages and those grown *in vitro* in rich media. Using a transcriptional microarray, the authors found that the gene encoding the glycolysis specific enzyme phosphofructokinase (*PFK1*) was down-regulated in intracellular *Paracoccidioides* yeasts. A separate transcriptional study that profiled *Paracoccidioides* yeasts from the lung identified a sugar transporter that was down-regulated relative to yeasts grown *in vitro* in a glucose-rich medium [2% glucose (Lacerda Pigosso et al., 2017)]. This suggests that glucose catabolism is not a primary metabolic pathway for *Paracoccidioides* intracellular growth. However, in the Tavares study (Tavares et al., 2007), RT-PCR data was unable to confirm the microarray results. Proteomic analysis of *Paracoccidioides* intracellular yeasts found that hexokinase (Hxk1) was down-regulated compared to yeast grown in a glucose-rich medium *in vitro* consistent with decreased metabolism of sugars (Parente-Rocha et al., 2015). The transcriptional signature of intracellular *Histoplasma* yeasts also shows down-regulation of a glycolytic response when growing within macrophages (Shen et al., 2020). As with *Paracoccidioides*, *PFK1* was down-regulated in *Histoplasma* yeasts. Genes encoding other glucose-catabolism factors including pyruvate kinase (*PYK1*) and the hexose/glucose kinases (*HXK1* and *GLK1)* were also down-regulated. The finding that multiple components of glycolysis showed decreased expression provides stronger support for the metabolism of alternative carbon sources during intracellular proliferation. As an independent indicator of the lack of hexose catabolism by intracellular *Histoplasma* yeasts, metabolic assays (i.e., Seahorse assays) of *Histoplasma* yeasts isolated from macrophages showed the yeasts were glycolytically inactive (Shen et al., 2020) consistent with the transcriptional profiles. Definitive evidence of the lack of hexose catabolism by intracellular yeasts came from the analysis of glycolysis-deficient *Histoplasma* yeasts. Simultaneous depletion of *Histoplasma*'s only hexose/glucose kinases (Hxk1 and Glk1) impaired the ability of *Histoplasma* yeast to grow on glucose as the carbon source *in vitro*, but Hxk1 and Glk1 loss did not prevent *Histoplasma* yeast growth within macrophages (Shen et al., 2020). Most revealing, the depletion of Hxk1 and Glk1 and no effect on *Histoplasma* respiratory infection *in vivo* (Shen et al., 2020). These data demonstrate that *Histoplasma* yeasts, and likely also *Paracoccidioides* yeasts, do not catabolize hexoses to grow within macrophages. As both *Histoplasma* and *Paracoccidioides* efficiently use glucose *in vitro*, this suggests that it is unlikely that hexoses are available to yeasts within the macrophage phagosome.

Gluconeogenesis

The lack of hexose utilization suggests that gluconeogenic substrates are likely metabolized by intracellular yeasts to provide energy and essential biomolecules including glucans for the polysaccharide-rich cell wall. A combined transcriptomic and proteomics study compared *Paracoccidioides* yeasts isolated from mouse lungs after 6 h of infection to yeasts grown in a glucose- and peptide-rich medium *in vitro* [Brain Heart Infusion medium (Lacerda Pigosso et al., 2017)]. The *PCK1* gene, encoding phosphoenolpyruvate carboxykinase which catalyzes the first committed step of gluconeogenesis, was transcriptionally up-regulated *in vivo*, suggesting the yeasts resided in a glucose-depleted environment. However, the proteomics analysis failed to detect Pck1 at the protein level in yeasts isolated from the lung. As only a portion of *Paracoccidioides* yeasts get internalized by phagocytes, it is unclear whether the up-regulation of *PCK1* reflects the intracellular or extracellular nutritional environment during *in vivo* infection and whether 6 h of infection is sufficient for transcriptional or proteomic adaptive responses. One of the limitations of this study was the recovery of low numbers of yeasts which could impact the sensitivity of their analyses. Many normally-abundant proteins were not detected in the proteomic data and key enzymes involved in the central carbon metabolism (i.e., pyruvate kinase, citrate synthase, and isocitrate dehydrogenase) that should be abundant in yeast cells, regardless of growth condition, were not recovered from the proteome data. No conclusions can be made from the absence of data, but an independent study of intramacrophage *Paracoccidioides* yeasts also showed up-regulation of the *PCK1* gene after 9 h of infection (Derengowski et al., 2008). In addition, Parente-Rocha et al. (2015) found that gluconeogenesis-specific enzyme fructose-1,6-bisphosphatase was modestly increased (1.5-fold) in *Paracoccidioides* yeasts recovered from macrophages, providing further support of gluconeogenesis-based metabolism in intracellular yeasts.

Studies of *Histoplasma* yeasts isolated from macrophages 24 h after infection shows *PCK1* expression is up-regulated in intracellular yeasts (Shen et al., 2020). Elimination of Pck1 activity prevents growth of *Histoplasma* yeasts within macrophages but not *in vitro* growth in glucose-containing medium confirming that the phagosome environment lacks hexose substrates (Shen et al., 2020). *Histoplasma* yeasts lacking Pck1 function are severely attenuated in a murine model of respiratory infection as early as 2 days post-infection and this growth defect *in vivo* persisted throughout the entire 8-day infection period, indicating that the *Histoplasma*-containing phagosome remains depleted of hexose substrates. The gluconeogenesis-specific fructose-1,6-bisphosphatase (Fbp1) is also required for *Histoplasma* yeast virulence in macrophages and in mice (Shen et al., 2020). These findings are consistent with the results that glycolytic enzymes are not required for *Histoplasma* full virulence *in vivo*. Collectively, these findings indicate that *Histoplasma* yeasts rely on metabolizing gluconeogenic carbon sources to proliferate within macrophages (**Figure 1**) and this metabolism likely characterizes intracellular *Paracoccidioides* yeasts.

Fatty Acids Utilization

What are the gluconeogenic substrates derived from the host that support yeast proliferation within phagosomes? One potential source is host fatty acids. These long-chain carbon molecules can be metabolized to acetyl-CoA (β-oxidation) which subsequently enters the TCA cycle to generate energy or can be assimilated into carbon biomass through the glyoxylate shunt. The up-regulation of the glyoxylate shunt can indicate utilization of fatty acids as the carbon source. In one study (Derengowski et al., 2008), the expression of key genes involved in glyoxylate shunt [isocitrate

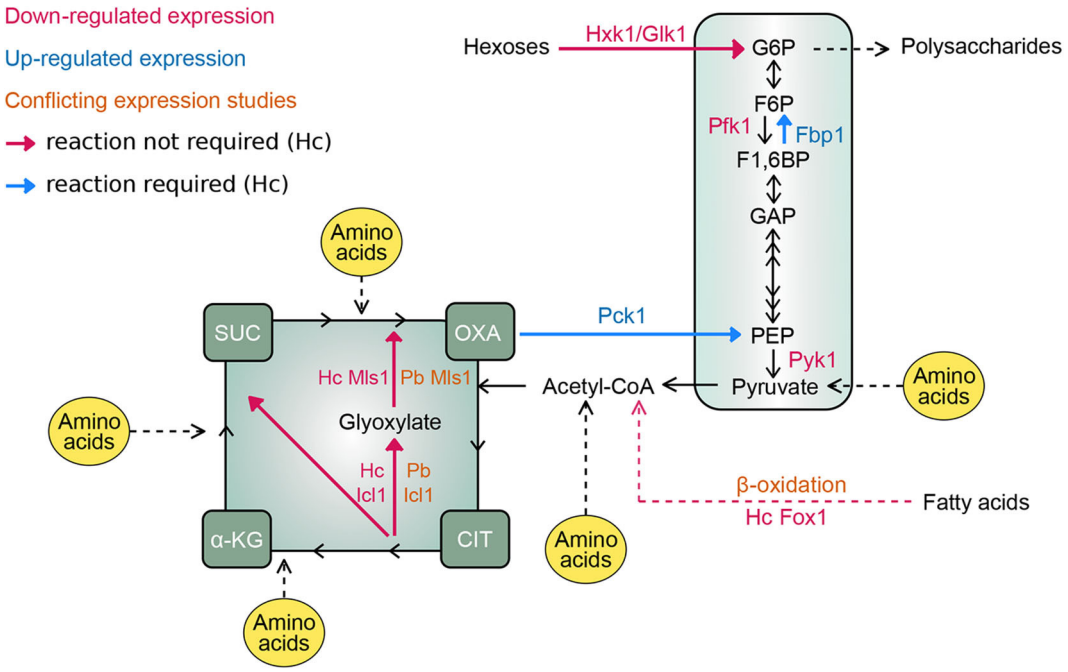

FIGURE 1 | Intramacrophage carbon metabolism of *Histoplasma* and *Paracoccidioides*. Schematic map depicts the central metabolic pathways for the metabolism of different carbon-containing molecules with key carbon intermediates shown. Enzymes catalyzing critical steps of glycolysis (Hxk1/Glk1, Pfk1, and Pyk1), gluconeogenesis (Pck1 and Fbp1), and fatty acid utilization (Fox1 for β-oxidation of fatty acids, and Icl1 and Mls1 for the glyoxylate cycle for incorporation of acetyl-CoA into biomolecules) are indicated. Names of enzymes are colored based on the down-regulation (magenta text) or up-regulation (blue text) in fungal cells within macrophages. *in situ*ations where expression data is conflicting, text is colored orange. For expression data that is discrepant between *Paracoccidioides* and *Histoplasma*, the respective genes are provided by a species prefix (Pb and Hc, respectively). Arrows indicate the flow of carbon through metabolic pathways. Enzymatic reactions that are not required for intracellular growth are indicated with magenta arrows. Reactions necessary for proliferation in the phagosome and for infection *in vivo* are indicated with blue arrows. Points of entry for amino acids as potential carbon substrates are indicated in yellow. Enzyme abbreviations: Hxk1, hexokinase; Glk1, glucokinase; Pfk1, phosphofructokinase; Pyk1, pyruvate kinase; Pck1, phosphoenolpyruvate carboxykinase; Fbp1, fructose 1,6-bisphosphatase; Fox1, fatty acyl-CoA oxidase; Icl1, isocitrate lyase. Metabolite abbreviations: G6P, glucose 6-phosphate; F6P, fructose 6-phosphate; F1, 6BP, fructose 1,6-bisphosphate; GAP, glyceraldehyde 3-phosphate; PEP, phosphoenolpyruvate; CIT, citrate; α-KG, α-ketoglutarate; SUC, succinate; OXA, oxaloacetate.

lyase (*ICL1*) and malate synthase (*MLS1*)] in *Paracoccidioides* yeasts was measured during infection of J774 macrophages using semi-quantitative RT-PCR. Expression of *ICL1* increased ∼3-fold in macrophages compared to growth in Fava-Neto medium (a rich medium containing high glucose, peptides, and amino acids). However, expression of *MLS1* showed only a minor increase in expression. Isocitrate lyase protein (Icl1) increased 1.6-fold in *Paracoccidioides* yeasts recovered from J774 macrophages (Parente-Rocha et al., 2015). The up-regulation of *ICL1* is consistent with results profiling *Candida albicans* and *Cryptococcus neoformans* yeasts when interacting with macrophages (Lorenz et al., 2004; Fan et al., 2005). However, Tavares et al. (2007) reported conflicting results that *ICL1* was not up-regulated in *Paracoccidioides* yeasts within peritoneal macrophages, possibly due to *in vitro* growth conditions used for comparison. Expression profiling of *Paracoccidioides* yeasts 6 h after infection of mice also found an indication of the up-regulation of the glyoxylate shunt, but only the *MLS1* gene, not *ICL1* (Lacerda Pigosso et al., 2017). Growth of *Paracoccidioides* yeasts on acetate *in vitro* increases both *ICL1* and *MSL1* expression by a similar magnitude (Derengowski et al., 2008), suggesting the one-sided increases in *ICL1* or *MLS1* expression by *Paracoccidioides* yeasts in macrophages or *in vivo* do not indicate simple induction of the glyoxylate cycle. These inconsistencies complicate inferences about the role of the glyoxylate cycle in intracellular *Paracoccidioides* yeasts.

As with the glyoxylate cycle, indications of fatty acid catabolism by *Paracoccidioides* yeasts are also variable. Enzymes catalyzing the breakdown of fatty acids via β-oxidation have been examined for *Paracoccidioides* yeasts both in macrophages and *in vivo*. While enoyl-CoA hydratase (which catalyzes the second step in fatty acid metabolism) was up-regulated in *Paracoccidioides* yeasts from J774 macrophages, 3-keyoacyl-CoA thiolase (which catalyzes the last step liberating acetyl-CoA) was down-regulated in these same intracellular yeasts (Parente-Rocha et al., 2015). Transcriptional profiling of *Paracoccidioides* yeast showed three different genes annotated as encoding acyl-CoA dehydrogenases, which catalyze the first step in fatty acid breakdown, were increased during respiratory infection of mice (Lacerda Pigosso et al., 2017). One of these was increased 13-fold over yeast grown *in vitro*. However, Parente-Rocha et al. (2015) did not detect any increased acyl-CoA dehydrogenases in *Paracoccidioides* yeasts resident within cultured macrophages. These inconsistencies as well as the potential profiling of a mixed

population of intra- and extracellular *Paracoccidioides* yeasts following infection of mice leave the role of fatty acid metabolism unclear for *Paracoccidioides*.

In contrast, *Histoplasma* yeasts within macrophages do not present hallmarks of fatty acid utilization. The transcription of genes encoding enzymes of the glyoxylate cycle (*ICL1* and *MLS1*) as well as the first step in fatty acid β-oxidation [fatty acyl-CoA oxidase (*FOX1)*] were all down-regulated in intracellular *Histoplasma* yeasts (Shen et al., 2020). *Histoplasma* yeasts are unable to metabolize exogenous fatty acids as the carbon source *in vitro*. Thus, changes in β-oxidation enzymes may reflect modulation of endogenous fatty acids unrelated to host carbon substrates. The most conclusive evidence of the lack of host fatty acid consumption by *Histoplasma* yeasts was obtained by functional studies with yeast strains depleted of key enzymes in fatty acid utilization. *Histoplasma* yeasts lacking Icl1 or lacking Fox1 are fully virulent in cultured macrophage infection as well as in respiratory infection of mice (Shen et al., 2020). The lack of any requirement for fatty acid utilization by intracellular *Histoplasma* yeasts differs from that of other fungal pathogens [e.g., *C. albicans* (Lorenz and Fink, 2001) and *C. neoformans* (Kretschmer et al., 2012)], which occupy diverse extracellular niches or are only transiently found within phagocytes. As *Histoplasma* yeasts are nearly all within phagocytes during infection, this suggests that *Histoplasma* yeasts have adapted to a more prolonged residence within the phagosome and do not utilize host fatty acids as a major carbon source, either because exogenous fatty acids are unavailable within the phagosome or because other carbon sources are more consistently obtained in this intracellular compartment. Whether intracellular *Paracoccidioides* yeast metabolism mirrors that of intracellular *Histoplasma* yeasts or if it follows the paradigm of transient occupants of the phagocyte remains to be determined.

Amino Acid Catabolism

The above studies indicate that both *Paracoccidioides* and *Histoplasma* yeasts exploit gluconeogenic substrates for intracellular proliferation. What are these alternative host carbon substrates obtained from the host macrophage, and specifically which are found within the phagosome? Carbon source utilization tests *in vitro* showed that the spectrum of carbon sources which can be metabolized by yeasts differs from those that are metabolized by *Histoplasma* mycelia, suggesting that the pathogenic yeasts are more metabolically streamlined (Shen et al., 2020). For example, *Histoplasma* yeasts can metabolize hexoses and hexosamines but not pentoses or disaccharides, some of which are metabolized by mycelia. In addition, *Histoplasma* yeasts can use a mix of amino acids as a non-carbohydrate carbon source. Given hexose-catabolism and fatty acids catabolism pathways are not required for *Histoplasma* intracellular proliferation, this focuses attention on amino acids as potential sources of carbon for pathogenic-phase yeasts within the phagosome. Indeed, the phagosome/phagolysosome is a degradative organelle harboring numerous proteases that could generate amino acids and short peptides through host protein degradation.

Expression of genes involved in amino acid biosynthesis hints to the absence of certain amino acids within the phagosome. Bailão et al. (2006) showed that the gene catalyzing the last step of glutamine synthesis (i.e., *GLN1*) in *Paracoccidioides* is up-regulated in fresh human blood, suggesting that glutamine in the human blood environment is not sufficient to support *Paracoccidioides* growth. However, the intracellular residence of *Paracoccidioides* is unknown in this study. In peritoneal macrophages, *Paracoccidioides* yeasts up-regulated the gene involved in methionine synthesis (*METG*) suggesting that methionine is not available within macrophages (Tavares et al., 2007). Differential gene expression of *Paracoccidioides* from respiratory infection showed genes encoding enzymes involved in the metabolism of glycine, serine, threonine, methionine, and lysine are down-regulated (Lacerda Pigosso et al., 2017). Also, down-regulated were genes encoding 4-hydroxyphenylpyruvate dioxygenase (*HPD1*) and homogentisate dioxygenase (*HGD1*), which are involved in phenylalanine and tyrosine degradation suggesting these aromatic amino acids are not consumed from the host. On the other hand, Parente-Rocha's study of *Paracoccidioides* yeasts from macrophages showed increased abundance of Hpd1 (Parente-Rocha et al., 2015) contradicting the *in vivo* gene expression study. Expression studies thus do not provide definitive answers, especially considering the interconversion of many amino acids. Functional evidence comes from a study that used the chemical compound CP1, which is known to inhibit chorismate synthase, the key enzyme in biosynthesis of aromatic amino acids (i.e., tyrosine, tryptophan, and phenylalanine). Treatment of *Paracoccidioides*-infected mice with CP1 reduced fungal burdens ∼10-fold compared to untreated mice (Rodrigues-Vendramini et al., 2019) suggesting that *Paracoccidioides* yeasts must synthesize at least one of the three to make up for the deficiency in the environment in which *Paracoccidioides* is found during lung infection.

Histoplasma yeasts can catabolize amino acids as the sole carbon source demonstrating the potential to use host amino acids within the phagosome. On the other hand, *Histoplasma* yeasts cannot utilize model host protein substrates for carbon (e.g., bovine serum albumin, gelatin, and hemoglobin). Prior digestion of these proteins with proteinases, including the phagosomal proteinase Cathepsin D, renders the proteins to a state that can support the growth of *Histoplasma* yeasts (Shen et al., 2020). Thus, it appears that *Histoplasma* yeasts can take up amino acids and select peptides to use as carbon but does not metabolize intact proteins. This would be consistent with residence within the phagosome where host proteinases may supply the degradative capacity to liberate amino acids for consumption by intraphagosomal *Histoplasma* yeasts. Indeed, the expression of many metabolic genes of *Histoplasma* yeasts within the macrophage is highly similar to the profile of *Histoplasma* yeasts growing on amino acids *in vitro* (Shen et al., 2020). The expression of various peptidases are increased in *Paracoccidioides* yeast within J774 macrophages (Parente-Rocha et al., 2015) and *Paracoccidioides* yeast secrete a serine proteinase during infection (Lacerda Pigosso et al., 2017), suggesting that proteins and peptides are hydrolyzed to amino acids before consumption. Nonetheless, not all amino acids are

sufficiently present in the phagosome to support fungal growth. A *Histoplasma* alanine auxotroph showed impaired virulence in both macrophages and *in vivo*, indicating alanine is deficient in the phagosomal environment (Shen et al., 2020). Combined with the lack of hexose and fatty acid catabolism described for *Histoplasma* yeasts above, it is likely that *Histoplasma* yeasts within the phagosome catabolize amino acids derived from the host which are then processed through gluconeogenic pathways to supply carbohydrates for biomass (**Figure 1**). Further investigations will be needed to define which amino acids are available within the phagosome and which are catabolized by the intracellular yeasts.

INTRAPHAGOSOMAL NITROGEN AND SULFUR

One of the advantages of amino acid catabolism within the phagosome is that amino acids provide yeasts not only carbon, but also a source of nitrogen and potentially sulfur. Consistent with amino acids providing nitrogen to intracellular yeasts, *Paracoccidioides* yeasts recovered from macrophages have increased abundance of various aminotransferases (Parente-Rocha et al., 2015). However, in *Paracoccidioides* yeasts from lung infections, a branched-chain amino acid aminotransferase is down-regulated again showing inconsistencies between the lung and the macrophage models. The transcriptome of yeasts from lungs showed increased expression of amino acid permeases and peptide transporters (Lacerda Pigosso et al., 2017) consistent with yeasts importing host amino acids and peptides during infection. Differential gene expression analysis of *Histoplasma* yeasts compared to mycelia also show three genes encoding aminotransferases are up-regulated in yeasts (Edwards et al., 2013). Interestingly, studies of *Paracoccidioides* yeasts consistently highlight formamidase as one of the most up-regulated genes or proteins increased in expression during infection of mice or cultured macrophages (Parente-Rocha et al., 2015; Lacerda Pigosso et al., 2017). This suggests formamidase is a central step in nitrogen acquisition and metabolism for *Paracoccidioides* yeast during infection. Alternatively, formamidase may be particularly repressed in the conditions used for *in vitro* growth used as comparison. While the *in vivo* substrate(s) for formamidase is/are unknown (e.g., formamide), arylformamidases are involved in tryptophan degradation which may signal utilization of tryptophan during infection.

Cysteine and methionine represent sulfur-containing amino acids that can provide organic sulfur to fungal pathogens. Changes in cysteine metabolism during transitions between *Histoplasma* yeast and mycelial phases are well-known (Stetler and Boguslawski, 1979; Maresca et al., 1981). Despite a pathway for inorganic sulfur assimilation (e.g., sulfate) that is operative in *Histoplasma* mycelia, *Histoplasma* yeasts require an organic sulfur source which can be supplied by cysteine (Salvin, 1949). Comparison of *Histoplasma* yeast and mycelial transcriptomes showed increased expression of a permease for methionine and cysteine (Hwang et al., 2003), suggesting the pathogenic yeast state is primed to uptake exogenous sulfur-containing amino acids. Despite the auxotrophy of *Histoplasma* yeasts for organic sulfur, *Histoplasma* is fully virulent indicating that organic sulfur is available to *Histoplasma* yeasts within the phagosome. While the ultimate source of organic sulfur for intracellular fungal growth remains unknown, cysteine is a logical candidate, which may be derived from protein degradation or even hydrolysis of abundant glutathione in the macrophage.

ACQUISITION OF MICRONUTRIENTS

Essential Vitamins

While required in smaller quantities than carbon or nitrogen, vitamins are essential micronutrients for growth. This nutritional requirement can be met either by vitamin acquisition from the host or through *de novo* synthesis by fungal cells. Biosynthesis of vitamins by *Paracoccidioides* and *Histoplasma* appears to be the primary source for these essential co-factors. *Paracoccidioides* yeasts infecting the murine lung up-regulate the gene involved in thiamine biosynthesis (*THI13*), suggesting that thiamine from the host is not available to yeasts during infection (Lacerda Pigosso et al., 2017). Parente-Rocha et al. (2015) similarly found that *Paracoccidioides* yeasts within macrophages have increased expression of enzymes involved in the synthesis of thiamine as well as pyridoxine and riboflavin. Although increased expression of these enzymes suggests yeasts synthesize vitamins from simpler metabolic intermediates during infection, expression was measured relative to yeast growth *in vitro* in a vitamin-rich medium. More direct evidence for the lack of vitamins within the macrophage host comes from functional studies in *Histoplasma*. A forward genetics screen for mutants unable to proliferate within macrophages isolated a mutant with a disruption of the *RIB2* gene, which encodes a deaminase catalyzing the third step of riboflavin biosynthesis (Garfoot et al., 2014). While *Histoplasma* yeast lacking Rib2 function could infect macrophages, they were severely attenuated for growth in macrophages as well as attenuated in lung infection. This indicates that *Histoplasma* cannot acquire sufficient exogenous riboflavin from the phagosomal environment to support its intracellular growth. In addition, depletion of the pantothenate biosynthesis enzyme, Pan6, impaired *Histoplasma* virulence in mice indicating that pantothenate is also scarce in the phagosomal environment (Garfoot et al., 2014). On the other hand, depletion of biotin biosynthesis did not affect *Histoplasma* virulence. Although this may suggest that host biotin can be scavenged within the phagosome, it is also possible that the *Histoplasma* yeast had stored sufficient biotin from the pre-growth. In support of this, depletion of biotin synthase (Bio2) did not impair growth *in vitro* until yeasts were passaged multiple times in biotin-deficient media. Thus, the macrophage phagosome compartment in general lacks essential vitamins thereby forcing intracellular yeasts to rely on *de novo* synthesis to meet this nutritional requirement.

Trace Metals

In addition to vitamin co-factors, trace metals are essential for yeast growth and are variably available within the phagosome depending on the activation state of macrophages. Iron

acquisition is essential for *Histoplasma* and *Paracoccidioides* virulence. Attenuation of *Paracoccidioides* and *Histoplasma* yeast growth in macrophages by chloroquine, which impairs phagosome acidification and availability of iron, is reversed by supplementation with exogenous iron (Newman et al., 1994; Dias-Melicio et al., 2006). In addition, supplementation of exogenous iron exacerbated *Paracoccidioides* infection in mice (Parente et al., 2011). Iron restriction of *Paracoccidioides* yeasts *in vitro* induces genes encoding enzymes involved in siderophore biosynthesis and transport (Parente et al., 2011; Silva-Bailão et al., 2014). However, induction of siderophore biosynthesis and transport was not observed in *Paracoccidioides* yeasts isolated from murine macrophages or *in vivo*. Among different iron acquisition mechanisms, *Histoplasma* yeasts secrete siderophores for scavenging rare iron (Hwang et al., 2008; Hilty et al., 2011). Genes encoding siderophore synthesis enzymes are located in a genetic cluster which is activated under low iron conditions through the action of Sre1, a GATA-family transcription factor (Hwang et al., 2008). Loss of siderophore biosynthesis impairs intracellular *Histoplasma* growth indicating the phagosome is a low iron compartment. However, studies of *Histoplasma* infection of mice indicate that siderophores are not required for proliferation of *Histoplasma* pathogenesis until 2-weeks post-infection which coincides with the adaptive immunity stage (Hwang et al., 2008). These results indicate that during early infection, sufficient iron is found within the macrophage phagosome, but after activation of host cells, iron becomes limiting for fungal growth.

Similar to iron, zinc levels in the phagosome can change depending on the activation state of macrophages. Initially, zinc is available for intracellular *Histoplasma* yeast growth, but becomes limiting as macrophages are activated by the GM-CSF cytokine to produce zinc-sequestering metallothioneines (Subramanian Vignesh et al., 2013). *Histoplasma* yeasts produce the Zrt2 zinc transporter to acquire zinc from the environment and this transporter is required for *Histoplasma* virulence in mice, but only after 3 days of infection (Dade et al., 2016). These data indicate that host macrophages can use restriction of trace metals from the phagosome to combat intracellular proliferation of yeasts, particularly after macrophage activation.

Host macrophages can use both abundance and restriction of available copper to curtail intracellular pathogen growth. Tavares et al. (2007) found that *Paracoccidioides* yeasts down-regulate a high-affinity copper transporter by 17-fold within cultured macrophages after 6 h, suggesting that the *Paracoccidioides*-containing phagosome has sufficient copper to support *Paracoccidioides* growth. This same down-regulation of the copper transporter was also observed during lung infection of mice at 6 h (Lacerda Pigosso et al., 2017) suggesting the lung environment has ample copper during early infection. The *Histoplasma* genome encodes a homologous copper transporter (Ctr3) whose transcription is induced at low copper concentrations (< 150 nM) (Shen et al., 2018). Through use of a transcriptional fusion of the copper-repressible *CTR3* promoter with a fluorescent protein, available copper levels within the *Histoplasma*-containing phagosome could be estimated. In resting macrophages, including alveolar macrophages which *Histoplasma* cells initially encounter during infection, phagosomal copper levels are roughly 300 nM. At this concentration, *Histoplasma* yeasts can acquire sufficient copper without needing the Ctr3 transporter. Upon activation of macrophages with IFN-γ, the available copper in the phagosome significantly decreases resulting in up-regulation of the Ctr3 transporter (Shen et al., 2018). Consistent with the phagosomal copper levels inferred from transcription studies, the Ctr3 transporter is not required for *Histoplasma* proliferation within resting macrophages (i.e., higher phagosomal copper levels) but becomes necessary following macrophage activation as phagosomal copper becomes restricted (**Figure 2**; Shen et al., 2018). These results indicate that copper availability in the macrophage phagosome, as well as that of iron and zinc, is dynamic and that activation of macrophages imposes a metal restriction strategy to impair the intracellular proliferation of yeasts.

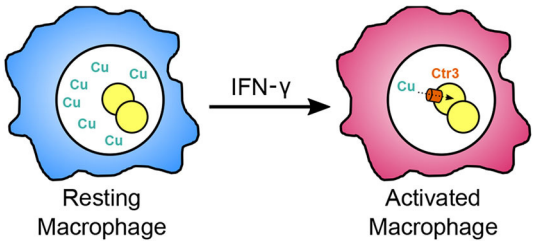

FIGURE 2 | Restriction of available copper within the phagosome following macrophage activation. During initial infection, *Histoplasma* infects resting macrophages (blue), and resides within a phagosomal compartment with sufficiently available copper (green Cu) for fungal proliferation without requiring the high affinity copper transporter Ctr3. Upon activation of macrophages by IFN-γ during adaptive immunity (magenta), copper in the phagosome becomes restricted forcing *Histoplasma* yeast to rely on Ctr3 to import copper.

CONCLUSION

Initial studies on fungal pathogens often focused on virulence mechanisms for host cell infection and survival. The studies highlighted above indicate that mechanisms of fungal metabolism are an integral component of intracellular fungal pathogenesis. While *in vitro* culture of fungi has typically used glucose- and peptone-rich media, the study of long-term phagosomal residents like *Histoplasma* and *Paracoccidioides* yeasts is revealing that alternate substrates, not hexoses, are available within the phagosome compartment. Furthermore, these dimorphic fungi have tuned their metabolism to exploit these resources during yeast infection of host cells. Consequently, media used for *in vitro* propagation of the yeasts should be re-evaluated for their physiological relevance to the nutritional conditions actually experienced by the yeast cells. The more-specialized metabolism used by yeasts within the phagosome creates opportunities for anti-fungal interventions. The finding that some micronutrient levels in the phagosome can change following macrophage activation and subsequent control of intracellular fungal proliferation further underscores the

potential of targeting metabolic pathways for therapeutic control of these primary pathogens.

AUTHOR CONTRIBUTIONS

QS and CR conceived of the review topic, performed the literature analysis, and composed the review article. All authors contributed to the article and approved the submitted version.

FUNDING

Research by QS and CR was supported by the National Institute of Allergy and Infectious Diseases of the National Institutes of Health under award numbers R21-AI137714 and R01-AI148561. The content is solely the responsibility of the authors and does not necessarily represent the official views of the National Institutes of Health.

REFERENCES

Allendoerfer, R., and Deepe, G. S. (1997). Intrapulmonary response to Histoplasma capsulatum in gamma interferon knockout mice. *Infect. Immun.* 65, 2564-2569.

Allendoerfer, R., and Deepe, G. S. (1998). Blockade of endogenous TNF-alpha exacerbates primary and secondary pulmonary histoplasmosis by differential mechanisms. *J. Immunol.* 160, 6072–6082.

Aristizabal, B. H., Clemons, K. V., Stevens, D. A., and Restrepo, A. (1998). Morphological transition of *Paracoccidioides brasiliensis* conidia to yeast cells: *in vivo* inhibition in females. *Infect. Immun.* 66, 5587–5591. doi: 10.1128/IAI.66.11.5587-5591.1998

Bailão, A. M., Schrank, A., Borges, C. L., Dutra, V., Walquíria Inês Molinari-Madlum, E. E., Soares Felipe, M. S., et al. (2006). Differential gene expression by *Paracoccidioides brasiliensis* in host interaction conditions: representational difference analysis identifies candidate genes associated with fungal pathogenesis. *Microbes Infect.* 8, 2686–2697. doi: 10.1016/j.micinf.2006.07.019

Beyhan, S., and Sil, A. (2019). Sensing the heat and the host: virulence determinants of *Histoplasma capsulatum*. *Virulence* 10, 793–800. doi: 10.1080/21505594.2019.1663596

Borges-Walmsley, M. I., Chen, D., Shu, X., and Walmsley, A. R. (2002). The pathobiology of *Paracoccidioides brasiliensis*. *Trends Microbiol.* 10, 80–87. doi: 10.1016/S0966-842X(01)02292-2

Calich, V. L. G., da Costa, T. A., Felonato, M., Arruda, C., Bernardino, S., Loures, F. V., et al. (2008). Innate immunity to *Paracoccidioides brasiliensis* infection. *Mycopathologia* 165, 223–236. doi: 10.1007/s11046-007-9048-1

da Silva, T. A., Roque-Barreira, M. C., Casadevall, A., and Almeida, F. (2016). Extracellular vesicles from *Paracoccidioides brasiliensis* induced M1 polarization *in vitro*. *Sci Rep* 6:35867. doi: 10.1038/srep35867

Dade, J., DuBois, J. C., Pasula, R., Donnell, A. M., Caruso, J. A., Smulian, A. G., et al. (2016). HcZrt2, a zinc responsive gene, is indispensable for the survival of *Histoplasma capsulatum in vivo*. *Med. Mycol.* 54, 865–875. doi: 10.1093/mmy/myw045

de Castro, L. F., Ferreira, M. C., da Silva, R. M., Blotta, M. H., Longhi, L. N., and Mamoni, R. L. (2013). Characterization of the immune response in human paracoccidioidomycosis. *J. Infect.* 67, 470–485. doi: 10.1016/j.jinf.2013.07.019

Deepe, G. S., Gibbons, R. S., and Smulian, A. G. (2008). *Histoplasma capsulatum* manifests preferential invasion of phagocytic subpopulations in murine lungs. *J. Leukoc. Biol.* 84, 669–678. doi: 10.1189/jlb.0308154

Derengowski, L. S., Tavares, A. H., Silva, S., Procópio, L. S., Felipe, M. S. S., and Silva-Pereira, I. (2008). Upregulation of glyoxylate cycle genes upon *Paracoccidioides brasiliensis* internalization by murine macrophages and *in vitro* nutritional stress condition. *Med. Mycol.* 46, 125–134. doi: 10.1080/13693780701670509

Dias-Melicio, L. A., Moreira, A. P., Calvi, S. A., and Soares, A. M. V. (2006). Chloroquine inhibits *Paracoccidioides brasiliensis* survival within human monocytes by limiting the availability of intracellular iron. *Microbiol. Immunol.* 50, 307–314. doi: 10.1111/j.1348-0421.2006.tb03798.x

Edwards, J. A., Chen, C., Kemski, M. M., Hu, J., Mitchell, T. K., and Rappleye, C. A. (2013). *Histoplasma* yeast and mycelial transcriptomes reveal pathogenic-phase and lineage-specific gene expression profiles. *BMC Genomics* 14:695. doi: 10.1186/1471-2164-14-695

Fan, W., Kraus, P. R., Boily, M. J., and Heitman, J. (2005). *Cryptococcus neoformans* gene expression during murine macrophage infection. *Eukaryotic Cell* 4, 1420–1433. doi: 10.1128/EC.4.8.1420-1433.2005

Garfoot, A. L., Shen, Q., Wüthrich, M., Klein, B. S., and Rappleye, C. A. (2016). The Eng1 β-glucanase enhances *Histoplasma* virulence by reducing β-Glucan exposure. *mBio* 7, e01388–e01315. doi: 10.1128/mBio.01388-15

Garfoot, A. L., Zemska, O., and Rappleye, C. A. (2014). *Histoplasma capsulatum* depends on *de novo* vitamin biosynthesis for intraphagosomal proliferation. *Infect. Immun.* 82, 393–404. doi: 10.1128/IAI.00824-13

Hilty, J., George Smulian, A., and Newman, S. L. (2011). *Histoplasma capsulatum* utilizes siderophores for intracellular iron acquisition in macrophages. *Med. Mycol.* 49, 633–642. doi: 10.3109/13693786.2011.558930

Holbrook, E. D., Smolnycki, K. A., Youseff, B. H., and Rappleye, C. A. (2013). Redundant catalases detoxify phagocyte reactive oxygen and facilitate *Histoplasma capsulatum* pathogenesis. *Infect. Immun.* 81, 2334–2346. doi: 10.1128/IAI.00173-13

Hwang, L., Hocking-Murray, D., Bahrami, A. K., Andersson, M., Rine, J., and Sil, A. (2003). Identifying phase-specific genes in the fungal pathogen *Histoplasma capsulatum* using a genomic shotgun microarray. *Mol. Biol. Cell* 14, 2314–2326. doi: 10.1091/mbc.e03-01-0027

Hwang, L. H., Mayfield, J. A., Rine, J., and Sil, A. (2008). *Histoplasma* requires *SID1*, a member of an iron-regulated siderophore gene cluster, for host colonization. *PLoS Pathog.* 4:e1000044. doi: 10.1371/journal.ppat.1000044

Kanetsuna, F., Carbonell, L. M., Azuma, I., and Yamamura, Y. (1972). Biochemical studies on the thermal dimorphism of *Paracoccidioides brasiliensis*. *J. Bacteriol.* 110, 208–218. doi: 10.1128/JB.110.1.208-218.1972

Kauffman, C. A. (2009). Histoplasmosis. *Clin. Chest Med.* 30, 217–225. doi: 10.1016/j.ccm.2009.02.002

Kretschmer, M., Wang, J., and Kronstad, J. W. (2012). Peroxisomal and mitochondrial β-oxidation pathways influence the virulence of the pathogenic fungus *Cryptococcus neoformans*. *Eukaryotic Cell* 11, 1042–1054. doi: 10.1128/EC.00128-12

Lacerda Pigosso, L., Baeza, L. C., Vieira Tomazett, M., Batista Rodrigues Faleiro, M., Brianezi Dignani de Moura, V. M., Melo Bailão, A., et al. (2017). *Paracoccidioides brasiliensis* presents metabolic reprogramming and secretes a serine proteinase during murine infection. *Virulence* 8, 1417–1434. doi: 10.1080/21505594.2017.1355660

Lorenz, M. C., Bender, J. A., and Fink, G. R. (2004). Transcriptional response of *Candida albicans* upon internalization by macrophages. *Eukaryotic Cell* 3, 1076–1087. doi: 10.1128/EC.3.5.1076-1087.2004

Lorenz, M. C., and Fink, G. R. (2001). The glyoxylate cycle is required for fungal virulence. *Nature* 412, 83–86. doi: 10.1038/35083594

Maresca, B., and Kobayashi, G. S. (1989). Dimorphism in *Histoplasma capsulatum*: a model for the study of cell differentiation in pathogenic fungi. *Microbiol. Rev.* 53, 186–209. doi: 10.1128/MMBR.53.2.186-209.1989

Maresca, B., Lambowitz, A. M., Kumar, V. B., Grant, G. A., Kobayashi, G. S., and Medoff, G. (1981). Role of cysteine in regulating morphogenesis and mitochondrial activity in the dimorphic fungus *Histoplasma capsulatum*. *Proc. Natl. Acad. Sci. U.S.A.* 78, 4596–4600. doi: 10.1073/pnas.78.7.4596

Medoff, G., Kobayashi, G. S., Painter, A., and Travis, S. (1987). Morphogenesis and pathogenicity of *Histoplasma capsulatum*. *Infect. Immun.* 55, 1355–1358. doi: 10.1128/IAI.55.6.1355-1358.1987

Newman, S. L., Bucher, C., Rhodes, J., and Bullock, W. E. (1990). Phagocytosis of *Histoplasma capsulatum* yeasts and microconidia by human cultured macrophages and alveolar macrophages. Cellular cytoskeleton requirement for attachment and ingestion. *J. Clin. Invest.* 85, 223–230. doi: 10.1172/JCI114416

Newman, S. L., Gootee, L., Brunner, G., and Deepe, G. S. (1994). Chloroquine induces human macrophage killing of *Histoplasma capsulatum* by limiting

the availability of intracellular iron and is therapeutic in a murine model of histoplasmosis. *J. Clin. Invest.* 93, 1422–1429. doi: 10.1172/JCI117119

Parente, A. F. A., Bailão, A. M., Borges, C. L., Parente, J. A., Magalhães, A. D., Ricart, C. A. O., et al. (2011). Proteomic analysis reveals that iron availability alters the metabolic status of the pathogenic fungus *Paracoccidioides brasiliensis*. *PLoS ONE* 6:e22810. doi: 10.1371/journal.pone.0022810

Parente-Rocha, J. A., Parente, A. F. A., Baeza, L. C., Bonfim, S. M. R. C., Hernandez, O., McEwen, J. G., et al. (2015). Macrophage interaction with *Paracoccidioides brasiliensis* yeast cells modulates fungal metabolism and generates a response to oxidative stress. *PLoS ONE* 10:e0137619. doi: 10.1371/journal.pone.0137619

Queiroz-Telles, F., and Escuissato, D. L. (2011). Pulmonary paracoccidioidomycosis. *Semin. Respir. Crit. Care Med.* 32, 764–774. doi: 10.1055/s-0031-1295724

Rappleye, C. A., Eissenberg, L. G., and Goldman, W. E. (2007). *Histoplasma capsulatum* alpha-(1,3)-glucan blocks innate immune recognition by the beta-glucan receptor. *Proc. Natl. Acad. Sci. U.S.A.* 104, 1366–1370. doi: 10.1073/pnas.0609848104

Rappleye, C. A., Engle, J. T., and Goldman, W. E. (2004). RNA interference in *Histoplasma capsulatum* demonstrates a role for alpha-(1,3)-glucan in virulence. *Mol. Microbiol.* 53, 153–165. doi: 10.1111/j.1365-2958.2004.04131.x

Rodrigues-Vendramini, F. A. V., Marschalk, C., Toplak, M., Macheroux, P., Bonfim-Mendonça, P., Svidzinski, T. I. E., et al. (2019). Promising new antifungal treatment targeting chorismate synthase from *Paracoccidioides brasiliensis*. *Antimicrob. Agents Chemother.* 63, e01097–18. doi: 10.1128/AAC.01097-18

Salvin, S. B. (1949). Cysteine and related compounds in the growth of the yeast like phase of *Histoplasma capsulatum*. *J. Infect. Dis.* 84, 275–283. doi: 10.1093/infdis/84.3.275

Salzer, H. J. F., Burchard, G., Cornely, O. A., Lange, C., Rolling, T., Schmiedel, S., et al. (2018). Diagnosis and management of systemic endemic mycoses causing pulmonary disease. *Respiration* 96, 283–301. doi: 10.1159/000489501

San-Blas, G., San-Blas, F., and Serrano, L. E. (1977). Host-parasite relationships in the yeastlike form of *Paracoccidioides brasiliensis* strain IVIC Pb9. *Infect. Immun.* 15, 343–346. doi: 10.1128/IAI.15.2.343-346.1977

Shen, Q., Beucler, M. J., Ray, S. C., and Rappleye, C. A. (2018). Macrophage activation by IFN-γ triggers restriction of phagosomal copper from intracellular pathogens. *PLoS Pathog.* 14:e1007444. doi: 10.1371/journal.ppat.1007444

Shen, Q., and Rappleye, C. A. (2017). Differentiation of the fungus *Histoplasma capsulatum* into a pathogen of phagocytes. *Curr. Opin. Microbiol.* 40, 1–7. doi: 10.1016/j.mib.2017.10.003

Shen, Q., Ray, S. C., Evans, H. M., Deepe, G. S., and Rappleye, C. A. (2020). Metabolism of gluconeogenic substrates by an intracellular fungal pathogen circumvents nutritional limitations within macrophages. *mBio* 11, e02712–19. doi: 10.1128/mBio.02712-19

Silva-Bailão, M. G., Bailão, E. F. L. C., Lechner, B. E., Gauthier, G. M., Lindner, H., Bailão, A. M., et al. (2014). Hydroxamate production as a high affinity iron acquisition mechanism in *Paracoccidioides* spp. *PLoS ONE* 9:e105805. doi: 10.1371/journal.pone.0105805

Soares, D. A., de Andrade, R. V., Silva, S. S., Bocca, A. L., Soares Felipe, S. M., and Petrofeza, S. (2010). Extracellular *Paracoccidioides brasiliensis* phospholipase B involvement in alveolar macrophage interaction. *BMC Microbiol.* 10:241. doi: 10.1186/1471-2180-10-241

Souto, J. T., Figueiredo, F., Furlanetto, A., Pfeffer, K., Rossi, M. A., and Silva, J. S. (2000). Interferon-gamma and tumor necrosis factor-alpha determine resistance to *Paracoccidioides brasiliensis* infection in mice. *Am. J. Pathol.* 156, 1811–1820. doi: 10.1016/S0002-9440(10)65053-5

Stetler, D. A., and Boguslawski, G. (1979). Cysteine biosynthesis in a fungus, *Histoplasma capsulatum*. *Sabouraudia* 17, 23–34. doi: 10.1080/00362177985380041

Subramanian Vignesh, K., Landero Figueroa, J. A., Porollo, A., Caruso, J. A., and Deepe, G. S. (2013). Granulocyte macrophage-colony stimulating factor induced Zn sequestration enhances macrophage superoxide and limits intracellular pathogen survival. *Immunity* 39, 697–710. doi: 10.1016/j.immuni.2013.09.006

Tavares, A. H. F. P., Silva, S. S., Dantas, A., Campos, E. G., Andrade, R. V., Maranhão, A. Q., et al. (2007). Early transcriptional response of *Paracoccidioides brasiliensis* upon internalization by murine macrophages. *Microbes Infect.* 9, 583–590. doi: 10.1016/j.micinf.2007.01.024

Tristão, F. S. M., Rocha, F. A., Carlos, D., Ketelut-Carneiro, N., Souza, C. O. S., Milanezi, C. M., et al. (2017). Th17-inducing cytokines IL-6 and IL-23 are crucial for granuloma formation during experimental paracoccidioidomycosis. *Front. Immunol.* 8:949. doi: 10.3389/fimmu.2017.00949

Van Dyke, M. C. C., Teixeira, M. M., and Barker, B. M. (2019). Fantastic yeasts and where to find them: the hidden diversity of dimorphic fungal pathogens. *Curr. Opin. Microbiol.* 52, 55–63. doi: 10.1016/j.mib.2019.05.002

Youseff, B. H., Holbrook, E. D., Smolnycki, K. A., and Rappleye, C. A. (2012). Extracellular superoxide dismutase protects *Histoplasma* yeast cells from host-derived oxidative stress. *PLoS Pathog.* 8:e1002713. doi: 10.1371/journal.ppat.1002713

Conflict of Interest: The authors declare that the research was conducted in the absence of any commercial or financial relationships that could be construed as a potential conflict of interest.

frontiers in Cellular and Infection Microbiology

REVIEW
published: 20 October 2020
doi: 10.3389/fcimb.2020.591970

Intracellular PRRs Activation in Targeting the Immune Response Against Fungal Infections

Grasielle Pereira Jannuzzi[1]*, *José Roberto Fogaça de Almeida*[1], *Larissa Neves Monteiro Paulo*[1], *Sandro Rogério de Almeida*[1] and *Karen Spadari Ferreira*[2]*

[1] Departamento de Análises Clínicas, Faculdade de Ciências Farmacêuticas da Universidade de São Paulo, São Paulo, Brazil, [2] Departamento de Ciências Biológicas do Instituto de Ciências Ambientais, Químicas e Farmacêuticas, Universidade Federal de São Paulo, Diadema, Brazil

The immune response against fungal infections is complex and exhibits several factors involving innate elements that participate in the interaction with the fungus. The innate immune system developed pattern recognition receptors that recognize different pathogen-associated molecular patterns present both on the surface of the fungi cell wall and on their genetic material. These receptors have the function of activating the innate immune response and regulating a subsequent adaptive immune response. Among pattern recognition receptors, the family of Toll-like receptors and C-type lectin receptors are the best described and characterized, they act directly in the recognition of pathogen-associated molecular patterns expressed on the wall of the fungus and consequently in directing the immune response. In recent years, the role of intracellular pattern recognition receptors (TLR3, TLR7, TLR8, and TLR9) has become increasingly important in the pathophysiology of some mycoses, as paracoccidioidomycosis, cryptococcosis, aspergillosis, and candidiasis. The recognition of nucleic acids performed by these receptors can be essential for the control of some fungal infections, as they can be harmful to others. Therefore, this review focuses on highlighting the role played by intracellular pattern recognition receptors both in controlling the infection and in the host's susceptibility against the main fungi of medical relevance.

Keywords: fungal infection, intracellular receptors, PRRs, innate immune response, nucleic acids

OPEN ACCESS

Edited by:
Carlos Pelleschi Taborda, University of São Paulo, Brazil

Reviewed by:
Toshiyuki Shimizu, The University of Tokyo, Japan
Lysangela Ronalte Alves, Carlos Chagas Institute (ICC), Brazil

***Correspondence:**
Grasielle Pereira Jannuzzi
grasi_jannuzzi@hotmail.com
Karen Spadari Ferreira
karenspadari@gmail.com

Specialty section:
This article was submitted to Fungal Pathogenesis, a section of the journal Frontiers in Cellular and Infection Microbiology

Received: *05 August 2020*
Accepted: *04 September 2020*
Published: *20 October 2020*

Citation:
Jannuzzi GP, de Almeida JRF, Paulo LNM, de Almeida SR and Ferreira KS (2020) Intracellular PRRs Activation in Targeting the Immune Response Against Fungal Infections. Front. Cell. Infect. Microbiol. 10:591970. doi: 10.3389/fcimb.2020.591970

INTRODUCTION

Fungi are eukaryotic cells with composition predominantly of carbohydrate polymers interspersed with glycoproteins and complex morphogenesis. Some fungal species have the capacity to present different forms depending on the temperature in which they are, in other words, they exhibit thermal dimorphism, which can facilitate the evasion of the immune response and dissemination in the host.

Depending on the morphotype, conidia or yeast, growth stage and of the species, the fungus can express different molecular patterns associated with pathogens (PAMPs) on the surface, which will be recognized by the cells of the immune system (Bowman and Free, 2006; Levitz, 2010; Romani, 2011; Gow and Hube, 2012; Gow et al., 2012).

The major fungi of medical relevance exhibit a wall composed mainly of β-glucans, chitins and mannans. β-glucans are glucose polymers, where in the β-(1,3)-glucan form is considered

to be its major fungal cell wall structure and has varying numbers of β-(1,6)-glucans, chitin is an *N*-acetylglucosamine polymer, and mannans is composed of chains with hundreds of mannose molecules that are added in the fungi proteins via *N* or *O*-linkages (Bowman and Free, 2006; Wheeler and Fink, 2006; Romani, 2011).

In addition to the fungal cell wall components, nucleic acids (NAs) are also considered to be true PAMPs capable of inducing strong stimuli to initiate a potent immune response (Bacci et al., 2002; Yordanov et al., 2005; Ramirez-Ortiz et al., 2008; Eberle et al., 2009; Freund et al., 2019). Pathogen derived NAs are recognized differently from self NAs, leading into account some types of parameters, such as location, sequence, structure, and molecular modifications. On the other hand, self NAs such as extranuclear DNA or extracellular RNA can be recognized as DAMPs because they are reliable indicators of cell damage (Pichlmair and Reis e Sousa, 2007; Chen and Nunez, 2010; Takeuchi and Akira, 2010; Barbalat et al., 2011).

The innate immune response uses its mechanisms quickly and conserved in response to a wide variety of fungal pathogens. Thus, the innate immune system developed receptors called pattern recognition receptors (PRRs), which are responsible for recognizing both PAMPs located on the surface of pathogens, and NAs that are located intracellularly.

The most well-characterized PRRs involved in sensing and recognition of fungal comprise 5 families, toll-like receptors (TLRs), C-type lectin-like receptors (CLRs), NOD-like receptors (NLR), galectins family proteins (Galectin-3), and scavenger receptors (such as CD5 and CD36) (Yoneyama et al., 2004; van de Veerdonk et al., 2008; Jouault et al., 2009; Bourgeois et al., 2010; Romani, 2011; Plato et al., 2015). Each of these receptors recognizes different PAMPs present on the fungal cell wall surface as well as its genetic material (**Table 1**).

The PRRs differ in signal transduction after the recognition of the fungal antigen and in its subcellular location. After the recognition of their respectives ligands, these receptors initiate the activation of the innate and adaptive immune response in order to induce a protective response against the fungus (Perruccio et al., 2005; Plato et al., 2015), but this is not always possible.

Among the PRRs, intracellular TLRs play an important role in the recognition of NAs from fungi and has been showing a potential activator of the immune response, which can mediate a protective response for the host or favor the escape of the fungus, with consequent dissemination and worsening of the disease (Carvalho et al., 2012; Menino et al., 2013; Jannuzzi et al., 2019). In addition to the pathophysiological context, the activation of intracellular TLR has been used as a promising technique for the treatment of some fungal infections (de Sousa et al., 2014; Morais et al., 2016; Freund et al., 2019). Thus, in this review, we will discuss the role of receptors involved in the recognition of fungal NAs, their location, signaling and the role played in the host's immune response.

ENDOSOMAL TLRs INVOLVED IN THE RECOGNITION OF FUNGAL NAs

The presence of TLRs in host defense has been described for several fungal pathogens such as *Candida albicans* (*C. albicans*) (Netea et al., 2002, 2006), *Aspergillus fumigatus* (*A. fumigatus*) (Meier et al., 2003; Dubourdeau et al., 2006), *Cryptococcus neoformans* (*C. neoformans*) (Yauch et al., 2004; Biondo et al., 2005), *Fonsecaea pedrosoi* (*F. pedrosoi*) (Sousa et al., 2011) and *Paracoccidioides brasiliensis* (*P. brasiliensis*) (Ferreira et al., 2007; Loures et al., 2015; Jannuzzi et al., 2019). These receptors act as a molecular button to trigger the activation of innate immunity and regulate a subsequent adaptive immune response, essential in the control of infections (Kawai and Akira, 2011).

TLRs are a family of receptors that comprise up to now 12 functional proteins identified in mice and 10 in humans, TLR1-9/TLR11-13, and TLR1-10, respectively (Akira et al., 2006; Medzhitov, 2007), of which TLR3, TLR7, TLR8, and TLR9 are found intracellularly, and recognize NAs derived from pathogens uptake by endocytosis or derivatives of autophagy and transferred to the endolysosomal compartment (Blasius and Beutler, 2010; Barbalat et al., 2011; Lee et al., 2012; Schuberth-Wagner et al., 2015).

Endosomal TLRs are synthesized in the endoplasmic reticulum and subsequently transported to Endosome or Lysosome with the help of the uncoordinated 93 homolog B1 (UNC93B1), which in addition to performing the transport it also cooperates with the expression and stabilization of the endosomal TLRs (Lee and Barton, 2014; Pelka et al., 2018). TLRs can be located in both endosomes and lysosomes, performing monitoring of endolysosomal contents or detecting NAs in the cytoplasm (Kawai and Akira, 2006; Barbalat et al., 2011) (**Figure 1**).

Intracellular TLRs recognize the different types of NAs liberated from fungi within the phagosome can stimulate or modulate the host response during infection. TLR3 recognizes double-stranded RNA (dsRNA) without requiring specific sequences, however, a minimum length of 40 base pairs is required for binding and hence induction of TLR3 responsiveness. TLR3 is activated by dsRNA from *A. fumigatus* conidia, yeast *C. albicans*, yeast *P. brasiliensis*, among others which will be discussed later (Bourgeois et al., 2011; Beisswenger et al., 2012; Carvalho et al., 2012; Jannuzzi et al., 2019). This receptor also recognizes polyinosine-polycytidylic acid [poly (I: C)] synthetic synthetic RNA (Alexopoulou et al., 2001; Liu et al., 2008).

Both TLR7 and TLR8 recognize single-stranded RNA (ssRNA), however this recognition exhibits distinction sequences motifs in ssRNA. While TLR7 recognizes GU-rich sequences (e.g., UUGU, GUUC), TLR8 requires AU-rich sequences (e.g., AUUU, UAUC) (Vollmer et al., 2005; Forsbach et al., 2008). TLR7 is involved in the recognition of ssRNA from *Candida spp* and *F. pedrosoi* (Bourgeois et al., 2011; Sousa et al., 2011).

TLR9 recognizes nomethylated cytosine-guanosine (CpG) motifs in DNA (Hemmi et al., 2000). CpG motifs were first described in bacterial DNA, evidencing their immunostimulatory

TABLE 1 | List of PRRs, their ligands, and respective fungi.

Receptor	Ligand	Most fungal species
TLR1/2	Triacylated lipoprotein	*A. fumigatus, C. albicans*
	GXM	*C. neoformans*
TLR2	Phospholipomannan	*C. albicans*
	β-1,2-oligomannoside	*C. albicans, S. schenkii, S. brasiliensis, P. brasiliensis*
TLR2/6	Diacylated lipoprotein	*A. fumigatus, C. albicans*
	GXM	*C. neoformans*
TLR3	dsRNA	*A. fumigatus, P. brasiliensis, C. neoformans*
TLR4	*O*-linked mannosyl, mannan	*C. albicans, S. serevisiae, S. brasiliensis, P. brasiliensis*
	GXM	*C. neoformans*
TLR7	ssRNA	*C. albicans*
TLR8	ssRNA	*C. albicans*
TLR9	DNA	*A. fumigatus, C. neoformans, Candida, P. brasiliensis, M. furfur*
Dectin-1	β-1,3-glucans	*A. fumigatus, C. albicans, P. carinii, S. schenckii, F. pedrosoi, C. neoformans, P. brasiliensis, H. capsulatum, Malassezia spp, S. cerevisiae, C. posadasii, T. mentagrophytes, F. solani, C. cladosporioides*
Dectin-2	High-mannose structures α-mannans	*C. albicans, C. glabrata C. neoformans, T. rubrum, Malassezia spp, H. capsulatum, F. pedrosoi, A. fumigatus* and *M. audouini*
Dectin-3	GXM	*C. neoformans serotype AD (C.n-AD)* and *C. gattii serotype B*
	α-mannans	*C. albicans*
Mannose receptor	α-glucans	*P. brasiliensis, C. yeast, C. neoformans Histoplama capsulatum, Blastomyces dermatitidis*
	Chitin	*Candida yeast, C. neoformans*
	Mananas	*A. fumigatus, S. cerevisiae, P. carinii, C. neoformans, P. brasiliensis, C. albicans, C. parapsilosis,* and *S. schenckii*
DC-SIGN	*N*-linked mannans	*Dermatophytes, A. fumigatus, S. cerevisiae, C. neoformans, C. albicans,* and *C. topicum*
	Galactomannans	*A. fumigatus*
MINCLE	a-mannose, glyceroglycolipid	*A. fumigatus, Malassezia spp., F. pedrosoi, P. carinii,* and *C. albicans*
	mannosyl fatty acids	*Malassezia spp P. carinii*
	MSG/gpA	*P. carinii*
Langerin	β-1,3-glucans	*M. furfur, S. cerevisia, C. albicans, C. glabrata, C. krusei, C. parapsilosis,* and *C. tropicalis*
Galectin-3	a-mannosides	*C. albicans*

GXM, Glucuronoxylomannan; dsRNA, Double-stranded RNA; ssRNA, Single-stranded RNA; MSG/gpA, glycoprotein of P. carinii.

capacity, however, it is now known that the recognition of these motifs is also related to many viruses and fungi (Hemmi et al., 2000; Souza et al., 2001; Barton, 2007). Among the studied fungal infections, TLR9 activation was related to DNA from *A. fumigattus*, *C. albicans*, *P. brasiliensis*, *S. cerevise*, *M. furfur*, and *C. neoformans* (Nakamura et al., 2008; Ramirez-Ortiz et al., 2008; Kasperkovitz et al., 2010, 2011; Menino et al., 2013).

ENDOSOMAL TLR-MEDIATED SIGNALING

After the recognition of NAs, a signaling cascade begins that will produce pro-inflammatory cytokines that are important for the recruitment and activation of immune cells (Kawai and Akira, 2010).

The recognition of endosomal TLRs by their ligands will induce the recruitment of different adapter proteins at the beginning of signaling. TLR7, 8, and 9 will recruit the adapter protein Myeloid differentiation primary response 88 (MYD88), which will activate the TNF receptor associated factor 6 (TRAF6) protein. TRAF6 can activate 3 distinct pathways, in which activating kappa-B kinase subunit alpha (IKKα) will induce the activation of interferon regulatory factor 7 (IRF7), which will be translocated to the nucleus inducing the production of Type I Interferons (type I IFN). If TRAF6 activates the IKKs it will generate the activation of the nuclear factor κB (NF-kB), which will be transcribed in the nucleus and induce the production of pro-inflammatory cytokines and chemokines. However, if TRAF6 activates mitogen-activated protein kinases (MAPKs), transcription of activator protein 1 (AP1) will occur, which will also result in the production of pro-inflammatory cytokines and chemokines. TLR3, on the other hand, recruits the adapter protein TIR-domain-containing adapter-inducing interferon-β (TRIF), which will activate the TRAF3 protein that can activate 2 different pathways, one that will have IKKε/IRAK activation and subsequent activation of IRF7, which will be transcribed in the nucleus and culminate in the production of type I IFN. The

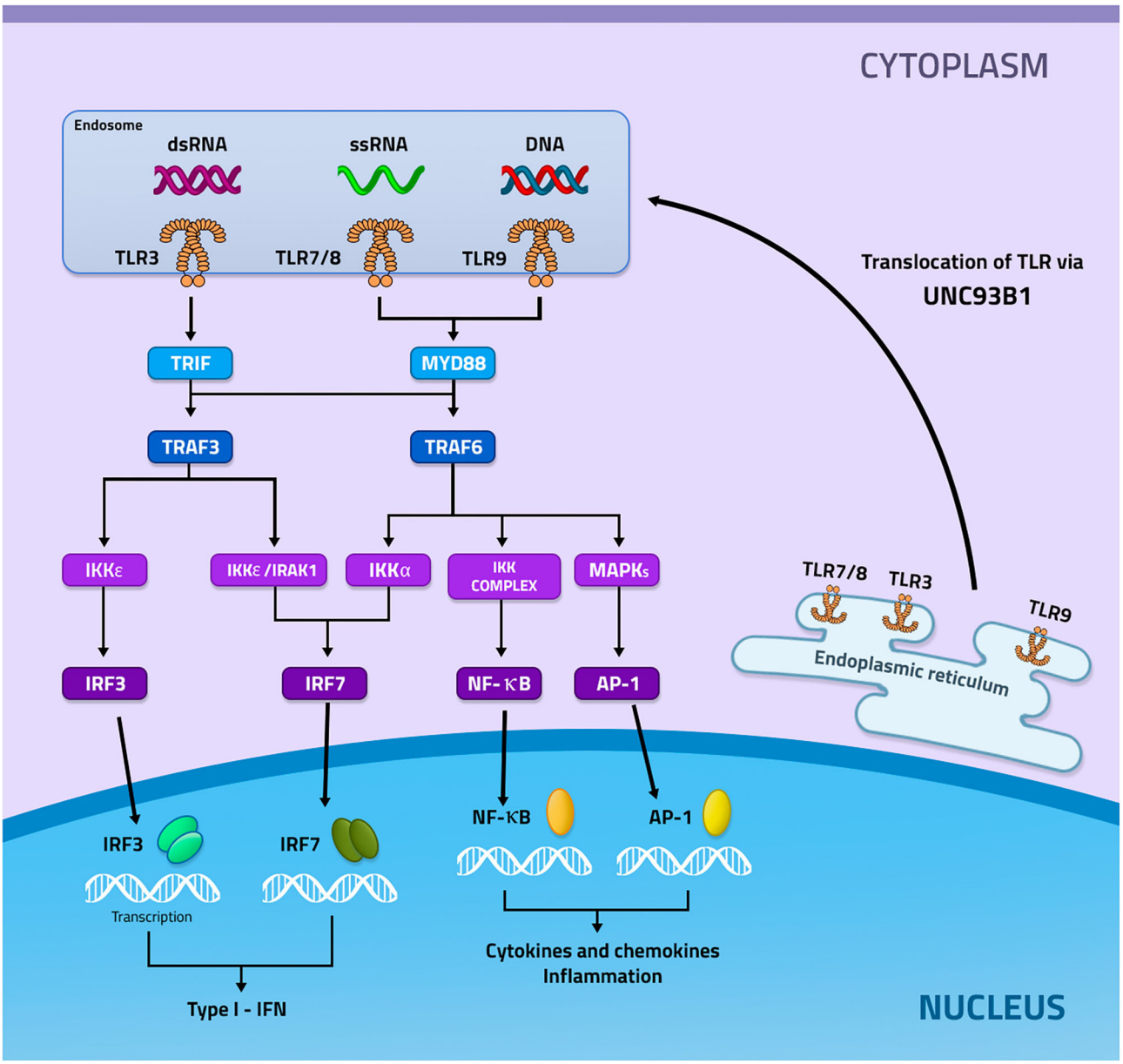

FIGURE 1 | Signaling mediated by the activation of TLR3, 7 and 9. TLRs 3, 7, and 9 are recruited from the endoplasmic reticulum through the UNC93b1 protein to the endosome. In the endosome these receptors will recognize their specific ligands, in which TLR3 recognizes dsRNA, while TLR7 ssRNA, and TLR9 DNA. Then each of these receivers, now activated, will start different signaling pathways. TLR3 recruits TRIF with subsequent activation of TRAF3. TRAF3 can activate two ways, the first IKKε will be activated and induce the activation of IRF3, while the second will occur activation of IKKε/IRAK1 which will result in the activation of IRF7. TLR7 and TLR9 recruit MYD88 which will result in the activation of TRAF6. TRAF6 may induce 3 different signals, the first will occur the activation of IRF7 through Ikka, the second will occur the activation of the IKKs complex that will induce the activation of NF-κB and the last will occur the activation of MAPKs that will mediate the activation of AP−1. IRF3 and IF7 will be transcribed in the nucleus inducing the production of type I IFN, whereas NF- κB and AP-1 will be transcribed and will mediate the production of inflammatory cytokines and chemokines.

other pathway will have IKKε/TBK1 activation which will induce the activation of IRF3, which will be transcribed in the nucleus and will also result in the production of type I IFN (**Figure 1**) (Fitzgerald et al., 2003; Meylan et al., 2004; Conze et al., 2008; Kawai and Akira, 2010; Lee et al., 2012; Yamashita et al., 2012; Gay et al., 2014).

EXPRESSION OF INTRACELLULAR TLRs IN CELLS OF THE IMMUNE SYSTEM

Intracellular TLRs are expressed mainly in phagocytes cells, TLR3 is expressed in myeloid dendritic cells, macrophages, epithelial cells, endothelial cells, and fibroblasts. Among the DC subtypes,

TLR3 is highly expressed in conventional DCs ($CD8\alpha^+$) from mice and human DCs ($CD141^+$), while plasmacytoid DCs express TLR7 and TLR9, but not TLR3 (Matsumoto and Seya, 2008; Beisswenger et al., 2012; Carvalho et al., 2012; Jannuzzi et al., 2019). Both TLR7 and TLR9 are expressed in monocytes, macrophages, DCs, and B lymphocytes (Ramirez-Ortiz et al., 2008; Mancuso et al., 2009; Biondo et al., 2011, 2012; Bourgeois et al., 2011; Kasperkovitz et al., 2011). TLR9 is also activated in neutrophils (Bellocchio et al., 2004), while TLR8 is expressed in all myeloid cells (Bellocchio et al., 2004; Ganguly et al., 2009).

PARTICIPATION OF INTRACELLULAR TLRs IN FUNGAL INFECTIONS

In this section, we will discuss the role of TLR3, TLR7, and TLR9 in the main fungal infections, such as candidiasis, aspergillosis, paracoccidioidomycosis, cryptococcosis, and histoplasmosis.

TLR3

TLR3 detects endogenous dsRNA released by cells in the death process from necrosis (Cavassani et al., 2008). Thus, it is possible that TLR3 is activated when observing damage in the host caused by an infectious process, and after its activation, it plays a role in regulating inflammatory, adaptive memory and tolerance response (Carvalho et al., 2012).

In aspergillosis, the TLR3 role in DCs is of great relevance, being critical both for its maturation and the production of type I IFN. TLR3 in both murine and human DCs by recognizing the fungus RNA effectively induces the CD8 T cell primer for an MHC-I restricted protective memory response against the fungus. The absence of TLR3 directly impacts the migration of murine DCs from the lung to the lymph nodes, due to the failure in the expression of *CCR7*, which leads to a deficient activation of T cells. In mice, the susceptibility to aspergillosis is increased in conditions of TLR3 absence, leading to an increase in the inflammatory process in murine aspergillosis, accompanied by a decrease in the production of IFN-γ, IL-10. In humans, the single nucleotide polymorphism (SNP) of TLR3 provides more invasive aspergillosis. Patients carrying a TLR3 +95C/A exhibit a phenotype of loss of function of DCs, which is correlated with a severe infection by *A. fumigatus* and deficiency in the activation of CD8 T cells (Carvalho et al., 2012). The therapeutic efficacy with micafungin in aspergillosis is strictly induced by the activation of the TLR2/dectin-1 and TLR3/TRIF signaling pathways, which regulate the inflammatory/anti-inflammatory balance during infection, mainly by increasing the production of IL-10 and decreased TNF-α (Moretti et al., 2014).

Human endothelial cells (ECs) express several genes after their interaction with *C. albicans* yeasts, such as genes involved in cell migration, proliferation, among others. TLR3 is involved as a mediator in the expression of the CXCL8/18 gene by ECs, such gene acts in the protective pro-inflammatory endothelial response in the candidiasis (Müller et al., 2007). Patients with the L412F genetic variant of TLR3 are more susceptible to chronic mucocutaneous candidiasis (CMCC). Human peripheral blood mononuclear cells (PBMCs) that carry L412F after interaction with *C. albicans* have a reduction in the production of TNF-α, type I IFN and IFN-γ (Nahum et al., 2012), these cytokines are extremely important for maintaining the innate and adaptive response against candidiasis (Gozalbo and Gil, 2009), this low production can strengthen the susceptibility of part of the patients with CMCC to infection with *C. albicans* (Nahum et al., 2012).

Contrary to other fungal infections, in paracoccidioidomycosis (PCM) TLR3 is used as an escape mechanism by *P. brasiliensis*, generating greater susceptibility to the disease. Although TLR3 does not play a role in the phagocytosis of *P brasiliensis* by murine BMDMs (Jannuzzi et al., 2019), as observed in the phagocytosis of *C. neoformans* by microglia cells (Redlich et al., 2013), in the absence of TLR3 BMDMs have greater microbicidal activity with increased NO and decreased fungal burden. In murine PCM, the absence of TLR3 generated greater resistance to infection, with decreased pulmonary fungal burden and an increased protective response mediated by IFN-γ and IL-17-producing CD8T cells (Jannuzzi et al., 2019). CD8 T lymphocytes, as well as IFN-γ, and IL-17 cytokines, are involved with the protective response of PCM (Loures et al., 2009, 2010, 2014; Jannuzzi et al., 2015). The role of TLR3 in each infection discussed in that session is summarized in **Table 2**.

TLR7

The involvement of TLR7 in ssRNA recognition and its role in the host's defenses against viruses and bacteria (Diebold et al., 2004; Mancuso et al., 2009) is well-known, it has recently been demonstrated that this receptor also plays an important role in the recognition and targeting of the immune response against some pathogens fungal (Biondo et al., 2012).

The recognition of *Candida* spp RNA by TLR7 proved to be crucial in inducing the type I IFN response in bone marrow-derived dendritic cells (BMDCs) (Bourgeois et al., 2011). The activation of the type I IFN response is essential for the maturation of DCs and participates in the polarization of the adaptive immune response, inducing the differentiation of Th cells (Stetson and Medzhitov, 2006). The release of high levels of IFN-β by BMDCs challenged with *Candida* spp depends on TLR7/MYD88/IRF1 and Src/Syk-mediated signaling. However, in a disseminated candidiasis model, type I IFN signaling promotes the persistence of *C. glabrata* in the host, being detrimental to the fungus clearance (Bourgeois et al., 2011). In a model of *C. albicans* infection, resistance to infection it was also correlated with the activation of TLR7 and the transcription factor IRF1 (Bacci et al., 2002; Biondo et al., 2012).

In studies with *Histoplasma capsulatum* (*H. capsulatum*) it has already been shown that macrophages and dendritic cells play different roles in control and infection evolution. While the fungus survives and replicates within the macrophages, in DCs its growth is restricted (Gildea et al., 2001). This fact may be related to the capacity of these cells to produce type I IFN since it was observed that macrophages stimulated with *H. capsulatum*

TABLE 2 | Response induced by TLR3 activation.

Disease	Effect	Outcome
Aspergillosis	Expression CCR7 in BMDC CD8 T cell primer for an MHC-I restricted protective memory response	Protective response
TLR3 + 95C/A SNP Invasive Aspergillosis	Improved phenotype and functions in Human DC CD8 T cell primer	Protective response
Candidiasis	Expression CXCL8/18 gene in Human EC	Protective response
L412F–TLR3 SNP Chronic mucocutaneous candidiase	Increase production of TNF-α, type I IFN and IFN-γ by Human PBMCs	Protective response
Cryptococcosis	No effect in Microglia	–
Paracoccidioidomycosis	Decrease both microbicidal activity, NO production and increase fungal burden by BMDM Decrease IFN-γ and IL-17-producing CD8T cells	Susceptibility

BMDC, bone marrow-derived dendritic cells; DC, dendritic cells; EC, endothelial cells; PBMCs, peripheral blood mononuclear cells; BMDM, bone marrow-derived macrophage.

do not produce this type of cytokine while DCs do it. The type I IFN mediated response is necessary for DCs to be able to restrict the growth of intracellular fungi and survive the fungal infection. Type I IFN production by BMDCs is directed by both TLR7 and TLR9. TLR7-deficient BMDCs exhibit a significant decrease of type I IFN when stimulated with yeast from *H. capsulatum*, the same could be observed with TLR9-deficient BMDCs, however, BMDCs deficient in both TLR7/TLR9 the levels of type I IFN are significantly reduced when compared to the deficient ones separately, this decrease is accompanied by increased fungal growth in the cell and cell lysis. In addition, these TLR7/TLR9 deficient BMDCs failed to induce activation of $CD4^+$ T cells. In the histoplasmosis model, TLR7/TLR9-deficient animals show a more aggressive infection, exhibiting increased neutrophil recruitment, increased lung damage, colonization in the brain, and consequently increased death (Van Prooyen et al., 2016).

The mechanisms present in the susceptibility of chromoblastommycosis are involved with a defect in the recognition of the pathogen by the innate immune response. The *F. pedrosoi* is recognized by CLRs, but there is a failure in the co-stimulation of TLRs leading to chronic infection. Thus, in an attempt to reverse this profile, in 2011, our group showed that animals infected with *F. pedrosoi* after being treated with topical administration of imiquimod, a TLR7 agonist, had a reduction in the fungal load on the skin, suggesting that the activation of TLR7 would be important in protecting the disease. In 2014, the administration of imiquimod was used in four patients with chromoblastomycosis who had a decrease in the diameter of the lesions and a clearing of the pathogen, confirming our previous hypothesis (de Sousa et al., 2014). The role of TLR7 in each infection discussed in that session is summarized in **Table 3**.

TLR9

The ability to induce phagosomal recruitment of TLR9 is conserved in distinct fungal taxonomic groups after phagocytosis, such as *A. fumigattus*, *C. albicans*, *S. cerevise*, *M. furfur*, and *C. neoformans* (Kasperkovitz et al., 2010, 2011). It has recently been shown that TLR9 recruitment and accumulation in the *A. fumigattus* and *C. albicans* phagosome is dependent on the recognition of β1,3-glucan by dectin-1/syk pathway. This pathway mediates phagosome acidification and allows recruitment and retention of TLR9 in this compartment. Knowing that TLR9 needs cysteine, L cathepsin and S cathepsin lysosomal proteases for their phagosome cleavage, it has been seen that blocking Dectin-1/syk-dependent phagosomal acidification therefore blocks the activation of lysosomal cathepsins, which will inhibit TLR9 cleavage. Thus, TLR9 can be recruited for the β1,3-glucan-containing phagosome, but if there is impairment in phagosome acidification there will be no cleavage it will not be activated. Thus, TLR9 modulates gene expression in a Dectin-1 dependent form in response to β1,3-glucan (Khan et al., 2016).

The DNA of *C. albicans*, when internalized, is located inside the endosomal and lysosomal compartments together with the CpG oligodeoxynucleotides (CpG-ODN). This DNA is capable of activating BMDCs through TLR9/MyD88-mediated signaling, but using a mechanism independent of the unmethylated CpG motif. The activation of BMDCs, by the DNA of *C. albicans*, induces immunostimulatory effects, such as IL-12p40 production, CD40 expression and NF-κB activation (Kasperkovitz et al., 2011). The same effects are also seen with the DNA of *C. neoformans* and *A. fumigatus* in BMDCs (Nakamura et al., 2008; Ramirez-Ortiz et al., 2008). In bone marrow-derived macrophages (BMDM), TLR9-mediated signaling with *C. albicans* DNA does not have an effect on their antifungal effector functions. However, the absence of TLR9 improves the effective antifungal response of both BMDM and PBMC, inducing an increased production of TNF-α, IL-6, and nitric oxide and decreasing the production of IL- 10, in addition to improving the microbicidal activity of BMDMs. Interestingly, the systemic infection by *C. albicans* in $TLR9^{-/-}$ mice did not show any difference in the fungi load of the analyzed organs or in their survival, when compared to the control group (van de Veerdonk et al., 2008; Miyazato et al., 2009). In contrast, TLR9 deficiency significantly increased resistance to mucosal candidiasis and reduced the growth of the fungal load on the analyzed organs

TABLE 3 | Response induced by TLR7 activation.

Disease	Effect	Outcome
Candidiasis (*C. albicans*)	Type I IFN production BMDCs	Protective response
Histoplasmosis	Improved Type I IFN production BMDCs	Protective response
Chromoblastommycosis	Reduction in the fungal load on the skin Decrease in the diameter of the lesions	Protective response

BMDC, bone marrow-derived dendritic cells.

(Bellocchio et al., 2004). The involvement of TLR9 during systemic infection by *C. albicans* yeasts may not impact the host's defense mechanism, being only related to the regulation of the immune response. The recognition of *C. albicans* suggests that multiple interactions between PAMPs and PRRs are integrated, acting synergistically and antagonistically, thus allowing the immune system to respond to this pathogen in a more specific way (Trinchieri and Sher, 2007; Netea et al., 2008; Miyazato et al., 2009).

The synthetic oligodeoxynucleotides (ODNs) containing CpG-rich motifs found in *A. fumigatus* DNA are capable of stimulating TLR9 influencing the host response to the fungal challenge. It was demonstrated that DNA obtained from *A. fumigatus* stimulates potently TLR9-dependent responses in BMDCs and human plasmacytoid dendritic cells, showing high production of proinflammatory cytokines like TNF-α and IL-12. The absence of TLR9 in BMDCs it abolished the production of these cytokines when stimulated with DNA from *A. fumigatus*, proving the role of TLR9 in the effector functions mediated by these cells (Ramirez-Ortiz et al., 2008). However, the activation of TLR9 in PMN does not play a role in the response against the fungus. Stimulation with CpG-ODN of *A. fumigatus* does not alter the antifungal effector functions in PMNs, the intracellular production of reactive oxygen intermediates (ROI), and the degranulation of these cells remaining unchanged. However, the absence of TLR9 in PMNs shows an increase in both conidiocidal activity and in hyphal damage activity, with increased azurophil granules degranulation (Bellocchio et al., 2004). In addition, $TLR9^{-/-}$ mice exhibit less pulmonary fungal load, accompanied by a milder pulmonary inflammatory process, in addition to having better survival compared to control animals. Suggesting that, although TLR9 activation plays a different role, depending on the cell analyzed, its absence generates a protective response against aspergillosis (Bellocchio et al., 2004; Ramirez-Ortiz et al., 2008). In humans, susceptibility to allergic bronchopulmonary aspergillosis has been associated with a SNP in the C allele at T-1237C, located within the putative promoter of the TLR9 gene (Carvalho et al., 2008).

The purified DNA of *P. brasiliensis* activates TLR9 in macrophages, leading to the expression of cytokines and promoting their phagocytic capacity, while stimulation of macrophages with *P. brasiliensis* yeasts exhibits low TLR9 activation. The absence of TLR9 in macrophages leads to a decrease in the phagocytic capacity of yeasts. This suggests under physiological conditions, TLR9 can recognize the DNA of *P. brasiliensis* released from the dead fungus in the extracellular environment or after the live cells of the fungus are phagocyted by the immune cells. This entire process would result in the activation of TLR9 and could contribute to targeting the host's defense response against *P. brasiliensis*. In the context of infection by *P. brasiliensis*, the absence of TLR9 increases the susceptibility of mice at the beginning of the infection (48 h), generating an exacerbated inflammatory response with the increased neutrophil influx and high levels of TNF-α at the site of infection (Menino et al., 2013). This condition is harmful to the host due to the excessive release of oxidants, proteases and the intense increase in neutrophils, which can be responsible for organ damage and fungal sepsis (Bellocchio et al., 2004; Zelante et al., 2007).

The use of CPG as an adjuvant in vaccines is a strategy widely used against some models of infection, as it has great potential to induce and increase Th1 type immune response through TLR9 activation (Klinman et al., 2004; Latz et al., 2004; Krieg, 2006). In paracoccidioidomycosis, the combination of CPG and rPb27, a recombinant protein from *P. brasiliensis*, has shown promise in protection in the early stages of the disease (30 DPI), with a 98% reduction in fungal burden. The activation of TLR9 with the adjuvant CPG directed an intense Th1 immune response, with increased recruitment of lymphocytes, and the production of pro-inflammatory cytokines. Regarding macrophages, CPG increased the phagocytic response and microbicidal activity, as well as induced the production of IL-1β, TNF-α, IL-6 and IL-12, however *in vivo* the adjuvant decreased its recruitment, possibly due to increased efficiency of these stimulated cells (Morais et al., 2016). The role of TLR9 in each infection discussed in that session is summarized in **Table 4**.

CONCLUSIONS

For years, the role of intracellular TLRs has been extensively studied in viral and bacterial infections (Diebold et al., 2004; Mancuso et al., 2009). However, these receptors have also been suggested for recognition and induction of immune responses against clinically relevant fungal pathogens (Bourgeois et al., 2010; Carvalho et al., 2012; Menino et al., 2013; Jannuzzi et al., 2019).

Intracellular TLRs are expressed mainly in phagocytic cells, such as macrophages and dendritic cells. These receptors are not necessary for the primary stage of detection and uptake of fungal

TABLE 4 | Response induced by TLR9 activation.

Disease	Effect	Outcome
Systemic candidiasis	IL-12p40 production, CD40 expression and NF- κB activation by BMDCs No effect in BMDM on their antifungal effector functions	No effect
Aspergillosis	Increase of TNF-α and IL-12 cytokine production by both BMDCs and human plasmacytoid dendritic cells No effect in PMN	Susceptibility
Paracoccidioidomycosis	Expression of cytokines and promoting phagocytic capacity in BMDM The combination of CPG and rPb27 induces 98% reduction in fungal burden	Protective response

BMDC, bone marrow-derived dendritic cells; PMN, polymorphonuclear; BMDM, bone marrow-derived macrophage; CPG, nomethylated cytosine-guanosine; rPb27, recombinant protein from P. brasiliensis.

pathogens (Bellocchio et al., 2004; Ramirez-Ortiz et al., 2008; Carvalho et al., 2012). However, after the recognition process on the surface of the phagocytic cells, the intracellular TLRs are recruited into phagosomes, and there perform the recognition of the NAs. The recognition of NAs, DNAs and RNAs, plays an important role in directing the murine immune response, both in innate and adaptive immunity. The type of induced response is particular for each fungus species and, depending on the recognized NAs, there will be the activation of a specific intracellular PRR that could culminate in a protective response or serve as an evasion mechanism of the immune system or, even, simply not influencing in the course of the disease (Bourgeois et al., 2010; Carvalho et al., 2012; Menino et al., 2013; Jannuzzi et al., 2019). Interestingly in humans, some SNRs in intracellular TLR are associated with greater susceptibility to fungal diseases in some types of immunocompromised patients (Carvalho et al., 2008, 2012). In addition the involvement in the immune response against fungal infections, the activation of these receptors is the target of therapeutic strategies, showing efficiency in the polarization of the protective response and resolution of signs and symptoms (de Sousa et al., 2014; Morais et al., 2016).

Based on the studies discussed in this review, we understand that although the signaling mediated by intracellular PRRs in fungal infections is not yet fully understood, the studies developed to date point to an important role in the activation of these TLRs. Thus, we suggest it is necessary to carry out further studies involving this type of signaling, which can help to better clarify the pathophysiology of fungal infections, in addition to contributing to the development of new therapeutic and prophylactic strategies.

AUTHOR CONTRIBUTIONS

The study was planned by KF, wrote by GJ and JA. The tables and figures were prepared by GJ, JA, and LP. The authors SA and KF discussed the session and the content covered. All authors reviewed the manuscript.

FUNDING

The present work was supported by FAPESP (2018/07073-7) and Doctoral Fellowship from CAPES.

ACKNOWLEDGMENTS

We sincerely thank that all Clinical Mycology Laboratory members of the Faculty of Pharmaceutical Sciences, University of São Paulo for helpful technical advice and discussions. We would like to thank Lucas Assis Sampaio de Souza for making **Figure 1** of the review.

REFERENCES

Akira, S., Uematsu, S., and Takeuchi, O. (2006). Pathogen recognition and innate immunity. *Cell* 124, 783–801. doi: 10.1016/j.cell.2006.02.015

Alexopoulou, L., Holt, A. C., Medzhitov, R., and Flavell, R. A. (2001). Recognition of double-stranded RNA and activation of NF-κB by Toll-like receptor 3. *Nature* 413, 732–738. doi: 10.1038/35099560

Bacci, A., Montagnoli, C., Perruccio, K., Bozza, S., Gaziano, R., Pitzurra, L., et al. (2002). Dendritic cells pulsed with fungal RNA induce protective immunity to *Candida albicans* in hematopoietic transplantation. *J. Immunol.* 168, 2904–2913. doi: 10.4049/jimmunol.168.6.2904

Barbalat, R., Ewald, S. E., Mouchess, M. L., and Barton, G. M. (2011). Nucleic acid recognition by the innate immune system. *Annu. Rev. Immunol.* 29, 185–214. doi: 10.1146/annurev-immunol-031210-101340

Barton, G. M. (2007). Viral recognition by Toll-like receptors. *Semin. Immunol* 19, 33–40. doi: 10.1016/j.smim.2007.01.003

Beisswenger, C., Hess, C., and Bals, R. (2012). *Aspergillus fumigatus* conidia induce interferon-β signaling in respiratory epithelial cells. *Eur. Respir. J.* 39, 411–418. doi: 10.1183/09031936.00096110

Bellocchio, S., Moretti, S., Perruccio, K., Fallarino, F., Bozza, S., Montagnoli, C., et al. (2004). TLRs govern neutrophil activity in aspergillosis. *J. Immunol.* 173, 7406–7415. doi: 10.4049/jimmunol.173.12.7406

Biondo, C., Malara, A., Costa, A., Signorino, G., Cardile, F., Midiri, A., et al. (2012). Recognition of fungal RNA by TLR7 has a nonredundant role in host defense against experimental candidiasis. *Eur. J. Immunol.* 42, 2632–2643. doi: 10.1002/eji.201242532

Biondo, C., Midiri, A., Messina, L., Tomasello, F., Garufi, G., Catania, M. R., et al. (2005). MyD88 and TLR2, but not TLR4, are required for host defense against *Cryptococcus neoformans*. *Eur. J. Immunol.* 35, 870–878. doi: 10.1002/eji.200425799

Biondo, C., Signorino, G., Costa, A., Midiri, A., Gerace, E., Galbo, R., et al. (2011). Recognition of yeast nucleic acids triggers a host-protective type I interferon response. *Eur. J. Immunol.* 41, 1969–1979. doi: 10.1002/eji.201141490

Blasius, A. L., and Beutler, B. (2010). Intracellular Toll-like receptors. *Immunity* 32, 305–315. doi: 10.1016/j.immuni.2010.03.012

Bourgeois, C., Majer, O., Frohner, I. E., Lesiak-Markowicz, I., Hildering, K. S., Glaser, W., et al. (2011). Conventional dendritic cells mount a type I IFN response against Candida spp. requiring novel phagosomal TLR7-mediated IFN-β signaling. *J. Immunol.* 186, 3104–3112. doi: 10.4049/jimmunol.1002599

Bourgeois, C., Majer, O., Frohner, I. E., Tierney, L., and Kuchler, K. (2010). Fungal attacks on mammalian hosts: pathogen elimination requires sensing and tasting. *Curr. Opin. Microbiol.* 13, 401–408. doi: 10.1016/j.mib.2010.05.004

Bowman, S. M., and Free, S. J. (2006) The structure and synthesis of the fungal cell wall. *Bioessays* 28, 799–808. doi: 10.1002/bies.20441

Carvalho, A., De Luca, A., Bozza, S., Cunha, C., D'Angelo, C., Moretti, S., et al. (2012). TLR3 essentially promotes protective class I-restricted memory $CD8^+$ T-cell responses to Aspergillus fumigatus in hematopoietic transplanted patients. *Blood* 119, 967–977. doi: 10.1182/blood-2011-06-362582

Carvalho, A., Pasqualotto, A. C., Pitzurra, L., Romani, L., Denning, D. W., and Rodrigues, F. (2008). Polymorphisms in Toll-like receptor genes and susceptibility to pulmonary aspergillosis. *J. Infect. Dis.* 197, 618–621. doi: 10.1086/526500

Cavassani, K. A., Ishii, M., Wen, H., Schaller, M. A., Lincoln, P. M., Lukacs, N. W., et al. (2008). TLR3 is an endogenous sensor of tissue necrosis during acute inflammatory events. *J. Exp. Med.* 205, 2609–2621. doi: 10.1084/jem.20081370

Chen, G. Y., and Nunez, G. (2010). Sterile inflammation: sensing and reacting to damage. *Nat. Rev. Immunol.* 10, 826–837. doi: 10.1038/nri2873

Conze, D. B., Wu, C. J., Thomas, J. A., Landstrom, A., and Ashwell, J. D. (2008). Lys63-linked polyubiquitination of IRAK-1 is required for interleukin-1receptor- and Toll-like receptor-mediated NF-kappaB activation. *Mol. Cell.Biol.* 28, 3538–3547. doi: 10.1128/MCB.02098-07

de Sousa, M., Belda, W. Jr., Spina, R., Lota, P. R., Valente, N. S., Brown, G. D., et al. (2014). Topical application of imiquimod as a treatment for chromoblastomycosis. *Clin. Infect. Dis.* 58, 1734–1737. doi: 10.1093/cid/ciu168

Diebold, S. S., Kaisho, T., Hemmi, H., Akira, S., and Reis Sousa, C. (2004). Innate antiviral responses by means of TLR7-mediated recognition of singlestranded RNA. *Science* 303, 1529–1531. doi: 10.1126/science.1093616

Dubourdeau, M., Athman, R., Balloy, V., Huerre, M., Chignard, M., Philpott, D. J., et al. (2006). *Aspergillus fumigatus* induces innate immune responses in alveolar macrophages through the MAPK pathway independently of TLR2 and TLR4. *J. Immunol.* 177, 3994–4001. doi: 10.4049/jimmunol.177.6.3994

Eberle, F., Sirin, M., Binder, M., and Dalpke, A. H. (2009). Bacterial RNA isrecognized by different sets of immunoreceptors. *Eur. J. Immunol.* 39, 2537–2547. doi: 10.1002/eji.200838978

Ferreira, K. S., Bastos, K. R., Russo, M., and Almeida, S. R. (2007). Interaction between *Paracoccidioides brasiliensis* and pulmonary dendritic cells induces interleukin-10 production and Toll-like receptor-2 expression: possible mechanisms of susceptibility. *J. Infect.* 196, 1108–1115. doi: 10.1086/521369

Fitzgerald, K. A., Rowe, D. C., Barnes, B. J., Caffrey, D. R., Visintin, A., Latz, E., et al. (2003). LPS-TLR4 signaling to IRF-3/7 and NF-kappaB involves the Toll adapters TRAM and TRIF. *J. Exp. Med.* 198, 1043–1055. doi: 10.1084/jem.20031023

Forsbach, A., Nemorin, J. G., Montino, C., Müller, C., Samulowitz, U., Vicari, A. P., et al. (2008). Identification of RNA sequence motifs stimulating sequence-specific TLR8-dependent immune responses. *J. Immunol.* 180, 3729–3738. doi: 10.4049/jimmunol.180.6.3729

Freund, I., Eigenbrod, T., Helm, M., and Dalpke, A. H. (2019). RNA modifications modulate activation of innate Toll-like receptors. *Genes* 10:92. doi: 10.3390/genes10020092

Ganguly, D., Chamilos, G., Lande, R., Gregorio, J., Meller, S., Facchinetti, V., et al. (2009). Self-RNA-antimicrobial peptide complexes activate human dendritic cells through TLR7 and TLR8. *J. Exp. Med.* 206, 1983–1994. doi: 10.1084/jem.20090480

Gay, N. J., Symmons, M. F., Gangloff, M., and Bryant, C. E. (2014). Assembly and localization of Toll-like receptor signalling complexes. *Nat. Rev. Immunol.* 14, 546–558. doi: 10.1038/nri3713

Gildea, L. A., Morris, R. E., and Newman, S. L. (2001). Histoplasma capsulatum yeasts are phagocytosed via very late antigen-5, killed, and processed for antigen presentation by human dendritic cells. *J. Immunol.* 166, 1049–1056. doi: 10.4049/jimmunol.166.2.1049

Gow, N. A., and Hube, B. (2012). Importance of the *Candida albicans* cell wall during commensalism and infection. *Curr. Opin. Microbiol.* 15, 406–412. doi: 10.1016/j.mib.2012.04.005

Gow, N. A., Van De Veerdonk, F. L., Brown, A. J., and Netea, M. G. (2012). *Candida albicans* morphogenesis and host defence: discriminating invasion from colonization. *Nat. Rev. Microbiol.* 10, 112–122. doi: 10.1038/nrmicro2711

Gozalbo, D., and Gil, M. L. (2009). IFN-gamma in *Candida albicans* infections. *Front. Biosci.* 14, 1970–1978. doi: 10.2741/3356

Hemmi, H., Takeuchi, O., Kawai, T., Kaisho, T., Sato, S., Sanjo, H., et al. (2000). A Toll-like receptor recognizes bacterial DNA. *Nature* 408, 740–745. doi: 10.1038/35047123

Jannuzzi, G. P., de Almeida, J., Amarante-Mendes, G. P., Romera, L., Kaihami, G. H., Vasconcelos, J. R., et al. (2019). TLR3 is a negative regulator of immune responses against *Paracoccidioides brasiliensis*. *Front. Cell. Infect. Microbiol.* 8:426. doi: 10.3389/fcimb.2018.00426

Jannuzzi, G. P., Tavares, A. H., Kaihami, G. H., de Almeida, J. R., Almeida, S. R., and Ferreira, K. S. (2015). scFv from antibody that mimics gp43 modulates the cellular and humoral imune responses during experimental paracoccidioidomycosis. *PLoS ONE* 10:e0129401. doi: 10.1371/journal.pone.0129401

Jouault, T., Sarazin, A., Martinez-Esparza, M., Fradin, C., Sendid, B., and Poulain, D. (2009). Host responses to a versatile commensal: PAMPs and PRRs interplay leading to tolerance or infection by *Candida albicans*. *Cell. Microbiol.* 11, 1007–1015. doi: 10.1111/j.1462-5822.2009.01318.x

Kasperkovitz, P. V., Cardenas, M. L., and Vyas, J. M. (2010). TLR9 is actively recruited to *Aspergillus fumigatus* phagosomes and requires the N-terminal proteolytic cleavage domain for proper intracellular trafficking. *J. Immunol.* 185, 7614–7622. doi: 10.4049/jimmunol.1002760

Kasperkovitz, P. V., Khan, N. S., Tam, J. M., Mansour, M. K., Davids, P. J., and Vyas, J. M. (2011). Toll-like receptor 9 modulates macrophage antifungal effector function during innate recognition of Candida albicans and Saccharomyces cerevisiae. *Infect. Immun.* 79, 4858–4867. doi: 10.1128/IAI.05626-11

Kawai, T., and Akira, S. (2006). TLR signaling. *Cell Death. Differ.* 13, 816–825. doi: 10.1038/sj.cdd.4401850

Kawai, T., and Akira, S. (2010). The role of pattern-recognition receptors in innate immunity: update on Toll-like receptors. *Nat. Immunol.* 11, 373–384. doi: 10.1038/ni.1863

Kawai, T., and Akira, S. (2011). Toll-like receptors and their crosstalk with other innate receptors in infection and immunity. *Immunity* 34, 637–650. doi: 10.1016/j.immuni.2011.05.006

Khan, N. S., Kasperkovitz, P. V., Timmons, A. K., Mansour, M. K., Tam, J. M., Seward, M. W., et al. (2016). Dectin-1 controls TLR9 trafficking to phagosomes containing β-1,3 Glucan. *J. Immunol.* 196, 2249–2261. doi: 10.4049/jimmunol.1401545

Klinman, D. M., Currie, D., Gurse, I., and Verthelyi, D. (2004). Use of CPG oligodeoxynucleotides as immune adjuvants. *Immunol. Rev.* 199, 201–216. doi: 10.1111/j.0105-2896.2004.00148.x

Krieg, A. M. (2006). Therapeutic potential of Toll-like receptor 9 activation. *Nat. Rev. Drug Discov.* 5, 471–484. doi: 10.1038/nrd2059

Latz, E., Schoenemeyer, A., Visintin, A., Fitzgerald, K. A., Monks, B. G., Knetter, C. F., et al. (2004). TLR9 signals after translocating from the ER to CpG DNA in the lysosome. *Nat. Immunol.* 5, 190–198. doi: 10.1038/ni1028

Lee, B. L., and Barton, G. M. (2014). Trafficking of endosomal Toll-like receptors. *Trends Cell Biol.* 24, 360–369. doi: 10.1016/j.tcb.2013.12.002

Lee, Y. A., Choi, H. M., Lee, S. H., Yang, H. I., Yoo, M. C., Hong, S. J., et al. (2012). Synergy between adiponectin and interleukin-1β on the

expression of interleukin-6, interleukin-8, and cyclooxygenase-2 in fibroblast-like synoviocytes. *Exp. Mol. Med.* 44, 440–447. doi: 10.3858/emm.2012.44.7.049

Levitz, S. M. (2010). Innate recognition of fungal cell walls. *PLoS Pathog.* 6:e1000758. doi: 10.1371/journal.ppat.1000758

Liu, L., Botos, I., Wang, Y., Leonard, J. N., Shiloach, J., Segal, D. M., et al. (2008). Structural basis of Toll-like receptor 3 signaling with double-stranded RNA. *Science* 320, 379–381. doi: 10.1126/science.1155406

Loures, F. V., Araújo, E. F., Feriotti, C., Bazan, S. B., and Calich, V. L. (2015). TLR-4 cooperates with Dectin-1 and mannose receptor to expand Th17 and Tc17 cells induced by *Paracoccidioides brasiliensis* stimulated dendritic cells. *Front. Microbiol.* 31:261. doi: 10.3389/fmicb.2015.00261

Loures, F. V., Araújo, E. F., Feriotti, C., Bazan, S. B., Costa, T. A., Brown, G. D., et al. (2014). Dectin-1 induces M1 macrophages and prominent expansion of $CD8^{+}IL17^{+}$ cells in pulmonar paracoccidioidomycosis. *J. Infect. Dis.* 210, 762–773. doi: 10.1093/infdis/jiu136

Loures, F. V., Pina, A., Felonato, M., Araújo, E. F., Leite, K. R., and Calich, V. L. (2010). TLR4 signaling leads to a more severe fungal infection associated with enhanced proinflammatory immunity and impaired expansion of regulatory T cells. *Infect. Immun.* 78, 1078–1088. doi: 10.1128/IAI.01198-09

Loures, F. V., Pina, A., Felonato, M., and Calich, V. L. (2009). TLR2 is a negative regulator of Th17 cells and tissue pathology in a pulmonary model of fungal infection. *J. Immunol.* 183, 1279–1290. doi: 10.4049/jimmunol.0801599

Mancuso, G., Gambuzza, M., Midiri, A., Biondo, C., Papasergi, S., Akira, S., et al. (2009). Bacterial recognition by TLR7 in the lysosomes of conventional dendritic cells. *Nat. Immunol.* 10, 587–594. doi: 10.1038/ni.1733

Matsumoto, M., and Seya, T. (2008). TLR3: interferon induction by double-stranded RNA including poly(I:C). *Adv. Drug Deliv. Rev.* 60, 805–812. doi: 10.1016/j.addr.2007.11.005

Medzhitov, R. (2007). Recognition of microorganisms and activation of the immune response. *Nature* 449, 819–826. doi: 10.1038/nature06246

Meier, A., Kirschning, C. J., Nikolaus, T., Wagner, H., Heesemann, J., and Ebel, F. (2003). Toll-like receptor (TLR) 2 and TLR4 are essential for *Aspergillus*-induced activation of murine macrophages. *Cell. Microbiol.* 5, 561–570. doi: 10.1046/j.1462-5822.2003.00301.x

Menino, J. F., Saraiva, M., Gomes-Alves, A. G., Lobo-Silva, D., Sturme, M., Gomes-Rezende, J., et al. (2013). TLR9 activation dampens the early inflammatory response to Paracoccidioides brasiliensis, impacting host survival. *PLoS Negl. Trop. Dis.* 7:e2317. doi: 10.1371/journal.pntd.0002317

Meylan, E., Burns, K., Hofmann, K., Blancheteau, V., Martinon, F., Kelliher, M., et al. (2004). RIP1 is an essential mediator of Toll-like receptor 3-induced NF-kappa B activation. *Nat. Immunol.* 5, 503–507. doi: 10.1038/ni1061

Miyazato, A., Nakamura, K., Yamamoto, N., Mora-Montes, H. M., Tanaka, M., Abe, Y., et al. (2009). Toll-like receptor 9-dependent activation of myeloid dendritic cells by Deoxynucleic acids from Candida albicans. *Infect. Immun.* 77, 3056–3064. doi: 10.1128/IAI.00840-08

Morais, E. A., Chame, D. F., Melo, E. M., Oliveira, J. A. C., Paula, A. N. C., Peixoto, A. C., et al. (2016). TLR 9 involvement in early protection induced by immunization with rPb27 against Paracoccidioidomycosis. *Microbes Infect.* 18, 137–147. doi: 10.1016/j.micinf.2015.10.005

Moretti, S., Bozza, S., Massi-Benedetti, C., Prezioso, L., Rossetti, E., Romani, L., et al. (2014). An immunomodulatory activity of micafungin in preclinical aspergillosis. *J. Antimicrob. Chemother.* 69, 1065–1074. doi: 10.1093/jac/dkt457

Müller, V., Viemann, D., Schmidt, M., Endres, N., Ludwig, S., Leverkus, M., et al. (2007). Candida albicans triggers activation of distinct signaling pathways to establish a proinflammatory gene expression program in primary human endothelial cells. *J. Immunol.* 179, 8435–8445. doi: 10.4049/jimmunol.179.12.8435

Nahum, A., Dadic, H., Batesc, A., Roifman, C. M. (2012). The biological significance of TLR3 variant, L412F, in conferring susceptibility to cutaneous candidiasis, CMV and autoimmunity. *Autoimmun. Rev.* 5, 341–347. doi: 10.1016/j.autrev.2011.10.007

Nakamura, K., A., Miyazato, G., Xiao, M., Hatta, K., Inden, T., Aoyagi, K., et al. (2008). Deoxynucleic acids from *Cryptococcus neoformans* activate myeloid dendritic cells via a TLR9- dependent pathway. *J. Immunol.* 180, 4067–4074. doi: 10.4049/jimmunol.180.6.4067

Netea, M. G., Brown, G. D., Kullberg, B. J., and Gow, N. A. R. (2008). An integrated model of the recognition of Candida albicans by the innate immune system. *Nat. Rev. Microbiol.* 6, 67–78. doi: 10.1038/nrmicro1815

Netea, M. G., Ferwerda, G., van der Graaf, C. A., Van der Meer, J. W., and Kullberg, B. J. (2006). Recognition of fungal pathogens by Toll-like receptors. *Curr. Pharm. Design* 12, 4195–4201. doi: 10.2174/138161206778743538

Netea, M. G., Van Der Graaf, C. A., Vonk, A. G., Verschueren, I., Van Der Meer, J. W., and Kullberg, B. J. (2002). The role of Toll-like receptor (TLR) 2 and TLR4 in the host defense against disseminated candidiasis. *J. Infect. Dis.* 185, 1483–1489. doi: 10.1086/340511

Pelka, K., Bertheloot, D., Reimer, E., Phulphagar, K., Schmidt, S. V., Christ, A., et al. (2018). The chaperone UNC93B1 regulates Toll-like receptor stability independently of endosomal TLR transport. *Immunity* 48, 911–922.e7. doi: 10.1016/j.immuni.2018.04.011

Perruccio, K., Tosti, A., Burchielli, E., Topini, F., Ruggeri, L., Carotti, A., et al. (2005). Transferring functional immune responses to pathogens after haploidentical hematopoietic transplantation. *Blood.* 106, 4397–4406. doi: 10.1182/blood-2005-05-1775

Pichlmair, A., and Reis e Sousa, C. (2007). Innate recognition of viruses. *Immunity* 27, 370–383. doi: 10.1016/j.immuni.2007.08.012

Plato, A., Hardison, S. E., and Brown, G. D. (2015). Pattern recognition receptors in anti-fungal immunity. *Semin. Immunopathol.* 37, 97–106. doi: 10.1007/s00281-014-0462-4

Ramirez-Ortiz, Z. G., Specht, C. A., Wang, J. P., Lee, C. K., Bartholomeu, D. C., Gazzinelli, R. T., et al. (2008). Toll-like receptor 9-dependent immune activation by unmethylated CpG motifs in Aspergillus fumigatus DNA. *Infect. Immun.* 76, 2123–2129. doi: 10.1128/IAI.00047-08

Redlich, S., Ribes, S., Schutze, S., Eiffert, H., and Nau, R. (2013). Toll-like receptor stimulation increases phagocytosis of *Cryptococcus neoformans* by microglial cells. *J. Neuroinflammation* 10:71. doi: 10.1186/1742-2094-10-71

Romani, L. (2011). Immunity to fungal infections. *Nat. Rev. Immunol.* 11, 275–287. doi: 10.1038/nri2939

Schuberth-Wagner, C., Ludwig, J., Bruder, A. K., Herzner, A. M., Zillinger, T., Goldeck, M., et al. (2015). A conserved histidine in the RNA sensor RIG-I controls immune tolerance to N1-2'O-methylated self RNA. *Immunity* 43, 41–51. doi: 10.1016/j.immuni.2015.06.015

Sousa, M., Reid, D. M., Schweighoffer, E., Tybulewicz, V., Ruland, J., Langhorne, J., et al. (2011). Restoration of pattern recognition receptor costimulation to treat chromoblastomycosis, a chronic fungal infection of the skin. *Cell Host Microbe* 9, 436–443. doi: 10.1016/j.chom.2011.04.005

Souza, M. C., Corrêa, M., Almeida, S. R., Lopes, J. D., and Camargo, Z. P. (2001). Immunostimulatory DNA from Paracoccidioides brasiliensis acts as T-helper 1 promoter in susceptible mice. *Scand. J. Immunol.* 54, 348–356. doi: 10.1046/j.1365-3083.2001.00937.x

Stetson, D. B., and Medzhitov, R. (2006). Type I interferons in host defense. *Immunity* 25, 373–381. doi: 10.1016/j.immuni.2006.08.007

Takeuchi, O., and Akira, S. (2010). Pattern recognition receptors and inflammation. *Cell* 140, 805–820. doi: 10.1016/j.cell.2010.01.022

Trinchieri, G., and Sher, A. (2007). Cooperation of Toll-like receptor signals in innate immune defence. *Nat. Rev. Immunol.* 7, 179–190. doi: 10.1038/nri2038

van de Veerdonk, F. L., Netea, M. G., Jansen, T. J., Jacobs, L., Verschueren, I., van der Meer, J. W., et al. (2008). Redundant role of TLR9 for anti-*Candida* host defense. *Immunobiology* 213, 613–620. doi: 10.1016/j.imbio.2008.05.002

Van Prooyen, N., Henderson, C. A., Hocking Murray, D., and Sil, A. (2016). CD103+ Conventional dendritic cells are critical for TLR7/9-dependent host defense against histoplasma capsulatum, an endemic fungal pathogen of humans. *PLoS Pathog.* 12:e1005749. doi: 10.1371/journal.ppat.1005749

Vollmer, J., Tluk, S., Schmitz, C., Hamm, S., Jurk, M., Forsbach, A., et al. (2005). Immune stimulation mediated by autoantigen binding sites within small nuclear RNAs involves Toll-like receptors 7 and 8. *J. Exp. Med.* 202, 1575–1585. doi: 10.1084/jem.20051696

Wheeler, R. T., and Fink, G. R. (2006) A drug-sensitive genetic network masks fungi from the immune system. *PLoS Pathog.* 2:e35. doi: 10.1371/journal.ppat.0020035

Yamashita, M., Chattopadhyay, S., Fensterl, V., Saikia, P., Wetzel, J. L., and Sen, G. C. (2012). Epidermal growth factor receptor is essential for Toll-like receptor 3 signaling. *Sci. Signal.* 5:ra50. doi: 10.1126/scisignal.2002581

Yauch, L. E., Mansour, M. K., Shoham, S., Rottman, J. B., and Levitz, S. M. (2004). Involvement of CD14, Toll-like receptors 2 and 4, and MyD88 in the host response to the fungal pathogen *Cryptococcus neoformans*

in vivo. *Infect. Immun.* 72, 5373–5382. doi: 10.1128/IAI.72.9.5373-5382.2004

Yoneyama, M., Kikuchi, M., Natsukawa, T., Shinobu, N., Imaizumi, T., Miyagishi, M., et al. (2004). The RNA helicase RIG-I has an essential function in double-stranded RNA-induced innate antiviral responses. *Nat. Immunol.* 5, 730–737. doi: 10.1038/ni1087

Yordanov, M., Dimitrova, P., Danova, S., and Ivanovska., N. (2005). *Candida albicans* double-stranded DNA can participate in the host defense against disseminated candidiasis. *Microbes Infect.* 7, 178–186. doi: 10.1016/j.micinf.2004.10.011

Zelante, T., De Luca, A., Bonifazi, P., Montagnoli, C., Bozza, S., Moretti, S., et al. (2007). IL-23 and the Th17 pathway promote inflammation and impair antifungal immune resistance. *Eur. J. Immunol.* 37, 2695–2706. doi: 10.1002/eji.200737409

Conflict of Interest: The authors declare that the research was conducted in the absence of any commercial or financial relationships that could be construed as a potential conflict of interest.

The handling editor declared a shared affiliation with several of the authors GJ, JA, LP, and KF at the time of review.

frontiers in Cellular and Infection Microbiology

ORIGINAL RESEARCH
published: 29 October 2020
doi: 10.3389/fcimb.2020.591974

Cytological and Histopathological Spectrum of Histoplasmosis: 15 Years of Experience in French Guiana

Kinan Drak Alsibai[1,2*], *Pierre Couppié*[3,4], *Denis Blanchet*[5], *Antoine Adenis*[6], *Loïc Epelboin*[7], *Romain Blaizot*[3], *Dominique Louvel*[8], *Félix Djossou*[7], *Magalie Demar*[5,9] *and Mathieu Nacher*[4,6]

[1] Department of Pathology, Centre Hospitalier de Cayenne Andrée Rosemon, Cayenne, French Guiana, [2] Centre of Biological Resource (CRB Amazonie), Centre Hospitalier de Cayenne Andrée Rosemon, Cayenne, French Guiana, [3] Department of Dermatology, Centre Hospitalier de Cayenne Andrée Rosemon, Cayenne, French Guiana, [4] DFR Santé, Université de Guyane, Cayenne, French Guiana, [5] Laboratory, Centre Hospitalier de Cayenne Andrée Rosemon, Cayenne, French Guiana, [6] CIC INSERM 1424, Centre Hospitalier de Cayenne Andrée Rosemon, Cayenne, French Guiana, [7] 1 Service des Maladies Infectieuses et Tropicales, Centre Hospitalier de Cayenne Andrée Rosemon, Cayenne, French Guiana, [8] Service de Médecine B, Centre Hospitalier de Cayenne Andrée Rosemon, Cayenne, French Guiana, [9] UMR Tropical Biome and Immunopathology, Université de Guyane, Cayenne, French Guiana

OPEN ACCESS

Edited by:
Carlos Pelleschi Taborda, University of São Paulo, Brazil

Reviewed by:
Rosely Maria Zancopé-Oliveira, Oswaldo Cruz Foundation (Fiocruz), Brazil
Beatriz L. Gómez, Rosario University, Colombia

***Correspondence:**
Kinan Drak Alsibai
kdrak.alsibai@doctor.com

Specialty section:
This article was submitted to Fungal Pathogenesis, a section of the journal Frontiers in Cellular and Infection Microbiology

Received: *05 August 2020*
Accepted: *07 October 2020*
Published: *29 October 2020*

Citation:
Drak Alsibai K, Couppié P, Blanchet D, Adenis A, Epelboin L, Blaizot R, Louvel D, Djossou F, Demar M and Nacher M (2020) Cytological and Histopathological Spectrum of Histoplasmosis: 15 Years of Experience in French Guiana. Front. Cell. Infect. Microbiol. 10:591974. doi: 10.3389/fcimb.2020.591974

Background: Disseminated histoplasmosis remains a major killer of immunocompromised patients in Latin America. Cytological and histological methods are usually present in most hospitals and may represent a precious diagnostic method. We report 15 years of experience of the department of pathology of the Centre Hospitalier de Cayenne Andrée Rosemon in French Guiana.

Methods: Specimens from live patients from January 2005 to June 2020 with the presence of *H. capsulatum* on cytological and/or histological analysis were analyzed. All specimens were examined by an experienced pathologist. The analysis was descriptive.

Results: Two hundred two cytological and histological samples were diagnosed with histoplasmosis between January 2005 and June 2020. The 202 samples included 153 (75.7%) histopathological formalin-fixed and paraffin-embedded tissues (biopsy or surgical specimens) and 49 (24.3%) cytological analysis from all organs. One hundred thirty-four patients (82.7%) were HIV-positive, 15 patients (9.3%) had immunosuppressant treatment, and 13 patients (8%) were immunocompetent. Seventy-eight of 202 (38.5%) were samples from the digestive tract, mostly the colon (53/78 cases, 70%) and small intestine (14/78 cases, 18%). Microorganisms were more numerous in digestive samples (notably the colon) than in other organs. Lymphocyte and histiocyte inflammation of moderate to marked intensity were observed in all positive specimens. Tuberculoid epithelioid granuloma were present in 16/78 (20,5%) specimens including 14 colon and 2 small intestine specimens. There were 11/202 cases of liver histoplasmosis, 26/202 (12,8%) cases of pulmonary histoplasmosis. Bone marrow involvement was diagnosed in 14 (2%) specimens (8 aspiration and 6 biopsies). Lymph

nodes were positive in 42 specimens (31 histology and 11 cytology). Histopathological analysis of the 31 lymph nodes showed a variable histological appearance. Tuberculoid forms were most frequent (24/31, 77,4%).

Conclusions: From the pathologist perspective, this is the largest series to date showing that digestive involvement was the most frequent, usually with a tuberculoid form and a greater load of *Histoplasma*. With awareness and expertise, cytology and pathology are widely available methods that can give life-saving results in a short time to help orient clinicians facing a potentially fatal infection requiring prompt treatment.

Keywords: histoplasmosis, pathology, HIV, French Guiana, tuberculoid granuloma, diagnosis

INTRODUCTION

H. capsulatum is a dimorphic saprophytic fungus which exists in its mycelial form in soil at moderate temperature, ideally in a moist environment. As a soil fungus, it is well adapted to be pathogenic to humans because it does not need to interact with a mammalian host as part of its life cycle. In tissues and after inhalation of airborne conidia, *H. capsulatum* remains in the blastospore state and does not produce filaments, and is usually intracellular (Woods et al., 2001). Morphologically, *H. capsulatum* is a small spherical or ovoid yeasts measuring 2 to 6 μm (Silverman et al., 1955). It is characterized by its ability to make a dimorphic transition from must-leaven to yeast, to enter host macrophages (also called histiocytes in tissues), and to survive intracellularly. It is also able to proliferate during active infection, and to persist during clinically inapparent infection, and has the ability to reactivate (Woods et al., 2001).

Histoplasmosis was first described by Samuel Taylor Darling by examining the autopsies of two Caribbean and one Asian persons living and working in Panama who developed disseminated histoplasmosis (Darling, 1906). Since then, histoplasmosis has been attributed to *H. capsulatum*. Until recently, following different clinical and epidemiological profiles, the classification entailed *Histoplasma capsulatum* var. *capsulatum* (*H. capsulatum*), which causes classic histoplasmosis, *Histoplasma capsulatum* var. *duboisii* (*H. duboisii*) which causes African histoplasmosis, and *H. capsulatum* var. *farciminosum*, which causes lymphangitis in horses in the Old World. Insights from phylogenetic studies have now replaced this classical denomination and shown that the causal pathogens of histoplasmosis include different regionally specific cryptic species, a classification that gradually gains in detail as the sampling of isolates from different parts of the world grows (Teixeira et al., 2016; Sepúlveda et al., 2017; Damasceno et al., 2019). African histoplasmosis, is located primarily in cutaneous and subcutaneous tissue (Cockshott and Lucas, 1964). Its evolution is slow and the prognosis is benign, and the spread to the viscera remains exceptional (Zida et al., 2015).

For American Histoplasmosis, different genotypes may be associated with differences in clinical phenotype, with South American genetic lineages being more dermotropic, and leading to acute pulmonary diseases whereas North American strains would be linked to more chronic pulmonary disease. These differences however, may be confounded by differences in access to care and further studies are still needed to disentangle what is attributable to differences in Histoplasma genetics and patient health care trajectories (Couppie et al., 2006; Morote et al., 2020; Rodrigues et al., 2020).

The severity of disease after inhalation of *H. capsulatum* varies, with the intensity of exposure and the host's immunity. This may lead to asymptomatic infections or mild pulmonary disease for low-intensity exposures in immunocompetent individuals, whereas heavy exposures may lead to severe pulmonary infections. Among patients with underlying lung disease, a chronic lung infection may develop with gradual loss of pulmonary function, and if untreated, frequent death. Among immunocompromised patients the infection progressively disseminates to other organs leading to non-specific syndromes. Various organs such as the lungs, gastrointestinal tract, liver or lymph nodes may thus be involved in the same patient. Immunocompromised patients infected with *Histoplasma* are 10 to 15 times more likely to develop a disseminated form of the disease, which is invariably fatal if left untreated. Hence, HIV-infected patients with disseminated histoplasmosis usually have CD4 counts under 200 per mm^3 and mostly under 50 per mm^3. In the past four decades, the acquired immune deficiency syndrome (AIDS) pandemic and the rise in the number of pharmacologically immunosuppressed patients have led to an increase of the population of patients susceptible to progressive disseminated histoplasmosis, and a high number of resulting fatalities in a context where diagnosis is difficult and antifungal treatment is often absent or late (Pan American Health Organization, 2020).

Histoplasmosis has thus become a major opportunistic infection in patients with advanced HIV infection in endemic areas, where it has often been ranked as the most common AIDS-defining infection and cause of death for patients with CD4 cell counts <200 cells/mm^3 (Nacher et al., 2011; Nacher et al., 2020).

French Guiana combines a favorable environment for the growth of fungi with a high prevalence of HIV infection (Nacher et al., 2018a). Epidemiological statistics suggest that the incidence of disseminated histoplasmosis in HIV patients is as high as 1.5 per 100 persons-years overall, and greater than 10 per 100 persons-years in patients with CD4 counts under 50/mm^3 (Nacher et al., 2011; Nacher et al., 2014). In South America,

histoplasmosis is a common diagnosis, frequently considered by physicians confronted with HIV patients with symptoms of an infectious disease, and pulmonary or digestive symptoms (Couppié et al., 2019).

Before the advent of the AIDS epidemic, histoplasmosis data were obtained from animal samples (Emmons and Ashburn, 1948) or by including autopsy specimens sometimes several decades after the initial diagnosis (Queiroz and Siqueira, 1975).

Various techniques have been used to detect Histoplasma infection. The reference methods are cytological and histological examination and fungal culture with a sensitivity of 65 and 80% respectively in immunocompromised patients (Wheat, 2003; Wheat, 2006; Nacher et al., 2018b). Other common procedures include DNA detection by polymerase chain reaction (PCR), and serological detection in plasma. However, the sensitivity of histoplasmosis detection methods reported in the literature are highly variable, and may differ geographically and according to the experience and the laboratory method used in each center (Wheat, 2003; Tobon et al., 2005; Huber et al., 2008; Mata-Essayag et al., 2008). In addition, the relevance of different tests may vary according to the organs retrieved or the immune status of the patient (Tobon et al., 2005; Weydert et al., 2007). Interestingly, the detection of the *H. capsulatum* antigen in serum or urine has shown a higher sensitivity, estimated at 90% on American strains. However, access to this method is limited and is only available in certain North American laboratories. Because of the diagnostic gap in most countries, most studies highlighting pathological findings of histoplasmosis are usually presented in the form of case reports. Some cohorts with larger numbers of patients have been assembled in the United States in successive epidemics of the east-central regions concerning mainly immunocompetent patients (Cano and Hajjeh, 2001). At the same time, the incidence has been steadily increasing in parts of South America, where access to medical care may be more difficult. Whereas fungal culture, antigen detection, or PCR are often not available, cytological and histological methods are usually present in most hospitals in endemic countries and may represent a precious diagnostic alternative. In this review, we report the experience of the department of pathology of the Centre Hospitalier de Cayenne Andrée Rosemon in French Guiana in terms of microscopic diagnosis of *H. capsulatum* histoplasmosis for more than 15 years (2005 and 2020) carried out on cytological and histological samples.

METHODS

We analyzed specimens from live patients diagnosed with histoplasmosis from January 2005 to June 2020 at the Centre Hospitalier de Cayenne Andrée Rosemon in the department of pathology (Cayenne, French Guiana). The inclusion criteria were the confirmed presence of *H. capsulatum* histoplasmosis on cytological and/or histological analysis. All specimens were examined by an experienced pathologist to confirm the initial diagnosis by looking for *H. capsulatum* organisms, such as the typical round intracellular yeast 2–6 μm with buds. All solid tissue samples were fixed in 10% buffered formalin, embedded in paraffin, sectioned at 4 μm and stained with routine Hematoxylin-Eosin-Safran (HES) stain as well as with Silver Methenamine Gomori-Grocott (Gomori-Grocott) and/or Periodic-Acid-Schiff (PAS) stain. The yeasts of *H. capsulatum* are usually colored red-violet and surrounded by a light halo by PAS stain, and colored brown-black by the Gomori-Grocott stain.

The histopathological lesions correspond to the host reactions against *H. capsulatum* and its immune status, and are classified into 4 categories: (i) the tuberculoid form, (ii) the anergic form, (iii) the mixed form, and (iv) the sequelae form.

The tuberculoid form usually corresponds to a low inoculation and effective tissue response of the host. The tissue shows an inflammatory infiltrate rich in activated macrophages and lymphocytes mostly of T-helper CD4+ phenotype progressively recruited *in vivo*. Granulomas with epithelioid cells with/without giant cells can also be observed. The evolution of this form, by analogy with tuberculosis, is caseous necrosis. Here, the histoplasmas are usually few in number and are located in the cytoplasm of histiocytes (intracellular).

The anergic form is observed in HIV patients and shows little or no tissue response. Local macrophages remain inactive. The typical appearance is that of an abundance of intracellular and extracellular yeast.

The mixed form represents an intermediate form between the tuberculoid form and the anergic form. Finally, in the sequelae form, the scarring fibrosis are predominates and the inflammation is mild. In this form, rare yeasts can be found that can correspond to a relapse case or eventual reactivation.

Ethical and Regulatory Aspects

HIV-infected patients were enrolled in the French Hospital Database for HIV (FHDH). The database includes most patients followed in French Guiana and nearly all AIDS cases. Patients in the FHDH gave informed consent for using their anonymized data and for publishing anonymized results. This data collection was approved by the Commission Nationale Informatique et Libertés (CNIL) since 1992 and this cohort has led to multiple international publications. For HIV-negative patients, posters and leaflets in a range of language were posted in laboratories and wards to inform patients that their anonymized results may be used in ancillary studies and that they have a right to refuse without any impact on access and quality of care.

RESULTS

Two hundred two cytological and histological samples (from 162 patients) of *H. capsulatum* histoplasmosis were diagnosed in our department between January 2005 and June 2020. The 202 samples included 153 (75.7%) histopathological formalin-fixed and paraffin-embedded tissues (biopsy or surgical specimens) and 49 (24.3%) cytological analysis from all organs. One hundred

thirty-four patients (82.7%) were HIV-positive, 15 patients (9.3%) had immunosuppressant treatment (long-term steroids, anti-TNF and chemotherapy), and 13 patients (8%) were immunocompetent with no known immunodeficiency status at the time of diagnosis. In HIV cases, the CD4+ cell count at the time of cytological or histopathological diagnosis ranged from 0 to 668 mm^3. **Table 1** summarizes histopathological data of 153 *H. capsulatum* positive tissues and **Table 2** summarizes the 49 cytological techniques used for detection of *H. capsulatum*.

Pulmonary Histoplasmosis

We diagnosed pulmonary histoplasmosis in 26/202 (12,8%) specimens consisting of 24 BAL and 2 bronchial biopsies. The two bronchial biopsies involved two HIV patients with CD4 at 124 and 30 mm^3. Both samples revealed a tuberculoid form associated with intra-cellular *H. capsulatum* (PAS+ and/or Gomori-Grocott +).

The 24 BAL fluid concerned 23 immunocompromised patients and one immunocompetent patient. Among the 23 immunocompromised patients with a BAL, there were 22 HIV patients and one post-renal transplant patient treated with immunosuppressant drugs who had a BAL because he was suffering from fever and diffuse pulmonary micronodules.

The cellular formula of all the 24 pathologic BAL consisted essentially of macrophages with a percentage ranging from 55 to 85% of cellularity (normal >80%). Neutrophils were in second place with 2 to 30% of cellularity (normal <5%), followed by lymphocytes with 8 to 18% of cellularity (normal <10%). The presence of plasmocytes and eosinophils was occasional. **Figure 1** shows a case of pulmonary histoplasmosis diagnosed on BAL.

We routinely performed Ziehl-Neelsen staining and immunochemistry study with the anti-*Pneumocystis jiroveci* antibody on BAL and bronchial biopsies of HIV patients to look for a co-infection with tuberculosis and pneumocystosis respectively. Histoplasmosis was associated with the presence of *Mycobacterium tuberculosis* on the same cytology specimen in two cases, *Pneumocystis jiroveci* in one case and candidiasis in two cases.

Bone Marrow Histoplasmosis

Bone marrow involvement by histoplasmosis was diagnosed in 14 (2%) specimens (8 aspiration and 6 biopsies). It was frequently associated with cytopenia (anemia, neutropenia, and thrombocytopenia) and sometimes with pancytopenia. The tuberculoid form without necrosis was present in 4 of 6 bone marrow biopsies. The two remaining biopsies revealed an anergic form in one case, and intermediate form in the second. **Figure 1** shows a case of disseminated histoplasmosis diagnosed from a blood smear.

Lymph Node Histoplasmosis

Microscopic analysis confirmed lymph node involvement by *H. capsulatum* in 42 specimens (31 histology and 11 cytology). The 11 histological samples consisted of 2 biopsies and 9 surgical specimens of lymph nodes. Histopathological analysis of the 31 lymph nodes showed a variable histological appearance. The tuberculoid form was the most frequent (24/31, 77,4%). Interestingly, a histological variant perfectly mimicking tuberculosis with epithelioid granulomas, multinucleated giant cells, and caseous necrosis was found in 10 of the 24 tuberculoid forms, followed by a less typical granulomatous variant where giant cells and necrosis were absent in 8 cases, and then a non-granulomatous histiocytic inflammation form in 6 cases (**Figure 2**). The remaining 7 lymph nodes showed non-specific follicular or sinusal histiocytic hyperplastic lymphadenitis.

In lymph node involvement (cytological and histological specimens), *H. capsulatum* were found with Gomori-Grocott and PAS+ special staining, which were routinely performed in HIV patients.

The Ziehl-Neelsen stain allowed the diagnosis of a histoplasmosis-tuberculosis coinfection in 3 cases. One case of

TABLE 2 | This table summarizes the 49 cytological techniques used for detection of *H. capsulatum* in our series.

Organ	N°	Cytological technique
Lung	24 (49%)	Bronchoalveolar lavage (BAL)
Bone marrow	8 (16.3)	Bone marrow aspiration
Lymph node	11 (22.5%)	Fine needle aspiration (FNA) of lymph node
CNS	1 (2%)	Cerebro-spinal fluid/cytology
Peritoneum	3 (6.2%)	Peritoneal fluid/cytology
Prostate	1 (2%)	Fine needle aspiration (FNA) of inflammatory prostatic lesion
Blood	1 (2%)	Peripheral blood smear
TOTAL	**49**	

TABLE 1 | This table summarizes histopathological data of 153 *H. capsulatum* positive tissues.

Organ/histological type	N°	Tuberculoid type	Anergic type	Intermediate type	Sequelae type
Gastro-intestinal tract	78	16/78 (20,5%)	17/78 (21.8%)	40/78 (51.2%)	5/78 (6.5%)
Liver	11	9/11 (82%)	2/11 (18%)	0/11 (0%)	0/11 (0%)
Lung	2	2/2 (100%)	0/2 (0%)	0/2 (0%)	0/2 (0%)
Bone marrow	6	4/6 (66,6%)	1/6 (16.7%)	1/6 (16.7%)	0/6 (0%)
Lymph node	31	24/31 (77,4)	4/31 (12.9%)	3/31 (9.7%)	0/31 (0%)
Skin	16	9/16 (56,3)	2/16 (12.5%)	4/16 (25%)	1/16 (6.2%)
ENT	7	4/7 (57,1%)	1/7 (14.3%)	2/7 (28.6%)	0/7 (0%)
Joints	2	1/2 (50%)	0/2 (0%)	1/2 (50%)	0/2 (0%)
TOTAL	**153**	**69/153**	**27/153**	**51/135**	**6/153**

The histopathological lesions correspond to the host reactions against H. capsulatum and its immune status, and are classified into 4 categories: (a) the tuberculoid type, (b) the anergic type, (c) the intermediate type, and (d) the sequelae type.

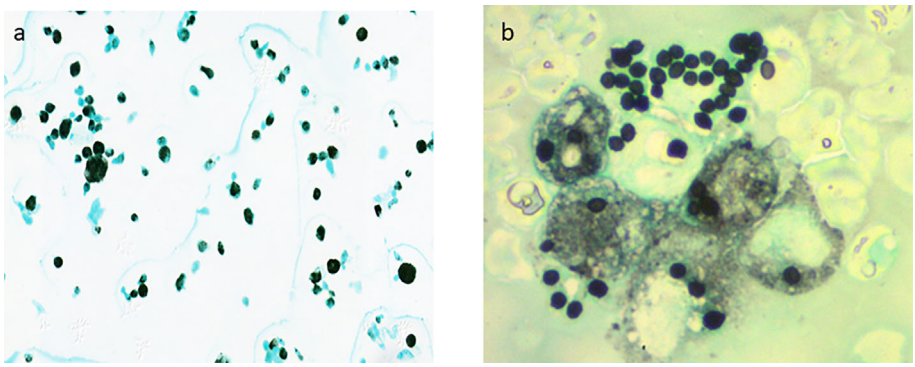

FIGURE 1 | *H. capsulatum* is a small spherical or ovoi yeasts measuring 2 to 6 µm characterized by its ability to make a dimorphic transition to enter host macrophages and to survive intracellularly and proliferate during active infection. **(A)** Pulmonary histoplasmosis: BAL cytology shows macrophages with numerous intracellular *H. capsulatum* (Gomori-Grocott stain x400). **(B)** Disseminated histoplasmosis: Extracellular *H. capsulatum* from blood smear (Gomori-Grocott stain x1500).

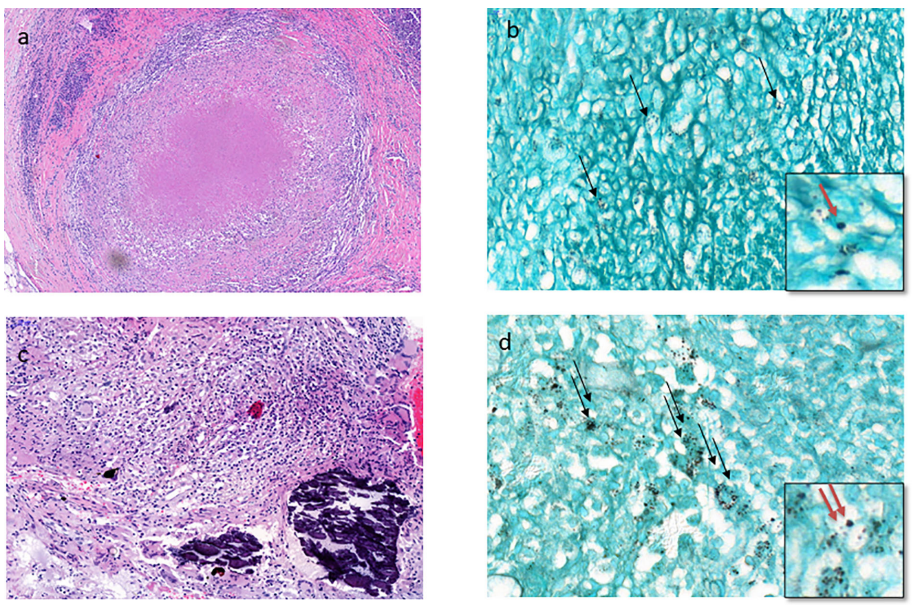

FIGURE 2 | The tuberculoid type of histoplasmosis. **(A)** Lymph node tuberculoid granuloma perfectly mimicking tuberculosis with epithelioid cells, multinucleated giant cells, and caseous necrosis (HES stain x200). **(B)** Few intracellular *H. capsulatum* (black arrow) in the peripheral layers of tuberculoid granuloma of the lymph node (Gomori-Grocott stain x 400) with focus spot (red arrow x1000). **(C)** Branchial biopsy shows less typical granuloma with macrophages, some epithelioid cells, and few multinucleated giant cells and calcifications without necrosis (HES stain x400). **(D)** Moderate number of intracellular *H. capsulatum* (two black arrows) from the same branchial biopsy (Gomori-Grocott stain x 600) with focus spot (two red arrows x1000).

lymph node histoplasmosis was associated with T-cell lymphoma in a patient with HTLV-1 infection.

Digestive Histoplasmosis

In our experience the digestive tract was the most affected organ by histoplasmosis. Seventy-eight of 202 positives samples (38.5%) belonged to the digestive tract (73 biopsies and 5 surgical specimens). Multiple ulcers of the digestive mucosa were the most common endoscopic findings (56/78 cases, 71.7%). Three of the five surgical specimens involved a parietal perforation and two cases involved a pseudotumoral fibro-inflammatory intestinal occlusion.

The colon was the organ most affected by histoplasmosis (53/78 cases, 70%) followed by the small intestine (14/78 cases, 18%). The other sites were less frequently involved: esophagus (3/78 cases, 3.8%), stomach (4/78 cases, 5.2%), rectum (2/78 cases, 2.5%), and anal region (2/78 cases, 2.5%). Concomitant colic and intestinal involvement were observed in 6 cases, and both colic and esophageal involvement in only 1 case.

The numbers of microorganisms were higher in digestive histoplasmosis than in other organs, with a maximum for colonic biopsies (number of *H. capsulatum* per light microscope field at magnification ×400). In addition, in these samples, *histoplasma* were observed in the cytoplasm of histiocytes or free in the stroma. Lymphocyte and histiocyte inflammation of moderate to marked intensity were observed in all positive specimens. Nevertheless, the tuberculoid epithelioid granulomatous form was present in 16/78 (20,5%) specimens including 14 colon and 2 small intestine specimens. The presence of multinucleated giant cells was observed in only 3 of the 16 cases. *H. capsulatum* yeasts were present mainly in the peripheral layers near the granuloma. No granulomas were found in the upper gastrointestinal tract. In addition, mixed inflammatory infiltrate contained plasma cells, neutrophils, and eosinophils were observed. **Figure 3** shows an anergic form of histoplasmosis in the colon.

Liver Histoplasmosis

Eleven cases of liver histoplasmosis were diagnosed in our department in the last 15 years. All eleven patients were HIV-positive and had fever, cholestasis and an altered general condition. On histological examination, the hepatic tissue was the site of moderate to marked lymphohistiocytic inflammatory infiltrates and/or epithelioid granulomas without necrosis (tuberculoid form) in 9 out of 11 cases. The two remaining cases corresponded to a rather anergic form. Sinusoidal hyperplasia of Kupffer cells was also observed in 5 cases. *H. capsulatum* were intra-cellular and occasionally observed in the sinusoid lumen in both cases of the anergic form.

Mucocutaneous Histoplasmosis

Histological analysis revealed the presence of *H. capsulatum* microorganisms in 16 mucocutaneous biopsies (12 skin biopsies, 3 oral mucosa biopsies, and 1 genital mucosa biopsy). Interestingly, the tuberculoid form associating epithelioid granulomas and multinucleated giant cells was the most frequent form (9/15, 60%). Necrosis was consistently absent. The intermediate form was observed in 6 cases (40%). **Figure 4** shows intermediate and sequelae cases of cutaneous histoplasmosis.

Diverse localizations of histoplasmosis were diagnosed by the Pathology Department in the last 15 years including cerebrospinal fluid which correspond to central nervous system involvement (1 case), peritoneal fluid (3 cases), cytology from a prostatic lesion (1 case), and peripheral blood smear in a patient with disseminated histoplasmosis. Seven biopsy specimens of ENT histoplasmosis were observed in our series (3 larynx, 1 cavum, 1 nasal fossa, 1 tonsil, and 1 tongue). We also diagnosed two synovial histoplasmoses, one of them was the subject of a recent case report (Gaume et al., 2017).

DISCUSSION

In the pathology department of the Centre Hospitalier de Cayenne Andrée Rosemon in French Guiana, consecutive patients diagnosed with histoplasmosis were almost exclusively immunocompromised, mainly from advanced HIV-infection. The appearance of histoplasmosis in patients suffering from cancer or treated with immunosuppressive drugs also emphasizes that this infection should be systematically suspected in endemic areas, a suspicion that should lead to specific explorations to identify it.

In this review of over 15 years of activity in the main hospital in French Guiana, we have reported the cytopathological and histopathological aspects of histoplasmosis diagnosed by light microscopy. To our knowledge, this is the largest series of pathological specimens diagnosed with histoplasmosis. The frequency of different types of samples may have reflected local organizational specificities. Hence, first clinicians must be proactive to obtain tissue samples for fungal culture or pathology. When the sample is taken it should be divided and immersed in formalin for pathology whereas it should not for fungal culture. These aspects are not trivial, they require awareness and a specific organization that allows patients and physicians to benefit from at least two complementary diagnostic methods. In French Guiana early on, physicians, and notably gastroenterologists have always been prompt to perform endoscopies to explore diarrheal diseases of HIV thereby identifying a significant number of cases of histoplasmosis, which presumably explains the large number of cases in the digestive tract.

We described the pathological findings in an immunodeficient population whose immune condition may have specificities.

We revealed that *Histoplasma* can be found in and beneath the gastrointestinal mucosa in patients who present multiple

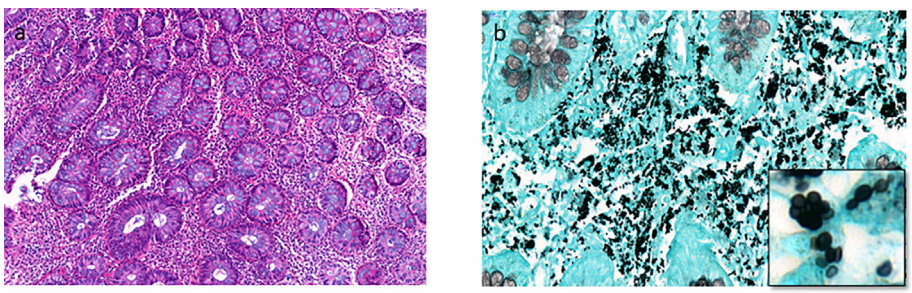

FIGURE 3 | The anergic type of histoplasmosis. **(A)** Colon biopsy shows interstitial moderate and polymorph inflammatory infiltrate including lymphocytes, plasmocytes, and some macrophages (HES stain x200). **(B)** Numerous intracellular and extracellular *H. capsulatum* from the same biopsy (Gomori-Grocott stain x600, with focus spot x1500).

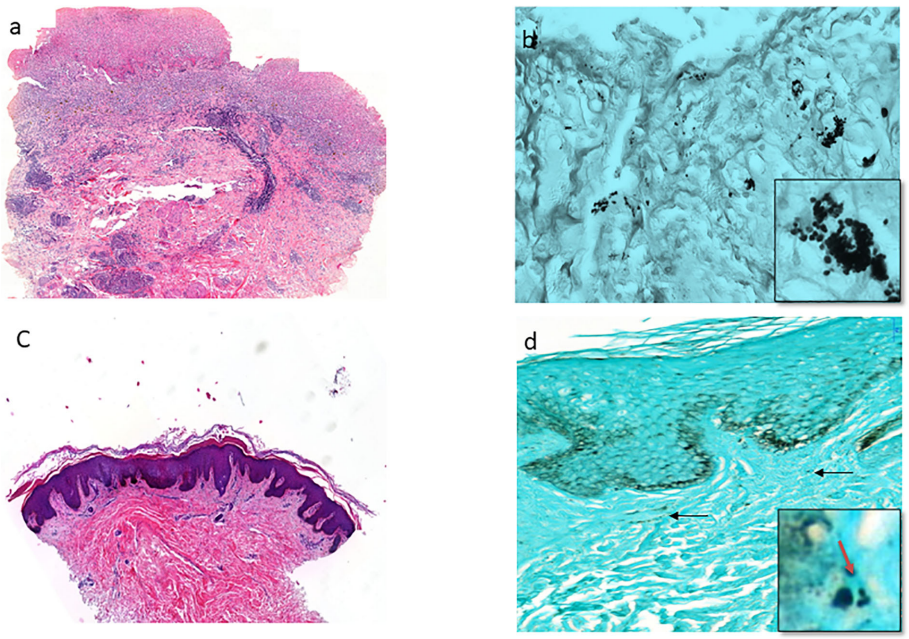

FIGURE 4 | The cutaneous histoplasmosis (intermediate and sequalae types). **(A)** Ulcerative skin biopsy shows marked polymorph dermatitis including neutrophils, lymphocytes, plasmocytes, eosinophils, and few macrophages (HES stain x200). **(B)** Presence of moderate number of intracellular and extracellular *H. capsulatum* in the dermis from the same biopsy (Gomori-Grocott stain x600, with focus spot x1000). **(C)** Skin biopsy shows a particularly fibrous dermis without significant inflammatory infiltration in an HIV patient (HES stain x100). Gomori-Grocott staining shows very rare *H. capsulatum* (black arrow) in the dermis (Gomori-Grocott stain x600, with focus spot and red arrow x1000).

endoscopic ulcers. The ulcers were associated with a large number of *H. capsulatum* yeasts and fever. In ulcers, yeast was often present outside the macrophages or even linked in small chains, a likely sign of intense fungal replication and/or tissue necrosis.

The tuberculoid form was the most common histological form found across all organs. This granulomatous form is found in both immunocompetent and immunocompromised patients. Nevertheless, the typical tuberculoid appearance associating both well-formed epithelioid granulomas and multinucleated giant cells with or without caseous necrosis was not so frequent, a finding that has already been highlighted by previous studies performed only on digestive and hepatic histoplasmosis (Lamps et al., 2000). Granulomas are strongly associated with a high fungal load, which easily leads to diagnosis. However, low fungal loads with <1 *H. capsulatum* yeast per microscopic field ×400, without any real inflammatory infiltrate, are not uncommon and should be diagnosed using the Gomori-Grocott stain, an oil lens with a higher magnification (×1,000) to avoid confusion with other fungal yeasts.

In this series, we reported two cases of histoplasmosis diagnosed following colon and small intestine occlusion by chronic fibro-inflammatory masses of pseudotumoral appearance. Given the diversity of the fungal load and inflammation on the slides, pathologists must be experienced in the identification of this yeast. Overall, the rarity of fibrosis and predominance of tuberculoid forms suggests that the evolution of infections may usually be subacute (1 to 3 months) because fibrotic lesions are usually associated with chronic infections (6 months). The rarity of fibrosis is presumably also a consequence of immune suppression which reduces inflammation. This is consistent with the observation of seasonality which suggested that a significant proportion of histoplasmosis cases were *de novo* infections (Hanf et al., 2010).

The diagnosis of histoplasmosis is not always simple. Most data have been provided from epidemics in predominantly immunocompetent North American populations with lung involvement. Patients in South America and in our series in French Guiana were mostly immunocompromised. While culture provides the strongest evidence of infection, it can be slow, despite recent improvements in culture media, and it requires BSL 3 laboratories. In addition, the antibodies currently in use are based on *H. capsulatum* strains from the United States, which may not be accurate enough for Amazonian strains. Studies have shown a remarkable polymorphism of *H. capsulatum* strains in Brazil, with genetic differences with the American strains leading to possible differences in clinical and laboratory results (Karimi et al., 2002; Zancopé-Oliveira et al., 2005).

A US study of 16 immunocompromised patients suggested that histology was the most useful diagnostic procedure (Kaufman, 1992). Since most of our patients present with severe systemic symptoms that require immediate care, a combination of several laboratory techniques such as direct MGG-stained examination, culture on Sabouraud dextrose agar, examination of pathological specimens (cytology and histology) stained by PAS or Gomori-Grocott, PCR, *Histoplasma* antigen (galactomannan antigen), or serology seems necessary. Information on the efficacy of histopathological examinations in the diagnosis of histoplasmosis

is scarce. Figures found in the literature refer mainly to results obtained mainly from lung samples during the Indiana epidemics and acknowledge a sensitivity of about 60% in immunocompromised patients (Wheat, 2006). On the contrary, the results obtained in the endemic population of South America show a remarkable initial sensitivity in 158 patients including 27 immunocompromised patients (Mata-Essayag et al., 2008). This result highlights the need for pathologists experienced in the diagnosis of infectious agents.

Previous studies based on autopsy results confirm that gastrointestinal involvement was common in disseminated histoplasmosis (Silverman et al., 1955; Queiroz and Siqueira, 1975; Goodwin et al., 1980). However, it caused symptoms in only a few patients (3–12%) in older studies involving mainly immunocompetent patients (Suh et al., 2001), which probably explains why gastrointestinal specimens are rarely considered for the diagnosis of histoplasmosis in daily practice in non-endemic areas.

The gastrointestinal tract was commonly involved in the histoplasma infection. In case of suspicion of histoplasmosis in patients reporting diarrhea or other digestive symptoms, upper tract endoscopy and ileocolonoscopy were often performed in our institute. While upper gastrointestinal specimens taken at the same time of diagnosis often yielded negative results, the ileum and colon were a common site of infection. Histopathology provided valuable information and proved to be very sensitive, probably due to the high number of yeasts found there. Histological examination for digestive histoplasmosis can provide a rapid diagnosis and avoid false negativity due to possible contaminating fungal organisms such as *Candida* yeast, which grow faster than histoplasmosis in the culture broth.

Similarly, cytological and histopathological examinations showed a high sensitivity in pulmonary histoplasmosis. In our experience, cytological examination of BAL fluid allows the diagnosis of pulmonary histoplasmosis and reveals *H. capsulatum* microorganisms within macrophages by PAS and/or Gomori-Grocott staining.

In our series the tuberculoid form was the most common histopathologic findings in liver histoplasmosis biopsies (9/11 specimens, 81,8%). These data are interesting because, unlike most previously published cases, this series involved hepatic tissue samples involved living hospitalized patients and not autopsy specimens.

Bone marrow aspiration was very effective in diagnosing *H. capsulatum*, and was easily able to detect the Gomori-Grocott positive yeast.

Finally, when looking for *H. capsulatum*, the search for other pathogens especially in immunocompromised patients should not be neglected. In our series histoplasmosis was associated with other infectious diseases including toxoplasmosis, *cytomegalovirus*, *Epstein-Barr virus*, *Pneumocystis*, genital herpes, leishmaniasis, syphilis, Chagas disease, local or systemic candidiasis, hookworm disease, dengue fever, leprosy, and cryptococcosis. The discovery of systemic bacterial infection like *Salmonella*, *Pseudomonas*, and *Klebsiella* was also common during hospitalization.

Overall, our results show the good performance of pathological analyses in a population which had a predominance of immunocompromised patients, by the high number of positive cytological and histological samples, and the experience acquired by the pathology team in the daily search for *Histoplasma* microorganisms. Cytological and/or histopathological analysis with an average of 3 days between sample collection and results is a relatively rapid and reliable diagnostic tool for histoplasmosis. In combination with other laboratory analyses the pathological analysis using special routine stains (PAS and Gomori-Grocott) is particularly useful and accurate in gastrointestinal histoplasmosis of the lower digestive tract and in the lungs, but also in other locations of histoplasmosis such as liver, bone marrow, lymph nodes, and skin. Given the diversity of fungal load and the cytological and histological findings on the analyzed specimens, the pathologist must have sufficient experience to identify *H. capsulatum* and think systematically about histoplasmosis as a differential diagnosis in HIV patients. Clinicians must also be aware of the possibility of histoplasmosis and should strive to obtain tissue samples adequately processed so that both fungal culture and cyto-pathology can be performed. Hence, guided by the clinical presentation, digestive endoscopies, bone marrow and lymph node aspiration, and biopsies were contributive standard explorations. Although great hopes have emerged for the scale-up of new rapid diagnostic methods clinicians should make full use of classical methods that are available and that can help save lives.

DATA AVAILABILITY STATEMENT

The original contributions presented in the study are included in the article/supplementary material. Further inquiries can be directed to the corresponding author.

AUTHOR CONTRIBUTIONS

KD: study design, analysis, first draft. MN: editing and final draft. PC, DB, LE, FD, AA, RB, DL, MD: data collection and validation of analysis and manuscript. All authors contributed to the article and approved the submitted version.

REFERENCES

Cano, M. V., and Hajjeh, R. A. (2001). The epidemiology of histoplasmosis: a review. *Semin. Respiratory Infect* 16 (2), 109–118. doi: 10.1053/srin.2001.24241

Cockshott, W. P., and Lucas, A. O. (1964). Histoplasmosis duboisii. *Q. J. Med.* 33, 223–238.

Couppie, P., Aznar, C., Carme, B., and Nacher, M. (2006). American histoplasmosis in developing countries with a special focus on patients with HIV: diagnosis, treatment, and prognosis. *Curr. Opin. Infect. Dis.* 19, 443–449. doi: 10.1097/01.qco.0000244049.15888.b9

Couppié, P., Herceg, K., Bourne-Watrin, M., Thomas, V., Blanchet, D., Alsibai, K. D., et al. (2019). The Broad Clinical Spectrum of Disseminated Histoplasmosis in HIV-Infected Patients: A 30 Years' Experience in French Guiana. *J. Fungi* 5, 115. doi: 10.3390/jof5040115

Damasceno, L. S., de Melo Teixeira, M., Barker, B. M., Almeida, M. A., de Medeiros Muniz, M., Pizzini, C. V., et al. (2019). Novel clinical and dual

infection by Histoplasma capsulatum genotypes in HIV patients from Northeastern, Brazil. *Sci. Rep.* 9, 1–12. doi: 10.1038/s41598-019-48111-6

Darling, S. T. (1906). A protozoon general infection producing pseudotubercules in the lungs and focal necroses in the liver, spleen and lymphnodes. *J. Am. Med. Assoc.* 46, 1283–1285. doi: 10.1001/jama.1906.62510440037003

Emmons, C. W., and Ashburn, L. L. (1948). Histoplasmosis in wild rats: Occurrence and histopathology. *Public Health Rep. (1896-1970)* 63, 1416–1422. doi: 10.2307/4586744

Gaume, M., Marie-Hardy, L., Larousserie, F., Lavielle, M., Roux, C., Leclerc, P., et al. (2017). Histoplasmose ostéo-articulaire à Histoplasma capsulatum. *Med Maladies Infectieuses* 47, 554–557. doi: 10.1016/j.medmal.2017.05.009

Goodwin, R. A.Jr, Shapiro, J. L., Thurman, G. H., Thurman, S. S., and Desprez, R. M. (1980). Disseminated histoplasmosis: clinical and pathologic correlations. *Medicine* 59, 1–33. doi: 10.1097/00005792-198001000-00001

Hanf, M., Adenis, A., Couppie, P., Carme, B., and Nacher, M. (2010). HIV-associated histoplasmosis in French Guiana: recent infection or reactivation? *AIDS* 24, 1777–1778. doi: 10.1097/QAD.0b013e32833999c9

Huber, F., Nacher, M., Aznar, C., Pierre-Demar, M., El Guedj, M., Vaz, T., et al. (2008). AIDS-related Histoplasma capsulatum var. capsulatum infection: 25 years experience of French Guiana. *AIDS* 22, 1047–1053. doi: 10.1097/QAD.0b013e3282ffde67

Karimi, K., Wheat, L. J., Connolly, P., Cloud, G., Hajjeh, R., Wheat, E., et al. (2002). Differences in Histoplasmosis in Patients with Acquired Immunodeficiency Syndrome in the United States and Brazil. *J. Infect. Dis.* 186, 1655–1660. doi: 10.1086/345724

Kaufman, L. (1992). Laboratory methods for the diagnosis and confirmation of systemic mycoses. *Clin. Infect. Dis.* 14, S23–S29. doi: 10.1093/clinids/14.Supplement_1.S23

Lamps, L. W., Molina, C. P., West, A. B., Haggitt, R. C., and Scott, M. A. (2000). The pathologic spectrum of gastrointestinal and hepatic histoplasmosis. *Am. J. Clin. Pathol.* 113, 64–72. doi: 10.1309/X0Y2-P3GY-TWE8-DM02

Mata-Essayag, S., Colella, M. T., Roselló, A., de Capriles, C. H., Landaeta, M. E., de Salazar, C. P., et al. (2008). Histoplasmosis: a study of 158 cases in Venezuela 2000-2005. *Medicine* 87, 193–202. doi: 10.1097/MD.0b013e31817fa2a8

Morote, S., Nacher, M., Blaizot, R., Ntab, B., Blanchet, D., Drak Alsibai, K., et al. (2020). Temporal trends of cutaneo-mucous histoplasmosis in persons living with HIV in French Guiana: early diagnosis defuses South American strain dermotropism. *PloS Negl. Trop. Dis.* 14 (10), e0008663. doi: 10.1371/journal.pntd.0008663

Nacher, M., Adenis, A., Adriouch, L., Dufour, J., Papot, E., Hanf, M., et al. (2011). What is AIDS in the Amazon and the Guianas? Establishing the burden of disseminated histoplasmosis. *Am. J. Trop. Med. Hyg* 84, 239–240. doi: 10.4269/ajtmh.2011.10-0251

Nacher, M., Adenis, A., Blanchet, D., Vantilcke, V., Demar, M., Basurko, C., et al. (2014). Risk factors for disseminated histoplasmosis in a cohort of HIV-infected patients in French Guiana. *PloS Negl. Trop. Dis.* 8, e2638. doi: 10.1371/journal.pntd.0002638

Nacher, M., Adriouch, L., Huber, F., Vantilcke, V., Djossou, F., Elenga, N., et al. (2018a). Modeling of the HIV epidemic and continuum of care in French Guiana. *PloS One* 13, e0197990. doi: 10.1371/journal.pone.0197990

Nacher, M., Blanchet, D., Bongomin, F., Chakrabarti, A., Couppié, P., Demar, M., et al. (2018b). Histoplasma capsulatum antigen detection tests as an essential diagnostic tool for patients with advanced HIV disease in low and middle income countries: A systematic review of diagnostic accuracy studies. *PloS Negl. Trop. Dis.* 12, e0006802. doi: 10.1371/journal.pntd.0006802

Nacher, M., Adenis, A., Guarmit, B., Lucarelli, A., Blanchet, D., Demar, M., et al. (2020). What is AIDS in the Amazon and the Guianas in the 90-90-90 era? *PLoS One* 15 (7), e0236368. doi: 10.1371/journal.pone.0236368

Pan American Health Organization (2020). *Guidelines for Diagnosing and Managing Disseminated Histoplasmosis among People Living with HIV*. Available at: https://iris.paho.org/handle/10665.2/52304#:~:text=Histoplasmosis%20is%20one%20of%20the,every%20year%20in%20this%20Region

Queiroz, A. C., and Siqueira, L. A. (1975). Histoplasmose em material de autópsia. *Rev. Patol Trop.* 4, 107–114.

Rodrigues, A. M., Beale, M. A., Hagen, F., Fisher, M. C., Della Terra, P. P., de Hoog, S., et al. (2020). The global epidemiology of emerging Histoplasma species in recent years. *Stud. Mycol.* doi: 10.1016/j.simyco.2020.02.001

Sepúlveda, V. E., Márquez, R., Turissini, D. A., Goldman, W. E., and Matute, D. R. (2017). Genome sequences reveal cryptic speciation in the human pathogen Histoplasma capsulatum. *MBio* 8 (6), e01339-17. doi: 10.1128/mBio.01339-17

Silverman, F. N., Schwartz, J., Lahey, M. E., and Carson, R. P. (1955). Histoplasmosis. *Am. J. Med.* 19, 410. doi: 10.1016/0002-9343(55)90129-7

Suh, K. N., Anekthananon, T., and Mariuz, P. R. (2001). Gastrointestinal histoplasmosis in patients with AIDS: case report and review. *Clin. Infect. Dis.* 32, 483–491. doi: 10.1086/318485

Teixeira, M. de M., Patané, J. S. L., Taylor, M. L., Gómez, B. L., Theodoro, R. C., de Hoog, S., et al. (2016). Worldwide Phylogenetic Distributions and Population Dynamics of the Genus Histoplasma. *PloS Neglected Trop. Dis.* 10, e0004732. doi: 10.1371/journal.pntd.0004732

Tobon, A. M., Agudelo, C. A., Rosero, D. S., Ochoa, J. E., De Bedout, C., Zuluaga, A., et al. (2005). Disseminated histoplasmosis: a comparative study between patients with acquired immunodeficiency syndrome and non-human immunodeficiency virus-infected individuals. *Am. J. Trop. Med. Hyg* 73, 576–582. doi: 10.4269/ajtmh.2005.73.576

Weydert, J. A., Van Natta, T. L., and DeYoung, B. R. (2007). Comparison of fungal culture versus surgical pathology examination in the detection of Histoplasma in surgically excised pulmonary granulomas. *Arch. Pathol. Lab. Med.* 131, 780–783. doi: 131[780:COFCVS]2.0.CO;2

Wheat, L. J. (2003). Current diagnosis of histoplasmosis. *Trends Microbiol.* 11, 488–494. doi: 10.1016/j.tim.2003.08.007

Wheat, L. J. (2006). Improvements in diagnosis of histoplasmosis. *Expert Opin. Biol. Ther.* 6, 1207–1221. doi: 10.1517/14712598.6.11.1207

Woods, J. P., Heinecke, E. L., Luecke, J. W., Maldonado, E., Ng, J. Z., Retallack, D. M., et al. (2001). Pathogenesis of Histoplasma capsulatum. *Semin. Respir. Infect.* 16 (2), 91–101. doi: 10.1053/srin.2001.24239

Zancopé-Oliveira, R. M., Morais e Silva Tavares, P., and de Medeiros Muniz, M. (2005). Genetic diversity of Histoplasma capsulatum strains in Brazil. *FEMS Immunol. Med. Microbiol.* 45, 443–449. doi: 10.1016/j.femsim.2005.05.018

Zida, A., Niamba, P., Barro-Traoré, F., Korsaga-Some, N., Tapsoba, P., Briegel, J., et al. (2015). Disseminated histoplasmosis caused by Histoplasma capsulatum var. duboisii in a non-HIV patient in Burkina Faso: Case report. *J. Mycol Med* 25, 159–162. doi: 10.1016/j.mycmed.2015.03.002

Conflict of Interest: The authors declare that the research was conducted in the absence of any commercial or financial relationships that could be construed as a potential conflict of interest.

frontiers in Cellular and Infection Microbiology

ORIGINAL RESEARCH
published: 29 October 2020
doi: 10.3389/fcimb.2020.591121

Immunoproteomics Reveals Pathogen's Antigens Involved in *Homo sapiens–Histoplasma capsulatum* Interaction and Specific Linear B-Cell Epitopes in Histoplasmosis

Marcos Abreu Almeida[1], *Rodrigo Almeida-Paes*[1], *Allan Jefferson Guimarães*[2], *Richard Hemmi Valente*[3], *Célia Maria de Almeida Soares*[4] *and Rosely Maria Zancopé-Oliveira*[1*]

[1] Laboratório de Micologia, Instituto Nacional de Infectologia Evandro Chagas, Fundação Oswaldo Cruz, Rio de Janeiro, Brazil, [2] Departamento de Microbiologia e Parasitologia, Instituto Biomédico, Universidade Federal Fluminense, Niterói, Brazil, [3] Laboratório de Toxinologia, Instituto Oswaldo Cruz, Fundação Oswaldo Cruz, Rio de Janeiro, Brazil, [4] Instituto de Ciências Biológicas, Universidade Federal de Goiás, Goiânia, Brazil

OPEN ACCESS

Edited by:
Carlos Pelleschi Taborda, University of São Paulo, Brazil

Reviewed by:
Diego Hernando Caceres, Centers for Disease Control and Prevention (CDC), United States
Alexandre Alanio, Université Paris Diderot, France

***Correspondence:**
Rosely Maria Zancopé-Oliveira
rosely.zancope@ini.fiocruz.br

Specialty section:
This article was submitted to Fungal Pathogenesis, a section of the journal Frontiers in Cellular and Infection Microbiology

Received: 03 August 2020
Accepted: 07 October 2020
Published: 29 October 2020

Citation:
Almeida MA, Almeida-Paes R, Guimarães AJ, Valente RH, Soares CMA and Zancopé-Oliveira RM (2020) Immunoproteomics Reveals Pathogen's Antigens Involved in Homo sapiens–Histoplasma capsulatum Interaction and Specific Linear B-Cell Epitope in Histoplasmosis. Front. Cell. Infect. Microbiol. 10:591121. doi: 10.3389/fcimb.2020.591121

Histoplasmosis is one of the most frequent systemic mycosis in HIV patients. In these patients, histoplasmosis has high rates of morbidity/mortality if diagnosis and treatment are delayed. Despite its relevance, there is a paucity of information concerning the interaction between *Histoplasma capsulatum* and the human host, especially regarding the B-cell response, which has a direct impact on the diagnosis. Culture-based "gold-standard" methods have limitations, making immunodiagnostic tests an attractive option for clinical decisions. Despite the continuous development of those tests, improving serological parameters is necessary to make these methods efficient tools for definitive diagnosis of histoplasmosis. This includes the determination of more specific and immunogenic antigens to improve specificity and sensitivity of assays. In this study, we performed a co-immunoprecipitation assay between a protein extract from the yeast form of *H. capsulatum* and pooled sera from patients with proven histoplasmosis, followed by shotgun mass spectrometry identification of antigenic targets. Sera from patients with other pulmonary infections or from healthy individuals living in endemic areas of histoplasmosis were also assayed to determine potentially cross-reactive proteins. The primary structures of *H. capsulatum* immunoprecipitated proteins were evaluated using the DNAStar Protean 7.0 software. In parallel, the online epitope prediction server, BCPREDS, was used to complement the B-epitope prediction analysis. Our approach detected 132 reactive proteins to antibodies present in histoplasmosis patients' sera. Among these antigens, 127 were recognized also by antibodies in heterologous patients' and/or normal healthy donors' sera. Therefore, the only three antigens specifically recognized by antibodies of histoplasmosis patients were mapped as potential

antigenic targets: the M antigen, previously demonstrated in the diagnosis of histoplasmosis, and the catalase P and YPS-3 proteins, characterized as virulence factors of *H. capsulatum*, with antigenic properties still unclear. The other two proteins were fragments of the YPS-3 and M antigen. Overlapping results obtained from the two aforementioned bioinformatic tools, 16 regions from these three proteins are proposed as putative B-cell epitopes exclusive to *H. capsulatum*. These data reveal a new role for these proteins on *H. capsulatum* interactions with the immune system and indicate their possible use in new methods for the diagnosis of histoplasmosis.

Keywords: *Histoplasma capsulatum*, *Homo sapiens*, immunoproteome, mass spectrometry, epitopes, M antigen, YPS-3, catalase P

INTRODUCTION

Histoplasmosis is a life-threatening systemic mycosis with worldwide distribution, with predominance areas in the Americas (Wheat et al., 2016), caused by the dimorphic fungus *Histoplasma capsulatum* (Teixeira et al., 2016). The mycelial form of *H. capsulatum* is found in the environment and the yeast form is observed during parasitism. Under laboratory conditions, the mycelium form can be cultivated from 25 to 30°C; a temperature switch—up to between 35 and 37°C—in enriched media can reversibly induce the yeast morphotype in this fungus (Sahaza et al., 2020).

In general, infection starts upon inhalation of airborne infectious propagules of *H. capsulatum* that are highly resistant to adverse environmental factors (Frías-De-León et al., 2017). Microconidia are the most frequent infectious elements because of their small size, which facilitates penetration into the pulmonary alveoli. This event is followed by the conversion of the fungus into yeasts, which has been considered a critical factor for the pathogenicity of *H. capsulatum* (Knox and Hage, 2010).

The infection by *H. capsulatum* depends on a complex interaction between the fungus and the mammalian host, with disease prognosis determined by factors such as immune status of the host, strain virulence, and inhaled fungal burden (Sepúlveda et al., 2014). Although histoplasmosis affects either immunologically intact or deficient hosts, individuals with compromised cellular immune response presents more severe manifestations of this disease (Mittal et al., 2019). The yeast cells of *H. capsulatum* are highly adapted to the host since they can survive and reproduce within phagocytic cells (Garfoot and Rappleye, 2016). *Histoplasma capsulatum* strategies against macrophages include evasion from the immune response on entry, inactivation of nitrogen and oxygen reactive species, prevention of phagolysosomal fusion, hindrance of lysosomal pH reduction, siderophore production, and induction of apoptosis for escape and dissemination into the host (Long et al., 2003; Missall et al., 2004; Guimarães et al., 2011; Hilty et al., 2011; Mittal et al., 2019).

Although the cellular immune response is long recognized as relevant in the control of *H. capsulatum* infection, roles for antibodies in the pathogenesis of histoplasmosis have been proposed. In fact, a monoclonal antibody reactive against a cell surface histone-like protein has proved to be protective in a murine histoplasmosis model (Nosanchuk et al., 2003). Also, monoclonal antibodies against heat shock protein 60 (HSP60) can alter the fate of the fungus within phagocytic cells and change host cytokine production profiles (Guimarães et al., 2009), as well as modify qualitatively and quantitatively the gene expression and contents of extracellular vesicles secreted by yeast cells of the fungus, impacting on the effector functions of bone-marrow derived macrophages (Baltazar et al., 2018; Burnet et al., 2020). Moreover, antibodies against the M and H antigens, a catalase B and beta-glucosidase, respectively, are consistently produced by patients with different clinical forms of histoplasmosis and, therefore, are largely applied in serodiagnostic tests (Pizzini et al., 1999; Guimarães et al., 2004; Almeida et al., 2016; Almeida et al., 2019).

Routine serodiagnosis of histoplasmosis is usually performed with the crude supernatant of *H. capsulatum* mycelial cultures known as histoplasmin. This is composed predominantly by C, H, and M antigens. The C antigen is a galactomannan responsible for the cross-reactions observed with other fungal species. The H antigen is a β-glucosidase and the M antigen is a catalase. These last two proteins are widely used as targets for antibody detection in the diagnosis of histoplasmosis (Guimarães et al., 2006).

The use of proteomic methodologies can assist in the identification of proteins involved in the parasite-host interaction process (Pastorelli et al., 2006). Besides clarifying the pathogenesis of mycotic diseases, the recognition of immunologically reactive molecules can aid in the development of more efficient serological tests for diagnosis of infections and differentiation of close-related species (Moreira et al., 2020). Immunoproteomic approach has been successfully applied to identify specific antigens in infectious diseases, as demonstrated for several fungal pathogens such as *Aspergillus fumigatus* (Virginio et al., 2014), *Candida albicans* (Pitarch et al., 2016), *Coccidioides posadasii* (Tarcha et al., 2006), *Cryptococcus gattii* (Martins et al., 2013), *Cryptococcus neoformans* (Neuville et al., 2000), *Paracoccidioides* spp. (Moreira et al., 2020), and *Sporothrix schenckii* (Rodrigues et al., 2015).

In this work, an immunoproteomic approach was employed to characterize *H. capsulatum* proteins specifically recognized by antibodies exclusively present in histoplasmosis patient's serum samples and, therefore with a role in the host-pathogen interaction. Moreover, these specific antigens were identified

and their B-epitopes characterized. Consequently, their applications could improve the serodiagnosis of histoplasmosis.

MATERIALS AND METHODS

Microorganism and Culture Conditions

Histoplasma capsulatum G-217B (ATCC 26032) was used in this study. This is a reference strain used by different research groups worldwide. It has been genotyped and classified in the NAm2 phylogenetic group, which has been proposed to be renamed as the cryptic species *Histoplasma ohiense* (Sepúlveda et al., 2017). The fungus was grown in Ham's F-12 medium supplemented with glucose (18.2 g/L), glutamic acid (1 g/L), 4- (2-hydroxyethyl) -1-piperazinoethanesulfonic acid [HEPES (6 g/L)], and cysteine (8.4 mg/L), pH 7.5. Yeast cells were grown at 36°C for 72 h under constant agitation (150 rpm).

Human Sera

The serum samples used were obtained from patients recruited at the Evandro Chagas National Institute of Infectious Diseases, a reference center for Infectious Diseases in Rio de Janeiro, Brazil. The study included samples from three groups: (i) 10 independent patients with histoplasmosis—confirmed by the isolation of *H. capsulatum* in culture—presenting different clinical manifestations [pulmonary (n = 3), mediastinal (n = 2), and disseminated (n = 5)], (ii) 10 independent patients with culture-proven diseases other than histoplasmosis [aspergillosis (n = 2), coccidioidomycosis (n = 2), cryptococcosis (n = 2), and paracoccidioidomycosis (n = 2)], as well as tuberculosis (n = 2), and (iii) Group NHS—10 samples from different healthy individuals were also included in this study. One serum sample was collected from each participant of the study. These serum samples were stored at −20°C until use. Three pools of sera were built with the samples included in this study and named as follows: (i) histoplasmosis (HPM), (ii) heterologous (HET), and (iii) normal healthy sera (NHS). The use of these samples was approved by the Research Ethics Committee of the Evandro Chagas National Institute of Infectious Diseases–Fiocruz, accession number CAAE 0029.0.009.000-11.

Preparation of Protein Extract

Yeast cells were collected by centrifugation (10.000 g, 10 min, 4°C) and washed three times with phosphate buffered saline (PBS; 1.4 mM KH_2PO_4, 8 mM Na_2HPO_4, 140 mM NaCl, 2.7 mM KCl; pH 7.2). The protein extracts were obtained by mechanical maceration in the presence of liquid nitrogen until complete cell disruption, monitored by light microscopy. Next, extraction buffer (20mM Tris-HCl pH 8.8, 2mM $CaCl_2$) supplemented with protease inhibitors (Complete Mini®, Roche Diagnostics, Manheim, Germany) and zirconia beads (0.5 mm) were added. The material was subjected to vigorous agitation in a Mini-Beadbeater (Biospec products, Bartlesville, OK, USA) for five 30 s cycles, intercalated with 1 min ice bath incubation. The lysate was then subjected to centrifugation at 10.000 g for 15 min at 4°C and the protein concentration (supernatant) was determined by the Bradford method, using bovine serum albumin as standard (Bradford, 1976). Samples were submitted to sodium dodecyl sulfate-polyacrylamide gel electrophoresis (1D SDS-PAGE) according to Laemmli (1970) and two-dimensional gel electrophoresis (2DE). Regarding 2DE, isoelectric focusing was carried out on 11-cm immobilized 3–10 pH gradient gel strips (Immobiline DryStrip gels, GE Healthcare Biosciences). Each protein extract (200 μg) was solubilized in 200 μl of rehydration solution [8 M urea, 2% (w/v) 3-[(3-cholamidopropyl)-dimethyl-ammonio]-1-propane sulfonate (CHAPS), 1% (w/v) ampholytes (IPG Buffer 3–10 linear), 0.1 M dithiotreitol (DTT), and 0.002% (w/v) bromophenol blue (BFB)]. The active rehydration and isoelectric focusing steps were performed in an Ettan IPGphor system (GE Healthcare Biosciences) under the following conditions: 30 V for 12 h, 200 V for 1 h, 500 V for 1 h, 1,000 V for 1 h, 3,500 V for 30 min, and 6,000 V for 6 h. For the second dimension, proteins were reduced with 0.1% (w/v) DTT followed by alkylation with 0.4% (w/v) iodoacetamide; both steps in equilibrium buffer [1.5 M Tris-HCl pH 8.8; 6 M urea, 30% (v/v) glycerol, 2% (w/v) SDS, and 0.002% (w/v) BFB] at constant agitation for 15 min each step. After this preparation, the strips were placed on the top of 12% polyacrylamide gels with SDS (Laemmli, 1970) and the system sealed with 0.5% (w/v) agarose in Tris-glycine buffer. The electrophoretic run was carried out at 15°C on a Protean II system (Bio-Rad) under the following conditions: 3 mA for 30 min and 25 mA until the end of the run. The proteins were colloidal Coomassie blue- or silver-stained.

Serological Tests

All sera included in this study were individually tested through the Outcherlony double immunodiffusion test using histoplasmin as an antigen (Guimarães et al., 2006). In addition, a Western blot assay (Pizzini et al., 1999) was performed to check the individual reactivity of the 30 included serum samples, as well as the three pool of sera described previously, against the protein extract prepared from the yeast cells of G217B *H. capsulatum* strain. Moreover, to check whether inespecific reactions could occur between the secondary antibody (alkaline phosphatase-conjugated AffiniPure goat anti-human IgG, Fc fragment specific, Jackson ImmunoResearch, West Grove, PA, USA) and the protein extract, a conjugate control was performed, where only the secondary antibody was added to the nitrocellulose strip with the antigen.

Co-Immunoprecipitation Assay

For the co-immunoprecipitation step, magnetic microspheres—Dynabeads® Protein G (Invitrogen, California, USA)—were used, following a previously described protocol (Moura et al., 2011). In the antibody-binding step, 50 μl of the solution containing the microspheres were resuspended and separated on a magnetic platform for 5 min and the supernatant was removed. The microspheres were washed three times (5 min each) in 200 μl of PBS with 0.1% Tween 20 (PBS-T). Ten micrograms of protein from each serum pool (HPM, HET, and NHS) were individually analyzed. As an additional control, the microspheres were incubated with PBS only (CON). Experimental triplicates were performed for each condition. Each serum pool was diluted to 50

μg/ml of total proteins in PBS and 200 μl of the dilution was applied to the beads and incubated for 2 h at room temperature under rotation. Again, the microspheres were separated, and washed three times in PBS-T after supernatant disposal. For the crosslinking step, 200 μl of a 13 mg/ml DMP (dimethyl pimelimidate) solution in PBS (pH 9.0) were added and incubated for 15 min under rotation at room temperature. The microspheres were subjected to three washes in PBS-T, as described above. At the immunoprecipitation stage, 25 μg of *H. capsulatum* protein extract, prepared as described above, diluted in 200 μl of PBS-T were incubated with the magnetic microspheres and submitted to rotation at room temperature for 2 h. Again, microsphere separation and washing steps were carried out. For the elution step, the microspheres were resuspended in 100 μl of PBS-T and transferred to a new tube. The polypeptides were eluted in 50 μl of a solution containing 0.1 M glycine (pH 2.8) incubated for 5 min at room temperature under rotation. The microspheres were separated for 5 min, the supernatant removed, and the pH adjusted to 7.0. Subsequently, the samples were dried on a centrifugal vacuum concentrator (Speed-Vac, Thermo) and stored at −20°C until further processing.

Shotgun Mass Spectrometry (MS) Protein Identification

For each dried sample resulting from the coimmunoprecipitation assays (above), 100 μg of protein were submitted to trypsin digestion. Samples were initially resuspended in 20 μl of a solution containing 0.4 M ammonium bicarbonate, 8 M urea, followed by addition of 5 μl of 0.1 M dithiotreitol and incubation at 37°C for 30 min. Then, 5 μl of 0.4 M iodoacetamide were added and incubated for 15 min at room temperature in the dark. Samples were diluted by addition of 130 μl of Milli-Q water followed by trypsin (Promega, Wisconsin, USA) addition at 1/50 (m/m) of enzyme to substrate; first incubation for 16 h at 37°C and second incubation at 56°C for 45 min; reaction was stopped with 20 μl of 10% (v/v) formic acid. Samples were then desalted with in-lab-generated columns packed with Poros R2 resin (Life Technologies). Columns were initially activated with 100% acetonitrile (CH_3CN), followed by equilibration with 1% (v/v) trifluoroacetic acid (TFA). Samples were applied to the columns and subjected to five washes with 0.1% TFA solution. The elutions were carried out with four washes of 0.1% TFA in 70% CH_3CN. Samples were dried on a centrifugal vacuum concentrator (SpeedVac, Thermo) and stored at −20°C until use. Prior to MS, each sample was resuspended in 20 μl of 1% formic acid. MS analysis was conducted in technical triplicate (4 μl injection per replicate) for samples HPM, HET, and NHS and technical duplicate for sample CON. Briefly, peptides were submitted to reversed-phase nanochromatography (EASY-nLC II, Thermo) coupled to a high-resolution nano-electrospray ionization mass spectrometer (LTQ Orbitrap XL, Thermo), using the data-dependent analysis mode with MS1 spectra being acquired in the orbitrap analyzer and MS2 spectra in the linear trap. Detailed experimental settings were the same as previously described (Brunoro et al., 2015), to the exception of column length, gradient duration, and number of most intense ions submitted to CID for each spectra, which were 20 cm, 168 min, and 7 ions/spectra, respectively, in the present work.

Data Analysis

All MS/MS spectra were analyzed using PEAKS Studio 8.5 (Bioinformatics Solutions, Canada). After data refinement with the precursor (mass only) correction option, PEAKS DE NOVO analysis was run assuming trypsin digestion, with a fragment ion mass tolerance of 0.60 Da and a parent ion tolerance of 10 ppm. Cysteine carbamidomethylation (+57.02 Da) was set as fixed modification and methionine oxidation (+15.99 Da) as variable modification; a maximum of three variable modifications per peptide was allowed. PEAKS DB analysis was performed using these same parameters plus the possibility of up to two missed enzyme cleavages and non-specific cleavage at one side of the peptides. Searches were made against an NCBInr database subset for "*H. capsulatum*" (37,754 entries). False discovery rates (FDR) were estimated through the PEAKS decoy fusion approach, and only peptide/protein identifications with FDR values ≤1% were accepted. Identified proteins were subjected to *in silico* analysis using UniProt database (www.uniprot.org) and WoLF PSORT server (https://wolfpsort.hgc.jp/). UniProt database was used to categorize the proteins according to their function and WoLF PSORT server to predict subcellular localization of the proteins. Presence of the proteins within *H. capsulatum* extracellular vesicles (EVs) was performed comparing our proteomic data with data previously described on proteomics of EVs (Albuquerque et al., 2008; Baltazar et al., 2018). After that Venn diagrams were created using the Venny 2.1 tool (http://bioinfogp.cnb.csic.es/tools/venny/) to determine which proteins were recognized by the serum pool of patients with histoplasmosis (HPM) detected in the three experimental replicates. From this intercession, new Venn diagrams were constructed with all proteins recognized by the serum pool of patients with other infections (HET), serum pool of normal healthy sera (NHS), and with all proteins recognized in the control experiment. In the HET, NHS, and control conditions, proteins identified in at least one of the replicates were considered in the exclusion analysis, in order to determine which proteins were specifically recognized by antibodies present in serum samples from patients with histoplasmosis. Proteome data could be found on: 10.17605/OSF.IO/FVMGE.

In Silico Protein Similarity and Antigenicity Analysis

The polypeptide sequences of proteins identified from coimmunoprecipitation, and which reacted specifically with the HPM serum pool, were submitted to the basic local alignment search tool for proteins (BLASTp) to search for sequence similarity. For antigenicity analysis, the amino acid sequences were evaluated using the software DNAStar Protean 7.0 (DNASTAR Inc.), by the Jameson-Wolf algorithm, associated with the hydrophobicity index (Kyte-Doolittle) and the surface accessibility probability of the protein (Emini). In parallel, in order to complement the B epitope prediction, the amino acid

sequences were analyzed by the epitope prediction online server, BCPREDS (http://ailab.ist.psu.edu/bcpred/index.html). The primary sequences of the proteins were given as input and the prediction of B cell epitopes was restricted to epitopes of fixed length of 20 amino acids. The standard specificity of 75% was used, and for the output of the results, the option of presenting only non-overlapping epitopes. The sequences of antigenic proteins and its possible epitopes demonstrated by analysis in bioinformatics tools had their homology analyzed against proteins from other pathogenic organisms that could have a confounding factor with histoplasmosis, using BLASTp.

RESULTS

Profile of Proteic Extract

Histoplasma capsulatum yeast protein extract was analyzed by SDS-PAGE and 2DE. Even though no quantitative evaluation was made, the extract displayed a heterogeneous proteic migration profile (as expected), with a broad distribution of molecular masses (**Figure 1A**, lane 2 and **Figure 1B**, vertical axis) and most proteins focusing in the *ca.* 5 to 8 pI range, although several proteins displayed high pI (>8) migration; this was not the case for the acidic region (pI < 5) (**Figure 1B**, horizontal axis).

Immunoreactivity of Individual Serum Samples

All but one serum sample (HPM6) from patients with histoplasmosis were reactive in the double immunodiffusion test against histoplasmin, while all heterologous and normal human sera were negative in this regular serodiagnostic test. When the reactivity of these sera was tested against the protein extract produced in this study a diverse profile of antigenic recognition was observed among the individual sera, with patients with histoplasmosis presenting more recognized antigens than healthy individuals, as expected. Patients with paracoccidioidomycosis and aspergilosis also presented reactivity against a large number of antigenic proteins, while the reactivity was lower in sera from patients with cryptococcosis, coccidioidomycosis, and tuberculosis (**Supplementary Figure 1**).

Immunoproteomics

Proteomic analysis of potential antigen recognition by antibodies present in the pooled sera of patients with different clinical forms of histoplasmosis (HPM) identified a total 247 proteins (**Table S1**). However, only 132 antigenic proteins were commonly detected among the three biological replicates analyzed, were selected for further studies (**Figure 2A** and **Table S5**). Assays with heterologous pooled sera of patients with other mycoses or tuberculosis (HET), pooled normal healthy donors sera (NHS), and mock PBS control (CON) identified 355 (**Table S2**), 165 (**Table S3**), and 38 (**Table S4**) proteins, respectively.

The 132 proteins recognized in all HPM immunoproteomics data (**Table S5**) were classified according to the functional categories and subcellular localization, based on the UniProt database and WoLF PSORT server, respectively (**Figure 3** and **Table S6**). **Figure 3A** shows that most proteins were related to protein synthesis (47; 35.60%), followed by transcription (30; 22.70%), energy (20; 15.20%), metabolism (7; 5.30%), cell cycle and DNA processing (7; 5.30%), protein fate (4; 3.00%), cell rescue, defense, and virulence (3; 2.30%), and cellular transport (1; 0.80%). Thirteen proteins with unknown function totalized

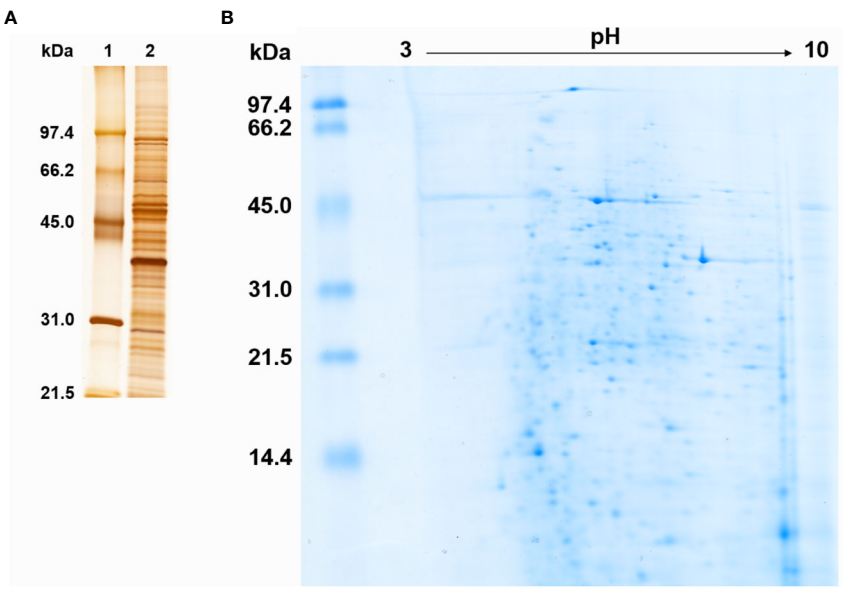

FIGURE 1 | Protein profile of *Histoplasma capsulatum* yeast cell extract. **(A)** Silver stained SDS-PAGE under reducing conditions. 1, Molecular mass standard; 2, Yeast cell extract of *H. capsulatum*. Numbers on the left correspond to the molecular mass (kDa) of the standards. **(B)** Colloidal Coomassie blue stained 2DE. The linear pH gradient range is indicated above the gel and the molecular mass standards (kDa) are on the left.

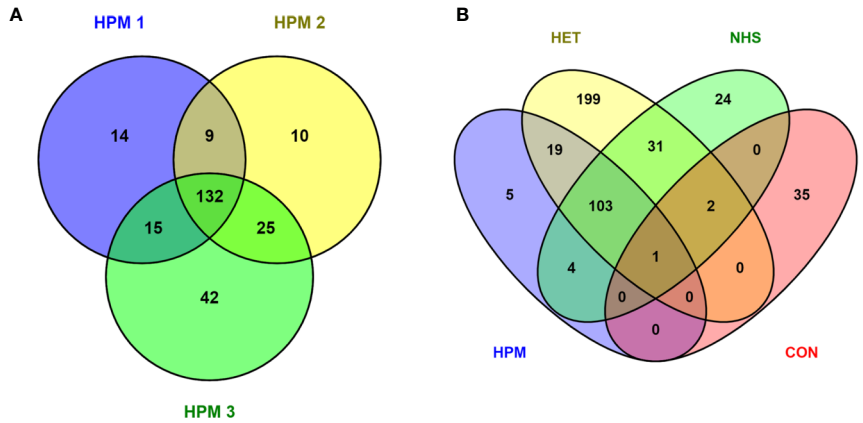

FIGURE 2 | Venn diagrams depicting *Histoplasma capsulatum* proteins (potential antigens) recognized by the different pooled sera groups. **(A)** Number of proteins recognized by the pooled sera of patients with histoplasmosis (HPM) for the three biological replicates analyzed (HPM 1, HPM 2, and HPM 3); **(B)** The 132 proteins in common to all conditions in panel A were compared to the total list of proteins detected in at least one of the biological replicates for the other conditions: HET, pooled sera of patients with other fungal infections or tuberculosis; NHS, pooled sera of normal healthy donors; CON, mock control: phosphate buffered saline.

9.80%. The prediction of subcellular localization of proteins revealed that most of them were classified as mitochondrial (91; 68.94%), followed by nuclear (24; 18.18%), cytoplasmic (9; 6.82%), extracellular (4; 3.02%), peroxisomal (2; 1.52%), plasma membrane (1; 0.76%), and cytoskeleton (1; 0.76%), as shown in **Figure 3B**.

Among the 132 antigenic proteins recognized by antibodies present in sera from patients with histoplasmosis, five protein entries were specifically recognized by these antibodies, without cross-reaction with antibodies present in sera from other conditions (**Figure 2B** and **Table S5**), namely: catalase (C0NVF6), catalase B (Q9Y7C2), M antigen (O13373), Yeast phase specific protein (Q8J1T0), and YPS-3 protein (Q00950). A BLASTp analysis of the identified catalase (C0NVF6) revealed 100% identity and query cover with the catalase isozyme P of *H. capsulatum* (accession number EEH04495), and therefore we refer to this protein as catalase P from now on. When the sequences from these five protein entries were compared, using the BLASTp, results showed that two of these entries consisted of fragments from larger proteins, which were also identified as specific through the strategy herein employed. Thus, after the removal of duplications, there were only three proteins supposedly with antigenic activity and specifically recognized by antibodies in sera of histoplasmosis patients, with high applicability on the diagnosis of histoplasmosis: catalase P, M antigen, and YPS-3.

B-Cell Epitope Prediction of Specific Antigens of *Histoplasma capsulatum*

The three specific candidate proteins as antigenic targets were then analyzed by the DNAStar software, combining the determination of antigenicity indexes (Jameson-Wolf algorithm), the hydrophobicity index (Kyte-Doolitle algorithm), and the probability of accessibility to the surface of the protein (Emini algorithm). As an additional analysis, an epitope prediction software (BCPREDS) was used, and 13 regions were proposed as possible B epitopes within the M antigen, 12 regions in the catalase P, and only 3 regions in the YPS-3 protein (**Table S7**). For identification of possible specific *H. capsulatum* B cell epitopes, the results obtained in the two bioinformatics tools (DNAStar and BCPREDS) were overlapped. Taking into account regions with high antigenic indices, combined with the hydrophobicity index and the probability of localization on the surface of the molecule, and considering only B cell epitopes having a BCPREDS score >0.8, sixteen regions have been proposed as the most immunogenic. Seven regions in M antigen, seven in catalase P, and two in YPS-3 protein, as shown in **Figure 4**. Finally, for further evaluation of the specificity of these epitopes, we performed an *in silico* analysis of their homology with proteins from other pathogens causing fungal diseases or infectious diseases that can be misdiagnosed as histoplasmosis. These data are presented in **Table S8**. In brief, it was observed a degree of similarity among epitopes previously showed in *Blastomyces dermatitidis* and *Tallaromyces marneffei*. However, four epitopes, two from catalase P (epitopes 1 and 12), one from the M antigen (epitope 1), and one from YPS-3 (epitope 1) presented low sequence identity with the organisms tested and could be considered specific for *H. capsulatum* (**Table S8**).

DISCUSSION

Histoplasmosis is a systemic mycosis much more widespread than the literature and epidemiological reports demonstrate (Antinori, 2014). Although a high endemicity was demonstrated in the Americas, the current knowledge of its distribution is incomplete (Bahr et al., 2015). Despite the relevance of this disease, there is a paucity of information regarding the interaction between *H. capsulatum* and the human host, especially regarding the B-cell response, which has a direct impact on the diagnosis of the infection.

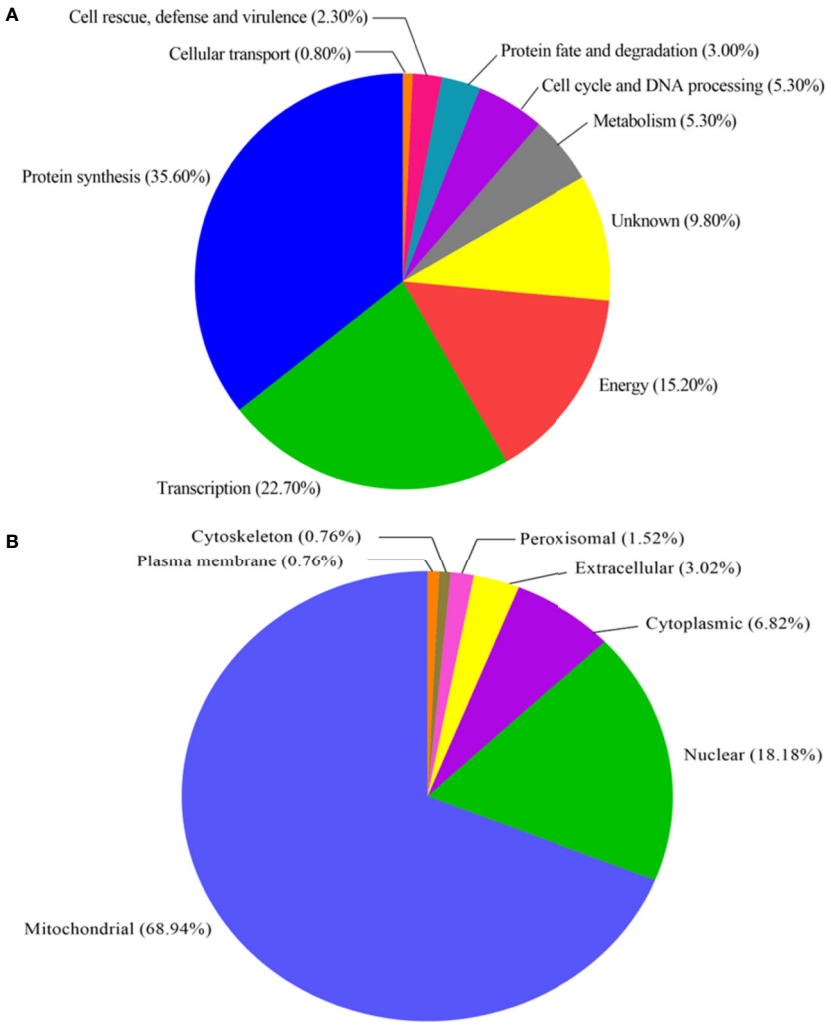

FIGURE 3 | Functional classification and subcellular localization of immunoreactive proteins identified in *Histoplasma capsulatum*. **(A)** Functional classification of proteins based on UniProt database; **(B)** Subcellular localization of proteins based on the WoLF PSORT server.

The gold standard diagnosis of histoplasmosis occurs by demonstration of the yeast-like *H. capsulatum* cells on microscopic examination and isolation of the fungus in culture of clinical specimens. However, these methods may require invasive medical procedures, the culture test is time-consuming, and conversion to the yeast form is essential, requiring up to 8 weeks to reveal fungal growth. Thus, in many situations, the diagnosis of histoplasmosis is based on serological tests to detect antibodies and/or antigens (Almeida et al., 2019). On the other hand, much remains to be done to improve the laboratory diagnosis. The serological tests available still have limitations (Azar and Hage, 2017), and the discovery of new antigenic targets would be essential to improve the diagnosis of histoplasmosis and possible development of vaccines, since there is still no vaccine available against *H. capsulatum* (Roth et al., 2019).

The use of proteomic tools for the identification of proteins involved in the parasite-host interaction, and presumed to be antigenic targets, has been applied to pathogenic fungi studies (Crockett et al., 2012; Ball et al., 2019; Moreira et al., 2020). Thus, our work used co-immunoprecipitation followed by mass spectrometry to identify proteins involved the interplay between host and pathogen, specifically those recognized by B-cell receptor and their B-cell antibodies products, as with the identification of presumed antigenic targets with possible application in diagnostic tests.

A total of 132 antigenic proteins were recognized by antibodies from patients with histoplasmosis. Most of these molecules were ribosomal proteins related to protein synthesis and transcription. However, proteins with relevant roles in the parasite-host interaction have also been identified within this pooled. The list included proteins that contribute to the survival of *H. capsulatum* after oxidative stress produced by the innate immune system, such as the alternative oxidase and catalases B and P, may be important for virulence of this fungus (Johnson et al., 2003; Holbrook et al., 2013). Also, a cell surface antigen of

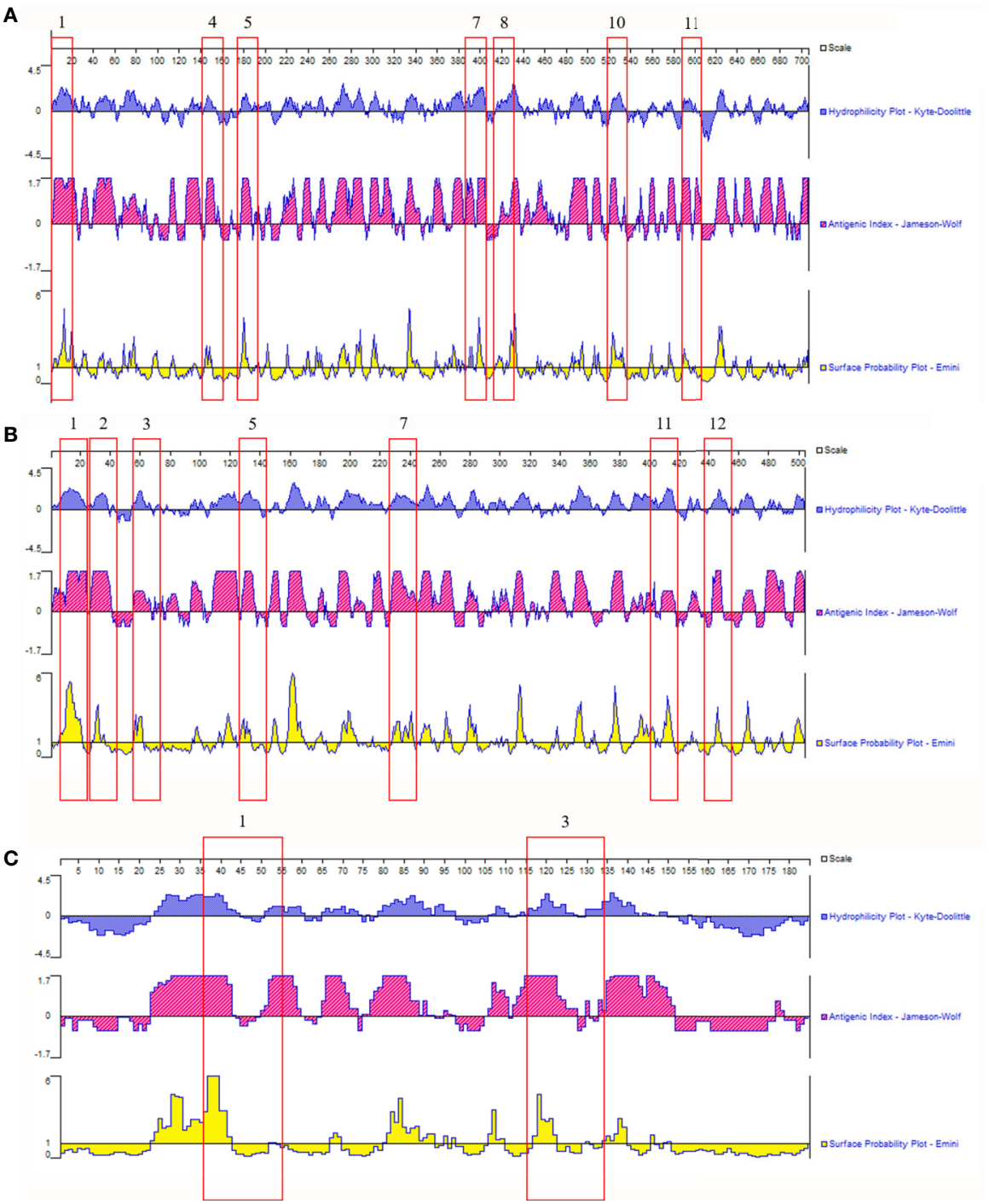

FIGURE 4 | *In silico* evaluation of putative B epitopes on candidate proteins for antigenic targets for the diagnosis of histoplasmosis. Results obtained from overlapping data from two bioinformatics tools: the software DNAStar Protean 7.0 and BCPREDS server. **(A)** M antigen; **(B)** Catalase P; **(C)** YPS-3. The flagged numbers refer to the peptides described in **Table S7**.

H. capsulatum, histone 2B, related with binding to host cells and that has the ability to modulate the intracellular fate of the fungus (Nosanchuk et al., 2012), was identified. Another find was YPS-3 protein, localized in the cell wall and culture supernatants of *H. capsulatum*, which may influence the dimorphic transition. The *yps-3* gene expression is not fundamental for the transformation to the yeast phase, but it may facilitate adaptive processes that allow mycelium-to-yeast transition and survival at elevated host

temperatures. Moreover, YPS-3 has already been associated with increased fungal burden in phagocyte-rich tissues (Keath et al., 1989; Weaver et al., 1996; Bohse and Woods, 2007).

Other proteins identified in this study with reactivity to the sera of patients with histoplasmosis have already had their functions described in other models. The nascent polypeptide-associated complex (α, β_1 and β_3 subunits) was found in *Saccharomyces cerevisiae*, in which the deletion of one subunit causes downregulation of the remaining subunits at physiological growth temperature. Cells lacking both β -subunits are have not been able to grow at 37°C (Reimann et al., 1999). Mills and colleagues (2016) proposed that increased mitochondrial oxidation of succinate *via* succinate dehydrogenase and an elevation of mitochondrial membrane potential combine to drive mitochondrial reactive oxygen species production. Thus, the same could happen in *H. capsulatum*, since succinate dehydrogenase was reactive to sera from patients with histoplasmosis in this study. However, *H. capsulatum* produces catalases that break down H_2O_2 into H_2O and O_2, working as a protection against oxidative mechanisms of the host (Maresca and Kobayashi, 2000).

The dihydrolipoamide succinyltransferase protein has already been described as immunogenic and potentially protective in some bacteria (Nguyen et al., 1999; Zygmunt et al., 2001; Gilmore et al., 2003). In our study dihydrolipoamide succinyltransferase also showed antigenicity, even though not specific to *H. capsulatum*. This protein was also recognized by heterologous pooled sera and the normal healthy pooled sera.

It was surprising that most immunoreactive *H. capsulatum* proteins were predicted with intracellular localization. In fact, *in silico* analysis regarding the cellular location of these proteins revealed that most of them were present in mitochondria. However, we found literature data (Albuquerque et al., 2008; Baltazar et al., 2018) supporting that approximately 57% of the proteins found in our study have already been identified by proteomic tools when analyzing macromolecules secreted within extracellular vesicles of *H. capsulatum* (**Tables S6**). These proteins could, through EVs transport, be accessed by the immune system and activate B-cells.

Since the contents of the *H. capsulatum* EVs produced during parasitism are not fully characterized and such contents change, depending on the microenvironment (Baltazar et al., 2018; Cleare et al., 2020), it is possible that the intracellular proteins detected as immunogenic in our proteomic approach become available to the immune system through EVs produced in the mammalian host. Future studies should be performed to test such hypothesis.

Surprisingly, beta-glucosidase, also known as H antigen, was not identified in our proteomic approach. This molecule is reported as a secreted protein of mycelium and yeast cells of *H. capsulatum*, and high levels of the H antigen were detected in supernatants of G217B yeast cell cultures. However, antibodies anti-H are found in less than 20% of patients with histoplasmosis (Azar and Hage, 2017). This fact could explain the absence of this protein in our immunoproteomic assay.

Although a high number of *H. capsulatum* proteins are recognized by antibodies present in pooled sera from patients with histoplasmosis, most of them are also recognized by antibodies from patients with other infectious diseases or healthy individuals, indicating a certain degree of similarity on the immunopathogenesis of these diseases. Three proteins are proposed as specific antigenic targets: M antigen, catalase P, and YPS-3.

In previous studies, the M antigen had its biological nature identified, was structurally characterized and its expression was detected on the yeast cell surface; in addition, it was characterized as a useful exoantigen in the diagnosis of histoplasmosis (Zancopé-Oliveira et al., 1999; Guimarães et al., 2008). However, catalase P and YPS-3 protein have been studied and characterized as virulence factors in *H. capsulatum* (Johnson et al., 2002; Bohse and Woods, 2007), but not yet described as antigenic targets.

In *H. capsulatum*, catalase P has already been described as a virulence factor and is involved in the response to oxidative stress. It is referred to as a protein with similarity to the well-known peroxisomal catalases of animals and yeasts of the order *Saccharomycotina* (Johnson et al., 2002). The transcriptional expression of the *H. capsulatum* CATB (M antigen) and CATP (catalase P) genes was assessed by Northern blot and the results at the transcript levels are shown for three conditions: cell morphology, carbon source, and response to oxidative stress. These results demonstrated regulation of CATB and CATP only by the availability of different carbon sources (Johnson et al., 2002).

Histoplasma capsulatum was grown in different concentrations of H_2O_2 to evaluate the role of catalases in oxidative stress *in vitro*, presenting progressive reduction in growth with increased concentrations of hydrogen peroxide from 1.0 mM up to 1.6 mM. However, no growth occurred by 120 h in concentrations higher than 1.6 mM (Guimarães et al., 2008).

The YPS-3 protein, present in the cell wall and also released in culture medium, is produced only by the yeast phase of *H. capsulatum* (Bohse and Woods, 2005). Its location suggests that YPS3 is a protein capable of being recognized by antibodies and the results of the present study show for the first time the antigenic potential of this protein. A previous study proposed YPS3 to be virulence factor involved in the progression of the disseminated disease, since, when its production was blocked by interference RNA in animal infection, the mutants showed a significant decrease in fungal dissemination (Bohse and Woods, 2007).

Our data suggest that the three proteins identified as antigenic targets could be used in the development of alternative methods of histoplasmosis diagnosis. However, when assessing homology with other infectious agents, some B cell epitopes of M antigen and catalase P showed high rates of sequence identity with regions of *Blastomyces dermatitidis* and *Talaromyces marneffei*, reaching up to 100% identity (such as epitope 2 of catalase P, and epitopes 5, 8 and 10 of M antigen). This could be a problem in regions where there is an overlap of endemic areas of these diseases. However, we could not demonstrate this situation since serum samples from patients with blastomycosis, frequent in the Mississippi and Ohio River valleys (US) and Midwestern states and Canadian provinces that border the Great Lakes, and areas adjacent to the Saint Lawrence

Seaway (Castillo et al., 2016), and talaromycosis endemic to Southeast Asia (Chan et al., 2016) are not available in our country. Consequently, they were not included in the heterologous pooled sera being a limitation of this study. In order to circumvent this limitation, avoiding possible cross reactions, more specific B cell epitopes could be used as targets in possible immunoassays, such as epitopes 1 and 12 of catalase P, and epitope 1 of M antigen, which showed low identity (values between 42 and 78% of identity) with regions of *B. dermatitidis* and *T. marneffei*. Future studies regarding the application of YPS-3 and the aforementioned epitopes of M antigen and catalase P are necessary to improve the immunodiagnosis of histoplasmosis.

Another relevant limitation of the study is that only one *H. capsulatum* strain was evaluated. This strain is the holotype of the proposed *H. ohiense* cryptic species and one of the most studied *Histoplasma* strains around the world. It is possible that different proteins are involved in the host-pathogen interaction of other phylogenetic clades. Future studies with different clades and cryptic species are necessary to a deeper knowledge of the immunopathogenesis of histoplasmosis.

The major aim in this study was to detect specific antigenic proteins that could be used to develop future assays to be employed in endemic areas of histoplasmosis. Therefore, the use of a control group from an endemic area would improve the detection of such proteins. It is expected that individuals living in non-endemic areas of histoplasmosis have less cross-reacting antibodies against *H. capsulatum*, and therefore, the three proteins identified as specific in this study (M antigen, catalase P, and YSP-3) should be also suitable as diagnostic markers in non-endemic areas of this mycosis.

CONCLUSION

The diagnosis and management of histoplasmosis remains a major public health problem in several countries. The knowledge the interplay between host and pathogen during infection and the ability to definitively diagnose histoplasmosis has become even more important due to the increasing number of patients susceptible to this disease. Proteomic tools could elucidate the mechanisms of fungal pathogenesis, the relationship between host and pathogen during infection, and also identify of antigenic targets.

This is the first study to use immunoproteomic approaches to identify proteins with a high antigenic index and map specific epitopes for the diagnosis of histoplasmosis. Besides that, bioinformatic tools made it possible to carry out other analyzes, such as functional classification and subcellular localization.

Three antigenic proteins of *H. capsulatum* are described in this study as putative candidates for the immunodiagnostic of histoplasmosis: catalase P, M antigen, and YPS-3. Also, 16 epitopes proposed as exclusive of *H. capsulatum* were mapped using bioinformatics. Among these, four epitopes are proposed as the most promising candidate once it shows lowest homology with proteins of other pathogens that could be misdiagnosed with histoplasmosis.

In conclusion, the three immunogenic proteins described in this work may be applied to histoplasmosis immunodiagnosis, as well as patient follow-ups, treatment, and putative vaccine candidate.

DATA AVAILABILITY STATEMENT

The original contributions presented in the study are included in the article/**Supplementary Material**. Further inquiries can be directed to the corresponding author.

ETHICS STATEMENT

The studies involving human participants were reviewed and approved by the Research Ethics Committee of the Evandro Chagas National Institute of Infectious Diseases–Fiocruz, accession number CAAE 0029.0.009.000-11. Written informed consent for participation was not required for this study in accordance with the national legislation and the institutional requirements.

AUTHOR CONTRIBUTIONS

MAA, RA-P, and AJG performed the experiments. MAA, RA-P, AJG, and RHV analyzed and interpreted the data. CMAS and RMZ-O participated in the design of the study and revised this manuscript. All authors contributed to the article and approved the submitted version.

FUNDING

This work was supported by grants from Conselho Nacional de Desenvolvimento Científico e Tecnológico (CNPq), Fundação de Amparo à Pesquisa do Estado do Rio de Janeiro (FAPERJ), and Fundação de Amparo à Pesquisa do Estado de Goiás (FAPEG). RA-P was supported in part by CNPq (305487/2015-9). AG was supported by CNPq (311470/2018-1) and FAPERJ (E-26/202.696/2018). RV is a fellow from CNPq (Grant 304523/2019-4). CS was supported by FAPEG/INCT (10267000022). RZ-O was supported in part by CNPq (302796/2017-7) and FAPERJ (E-26/202.527/2019). We are grateful for support from the Coordination for the Improvement of Higher Education Personnel (CAPES).

SUPPLEMENTARY MATERIAL

The Supplementary Material for this article can be found online at: https://www.frontiersin.org/articles/10.3389/fcimb.2020.591121/full#supplementary-material

SUPPLEMENTARY FIGURE 1 | Immunologic reactivity of individual serum samples against the yeast protein extract of *H. capsulatum* G217B. Serum samples of patients with histoplasmosis (HPM1 to HPM10), paracoccidioidomycosis (HET1 and HET2), aspergilosis (HET3 and HET4), cryptococcosis (HET5 and HET6),

coccidioidomycosis (HET7 and HET8), and tuberculosis (HET9 and HET10), as well as serum samples from healthy individuals (NHS1 to NHS10) were tested through a Western blot assay against the protein extract used in this study. The reactivity of the three pool of sera used in the coimmunoprecipitation assay (HPM*, HET*, and NHS*) was also tested. MM, molecular mass standard (BioRad Laboratories Inc, Hercules, CA, USA); CC, conjugate control.

REFERENCES

Albuquerque, P. C., Nakayasu, E. S., Rodrigues, M. L., Frases, S., Casadevall, A., Zancope-Oliveira, R. M., et al. (2008). Vesicular transport in *Histoplasma capsulatum*: an effective mechanism for trans-cell wall transfer of proteins and lipids in ascomycetes. *Cell Microbiol.* 10, 1695–1710. doi: 10.1111/j.1462-5822.2008.01160.x

Almeida, M. A., Pizzini, C. V., Damasceno, L. S., Muniz, M. M., Almeida-Paes, R., Peralta, R. H., et al. (2016). Validation of western blot for *Histoplasma capsulatum* antibody detection assay. *BMC Infect. Dis.* 16, 87. doi: 10.1186/s12879-016-1427-0

Almeida, M. A., Damasceno, L. S., Pizzini, C. V., Muniz, M. M., Almeida-Paes, R., and Zancopé-Oliveira, R. M. (2019). Role of western blot assay for the diagnosis of histoplasmosis in AIDS patients from a National Institute of Infectious Diseases in Rio de Janeiro, Brazil. *Mycoses* 62, 261–267. doi: 10.1111/myc.12877

Antinori, S. (2014). *Histoplasma capsulatum*: more widespread than previously thought. *Am. J. Trop. Med. Hyg.* 90, 982–983. doi: 10.4269/ajtmh.14-0175

Azar, M. M., and Hage, C. A. (2017). Clinical Perspectives in the Diagnosis and Management of Histoplasmosis. *Clin. Chest Med.* 38, 403–415. doi: 10.1016/j.ccm.2017.04.004

Bahr, N. C., Antinori, S., Wheat, L. J., and Sarosi, G. A. (2015). Histoplasmosis infections worldwide: thinking outside of the Ohio River valley. *Curr. Trop. Med. Rep.* 2, 70–80. doi: 10.1007/s40475-015-0044-0

Ball, B., Bermas, A., Carruthers-Lay, D., and Geddes-McAlister, J. (2019). Mass Spectrometry-Based Proteomics of Fungal Pathogenesis, Host-Fungal Interactions, and Antifungal Development. *J. Fungi (Basel)* 5, 52. doi: 10.3390/jof5020052

Baltazar, L. M., Zamith-Miranda, D., Burnet, M. C., Choi, H., Nimrichter, L., Nakayasu, E. S., et al. (2018). Concentration-dependent protein loading of extracellular vesicles released by *Histoplasma capsulatum* after antibody treatment and its modulatory action upon macrophages. *Sci. Rep.* 8, 8065. doi: 10.1038/s41598-018-25665-5

Bohse, M. L., and Woods, J. P. (2005). Surface localization of the Yps3p protein of *Histoplasma capsulatum*. *Eukaryot. Cell.* 4, 685–693. doi: 10.1128/EC.4.4.685-693.2005

Bohse, M. L., and Woods, J. P. (2007). Expression and interstrain variability of the YPS3 gene of *Histoplasma capsulatum*. *Eukaryot. Cell.* 6, 609–615. doi: 10.1128/EC.00010-07

Bradford, M. M. (1976). A rapid and sensitive method for the quantitation of microgram quantities of protein utilizing the principle of protein-dye binding. *Anal. Biochem.* 72, 248–254. doi: 10.1006/abio.1976.9999

Brunoro, G. V., Caminha, M. A., Ferreira, A. T., Leprevost, F. V., Carvalho, P. C., Perales, J., et al. (2015). Reevaluating the *Trypanosoma cruzi* proteomic map: The shotgun description of bloodstream trypomastigotes. *J. Proteomics* 115, 58–65. doi: 10.1016/j.jprot.2014.12.003

Burnet, M. C., Zamith-Miranda, D., Heyman, H. M., Weitz, K. K., Bredeweg, E. L., Nosanchuk, J. D., et al. (2020). Remodeling of the *Histoplasma capsulatum* Membrane Induced by Monoclonal Antibodies. *Vaccines (Basel)* 8, 269. doi: 10.3390/vaccines8020269

Castillo, C. G., Kauffman, C. A., and Miceli, M. H. (2016). Blastomycosis. *Infect. Dis. Clin. North Am.* 30, 247–264. doi: 10.1016/j.idc.2015.10.002

Chan, J. F., Lau, S. K., Yuen, K. Y., and Woo, P. C. (2016). *Talaromyces (Penicillium) marneffei* infection in non-HIV-infected patients. *Emerg. Microbes Infect.* 5, e19. doi: 10.1038/emi.2016.18

Cleare, L. G., Zamith, D., Heyman, H. M., Couvillion, S. P., Nimrichter, L., Rodrigues, M. L., et al. (2020). Media matters! Alterations in the loading and release of *Histoplasma capsulatum* extracellular vesicles in response to different nutritional milieus. *Cell Microbiol.* 22, e13217. doi: 10.1111/cmi.13217

Crockett, D. K., Kushnir, M. M., Cloud, J. L., Ashwood, E. R., and Rockwood, A. L. (2012). Identification of *Histoplasma*-specific peptides in human urine. *Int. J. Pept.* 2012:621329. doi: 10.1155/2012/621329

Frías-De-León, M. G., Ramírez-Bárcenas, J. A., Rodríguez-Arellanes, G., Velasco-Castrejón, O., Taylor, M. L., and Reyes-Montes, M. D. R. (2017). Usefulness of molecular markers in the diagnosis of occupational and recreational histoplasmosis outbreaks. *Folia Microbiol. (Praha)* 62, 111–116. doi: 10.1007/s12223-016-0477-4

Garfoot, A. L., and Rappleye, C. A. (2016). *Histoplasma capsulatum* surmounts obstacles to intracellular pathogenesis. *FEBS J.* 283, 619–633. doi: 10.1111/febs.13389

Gilmore, R. D., Carpio, A. M., Kosoy, M. Y., and Gage, K. L. (2003). Molecular characterization of the sucB gene encoding the immunogenic dihydrolipoamide succinyltransferase protein of *Bartonella vinsonii* subsp. *berkhoffii* and *Bartonella quintana*. *Infect. Immun.* 71, 4818–4822. doi: 10.1128/iai.71.8.4818-4822.2003

Guimarães, A. J., Pizzini, C. V., Guedes, H. L. M., Albuquerque, P. C., Peralta, J. M., Hamilton, A. J., et al. (2004). ELISA for early diagnosis of histoplasmosis. *J. Med. Microbiol.* 53, 509–514. doi: 10.1099/jmm.0.05469-0

Guimarães, A. J., Nosanchuk, J. D., and Zancopé-Oliveira, R. M. (2006). Diagnosis of histoplasmosis. *Braz. J. Microbiol.* 37, 1–13. doi: 10.1590/S1517-83822006000100001

Guimarães, A. J., Hamilton, A. J., Guedes, H. L. M., Nosanchuk, J. D., and Zancopé-Oliveira, R. M. (2008). Biological function and molecular mapping of M antigen in yeast phase of *Histoplasma capsulatum*. *PloS One* 3, e3449. doi: 10.1371/journal.pone.0003449

Guimarães, A. J., Frases, S., Gomez, F. J., Zancopé-Oliveira, R. M., and Nosanchuk, J. D. (2009). Monoclonal antibodies to heat shock protein 60 alter the pathogenesis of *Histoplasma capsulatum*. *Infect. Immun.* 77, 1357–1367. doi: 10.1128/IAI.01443-08

Guimarães, A. J., Nakayasu, E. S., Sobreira, T. J., Cordero, R. J., Nimrichter, L., Almeida, I. C., et al. (2011). *Histoplasma capsulatum* heat-shock 60 orchestrates the adaptation of the fungus to temperature stress. *PloS One* 6, e14660. doi: 10.1371/journal.pone.0014660

Hilty, J., Smulian, A. G., and Newman, S. L. (2011). *Histoplasma capsulatum* utilizes siderophores for intracellular iron acquisition in macrophages. *Med. Mycol.* 49, 633–642. doi: 10.3109/13693786.2011.558930

Holbrook, E. D., Smolnycki, K. A., Youseff, B. H., and Rappleye, C. A. (2013). Redundant catalases detoxify phagocyte reactive oxygen and facilitate *Histoplasma capsulatum* pathogenesis. *Infect. Immun.* 81, 2334–2346. doi: 10.1128/IAI.00173-13

Johnson, C. H., Klotz, M. G., York, J. L., Kruft, V., and McEwen, J. E. (2002). Redundancy, phylogeny and differential expression of *Histoplasma capsulatum* catalases. *Microbiology* 148, 1129–1142. doi: 10.1099/00221287-148-4-1129

Johnson, C. H., Prigge, J. T., Warren, A. D., and McEwen, J. E. (2003). Characterization of an alternative oxidase activity of *Histoplasma capsulatum*. *Yeast* 20, 381–388. doi: 10.1002/yea.968

Keath, E. J., Painter, A. A., Kobayashi, G. S., and Medoff, G. (1989). Variable expression of a yeast-phase-specific gene in *Histoplasma capsulatum* strains differing in thermotolerance and virulence. *Infect. Immun.* 57, 1384–1390. doi: 10.1128/IAI.57.5.1384-1390.1989

Knox, K. S., and Hage, C. A. (2010). Histoplasmosis. *Proc. Am. Thorac. Soc.* 7, 169–172. doi: 10.1513/pats.200907-069AL

Laemmli, U. K. (1970). Cleavage of structural proteins during the assembly of the head of bacteriophage T4. *Nature* 227, 680–685. doi: 10.1038/227680a0

Long, K. H., Gomez, F. J., Morris, R. E., and Newman, S. L. (2003). Identification of heat shock protein 60 as the ligand on *Histoplasma capsulatum* that mediates binding to CD18 receptors on human macrophages. *J. Immunol.* 170, 487–494. doi: 10.4049/jimmunol.170.1.487

Maresca, B., and Kobayashi, G. S. (2000). Dimorphism in *Histoplasma capsulatum* and *Blastomyces dermatitidis*. *Contrib. Microbiol.* 5, 201–216. doi: 10.1159/000060346

Martins, L. M., Andrade, H. M., Vainstein, M. H., Wanke, B., Schrank, A., Balaguez, C. B., et al. (2013). Immunoproteomics and immunoinformatics analysis of *Cryptococcus gattii*: novel candidate antigens for diagnosis. *Future Microbiol.* 8, 549–563. doi: 10.2217/fmb.13.22

Mills, E. L., Kelly, B., Logan, A., Costa, A. S. H., Varma, M., Bryant, C. E., et al. (2016). Succinate Dehydrogenase Supports Metabolic Repurposing of Mitochondria to Drive Inflammatory Macrophages. *Cell* 167, 457–470.e413. doi: 10.1016/j.cell.2016.08.064

Missall, T. A., Lodge, J. K., and McEwen, J. E. (2004). Mechanisms of resistance to oxidative and nitrosative stress: implications for fungal survival in mammalian hosts. *Eukaryot. Cell.* 3, 835–846. doi: 10.1128/EC.3.4.835-846.2004

Mittal, J., Ponce, M. G., Gendlina, I., and Nosanchuk, J. D. (2019). *Histoplasma capsulatum*: Mechanisms for Pathogenesis. *Curr. Top. Microbiol. Immunol.* 422, 157–191. doi: 10.1007/82_2018_114

Moreira, A. L. E., Oliveira, M. A. P., Silva, L. O. S., Inácio, M. M., Bailão, A. M., Parente-Rocha, J. A., et al. (2020). Immunoproteomic Approach of Extracellular Antigens From *Paracoccidioides* Species Reveals Exclusive B-Cell Epitopes. *Front. Microbiol.* 10:2968. doi: 10.3389/fmicb.2019.02968

Moura, H., Terilli, R. R., Woolfitt, A. R., Gallegos-Candela, M., McWilliams, L. G., Solano, M.II, et al. (2011). Studies on botulinum neurotoxins type /C1 and mosaic/DC using Endopep-MS and proteomics. *FEMS Immunol. Med. Microbiol.* 61, 288–300. doi: 10.1111/j.1574-695X.2010.00774.x

Neuville, S., Lortholary, O., and Dromer, F. (2000). Do Kinetics of the Humoral Response to CryptococcusProtein During Murine Cryptococcosis Reflect Outcome? *Infect. Immun.* 68, 3724–3726. doi: 10.1128/iai.68.6.3724-3726.2000

Nguyen, S. V., Yamaguchi, H. T. T., Fukushi, H., and Hirai, K. (1999). Characterization of the *Coxiella burnetti* sucB gene encoding an immunogenic dihydrolipoamide succinyltransferase. *Microbiol. Immunol.* 43, 743–749. doi: 10.1111/j.1348-0421.1999.tb02465.x

Nosanchuk, J. D., Steenbergen, J. N., Shi, L., Deepe, G. S., and Casadevall, A. (2003). Antibodies to a cell surface histone-like protein protect against *Histoplasma capsulatum*. *J. Clin. Invest.* 112, 1164–1175. doi: 10.1172/JCI19361

Nosanchuk, J. D., Zancopé-Oliveira, R. M., Hamilton, A. J., and Guimarães, A. J. (2012). Antibody therapy for histoplasmosis. *Front. Microbiol.* 3, 21. doi: 10.3389/fmicb.2012.00021

Pastorelli, R., Carpi, D., Campagna, R., Airoldi, L., Pohjanvirta, V., Viluksela, M., et al. (2006). Differential expression profiling of the hepatic proteome in a rat model of dioxin resistance: correlation with genomic and transcriptomic analyses. *Mol. Cell Proteomics* 5, 882–894. doi: 10.1074/mcp.M500415-MCP200

Pitarch, A., Nombela, C., and Gil, C. (2016). Seroprofiling at the *Candida albicans* protein species level unveils an accurate molecular discriminator for candidemia. *J. Proteomics* 134, 144–162. doi: 10.1016/j.jprot.2015.10.022

Pizzini, C. V., Zancopé-Oliveira, R. M., Reiss, E., Hajjeh, R., Kaufman, L., and Peralta, J. M. (1999). Evaluation of a western blot test in an outbreak of acute pulmonary histoplasmosis. *Clin. Diagn. Lab. Immunol.* 6, 20–23. doi: 10.1128/CDLI.6.1.20-23.1999

Reimann, B., Bradsher, J., Franke, J., Hartmann, E., Wiedmann, M., Prehn, S., et al. (1999). Initial characterization of the nascent polypeptide-associated complex in yeast. *Yeast* 15, 397–407. doi: 10.1002/(SICI)1097-0061(19990330)15:5<397::AID-YEA384>3.0.CO;2-U

Rodrigues, A. M., Kubitschek-Barreira, P. H., Fernandes, G. F., Almeida, S. R., Lopes-Bezerra, L. M., and Camargo, Z. P. (2015). Immunoproteomic analysis reveals a convergent humoral response signature in the *Sporothrix schenckii* complex. *J. Proteomics* 115, 8–22. doi: 10.1016/j.jprot.2014.11.013

Roth, M. T., Zamith-Miranda, D., and Nosanchuk, J. D. (2019). Immunization Strategies for the Control of Histoplasmosis. *Curr. Trop. Med. Rep.* 6, 35–41. doi: 10.1007/s40475-019-00172-3

Sahaza, J. H., Rodríguez-Arellanez, G., Canteros, C. E., Reyes-Montes, M. D. R., and Taylor, M. L. (2020). Thermotolerance of Histoplasma capsulatum at 40°C predominates among clinical isolates from different Latin American regions. *Braz. J. Infect. Dis.* 24, 44–50. doi: 10.1016/j.bjid.2019.12.007

Sepúlveda, V. E., Williams, C. L., and Goldman, W. E. (2014). Comparison of phylogenetically distinct *Histoplasma* strains reveals evolutionarily divergent virulence strategies. *mBio* 5, e01376–e01314. doi: 10.1128/mBio.01376-14

Sepúlveda, V. E., Márquez, R., Turissini, D. A., Goldman, W. E., and Matute, D. R. (2017). Genome Sequences Reveal Cryptic Speciation in the Human Pathogen *Histoplasma capsulatum*. *mBio* 5, e01339–e01317. doi: 10.1128/mBio.01339-17

Tarcha, E. J., Basrur, V., Hung, C. Y., Gardner, M. J., and Cole, G. T. (2006). Multivalent recombinant protein vaccine against coccidioidomycosis. *Infect. Immun.* 74, 5802–5813. doi: 10.1128/IAI.00961-06

Teixeira, M. M., Patané, J. S., Taylor, M. L., Gómez, B. L., Theodoro, R. C., de Hoog, S., et al. (2016). Worldwide Phylogenetic Distributions and Population Dynamics of the Genus *Histoplasma*. *PloS Negl. Trop. Dis.* 10, e0004732. doi: 10.1371/journal.pntd.0004732

Virginio, E. D., Kubitschek-Barreira, P. H., Batista, M. V., Schirmer, M. R., Abdelhay, E., Shikanai-Yasuda, M. A., et al. (2014). Immunoproteome of *Aspergillus fumigatus* using sera of patients with invasive aspergillosis. *Int. J. Mol. Sci.* 15, 14505–14530. doi: 10.3390/ijms150814505

Weaver, C. H., Sheehan, K. C., and Keath, E. J. (1996). Localization of a yeast-phase-specific gene product to the cell wall in *Histoplasma capsulatum*. *Infect. Immun.* 64, 3048–3054. doi: 10.1128/IAI.64.8.3048-3054.1996

Wheat, L. J., Azar, M. M., Bahr, N. C., Spec, A., Relich, R. F., and Hage, C. (2016). Histoplasmosis. *Infect. Dis. Clin. North Am.* 30, 207–227. doi: 10.1016/j.idc.2015.10.009

Zancopé-Oliveira, R. M., Reiss, E., Lott, T. J., Mayer, L. W., and Deepe, G. S. (1999). Molecular cloning, characterization, and expression of the M antigen of *Histoplasma capsulatum*. *Infect. Immun.* 67, 1947–1953. doi: 10.1128/IAI.67.4.1947-1953.1999

Zygmunt, M. S., Díaz, M. A., Teixeira-Gomes, A. P., and Cloeckaert, A. (2001). Cloning, nucleotide sequence, and expression of the *Brucella melitensis* sucB gene coding for an immunogenic dihydrolipoamide succinyltransferase homologous protein. *Infect. Immun.* 69, 6537–6540. doi: 10.1128/IAI.69.10.6537-6540.2001

Conflict of Interest: The authors declare that the research was conducted in the absence of any commercial or financial relationships that could be construed as a potential conflict of interest.

frontiers in Cellular and Infection Microbiology

ORIGINAL RESEARCH
published: 30 October 2020
doi: 10.3389/fcimb.2020.590025

Exoantigens of *Paracoccidioides* spp. Promote Proliferation and Modulation of Human and Mouse Pulmonary Fibroblasts

Débora de Fátima Almeida Donanzam[1,2], *Tatiani Ayako Goto Donato*[3], *Karoline Haghata dos Reis*[2], *Adriely Primo da Silva*[2], *Angela Carolina Finato*[2], *Amanda Ribeiro dos Santos*[1,2], *Ricardo Souza Cavalcante*[2], *Rinaldo Poncio Mendes*[1,2] *and James Venturini*[1,2*]

[1] Faculdade de Medicina, Universidade Federal do Mato Grosso do Sul, Campo Grande, Brazil, [2] Faculdade de Medicina, Departamento de Doenças Tropicais e Diagnóstico por Imagem, UNESP, Botucatu, Brazil, [3] Faculdade de Ciências, UNESP, Bauru, Brazil

OPEN ACCESS

Edited by:
Carlos Pelleschi Taborda,
University of São Paulo, Brazil

Reviewed by:
Juan G. McEwen,
University of Antioquia, Colombia
Anamelia Lorenzetti Bocca,
University of Brasilia, Brazil
Gustavo Alexis Niño-Vega,
University of Guanajuato, Mexico
Sandro Rogerio Almeida,
University of São Paulo, Brazil

***Correspondence:**
James Venturini
james.venturini@ufms.br

Specialty section:
This article was submitted to Fungal Pathogenesis, a section of the journal Frontiers in Cellular and Infection Microbiology

Received: 31 July 2020
Accepted: 07 October 2020
Published: 30 October 2020

Citation:
Almeida Donanzam DF, Donato TAG, Reis KH, Silva AP, Finato AC, Santos AR, Cavalcante RS, Mendes RP and Venturini J (2020) Exoantigens of Paracoccidioides spp. Promote Proliferation and Modulation of Human and Mouse Pulmonary Fibroblasts. Front. Cell. Infect. Microbiol. 10:590025. doi: 10.3389/fcimb.2020.590025

Paracoccidioidomycosis (PCM) is a systemic granulomatous fungal infection caused by thermally dimorphic fungi of the genus *Paracoccidioides*. Endemic in Latin America, PCM presents with high incidence in Brazil, Colombia, and Venezuela, especially among rural workers. The main clinical types are acute/subacute (AF) form and chronic form (CF). Even after effective antifungal treatment, patients with CF usually present sequelae, such as pulmonary fibrosis. In general, pulmonary fibrosis is associated with dysregulation wound healing and abnormal fibroblast activation. Although fibrogenesis is recognized as an early process in PCM, its mechanisms remain unknown. In the current study, we addressed the role of *Paracoccidioides* spp. exoantigens in pulmonary fibroblast proliferation and responsiveness. Human pulmonary fibroblasts (MRC-5) and pulmonary fibroblasts isolated from BALB/c mice were cultivated with 2.5, 5, 10, 100, and 250 μg/ml of exoantigens produced from *P. brasiliensis* (Pb18 and Pb326) and *P. lutzii* (Pb01, Pb8334, and Pb66) isolates. Purified gp43, the immunodominant protein of *P. brasiliensis* exoantigens, was also evaluated at concentrations of 5 and 10 μg/ml. After 24 h, proliferation and production of cytokines and growth factors by pulmonary fibroblasts were evaluated. Each exoantigen concentration promoted a different level of interference of the pulmonary fibroblasts. In general, exoantigens induced significant proliferation of both murine and human pulmonary fibroblasts ($p < 0.05$). All concentrations of exoantigens promoted decreased levels of IL-6 ($p < 0.05$) and VEGF ($p < 0.05$) in murine fibroblasts. Interestingly, decreased levels of bFGF ($p < 0.05$) and increased levels of TGF-β1 ($p < 0.05$) and pro-collagen I ($p < 0.05$) were observed in human fibroblasts. The gp43 protein induced increased TGF-β1 production by human cells ($p = 0.02$). In conclusion, our findings showed for the first time that components of *P. brasiliensis* and *P. lutzii* interfered in fibrogenesis by directly acting on the biology of pulmonary fibroblasts.

Keywords: pulmonary fibroblast, pulmonary fibrosis, paracoccidioidomycosis, cell response, growth factors

INTRODUCTION

Paracoccidioidomycosis (PCM) is a systemic granulomatous fungal infection caused by thermally dimorphic fungi of the genus Paracoccidioides (Teixeira et al., 2009). The infection occurs after inhalation of conidia or mycelia fragments that reach the lungs and morphologically switch to yeast forms (Restrepo et al., 2012). Clinically, PCM is mainly of two types, acute/subacute form (AF) and chronic form (CF) (Mendes et al., 2017). CF is the most common with clinical manifestations predominantly in the lungs and upper aerodigestive tract (Shikanai-Yasuda et al., 2017). Most CF-PCM patients exhibit pulmonary fibrosis (PF) as a sequela of chronic inflammation (Tobón et al., 2003). PF is observed in patients with PCM even before treatment as necroscopic findings reveal the presence of fibrosis characterized by extensive areas of collagen deposition near the hilar region and involving other structures, such as lymph nodes, bronchi, and arteries. Furthermore, collagen fibers are found on the periphery of granulomas and extend to nearby bronchi and blood vessels (Tuder et al., 1985). Fibrotic sequelae alter respiratory function and may incapacitate patients (Mendes et al., 2017). Usually, fibrotic sequelae is observed disproportionately in patients with ventilation/perfusion and alveolar-capillary blockade causing dyspnea (Campos and Cataneo, 1986). The most common abnormalities are architectural distortion and interlobular septal thickening and reticulate (Costa et al., 2013) with residual lesions occurring in up to 53% of treated patients (Tobón et al., 2003). Furthermore, emphysema, possibly due to smoking, may also be present in these patients. As a result of all these changes, an obstructive pattern is observed in lung function tests (Lemle et al., 1983).

The development of PF is generally related to a dysregulation of wound healing (Witte and Barbul, 1997). During homeostatic wound healing, fibroblasts proliferate and produce factors related to tissue repair, such as transforming growth factor beta 1 (TGF-β1), which act in paracrine and autocrine fashions to induce the differentiation of fibroblasts to myofibroblasts (Thannickal et al., 2003; Midwood et al., 2004). Myofibroblasts are cells involved in the production of extracellular matrix, fibronectin, and collagen and are characterized by the expression of alpha smooth actin (α-SMA), a protein that integrates actin filaments and proportionate the contractile phenotype of these cells (Hinz et al., 2001; Peyton et al., 2008). Although beneficial in the beginning, tissue repair can become pathogenic if it occurs rampantly, resulting in extracellular matrix remodeling and permanent scarring.

Evaluation of PF in PCM has been limited. A well-established granuloma surrounded by intense deposition of collagen type I and III in the lung parenchyma is typically observed in *P. brasiliensis*-infected mice after 4–8 weeks of fungal inoculation (Cock et al., 2000). Finato et al. (2020) also observed high concentrations of profibrotic mediators, such as IL-6, IL-1β, CCL3, IL-10, TGF-β1, VEGF, and interferon (IFN)-γ in the lungs of *P. brasiliensis*-infected mice on the eighth week of infection. High production of TGF-β1 and bFGF by *P. brasiliensis* exoantigens-stimulated monocytes from monocytes of untreated CF PCM patients has been described (Venturini et al., 2014). Araujo et al. (2011) verified PF in patients that do not received treatment. Furthermore, Tuder et al. (1985) verified the proliferation of reticular fibers in remote areas of granulomatous reactions, leading to the hypothesis that fungal components may promote collagen production. Despite this evidence, the interaction between *Paracoccidioides* spp. and pulmonary fibroblasts has not yet fully elucidated.

On the other hand, the interaction of *P. brasiliensis* and host cells has been investigated regarding the mechanisms involved in adherence and escape (Vicentini et al., 1994; Mendes-Giannini et al., 2008; Ywazaki et al., 2011). Vicentini et al. (1994) demonstrated that extracellular matrix protein laminin binds specifically to yeast forms of *P. brasiliensis* and enhances adhesion of the fungus to the surface of epithelial cells. Ywazaki et al. (2011) showed the adhesion of *P. brasiliensis* to GM1 and GM3 gangliosides of human pulmonary fibroblasts, which may be the path of bound/infection by the fungus. In another study, Mendes-Giannini et al. (2008) reported interactions between *P. brasiliensis* and epithelial Vero and A549 cells and suggested that the adhesion and invasion of these cells could represent an escape mechanism and contribute to the spread of infection.

Considering the possible influences of *Paracoccidioides* spp. on the activity of pulmonary fibroblasts and development of fibrosis in lungs, we investigated the influence of *Paracoccidioides* spp. exoantigens on the proliferation and responsiveness of human and murine pulmonary fibroblasts.

MATERIALS AND METHODS

Paracoccidioides spp. Isolates

The *Paracoccidioides* spp. isolates were obtained from mycology collection of Laboratório de Pesquisa em Moléstias Infecciosas (UNESP, Botucatu, SP, Brazil). Were used in the study *P. brasiliensis* isolates Pb18 and Pb326, isolated from a patient from Botucatu, SP, Brazil, and *P. lutzii* isolates Pb01, Pb66, and Pb8334. The isolates were maintained by frequent subculture at 36°C in semi-solid GPY media containing 2% glucose, 1% peptone, 0.5% yeast extract, and 2% agar.

Exoantigen Production

Total exoantigen was produced according to Camargo et al. (2003) with minor modifications. Briefly, yeast forms of *Paracoccidioides* spp. were subcultured in Sabouraud broth containing 2% dextrose (Sigma-Aldrich, St. Louis, MO, USA) and supplemented with 0.01% thiamine (Sigma-Aldrich) and 0.14% L-asparagine (Sigma-Aldrich) and maintained at 37°C for 3 days. The fungi were cultivated in supplemented Sabouraud broth for 3 days shaking at 50 rpm at 37°C. Next, more supplemented Sabouraud broth was added and the cultures cultivated for 7 more days at 37°C with shaking at 50 rpm. The fungi were killed by the addition of sodium merthiolate (0.2 g/L) for 24 h at 4°C and filtered using Whatman™ filter paper #1. The filtrate was dialyzed against several changes of distilled water for 24 h at 4°C. The dialysate was then filtered and concentrated

by centrifugation at 4,000 rpm for 30 min at 4°C using an Amicon® Ultra 15 Filter (Millipore, Billerica, MA, USA). Protein concentrations were determined using a Pierce™ BCA Protein Assay Kit (Thermo Fisher Scientific, Waltham, MA, USA). The gp43 protein was obtained by of *P. brasiliensis* B-339 according Saraiva et al. (1996) and kindly provided by Dr. Zoilo Pires de Camargo (Federal University of São Paulo, UNIFESP, Brazil).

Human Lung Fibroblasts

The human lung fibroblast cell line MRC5 (ATCC CCL-171) was purchased from Banco de Células do Rio de Janeiro, RJ, Brazil. Fibroblasts were incubated at 37°C in a humidified 5% CO_2/95% air atmosphere in complete Dulbecco's Modified Eagle Medium (DMEM; Sigma-Aldrich) containing 10% fetal bovine serum (FBS; Sigma-Aldrich), 100 U/ml penicillin, and 100 μg/m; streptomycin (Sigma-Aldrich). When the cell cultures reached 80% confluence, the cells were dispersed using trypsin-EDTA (Sigma-Aldrich) for 5 min and then transferred to new culture flasks (Greiner BioOne, Frickenhausen, BW, GER).

Isolation of Murine Pulmonary Fibroblasts

Pulmonary fibroblasts were isolated from mice using their differential adherent properties as described previously (Trentin et al., 2015; Verma et al., 2016) with modifications. Male BALB/c mice, 4 weeks old, were obtained from Instituto Lauro de Souza Lima, Bauru, SP, Brazil. All mice received a sterile balanced diet and water *ad libitum* and were kept in a ventilated shelf ALERKS-56 housing system (Alesco®, Monte Mor, SP, Brazil). The experimental protocol was performed in accordance with the ethical principles for animal research adopted by the National Council for the Control of Animal Experimentation (CONCEA). Briefly, *naïve* young mice (4-week-old) were euthanized by intraperitoneal administration of ketamine and xylazine. After thoracotomy under aseptic conditions, the lungs were perfused with sterile phosphate-buffered saline. The perfused lungs were then removed and cut into small pieces and underwent two rounds of enzymatic digestion using collagenase type II (Gibco, Life Technologies, Paisley, UK) and trypsin (0.25%; Gibco, Life Technologies). Cell viability was determined using 0.1% trypan blue staining. The cells were then aliquoted into 25 cm^2 cell culture flasks (Corning Costar, New York, NY, USA) at a proportion of 1 lung/flask in 1 ml. Then, 4.0 ml of DMEM supplemented with 20% fetal calve serum was added and the cells incubated at 37°C with 5% CO_2 in a humidified chamber. After 24 h, the medium was changed to remove non-adherent cells. Once the cell culture reached 70% confluence, they were dispersed using trypsin-EDTA (Sigma-Aldrich) for 5 min and then resuspended in supplemented DMEM. Fibroblast isolation was confirmed using by immunofluorescence staining based on CD90 expression (**Supplementary Figure 1**). Fibroblasts were used after two to three passages.

Fibroblast Cell Cultures

Human and murine fibroblasts were incubated with exoantigens of *P. brasiliensis* and *P. lutzii* at concentrations of 2.5, 5, 10, 100, and 250 μg/ml and gp43 at concentrations of 5 and 10 μg/ml. The protein gp43 is the immunodominant antigen of *P. brasiliensis*. (Puccia et al., 1986). After 24 h, the cells were analyzed using proliferation assays and cell-free supernatants were evaluated for cytokines.

Proliferation Assays/Viability Assay

Cell viability and proliferation were measured using MTT assays according to Mosmann (1983). Briefly, fibroblasts were seeded into 96-well culture plates in octuplicate at 2×10^4 murine pulmonary fibroblast/well and 1×10^4 human pulmonary fibroblasts/well. After 24 h of incubation, the cells were stimulated with *Paracoccidioides* spp. exoantigens. At 24-h post-stimulation, the supernatants were collected and the cells then incubated in complete DMEM containing MTT (5 mg/ml). The plate was incubated for 2 h at 37°C in 5% CO_2 and then centrifuged for 5 min at 1,500 rpm. The supernatants were removed and the cells in each well resuspended in 100 ml of dimethyl sulfoxide (DMSO). After 5 min, the plate was read at 540 nm using a spectrophotometer reader. The percentage of proliferation was calculated according to the ratio between the treated and control cultures multiplied by 100.

Functional Analyses

Levels of human basic fibroblast growth factor (bFGF), TGF-β1, interleukin (IL)-1β, tumor necrosis factor alpha (TNF-α), and pro-collagen I and mouse levels of TGF-β1, IL-1β, IL-6, and vascular endothelial growth factor (VEGF) were measured in the cell-free supernatants using a Duo-Set Kit (R&D Systems, Minneapolis, MI, USA), according to the manufacturer's instructions. Results were expressed as pg/ml and determined using standard curves established for each assay.

Ethical Aspects

The study was approved by the Research Ethics Committees of Botucatu Medical School, UNESP (CAEE #62177516.3.0000.5411) and the experimental approach was approved by the Ethical Committee of School of Sciences (Proc. #760/2016; UNESP, Bauru, São Paulo, Brazil).

Statistical Analyses

The two matched groups were compared using the paired t-test. Multiple group comparisons were performed using one-way analysis of variance (ANOVA) with Dunnet's *post hoc* tests. All statistical analyses were performed using GraphPad Prism 5.0 software (GraphPad Software. Inc., San Diego, California, USA) at a significance level of 5% ($p < 0.05$) (Zar, 2010).

RESULTS

Paracoccidioides spp. Exoantigens Induced Enhanced Proliferation in Murine Pulmonary Fibroblasts and Discrete Proliferation in Human Pulmonary Fibroblasts

The behavior of murine pulmonary fibroblasts was similar when stimulated with the exoantigens prepared from different

Paracoccidioides species and isolates. Exoantigens from all *P. lutzii* isolates (Pb01, Pb66, and Pb8334) induced cell proliferation at the lower concentrations of 2.5 and 5 μg/ml represented by increase percentage of viable cell compared to non-stimulated culture (**Figure 1A**). Isolate Pb8334 exoantigen also promoted cell proliferation at 100 μg/ml and the exoantigen of Pb66 promoted cell proliferation at 10 μg/ml. The exoantigen of isolate Pb01 was cytotoxic at the higher concentration of 250 μg/ml. *P. brasiliensis* exoantigens also promoted cell proliferation at different concentrations depending on the particular isolate. For instance, Pb18 exoantigen promoted cell proliferation at 2.5 and 100 μg/ml, whereas Pb326 exoantigen promoted proliferation at 5 and 10 μg/ml. Neither of the *P. brasiliensis* exoantigens was cytotoxic to murine pulmonary fibroblasts at the concentrations tested (**Figure 1A**).

Human pulmonary fibroblasts were more sensitive to *Paracoccidioides* spp. exoantigens compared to that of murine fibroblasts, exhibiting discrete proliferation and cytotoxicity at the higher concentrations (100 and 250 μg/ml) of both species tested (**Figure 1B**). Pb01 exoantigen induced cell proliferation at the lowest concentrations tested of 2.5, 5, and 10 μg/ml. In contrast, Pb18 exoantigen induced proliferation at only 5 μg/ml. For the two *P. brasiliensis* isolates, Pb18 exoantigen induced cell proliferation at 10 μg/ml, while Pb326 exoantigen induced cell proliferation at a concentration of 2.5 μg/ml but was cytotoxic at 10 μg/ml (**Figure 1B**).

Paracoccidioides spp. Exoantigens Decreased IL-6 and VEGF Production by Murine Pulmonary Fibroblasts

To evaluate the effects of exoantigens of the activity of murine pulmonary fibroblast, we measured the levels of cytokines and growth factors involved in inflammation and wound healing. All exoantigens of *P. brasiliensis* and *P. lutzii* caused decreased levels of VEGF compared to that of the control group at all exoantigen concentrations tested (**Figure 2**). Also, decreased levels of IL-6 were observed in murine pulmonary fibroblasts stimulated with 2.5 and 10 μg/ml of Pb01 and Pb66 exoantigens (**Figures 2A, B**) and 2.5, 5, and 10 μg/ml of Pb8334 exoantigen (**Figure 2C**) compared to that of the control group. Exoantigen from the *P. brasiliensis* isolate Pb18 at 5 μg/ml induced decreased levels of IL-6 (**Figure 2D**). Meanwhile, compared with that of the control group, exoantigen from the *P. brasiliensis* isolate Pb326 was also shown to decrease levels of IL-6 at 2.5 and 5 μg/ml as well as decrease levels of TGF-β1 at 2.5 μg/ml, but increased levels of TGF-β1 at 5 and 10 μg/ml (**Figure 2E**). Levels of IL-1β were not detected in the supernatants of murine fibroblast cultures.

Intense Production of Pro-collagen I and TGF-β1 by Human Pulmonary Fibroblast Was Induced by *Paracoccidioides* spp. Exoantigens

Functional analyses of human pulmonary fibroblasts compared to that of non-stimulated cells (control group) revealed intense pro-collagen I production in cells stimulated with Pb01 exoantigen at 10 μg/ml (**Figure 3A**), Pb18 exoantigen at 2.5, 5, and 10 μg/ml (**Figure 3D**), and Pb326 exoantigen at 10 μg/ml (**Figure 3E**). Decreased pro-collagen I production was also seen in cells stimulated with 10 μg/ml of Pb8334 exoantigen compared to that in non-stimulated cells (**Figure 3C**). No difference in pro-collagen I production was observed in cells stimulated with Pb66 exoantigen. In addition, increased TGF-β1 production was detected in cells stimulated with 10 μg/ml Pb66 exoantigen (**Figure 3B**), 2.5, 5, and 10 μg/ml Pb8334 exoantigen (**Figure 3C**), and 10 μg/ml Pb326 exoantigen (**Figure 3E**) compared to that in the control group. In contrast, decreased TGF-β1 levels was seen in cells stimulated with 10 μg/ml Pb01 exoantigen (**Figure 3A**) and 2.5, 5, and 10 μg/ml Pb18 exoantigen (**Figure 3D**). Decreased bFGF levels were observed in fibroblasts stimulated with Pb01 exoantigen (**Figure 3A**) and 2.5, 5, and 10 μg/ml Pb18 exoantigen (**Figure 3D**). IL-1β was not detected in the supernatants of human pulmonary fibroblasts.

Gp43 Was Cytotoxic and Increased TGF-β1 Levels Only in Human Pulmonary Fibroblasts

We also analyze the influence of gp43 on pulmonary fibroblast function. No differences in viability (**Figure 4**) or cytokine production (**Figure 5**) were observed in murine pulmonary fibroblasts at any concentration of gp43 tested. No IL-1β was not detected in the supernatants of mouse pulmonary fibroblasts. In human pulmonary fibroblasts, gp43 was cytotoxic at 5 and 10 μg/ml compared to that in non-stimulated cells (**Figure 4**). Decreased pro-collagen I levels and increased TGF-β1 production were also observed in human pulmonary fibroblasts treated with 10 μg/ml gp43 (**Figures 5A–B**). No significant difference was observed in bFGF production. Consistent with the supernatants of mouse pulmonary fibroblasts, no IL-1β was not detected in supernatants of human pulmonary fibroblasts.

DISCUSSION

In the current study, we showed for the first-time interactions of *Paracoccidioides* spp. exoantigens with human and murine pulmonary fibroblasts. Exoantigens of both *Paracoccidioides* species, *P. lutzii* and *P. brasiliensis*, induced proliferation of human and murine fibroblasts. Interestingly, in murine pulmonary fibroblasts *P. lutzii* isolates Pb01 and Pb66 and *P. brasiliensis* isolate Pb326 increased cell proliferation at the lowest concentrations of exoantigen tested. This was in conjunction with reduced viability of cells stimulated with the higher concentrations of the exoantigens, suggesting a dose-dependent effect. In human pulmonary fibroblasts, we also observed increased proliferation induced by the lowest concentrations of exoantigens; however, Pb66 exoantigen reduced cell viability at every concentration tested. Pb18 and Pb8334 exoantigens seemed to not cause the same effect as the exoantigens from the other isolates. These exoantigens induced cell proliferation at different concentrations, but without it being a dose-dependent effect. Diversity among isolated *Paracoccidioides* species has been previously explored. For instance, Machado et al. (2013) reported

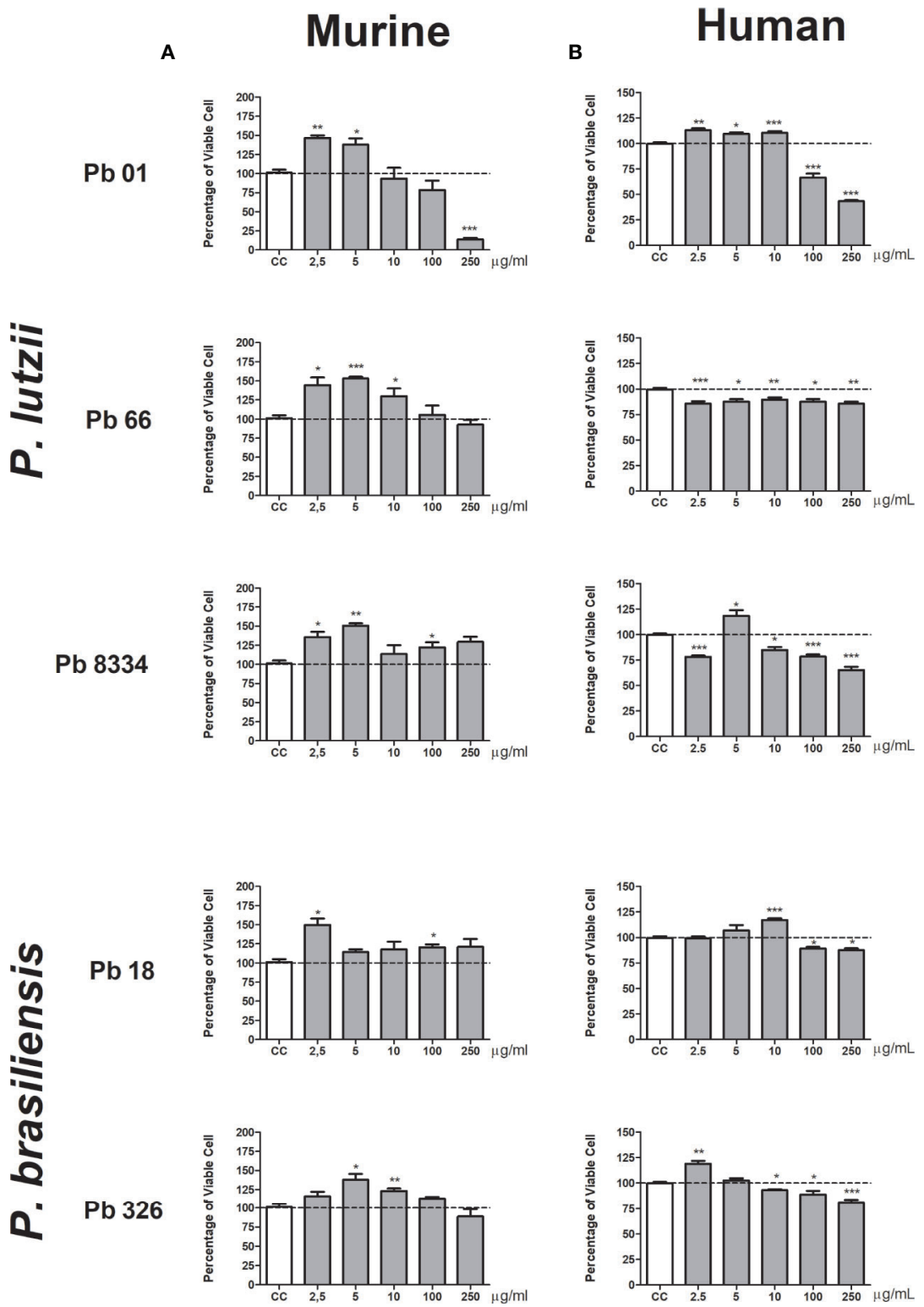

FIGURE 1 | Percentage of viable pulmonary fibroblasts stimulated with *Paracoccidioides* spp. exoantigens. Fibroblasts were cultured in the presence or absence of *Paracoccidioides* spp. exoantigens and evaluated 24 h post-treatment using MTT assays. **(A)** Murine pulmonary fibroblasts. **(B)** Human pulmonary fibroblasts. Fibroblast proliferation was measured according to the ratio of test culture cells (challenged with exoantigens) to untreated culture control (CC) cells. Values above 100% of viability represent cell proliferation. Results are expressed as mean ± SEM; paired t-test, $^{*}p < 0.05$, $^{**}p < 0.01$, $^{***}p < 0.001$; n = 4.

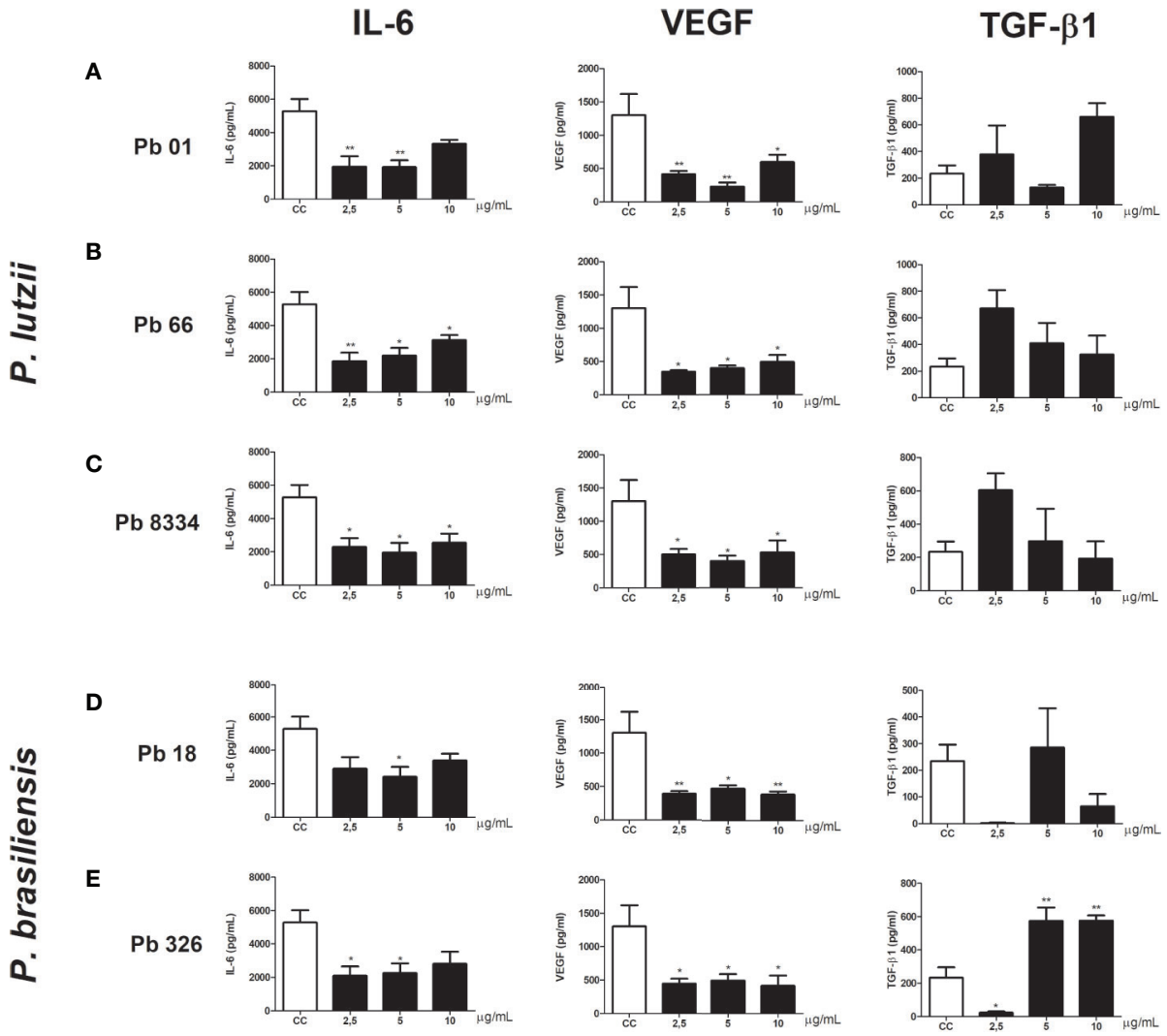

FIGURE 2 | Murine pulmonary fibroblast activity stimulated by *Paracoccidioides* spp. exoantigens. Fibroblasts were cultured in the presence or absence of *Paracoccidioides* spp. exoantigens and levels of IL-6, VEGF, and TGF-β1 in the cell-free supernatants were determined 24 h post-treatment. **(A)** Pb01 exoantigen. **(B)** Pb66 exoantigen. **(C)** Pb8334 exoantigen. **(D)** Pb18 exoantigen. **(E)** Pb326 exoantigen. Results are expressed as means ± SEM; ANOVA with Dunnett's *post hoc* test; $^{*}p < 0.05$, $^{**}p < 0.01$; n = 4.

differences in exoantigen composition of Pb01, Pb8334, Pb18, Epm83, and Pb265 isolates. They also demonstrated that *P. lutzii* expresses lower amounts of gp43 compared to that of *P. brasiliensis*. Furthermore, de Oliveira et al. (2018) analyzed the secretome of isolates Pb01 and Epm83 and showed that isolates of the *Paracoccidioides* complex are able to secrete different proteins, mainly those related to adhesion and virulence.

The mainly pathological pulmonary characteristic in CF-PCM is the granulomatous inflammatory process (Queiroz-Telles and Escuissato, 2011) with lesions typically surrounded by fibroblasts and collagen fibers after 2–3 weeks of fungal infection (Kerr et al., 1988; Cock et al., 2000). Fibroblasts are directly involved with collagen production and the establishment of fibrosis during chronic inflammation (Wick et al., 2013). Therefore, our results provide evidence that *Paracoccidioides* spp. may influence the modulation of pulmonary fibroblasts by inducing cell proliferation and acting directly on the development of non-regulated wound healing, which could support the establishment of fibrosis. Other investigators suggest other main roles for fibroblasts and myofibroblasts during infections. For instance, the pathophysiological basis of inflammatory myofibroblastic tumors (IMTs) is related to an uncontrolled response to tissue damage or chronic inflammation. Furthermore, the development of IMTs have previously been related to chronic inflammation caused by histoplasmosis (Cassivi and Wylam, 2006). Rosa et al. (2019), using an experimental model, showed that *Cryptococcus gatti* infection increases the expression in the lungs of proteins related to energy metabolism, leading to activation of the glycolytic pathway. In the same study, these authors confirmed the

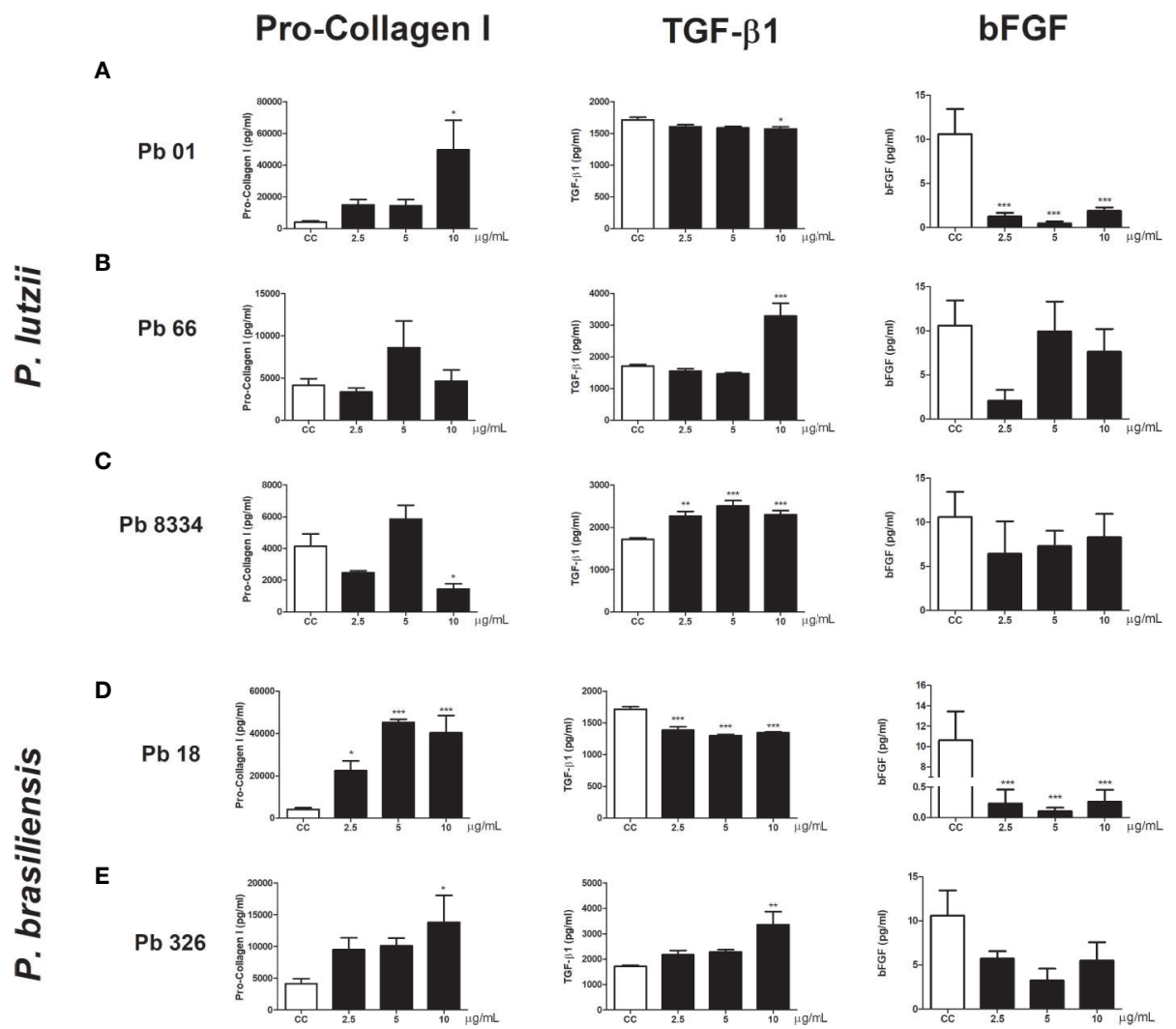

FIGURE 3 | Human pulmonary fibroblast activity stimulated by *Paracoccidioides* spp. exoantigens. Fibroblasts were cultured in the presence or absence of *Paracoccidioides* spp. exoantigens and levels of pro-collagen I, TGF-β1, and bFGF in the cell-free supernatants were determined 24 h post-treatment. **(A)** Pb01 exoantigen. **(B)** Pb66 exoantigen. **(C)** Pb8334 exoantigen. **(D)** Pb18 exoantigen. **(E)** Pb326 exoantigen. Results are expressed as means ± SEM; ANOVA with Dunnett's *post hoc* test; $^{*}p < 0.05$, $^{**}p < 0.01$, $^{***}p < 0.001$; n = 4.

activation of glycolysis in human pulmonary fibroblasts, culminating in the Warburg effect (WE). Interestingly, WE is known for its involvement with cell proliferation, mainly tumor cells. A similar change has been observed in a murine model of pulmonary infection by *Mycobacterium tuberculosis* in which the authors described as an infection-induced WE (Shi et al., 2015). Furthermore, an *in vitro* study showed that *M. tuberculosis* stimulates murine lung fibroblasts to proliferate and differentiate into myofibroblasts (Verma et al., 2016).

Fibroblasts play a key role in the tissue repair process, but may also impact immune responses (Buechler and Turley, 2018). In rheumatoid arthritis, IL-6 produced by synovial fibroblasts contributes to the autoimmunity associated with this disease (Nguyen et al., 2017; Buechler and Turley, 2018). Meanwhile, lung fibroblasts can recruit dendritic cells into airway lymph nodes through an integrin-mediated inflammatory signaling (Kitamura et al., 2011; Buechler and Turley, 2018). Liver fibroblasts infected by *Leishmania donovani* induce the generation of T-regulatory (Treg) lymphocytes. The depletion of liver fibroblasts *in vivo* reduces the number of Treg lymphocytes and decreases the parasitic burden (Khadem et al., 2016; Buechler and Turley, 2018). Patients with CF-PCM commonly present with lung fibrosis and persistent nonspecific inflammatory responses (Mendes et al., 2017). Similar to PCM, other infectious agents can cause chronic inflammation and the establishment of fibrosis. In necropsies of acquired immunodeficiency syndrome (AIDS) patients with pneumocystosis, it is possible to detect chronic inflammation and interstitial fibrosis in the lungs (Foley et al., 1993). In chronic pulmonary histoplasmosis, it is common for pulmonary inflammation to lead to fibrosis and

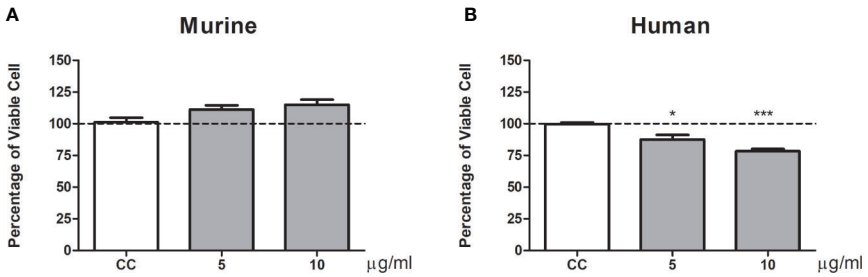

FIGURE 4 | Percentage of viable pulmonary fibroblasts stimulated by gp43. Fibroblasts were cultured in the presence or absence of gp43 and proliferation evaluated 24 h post-treatment using MTT assays. **(A)** Murine pulmonary fibroblasts. **(B)** Human pulmonary fibroblasts. Fibroblast proliferation was measured according to the ratio of test culture cells (challenged with exoantigens) to untreated culture control (CC) cells. Results are expressed as mean ± SEM; paired t-test; $^{*}p < 0.05$, $^{***}p < 0.001$; n = 4.

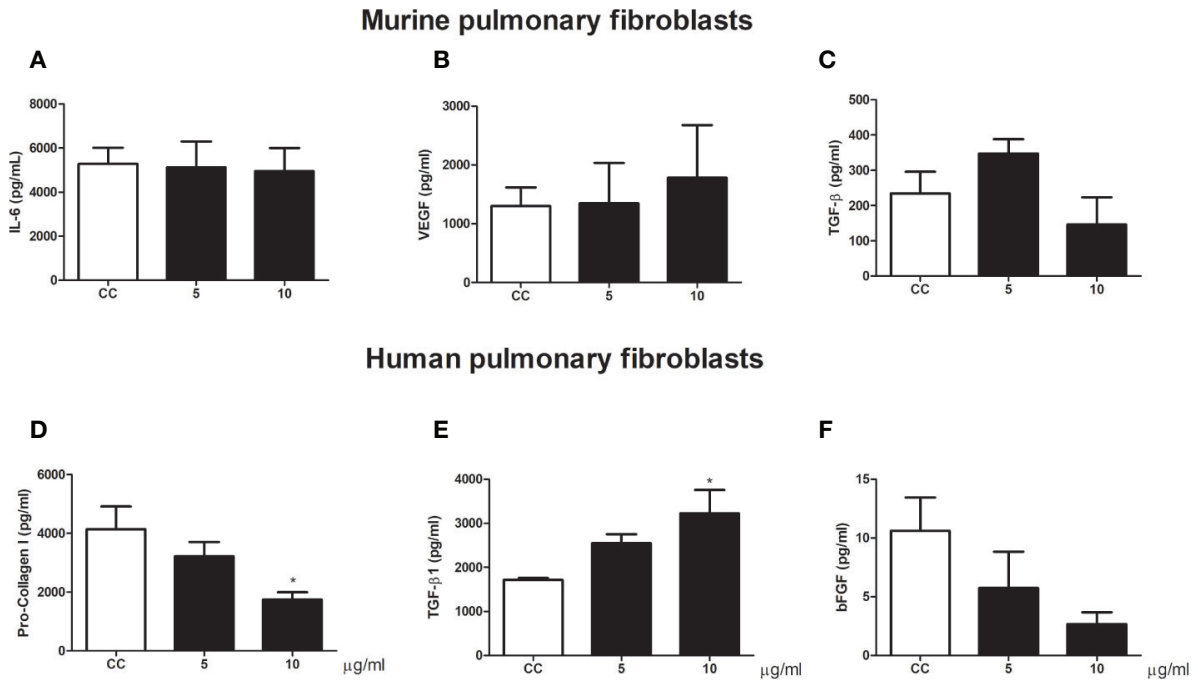

FIGURE 5 | Pulmonary fibroblast activity stimulated by gp43. Human and murine fibroblasts were cultured in the presence or absence of gp43 and IL-6, VEGF, TGF-β1, pro-collagen I, and bFGF levels in the cell-free supernatants were determined 24 h post-treatment. **(A)** IL-6. **(B)** VEGF. **(C)** TGF-β1. **(D)** Pro-collagen I. **(E)** TGF-β1. **(F)** bFGF. Results are expressed as means ± SEM; ANOVA with Dunnett's *post hoc* test; $^{*}p < 0.05$; n = 4.

volume loss with compensatory enlargement of cavities and pleural thickening. In rare cases, mediastinal fibrosis may occur, which is an abnormal and exuberant post-infection fibrotic response for which the mechanism has not been elicited (Wheat et al., 2016).

To investigate the link between immune responses and fibrosis in PCM, we evaluated fibroblasts for the production of targeted cytokine related to inflammation and tissue repair. In murine cells, we determined that all *Paracoccidioides* exoantigens promoted decreased levels of IL-6 and VEGF, but interestingly Pb326 exoantigen induced increased levels of TGF-β1. In human pulmonary fibroblasts, we also observed increased levels of TGF-β1 produced by cells stimulated with Pb66, Pb8334, and Pb326 exoantigens and increased levels of pro-collagen I produced by cells stimulated with Pb01, Pb18, and Pb326 exoantigens. We also observed increased proliferation of human fibroblasts, but bFGF levels were lower than that of the untreated control cells. Venturini et al. (2014) showed that *P. brasiliensis* antigens increase the production of IL-1β, TNF-α, TGF-β1, and bFGF by peripheral blood monocytes of CF-PCM patients, suggesting fungal metabolites may play an important role in the activation of these cells. Therefore, *Paracoccidioides* spp. exoantigens may also participate in the establishment of fibrosis in PCM. This could occur by activating monocytes to produce high levels of

bFGF and TGF-β1 and activating fibroblasts to produce TGF-β1 and pro-collagen I. TGF-β1 is a potent pro-mitotic factor that contributes to increased collagen production and others extracellular matrix compounds (Midwood et al., 2004) and is also involved in the transformation of fibroblasts into myofibroblasts (Thannickal et al., 2003). Pulmonary fibrosis is characterized by the loss of lung epithelial cells and the proliferation of fibroblasts (Mendes-Giannini et al., 2008). Also, *P. brasiliensis* may modulate apoptosis of epithelial cells A549 by the expression of apoptotic molecules such as Bcl-2, Bak, and caspase-3, confirming the inducing of apoptosis by the fungus which can then survive and spread to other parts of the body (Del Vecchio et al., 2009). This suggests that exoantigens may have a role in the mechanisms that regulate fibrosis in PCM. An interesting fact regarding *Paracoccidioides* spp. is that they are capable of surviving in hypoxic environments (Lima et al., 2015), such as granulomatous centers. Hypoxia directly influences wound repair by activation of HIF-1α, transformation of fibroblasts into myofibroblasts, increased expression of α-SMA, collagen I, and collagen III, and activation of SMAD3 (Zhao et al., 2017). Mendes et al. (2017) discuss the pathogenesis and the role of host's immune in PCM, and one of the cases is when after infection, the inflammatory reaction recedes and scars are formed, which may be sterile or contain viable, albeit latent fungi. So, the fungi may remain latent for many years, however, any imbalance may result in reactivation of latent foci, a phenomenon known as endogenous reinfection, which triggers disease. Restrepo (2000) also mentions and discuss about cases where the infection results in residual foci containing viable fungi that may outcome in endogenous reactivation, as shown by cases diagnosed outside of the geographic limits of the mycosis. Taken together, this data provides evidence for *Paracoccidioides* spp. being able to potentiate tissue repair functions of fibroblasts, resulting in cell proliferation and increased collagen production, which can lead to changes in the lung structure and low oxygen circulation. This new environment would be conducive to fungal survival and escape from the immune system with the fungi being hidden for prolonged periods in granulomatous centers.

Gp43 is a high mannose glycoprotein, the main antigen secreted by *P. brasiliensis*, and is usually used as a diagnostic antigen (Flavia Popi et al., 2002). It has been shown in an experimental model that gp43 is able to inhibit the fungicidal ability of macrophages, suggesting that the avoidance mechanisms of *Paracoccidioides* spp. may favor the primary infection status of susceptible hosts (Flavia Popi et al., 2002). Therefore, we investigated the possible influences of gp43 on pulmonary fibroblasts. Our results failed to show an important role for gp43 in the induction of murine pulmonary fibroblast proliferation. However, we did observe that gp43 promoted decreased cell viability and increase TGF-β1 production in human pulmonary fibroblasts. Curiously, gp43 strongly stimulates granuloma formation in a murine model using peritoneal macrophages and B-1 cells isolated from A/J mice (Vigna et al., 2006). It is important to highlight that *P. lutzii* has an ortholog glycoprotein called Plp43 that presents a peptide sequence only of 81% identical with *P. brasiliensis* (Leitão et al., 2014). Thus, *P. lutzii* exoantigens represents a control of enriched gp43 exoantigen.

Our results require further investigation. Despite the evidence that exoantigens of *Paracoccidioides* spp. modulate the function of human and mouse pulmonary fibroblasts, we did not evaluated different antigenic components from both fungal strain. Other limitations were we did not prove if chosen concentration range has any physiological meaning, the maturation of fibroblasts into myofibroblasts, or the presence of other factors that may influence fibrogenesis, such as the downregulation of metalloproteinases. While our study may not present a comprehensive model defining all the mechanisms of how *Paracoccidioides* spp. exoantigens modulate the pulmonary fibroblasts, we believe that it is an important source to start understanding how this fungus influences tissue repair function of these cells.

In summary, our results demonstrate, for the first time, that *Paracoccidioides* spp. exoantigens may promote pulmonary fibroblast proliferation and gp43, the immunodominant antigen of *P. brasiliensis*, is not related to the stimulation of fibroblast proliferation, but may have a role in the maturation of fibroblasts into myofibroblasts. Further studies are needed to better understand the mechanistic process in greater detail.

DATA AVAILABILITY STATEMENT

The original contributions presented in the study are included in the article/**Supplementary Materials**. Further inquiries can be directed to the corresponding author.

ETHICS STATEMENT

The animal study was reviewed and approved by National Council for the Control of Animal Experimentation.

AUTHOR CONTRIBUTIONS

Conception and design of the experiments: DA, TD, RC, RM, APS, and JV. Performance of the experiments: DA, KR, ARS, AF, and APS. Analysis of the data: DA and JV. Preparation of the manuscript: DA and JV. All authors contributed to the article and approved the submitted version.

FUNDING

This study was financially supported in part by the Fundação da Universidade Federal do Mato Grosso do Sul, UFMS/MEC, BRASIL. This study was also supported by the Coordenação de Aperfeiçoamento de Pessoal de Nível Superior, Brasil (CAPES; Finance Code 001) and Conselho Nacional de Desenvolvimento Científico e Tecnológico (CNPq; Grant #470221/2014-3).

ACKNOWLEDGMENTS

The authors wish to thank Coordenação de Aperfeiçoamento de Pessoal de Nível Superior (CAPES) for the D.F.A.D. Master Scholarship. The content of this manuscript has been published [in part] as part of the master thesis of Débora de Fátima Almeida [Almeida (2017) Fibrose pulmonar na paracoccidioidomicose: influência do fungo e do hospedeiro na fibrogênese. [dissertation/master's thesis]. [Botucatu (SP)]: UNESP. Available at: https://repositorio.unesp.br/handle/11449/151552. [Accessed July 06, 2020]].

SUPPLEMENTARY MATERIAL

The Supplementary Material for this article can be found online at: https://www.frontiersin.org/articles/10.3389/fcimb.2020.590025/full#supplementary-material

REFERENCES

Almeida, D. F. (2017). *Fibrose pulmonar na paracoccidioidomicose: influência do fungo e do hospedeiro na fibrogênese. [dissertation/master"s thesis]. [Botucatu (SP)]: UNESP*. Available at: https://repositorio.unesp.br/handle/11449/151552 (Accessed July 06, 2020).

Araujo, S. A. (2011). *Contribuição ao estudo anátomo-clínico da Paracoccidioiodomicose em Minas Gerais. meio século de experiência - avaliação das necrópsias realizadas no período compreendido entre 1944 até 1999, no departamento de anatomia patológica e medicina legal, da Faculdade de Medicina da Universidade Federal de Minas Gerais*. Available at: http://www.bibliotecadigital.ufmg.br/dspace/handle/1843/BUOS-8KVLVK (Accessed October 28, 2015).

Buechler, M. B., and Turley, S. J. (2018). A short field guide to fibroblast function in immunity. *Semin. Immunol.* 35, 48–58. doi: 10.1016/j.smim.2017.11.001

Camargo, Z. P., Berzaghi, R., Amaral, C. C., and Silva, S. H. M. (2003). Simplified method for producing Paracoccidioides brasiliensis exoantigens for use in immunodiffusion tests. *Med. Mycol.* 41, 539–542. doi: 10.1080/13693780310001615358

Campos, E. P., and Cataneo, A. J. (1986). [Pulmonary function in 35 patients with paracoccidioidomycosis]. *Rev. Inst. Med. Trop. Sao Paulo* 28, 330–336. doi: 10.1590/S0036-46651986000500008

Cassivi, S. D., and Wylam, M. E. (2006). Pulmonary inflammatory myofibroblastic tumor associated with histoplasmosis. *Interact. Cardiovasc. Thorac. Surg.* 5, 514–516. doi: 10.1510/icvts.2006.129809

Cock, A. M., Cano, L. E., Vélez, D., Aristizábal, B. H., Trujillo, J., and Restrepo, A. (2000). Fibrotic sequelae in pulmonary paracoccidioidomycosis: histopathological aspects in BALB/c mice infected with viable and non-viable paracoccidioides brasiliensis propagules. *Rev. Inst. Med. Trop. Sao Paulo* 42, 59–66. doi: 10.1590/S0036-46652000000200001

Costa, A. N., Benard, G., Albuquerque, A. L. P., Fujita, C. L., Magri, A. S. K., Salge, J. M., et al. (2013). The lung in paracoccidioidomycosis: new insights into old problems. *Clinics (Sao Paulo)* 68, 441–448. doi: 10.6061/clinics/2013(04)02

de Oliveira, A. R., Oliveira, L. N., Chaves, E. G. A., Weber, S. S., Bailão, A. M., Parente-Rocha, J. A., et al. (2018). Characterization of extracellular proteins in members of the Paracoccidioides complex. *Fungal Biol.* 122, 738–751. doi: 10.1016/j.funbio.2018.04.001

Del Vecchio, A., Silve Jde, F., Silva, J., Andreotti, P. F., Soares, C. P., Benard, G., et al. (2009). Induction of apoptosis in A549 pulmonary cells by two Paracoccidioides brasiliensis samples. *Mem. Inst. Oswaldo Cruz* 104, 749–754. doi: 10.1590/s0074-02762009000500015

Finato, A. C., Almeida, D. F., Dos Santos, A. R., Nascimento, D. C., Cavalcante, R. S., Mendes, R. P., et al. (2020). Evaluation of antifibrotic and antifungal combined therapies in experimental pulmonary paracoccidioidomycosis. *Med. Mycol.* 58, 667–678. doi: 10.1093/mmy/myz100

Flavia Popi, A. F., Lopes, J. D., and Mariano, M. (2002). GP43 from Paracoccidioides brasiliensis inhibits macrophage functions. An evasion mechanism of the fungus. *Cell. Immunol.* 218, 87–94. doi: 10.1016/s0008-8749(02)00576-2

Foley, N. M., Griffiths, M. H., and Miller, R. F. (1993). Histologically atypical Pneumocystis carinii pneumonia. *Thorax* 48, 996–1001. doi: 10.1136/thx.48.10.996

Hinz, B., Celetta, G., Tomasek, J. J., Gabbiani, G., and Chaponnier, C. (2001). Alpha-smooth muscle actin expression upregulates fibroblast contractile activity. *Mol. Biol. Cell* 12, 2730–2741. doi: 10.1091/mbc.12.9.2730

Kerr, I. B., Araripe, J. R., Oliveira, P. C., and Lenzi, H. L. (1988). Paracoccidioidomycosis: a sequential histopathologic study of lesions in experimentally-infected rats. *Rev. Inst. Med. Trop. S Paulo* 30, 336–350. doi: 10.1590/S0036-46651988000500003

Khadem, F., Gao, X., Mou, Z., Jia, P., Movassagh, H., Onyilagha, C., et al. (2016). Hepatic stellate cells regulate liver immunity to visceral leishmaniasis through P110δ-dependent induction and expansion of regulatory T cells in mice. *Hepatology* 63, 620–632. doi: 10.1002/hep.28130

Kitamura, H., Cambier, S., Somanath, S., Barker, T., Minagawa, S., Markovics, J., et al. (2011). Mouse and human lung fibroblasts regulate dendritic cell trafficking, airway inflammation, and fibrosis through integrin αvβ8–mediated activation of TGF-β. *J. Clin. Invest.* 121, 2863–2875. doi: 10.1172/JCI45589

Leitão, N. P., Vallejo, M. C., Conceição, P. M., Camargo, Z. P., Hahn, R., Puccia, R., et al. (2014). Paracoccidioides lutzii Plp43 Is an Active Glucanase with Partial Antigenic Identity with P. brasiliensis gp43. *PlLoS Negl. Trop. Dis.* 8, 1–9. doi: 10.1371/journal.pntd.0003111

Lemle, A., Wanke, B., Miranda, J. L., Kropf, G. L., Mandel, M. B., and Mandel, S. (1983). Pulmonary function in paracoccidioidomycosis (South American blastomycosis). An analysis of the obstructive defect. *Chest* 83, 827–828. doi: 10.1378/chest.83.5.827

Lima, P. S., Chung, D., Bailão, A. M., Cramer, R. A., and Soares, C. M. (2015). Characterization of the Paracoccidioides Hypoxia Response Reveals New Insights into Pathogenesis Mechanisms of This Important Human Pathogenic Fungus. *PLoS Negl. Trop. Dis.* 9, e0004282. doi: 10.1371/journal.pntd.0004282

Machado, G. C., Moris, D. V., Arantes, T. D., Silva, L. R. F., Theodoro, R. C., Mendes, R. P., et al. (2013). Cryptic species of Paracoccidioides brasiliensis: impact on paracoccidioidomycosis immunodiagnosis. *Mem. Inst. Oswaldo Cruz* 108, 637–643. doi: 10.1590/0074-0276108052013016

Mendes, R. P., Cavalcante, R. S., Marques, S. A., Marques, M. E. A., Venturini, J., Sylvestre, T. F., et al. (2017). Paracoccidioidomycosis: Current Perspectives from Brazil. *Open Microbiol. J.* 11, 224–282. doi: 10.2174/1874285801711010224

Mendes-Giannini, M. J. S., Monteiro da Silva, J. L., de Fátima da Silva, J., Donofrio, F. C., Miranda, E. T., Andreotti, P. F., et al. (2008). Interactions of Paracoccidioides brasiliensis with host cells: recent advances. *Mycopathologia* 165, 237–248. doi: 10.1007/s11046-007-9074-z

Midwood, K. S., Williams, L. V., and Schwarzbauer, J. E. (2004). Tissue repair and the dynamics of the extracellular matrix. *Int. J. Biochem. Cell Biol.* 36, 1031–1037. doi: 10.1016/j.biocel.2003.12.003

Mosmann, T. (1983). Rapid colorimetric assay for cellular growth and survival: application to proliferation and cytotoxicity assays. *J. Immunol. Methods* 65, 55–63. doi: 10.1016/0022-1759(83)90303-4

Nguyen, H. N., Noss, E. H., Mizoguchi, F., Huppertz, C., Wei, K. S., Watts, G. F. M., et al. (2017). Autocrine Loop Involving IL-6 Family Member LIF, LIF Receptor, and STAT4 Drives Sustained Fibroblast Production of Inflammatory Mediators. *Immunity* 46, 220–232. doi: 10.1016/j.immuni.2017.01.004

Peyton, S. R., Kim, P. D., Ghajar, C. M., Seliktar, D., and Putnam, A. J. (2008). The effects of matrix stiffness and RhoA on the phenotypic plasticity of smooth muscle cells in a 3-D biosynthetic hydrogel system. *Biomaterials* 29, 2597–2607. doi: 10.1016/j.biomaterials.2008.02.005

Puccia, R., Schenkman, S., Gorin, P. A., and Travassos, L. R. (1986). Exocellular components of Paracoccidioides brasiliensis: identification of a specific antigen. *Infect. Immun.* 53, 199–206. doi: 10.1128/IAI.53.1.199-206.1986

Queiroz-Telles, F., and Escuissato, D. L. (2011). Pulmonary Paracoccidioidomycosis. *Semin. Respir. Crit. Care Med.* 32, 764–774. doi: 10.1055/s-0031-1295724

Restrepo, A., Gómez, B. L., and Tobón, A. (2012). Paracoccidioidomycosis: Latin America's Own Fungal Disorder. *Curr. Fungal Infect. Rep.* 6, 303–311. doi: 10.1007/s12281-012-0114-x

Restrepo, A. (2000). Morphological aspects of Paracoccidioides brasiliensis in lymph nodes: implications for the prolonged latency of paracoccidioidomycosis? *Med. Mycol.* 38, 317–322. doi: 10.1080/mmy.38.4.317.322

Rosa, R. L., Berger, M., Santi, L., Driemeier, D., Barros Terraciano, P., Campos, A. R., et al. (2019). Proteomics of Rat Lungs Infected by Cryptococcus gattii Reveals a Potential Warburg-like Effect. *J. Proteome Res.* 18, 3885–3895. doi: 10.1021/acs.jproteome.9b00326

Saraiva, E. C., Altemani, A., Franco, M. F., Unterkircher, C. S., and Camargo, Z. P. (1996). *Paracoccidioides brasiliensis*-gp43 used as paracoccidioidin. *J. Med. Vet. Mycol.* 34, 155–161. doi: 10.1080/02681219680000261

Shi, L., Salamon, H., Eugenin, E. A., Pine, R., Cooper, A., and Gennaro, M. L. (2015). Infection with Mycobacterium tuberculosis induces the Warburg effect in mouse lungs. *Sci. Rep.* 5:18176. doi: 10.1038/srep18176

Shikanai-Yasuda, M. A., Mendes, R. P., Colombo, A. L., Queiroz-Telles, F., Kono, A. S. G., Paniago, A. M., et al. (2017). Brazilian guidelines for the clinical management of paracoccidioidomycosis. *Rev. Soc Bras. Med. Trop*. 5, 715–740 doi: 10.1590/0037-8682-0230-2017

Teixeira, M. M., Theodoro, R. C., de Carvalho, M. J. A., Fernandes, L., Paes, H. C., Hahn, R. C., et al. (2009). Phylogenetic analysis reveals a high level of speciation in the Paracoccidioides genus. *Mol. Phylogenet. Evol.* 52, 273–283. doi: 10.1016/j.ympev.2009.04.005

Thannickal, V. J., Lee, D. Y., White, E. S., Cui, Z., Larios, J. M., Chacon, R., et al. (2003). Myofibroblast differentiation by transforming growth factor-beta1 is dependent on cell adhesion and integrin signaling via focal adhesion kinase. *J. Biol. Chem.* 278, 12384–12389. doi: 10.1074/jbc.M208544200

Tobón, A. M., Agudelo, C. A., Osorio, M. L., Alvarez, D. L., Arango, M., Cano, L. E., et al. (2003). Residual pulmonary abnormalities in adult patients with chronic paracoccidioidomycosis: prolonged follow-up after itraconazole therapy. *Clin. Infect. Dis.* 37, 898–904. doi: 10.1086/377538

Trentin, P. G., Ferreira, T. P. T., Arantes, A. C. S., Ciambarella, B. T., Cordeiro, R. S. B., Flower, R. J., et al. (2015). Annexin A1 mimetic peptide controls the inflammatory and fibrotic effects of silica particles in mice. *Br. J. Pharmacol.* 172, 3058–3071. doi: 10.1111/bph.13109

Tuder, R. M., el Ibrahim, R., Godoy, C. E., and De Brito, T. (1985). Pathology of the human pulmonary paracoccidioidomycosis. *Mycopathologia* 92, 179–188. doi: 10.1007/BF00437631

Venturini, J., Cavalcante, R. S., Golim Mde, A., Marchetti, C. M., Azevedo, P. Z., Amorim, B. C., et al. (2014). Phenotypic and functional evaluations of peripheral blood monocytes from chronic-form paracoccidioidomycosis patients before and after treatment. *BMC Infect. Dis.* 14:552. doi: 10.1186/s12879-014-0552-x

Verma, S. C., Agarwal, P., and Krishnan, M. Y. (2016). Primary mouse lung fibroblasts help macrophages to tackle Mycobacterium tuberculosis more efficiently and differentiate into myofibroblasts up on bacterial stimulation. *Tuberculosis* 97, 172–180. doi: 10.1016/j.tube.2015.10.009

Vicentini, A. P., Gesztesi, J. L., Franco, M. F., de Souza, W., de Moraes, J. Z., Travassos, L. R., et al. (1994). Binding of Paracoccidioides brasiliensis to laminin through surface glycoprotein gp43 leads to enhancement of fungal pathogenesis. *Infect. Immun.* 62, 1465–1469. doi: 10.1128/IAI.62.4.1465-1469.1994

Vigna, A. F., Almeida, S. R., Xander, P., Freymüller, E., Mariano, M., and Lopes, J. D. (2006). Granuloma formation in vitro requires B-1 cells and is modulated by Paracoccidioides brasiliensis gp43 antigen. *Microbes Infect.* 8, 589–597. doi: 10.1016/j.micinf.2005.06.033

Wheat, L. J., Azar, M. M., Bahr, N. C., Spec, A., Relich, R. F., and Hage, C. (2016). Histoplasmosis. *Infect. Dis. Clinics North Am* 30, 207–227. doi: 10.1016/j.idc.2015.10.009

Wick, G., Grundtman, C., Mayerl, C., Wimpissinger, T.-F., Feichtinger, J., Zelger, B., et al. (2013). The immunology of fibrosis. *Annu. Rev. Immunol.* 31, 107–135. doi: 10.1146/annurev-immunol-032712-095937

Witte, M. B., and Barbul, A. (1997). General principles of wound healing. *Surg. Clin. North Am.* 77, 509–528. doi: 10.1016/S0039-6109(05)70566-1

Ywazaki, C. Y., Maza, P. K., Suzuki, E., Takahashi, H. K., and Straus, A. H. (2011). Role of host glycosphingolipids on Paracoccidioides brasiliensis adhesion. *Mycopathologia* 171, 325–332. doi: 10.1007/s11046-010-9376-4

Zar, J. H. (2010). *Biostatistical analysis*. *5th ed* (Upper Saddle River, N.J: Prentice-Hall/Pearson).

Zhao, B., Guan, H., Liu, J.-Q., Zheng, Z., Zhou, Q., Zhang, J., et al. (2017). Hypoxia drives the transition of human dermal fibroblasts to a myofibroblast-like phenotype via the TGF-β1/Smad3 pathway. *Int. J. Mol. Med.* 39, 153–159. doi: 10.3892/ijmm.2016.2816

Conflict of Interest: The authors declare that the research was conducted in the absence of any commercial or financial relationships that could be construed as potential conflicts of interest.

frontiers in Cellular and Infection Microbiology

REVIEW
published: 11 November 2020
doi: 10.3389/fcimb.2020.581101

Host Response to *Coccidioides* Infection: Fungal Immunity

Anh L. Diep[1] *and Katrina K. Hoyer*[1,2,3]*

[1] Quantitative and Systems Biology, Graduate Program, University of California Merced, Merced, CA, United States, [2] Department of Molecular and Cell Biology, School of Natural Sciences, University of California Merced, Merced, CA, United States, [3] Health Sciences Research Institute, University of California Merced, Merced, CA, United States

Coccidioidomycosis is a fungal, respiratory disease caused by *Coccidioides immitis* and *Coccidioides posadasii*. This emerging infectious disease ranges from asymptomatic to pulmonary disease and disseminated infection. Most infections are cleared with little to no medical intervention whereas chronic disease often requires life-long medication with severe impairment in quality of life. It is unclear what differentiates hosts immunity resulting in disease resolution versus chronic infection. Current understanding in mycology-immunology suggests that chronic infection could be due to maladaptive immune responses. Immunosuppressed patients develop more severe disease and mouse studies show adaptive Th1 and Th17 responses are required for clearance. This is supported by heightened immunosuppressive regulatory responses and lowered anti-fungal T helper responses in chronic *Coccidioides* patients. Diagnosis and prognosis is difficult as symptoms are broad and overlapping with community acquired pneumonia, often resulting in misdiagnosis and delayed treatment. Furthermore, we lack clear biomarkers of disease severity which could aid prognosis for more effective healthcare. As the endemic region grows and population increases in endemic areas, the need to understand *Coccidioides* infection is becoming urgent. There is a growing effort to identify fungal virulence factors and host immune components that influence fungal immunity and relate these to patient disease outcome and treatment. This review compiles the known immune responses to *Coccidioides* spp. infection and various related fungal pathogens to provide speculation on *Coccidioides* immunity.

Keywords: *Coccidioides immitis*, *Coccidioides posadasii*, Coccidioidomycosis, Valley fever, host pathogen interactions, fungal immunity

OPEN ACCESS

Edited by:
Carlos Pelleschi Taborda, University of São Paulo, Brazil

Reviewed by:
Marcus De Melo Teixeira, University of Brasilia, Brazil
Marley C. Caballero Van Dyke, Northern Arizona University, United States

***Correspondence:**
Katrina K. Hoyer
khoyer2@ucmerced.edu

Specialty section:
This article was submitted to Fungal Pathogenesis, a section of the journal Frontiers in Cellular and Infection Microbiology

Received: *07 July 2020*
Accepted: *15 October 2020*
Published: *11 November 2020*

Citation:
Diep AL and Hoyer KK (2020) Host Response to Coccidioides Infection: Fungal Immunity. Front. Cell. Infect. Microbiol. 10:581101. doi: 10.3389/fcimb.2020.581101

INTRODUCTION

Coccidioidomycosis is a fungal lung disease caused by inhalation of *Coccidioides immitis* and *Coccidioides posadasii*. It is a disease endemic to the Southwestern United States, Central America, and South America and is typically transmitted from the soil *via* wind (Johnson et al., 2014). In endemic regions of the American Southwest alone (California, Nevada, Utah, Arizona, and New Mexico) the estimated incidence is 122.7 cases per 100,000 (Benedict et al., 2019). Fungal arthroconidia enter the lungs and differentiate into a spherule state that replicates *via* endosporulation. Subsequent endospore rupture spreads the fungus, resulting in tissue damage

and inflammation (Ternovoĭ and Golotina, 1977). Clinically, coccidioidomycosis is often misdiagnosed as pneumonia or lung cancer (Nguyen et al., 2013; Saenz-Ibarra et al., 2018). When the host immune system is unable to clear infection, it develops into a chronic state sometimes disseminating into other organs (Nguyen et al., 2013). In 60% of cases, infection remains asymptomatic or presents mild flu-like symptoms and is cleared by the host with little to no medical intervention (Saubolle et al., 2007). In 40% of cases, patients present moderate to severe flu-like symptoms that can become chronic. One percent of symptomatic cases develop severe disseminated infection (Saubolle et al., 2007).

In large part due to biosafety regulations, *Coccidioides* has been much less explored than other fungal pathogens. Though first reported in 1892, and with research dating back to the early 1900s, focus on the immune response against *Coccidioides* did not begin until the 1980s (Smith, 1940). A small but dedicated group of immunologists focus on fungal pathogens and host responses, but there is a critical need for further research into host responses to *Coccidioides*. There is little understanding of the immune events and players that contribute to disease resolution or chronic infection. Clinicians currently rely on symptom-based diagnosis, antibody-antigen assays, and imaging (chest x-rays and CT scans) to diagnose *Coccidioides*-infected patients, but these methods are limited in their ability to assess disease progression and host clearance capacity (Johnson et al., 2012; Wack et al., 2015). This review explores the initiation of innate immune responses and the development of adaptive immune responses to *Coccidioides*. Where gaps in *Coccidioides* knowledge exists, closely related fungal pathogens are used to extrapolate.

DISEASE AND EPIDEMIOLOGY

Coccidioides is endemic in regions with heavy intermittent rains along with the hot, arid summers (Johnson et al., 2014; Coopersmith et al., 2017; McCotter et al., 2019) It is found primarily in alkaline soils with high surface salinity (Elconin et al., 1964; Swatek, 1970; Lacy and Swatek, 1974). During wet, rainy months, filamentous threads composed of barrel-like subunits called arthroconidia expand within the soil. Environmental stresses, such as heat or digging, disrupts the soil and aerosolize the arthroconidia, making it airborne (McCotter et al., 2019). Infection occurs when arthroconidia are inhaled into the lungs and temperature and moisture differences trigger morphological change from arthroconidia to spherule to endospore (Johannesson et al., 2006). The fungal spherule develops into an endospore, capable of maturing and bursting to release more spores (Nguyen et al., 2013). As fungi develop, the host presents generic flu-like symptoms including headache, fever, body ache, coughing, and respiratory distress (Johnson et al., 2012; Wack et al., 2015).

Coccidioides infection also occurs in non-human animals, spanning across taxonomical classes from reptiles to mammals (Fisher et al., 2007; del Rocío Reyes-Montes et al., 2016). Animal carcasses are often found positive for *Coccidioides* while the surrounding soil environments test negative for the fungi (del Rocío Reyes-Montes et al., 2016). Originally, animals were believed to be accidental hosts, but genomic analysis indicates that *Coccidioides* code for several animal peptidases and lack enzymes associated with plant-decomposing fungi (Fisher et al., 2007; del Rocío Reyes-Montes et al., 2016; Taylor and Barker, 2019). This suggests that *Coccidioides* infected animals can act as fungal distributors, transporting the fungus from the initial infection site and upon animal death returning the fungus to new soil. Animal carcasses may also act as a protective, nutrient rich nursery for *Coccidioides* growth. Peptidase expression suggests that *Coccidioides* evolved methods to infect and thrive inside a protein rich environment, perhaps contributing to its success in surviving in harsh, alkaline environments. Wind and disturbance from other scavenging animals can then further disseminate the fungus driving human infection.

Agricultural, construction, and fieldwork in endemic regions are risk factors for fungal exposure. San Joaquin Valley (SJV) in California is an agricultural hub, supporting over 180,000 agricultural and 100,000 construction/labor jobs (Garcia and Young; Nicas, 2018). Solar energy field expansion puts solar-panel workers at risk for fungal exposure (Wilken et al., 2015; Laws et al., 2018). Legislative efforts in California have mandated *Coccidioides* risk education and safety protective equipment for at-risk workers in endemic areas (Salas, 2019). In Arizona, disease incidence increases with age, with those over the age of 70 experiencing the highest rate of disease (McCotter et al., 2019). Disease susceptibility for coccidiomycosis has been correlated with increasing age, with the elderly being much more susceptibility to infection and severe disease (Saubolle et al., 2007; Johnson et al., 2012; Nguyen et al., 2013; Wack et al., 2015). The high disease incidence in Arizona has been credited to the steady influx of new settlers over the last few decades and the increasing popularity of the state amongst retirees (McCotter et al., 2019).

Disease impact is further complicated by socioeconomic constraints. In California's SJV, Hmong and Latino minorities make up a large percentage of field workers and soil-based laborers (Johnson et al., 2014). These populations tend to fall into the lowest wealth bracket with little to no access to healthcare, thus representing those with the least availability and opportunity to seek medical care, and the most exposed to *Coccidioides* (Mobed et al., 1992). Health care practioners working in the are often trained outside the endemic region and are initially unfamiliar with disease symptoms (Saenz-Ibarra et al., 2018). In 2007 in Arizona, only 50% of health care providers surveyed were confident in treating *Coccidioides* infection and only 21% correctly answered treatment questions (Chen et al., 2011). Since then, Arizona has implemented specialized coccidioidomycosis continuing medical education for in-state practioners, resulting in health care providers being twice as likely to answer treatment questions correctly compared to their untrained cohort. In California, outreach programs throughout endemic regions are providing disease awareness for physicians and patients, while legislative efforts aim to

mandate coccidioidomycosis centric continuing medical education courses to provide specialized regional training (Salas, 2018).

INNATE IMMUNITY

Innate Detection and Immune Evasion

The lungs maintain many defense mechanisms to survey and eliminate airborne threats. Lung epithelial cells (LECs) secrete anti-microbial peptides, complement proteins, and defensins which enhance granulocyte activity and create a less hospitable environment for *Coccidioides* (Hernández-Santos et al., 2018). To survive, *Coccidioides* must successfully avoid detection from surveying and patrolling innate immune cells. Lung-resident macrophages, also known as alveolar macrophages, comprise up to 95% of pulmonary leukocytes and participate in early immune detection of pathogens and maintain the lung microenvironment (Wynn and Vannella, 2016). In *Aspergillus* infections, tissue-specific neutrophils are recruited by LECs and enter the lung early after infection due to β-glucan and chitin (Dubey et al., 2014). Innate leukocytes control early pathogen invasion *via* phagocytosis and production of reactive oxide and reactive nitrogen species (RNS) (Xu and Shinohara, 2017). β-glucan and chitin are conserved across many fungal species, including *Coccidioides*, so these molecules could interact with epithelial cells and aid in neutrophil recruitment. In cases where host immune responses cannot control infection, disease becomes chronic. Host responses sometimes control infections through granuloma formation in the lung as fungi is walled off instead of destroyed (Nguyen et al., 2013; Johnson et al., 2014; Wynn and Vannella, 2016).

To survive lung defenses and evade innate immune responses, *Coccidioides* expresses virulence factors for immune evasion and survival. Inside the lung, arthroconidia express ornithine decarboxylase, an enzyme implicated during growth from arthroconidia to spherule state (Guevara-Olvera et al., 2000). During transition, the spherule internal cell wall segments bud off into endospores. Lifecycle transition allows vulnerable, easily phagocytosed, arthroconidia to develop into phagocytosis-resistant spherules (Hung et al., 2002; Gonzalez et al., 2011; Nguyen et al., 2013). Arthroconidia are vulnerable to RNS while mature spherules suppress nitric oxide species (NOS) and inducible NOS expression in macrophages (**Figure 1**) (Gonzalez et al., 2011). Mature spherules are too large for most host phagocytic activity, allowing *Coccidiodes* to evade early immune detection (Hung et al., 2002). *Coccidioides* induces host expression of arginase resulting in ornithine and urea production, important components for transition from arthroconidia to spherule (Hung et al., 2007).

In the spherule state, *Coccidioides* secretes metalloproteinase 1 (Mep1) which digests an immunodominant antigen spherical outer wall glycoprotein (SOWgp) on the fungal surface (**Figure 1**) (Hung et al., 2005). Phagocytotic granulocytes rely on pathogen associated molecular patterns such as SOWgp, thus Mep1 secretion prevents detection by innate immune cells (Hung et al., 2005). *Coccidioides* upregulates nitrate reductase during development, an enzyme that converts nitrate to nitrite, thereby enhancing *Coccidioides* survival in anoxic conditions, such as those found inside a granuloma (Johannesson et al., 2006). Early detection to inhaled fungus is critical for host response. Macrophages and neutrophils detect *Coccidioides* arthroconidia and immature spherules *via* receptors Dectin-1, Dectin-2, and Mincle interacting with SOWgp (Hung et al., 2002; Nguyen et al., 2013). Endothelial lung cells use these same receptors to regulate defensin secretion.

Toll-like receptors (TLRs) and c-type lectin receptors (CLRs) interact with major pathogen-associated molecular patterns to detect *Coccidioides* (Romani, 2004; Viriyakosol et al., 2008;

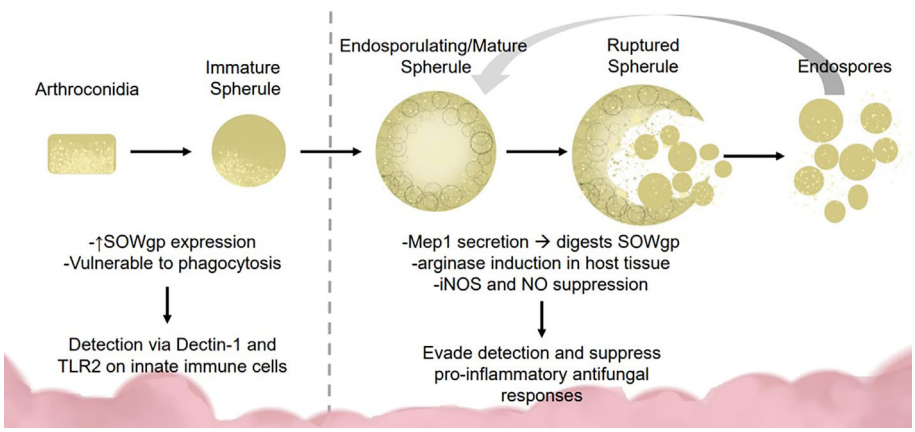

FIGURE 1 | Fungal dimorphism presents challenges for immune detection and activation. Early infection: *Coccidioides* is vulnerable to immune detection during early infection due to the smaller size (2–5 μM) and SOWgp expression which is detected *via* Dectin-1 and TLR2 on innate immune cells. These interactions mediate clearance *via* phagocytosis and reactive oxide species production. Later infection: As *Coccidioides* sporulates, it secretes MEP1 which digests SOWgp from the fungal surface, hampering immune detection. Spherules induce arginase expression in host tissues, suppressing NOS/NO production *via* an unknown mechanism, contributing to immune suppression.

Viriyakosol et al., 2013). Like most fungi, *Coccidioides* expresses β-glucans, chitins, and mannans in the outer cell wall (Nguyen et al., 2013). These cell components are recognized by a variety of TLRs and CLRs and elicit strong inflammatory responses from local immune cells. *Coccidioides* interactions with TLR2 and Dectin-1 on macrophages activate production of reactive oxide species (ROS) and inflammatory cytokines, such as interleukin-6 (IL-6) and tumor necrosis factor-alpha (TNFα) (Viriyakosol et al., 2008; Viriyakosol et al., 2013). There are no known nucleotide-binding oligomerization domain-like (NOD-like) receptors yet associated with *Coccidioides* detection.

In humans, polymorphisms in IFNγ/IL-12 signaling pathway result in a STAT1 gain of function mutations that associate with increased disease severity in *Coccidioides*, *Histoplasma*, and *Candida* infection (Sampaio et al., 2013). In disseminated *Coccidioides*, patients with severe disease were found to have a STAT3 mutation (Odio et al., 2015). STAT 3 mediates IL-23 signaling, critical for IFNγ, IL-12, and IL-17 production while STAT1 signaling induces Th1 cell differentiation in response to IL-12 to produce IFNγ; IFNγ, in turn, inhibits Th17 differentiation (Yeh et al., 2014). IL-12β1 receptor deficiency is associated with increased risk of disseminated coccidioidomycosis (Yeh et al., 2014). In chronic mucocutaneous candidiasis, gain of function mutations in STAT1 and STAT3 correlates to more severe disease and poor TH17 responses (Zheng et al., 2015). These observations suggest that STAT1 and STAT3 immune signaling is critical in host control of Th1/Th17 cytokine balance and is required for protection and *Coccidioides* fungal control.

In *Blastomyces dermatitidis* infection, LECs regulate collaborative killing between alveolar macrophages, dendritic cells (DC), and neutrophils (Hussell and Bell, 2014; Hernández-Santos et al., 2018). Upon LECs ablation, *B. dermatitidis* phagocytosis is reduced, and viable yeast numbers increase. Other data suggests that IL-1/IL-1R interactions regulate CCL20 expression in LECs. Chemokine CCL20 strongly recruits lymphocytes and weakly recruits neutrophils (Hernández-Santos et al., 2018). IL-1R-deficient mice express less CCL20 and lung Th17 cells are reduced, suggesting that IL-1/IL-1R signaling in LECs could regulate adaptive immune functions (Hernández-Santos et al., 2018). IL-1R is critical for vaccine induced resistance to *Coccidioides* infection *via* MyD88 induction of Th17 responses (Hung et al., 2014a; Hung et al., 2016a). Though it has not been explored, LECs could mediate early responses to *Coccidioides* through IL-1R, suggesting another innate immune cell role in anti-fungal responses within the lung tissues.

Alveoli structure likely helps shape local immune responses. Three dominant cell types exist within and around the alveoli structure: Type 1 and Type 2 pneumocytes (also known as alveolar epithelial cells, AECs), and tissue-resident alveolar macrophages (Guillot et al., 2013; Hussell and Bell, 2014). Type 1 pneumocytes (AECI) secrete IL-10 constitutively, which bind to IL-10R on alveolar macrophages to maintain an anti-inflammatory state. Type 2 pneumocytes (or AECII) express CD200 which interacts with CD200R on alveolar macrophage to inhibit pro-inflammatory phenotype (Guillot et al., 2013; Hernández-Santos et al., 2018). Alveolar macrophages express TGFβ-receptors that bind to pneumocyte-expressed αvβ6 integrin, tethering them in the alveolar airspace. In inflammatory conditions, AECIs upregulate TLRs and AECIIs increase SP-A and SP-D production (Guillot et al., 2013). These surfactant proteins are known to enhance pathogen opsonization and phagocytosis, and are capable of binding to *Coccidioides* antigen (Awasthi et al., 2004). *Coccidioides* infected mice expressed less SP-A and SP-D protein in their bronchial lavage fluid compared to uninfected and vaccinated controls, demonstrating the pathogen's capability of altering the lung mucosa (Awasthi et al., 2004). AECII secreted production of surfactant proteins may be influenced by *Coccidioides* allowing fungal escape of phagocytosis and prolonged survival.

Neutrophils

Neutrophils are the first responders and most abundant granulocytes in the immune system, making up 40%–70% of the total leukocyte population at homeostasis (Kolaczkowska and Kubes, 2013). Neutrophils destroy pathogens *via* phagocytosis, secretion of anti-microbial peptides, and extracellular traps, and provide signals for monocyte entry to sites of infection (Schaffner et al., 1986; Jain et al., 2016). In a 1:1 neutrophil to *Coccidioides* endospore interaction, human neutrophils readily phagocytose *Coccidioides* endospores and exhibit partial phagocytosis of larger spherules, coined "frustrated phagocytosis" (Lee et al., 2015). Neutrophils from healthy patients and chronic coccidioidomycosis patients exhibit similar neutrophil phagocytosis capabilities; however, high neutrophil presence is associated with chronic *Coccidioides* infection (Lee et al., 2015; Davini et al., 2018). This suggests that expanded neutrophil presence is detrimental for *Coccidioides* clearance perhaps due to their persistence into later stages of infection that may preclude other more effective responses (Davini et al., 2018). This in combination with neutrophil inability to fully phagocytose large endospores may make neutrophils ineffective, allowing prolonged fungal infection.

Neutrophil presence in tissue is typically associated with inflammatory tissue damage and pro-inflammatory cytokine expression such as IL-6 and IL-1β (Kolaczkowska and Kubes, 2013). Neutrophils follow C3a, C5a, IL-8, and IFNγ gradients toward sites of inflammation (Kolaczkowska and Kubes, 2013; Liu et al., 2017). However, chemoattractive molecules have limited stability and diffusion capabilities through tissues, suggestive that high neutrophil recruitment requires robust and/or steady expression of chemokines, which may also cause more inflammatory tissue damage. Until recently, it was believed that neutrophils migrate to infected tissue to mediate pathogen clearance and die within infected tissue after a few hours. Newer evidence suggests neutrophils re-enter circulation from the site of infection and may disseminate inflammation from the original recruitment site (Jain et al., 2016). For *Coccidioides* infection, this suggests a potential novel method for neutrophil dissemination of infection from the lungs where neutrophilia might promote disseminated disease. Depletion of neutrophils in *Paracoccidioides brasiliensis* infection results in decreased IFNγ

and IL-17 with almost all infected mice succumbing to infection (Pino-Tamayo et al., 2016). This highlights the delicate balance of helpful versus harmful responses that pro-inflammatory innate immune cells play during disease clearance. In murine models of disseminated fungal infection with *Blastomyces*, *Aspergillus*, and *Candida*, neutrophils transdifferentiate into specialized hybrid neutrophil-DCs, and *in vitro*, neutrophil-DCs retain microbicidal, neutrophil-like function while also stimulating CD4+ T cell differentiation (Fites et al., 2018). This suggests a dual role for neutrophils in coccidioidomycosis, where too much neutrophil presence could contribute to disseminated disease and tissue damage, while some appropriate level response allows stimulation of adaptive immunity. *In vivo* examination and characterization of neutrophil-DC hybrids may provide a better understanding of innate immune cell influence on adaptive immune cell responses in *Coccidioides* infection. *In vivo* examination of neutrophil migration may unveil dissemination mechanisms, allowing for targeted therapeutics to prevent severe, disseminated coccidioidomycosis.

Macrophages and Alveolar Macrophages

Macrophages engulf fungi and generate ROS and NOS that aid in degrading pathogens (Hussell and Bell, 2014). Fungicidal activity against *Coccidioides in vitro* by murine alveolar macrophages is enhanced in the presence of IFNγ (Beaman, 1987). IFNγ enhances and promotes phagocytosis, oxide species generation, pro-inflammatory cytokine production, and macrophage differentiation into the M1 phenotype for pathogen clearance and recruitment of other pro-inflammatory cells (Gentek et al., 2014). Pathogen recognition receptors on macrophages bind to targets for phagocytosis. Specifically, Dectin-1 and TLR2 interactions with *Coccidioides* facilitates clearance by macrophages by promoting oxide species and pro-inflammatory cytokine production (Viriyakosol et al., 2005; Tam et al., 2014).

Lung resident alveolar macrophages reside in air-exposed tissue compartments of the alveoli. Alveolar macrophages remove and clear particulates such as dust, pollutants, or airborne microorganisms in the respiratory mucosal surfaces (Lohmann-Matthes et al., 1994; Hussell and Bell, 2014). Alveolar macrophage-depleted mice challenged with *Aspergillus fumigatus* had higher fungal burden than wild-type mice (Gonzalez et al., 2011). When alveolar macrophages and DCs are ablated during *Aspergillus* infection, neutrophil infiltration increases (Lohmann-Matthes et al., 1994). This suggests alveolar macrophages and DCs may inhibit neutrophil recruitment during productive immunity to fungal lung infections.

Alveolar macrophages also promote tolerance to commonly encountered lung antigens (Hussell and Bell, 2014). Resting alveolar macrophages closely resemble an M2 or alternatively activated macrophage (Hussell and Bell, 2014). It is theorized that these cells require cooperation between many receptors to override the basal anti-inflammatory, tolerogenic state found in the lungs (Wilken et al., 2015). Once activated, alveolar macrophages exhibit higher respiratory burst, phagocytotic capabilities, and inflammatory cytokine production (Lohmann-Matthes et al., 1994). These cells are regulated through interactions with IL-10R, CD200R, TGFβ-R, mannose receptors, and triggering receptors (TREM1 and TREM2), which all dampen proinflammatory signaling pathways (Hussell and Bell, 2014). Following inflammation caused by high viral infection, murine alveolar macrophages have decreased TLR2 responsiveness, low mannose receptor and high CD200R expression (Hussell and Bell, 2014). Acute inflammation seems to irreversibly change the overall alveolar macrophage responsiveness toward pathogen invaders. This has interesting implications for *Coccidioides* infection in patients with chronic inflammatory lung diseases such as asthma, chronic obstructive pulmonary disease (COPD), or high pollution exposure. In coccidioidomycosis, it is possible that M1 macrophages may be required for pathogen clearance, but instead become M2 due to signals from fungal factors (**Figure 2A**). Studies examining macrophages recruited following *Coccidioides* infection would help characterize the macrophage subtypes needed for fungal clearance. Such data may identify novel macrophage targets to treat *Coccidioides* infection by influencing macrophage differentiation.

Eosinophils

Eosinophils are granulocytes associated with parasite infection, allergy, and asthma (Uhm et al., 2012). They make up 1%–3% of the leukocytes in the immune system and migrate to sites of inflammation *via* IL-5 chemotaxis (Yamaguchi et al., 1988; Uhm et al., 2012). Though not typically associated with an anti-fungal innate response, immunocompromised patients with allergic bronchopulmonary aspergillosis have high eosinophil lung infiltration during fungal infection, suggestive of maladaptive immunity (Chong et al., 2006). In chronic *Coccidioides*, infection correlates with peripheral blood eosinophilia (Harley and Blaser, 1994; Davini et al., 2018). Clinical observations from a *Coccidioides* case study highlight a correlation between asthma and poor fungal clearance, marked by high eosinophil lung infiltrate (Lombard et al., 1987). Increased IL-5 secretion in TNFα-deficient mice results in high eosinophil numbers and decreased IL-17A production, linking eosinophil changes to reduced adaptive responses (Fei et al., 2011). In acute *Paracoccidioides brasiliensis* infection, eosinophil recruitment is modest compared to uninfected mice but upon neutrophil depletion, eosinophil numbers increase significantly in the lungs (Pino-Tamayo et al., 2016). However, even with increased eosinophil presence, these mice still succumbed to infection with higher fungal burden. These data suggest that eosinophils could be recruited in the absence of neutrophils as a compensatory mechanism but unfortunately are not as protective as neutrophils.

Eosinophil presence in pulmonary coccidioidomycosis inversely correlates to neutrophil frequency (Lombard et al., 1987; Lee et al., 2015). In *Aspergillus*-allergy asthma murine models, lung DCs secrete TNFα which preferentially recruits neutrophils over eosinophils in the lung (Fei et al., 2011). This suggests local lung leukocytes influence immune cell recruitment and potentially control *Coccidioides* infection by establishing a different lung microenvironment (Fei et al., 2011). It is unknown whether asthma contributes to poor *Coccidioides* clearance, and asthma

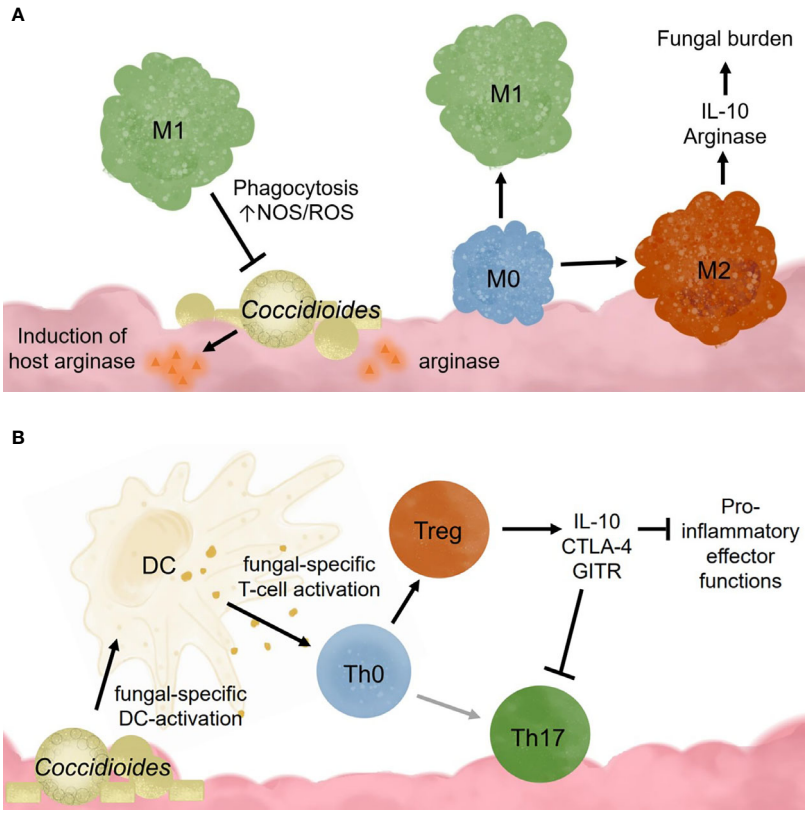

FIGURE 2 | Innate immune cell responses to *Coccidioides* influence adaptive immune cell activation and effector functions. **(A)** *Coccidioides* may evade innate immune cell clearance and influence immune functions. **(B)** Dendritic cells are critical for activating adaptive responses and influencing adaptive immune cell population differentiation.

rates are high in current endemic regions. It could be that eosinophil and neutrophil recruitment varies between acute and chronic coccidiomycosis patients due to predisposed lung conditions such as allergies and asthma. Therefore, exploring pre-existing health conditions and disease progression may provide important clues to define effective clearance mechanisms.

Dendritic Cells

DCs are professional antigen presenting cells, responsible for the initiation, regulation, and maintenance of adaptive immune responses (Desch et al., 2013). Lung-resident DCs must also maintain a balance between activation against invading pathogens and tolerance to continuous antigen exposure. DCs are adept at identifying fungal pathogens and promoting pathogen clearance, due to their powerful ability to activate naïve T lymphocytes (Romani et al., 2002). *Coccidioides* spherule recognition induces human DC maturation and activation resulting in elevated CD40 and CD80/CD86 (B7.1/B7.2) surface expression and heightened T lymphocyte stimulation (Dionne et al., 2006). DCs from healthy human patients, pulsed with *Coccidioides* spherule lysate, induce antigen-specific T cell activation (Richards et al., 2001).

There are many DC subsets with distinct functionality (Segura, 2016). Some promote inflammatory immune activation while others induce tolerance and tissue regeneration. Conventional DCs (cDC) versus monocyte-derived DCs (mDCs), exhibit opposing migration capacity to the lungs (Nakano et al., 2013). cDCs travel into the lung during homeostasis, whereas mDCs only migrate into lung tissue during active inflammation (Segura, 2016). Lung endothelial cells secrete IL-10, which maintains an anti-inflammatory, tolerogenic state and promotes anti-inflammatory DC function (Segura, 2016; Teitz-Tennenbaum et al., 2018). In IL-10 deficient mice infected with *Cryptococcus*, DCs upregulate inducible NOS expression and recruit neutrophils and M1 macrophages to the lungs during infection (Teitz-Tennenbaum et al., 2018). In contrast, IL-10-sufficient DCs express high arginase and CD206 (mannose receptor) which promotes tolerance within the lung by inducing IL-10 expression within endothelial tissues (Teitz-Tennenbaum et al., 2018). Maintaining an anti-inflammatory state within the lungs is critical for preventing unnecessary tissue damage to the delicate airspace architecture. Tolerance and anti-inflammatory signals are thus critical for ensuring that tissue-damaging inflammation does not occur unless pathogenic danger is imminent. Since DCs are responsible for controlling adaptive immune responses, understanding tissue-resident DCs and lung-microenvironmental influences is critical for understanding immune activation choices during pathogen detection and clearance.

DCs possess phagocytotic and pathogen clearance capabilities and act as professional antigen presenters to adaptive immune cells. Like macrophages that polarize into pro-inflammatory or anti-inflammatory subsets, DCs also exhibit polarization and DC polarization skews helper T cell differentiation toward specific subtypes (de Jong et al., 2005). *Cryptococcus neoformans* promotes an anti-inflammatory DC phenotype which suppresses inflammatory innate cells activation, allowing fungal persistence (Teitz-Tennenbaum et al., 2018). IL-10 blockade results in DCs with higher expression of costimulatory molecules and pro-inflammatory cytokines (Segura, 2016). In *Histoplasma capsulatum infection*, CD8α+ pro-inflammatory DCs were found to be critical for fungal clearance by inducing CD4+ T helper 1 (Th1) cells and CD8+ T cells (Lin et al., 2005).

DCs regulate T cell responses and immunological memory generation required for effective vaccines. Creating vaccines for dimorphic fungal pathogens is difficult as T lymphocytes recognize specific antigens and polymorphic fungal pathogens express different antigens throughout their life cycle. DCs have the unique challenge of presenting and mounting an effective immune response against *Coccidioides* regardless of morphological stage. Recent attempts at DC-based vaccinations show promising success in mouse models. Adoptive transfer of *Coccidioides*-antigen loaded DCs reduces murine fungal burden by live, virulent *Coccidioides* challenge (Awasthi, 2007). Disseminated coccidioidomycosis patient DCs loaded with T2K antigen overcame T cell anergy, driving T cell proliferation (Richards et al., 2002). This highlights a potential therapeutic where patients' immune responses could be reactivated for fungal clearance. In murine vaccine studies, *Coccidioides* antigens delivered with glucan-chitin particles (GCP) effectively stimulate DC inflammatory responses. DCs loaded with GCP-antigen complex induce a mixed T helper 1 and T helper 17 response against *Coccidioides* infection, thought to be critical for effective fungal clearance (Hung et al., 2018a). These studies suggest that manipulating DC responses may be a viable route to creating vaccines that induce strong and specific immunity and may overcome pre-existing T cell anergy. The antigen subunit studies suggest effective DC activation requires multi-variant antigen interactions, and that multi-antigen vaccine therapies are promising strategies against *Coccidioides*.

INTRODUCTION TO ADAPTIVE IMMUNITY

Unlike innate immunity, adaptive immunity offers higher pathogen specificity, more powerful pathogen control mechanisms, and the ability to establish memory against future infections. Infection persistence implies a breakdown in immunity effectiveness or host feedback mechanisms protecting against damaging responses. To understand why chronic *Coccidioides* infections occur, we must first understand effective immunity to *Coccidioides*.

B Cells

Protective immunity against *Coccidioides* is mediated predominantly by T cells (Hung et al., 2018a). *Coccidioides*-specific antibodies are observed in human and mouse studies, indicating that B cells also recognize and interact with *Coccidioides* antigen. IgG antibody is the prominent antibody isotype observed in humoral mediated responses to *Coccidioides* infection, indicative that class-switching occurs (Magee et al., 2005). Screening patients infected with *Coccidioides*, *Histoplasma*, and/or *Blastomycoses* with complement-fixing assays identified IgG1 as the predominant isotype generated.

Thirty days post-infection, mice have no neutralizing or complement-fixing antibodies in their sera against *Coccidioides* antigen and adoptive transfer of B cells from immunized mice into naïve mice does not confer protection (Beaman et al., 1979). In a contrasting study, T cell rich, B-cell deficient transfer conferred early protection, but the mice ultimately succumbed to disease 34 days post-infection (Magee et al., 2005). Mice that received whole splenocyte (mixed T cell, B cell, and other immune cell populations) transfers survived the longest. This could be due to the inclusion of B cells or other immune populations in the transfer. Vaccination with formalin fixed *Coccidioides* spherules and secondary intranasal challenge with live, virulent *Coccidioides* in BALB/c mice causes a marked increase in B cell-specific genes within whole lung tissue and generation of *Coccidioides*-specific serum antibodies (Magee et al., 2005). These studies suggest that B cells have a protective role in *Coccidioides* response and may even increase in frequency within the lung as suggested by bulk gene expression analysis data where B cell specific genes increased in expression in *Coccidioides* infected lung tissue compared to uninfected lung (Magee et al., 2005).

IgG generation requires CD4+ T cell-mediated class-switching and may explain the discrepancy between the B cell studies described above: T cells might provide initial protection, but without B cells there is no sustained antibody protection. Some *Coccidioides* antigens stimulate both T and B cell responses (Zhu et al., 1997). SOWgp is the best known immunostimulating *Coccidioides* antigen, eliciting a humoral response and innate immune cell activation (Hung et al., 2000). Disagreement around B cells in protective immunity against *Coccidioides* might be partially explained due to varied use of live-wildtype, live-attenuated, or formalin-fixed *Coccidioides* between studies, and the purity of cell populations utilized. *Coccidioides* is polymorphic and expresses multiple antigen types throughout its lifecycle, thus effective neutralizing antibodies and class-switching may be required at different stages of the immune response. High affinity antibody generation requires affinity maturation *via* somatic mutation, processes reliant on CD4+ T cell help. Considering all these data together, B cells likely contribute to adaptive and humoral immunity against *Coccidioides*, but further work is needed to definitively define the contribution to disease progression and control.

T Cells and Effector Cytokines

Patients that recover from coccidioidomycosis with little to no medical intervention have polyfunctional T lymphocytes in circulation (Nesbit et al., 2010). Upon *Coccidioides* antigen stimulation, peripheral human CD4+ and CD8+ T lymphocytes secrete pro-inflammatory cytokines, such as IL-2,

TNFα, and IFNγ (Nesbit et al., 2010). In humans, HIV and immunosuppression are risk factors for severe, disseminated infection and this risk is associated with decreased CD4+ T cell numbers (Saubolle et al., 2007; Johnson et al., 2012; Wack et al., 2015). In T cell-deficient mice, infection is severe, and effector T cell transfer protects mice against virulent infection (Fierer et al., 2006). CD4+ T cells from immunized C57BL/6 mice transferred into non-immunized CD40-deficient mice confer protection and prolong survival (Zhu et al., 1997). Vaccination with an attenuated *C. immitis* laboratory strain in CD4-deficient mice is protective, suggesting that CD8+ T cells can protect against *Coccidioides* (Fierer et al., 2006). No other studies show direct CD8+ T cells contribution to *Coccidioides* immunity. However, the CD8+ T cell study used an intraperitoneal infection, not intranasal delivery, so translation to pulmonary infection is unclear. In other fungal infections such as *Blastomyces* and *Histoplasma*, IL-17 producing CD8+ T cells provide protection and fungal clearance even in CD4-deficient mouse models (Nanjappa et al., 2012; Hung et al., 2016b). Overall, CD8α+ T cells may contribute to *Coccidioides* immunity, but further work is needed to characterize their anti-fungal mechanisms.

T cell differentiation into subsets allows targeted and tailored immune responses to different pathogen classes. For anti-fungal responses, T helper 1 (Th1) and T helper 17 (Th17) cells are especially critical in *Coccidioides* murine infections (Nanjappa et al., 2012). Loss of either of these T helper subtypes, or their associated cytokines, results in impaired immune responses and impaired fungal clearance. In human *Coccidioides* infection, Th17 cells are protective and acute coccidioidomycosis patients have high Th17 promoting serum cytokine levels (Davini et al., 2018). *In vitro Coccidioides* antigen stimulation of peripheral blood cells from acute disease patients yields robust IL-17 production (Hung et al., 2016b). *Coccidioides*-induced Th1 and Th17 cells secrete cytokines that mobilize innate immune cells to the site of infection, promote the activation and differentiation of immune cells, and induce anti-microbial peptides in endothelial cells (Hung et al., 2016b). This crossroad in innate immunity mediated by Th17 is observed in other fungal pathogens that infect mucosal tissues (Khader et al., 2009). Th1 cells make cytokines that enhance macrophage phagocytosis and ROS generation.

Coccidioides-resistant DBA/2 mice mount strong Th1 responses against *Coccidioides*, with increased serum IL-12 production (Magee and Cox, 1996). IL-12 administration to *Coccidioides*-susceptible BALB/c mice results in lowered fungal burden in lungs and spleen, whereas IL-12 blockage dramatically increases fungal burden across tissues, suggesting that IL-12 is protective against *Coccidioides* (Magee and Cox, 1996). DBA/2 mice express fully formed C-type lectin receptors, Dectin-1, unlike susceptible C56BL/6 mice with truncated Dectin-1. Dectin-1 is critical in fungal pathogen recognition and loss of dectin-1 correlates to increased fungal burden and decreased adaptive immune responses (Vautier et al., 2010) Dectin-1 interacts with *Coccidioides* β-1,3-glucans located in the outer cell wall and induces antibody class-switching and production, and CD8+ T cell activation (Viriyakosol et al., 2013). Dectin-1 binding to its ligand induces antigen presenting cell secretion of IL-1β, IL-23, IL-6, and TGFβ, cytokines necessary for Th17 cell differentiation. It is theorized that CARD9, an adaptor molecule downstream of Dectin-1 signaling, promotes intracellular signaling required for Th17 differentiation. CARD9-deficient mice are unable to clear pulmonary and subcutaneous infections with a highly virulent strain of *Coccidioides posadasii* (C735) (Hung et al., 2016a). These data emphasize the importance of fungal sugar pattern recognition receptor interactions for supporting Th1 and Th17 responses in adaptive immunity. In a multivalent vaccine study, CARD9 mediated Dectin-1 and Dectin-2 interactions were critical for establishing protection against *C. posadasii* infection (Campuzano et al., 2020). Mice not expressing CARD9, Dectin-1, or Dectin-2 all have significantly lower inflammatory cytokine responses and fail to mount Th17 responses within the lung. These data emphasize that though adaptive immune responses are critical, innate-associated receptors are required for establishing adaptive immunity, emphasizing that early innate interactions set the state for later adaptive responses.

C57BL/6 and BALB/c mice infected with an attenuated strain of *Coccidioides posadasii* (ΔT) have increased Th1 and Th17 frequencies and reduced fungal lung burden, further supporting the observation that these T helper responses are necessary for anti-fungal protection (Hung et al., 2016b). In other fungal pathogen studies, IL-17, IL-21, and IL-22 secretion by Th17 cells was vital for protection. IL-17 stimulates neutrophil and macrophage pro-inflammatory abilities and stimulates epithelial cells to secrete β-defensins (Khader et al., 2009). IL-21 acts as an autocrine regulator and promoter of Th17 proliferation, IL-22 induces host-secreted anti-microbial peptides, and TNFα promotes multiple proinflammatory pathways through NF-κβ and MAPK (Khader et al., 2009). These functions make Th17 cells and their effector cytokines very powerful against fungal pathogens. IL-1R deletion results in a significant decrease in Th17 numbers in *Coccidioides*-infected lungs, while Th1 numbers remain unchanged (Hung et al., 2014a). Lung Th17 numbers decrease in *Coccidioides*-infected IL-1R deficient mice relative to WT mice while Th1 numbers remain unchanged. In a human population study analyzing genetic susceptibility to *Blastomyces* infection, researchers found that IL-6 loss of function mutations increases susceptibility against *Blastomyces* infection (Merkhofer et al., 2019). IL-6 knock-out mice had lower Th17 responses and increased fungal burden within the lungs. These data emphasize the importance of Th17 responses against fungal infection while highlighting the complexity of cytokine networks needed to establish and regulate anti-fungal responses.

Th17 cells also participate in memory responses. In chronic pulmonary disease and fungal infection (*C. posadasii*, *H. capsulatum*, and *B. dermatitidis*), vaccine induced Th17 cells are sufficient for overcoming secondary challenge (Zelante et al., 2007). However, in *C. albican*s and *A. fumigatus* infection, Th17 cells are detrimental for fungal clearance, highlighting the variable role Th17 cells play in adaptive immunity. Th17 cells dampen neutrophil function and recruitment but also induce

hyperinflammatory responses depending on the immune context (Zelante et al., 2007). There are two known Th17 subsets: pathogenic (GM-CSF producing) Th17 and non-pathogenic (IL-10 producing) Th17 (El-Behi et al., 2011; Bystrom et al., 2019). While advances have been made in defining effector T cell functions during chronic fungal infection, much more work is needed to understand how chronic inflammation alters function. This may explain why Th17 cells are critical for memory responses, host survival and fungal clearance in some fungal infections but damaging and ineffective in others.

In a *Coccidioides* vaccine study, loss of Th17 immunity increased infection susceptibility while loss of Th1 and Th2 immunity did not, implying that Th1 and Th2 cells are not critical for protection (Hung et al., 2011). The underlying mechanisms for this protection are less clear. For example, Th2 cells can promote alternatively activated macrophages which secrete collagen and assist in tissue repair. Alternatively activated macrophages are often recruited to sites of infection where their collagen production assists in establishing granulomatous structures. Virulent and avirulent *Coccidioides* strains form granulomas *in vivo*, and while morphologies have been characterized. we do not know what cells are recruited to the granuloma, what signals form and maintain the granuloma structure, nor details on the immune microenvironment within the granuloma interior (Narra et al., 2016). Exploring granuloma immunity is imperative for understanding infection chronicity as *Coccidioides* infection often presents with granuloma formation. Such knowledge could inform diagnosis and provide markers that distinguish fungal granulomas from cancer nodules and bacterial granulomas.

CD4+ T cell subset frequency is also correlated with infection outcome in human patients. In a pediatric coccidioidomycosis study, high regulatory T cell (Treg) frequency correlated with chronic disease (Davini et al., 2018). Patients with a similar fungal infection, *Paracocidioides brasiliensis*, have a higher %Tregs than healthy controls, and the Tregs are more suppressive (Odio et al., 2015). In mouse models, Treg depletion after infection with *Paracoccidioides brasiliensis* resulted in decreased fungal burden and enhanced survival (Galdino et al., 2018). Chronic *Coccidioides* patients also express heightened serum IL-10 cytokine levels. IL-10 is an effector cytokine used by Tregs to suppress immune activation and reduce inflammation (Cavassani et al., 2006). In the absence of IL-10, susceptible mice develop a protective immune response and lasting immune memory against virulent *Coccidioides posadasii* (Hung et al., 2014b). Tregs regulate immune responses by controlling immune cell activation to prevent hyperinflammatory, damaging responses (Montagnoli et al., 2002; Wing et al., 2008). The mechanisms underlying Treg association with chronic *Coccidioides* disease outcome are unknown. Elevated Treg frequency may block effector responses by overwhelming effector cells, Tregs may be more suppressive, or Tregs may develop at the expense of Th17 responses (Davini et al., 2018). Treg and Th17 differentiation are inversely regulated; the signals required for Treg development block Th17 differentiation (Khader et al., 2009; Yeh et al., 2014). Under inflammatory conditions Tregs can lose regulatory, and gain effector, functions promoting chronic inflammation (Wing et al., 2008). *Coccidioides*-resistant DBA/2 mice have lower lung Treg frequency that produce less IL-10 upon stimulation *ex vivo* compared to susceptible mice (**Table 1**) (Fierer et al., 1998; Viriyakosol et al., 2008; Hung et al., 2014b). These studies suggest a detrimental role for Tregs in *Coccidioides* clearance and emphasize a need to explore their function and plasticity during *Coccidioides* infection. It is unlikely that gain of effector functionality is occurring during chronic *Coccidioides* infection as T helper cells enhance fungal control. Further work must be done to determine whether Treg presence and functionality direct adaptive immune responses and reduce *Coccidioides* control.

In better studied models of chronic inflammation, such as chronic viral infections and cancer, T cells upregulate inhibitory receptors, reducing effector function, in a process termed exhaustion (Wherry and Kurachi, 2015). Chronic antigen exposure is sufficient to drive T cells toward exhaustion, often marked by elevated PD-1 and PD-L1 surface expression (Wherry and Kurachi, 2015). There is very little work examining T cell exhaustion in the context of chronic fungal infections, but existing works that look at chronic *Candida* sepsis patients supports the general observation that exhaustion is detrimental to host health and fungal clearance (Lázár-Molnár et al., 2008; Spec et al., 2016). In *Histoplasma* infections, mice lacking PD-1/PD-L1 survive severe infection while wild-type do not (Lázár-Molnár et al., 2008). *Candida* sepsis patients have elevated circulating PD-1/PD-L1 high T cell frequency (Spec et al., 2016).

TABLE 1 | Resistance to *Coccidioides* infection in specific strains could be due to immune cellularity differences.

Mouse Background	Susceptibility to *Coccidioides* Infection	Alveolar Macrophage Freq.	Lung-resident DC Freq.	Respiratory Leukocyte TNFα production	Respiratory Leukocyte IL-10 production	Lung CD4+CD25+FOXP3+ (Treg) Freq.	Reference Numbers
C57BL/6	Susceptible	Base	Base	Base	Base	Base	(Fierer et al., 1998; Viriyakosol et al., 2008; Viriyakosol et al., 2013; Hung et al., 2014b)
BALB/C	Susceptible	No Δ	No Δ	↑↑	↑↑	↑↑	(Fierer et al., 1998; Viriyakosol et al., 2008; Hung et al., 2014b)
DBA/2	Resistant	No Δ	No Δ	No Δ	↓	↓	(Fierer et al., 1998; Viriyakosol et al., 2008; Viriyakosol et al., 2013; Hung et al., 2014b)

The base frequency of cells or cytokine production is in reference to C57BL/6 mice; denoted changes are relative to this strain. Cytokine production was measured post stimulation ex vivo. No Δ, no change from base level; ↑↑, higher than base; ↓, less than base.

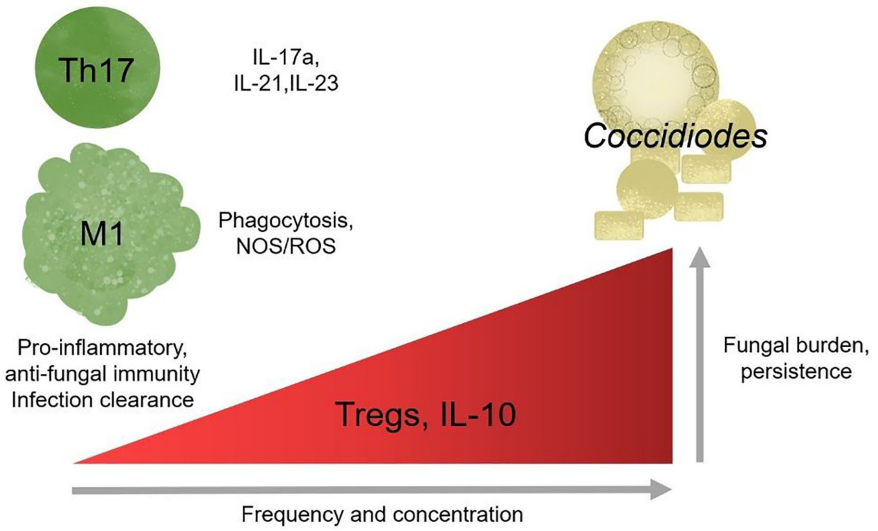

FIGURE 3 | Regulatory responses correlate with chronic disease outcome. Th17 cells and pro-inflammatory responses are protective against *Coccidioides* and loss of responses results in increase susceptibility in mice. Modulating effector and regulatory responses might be a potential therapy for chronic infection.

In paracoccidiomycosis, T cells overexpress PD-1 suggestive of early stage exhaustion during chronic infection (Cacere et al., 2008). It is unknown whether chronic coccidioidomycosis may occur due to T cell exhaustion and maintenance by inappropriately mounted regulatory responses; if so, immune checkpoint blockade could benefit patients with fungal induced T cell exhaustion and promote fungal clearance (**Figure 3**).

VACCINATIONS AND IMMUNE MEMORY

There is currently no fungal vaccine clinically available for humans. Fungal pathogens are eukaryotic, sharing many conserved molecules with humans, making drug and vaccine targeting highly difficult without targeting human cells (Johannesson et al., 2006; Nguyen et al., 2013). *Coccidioides* is dimorphic; the soil and host forms express different surface molecules (Johannesson et al., 2006; Saubolle et al., 2007; Nguyen et al., 2013; Johnson et al., 2014). Thus, effective vaccine strategies must include components that would elicit both a strong and effective immune response without selecting temporal life cycle antigen targets. A *C. albicans* vaccine, NDV-3A, in stage 1b/2a clinical trial that shows promise in protecting patients from recurring vulvovaginal candidiasis (Alqarihi et al., 2019). NDV-3A success demonstrates the major strides made in fungal vaccine research and highlight how much further we have to go. The field has made remarkable progress in identifying adjuvants, antigens, and target cells for vaccine therapies, but further work must be done to demonstrate reliable efficacy between animal models and human use, especially in less studied fungal pathogens such as *Coccidioides*.

Several labs have generated live, attenuated strains of *Coccidioides* that successfully confer protection against secondary challenges with virulent, wild-type *Coccidioides* in susceptible mouse strains (Xue et al., 2009; Hung et al., 2011). The attenuations hinder fungal replication within the host, pausing *Coccidioides* growth at the spherule state. Mice vaccinated with attenuated *Coccidioides* strain ΔT mount Th1 and Th2 effector responses and survive longer than non-vaccinated littermates during post-secondary challenge (Xue et al., 2009). Protein component vaccination with antigen2/PRA (a deglycosylated, proline-rich antigen expressed in *Coccidioides* spherules) is protective when administered subcutaneously or intranasally in susceptible mice (Shubitz et al., 2002). However, this protection decreases at higher fungal doses and only intranasal administration of antigen2/PRA confers protection to both C57BL/6 and BALB/C mice. This component vaccine prolongs survival, but immune cell response to antigen2/PRA has yet to be characterized (Shubitz et al., 2002). Following up on antigen2/PRA as a promising vaccine strategy, mouse bone marrow derived DCs presenting the antigen2/PRA epitope, were intranasally transferred into mice and their immune response analyzed (Awasthi et al., 2019). Lymphocytes and leukocytes from immunized mice express more IFNγ, IL-4, and IL-17 compared to mice that receive control DCs. While this study did not challenge mice with *Coccidioides* post-immunization, it demonstrates the possibility of immune-cell transfer as a vaccination strategy. ΔT vaccination studies show a mixed Th1, Th2, and Th17 response in immunized mice and conferred protection in susceptible C57BL/6 mice (El-Behi et al., 2011). This vaccine's success emphasizes adaptive immunity's importance in protection. Maize provides more efficient generation of antigen2, and a maize-produced subunit vaccine along with the previously discussed glucan-chitin particle delivery

method protected mice against *Coccidioides* and yielded lower fungal burden (Hayden et al., 2019).

The most effective vaccines include adjuvants and additives that enhance immunity and memory. Most notably, adding an agonist of human fragment C5a enhances vaccine immunity against *Coccidioides* infection in mice (Hung et al., 2012). Human C5a added during ΔT vaccination in BALB/c mice, causes heightened Th1 and Th17 responses and circulating effector cytokines; furthermore, humanC5a/ΔT vaccinated mice express higher titers of IgG1 and IgG2 specific to *Coccidioides* and survive longer compared to BALB/c mice vaccinated with ΔT alone (Hung et al., 2012). Ablating IL-10 with ΔT vaccination increases survival and protection against virulent *Coccidioides* infection and increases recall protection post infection (Hung et al., 2014b). These studies further reinforce Th1/Th17 cells in immunity against *Coccidioides* while IL-10 plays a negative role in clearance. This suggests *Coccidioides* immunity requires robust pro-inflammatory responses, while immunosuppression leads to infection persistence.

To complement vaccine research, we need to understand the memory responses vital for sustained immunity. While memory responses have been observed in *Coccidioides* vaccine experiments, tissue-resident memory, effector memory, and central memory subtypes have not been characterized in *Coccidioides* infection. Memory research has made great strides in characterizing cytokine recall responses, but further characterization is required to identify the source of the memory cells. In *Candida* infection, skin-resident memory T cells remain after infection and reactivate upon reinfection (Iannitti et al., 2012). Since many fungal infections occur within mucosal tissues and effective clearance requires tissue specific responses, fungal vaccine development could benefit from exploring tissue-specific memory (Iannitti et al., 2012). In tuberculosis, a bacterial infection associated with granuloma formation, intranasal vaccination with attenuated mycobacterium induces protective CD4+ and CD8+ T cells and mucosa associated lymphoid responses (Walrath et al., 2005). Further analysis revealed tissue resident memory responses from lung parenchyma are critical for protection against virulent mycobacterium (Walrath et al., 2005; Sakai et al., 2014). This validates intranasal delivery as an effective method of vaccination for stimulating tissue resident memory development. While tuberculosis is a bacterial infection, similarities between tuberculosis granulomas and coccidioidomycosis granulomas highlight tissue-resident memory responses as a key for long-lasting immunity in chronic lung infections. Coccidiomycosis starts as a localized respiratory infection, so tissue-resident memory could be critical for providing long lasting protection and warrants further study.

Current work suggests fungal sugar receptors are highly important for the development of anti-fungal recall responses (Shubitz et al., 2002; Cavassani et al., 2006; Hung et al., 2018b). However, much of what we know about memory immunity to *Coccidioides* has used live-attenuated laboratory strains, fungal-derived antigens, and fungal sugar adjuvants to achieve protective immune responses. Characterizing the memory response to live, whole, virulent *Coccidioides* might help to define how memory is generated, or perhaps blocked from generation, in natural infections. Such immunological questions would aid vaccine development, providing a broader context of *Coccidioides*-specific challenges for effective memory responses where our more defined, specific studies are lacking Together, these studies would allow for an elevated understanding of *Coccidioides* immunity as a whole, generating the specific antigen knowledge for vaccine development and broad characterization for better patient treatment.

CONCLUSION: CLINICAL SIGNIFICANCE AND URGENCY

Valley fever research is at a critical point. California's highest endemic region for Valley fever, SJV, has one of the lowest physicians to citizen ratios, adding a barrier to health care access (Petterson et al., 2012). Drugs used to treat chronic Valley fever cause debilitating side-effects in patients such as, but not limited to, headaches, lethargy, seizures, severe hair lost, extreme exhaustion, and nerve pain (Saubolle et al., 2007; Saenz-Ibarra et al., 2018). Due to its generic flu-like symptoms, it is often misdiagnosed as other respiratory infections, leading to late stage diagnosis when more severe symptoms of chronic infection manifest. Since disease clearance or progression determinants are unknown, early diagnosis is invaluable for planning patient treatment. Susceptibility marker identification would help determine those vulnerable to chronic disease. Understanding how the innate and adaptive immune system responds to Valley fever is necessary for optimal diagnoses, treatments, disease progression predictions, and vaccine development. Such studies will inform accurate diagnoses and perhaps provide novel drug targets for therapy. It is unclear whether *Coccidioides* infection becomes chronic because i) the host has high regulatory responses and thus suppresses pro-inflammatory responses, ii) *Coccidioides* is manipulating and influencing host innate immunity to block inflammatory responses, which, in turn, promotes ineffective helper responses, or iii) a combination of host and pathogen influences (**Figures 2A, B**). These observations emphasize the importance of a pro-inflammatory response and suggest that inhibition of pro-inflammatory players promote infection persistence. Tregs seem especially pertinent given supportive pediatric patient and depletion data in *Paracoccidioides* (Felonato et al., 2012). In some settings, Tregs retain their suppressive function yet cannot control T effector responses. This is because T effector cells become refractory to Treg suppression. While this has not been assessed, it is possible that T effector cells could become more sensitive to suppression by Tregs, reducing their effector functionality. Characterizing innate immune cells activation and recruitment of adaptive responses may define how *Coccidioides* eludes clearance and shed light on the role of pro-inflammatory and regulatory responses in disease progression (**Figure 3**).

Until the last 30 years, fungal pathogens have not been as well studied as their viral or bacterial counterparts. The field is at a critical and exciting time as we work together to close gaps in fungal pathogen host immune knowledge. Climate change models predict *Coccidioides*' endemic regions will spread to the American Midwest

by 2050. Thus *Coccidioides* is anticipated to spread significantly beyond the current regions of endemicity (Coopersmith et al., 2017; Gorris et al., 2019). Though severe disease is rare, it is unknown what factors indicate infection susceptibility and disease progression. As antifungal resistance, fungal disease frequency, and regions of endemicity increase, the urgency and need for effective vaccines and better therapeutics also rise. Due to current lack of effective treatment options for chronic disease, the inability to determine likelihood of disease progression toward chronicity at time of diagnosis, and the growing spread of the endemic region, there is a dire need to fully understand host immune response for improved diagnoses and treatment.

AUTHOR CONTRIBUTIONS

AD: conceptualization, literature evaluation, original draft writing, and generated and visualized figures. KH: conceptualization, writing and review, visualization, funding acquisition, and supervision. All authors contributed to the article and approved the submitted version.

FUNDING

This work was supported by the University of California (UC) Office of the President grant VFR-19-633952 and UC Multicampus Research Programs and Initiatives grant 17-454959, and a private donation from Robert Hayden and Betty Dawson.

ACKNOWLEDGMENTS

The authors thank Austin M. Perry, Dr. Melanie Ikeh, and Hoyer lab members for their expertise and critical evaluation of the manuscript.

REFERENCES

Alqarihi, A., Singh, S., Edwards, J. E., Ibrahim, A. S., and Uppuluri, P. (2019). NDV-3A vaccination prevents C. albicans colonization of jugular vein catheters in mice. *Sci. Rep.* 9 (1), 1–6. doi: 10.1038/s41598-019-42517-y

Awasthi, S., Magee, D. M., and Coalson, J. J. (2004). Coccidioides posadasii infection alters the expression of pulmonary surfactant proteins (SP)-A and SP-D. *Respir. Res.* 5 (1), 1–8. doi: 10.1186/1465-9921-5-28

Awasthi, S., Vilekar, P., Conkleton, A., and Rahman, N. (2019). Dendritic cell-based immunization induces Coccidioides Ag2/PRA-specific immune response. *Vaccine* 37 (12), 1685–1691. doi: 10.1016/j.vaccine.2019.01.034

Awasthi, S. (2007). Dendritic Cell-Based Vaccine against Coccidioides Infection. *Ann. N. Y. Acad. Sci.* 1111 (1), 269–274. doi: 10.1196/annals.1406.013

Beaman, L. V., Pappagianis, D., and Benjamini, E. (1979). Mechanisms of resistance to infection with Coccidioides immitis in mice. *Infect. Immun.* 23 (3), 681–685. doi: 10.1128/IAI.23.3.681-685.1979

Beaman, L. (1987). Fungicidal activation of murine macrophages by recombinant gamma interferon. *Infect. Immun.* 55 (12), 2951–2955. doi: 10.1128/IAI.55.12.2951-2955.1987

Benedict, K., McCotter, O. Z., Brady, S., Komatsu, K., Cooksey, G. L. S., Nguyen, A., et al. (2019). Surveillance for Coccidioidomycosis—United States, 2011–2017. *MMWR Surveill. Summaries* 68 (7), 1. doi: 10.15585/mmwr.ss6807a1

Bystrom, J., Clanchy, F.II, Taher, T. E., Al-Bogami, M., Ong, V. H., Abraham, D. J., et al. (2019). Functional and phenotypic heterogeneity of Th17 cells in health and disease. *Eur. J. Clin. Invest.* 49 (1), e13032. doi: 10.1111/eci.13032

Cacere, C. R., Mendes-Giannini, M. J., Fontes, C. J., Kono, A., Duarte, A. J., and Benard, G. (2008). Altered expression of the costimulatory molecules CD80, CD86, CD152, PD-1 and ICOS on T-cells from paracoccidioidomycosis patients: lack of correlation with T-cell hyporesponsiveness. *Clin. Immunol.* 129 (2), 341–349. doi: 10.1016/j.clim.2008.07.008

Campuzano, A., Zhang, H., Ostroff, G. R., dos Santos Dias, L., Wüthrich, M., Klein, B. S., et al. (2020). CARD9-Associated Dectin-1 and Dectin-2 Are Required for Protective Immunity of a Multivalent Vaccine against Coccidioides posadasii Infection. *J. Immunol.* 204 (12), 3296–3306. doi: 10.4049/jimmunol.1900793

Cavassani, K. A., Campanelli, A. P., Moreira, A. P., Vancim, J. O., Vitali, L. H., Mamede, R. C., et al. (2006). Systemic and local characterization of regulatory T cells in a chronic fungal infection in humans. *J. Immunol.* 177 (9), 5811–5818. doi: 10.4049/jimmunol.177.9.5811

Chen, S., Erhart, L. M., Anderson, S., Komatsu, K., Park, B., Chiller, T., et al. (2011). Coccidioidomycosis: knowledge, attitudes, and practices among healthcare providers—Arizona, 2007. *Med. Mycol.* 49 (6), 649–656. doi: 10.3109/13693786.2010.547995

Chong, S., Lee, K. S., Chin, A. Y., Chung, M. J., Kim, T. S., and Han, J. (2006). Pulmonary fungal infection: imaging findings in immunocompetent and immunocompromised patients. *Eur. J. Radiol.* 59 (3), 371–383. doi: 10.1016/j.ejrad.2006.04.017

Coopersmith, E. J., Bell, J. E., Benedict, K., Shriber, J., McCotter, O., and Cosh, M. H. (2017). Relating coccidioidomycosis (valley fever) incidence to soil moisture conditions. *GeoHealth* 1 (1), 51–63. doi: 10.1002/2016GH000033

Davini, D., Naeem, F., Phong, A., Al-Kuhlani, M., Valentine, K. M., McCarty, J., et al. (2018). Elevated regulatory T cells at diagnosis of Coccidioides infection associates with chronicity in pediatric patients. *J. Allergy Clin. Immunol.* 142 (6), 1971–1974. doi: 10.1016/j.jaci.2018.10.022

de Jong, E. C., Smits, H. H., and Kapsenberg, M. L. (2005). "Dendritic cell-mediated T cell polarization," in *Springer seminars in immunopathology*, vol. 26. (Germany: Springer-Verlag), 289–307.

del Rocío Reyes-Montes, M., Pérez-Huitrón, M. A., Ocaña-Monroy, J. L., Frías-De-León, M. G., Martínez-Herrera, E., Arenas, R., et al. (2016). The habitat of Coccidioides spp. and the role of animals as reservoirs and disseminators in nature. *BMC Infect. Dis.* 16 (1), 1–8. doi: 10.1186/s12879-016-1902-7

Desch, A. N., Henson, P. M., and Jakubzick, C. V. (2013). Pulmonary dendritic cell development and antigen acquisition. *Immunol. Res.* 55 (1-3), 178–186. doi: 10.1007/s12026-012-8359-6

Dionne, S. O., Podany, A. B., Ruiz, Y. W., Ampel, N. M., Galgiani, J. N., and Lake, D. F. (2006). Spherules derived from Coccidioides posadasii promote human dendritic cell maturation and activation. *Infect. Immun.* 74 (4), 2415–2422. doi: 10.1128/IAI.74.4.2415-2422.2006

Dubey, L. K., Moeller, J. B., Schlosser, A., Sorensen, G. L., and Holmskov, U. (2014). Induction of innate immunity by Aspergillus fumigatus cell wall polysaccharides is enhanced by the composite presentation of chitin and beta-glucan. *Immunobiology* 219 (3), 179–188. doi: 10.1016/j.imbio.2013.10.003

El-Behi, M., Ciric, B., Dai, H., Yan, Y., Cullimore, M., Safavi, F., et al. (2011). The encephalitogenicity of TH 17 cells is dependent on IL-1-and IL-23-induced production of the cytokine GM-CSF. *Nat. Immunol.* 12 (6), 568–575. doi: 10.1038/ni.2031

Elconin, A. F., Egeberg, R. O., and Egeberg, M. C. (1964). Significance of soil salinity on the ecology of Coccidioides immitis. *J. Bacteriol.* 87.3, 500–503. doi: 10.1128/JB.87.3.500-503.1964

Fei, M., Bhatia, S., Oriss, T. B., Yarlagadda, M., Khare, A., Akira, S., et al. (2011). TNF-α from inflammatory dendritic cells (DCs) regulates lung IL-17A/IL-5 levels and neutrophilia versus eosinophilia during persistent fungal infection. *Proc. Natl. Acad. Sci.* 108 (13), 5360–5365. doi: 10.1073/pnas.1015476108

Felonato, M., Pina, A., de Araujo, E. F., Loures, F. V., Bazan, S. B., Feriotti, C., et al.. (2012). Anti-CD25 treatment depletes Treg cells and decreases disease severity in susceptible and resistant mice infected with Paracoccidioides brasiliensis. *PLoS One* 7 (11), e51071. doi: 10.1371/journal.pone.0051071

Fierer, J., Walls, L., Eckmann, L., Yamamoto, T., and Kirkland, T. N. (1998). Importance of interleukin-10 in genetic susceptibility of mice to Coccidioides immitis. *Infect. Immun.* 66 (9), 4397–4402. doi: 10.1128/IAI.66.9.4397-4402.1998

Fierer, J., Waters, C., and Walls, L. (2006). Both CD4+ and CD8+ T cells can mediate vaccine-induced protection against Coccidioides immitis infection in mice. *J. Infect. Dis.* 193 (9), 1323–1331. doi: 10.1086/502972

Fisher, F. S., Bultman, M. W., Johnson, S. M., Pappagianis, D., and Zaborsky, E. (2007). Coccidioides niches and habitat parameters in the southwestern United States: a matter of scale. *Ann. N. Y. Acad. Sci.* 1111 (1), 47–72. doi: 10.1196/annals.1406.031

Fites, J. S., Gui, M., Kernien, J. F., Negoro, P., Dagher, Z., Sykes, D. B., et al. (2018). An unappreciated role for neutrophil-DC hybrids in immunity to invasive fungal infections. *PLoS Pathog.* 14 (5), e1007073. doi: 10.1371/journal.ppat.1007073

Galdino, N. A., Loures, F. V., de Araújo, E. F., da Costa, T. A., Preite, N. W., and Calich, V. L. G. (2018). Depletion of regulatory T cells in ongoing paracoccidioidomycosis rescues protective Th1/Th17 immunity and prevents fatal disease outcome. *Sci. Rep.* 8 (1), 1–15. doi: 10.1038/s41598-018-35037-8

Garcia, E., and Young, K. O. (2015). "Assembly Committee on Jobs, Economic Development, and the Economy," in *Assembly California* (California State Assembly Committee on Jobs, Economic Development and the Economy). Available at: https://ajed.assembly.ca.gov/sites/ajed.assembly.ca.gov/files/Final%20JEDE%202.11.15%20Report%20ELECTRONIC%20VERSION.pdf.

Gentek, R., Molawi, K., and Sieweke, M. H. (2014). Tissue macrophage identity and self-renewal. *Immunol. Rev.* 262 (1), 56–73. doi: 10.1111/imr.12224

Gonzalez, A., Hung, C.-Y., and Cole, G. T. (2011). Coccidioides releases a soluble factor that suppresses nitric oxide production by murine primary macrophages. *Microb. Pathogenesis* 50.2, 100–108. doi: 10.1016/j.micpath.2010.11.006

Gorris, M. E., Treseder, K. K., Zender, C. S., and Randerson, J. T. (2019). Expansion of coccidioidomycosis endemic regions in the United States in response to climate change. *GeoHealth* 3 (10), 308–327. doi: 10.1029/2019GH000209

Guevara-Olvera, L., Hung, C. Y., Yu, J. J., and Cole, G. T. (2000). Sequence, expression and functional analysis of the Coccidioides immitis ODC (ornithine decarboxylase) gene. *Gene* 242 (1-2), 437–448. doi: 10.1016/S0378-1119(99)00496-5

Guillot, L., Nathan, N., Tabary, O., Thouvenin, G., Le Rouzic, P., Corvol, H., et al. (2013). Alveolar epithelial cells: master regulators of lung homeostasis. *Int. J. Biochem. Cell Biol.* 45 (11), 2568–2573. doi: 10.1016/j.biocel.2013.08.009

Harley, W. B., and Blaser, M. J. (1994). Disseminated coccidioidomycosis associated with extreme eosinophilia. *Clin. Infect. Dis.* 18 (4), 627–629. doi: 10.1093/clinids/18.4.627

Hayden, C. A., Hung, C. Y., Zhang, H., Negron, A., Esquerra, R., Ostroff, G., et al. (2019). Maize-produced Ag2 as a subunit vaccine for valley fever. *J. Infect. Dis.* 220 (4), 615–623. doi: 10.1093/infdis/jiz196

Hernández-Santos, N., Wiesner, D. L., Fites, J. S., McDermott, A. J., Warner, T., Wüthrich, M., et al. (2018). Lung epithelial cells coordinate innate lymphocytes and immunity against pulmonary fungal infection. *Cell Host Microbe* 23 (4), 511–522. doi: 10.1016/j.chom.2018.02.011

Hung, C. Y., Ampel, N. M., Christian, L., Seshan, K. R., and Cole, G. T. (2000). A major cell surface antigen of Coccidioides immitis which elicits both humoral and cellular immune responses. *Infect. Immun.* 68 (2), 584–593. doi: 10.1128/IAI.68.2.584-593.2000

Hung, C. Y., Yu, J. J., Seshan, K. R., Reichard, U., and Cole, G. T. (2002). A parasitic phase-specific adhesin of Coccidioides immitis contributes to the virulence of this respiratory fungal pathogen. *Infect. Immun.* 70 (7), 3443–3456. doi: 10.1128/IAI.70.7.3443-3456.2002

Hung, C. Y., Seshan, K. R., Yu, J. J., Schaller, R., Xue, J., Basrur, V., et al. (2005). A metalloproteinase of Coccidioides posadasii contributes to evasion of host detection. *Infect. Immun.* 73 (10), 6689–6703. doi: 10.1128/IAI.73.10.6689-6703.2005

Hung, C. Y., Xue, J., and Cole, G. T. (2007). Virulence mechanisms of Coccidioides. *Ann. N. Y. Acad. Sci.* 1111 (1), 225–235. doi: 10.1196/annals.1406.020

Hung, C. Y., Gonzalez, A., Wüthrich, M., Klein, B. S., and Cole, G. T. (2011). Vaccine immunity to coccidioidomycosis occurs by early activation of three signal pathways of T helper cell response (Th1, Th2, and Th17). *Infect. Immun.* 79 (11), 4511–4522.

Hung, C. Y., Hurtgen, B. J., Bellecourt, M., Sanderson, S. D., Morgan, E. L., and Cole, G. T. (2012). An agonist of human complement fragment C5a enhances vaccine immunity against Coccidioides infection. *Vaccine* 30 (31), 4681–4690. doi: 10.1016/j.vaccine.2012.04.084

Hung, C. Y., del Pilar Jiménez-Alzate, M., Gonzalez, A., Wüthrich, M., Klein, B. S., and Cole, G. T. (2014a). Interleukin-1 receptor but not Toll-like receptor 2 is essential for MyD88-dependent Th17 immunity to Coccidioides infection. *Infect. Immun.* 82 (5), 2106–2114. doi: 10.1128/IAI.01579-13

Hung, C. Y., Castro-Lopez, N., and Cole, G. T. (2014b). Vaccinated C57BL/6 mice develop protective and memory T cell responses to Coccidioides posadasii infection in the absence of interleukin-10. *Infect. Immun.* 82 (2), 903–913. doi: 10.1128/IAI.01148-13

Hung, C. Y., Castro-Lopez, N., and Cole, G. T. (2016a). Card9-and MyD88-mediated gamma interferon and nitric oxide production is essential for resistance to subcutaneous Coccidioides posadasii infection. *Infect. Immun.* 84 (4), 1166–1175. doi: 10.1128/IAI.01066-15

Hung, C. Y., Wozniak, K. L., and Cole, G. T. (2016b). "Flow Cytometric Analysis of Protective T-Cell Response Against Pulmonary Coccidioides Infection," in *Vaccine Design* (New York, NY: Humana Press), 551–566.

Hung, C. Y., Zhang, H., Castro-Lopez, N., Ostroff, G. R., Khoshlenar, P., Abraham, A., et al. (2018a). Glucan-chitin particles enhance Th17 response and improve protective efficacy of a multivalent antigen (rCpa1) against pulmonary Coccidioides posadasii infection. *Infect. Immun.* 86 (11), e00070–18. doi: 10.1128/IAI.00070-18

Hung, C. Y., Zhang, H., Campuzano, A., Ostroff, G., and Yu, J. J. (2018b). An multivalent vaccine elicits protective Th17 response via activation of C-type lectin receptor-and Card9-mediated signal against pulmonary Coccidioides posadasii infection. *J. Immunol.* 200 (1 Supplement) 125.4.

Hussell, T., and Bell, T. J. (2014). Alveolar macrophages: plasticity in a tissue-specific context. *Nat. Rev. Immunol.* 14 (2), 81–93. doi: 10.1038/nri3600

Iannitti, R. G., Carvalho, A., and Romani, L. (2012). From memory to antifungal vaccine design. *Trends Immunol.* 33 (9), 467–474.

Jain, R., Tikoo, S., and Weninger, W. (2016). Recent advances in microscopic techniques for visualizing leukocytes in vivo. *F1000Research* 5. doi: 10.12688/f1000research.8127

Johannesson, H., Kasuga, T., Schaller, R. A., Good, B., Gardner, M. J., Townsend, J P., et al. (2006). Phase-specific gene expression underlying morphological adaptations of the dimorphic human pathogenic fungus, Coccidioides posadasii. *Fungal Genet. Biol.* 43 (8), 545–559. doi: 10.1016/j.fgb.2006.02.003

Johnson, L., Gaab, E. M., Sanchez, J., Bui, P. Q., Nobile, C. J., Hoyer, K. K., et al. (2014). Valley fever: danger lurking in a dust cloud. *Microbes Infect.* 16 (8), 591–600. doi: 10.1016/j.micinf.2014.06.011

Johnson, R., Kernerman, S. M., Sawtelle, B. G., Rastogi, S. C., Nielsen, H. S., and Ampel, N. M. (2012). A reformulated spherule-derived coccidioidin (Spherusol) to detect delayed-type hypersensitivity in coccidioidomycosisexternal icon. *Mycopathologia.* 174 (5–6), 353–358.

Khader, S. A., Gaffen, S. L., and Kolls, J. K. (2009). Th17 cells at the crossroads of innate and adaptive immunity against infectious diseases at the mucosa. *Mucosal Immunol.* 2 (5), 403–411. doi: 10.1038/mi.2009.100

Kolaczkowska, E., and Kubes, P. (2013). Neutrophil recruitment and function in health and inflammation. *Nat. Rev. Immunol.* 13 (3), 159–175. doi: 10.1038/nri3399

Lacy, G. H., and Swatek, F. E. (1974). Soil ecology of Coccidioides immitis at Amerindian middens in California. *Appl. Microbiol.* 27 (2), 379–388. doi: 10.1128/AEM.27.2.379-388.1974

Laws, R. L., Cooksey, G. S., Jain, S., Wilken, J., McNary, J., Moreno, E., et al. (2018). Coccidioidomycosis outbreak among workers constructing a solar power farm—Monterey County, California, 2016–2017. *Morb. Mortality Wkly. Rep.* 67 (33), 931. doi: 10.15585/mmwr.mm6733a4

Lázár-Molnár, E., Gácser, A., Freeman, G. J., Almo, S. C., Nathenson, S. G., and Nosanchuk, J. D. (2008). The PD-1/PD-L costimulatory pathway critically

affects host resistance to the pathogenic fungus Histoplasma capsulatum. *Proc. Natl. Acad. Sci.* 105 (7), 2658–2663. doi: 10.1073/pnas.0711918105

Lee, C. Y., Thompson III, G. R., Hastey, C. J., Hodge, G. C., Lunetta, J. M., Pappagianis, D., et al. (2015). Coccidioides endospores and spherules draw strong chemotactic, adhesive, and phagocytic responses by individual human neutrophils. *PLoS One* 10 (6), e0129522. doi: 10.1371/journal.pone.0129522

Lin, J. S., Yang, C. W., Wang, D. W., and Wu-Hsieh, B. A. (2005). Dendritic cells cross-present exogenous fungal antigens to stimulate a protective CD8 T cell response in infection by Histoplasma capsulatum. *J. Immunol.* 174, 6282–6291. doi: 10.4049/jimmunol.174.10.6282

Liu, J., Pang, Z., Wang, G., Guan, X., Fang, K., Wang, Z., et al. (2017). Advanced role of neutrophils in common respiratory diseases. *J. Immunol. Res* 2017, 21. doi: 10.1155/2017/6710278

Lohmann-Matthes, M. L., Steinmuller, C., and Franke-Ullmann, G. (1994). Pulmonary macrophages. *Eur. Respir. J.* 7 (9), 1678–1689. doi: 10.1183/09031936.94.07091678

Lombard, C. M., Tazelaar, H. D., and Krasne, D. L. (1987). Pulmonary eosinophilia in coccidioidal infections. *Chest* 91 (5), 734–736. doi: 10.1378/chest.91.5.734

Magee, D. M., and Cox, R. A. (1996). Interleukin-12 regulation of host defenses against Coccidioides immitis. *Infect. Immun.* 64 (9), 3609–3613. doi: 10.1128/IAI.64.9.3609-3613.1996

Magee, D. M., Friedberg, R. L., Woitaske, M. D., Johnston, S. A., and Cox, R. A. (2005). Role of B cells in vaccine-induced immunity against coccidioidomycosis. *Infect. Immun.* 73 (10), 7011–7013. doi: 10.1128/IAI.73.10.7011-7013.2005

McCotter, O. Z., Benedict, K., Engelthaler, D. M., Komatsu, K., Lucas, K. D., Mohle-Boetani, J. C., et al. (2019). Update on the epidemiology of coccidioidomycosis in the United States. *Med. Mycol.* 57 (Supplement_1), S30–S40. doi: 10.15585/mmwr.ss6807a1

Merkhofer, R. M., O'Neill, M. B., Xiong, D., Hernandez-Santos, N., Dobson, H., Fites, J. S., et al. (2019). Investigation of genetic susceptibility to blastomycosis reveals interleukin-6 as a potential susceptibility locus. *MBio* 10 (3), e01224–19. doi: 10.1128/mBio.01224-19

Mobed, K., Gold, E. B., and Schenker, M. B. (1992). Occupational health problems among migrant and seasonal farm workers. *West. J. Med.* 157 (3), 367–373.

Montagnoli, C., Bacci, A., Bozza, S., Gaziano, R., Mosci, P., Sharpe, A. H., et al. (2002). B7/CD28-dependent CD4+ CD25+ regulatory T cells are essential components of the memory-protective immunity to Candida albicans. *J. Immunol.* 169 (11), 6298–6308. doi: 10.4049/jimmunol.169.11.6298

Nakano, H., Burgents, J. E., Nakano, K., Whitehead, G. S., Cheong, C., Bortner, C. D., et al. (2013). Migratory properties of pulmonary dendritic cells are determined by their developmental lineage. *Mucosal Immunol.* 6 (4), 678–691. doi: 10.1038/mi.2012.106

Nanjappa, S. G., Heninger, E., Wüthrich, M., Gasper, D. J., and Klein, B. S. (2012). Tc17 cells mediate vaccine immunity against lethal fungal pneumonia in immune deficient hosts lacking CD4+ T cells. *PLoS Pathog.* 8 (7), e1002771. doi: 10.1371/journal.ppat.1002771

Narra, H. P., Shubitz, L. F., Mandel, M. A., Trinh, H. T., Griffin, K., Buntzman, A. S., et al. (2016). A Coccidioides posadasii CPS1 deletion mutant is avirulent and protects mice from lethal infection. *Infect. Immun.* 84 (10), 3007–3016. doi: 10.1128/IAI.00633-16

Nesbit, L., Johnson, S. M., Pappagianis, D., and Ampel, N. M. (2010). Polyfunctional T lymphocytes are in the peripheral blood of donors naturally immune to coccidioidomycosis and are not induced by dendritic cells. *Infect. Immun.* 78 (1), 309–315. doi: 10.1128/IAI.00953-09

Nguyen, C., Barker, B. M., Hoover, S., Nix, D. E., Ampel, N. M., Frelinger, J. A., et al. (2013). Recent advances in our understanding of the environmental, epidemiological, immunological, and clinical dimensions of coccidioidomycosis. *Clin. Microbiol. Rev.* 26 (3), 505–525. doi: 10.1128/CMR.00005-13

Nicas, M. (2018). A point-source outbreak of Coccidioidomycosis among a highway construction crew. *J. Occup. Environ. Hyg.* 15 (1), 57–62. doi: 10.1080/15459624.2017.1383612

Odio, C. D., Milligan, K. L., McGowan, K., Spergel, A. K. R., Bishop, R., Boris, L., et al. (2015). Endemic mycoses in patients with STAT3-mutated hyper-IgE (Job) syndrome. *J. Allergy Clin. Immunol.* 136 (5), 1411–1413. doi: 10.1016/j.jaci.2015.07.003

Petterson, S. M., Liaw, W. R., Phillips, R. L., Rabin, D. L., Meyers, D. S., and Bazemore, A. W. (2012). Projecting US primary care physician workforce needs: 2010-2025. *Ann. Family Med.* 10 (6), 503–509. doi: 10.1370/afm.1431

Pino-Tamayo, P. A., Puerta-Arias, J. D., Lopera, D., Urán-Jiménez, M. E., and González, Á. (2016). Depletion of neutrophils exacerbates the early inflammatory immune response in lungs of mice infected with Paracoccidioides brasiliensis. *Mediators Inflamm.* 2016, 17. doi: 10.1155/2016/3183285

Richards, J. O., Ampel, N. M., Galgiani, J. N., and Lake, D. F. (2001). Dendritic cells pulsed with Coccidioides immitis lysate induce antigen-specific naive T cell activation. *J. Infect. Dis.* 184 (9), 1220–1224. doi: 10.1086/323664

Richards, J. O., Ampel, N. M., and Lake, D. F. (2002). Reversal of coccidioidal anergy in vitro by dendritic cells from patients with disseminated coccidioidomycosis. *J. Immunol.* 169 (4), 2020–2025. doi: 10.4049/jimmunol.169.4.2020

Romani, L., Bistoni, F., and Puccetti, P. (2002). Fungi, dendritic cells and receptors: a host perspective of fungal virulence. *Trends Microbiol.* 10 (11), 508–514. doi: 10.1016/S0966-842X(02)02460-5

Romani, L. (2004). Immunity to fungal infections. *Nat. Rev. Immunol.* 4 (1), 11–24. doi: 10.1038/nri1255

Saenz-Ibarra, B., Prieto, V. G., Torres-Cabala, C. A., Huen, A., Nagarajan, P., Tetzlaff, M. T., et al. (2018). Coccidioidomycosis involving lungs and skin: a mimicker of metastatic disease. *Am. J. Dermatopathol.* 40 (3), e41–e43. doi: 10.1097/DAD.0000000000000986

Sakai, S., Kauffman, K. D., Schenkel, J. M., McBerry, C. C., Mayer-Barber, K. D., Masopust, D., et al. (2014). Cutting edge: Control of Mycobacterium tuberculosis infection by a subset of lung parenchyma–homing CD4 T cells. *J. Immunol.* 192 (7), 2965–2969. doi: 10.4049/jimmunol.1400019

Salas, R. (2018). *"Bill Text." Bill Text - AB-1709 Valley Fever Education, Early Diagnosis, and Treatment Act*. (California State Assembly). Available at: https://leginfo.legislature.ca.gov/faces/billTextClient.xhtml?bill_id=201720180AB1790.

Salas, R. (2019). *"Bill Text." Bill Text - AB-203 Occupational Safety and Health: Valley Fever*. (California State Assembly). Available at: https://leginfo.legislature.ca.gov/faces/billTextClient.xhtml?bill_id=201920200AB203.

Sampaio, E. P., Hsu, A. P., Pechacek, J., Bax, H.II, Dias, D. L., Paulson, M. L., et al. (2013). Signal transducer and activator of transcription 1 (STAT1) gain-of-function mutations and disseminated coccidioidomycosis and histoplasmosis. *J. Allergy Clin. Immunol.* 131 (6), 1624–1634. doi: 10.1016/j.jaci.2013.01.052

Saubolle, M. A., McKellar, P. P., and Sussland, D. (2007). Epidemiologic, clinical, and diagnostic aspects of coccidioidomycosis. *J. Clin. Microbiol.* 45 (1), 26–30. doi: 10.1128/JCM.02230-06

Schaffner, A. C. T. M. H. A., Davis, C. E., Schaffner, T., Markert, M., Douglas, H., and Braude, A.II (1986). In vitro susceptibility of fungi to killing by neutrophil granulocytes discriminates between primary pathogenicity and opportunism. *J. Clin. Invest.* 78 (2), 511–524. doi: 10.1172/JCI112603

Segura, E. (2016). "Review of mouse and human dendritic cell subsets," in *Dendritic Cell Protocols* (New York, NY: Humana Press), 3–15.

Shubitz, L., Peng, T., Perrill, R., Simons, J., Orsborn, K., and Galgiani, J. N. (2002). Protection of mice against Coccidioides immitis intranasal infection by vaccination with recombinant antigen 2/PRA. *Infect. Immun.* 70 (6), 3287–3289. doi: 10.1128/IAI.70.6.3287-3289.2002

Smith, C. E. (1940). Epidemiology of acute coccidioidomycosis with erythema nodosum ("San Joaquin" or "Valley Fever"). *Am. J. Public Health Nations Health* 30 (6), 600–611. doi: 10.2105/AJPH.30.6.600

Spec, A., Shindo, Y., Burnham, C. A. D., Wilson, S., Ablordeppey, E. A., Beiter, E. R., et al. (2016). T cells from patients with Candida sepsis display a suppressive immunophenotype. *Crit. Care* 20 (1), 1–9. doi: 10.1186/s13054-016-1182-z

Swatek, F. E. (1970). Ecology of Coccidioides immitis. *Mycopathol. Mycol. Applicata* 41 (1-2), 3–12. doi: 10.1007/BF02051479

Tam, J. M., Mansour, M. K., Khan, N. S., Seward, M., Puranam, S., Tanne, A., et al. (2014). Dectin-1–dependent LC3 recruitment to phagosomes enhances fungicidal activity in macrophages. *J. Infect. Dis.* 210 (11), 1844–1854. doi: 10.1093/infdis/jiu290

Taylor, J. W., and Barker, B. M. (2019). The endozoan, small-mammal reservoir hypothesis and the life cycle of Coccidioides species. *Med. Mycol.* 57 (Supplement_1), S16–S20. doi: 10.1093/mmy/myy039

Teitz-Tennenbaum, S., Viglianti, S. P., Roussey, J. A., Levitz, S. M., Olszewski, M. A., and Osterholzer, J. J. (2018). Autocrine IL-10 signaling promotes dendritic cell type-2 activation and persistence of murine cryptococcal lung infection. *J. Immunol.* 201 (7), 2004–2015. doi: 10.4049/jimmunol.1800070

Ternovoĭ, V.II, and Golotina, N. B. (1977). Ultrastructure of parasitic forms of the agent of coccidioidomycosis. *Zhurnal Mikrobiol. Epidemiol. i Immunobiol.* 4), 71–77.

Uhm, T. G., Kim, B. S., and Chung, I. Y. (2012). Eosinophil development, regulation of eosinophil-specific genes, and role of eosinophils in the pathogenesis of asthma. *Allergy Asthma Immunol. Res.* 4 (2), 68–79. doi: 10.4168/aair.2012.4.2.68

Vautier, S., da Glória Sousa, M., and Brown, G. D. (2010). C-type lectins, fungi and Th17 responses. *Cytokine Growth Factor Rev.* 21 (6), 405–412. doi: 10.1016/j.cytogfr.2010.10.001

Viriyakosol, S., Fierer, J., Brown, G. D., and Kirkland, T. N. (2005). Innate immunity to the pathogenic fungus Coccidioides posadasii is dependent on Toll-like receptor 2 and Dectin-1. *Infect. Immun.* 73 (3), 1553–1560. doi: 10.1128/IAI.73.3.1553-1560.2005

Viriyakosol, S., Walls, L., Datta, S. K., Kirkland, T., Heinsbroek, S. E. M., Brown, G., et al. (2008). Susceptibility to Coccidioides species in C57BL/6 mice is associated with expression of a truncated splice variant of Dectin-1 (Clec7a). *Genes Immun.* 9 (4), 338–348. doi: 10.1038/gene.2008.23

Viriyakosol, S., del Pilar Jimenez, M., Gurney, M. A., Ashbaugh, M. E., and Fierer, J. (2013). Dectin-1 is required for resistance to coccidioidomycosis in mice. *MBio* 4 (1), 1147–1156. doi: 10.1128/mBio.00597-12

Wack, E. E., Ampel, N. M., Sunenshine, R. H., and Galgiani, J. N. (2015). The return of delayed-type hypersensitivity skin testing for coccidioidomycosisexternal icon. *Clin. Infect Dis.* 61 (5), 787–791.

Walrath, J., Zukowski, L., Krywiak, A., and Silver, R. F. (2005). Resident Th1-like effector memory cells in pulmonary recall responses to Mycobacterium tuberculosis. *Am. J. Respir. Cell Mol. Biol.* 33 (1), 48–55. doi: 10.1165/rcmb.2005-0060OC

Wherry, E. J., and Kurachi, M. (2015). Molecular and cellular insights into T cell exhaustion. *Nat. Rev. Immunol.* 15 (8), 486–499. doi: 10.1038/nri3862

Wilken, J. A., Sondermeyer, G., Shusterman, D., McNary, J., Vugia, D. J., McDowell, A., et al. (2015). Coccidioidomycosis among workers constructing solar power farms, California, USA, 2011–2014. *Emerg. Infect. Dis.* 21 (11), 1997. doi: 10.3201/eid2111.150129

Wing, K., Onishi, Y., Prieto-Martin, P., Yamaguchi, T., Miyara, M., Fehervari, Z., et al. (2008). CTLA-4 control over Foxp3+ regulatory T cell function. *Science* 322 (5899), 271–275. doi: 10.1126/science.1160062

Wynn, T. A., and Vannella, K. M. (2016). Macrophages in tissue repair, regeneration, and fibrosis. *Immunity* 44.3, 450–462. doi: 10.1016/j.immuni.2016.02.015

Xu, S., and Shinohara, M. L. (2017). Tissue-resident macrophages in fungal infections. *Front. Immunol.* 8, 1798. doi: 10.3389/fimmu.2017.01798

Xue, J., Chen, X., Selby, D., Hung, C. Y., Yu, J. J., and Cole, G. T. (2009). A genetically engineered live attenuated vaccine of Coccidioides posadasii protects BALB/c mice against coccidioidomycosis. *Infect. Immun.* 77 (8), 3196–3208. doi: 10.1128/IAI.00459-09

Yamaguchi, Y., Hayashi, Y., Sugama, Y., Miura, Y., Kasahara, T., Kitamura, S., et al. (1988). Highly purified murine interleukin 5 (IL-5) stimulates eosinophil function and prolongs in vitro survival. IL-5 as an eosinophil chemotactic factor. *J. Exp. Med.* 167 (5), 1737–1742. doi: 10.1084/jem.167.5.1737

Yeh, W.II, McWilliams, I. L., and Harrington, L. E. (2014). IFNγ inhibits Th17 differentiation and function via Tbet-dependent and Tbet-independent mechanisms. *J. Neuroimmunol.* 267 (1-2), 20–27. doi: 10.1016/j.jneuroim.2013.12.001

Zelante, T., De Luca, A., Bonifazi, P., Montagnoli, C., Bozza, S., Moretti, S., et al. (2007). IL-23 and the Th17 pathway promote inflammation and impair antifungal immune resistance. *Eur. J. Immunol.* 37 (10), 2695–2706. doi: 10.1002/eji.200737409

Zheng, J., van de Veerdonk, F. L., Crossland, K. L., Smeekens, S. P., Chan, C. M., Al Shehri, T., et al. (2015). Gain-of-function STAT1 mutations impair STAT3 activity in patients with chronic mucocutaneous candidiasis (CMC). *Eur. J. Immunol.* 45 (10), 2834–2846. doi: 10.1002/eji.201445344

Zhu, Y., Tryon, V., Magee, D. M., and Cox, R. A. (1997). Identification of a Coccidioides immitis antigen 2 domain that expresses B-cell-reactive epitopes. *Infect. Immun.* 65 (8), 3376–3380. doi: 10.1128/IAI.65.8.3376-3380.1997

Conflict of Interest: The authors declare that the research was conducted in the absence of any commercial or financial relationships that could be construed as a potential conflict of interest.

frontiers in Cellular and Infection Microbiology

ORIGINAL RESEARCH
published: 30 November 2020
doi: 10.3389/fcimb.2020.573097

Insights Into *Histoplasma capsulatum* Behavior on Zinc Deprivation

*Leandro do Prado Assunção[1], Dayane Moraes[1], Lucas Weba Soares[1], Mirelle Garcia Silva-Bailão[1], Janaina Gomes de Siqueira[1], Lilian Cristiane Baeza[2], Sônia Nair Báo[3], Célia Maria de Almeida Soares[1] and Alexandre Melo Bailão[1]**

[1] Molecular Biology and Biochemistry Laboratory, Institute of Biological Sciences II, Federal University of Goias (UFG), Goiania, Brazil, [2] Laboratory of Experimental Microbiology, State University of Western Paraná (Unioeste), Cascavel, Brazil, [3] Microscopy and Microanalysis Laboratory, Institute of Biological Sciences, Brasília University (UnB), Brasilia, Brazil

Histoplasma capsulatum is a thermodimorphic fungus that causes histoplasmosis, a mycosis of global incidence. The disease is prevalent in temperate and tropical regions such as North America, South America, Europe, and Asia. It is known that during infection macrophages restrict Zn availability to *H. capsulatum* as a microbicidal mechanism. In this way the present work aimed to study the response of *H. capsulatum* to zinc deprivation. *In silico* analyses showed that *H. capsulatum* has eight genes related to zinc homeostasis ranging from transcription factors to CDF and ZIP family transporters. The transcriptional levels of *ZAP1*, *ZRT1*, and *ZRT2* were induced under zinc-limiting conditions. The decrease in Zn availability increases fungicidal macrophage activity. Proteomics analysis during zinc deprivation at 24 and 48 h showed 265 proteins differentially expressed at 24 h and 68 at 48 h. Proteins related to energy production pathways, oxidative stress, and cell wall remodeling were regulated. The data also suggested that low metal availability increases the chitin and glycan content in fungal cell wall that results in smoother cell surface. Metal restriction also induces oxidative stress triggered, at least in part, by reduction in pyridoxin synthesis.

Keywords: fungal pathogenesis, Zn uptake, Zn and cell wall remodeling, proteomics, zinc homeostasis

OPEN ACCESS

Edited by:
Carlos Pelleschi Taborda, University of São Paulo, Brazil

Reviewed by:
George Samuel Deepe, University of Cincinnati, United States
Aylin Döğen, Mersin University, Turkey

***Correspondence:**
Alexandre Melo Bailão
alexandre.bailao@gmail.com

Specialty section:
This article was submitted to Fungal Pathogenesis, a section of the journal Frontiers in Cellular and Infection Microbiology

Received: *16 June 2020*
Accepted: *21 October 2020*
Published: *30 November 2020*

Citation:
Assunção LP, Moraes D, Soares LW, Silva-Bailão MG, de Siqueira JG, Baeza LC, Báo SN, Soares CMdA and Bailão AM (2020) Insights Into Histoplasma capsulatum Behavior on Zinc Deprivation. Front. Cell. Infect. Microbiol. 10:573097. doi: 10.3389/fcimb.2020.573097

INTRODUCTION

H. capsultatum is a thermal dimorphic fungus that causes histoplasmosis, a mycosis with worldwide incidence and prevalence in temperate and tropical climates (Aide, 2009). This disease is widely distributed in Central and North America, mainly in the United States, Panama, and Honduras. In Latin America, a high incidence of the disease is seen in countries such as Brazil and Argentina. However, isolated cases have been reported in countries in Europe, Africa, and Asia (Bahr et al., 2015). Some molecular factors produced by *H. capsulatum* yeast cells enable them to parasitize phagocytic immune cells. Fungal yeasts are capable to infect and survive in phagocytic cells, including alveolar macrophages, polymorphonuclear leukocytes, and dendritic cells (De Sanchez and Carbonell, 1975; Schaffner et al., 1986; Gildea et al., 2001). These phagocytes serve as both the host cell and the vector by which infection dissemination is mediated. After phagocytosis, the

fungus is exposed to stress conditions imposed by host defense mechanisms such as: deprivation of macro and micronutrients, production of reactive oxygen and nitrogen species, proteolytic enzymes, lipases, hypoxia and drastic changes in pHs. Among those, zinc deprivation has been identified as a microbicidal strategy used by host cells to control *H. capsulatum* infection (Garfoot and Rappleye, 2016; Shen and Rappleye, 2017).

Zinc is an important chemical element in all life kingdoms. This ion has different chemical characteristics from other metals because of its high ionization potential that favors the formation of covalent bonds (Alberts, 1998; Permyakov, 2009). This property allows the zinc to binds to two main protein classes: enzymes, in which constitute 3/5 of the zinc metalloproteins and transcription factors (Andreini et al., 2006; Andreini et al., 2009). Zinc-binding enzymes are distributed in all cellular components, with an emphasis on cytoplasm and mitochondria, where most of the metabolic processes occur (Tristão et al., 2014). In addition, zinc, in its free form within the cell, acts as an activator of cell signaling, regulating transporters that have the ability to capture zinc during deprivation or stress conditions (Auld, 2001; Permyakov, 2009). Thus, it is clear that small changes in zinc concentrations may alter cellular metabolism (Taylor et al., 2012). In *H. capsulatum*, the metabolic response during zinc deprivation is not well known. However, it is known that zinc is essential for the survival of this fungus during the infection process. Studies by Vignesh et al. (2013) showed that *H. capsulatum* undergoes zinc deprivation when inside of GM-CSF activated macrophages. One of the mechanisms of zinc deprivation controlled by GM-CSF exposed macrophages is the production of metallothioneins specific to this metal, which ends up reducing the amount of free zinc in the fungus (Vignesh et al., 2013). As a result, it is suggested that *H. capsulatum* developed zinc capture and storage strategies to increase the chances of survival in phagocytic cells (Shen and Rappleye, 2017).

The fungus defense against zinc deprivation is the activation of a very specific transcription factor, known as Zap1, which regulates zinc homeostasis. Zap1 and its orthologs have already been characterized in several fungal species such as *Saccharomycces cerevisiae* (Frey et al., 2011), *Cryptococcus gattii* (Schneider et al., 2015), *Aspergillus fumigatus* (known as ZafA) (Vicentefranqueira et al., 2018), and *Candida Albicans* (initially named Crs1) (Kim et al., 2008). This transcription factor increases the expression of the ZIP (Zrt/Irt type Proteins) and CDF (Cation Diffusion Facilitators) family of transporters capable of transporting zinc towards the cytoplasm or organelles, respectively. In some organisms, such as in *S. cerevisiae*, Zap1 is capable of auto regulation, inducing itself and also a range of proteins involved on the adaptation to different levels of zinc (Schneider et al., 2012; Wilson et al., 2012; Amich and Calera, 2014). In *H. capsulatum*, a member of the ZIP family (Zrt2) has been characterized. *HcZrt2* behaves as a high affinity transporter, being necessary for growth in zinc limiting condition as well as playing an important role during infection *in vivo* (Dade et al., 2016).

In some fungal species, there are also non-specific metal carriers or even different transcription factors. Fet4 and Pho84 for example, have binding sites for iron, copper, zinc, manganese, and magnesium. These transporters assist Zrts in regulating zinc homeostasis, where they also capture zinc from the extracellular medium to the intracellular medium. Loz1 is the only transcription factor that seems to behave similarly to Zap1 in fungi, capable of regulating homeostasis in zinc replete conditions in *Schizosaccharomyces pombe* (Corkins et al., 2013). In addition to plasma membrane transporters or transcription factors, there are also intracellular carriers, such as Zrc1, Cot1, and Zrt3 in *S. cerevisae*. The first two store zinc into the vacuole when the fungi is in conditions of high zinc availability or when preparing for "zinc shock", a term applied when the environment rapidly shifts from deplete to replete zinc condition in a short span. Zrt3 meanwhile, has an inverse function, in which it is able to export zinc stored in the vacuole to the cytoplasm when the environment has low availability of this metal (Eide, 2006; Wilson et al., 2012).

Unlike *S. cerevisiae* and *C. neoformans*, some fungi have alternative mechanisms for zinc homeostasis, being regulated not only by zinc, but by pH as well. Examples of this can be seen in *Aspergillus fumigatus* and *Candida albicans* (Vicentefranqueira et al., 2005; Wilson et al., 2012). In *A. fumigatus*, there are 18 genes related to zinc transport within the cell, of which two are transcription factors, ZafA (homologous to Zap1) and PacC, that, while not induced by zinc but rather pH, PacC influences expression of some of the remaining zinc transporters from the ZIP and CDF family (Moreno et al., 2007; Amich and Calera, 2014; Bertuzzi et al., 2014). *C. albicans*, has an extracellular zinc capture mechanism mediated by Pra (pH-regulated antigen 1) that has a high affinity for zinc and plays a role in alkaline conditions. It is known that this molecule is secreted in the extracellular medium to capture free zinc in the host cytoplasm or from storage proteins. Subsequently, the Pra–Zn complex makes the captured metal available to the cytoplasm through Zrt1 (Wilson et al., 2012). Pra1 was later found in *A. fumigatus* (named Aspf2) and *Blastomyces dermatitidis*, being also associated with a specific ZIP transporter, ZrfC and Zrt1, respectively.

Besides the control of zinc concentrations inside the cell, Zap1 also regulates multiple proteins involved in maintaining metabolic homeostasis such as enzymes related to aerobic metabolism, fermentation, and the biosynthesis of secondary compounds (Wilson and Bird, 2016). In addition to those, over 500 proteins linked to this metal have already been identified, and approximately 70% are enzymes (Permyakov, 2009). In *H. capsulatum*, current understanding of how those processes operate or what proteins are involved in the maintenance of optimal zinc concentrations is currently lacking. In the present work, we sought to elucidate *H. capsulatum's* general behavior during zinc starvation through genomic analysis and proteomic approaches.

MATERIALS AND METHODS

In Silico Analysis

Protein sequences of genes related to zinc homeostasis were obtained in Gene bank (https://www.ncbi.nlm.nih.gov/protein). The *in silico* homology analyses were performed using the tool

BLASTp (Basic Local Alignment Search Tool) (https://blast.ncbi.nlm.nih.gov/Blast.cgi). Sequences of zinc homeostasis proteins of *A. fumigatus*, *C. neoformans, P. brasiliensis*, and *S. cerevisiae* were used as templates. Additionally, STRING (https://string-db.org/) was used in analyses of protein interactions in *H. capsulatum* Nam1 and the BLASTp tool was used to find orthologs in G186AR strain.

H. capsulatum Growth Conditions

H. capsulatum yeasts (G186AR, ATCC26029) were maintained in a solid chemically defined medium McVeigh/Morton (MMcM) (Restrepo and Jimenez, 1980), supplemented with 20 μM $ZnSO_4$, 200 μM $FeSO_4$, and 30 μM $CuSO_4$ at 37°C under an atmosphere of 5% CO_2 for seven days. For zinc-limiting assays the yeast cells (10^8 cells/ml) were incubated in liquid MMcM with no zinc and supplemented with 100 μM of zinc chelator DTPA (diethylenetriaminepentaacetic acid, Sigma Aldrich), 200 μM $FeSO_4$, and 30 μM $CuSO_4$ to avoid unspecific metal-chelation promoted by DTPA, under agitation for 24 or 48 h. Cells incubated in MMcM with 20 μM of $ZnSO_4$ were used as controls. For analyses of pyridoxine on *H. capsulatum* growth, yeast cells were incubated under Zn deprivation and different concentrations of pyridoxine (0, 1, and 6 μM). The growth of *H. capsulatum* in liquid culture was quantified by measurement of culture turbidity using optical density (OD 595 nm). The cellular viability of *H. capsulatum* yeast cells was determined by the trypan blue method (Trypan Blue, Sigma Aldrich) using a Neubauer chamber at optical microscopy. The growth analyses were performed in triplicate.

RNA Extraction and qRT-PCR

The expression analysis of Zn homeostasis genes was performed by quantitative real time reverse transcription polymerase chain reaction (qRT-PCR) using cells grown during 3 and 24 h in control (MMcM supplemented with 20 μM of $ZnSO_4$) and Zn-limiting conditions. The cells were harvested and subjected to total RNA extraction by mechanical cell rupture using a BeadBeater (Mini-BeadBeather, Biospec Products Inc., Bartlesville, OK, USA), 0.5 μm diameter glass beads and TRIzol (TRI Reagent®, Sigma-Aldrich, St. Luois, MO, USA), according to the manufacturer's protocol. The RNAs were used to synthesize single stranded cDNAs (DNA complementary) using the High Capacity RNA-to-cDNA kit (Applied Biosystems, Foster City, CA) and oligo (dT) primer. The qRT-PCR was performed using SYBER green PCR master mix (Applied Biosystems, Foster City, CA) on the Applied Biosystems Step One Plus Real-Time PCR System (Applied Biosystems Inc.) with 10 pmol of each specific primer and 40 ng of template cDNA in a final volume of 25 μl. Melting curve analysis was performed to confirm a single PCR product. Standard curves were generated using 1:5 serial dilutions by pooling cDNAs of all conditions. The qRT-PCR assays were performed in triplicates. The levels of relative expression of the transcripts were calculated using the standard curve method for relative quantification (Bookout et al., 2006). The oligonucleotides used in the real time PCR analysis were constructed based on the structural genome of *H. capsulatum* (https://www.ncbi.nlm.nih.gov/protein, **Supplementary Table 1**).

Proteomic Analysis

Protein extracts of *H. capsulatum* were obtained from yeast cells lysed using a BeadBeater (Mini-BeadBeather, Biospec Products Inc., Bartlesville, OK, USA), 0.5 μm diameter glass beads and ammonium bicarbonate buffer (pH 8.5). The cells were disrupted six times for 30 s at maximum speed with 1 min intervals on ice. Then, the lysate was centrifuged five times at 10,000 × *g* for 10 min at 4°C to remove cell debris. The protein extracts were quantified using the Bradford method (BRADFORD, 1976) with bovine serum albumin solution as standard. The enzymatic digestion was performed based on Murad et al. (2011), using 150 μg of total protein extract in ammonium bicarbonate buffer (50 mM) and RapiGEST™ SF (Waters, Milford, MA, USA) for 15 min at 80°C. Then, dithiothreitol (DTT, GE Healthcare, Little Chalfont, UK, 100 mM) was added and samples incubated for 30 min at 60°C followed by addition of iodoacetamine (300 mM, GE Healthcare, Piscataway, NJ, USA) and incubation at room temperature in a dark room. The digestion was done by the addition of 30 μl of a 0.05 μg/μl trypsin solution (Promega, Madison, WI, USA) and incubation at 37°C for 16 h. Subsequently, 10 μl of 5% (v/v) triofluoracetic acid (TFA) was added, followed by incubation at 37°C for 90 min. The samples were centrifuged, and supernatant was lyophilized in the speed vacuum (Eppendorf, Hamburg, Germany). The tryptic peptides were separated by Ultra High Performance Liquid Chromatography according to Baeza et al. (2017), using the ACQUITY UPLC® M-Class system (Waters Corporation, Manchester, UK) coupled to Synapt G1 HDMS™ mass spectrometer (Waters Micromass, Manchester, UK). Rabbit phosphorylase B (MassPREP™ Digestion Standard) was used as internal standard and [GLU1]-Fibrinopeptide B (GFB) for calibration during the sample analysis. Mass spectra were processed using the ProteinLynx Global Server software version 3.0.2 (Waters, Manchester, UK) loaded with a specific database for *H. capsulatum* (Geromanos et al., 2009). Proteomic analyses were performed in triplicates for each sample. Identified proteins with at least 1.2 fold change difference between conditions were considered as regulated. Subsequently, online tools such as FungiDB (https://fungidb.org/fungidb/) and KEGG (https://www.genome.jp/kegg/pathway.html) were used to functionally categorize the regulated proteins.

Carbohydrate and Glucose Dosage

Total carbohydrate content from yeast cells grown in control and DTPA conditions was measured using the modified phenol-sulfuric acid reaction (Dubois et al., 1956). A harvest pellet from an aliquot of 1 ml culture sample was mixed with 800 μl of concentrated sulfuric acid (98%) and 50 μl of 80% phenol aqueous solution in a microtube. The samples were read at 490 nm on a 96 well microplate spectrophotometer. A standard curve was constructed using a serial dilution of a glucose solution (5 mg/ml) in water. The values were normalized, and the concentration was expressed in micrograms of carbohydrate per gram of cell dry weight. The assays were conducted in

triplicate. The glucose concentration in culture supernatants was determined using Bioclin Glucose Monoreagent kit (cat. no. K082, QUIBASA QUIMICA BÁSICA Ltda, Belo Horizonte, Brazil). *H. capsulatum* yeast cells (10^8cells/mL) were incubated under control and DTPA conditions, during 0, 24, 48, and 72 h. Then, the cells were centrifuged at 1,371 × *g*, and the supernatant was used for glucose measurement according to the manufacturer's instructions. A standard curve was constructed using MMcM medium with crescent glucose concentrations (0, 0.125, 0.250, 0.50, 0.75, and 1%). The dosages were performed in triplicate.

Quantification of Chitin, Glucan and ROS Content

H. capsulatum cells grown in control and Zn-limiting conditions were collected by centrifugation at 1,372 × *g* and washed with PBS. For chitin dosage the cells were treated for 30 min with calcofluor white (100 μg/ml). For glucan dosage the cells were treated for 5 min with aniline blue. After treatment, the cells were washed twice with PBS and analyzed under fluorescence microscope (Zeiss Axiocam MRc-Scope A1). Intracellular peroxide hydrogen (H_2O_2) was measured in *H. capsulatum* yeasts incubated under conditions of zinc and pyridoxine deprivation for 24 h. The fluorescence was obtained using 2′7′-dichlorofluorescein diacetate (DCFH-DA, 25 nM) for 25 min in the dark. The fluorescence intensity of yeast cells was measured using the AxioVision software (Carl Zeiss AG, Germany). The minimum of 30 cells for each microscope slide was used to calculate fluorescence intensity (in pixels). The assays were performed in triplicate.

Scanning Electron Microscopy

The *H. caspulatum* yeast cells were fixed with a solution containing 2% (v/v) glutaraldehyde and 2% (w/v) paraformaldehyde in 0.05 M sodium cacodylate buffer pH 7.4 overnight at room temperature. After, the cells were washed in sodium cacodylate buffer pH 7.2 and incubated for 1 h in 2% (w/v) osmium tetroxide (OsO_4) and 0.8% (w/v) potassium ferricyanide in 0.05 M sodium cacodylate buffer pH 7.4. Subsequently, the cells were washed to remove excess osmium tetroxide and dehydrated in ascending series of acetone solutions (v/v) ranging from 30, 50, 70, 90, to 100%. The samples were dried by the critical point Balzers CPD 30 and placed in stubs to be coated with gold in a Sputter Coater Balzers SCD 050 and then examined in a scanning electron microscope (7001F, JEOL, Tokyo, Japan).

Alcohol Dehydrogenase Activity

Fresh cell extracts from *H. capsulatum* yeasts incubated in control and Zn-limiting conditions were used to measure alcohol dehydrogenase (ADH) activity according to the NADH consumption at 350 nm. Briefly, 5 μg of protein extract was added to 180 ul of reaction mixture (100 mM MES buffer pH 6.1, 1 mM DTT, 5 mM $MgCl_2$, 0.2 mM NADH, and 20 mM acetaldehyde). The reactions were measured every 10 s over 10 min in a microplate reader. The ADH measurement assays were performed in triplicate.

Macrophage Infection Assays

Macrophages J774 1.6 were supplied by the Rio de Janeiro Cell Bank (BCRJ) of the Federal University of Rio de Janeiro (UFRJ). Macrophages were maintained in RPMI 1640 medium (Biowhittaker, Walkersville, Md.) supplemented with 10% (v/v) fetal bovine serum (FBS) (Citrocell/ Embriolife, Campinas, SP, Brazil), 1% (v/v) essential amino acid, and 50 ug/ml of gentamicin solution (Sigma Biochemical) at 36°C and 5% CO_2 until completely confluent. For fungal burden analysis, macrophages (3.75×10^6) cells were plated in 24-well plates (Greinner Bio-One, USA) with RPMI medium containing IFN-γ (1 U/ml) (Sigma Aldrich) for 24 h followed by incubation with RPMI medium containing DTPA or 20 μM of $ZnSO_4$ for 1 h. The cells were then washed twice with PBS. A control sample was incubated with the maintenance medium. After 1.8×10^7 *H. capsulatum* yeasts (MOI 1:5) were added to each well, and the plates were incubated for 24 h at 36°C and 5% CO_2. Each well was then washed with PBS, the macrophages were lysed with sterile cool water and the lysates plated on solid MMcM plates. The experiments were performed in triplicate.

Statistical Analysis

The data were analyzed using electronic spreadsheets and the statistical software R. In the present work, the t Student statistical test was used to analyze gene expression, proteomics, and microscopy data. Meanwhile, CFU's statistical tests were performed through analysis of variance (ANOVA) followed by Tukey test. In addition, in order to verify the quality of the proteomic data, multivariate principal component analysis was applied. Finally, factor analysis was performed with proteomic data to identify proteins regulated by treatment and time.

RESULTS

Growth and Fungal Viability in Zinc Deprivation

Since zinc limitation is one of the GM-CSF-activated macrophage strategies to control *H. capsulatum* infection (Vignesh et al., 2013), fungal growth was assessed in a zinc-limited environment. Spot dilution growth analysis infers a slight reduction in growth when the medium is supplemented with DTPA (**Figure 1A**). The treatment with DTPA did not affect the fungal growth in liquid medium. The growth differences between solid and liquid media may be explained by the fact that in solid medium the cell-nutrient contact is dependent on diffusion, which is less efficient then in liquid cultures. Also, the yeast cell viability is not affected by DTPA treatment (**Figure 1C**). Based on these findings, it may be concluded *H. capsulatum* is able to grow in a zinc poor environment and thus presents molecular machinery to deal with it, at least *in vitro*. Our data is consistent with previous findings that have shown DTPA treatment decreases fungal growth as assessed by tritiated leucine uptake assays (Winters et al., 2010).

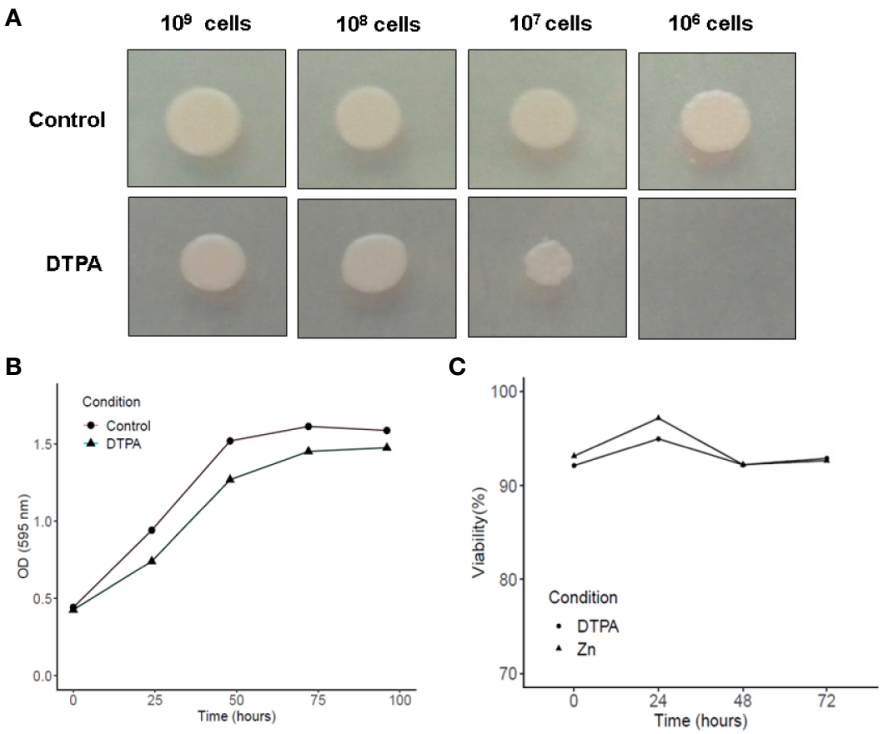

FIGURE 1 | Influence of Zn availability on *H. capsulatum* growth and viability. **(A)** Growth in solid MMcM medium during 5 days with 20 μM of $ZnSO_4$ or 100 μM DPTA. **(B)** Growth of *H. capsulatum* in liquid medium was measured by optical density at 595 nm. **(C)** Viability of *H. capsulatum* in liquid medium was assessed by trypan blue dye. Growth and viability experiments were carried out in biological triplicates.

Data Mining of Zinc Homeostasis Related Genes in *H. capsulatum* Genome

The genome of *H. capsulatum* G186 was screened for genes involved in the coordination of zinc content inside the cell and, with it, maintaining safe zinc levels (zinc homeostasis). The search was performed using genes already characterized in other fungi. The approach led to the identification of eight genes putatively related to zinc homeostasis (**Table 1**). Two transcription factors were found, Zap1 with an identity average of 56.8% and PacC with an identity average 62.8% when compared to regulators of other fungi. These two transcription factors have joint action in regulating zinc uptake transporters in different pH environments. In addition,

TABLE 1 | Identity of zinc homeostasis related genes of *H. capsulatum* G186 when compared to functionally characterized genes.

Accession number	Gene	*P. lutzii (Pb01)*	*P. brasiliensis (Pb03)*	*B. dermatitidis (ER-3)*	*C. immitis (RS)*	*A. fumigatus (Af293)*	*S. cerevisiae (S288C)*
HCBG_07321	*ZRT1*	62% (XP_002789372.1)	63% (EEH18665.1)	68% (EEQ92299.1)	63% (XP_001240918.1)	66% (XP_749518.1)	43% (NP_013231.1)
HCBG_08608	*ZRT2*	68% (XP_002794874.1)	68% (EEH17011.2)	78% (EEQ91531.1)	55% (XP_001241167.2)	51% (XP_751869.1)	30% (NP_013231.1)
HCBG_04549	*ZRT3*	65% (XP_015701767.1)	65% (EEH22486.1)	–	56% (XP_001247051.1)	49% (XP_755208.1)	41% (NP_012746.1)
HCBG_02465	*ZRC2*	70% (XP_015700796.1)	70% (EEH17306.2)	66% (EEQ87926.2)	–	54% (XP_748854.2)	30% (NP_014961.3)
HCBG_00193	*ZRC1*	69% (XP_015703463.1)	68% (EEH19201.2)	–	63% (XP_001240418.1)	61% (XP_755789.1)	48% (NP_013970.1)
HCBG_07376	*PACC*	61% (XP_015700598.1)	–	77% (EEQ84340.1)	61% (XP_001244284.1)	59% (XP_754424.1)	55% (NP_011836.1)
HCBG_03275	*ZAP1*	62% (XP_015701851.1)	63% (EEH21074.2)	68% (EEQ90390.2)	44% (XP_001239281.2)	65% (XP_752374.1)	45% (NP_012479.1)
HCBG_07983	*ZITB*	42% (XP_015701946.1)	45% (EEH17028.2)	53% (EEQ87344.2)	57% (XP_001249104.2)	64% (XP_751291.1)	41% (NP_010491.4)

-ortholog not found in H. capsulatum genome.

six zinc transporters were identified in the *H. capsulatum* genome, three belonging to the ZIP family. The first one was initially named *Zrt2* (Dade et al., 2016). However, experimental analysis showed that it behaves as *ZRT1* found in *S. cerevisiae*, being highly induced during zinc deprivation (**Figure 2**); hence, we saw it fit to name it accordingly. The second ZIP transporter holds a high identity to *A. fumigatus ZrfC* (60%). *ZrfC* is a transporter expressed at low zinc availability and high pH environments and it is tightly associated with a zinc extracellular captor (*Aspf2* in *A. fumigatus* and *PRA1* in *B. dermatitidis)* (Citiulo et al., 2012). Curiously, *PRA1*/Aspf2 was not found in the *H. capsulatum* genome. Furthermore, *HcZrfC* ortholog showed no apparent pH dependent regulation (data not shown). Given that, this transporter was named Zrt2, as so far it was shown to behave in a similar fashion to *ZrfA*, the low affinity zinc transporter in *A. fumigatus* (Vicentefranqueira et al., 2005). The remaining ZIP transporter showed significant identity (ranging from 41 to 74%) to *ZRT3*, the zinc exporter found in the vacuole (Wilson et al., 2012). The CDF family in *H. capsulatum* seems to be composed of *ZRC1*, the known vacuole exporter, *ZRC2*, a *ZrcA* ortholog in *A. fumigatus* (52% identity) and *ZITB*, a CDF found in *E. coli* (Grass et al., 2001), with its biological function not yet characterized in fungi.

In addition, the STRING tool was used in order to analyze the interaction of Zap1 with other proteins related to zinc homeostasis. With it, a network of interactions of the regulator with proteins related to Zn homeostasis was found (**Supplementary Figure 1**). The network shows interactions between Zap1 and Zrt1, as well as Zrt3. Furthermore, the network also showed interaction of Zap1 with transporters probably present in the membrane of organelles such as Zrc1 and Zrc2 that, under conditions of zinc availability, capture and store this metal in vacuoles. Interestingly, ZitB, a zinc carrier of the CDF family, was also found in the interaction network. By using the STRING approach, interactions between carriers Zrt1 and Zrt3 (ZIP family) with carriers of the CDF family (Zrc1 and Zrc2) were also identified. Similar analysis with PacC revealed no interactions with Zn-related genes.

Expression of Zinc Homeostasis Genes During Zinc Deprivation

The influence of Zn availability on transcriptional levels of *H. capsulatum* genes putatively related to Zn homeostasis was analyzed by qRT-PCR (**Figure 2**). The transcription factor *ZAP1*, genes from the ZIP family (*ZRT1, ZRT2, ZRT3*), and two genes from the CDF family (*ZRC2 and ZRC1*) were analyzed. qPCR assays showed that *ZAP1* transcripts increased after 24 h of Zn deprivation. The levels of *ZRT1* and *ZRT2* transcription were induced under Zn limiting conditions at both time points. *ZRT1* stands out as it was the transporter that presented the highest levels of expression among all transporter-genes analyzed. In comparison with *ZRT2*, *H. capsulatum ZRT1* showed a threefold increase in expression after 3 h exposure to a low zinc environment. In addition, *ZRT3* showed a significant difference only in zinc deprivation after 24 h when compared to control (**Figure 2**). These changes in gene expression are due to the Zn-deprivation promoted by DTPA since when Zn is added back to DTPA treated cells the *ZRT1* expression level decreases to

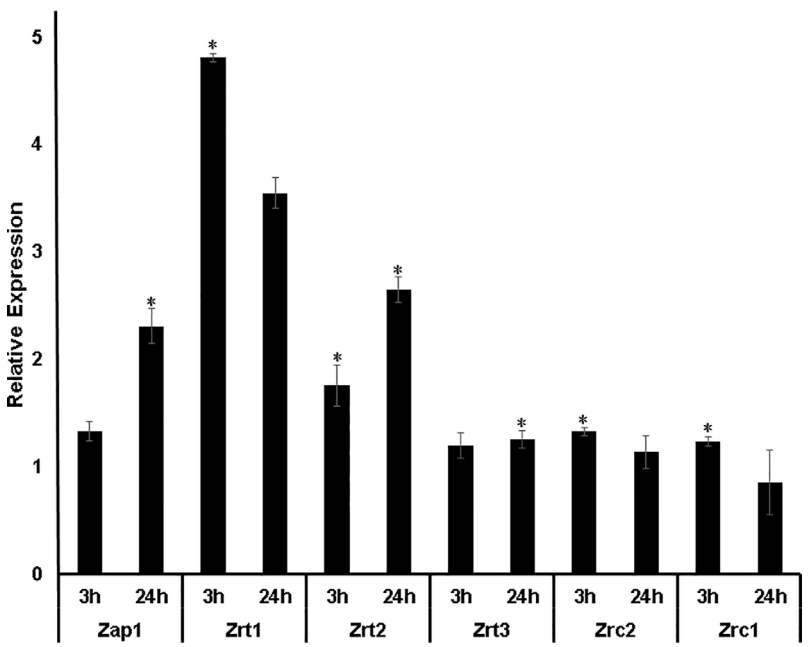

FIGURE 2 | Transcript levels of Zn homeostasis genes during Zn deprivation. ZAP1: transcription factor that regulates the expression of zinc transporters. ZRT11, ZRT2, and ZRT3: Zinc carriers of the ZIP family. ZRC1 and ZRC2: Zinc transporters of the CDF family. The DTPA transcript levels were normalized against the transcript levels of control condition. Transcriptional levels of Zn-related genes were measured in biological triplicates. *:p-value ≤ 0.05.

control the cells (**Figure S2**). Also, the changes promoted by DTPA are not due to chelation of other metals since DTPA does not regulate the expression levels of a high affinity copper transporter (*CTR3*, **Figure S2**). The fact that Zap1 mRNA levels increase at 24 h but its putative regulated transporter is induced at 3 h of Zn deprivation suggests that *H. capsulatum* already has baseline levels of *ZAP1* that acts quickly by increasing *ZRT1* expression. Although surprising, the non-concurrent ZAP1 induction compared to its regulated transporters is not uncommon. Such claims are validated by similar findings in different fungi such as *C. dubliniensis* (Bottcher et al., 2015). Therefore, these results suggest that carriers of the *H. capsulatum* ZIP family are regulated by the amount of zinc available in the cell. Regarding the genes of the CDF family, Zn depletion promotes slight changes in transcript levels of Zrc1 and Zrc2 transporters. Thus, the role of these genes on zinc homeostasis in *Histoplasma* must be approached by mutant based assays.

Influence of Zinc in *H. capsulatum* Survival in Macrophages

Transcript levels of *ZAP1* and *ZRT1* were measured during macrophage infection (**Figure 3A**). Since IFN-γ plays an essential role in fungicidal activity of macrophage (Allendoerfer and Deepe, 1997; Horwath et al., 2015), cells were pre-treated before infection. The data obtained showed that both Zap1 and Zrt1 were induced in fungal cells growing inside macrophages. These findings reinforce previous studies showing that *H. capsulatum* undergoes a Zn limiting environment inside GM-CSF exposed phagocytes (Vignesh et al., 2013). In order to confirm the influence of Zn availability on fungus survival during infection, colony-forming unit analysis was performed (**Figure 3B**). Pre-treatment of macrophages with DTPA reduces fungal survival. This fact is not an effect of DTPA on macrophages, since the viability of the cells is not affected by DTPA (**Figure 3C**). These data together with the increased expression of *ZAP1* and *ZRT1* suggest that *H. capsulatum* faces a low zinc environment as a microbicidal strategy of macrophages and counteracts it, activating high affinity Zn-uptake mechanism.

Proteomic Analysis of *H. capsulatum* During Zinc Deprivation

Since *H. capsulatum* is able to grow inside the intraphagosomal Zn-poor environment, the global response of the fungus to metal scarcity was accessed through proteomics. The approach identified 333 proteins regulated during zinc deprivation, 265 and 68 after 24 h and 48 h of treatment, respectively. According to statistical analysis, 119 proteins were induced at 24 h, and 146 were suppressed (**Supplementary Tables 2** and **3**), while at 48 h 47 proteins were induced and 21 repressed during zinc deprivation (transporter-genes). After 24 h, metabolic pathways related to fatty acid oxidation, energy production, oxidative phosphorylation, amino acid catabolism, biosynthesis of secondary metabolites (pyridoxine), and response to oxidative stress were induced, while glucose oxidation pathways, glyoxylate cycle, and fermentation were repressed (**Figure 4A**). Pathways with the greatest number of induced regulated proteins include fatty acid oxidation, energy production, oxidative phosphorylation, and cell wall carbohydrate biosynthesis (Chitin and Glucan), all after 48 h of Zn deprivation. Meanwhile, glycolysis and fermentation remained suppressed (**Figure 4B**).

In order to filter proteins regulated by the absence of zinc along time, a factor analysis was performed. With it, 22 proteins appeared under regular (control) and zinc deprivation conditions in both times (24 and 48 h) and therefore were included in the analysis (**Supplementary Figure 4**). The

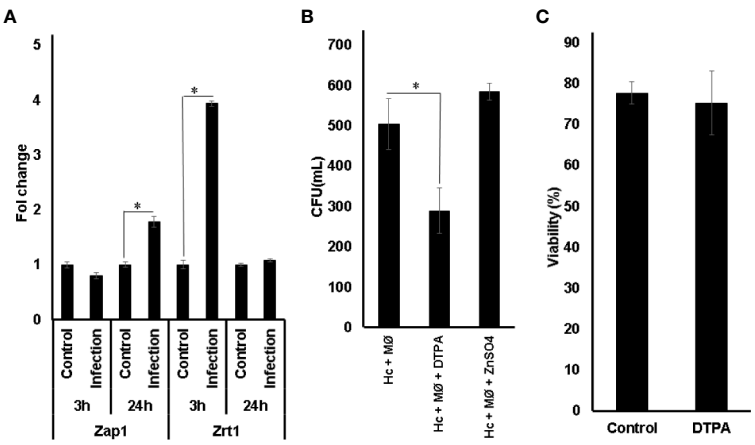

FIGURE 3 | Influence of Zn availability in *H. capsulatum* survival in macrophages. **(A)** Relative expression of Zap1 and Zrt1 in *H. capsulatum* during infection overtime. **(B)** Fungal burden of macrophages treated with (Hc + MØ), ZnSO4 (Hc + MØ + ZnSO4), and DTPA (Hc + MØ + DTPA) conditions. Control: *H. capsulatum* incubated in macrophage medium; Infection: macrophages infected with *H. capsulatum* yeasts. **(C)** Viability of macrophages in RPMI medium was measured by trypan blue dye. Statistical analysis was performed using t-test, one-way ANOVA, and the Tukey multiple comparison test with *p ≤ 0.05. All experiments were carried out in triplicates.

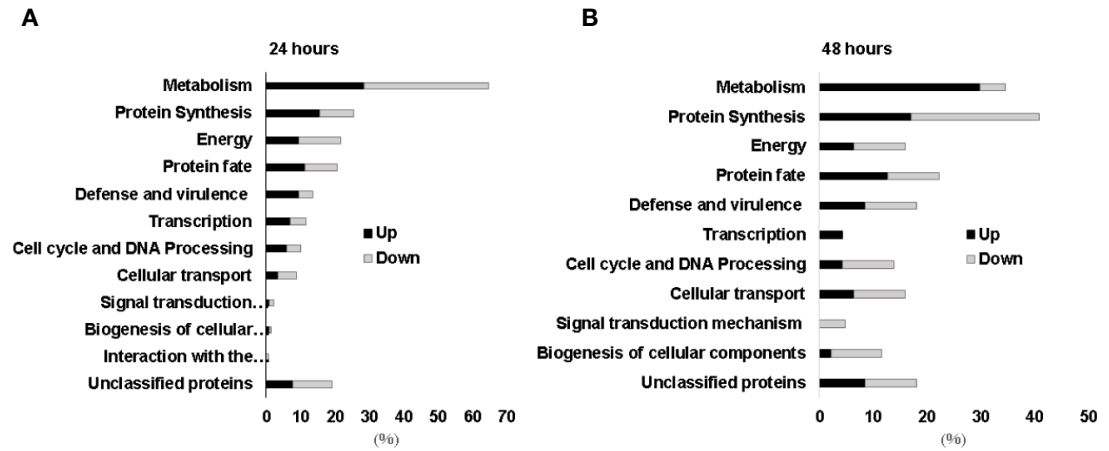

FIGURE 4 | Functional categorization of proteins identified during zinc deprivation at 24 h **(A)** and 48 h **(B)**. Up, upregulated proteins during zinc deprivation. Down, downregulated proteins during zinc deprivation.

TABLE 2 | Core proteins identified regulated by zinc and time.

Accession number	Protein	Control 24–48 h	DTPA 24–48h
HCBG_03816	Prefoldin subunit 4	0.34	0.05
HCBG_05072	Tyrosine-protein kinase	0.82	0.0000006
HCBG_03370	Glyoxylate reductase	0.83	0.0000019

Control 24–48 h, p values of the factor analysis for control conditions regulated over time. DTPA 24–48 h, p values of the factor analysis for DTPA condition regulated over time.

approach identified three proteins (Prefoldin subunit 4, Tyrosine Kinase, and Glyoxylate reductase) differentially regulated by zinc deprivation and also by time (**Table 2**). It is worth mentioning that glyoxylate reductase is increased at 24 h of zinc deprivation and is decreased at 48 h. Thus, it is likely that the enzyme produces the necessary amounts of precursors for the biosynthesis of other metabolites in zinc deprivation in the first 24 h, and therefore, this enzyme is important for early fungal adapting to Zn deprivation.

Proteomics showed a rearrangement of metabolic process in order to cope with reduced zinc availability. Enzymes such as hexokinase and phosphofrutokinase-1 were repressed, suggesting a reduction in glycolytic activity in the cell. Proteomic data also revealed that alcohol dehydrogenase (ADH) was suppressed during zinc deprivation, suggesting that the fungus relies on the anaerobic metabolism since ADH is a Zn-dependent enzyme (**Figure 5**). Furthermore, other enzymes related to energy production have also been observed, for example, carnitine-acyl transferase, an important regulator that dictates beta-oxidation. In addition, several enzymes of the citric acid cycle (malate dehydrogenase, succinate dehydrogenase, and isocitrate dehydrogenase) and ATP synthase from oxidative phosphorylation were induced (**Figure 5**). Therefore, these results suggest that the supply of acetyl-CoA for the Krebs cycle in zinc deprivation is not exclusively being provided through the glycolytic pathway but rather by the oxidation of fatty acids. Thus, it is suggested that *H. capsulatum* during zinc deprivation has the ability to modify its energy metabolism to survive the changes imposed by the host. In addition, it has been shown that this fungus has lipid reserves used in adverse conditions, such as during an infectious process. Changes in glycolate biosynthesis (a precursor of pyridoxine biosynthesis), has been revealed by factor analysis. Two enzymes related to pyridoxine production were induced in metal deficiency: pyridoxal 5P kinase and pyridoxal kinase (**Figure 5**). In addition, enzymes related to amino acid degradation such as alanine transaminase, which was induced in zinc deprivation, were also found in this work. This enzyme can help with energy metabolism since it led to the production of pyruvate, that may be directed to TCA cycle.

UDP-N-acetylgalactosamine pyrophosphorylase, an enzyme related to the synthesis of chitin, was induced during zinc deprivation at both time points (24 and 48 h). In addition, we also observed that the glyoxylate cycle was suppressed by zinc deprivation (**Figure 5**). Therefore, it appears that *H. capsulatum* increased the production of structural carbohydrates from glucose that is not consumed by the glycolytic pathway. The consumption of glucose in Zn deprivation is likely related to the remodeling of the wall since glycolysis and fermentation are reduced and beta-oxidation is induced.

Zinc Deprivation Decreases Fermentation in *H. capsulatum*

The proteomic analysis showed that enzymes such as hexokinase (HCBG_05633), enolase (HCBG_00056), pyruvate carboxylase (HCBG_00107), and alcohol dehydrogenase (HCBG_05406) were repressed in zinc deprivation. Such results indicate that anaerobic metabolism is suppressed at low zinc levels. Thus, to confirm these results, ADH activity was measured in *H. capsulatum* yeasts grown under control conditions and with Zn deficiency (**Figure 6A**). This approach showed that Zn

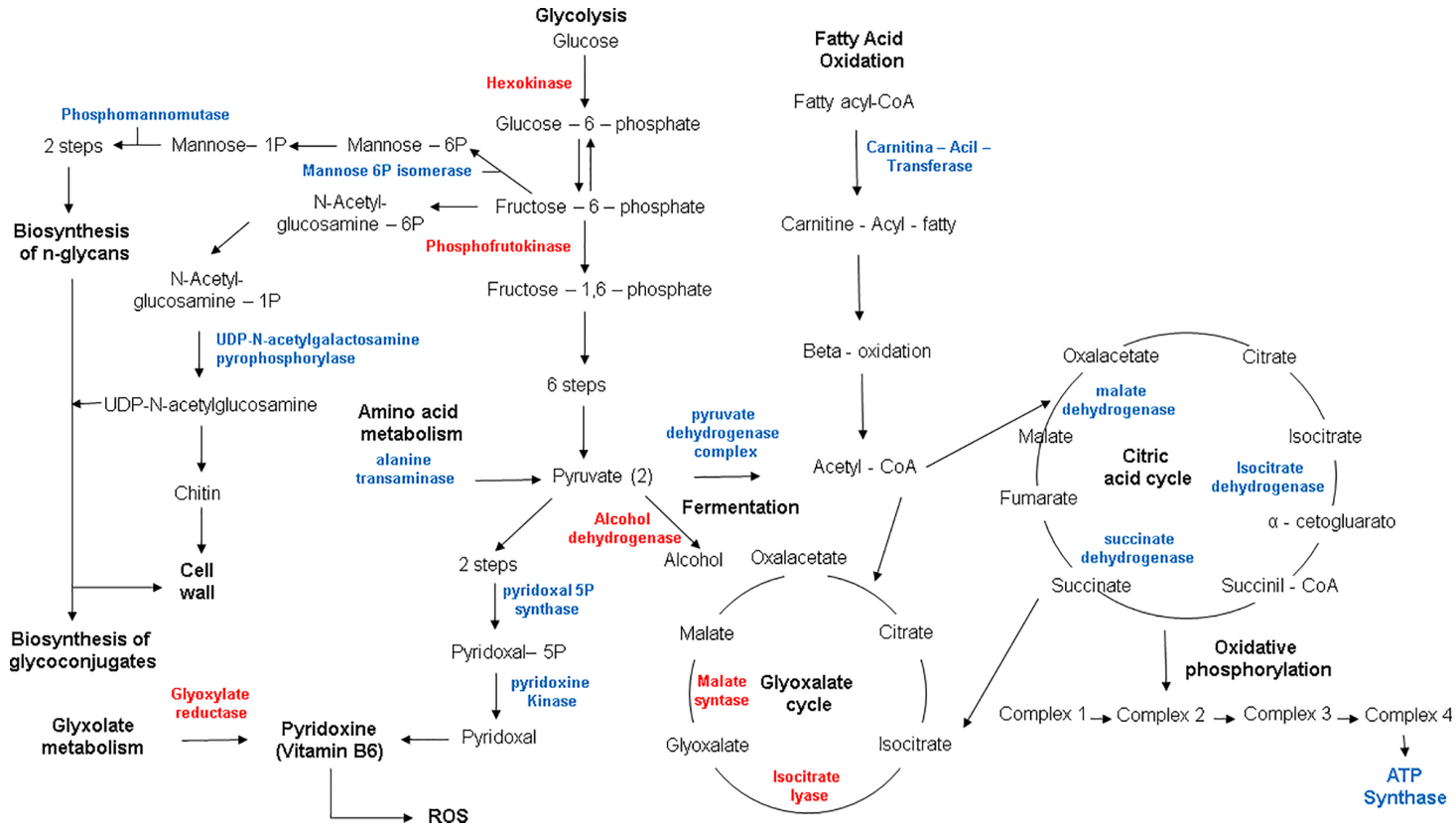

FIGURE 5 | Metabolic profile of *H. capsulatum* yeasts during zinc deprivation. Red: downregulated proteins; Blue: upregulated proteins.

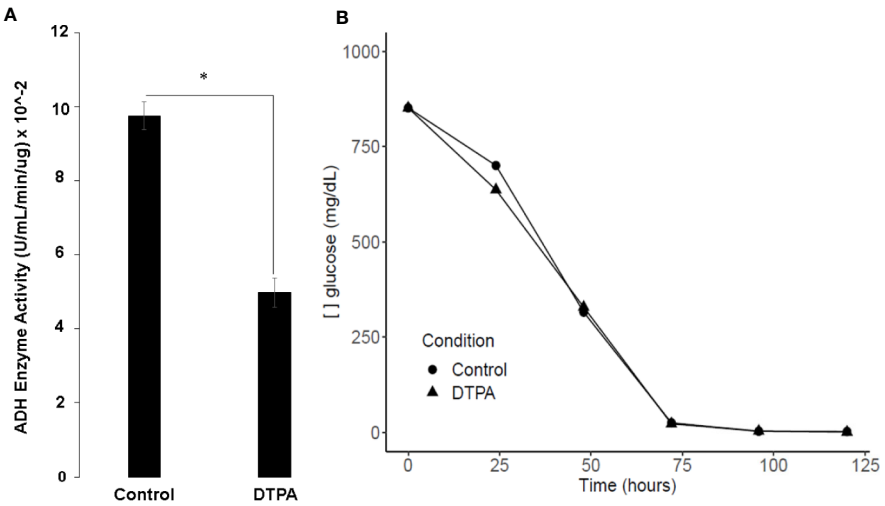

FIGURE 6 | Influence of zinc scarcity glucose metabolism of *H. capsulatum*. **(A)** Enzymatic activity of ADH during zinc deprivation in 24 h. **(B)** Glucose dosage in culture supernatants of cells grown in Zn replete or Zn depleted conditions. All experiments were carried out in biological triplicates. Student t test with *p ≤ 0.05.

limitation decreases ADH activity, corroborating with proteomic data. Therefore, it is likely that fermentation under conditions of low zinc availability was suppressed in *H. capsulatum*, and probably glucose flow through glycolytic pathway is decreased. In order to confirm that, assays were performed to measure glucose consumption by *H. capsulatum* in zinc deprivation. The glucose consumption did not change in Zn-depleted cells in comparison with control cells (**Figure 6B**), which reinforces the idea that glucose consumed by the fungus is being used for purposes other than energy production.

Zinc Deprivation Alters the Structural Carbohydrate Distribution in *H. capsulatum*

The decreased levels of glycolytic and fermentative enzymes allied to glucose consumption suggest the fungus may be directing glucose to structural purposes. This hypothesis is supported by an increase in enzymes related to the biosynthesis of wall precursors during Zn deprivation such as UDP-N-acetylglucosamine pyrophosphorylase (HCBG_00326), mannose-6-phosphate isomerase (HCBG_05577), and phosphomannomutase (HCBG_05577). Among them, UDP-N-acetylglucosamine pyrophosphorylase stands out as it is related to chitin biosynthesis. To assess that, *H. capsulatum* carbohydrate content was biochemically measured. Accordingly, an increase in carbohydrate content was observed under 24 h of Zn deprivation. However, after 48 h, there was no significant difference in the amount of carbohydrate present in the cell, suggesting an adaptation of *H. capsulatum* to zinc deprivation over time (**Figure 7A**).

In addition, the increase in the amount of glycan during zinc deprivation may also be related to the production of carbohydrates with structural function. Therefore, it was hypothesized that the glucose consumed by the fungus was being driven to structural carbohydrate biosynthesis. In order to test that hypothesis, the contents of chitin and glycan were measured by fluorescence microscopy. Indeed, Zn limitation induces chitin and glucan accumulation (**Figures 7B, C**). To further confirm those changes, cell wall structure was examined by scanning electron microscopy (**Figure 7D**). The results showed that *H. capsulatum* in the control condition presents a rougher cell wall when compared to zinc deprivation, suggesting that *H. capsulatum* alters cell wall structure and composition during zinc deprivation.

Zn Limitation and Pyridoxine Synthesis

Factor analysis results revealed that the glyoxylate reductase (HCBG_03370) was induced during zinc deprivation at 24 h when compared to cells in control condition. However, in 48 h we observed an inversion in the abundancy of the enzyme, in which it is repressed in zinc deficiency. Thus, it appears that the enzyme produced relevant amounts of glycolate during the first 24 h and later, still for unknown reasons, has its quantity reduced. In addition, two enzymes related to vitamin B6 synthesis, pyridoxal 5P synthase and pyridoxal kinase, were identified by proteomic approach. Both were induced after 48 h of zinc deprivation, suggesting an increase in pyridoxine biosynthesis. In order to verify the importance of pyridoxine in *H. capsulatum*, the effect of pyridoxine on fungal growth under Zn limitation was analyzed (**Figure 8A**). Surprisingly, *H. capsulatum* grows similarly when zinc is available regardless of pyridoxine availability. However, the growth in Zn deprivation was affected when no pyridoxine was provided. Therefore, it is suggested that there is an association between zinc homeostasis and vitamin B6 biosynthesis. Furthermore, it is known that pyridoxine is a chemical compound with a high affinity for reactive oxygen species (Matxain et al., 2006). In order to analyze the association of Zn-depletion and ROS stress, ROS labeling assays were performed. The data show that Zn-limitation itself increases the

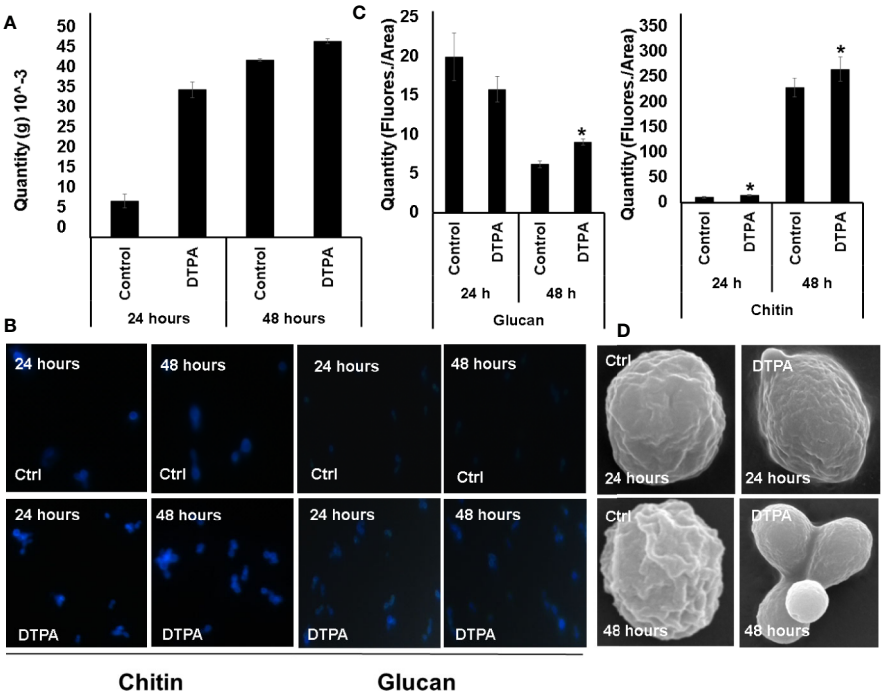

FIGURE 7 | Effect of Zn availability on *H. capsulatum* cell wall carbohydrates. **(A)** Dosage of total carbohydrate in *H. capsulatum* cells during zinc deprivation. **(B)** Fluorescence microscopy *H. capsulatum* grown under control and DTPA conditions. Calcofluor white and aniline blue were used to dosage chitin and glycan, respectively. **(C)** Measurement of glycan and chitin contents using fluorescence intensity. **(D)** Scanning electron microscopy of *H. capsulatum* during zinc deprivation. All experiments were carried out in biological triplicates. The comparisons were made using the Student t test with *p ≤ 0.05.

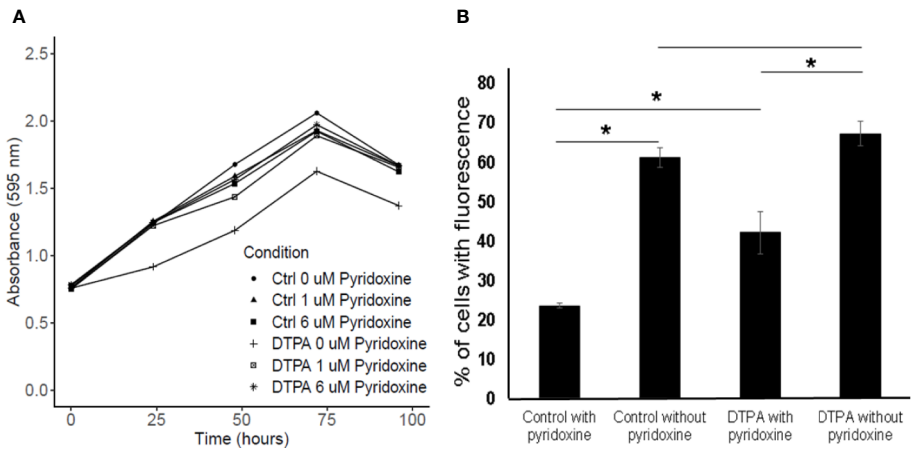

FIGURE 8 | Influence of pyridoxine on *H. capsulatum* growth and oxidative stress level. **(A)** Growth curve of *H. capsulatum* during zinc deprivation at different concentrations of pyridoxine. **(B)** ROS detection of *H. capsulatum* labeled with DCFH-DA. Ctrl, fungal cells grown in zinc; DTPA, fungal cells grown in DTPA. All experiments were carried out in biological triplicates. The comparison was made using the Student t test with *p ≤ 0.05.

number of labeled cells by twofold. The zinc limitation in absence of pyridoxine potentialize the ROS levels since teh number of labeled cells incresed by threefold. Therefore, it may be concluded that both pyridoxine and zinc are able to influence *H. capsulatum's* ability to control intracellular ROS levels (**Figure 8B**).

DISCUSSION

The *in silico* analysis identified eight orthologous genes putatively related to zinc homeostasis in *H. capsulatum*. Two of them are transcription factors (Zap1 and PacC), three belong

to the CDF zinc transporter family (Zrc1, Zrc2 and ZitB), and three belong to the ZIP family (Zrt1, Zrt2 and Zrt3). In *A. fumigatus*, zinc homeostasis is regulated by two transcription factors and zinc sensors that control the coordinated action of eight carriers belonging to the ZIP family and eight of the CDF family (Amich and Calera, 2014). In *C. gatti*, zinc carrier proteins of the ZIP family have already been described, such as ZIP1, ZIP2, and ZIP3. These proteins are orthologs of the Zrts/Zrfs found in *H. capsulatum* and *A. fumigatus* (Schneider et al., 2015). As previously mentioned, studies with *H. capsulatum* have shown the presence of a carrier called *Hc*Zrt2 (called here as Zrt1) that behaves in a similar manner to Zrt1 in *S. cerevisiae* (Dade et al., 2016). Thus, we propose the change since most high affinity transporters are named Zrt1, as in *C. albicans* (Crawford et al., 2018), *C. dubliniensis* (Bottcher et al., 2015), *B. dermatitidis* (Kujoth et al., 2018), and the already mentioned *S. cerevisiae* (Zhao and Eide, 1996). However, mutant based studies are required to properly characterize the remaining transporters. In addition to zinc uptake mechanisms mediated by carriers of the ZIP and CDF family, a novel zinc uptake protein was first identified in *C. albicans*. Pra1 acts as a "zincophore" similarly to siderophores (Fe carriers) found in bacteria and fungi (Miethke and Marahiel, 2007). This protein holds multiple zinc binding sites in its structure and is able to gather either free or protein associated zinc in the extracellular medium. Studies have shown that Pra1 is normally expressed under low zinc and alkaline conditions, similar to ZrfC in *A. fumigatus* and its orthologs Zrt1 in *C. albicans* where Pra1 has also shown to be associated with both through function, redirecting captured zinc to be transported by ZrfC/Zrt1 (Wilson et al., 2012). However, in *H. capsulatum*, no molecule homologous to Pra1 was found. Thus, from the *in silico* analysis it is suggested that *H. capsulatum* does not have a zinc capture mechanism mediated by zincophore. Finally, while our analyses showed that the genes mentioned are being influenced by zinc to different degrees, mutant studies are required to properly characterize their biological significance in *H. capsulatum.*

During infection, it is known that GM-CSF activated macrophages reduce the availability of free zinc in the *Histoplasma*-containing phagolysosome. This reduction is mediated by the production of metallothioneins that sequester cytoplasmic labile zinc and also pumps out Zn from *H. capsulatum* containing phagolysosome (Vignesh et al., 2013). Corroborating our data showed that fungal survival in macrophages under Zn limitation was decreased when compared to cells under Zn-homeostatic levels. As a successful pathogen, *H. capsulatum* is able to survive and proliferate in such condition. As depicted in this work, it is suggested that this mechanism of zinc capture and management is mediated by carriers of the ZIP and CDF family under the influence of Zap1. Experimentally, *H. capsulatum* captures zinc from the extracellular medium by a high affinity transporter, previously known as HcZrt2 (Dade et al., 2016). In addition, Dade et al. (2016) showed that the fungus in the absence of this gene lose part of its virulence. Therefore, this transporter is one of the evolutionary aspects developed by *H. capsulatum* to capture zinc and increase the chances of survival in hostile environments. As such, it is possible that Zrt1 (HcZrt2), Zrt2, and Zrt3 identified in this work are being induced by low zinc availability, and this induction may be promoted by Zap1.

Currently, it is known that the main mechanism of zinc regulation in fungi is mediated by the transcription factor Zap1. In *S. cerevisiae*, this transcription factor binds to Zinc Responsive Elements (ZREs) found on the promoter regions of genes such as *ZRT1*, *ZRT2*, and *FET3* (Zhao et al., 1998; Eide, 2009). In our gene expression experiments, an increase in Zap1 levels over 24 h was observed, while the high affinity Zn transporter ZRT1, controlled by ZAP1, was induced at 3 h. This uncorrelation of the regulator and its target genes is not a surprise since previous studies have shown that Zap1 protein levels are stable regardless of the transcript amount, being the regulation of zinc transporter mediated not only by Zap1, but also by zinc availability. With it, it is reasonable to assume that as zinc quantity drastically decreases, basal Zap1 levels are enough to quickly induce key transporters before itself. Additionally, expression analysis studies on Zap1 orthologs in previously mentioned fungi showed that the regulator was induced at the 24 h time period (Zhao and Eide, 1997; Schneider et al., 2012; Vicentefranqueira et al., 2018), similar to the results found in the present study. Thus, it is suggested that all these genes are working together to regulate zinc homeostasis, in which Zap1 induces the production of Zrt1, Zrt3, and Zrt2 in the absence of zinc as seen in *S. cerevisiae*, *C. gatti*, and *C. neoformans* (Eide, 2009; Schneider et al., 2012; Wilson et al., 2012; Bottcher et al., 2015). Regarding CDFs, it was observed that the transporters Zrc1 and Zrc2 showed a mild response in the absence of zinc. Thus, more specific studies are required in order to determine the roles of Zrc1 and Zrc2 in zinc homeostasis in *H. capsulatum*.

Proteomic data revealed a change in energy metabolism and biosynthesis of secondary compounds of *H. capsulatum* during zinc deprivation (**Figure 7**). In other fungi, such as *A. fumigatus, C. albicans, C. neoformans, C. gatti, and S. cerevisiae*, bioinformatics studies have shown that 12% of all zinc-binding proteins are involved in metabolic processes of carbohydrates and amino acids (Staats et al., 2013). In this work, changes in enzymes related to glycolysis, fermentation, glyoxylate cycle, amino acid synthesis/degradation, pyridoxine, and glycan biosynthesis were also observed (**Supplementary Tables 02–05**). Specifically, in glycolysis, two regulatory enzymes: hexokinase (HCBG_05633) and phosphofrutokinase-1 (HCBG_08430), were repressed, indicating that the glycolytic pathway was oxidizing glucose at a reduced rate. These results corroborate with Medina and Nicholas (1957) who showed a 70% reduction in the activity of *Neurospora crassa* hexokinase in zinc deprivation. Other pathways of energy production, such as beta-oxidation, amino acid degradation, citric acid cycle, and oxidative phosphorylation, were induced by zinc deprivation. Therefore, it is suggested that the energy metabolism remains active, as other sources of energy are being oxidized to compensate the decreased glycolysis activity. Unlike our findings, Parente et al. (2013), utilizing a similar approach, showed that the energy source in *P. brasiliensis* in zinc

deprivation occurred through the induction of enzymes in the glycolytic pathway.

Regarding fermentation, our results showed a reduction in the enzymatic activity of alcohol dehydrogenase, indicating a suppression of anaerobic metabolism. These data are consistent with the structural conformation of this protein, since zinc is a fundamental cofactor for the catalytic activity of alcoholic dehydrogenase (Culotta et al., 2006). Additionally, data obtained corroborate with *in silico* results showed by Tristão et al. (2014) in which they analyzed all zinc binding proteins of the *Paracoccidioides* complex, among which were found the enzymes alcohol dehydrogenase and hexokinase. A recent work demonstrated that *H. capsulatum* survival in macrophages is dependent on gluconeogenesis and that glycolysis is dispensable (Shen et al., 2020). Our data demonstrate Zn-depletion decreases glycolysis since the metal structurally composes some glycolytic enzymes. Thus, the non-activation of glycolysis in intraphagosomal milieu may be a phenomenon not only related to low glucose availability but also a result of a Zn poor environment (Vignesh et al., 2013).

Experiments on total carbohydrate dosage showed that, when zinc is deprived, the fungus accumulated this compound (**Figure 9**). The main molecules produced were related to structural carbohydrates, since the glycolytic pathway was repressed and enzymes belonging to synthesis of cell wall carbohydrates (Chitin and Glucan) were induced during zinc deprivation. Also, the amount of chitin and glucan in the cell wall of *H. capsulatum* was greater than that of the control. Our results complement those found by Rappleye et al. (2007), which has shown that during infection, *H. capsulatum* processes a large amount of α-(1,3)-glucan inside macrophages. High concentrations of glucan inhibit production of cytokines released by the host, such as, tumor necrosis factor alpha (αTNF). Therefore, *H. capsulatum* in the absence of zinc was using glucose for cell wall remodeling since this condition simulate the infectious process. On top of that, scanning microscopy analysis revealed that *H. capsulatum* in normal conditions has a more irregular cell surface when compared to the zinc deprivation condition. The smoother cell surface phenotype may be a direct effect of zinc depletion or a secondary event triggered by metal scarcity. The biological meaning of this cell surface morphology in virulence of *H. capsulatum* will be addressed in further studies. The changes in carbohydrate content differ from those found by de Curcio et al. (2017) in *P. brasiliensis*, in which Zn-limitation promotes a decreasing in chitin content in yeast cells. Such contrasting results may be explained by different pathogenic strategies used by the two fungi. Whereas *H. capsulatum* behaves as an intracellular microorganism, *P. brasiliensis* is not considered a classical intracellular pathogen, being then exposed to different conditions in the host.

Vitamin B6 synthesis reduction is associated with decreased Zn levels in the cell, since the enzyme pyridoxine kinase has a structural site that binds to a Zn–ATP complex (Li et al., 2002). Therefore, it is inferred that under zinc limiting conditions, the enzymatic activity of pyridoxine kinase is altered, resulting in a reduction in pyridoxine synthesis in *H. capsulatum* cells. These results are in agreement with those found by Churchich et al. (1989), in which the enzymatic activity of pyridoxine kinase reduces about 70% during zinc deprivation. This study also showed that pyridoxal kinase can instead be activated by zinc metallothioneins as a rapid response to vitamin B6 biosynthesis in adverse conditions (Karawya and Fonda, 1982). Our data also indicate that oxidative stress is increased in Zn-limitation and is magnified when pyridoxine is not available in the medium. Thus the reduced growth when both Zn and vitamin B6 are reduced is

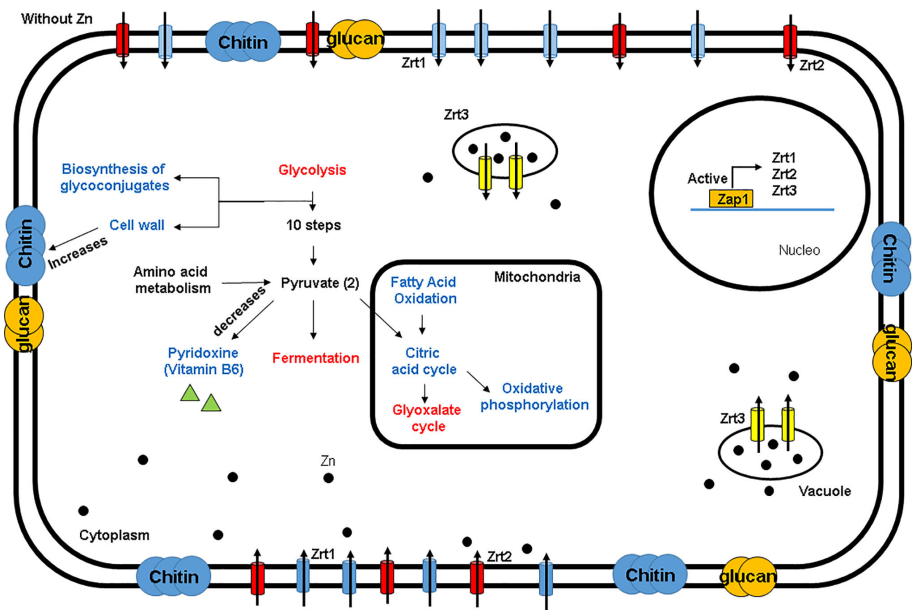

FIGURE 9 | Hypothetical model of *H. capsulatum* response to zinc deprivation.

probably due to a cascade effect, in which the lack of zinc reduces the production of vitamin B6 and, as a consequence, increases the amount of reactive oxygen species in *H. capsulatum* cells.

CONCLUSIONS

In this study, eight genes possibly involved in zinc homeostasis were identified in the *in silico* analysis. Proteomic analysis during zinc starvation revealed influence in several metabolic pathways, mainly in the metabolism of glucose, biosynthesis of structural carbohydrates, biosynthesis of pyridoxine and regulation of oxidative stress. Our data also suggest *H. capsulatum* takes glucose for cell wall remodeling. The absence of zinc interferes with pyridoxine biosynthesis, which increases oxidative stress in yeast cells (**Figure 9**). This study sets the groundwork for a deeper understanding of *H. capsulatum* behavior on zinc deprivation, a relevant condition often found during infection. Providing scientists with a new perspective on how *H. capsulatum* is able to thrive on such conditions can help on the establishment of future treatment options.

DATA AVAILABILITY STATEMENT

The original contributions presented in the study are publicly available. This data can be found here: http://www.ebi.ac.uk/pride, project accession PDX022039.

AUTHOR CONTRIBUTIONS

LA, JS, LB, and SB performed the experiments. LA, LS, DM, and MS-B performed data analysis. AB and MS-B designed the research. AB and CS contributed with reagents and/or funds for research. LA, DM, LS, AB, and MS-B contributed to data interpretation and manuscript writing. All authors contributed to the article and approved the submitted version.

FUNDING

This work received financial support from the National Council for Scientific and Technological Development (CNPQ, grant number 407666/2016-8), Goiás State Research Support Foundation (FAPEG), Coordination for the Improvement of Higher Education Personnel (CAPES) and the National Institute of Science and Technology of Host-Pathogen Interaction (INCT-IPH).

SUPPLEMENTARY MATERIAL

The Supplementary Material for this article can be found online at: https://www.frontiersin.org/articles/10.3389/fcimb.2020.573097/full#supplementary-material

SUPPLEMENTARY FIGURE 1 | Interaction network of genes related to zinc homeostasis. Zap1 was used as input sequence. Zap1: HCBG_03275; Zrt1: HCBG_07321; Zrt3: HCBG_04549; Zrc1: HCBG_00193; Zrc2: HCBG_00193; ZrfG: HCBG_05775 and ZitB: HCBG_07983. Light blue and purple lines are known interactions from experimental databases. Dark green, red, and dark blue lines are predicted interactions from neighborhood genes, gene fusions, and gene co-occurrence. The light green and black lines are the interactions by co-expression and homology of the protein.

SUPPLEMENTARY FIGURE 2 | DTPA promotes a Zn depleted environment. **(A)** Influence of DTPA on the growth of *H. capsulatum*. Optical density was measured at 595 nm. (**B**) Expression level of *ZRT1* in the control condition, DTPA and DTPA plus Zn (200 μM). (**C)** Expression level of *CTR3* in the control condition, DTPA and DTPA plus Zn (200 μM). All experiments were carried out in biological triplicates. The comparisons were made using the Student t test with *p ≤ 0.05.

REFERENCES

Aide, M. A. (2009). Chapter 4-histoplasmosis. *J. Bras Pneumol.* 35 (11), 1145–1151. doi: 10.1590/s1806-37132009001100013

Alberts, B. (1998). The cell as a collection of protein machines: preparing the next generation of molecular biologists. *Cell* 92 (3), 291–294. doi: 10.1016/S0092-8674(00)80922-8

Allendoerfer, R., and Deepe, G. S. (1997). Intrapulmonary response to *Histoplasma capsulatum* in gamma interferon knockout mice. *Infect. Immun.* 65 (7), 2564–2569. doi: 10.1128/IAI.65.7.2564-2569.1997

Amich, J., and Calera, J. A. (2014). Zinc acquisition: a key aspect in *Aspergillus fumigatus* virulence. *Mycopathologia* 178 (5-6), 379–385. doi: 10.1007/s11046-014-9764-2

Andreini, C., Banci, L., Bertini, I., and Rosato, A. (2006). Counting the zinc-proteins encoded in the human genome. *J. Proteome Res.* 5 (1), 196–201. doi: 10.1021/pr050361j

Andreini, C., Bertini, I., Cavallaro, G., Holliday, G. L., and Thornton, J. M. (2009). Metal-MACiE: a database of metals involved in biological catalysis. *Bioinformatics* 25 (16), 2088–2089. doi: 10.1093/bioinformatics/btp256

Auld, D. S. (2001). Zinc coordination sphere in biochemical zinc sites. *Biometals* 14 (3-4), 271–313. doi: 10.1023/a:1012976615056

Baeza, L. C., da Mata, F. R., Pigosso, L. L., Pereira, M., de Souza, G., Coelho, A. S. G., et al. (2017). Differential Metabolism of a Two-Carbon Substrate by Members of the *Paracoccidioides* Genus. *Front. Microbiol.* 8, 2308. doi: 10.3389/fmicb.2017.02308

Bahr, N. C., Antinori, S., Wheat, L. J., and Sarosi, G. A. (2015). Histoplasmosis infections worldwide: thinking outside of the Ohio River valley. *Curr. Trop. Med. Rep.* 2 (2), 70–80. doi: 10.1007/s40475-015-0044-0

Bertuzzi, M., Schrettl, M., Alcazar-Fuoli, L., Cairns, T. C., Munoz, A., Walker, L. A., et al. (2014). The pH-responsive PacC transcription factor of *Aspergillus fumigatus* governs epithelial entry and tissue invasion during pulmonary aspergillosis. *PLoS Pathog.* 10 (10), e1004413. doi: 10.1371/journal.ppat.1004413

Bookout, A. L., Cummins, C. L., Mangelsdorf, D. J., Pesola, J. M., and Kramer, M. F. (2006). High-throughput real-time quantitative reverse transcription PCR. *Curr. Protoc. Mol. Biol.* Chapter 15, Unit 15.18. doi: 10.1002/0471142727.mb1508s73

Bottcher, B., Palige, K., Jacobsen, I. D., Hube, B., and Brunke, S. (2015). Csr1/Zap1 Maintains Zinc Homeostasis and Influences Virulence in *Candida dubliniensis* but Is Not Coupled to Morphogenesis. *Eukaryot. Cell* 14 (7), 661–670. doi: 10.1128/EC.00078-15

Churchich, J. E., Scholz, G., and Kwok, F. (1989). Activation of pyridoxal kinase by metallothionein. *Biochim. Biophys. Acta* 996 (3), 181–186. doi: 10.1016/0167-4838(89)90245-8

Citiulo, F., Jacobsen, I. D., Miramon, P., Schild, L., Brunke, S., Zipfel, P., et al. (2012). *Candida albicans* scavenges host zinc via Pra1 during endothelial invasion. *PLoS Pathog.* 8 (6), e1002777. doi: 10.1371/journal.ppat.1002777

Corkins, M. E., May, M., Ehrensberger, K. M., Hu, Y. M., Liu, Y. H., Bloor, S. D., et al. (2013). Zinc finger protein Loz1 is required for zinc-responsive regulation of gene expression in fission yeast. *Proc. Natl. Acad. Sci. U. S. A.* 110 (38), 15371–15376. doi: 10.1073/pnas.1300853110

Crawford, A. C., Lehtovirta-Morley, L. E., Alamir, O., Niemiec, M. J., Alawfi, B., Alsarraf, M., et al. (2018). Biphasic zinc compartmentalisation in a human fungal pathogen. *PLoS Pathog.* 14 (5), e1007013. doi: 10.1371/journal.ppat.1007013

Culotta, V. C., Yang, M., and O'Halloran, T. V. (2006). Activation of superoxide dismutases: putting the metal to the pedal. *Biochim. Biophys. Acta* 1763 (7), 747–758. doi: 10.1016/j.bbamcr.2006.05.003

Dade, J., DuBois, J. C., Pasula, R., Donnell, A. M., Caruso, J. A., Smulian, A. G., et al. (2016). *Hc*Zrt2, a zinc responsive gene, is indispensable for the survival of *Histoplasma capsulatum in vivo*. *Med. Mycol.* 54 (8), 865–875. doi: 10.1093/mmy/myw045

de Curcio, J. S., Silva, M. G., Silva Bailao, M. G., Bao, S. N., Casaletti, L., Bailao, A. M., et al. (2017). Identification of membrane proteome of *Paracoccidioides lutzii* and its regulation by zinc. *Future Sci. OA* 3 (4), FSO232. doi: 10.4155/fsoa-2017-0044

De Sanchez, S. B., and Carbonell, L. M. (1975). Immunological studies on Histoplasma capsulatum. *Infect. Immun.* 11 (2), 387–394. doi: 10.1128/iai.11.2.387-394.1975

Dubois, M., Gilles, K. A., Hamilton, J. K., Rebers, P.T., and Smith, F. (1956). Colorimetric method for determination of sugars and related substances. *Anal. Chem.* 28 (3), 350–356. doi: 10.1021/ac60111a017

Eide, D. J. (2006). Zinc transporters and the cellular trafficking of zinc. *Biochim. Biophys. Acta* 1763 (7), 711–722. doi: 10.1016/j.bbamcr.2006.03.005

Eide, D. J. (2009). Homeostatic and adaptive responses to zinc deficiency in *Saccharomyces cerevisiae*. *J. Biol. Chem.* 284 (28), 18565–18569. doi: 10.1074/jbc.R900014200

Frey, A. G., Bird, A. J., Evans-Galea, M. V., Blankman, E., Winge, D. R., and Eide, D. J. (2011). Zinc-regulated DNA binding of the yeast Zap1 zinc-responsive activator. *PLoS One* 6 (7), e22535. doi: 10.1371/journal.pone.0022535

Garfoot, A. L., and Rappleye, C. A. (2016). Histoplasma capsulatum surmounts obstacles to intracellular pathogenesis. *FEBS J.* 283 (4), 619–633. doi: 10.1111/febs.13389

Geromanos, S. J., Vissers, J. P., Silva, J. C., Dorschel, C. A., Li, G. Z., Gorenstein, M. V., et al. (2009). The detection, correlation, and comparison of peptide precursor and product ions from data independent LC-MS with data dependant LC-MS/MS. *Proteomics* 9 (6), 1683–1695. doi: 10.1002/pmic.200800562

Gildea, L. A., Morris, R. E., and Newman, S. L. (2001). Histoplasma capsulatum yeasts are phagocytosed via very late antigen-5, killed, and processed for antigen presentation by human dendritic cells. *J. Immunol.* 166 (2), 1049–1056. doi: 10.4049/jimmunol.166.2.1049

Grass, G., Fan, B., Rosen, B. P., Franke, S., Nies, D. H., and Rensing, C. (2001). ZitB (YbgR), a Member of the Cation Diffusion Facilitator Family, Is an Additional Zinc Transporter in *Escherichia coli*. *J. Bacteriol.* 183 (15), 4664–4667. doi: 10.1128/JB.183.15.4664-4667.2001

Horwath, M. C., Fecher, R. A., and Deepe, G. S.Jr (2015). *Histoplasma capsulatum*, lung infection and immunity. *Future Microbiol.* 10 (6), 967–975. doi: 10.2217/fmb.15.25

Karawya, E., and Fonda, M. L. (1982). Physical and kinetic properties of sheep liver pyridoxine kinase. *Arch. Biochem. Biophys.* 216 (1), 170–177. doi: 10.1016/0003-9861(82)90201-6

Kim, M. J., Kil, M., Jung, J. H., and Kim, J. (2008). Roles of Zinc-responsive transcription factor Csr1 in filamentous growth of the pathogenic Yeast *Candida albicans*. *J. Microbiol. Biotechnol.* 18 (2), 242–247.

Kujoth, G. C., Sullivan, T. D., Merkhofer, R., Lee, T. J., Wang, H., Brandhorst, T., et al. (2018). CRISPR/Cas9-Mediated Gene Disruption Reveals the Importance of Zinc Metabolism for Fitness of the Dimorphic Fungal Pathogen *Blastomyces dermatitidis*. *MBio* 9 (2), e00412-18. doi: 10.1128/mBio.00412-18

Li, M. H., Kwok, F., Chang, W. R., Lau, C. K., Zhang, J. P., Lo, S. C., et al. (2002). Crystal structure of brain pyridoxal kinase, a novel member of the ribokinase superfamily. *J. Biol. Chem.* 277 (48), 46385–46390. doi: 10.1074/jbc.M208600200

Matxain, J. M., Ristila, M., Strid, A., and Eriksson, L. A. (2006). Theoretical study of the antioxidant properties of pyridoxine. *J. Phys. Chem. A* 110 (48), 13068–13072. doi: 10.1021/jp065115p

Medina, A., and Nicholas, D. J. (1957). Some properties of a zinc-dependent hexokinase from. *Neurospora Crassa Biochem. J.* 66 (4), 573–578. doi: 10.1042/bj0660573

Miethke, M., and Marahiel, M. A. (2007). Siderophore-based iron acquisition and pathogen control. *Microbiol. Mol. Biol. Rev.* 71 (3), 413–451. doi: 10.1128/MMBR.00012-07

Moreno, M. A., Amich, J., Vicentefranqueira, R., Leal, F., and Calera, J. A. (2007). Culture conditions for zinc- and pH-regulated gene expression studies in *Aspergillus fumigatus*. *Int. Microbiol.* 10 (3), 187–192.

Murad, A. M., Souza, G. H., Garcia, J. S., and Rech, E. L. (2011). Detection and expression analysis of recombinant proteins in plant-derived complex mixtures using nanoUPLC-MSE. *J. Sep. Sci.* 34 (19), 2618–2630. doi: 10.1002/jssc.201100238

Parente, A. F., de Rezende, T. C., de Castro, K. P., Bailao, A. M., Parente, J. A., Borges, C. L., et al. (2013). A proteomic view of the response of *Paracoccidioides* yeast cells to zinc deprivation. *Fungal Biol.* 117 (6), 399–410. doi: 10.1016/j.funbio.2013.04.004

Permyakov, E. (2009). *Metalloproteomics* (Hoboken, New Jersey: John Wiley & Sons) Vol. 2.

Rappleye, C. A., Eissenberg, L. G., and Goldman, W. E. (2007). *Histoplasma capsulatum* alpha-(1,3)-glucan blocks innate immune recognition by the beta-glucan receptor. *Proc. Natl. Acad. Sci. U. S. A.* 104 (4), 1366–1370. doi: 10.1073/pnas.0609848104

Restrepo, A., and Jimenez, B. E. (1980). Growth of *Paracoccidioides brasiliensis* east phase in a chemically defined culture medium. *J. Clin. Microbiol.* 12 (2), 279–281. doi: 10.1128/JCM.12.2.279-281.1980

Schaffner, A., Davis, C. E., Schaffner, T., Markert, M., Douglas, H., and Braude, A. I. (1986). In vitro susceptibility of fungi to killing by neutrophil granulocytes discriminates between primary pathogenicity and opportunism. *J. Clin. Invest.* 78 (2), 511–524. doi: 10.1172/jci112603

Schneider, R. O., Fogaca, N. S., Kmetzsch, L., Schrank, A., Vainstein, M. H., and Staats, C. C. (2012). Zap1 regulates zinc homeostasis and modulates virulence in *Cryptococcus gattii*. *PLoS One* 7 (8), e43773. doi: 10.1371/journal.pone.0043773

Schneider, R. O., Diehl, C., Dos Santos, F. M., Piffer, A. C., Garcia, A. W. A., Kulmann, M. I. R., et al. (2015). Effects of zinc transporters on *Cryptococcus gattii* virulence. *Sci. Rep.* 5:10104. doi: 10.1038/srep10104

Shen, Q., and Rappleye, C. A. (2017). Differentiation of the fungus Histoplasma capsulatum into a pathogen of phagocytes. *Curr. Opin. Microbiol.* 40, 1–7. doi: 10.1016/j.mib.2017.10.003

Shen, Q., Ray, S. C., Evans, H. M., Deepe, G. S., and Rappleye, C. A. (2020). Metabolism of Gluconeogenic Substrates by an Intracellular Fungal Pathogen Circumvents Nutritional Limitations within Macrophages. *mBio* 11 (2), e02712-19. doi: 10.1128/mBio.02712-19

Staats, C. C., Kmetzsch, L., Schrank, A., and Vainstein, M. H. (2013). Fungal zinc metabolism and its connections to virulence. *Front. Cell Infect. Microbiol.* 3, 65. doi: 10.3389/fcimb.2013.00065

Taylor, K. M., Hiscox, S., Nicholson, R. I., Hogstrand, C., and Kille, P. (2012). Protein kinase CK2 triggers cytosolic zinc signaling pathways by phosphorylation of zinc channel ZIP7. *Sci. Signal* 5 (210), ra11. doi: 10.1126/scisignal.2002585

Tristão, G. B., Assuncao Ldo, P., Dos Santos, L. P., Borges, C. L., Silva-Bailao, M. G., Soares, C. M., et al. (2014). Predicting copper-, iron-, and zinc-binding proteins in pathogenic species of the *Paracoccidioides* genus. *Front. Microbiol.* 5, 761. doi: 10.3389/fmicb.2014.00761

Vicentefranqueira, R., Moreno, M. A., Leal, F., and Calera, J. A. (2005). The *zrfA* and *zrfB* genes of *Aspergillus fumigatus* encode the zinc transporter proteins of a zinc uptake system induced in an acid, zinc-depleted environment. *Eukaryot. Cell* 4 (5), 837–848. doi: 10.1128/EC.4.5.837-848.2005

Vicentefranqueira, R., Amich, J., Marin, L., Sanchez, C. I., Leal, F., and Calera, J. A. (2018). The Transcription Factor ZafA Regulates the Homeostatic and Adaptive Response to Zinc Starvation in *Aspergillus fumigatus*. *Genes (Basel)* 9 (7), 318. doi: 10.3390/genes9070318

Vignesh, S. K., Figueroa, J., Porollo, A., Caruso, J. A., and Deepe, G. S.Jr. (2013). Granulocyte macrophage-colony stimulating factor induced Zn sequestration

enhances macrophage superoxide and limits intracellular pathogen survival. *Immunity* 39 (4), 697–710. doi: 10.1016/j.immuni.2013.09.006

Wilson, S., and Bird, A. J. (2016). Zinc sensing and regulation in yeast model systems. *Arch. Biochem. Biophys.* 611, 30–36. doi: 10.1016/j.abb.2016.02.031

Wilson, D., Citiulo, F., and Hube, B. (2012). Zinc exploitation by pathogenic fungi. *PLoS Pathog.* 8 (12), e1003034. doi: 10.1371/journal.ppat.1003034

Winters, M. S., Chan, Q., Caruso, J. A., and Deepe, G. S.Jr. (2010). Metallomic analysis of macrophages infected with *Histoplasma capsulatum* reveals a fundamental role for zinc in host defenses. *J. Infect. Dis.* 202 (7), 1136–1145. doi: 10.1086/656191

Zhao, H., and Eide, D. (1996). The yeast ZRT1 gene encodes the zinc transporter protein of a high-affinity uptake system induced by zinc limitation. *Proc. Natl. Acad. Sci. U. S. A.* 93 (6), 2454–2458. doi: 10.1073/pnas.93.6.2454

Zhao, H., and Eide, D. J. (1997). Zap1p, a metalloregulatory protein involved in zinc-responsive transcriptional regulation in. *Saccharomyces Cerevisiae Mol. Cell Biol.* 17 (9), 5044–5052. doi: 10.1128/mcb.17.9.5044

Zhao, H., Butler, E., Rodgers, J., Spizzo, T., Duesterhoeft, S., and Eide, D. (1998). Regulation of zinc homeostasis in yeast by binding of the ZAP1 transcriptional activator to zinc-responsive promoter elements. *J. Biol. Chem.* 273 (44), 28713–28720. doi: 10.1074/jbc.273.44.28713

Conflict of Interest: The authors declare that the research was conducted in the absence of any commercial or financial relationships that could be construed as a potential conflict of interest.

frontiers in Cellular and Infection Microbiology

REVIEW
published: 14 December 2020
doi: 10.3389/fcimb.2020.595301

The Role of the Interleukin-17 Axis and Neutrophils in the Pathogenesis of Endemic and Systemic Mycoses

Juan David Puerta-Arias[1,2], *Susana P. Mejía*[1,3] *and Ángel González*[4*]

[1] Medical and Experimental Mycology Group, Corporación para Investigaciones Biológicas (CIB), Universidad de Antioquia, Medellín, Colombia, [2] School of Health Sciences, Universidad Pontificia Bolivariana, Medellín, Colombia, [3] Max Planck Tandem Group in Nanobioengineering, Universidad de Antioquia, Medellin, Colombia, [4] Basic and Applied Microbiology Research Group (MICROBA), School of Microbiology, Universidad de Antioquia, Medellin, Colombia

Systemic and endemic mycoses are considered life-threatening respiratory diseases which are caused by a group of dimorphic fungal pathogens belonging to the genera *Histoplasma*, *Coccidioides*, *Blastomyces*, *Paracoccidioides*, *Talaromyces*, and the newly described pathogen *Emergomyces*. T-cell mediated immunity, mainly T helper (Th)1 and Th17 responses, are essential for protection against these dimorphic fungi; thus, IL-17 production is associated with neutrophil and macrophage recruitment at the site of infection accompanied by chemokines and proinflammatory cytokines production, a mechanism that is mediated by some pattern recognition receptors (PRRs), including Dectin-1, Dectine-2, TLRs, Mannose receptor (MR), Galectin-3 and NLPR3, and the adaptor molecules caspase adaptor recruitment domain family member 9 (Card9), and myeloid differentiation factor 88 (MyD88). However, these PRRs play distinctly different roles for each pathogen. Furthermore, neutrophils have been confirmed as a source of IL-17, and different neutrophil subsets and neutrophil extracellular traps (NETs) have also been described as participating in the inflammatory process in these fungal infections. However, both the Th17/IL-17 axis and neutrophils appear to play different roles, being beneficial mediating fungal controls or detrimental promoting disease pathologies depending on the fungal agent. This review will focus on highlighting the role of the IL-17 axis and neutrophils in the main endemic and systemic mycoses: histoplasmosis, coccidioidomycosis, blastomycosis, and paracoccidioidomycosis.

Keywords: IL-17, Neutrophils, *Paracoccidioides* spp., *Coccidioides* spp., *Histoplasma capsulatum*, *Blastomyces* spp

OPEN ACCESS

Edited by:
Yong-Sun Bahn,
Yonsei University, South Korea

Reviewed by:
Chiung-Yu Hung,
University of Texas at San Antonio, United States
Bruce Klein,
University of Wisconsin-Madison, United States

***Correspondence:**
Ángel González
angel.gonzalez@udea.edu.co

Specialty section:
This article was submitted to Fungal Pathogenesis, a section of the journal Frontiers in Cellular and Infection Microbiology

Received: *15 August 2020*
Accepted: *13 November 2020*
Published: *14 December 2020*

Citation:
Puerta-Arias JD, Mejía SP and González Á (2020) The Role of the Interleukin-17 Axis and Neutrophils in the Pathogenesis of Endemic and Systemic Mycoses. Front. Cell. Infect. Microbiol. 10:595301. doi: 10.3389/fcimb.2020.595301

INTRODUCTION

Systemic fungal infections are characterized by their ability to produce a potentially life-threatening respiratory disease. These systemic mycoses are caused by a group of thermally dimorphic fungal pathogens belonging to different genera of several species including *Histoplasma capsulatum*, *Coccidioides* spp., *Blastomyces* spp., *Paracoccidioides* spp., *Talaromyces marneffei* and the newly described pathogen *Emergomyces* spp. (Sepúlveda et al., 2017; Turissini et al., 2017; Kirkland and

Fierer, 2018; Cao et al., 2019; Schwartz et al., 2019; Schwartz and Kauffman, 2020). Additionally, these mycoses are usually geographically restricted; thus, histoplasmosis is found worldwide, coccidioidomycosis is endemic in some regions of the United States and some countries of Latin America, blastomycosis is endemic in North America and Africa, paracoccidioidomycosis is restricted to Latin America, talaromycosis is endemic in Asian countries, while emergomycosis has been reported in Africa, Europe, Asia, and North America (Sepúlveda et al., 2017; Turissini et al., 2017; Kirkland and Fierer, 2018; Cao et al., 2019; Schwartz et al., 2019; Schwartz and Kauffman, 2020).

In general, these systemic mycoses are acquired by inhalation of the conidia or spores that are produced in the mold phase; in the lungs, a temperature-dependent transformation occurs to the yeast phase, except for *Coccidioides* spp., which undergoes isotropic growth to form spherules initials (Hung et al., 2007). These fungal morphotypes are phagocytized by macrophages and can spread hematogenously to various organs, causing disseminated infection; nonetheless, the clinical presentation could vary from self-limited, or mild, to severe infection, which, in turn, depends on several factors including the immune response and the inoculum size, among others.

Several studies have confirmed the T-cell mediated immune response to some of these dimorphic fungal pathogens, especially those associated with T helper (Th)1 and Th17 responses that are essential for protection (Wüthrich et al., 2011; Nanjappa et al., 2012; Wu et al., 2013; Ketelut-Carneiro et al., 2019). Of note, Th17 and IL-17 protective responses, which also participate during the primary infections in the nonimmune host, are associated with recruiting and activating neutrophils and macrophages to the site of infection as well as with chemokine and proinflammatory cytokines production, a mechanism mediated by the fungal recognition of pattern recognition receptors (PRRs) present on the surface of the host cells, which lead to the activation of adaptor molecules and the subsequent downstream signaling (Wüthrich et al., 2011; Nanjappa et al., 2012; Wu et al., 2013; Ketelut-Carneiro et al., 2019). Nonetheless, both the Th17/IL-17 axis and neutrophils appear to play a dual role, being beneficial mediating fungal controls and detrimentally promoting disease pathology depending on the fungal agent (Loures et al., 2009; Wüthrich et al., 2011; Pino-Tamayo et al., 2016; Puerta-Arias et al., 2016; Ketelut-Carneiro et al., 2019).

In this review, we will discuss the current findings regarding the role of the IL-17 axis and neutrophils in the immune response against dimorphic fungal pathogens with special emphasis on the most studied endemic and systemic mycoses: histoplasmosis, coccidioidomycosis, blastomycosis, and paracoccidioidomycosis. Of note, the role of IL-17 and neutrophils on talaromycosis and emergomycosis have not been investigated so far or are incipient, reasons why these mycoses were not included in this review.

IL-17: SOURCES AND FUNCTION

The IL-17 family is a group of pleiotropic cytokines secreted mainly by a subset of CD4+T helper cells (Th) known as Th17 cells (Harrington et al., 2006). The differentiation and stimulation of Th17 from naïve CD4+ T-cells occurs in secondary lymphoid organs with the participation of IL-1β, IL-6, transforming growth factor β (TGFβ), and IL-23. The stimuli with cytokines trigger the downstream STAT3, promoting the activation of *RORγt*, the master transcriptional factor, which modulates the production of the hallmark cytokines IL-17A, IL-17F, and other cytokines such as IL-21, IL-22, and granulocyte-macrophage colony-stimulation factor (GM-CSF) (Hartupee et al., 2009; Isailovic et al., 2015; Monin and Gaffen, 2018). Moreover, polarized Th17 cells express CC chemokine receptor 6 (CCR6), which allows their migration into mucosal barrier sites (Abusleme and Moutsopoulos, 2017).

Moreover, other cell populations were also reported as important sources of IL-17A and IL-17F, such as the CD8+ T-cells and the innate immune cells including γδ T-cells (Takatori et al., 2008), innate lymphoid cells subset 3 (ILC3) (Geremia et al., 2011; Villanova et al., 2014), invariant natural killer cells (iNKT) (Michel et al., 2007), IL-17 innate lymphoid cells (ILC17) (Buonocore et al., 2010), and natural killer T (NKT) cells (Cella et al., 2009). Additionally, macrophages and dendritic cells are also important sources of IL-23 and IL-17, which are produced in response to the microorganism's invasion and inflammatory cytokines stimulation. Neutrophils and mast cells also contribute to IL-17 production (Hoshino et al., 2008; Lin et al., 2011; Monin and Gaffen, 2018; Schön and Erpenbeck, 2018).

The IL-17 family includes six related proteins, namely IL-17A, IL-17B, IL-17C, IL-17D, IL-17E (also known as IL-25), and IL-17F (Monin and Gaffen, 2018), IL-17A (commonly known as IL-17) being the most studied member of the IL-17 family. The functions of IL-17 are crucial to maintaining mucosal immunity against extracellular and intracellular pathogens through the induction of antimicrobial proteins and the recruitment of neutrophils to the site of infections. Furthermore, IL-17 increases mucosal barrier repair and maintenance by the production of tight junction proteins and the stimulation of epithelial cell proliferation (Valeri and Raffatellu, 2016).

IL-17 is recognized by the family of the IL-17 receptors (IL-17R), which is a multimeric receptor constituted by two subunits with five members: IL-17A-IL17E. The IL-17R is composed of a common IL-17RA chain and a second chain that determines the ligand and downstream signal. (Yao et al., 1995; Toy et al., 2006; Rickel et al., 2008; Ramirez-Carrozzi et al., 2011; Zhu et al., 2011). The IL-17RA is expressed on the surface of leukocytes, keratinocytes, fibroblasts, epithelial, mesothelial, and vascular endothelial cells. The expression of IL-17RA induces granulopoiesis, neutrophil recruitment, and inflammatory response (Tristão et al., 2017). The IL-17A and IL-17F share a high degree of similarity, with both playing a central role in the adaptive immune response, especially against bacteria and fungi. IL-17A and IL-17F induce an inflammatory response by stimulating the expression of proinflammatory cytokines and chemokines and matrix metalloproteinase (MMP) production, thus promoting a potent immune response with the recruitment of immune cells to the site of infection, mainly neutrophil accumulation (Tristão et al., 2017). IL-17A induces the production of the chemokines CXCL1, CXCL2, and CXCL8 (IL-8), which in turn attract neutrophils. In addition,

IL17A appears to have a protecting role against microorganisms through the induction of antimicrobial peptides, including β-defensins, S100A8, and lipocalin 2 (Onishi and Gaffen, 2010; Chen and Kolls, 2017).

Fungal infections have been particularly associated with the regulation of the Th17 immune response by the activation of CD4+ T - antigen-presenting cells *via* recognition of the components of the fungal cell wall by pattern recognition receptors (PRRs). The cell walls of fungal pathogens contain three major polysaccharides types: β-glucan, chitin, and mannan (Netea et al., 2008); meanwhile, PRRs include Dectin-1, Dectin-2, Dectin-3, Mincle, mannose receptor (MR), and *Toll*-like receptors (TLRs), among others; thus, Dectin-1 recognizes fungi *via* β-1,3-glucan. Dectin-2 and Mincle recognize mannose-like structures, while TLR2 recognizes mainly β-glucan and zymosan, and TLR4 recognizes mannan components (McGreal et al., 2006; Netea et al., 2006; Reid et al., 2009; Yamasaki et al., 2009; Saijo et al., 2010; Ishikawa et al., 2013). Once PRRs recognize fungal cells, these interactions trigger a cascade of signaling events, with the participation of cytosolic adaptors [mainly caspase adaptor recruitment domain family member 9 (Card9) and myeloid differentiation factor 88 (MyD88)] that transduce signals from these PRRs, that in turn activate the secretion of proinflammatory cytokines and the induction of T-cell differentiation (Drummond et al., 2011; Loures et al., 2011; Wüthrich et al., 2012).

On the whole, the activation of the Th17 immune response against fungal infection depends upon which receptors are involved and the degree of interaction (Netea et al., 2008; van de Veerdonk et al., 2009; Wang et al., 2016).

THE ROLE OF IL-17 AXIS IN THE DIMORPHIC FUNGAL INFECTIONS

It is known that the development of Th1 cells is crucial for protective immunity against dimorphic fungal pathogens including *H. capsulatum*, *Coccidioides* spp., *Blastomyces* spp., and *Paracoccidioides* spp.; however, the roles of the Th17 cell and IL-17 are controversial. In models of infection with the above fungal pathogens, some studies have shown that Th17/IL-17 axis mediate resistance, while others have shown that they promote disease pathology (Deepe and Gibbons, 2009; Loures et al., 2009; Loures et al., 2009; Wüthrich et al., 2011; Nanjappa et al., 2012; Wu et al., 2013; Wang et al., 2014; Pino-Tamayo et al., 2016; Puerta-Arias et al., 2016; Ketelut-Carneiro et al., 2019). In the case of histoplasmosis, coccidioidomycosis, and blastomycosis, it has been reported that mice vaccinated against these three fungal pathogens showed that Th1 immunity was dispensable, whereas the fungal-specific Th17 cells were sufficient for inducing protection against these systemic mycoses (Wüthrich et al., 2011). Subsequently, these results were confirmed using hosts lacking CD4+ cells, where CD8+ T-cell derived IL-17 was indispensable to develop immunity protection against these three endemic and systemic mycoses (Nanjappa et al., 2012).

In the dimorphic fungal infections, the induction of Th17 cells and the subsequent IL-17 production depends on the interactions of the PRRs present on the host cells' surfaces. The fungal pathogen-associated molecular patterns (PAMPs), TLRs and C-Type Lectin [including Dectin-1, Dectin-2, MR and Mincle] receptors have been the most studied PPRs so far. These interactions induce the secretion of proinflammatory cytokines and T cell differentiation. **Figure 1** shows the interactions of the main dimorphic fungal pathogens and PRRs with the subsequent signaling activation (with adaptor molecules participation), Th17 differentiation, and IL-17 production.

Histoplasmosis

Histoplasmosis is the most common endemic mycosis reported worldwide. The infection is acquired by the inhalation of aerosolized microconidia and mycelial fragments, but the severity of illness and the presence of clinical manifestations depend on the intensity of fungal burden exposure and the host´s immune status (Wheat et al., 2016). It is known that Th17 and its signature cytokine IL-17 play an important role and mediate a response in *H. capsulatum* infection; however, despite IL-17 not being necessary for survival, its neutralization alters inflammatory cell recruitment and elevates fungal burden in a murine model of histoplasmosis; therefore, it was demonstrated that this cytokine participates in the control of this fungal infection, particularly in the absence of IFN-γ (Deepe and Gibbons, 2009).

Among the different PRRs that participate in the recognition of *Histoplasma*, it has been reported that Dectin-1 and Dectin-2, but not Mincle, recognize and induce a protective Th17 immune response against *H. capsulatum* (Wüthrich et al., 2011; Viriyakosol et al., 2013; Wang et al., 2014); moreover, these interactions are mediated by Card9 and MyD88 signaling, which are indispensable for the development of this Th17 protective immune response (Wüthrich et al., 2011; Wang et al., 2014). Additionally, it has been demonstrated that the Galectin-3 (gal3) receptor, a member of the galectin family, negatively regulates IL-17A response through the inhibition of IL-23/IL-17 axis cytokine production by dendritic cells (DC) when infected with *H. capsulatum* (Wu et al., 2013). Similarly, it has been reported that the induction of IL-23 producing DCs depended on the activation of Dectin-1, which is mediated by β-glucan exposed in the cell walls of the fungal pathogens. Interestingly, the yeast form of *Histoplasma*, which lacks cell wall exposure of β-glucan, failed to induce IL-23 producing DCs, a fact that was confirmed using a mutant of *Histoplasma* in which β-glucan present in its cell wall was unmasked; thus, the interaction of DC with this mutant not only abrogated the pathogenicity of this fungus but also triggered the induction of IL-23 producing DCs (Chamilos et al., 2010); this study indicated that β-glucan exposure in the fungal cell wall is essential for the generation of IL-23 producing DCs and Th17 immune responses and may represent an evasion mechanism exerted by *Histoplasma*.

It is known that the differentiation of Th17 cells and their IL-17 production are mediated by IL-6 and TGF-β signaling, a process that is amplified and sustained by IL-21 and IL-23, respectively (Korn et al., 2009; Zhu et al., 2010). Along these lines, in *Histoplasma* infection, it has been described that the Th17 response is associated with cytokines that include IL-6, IL-23, and IL-17 and that CD4+ and CD8+ T cells expressing CD25

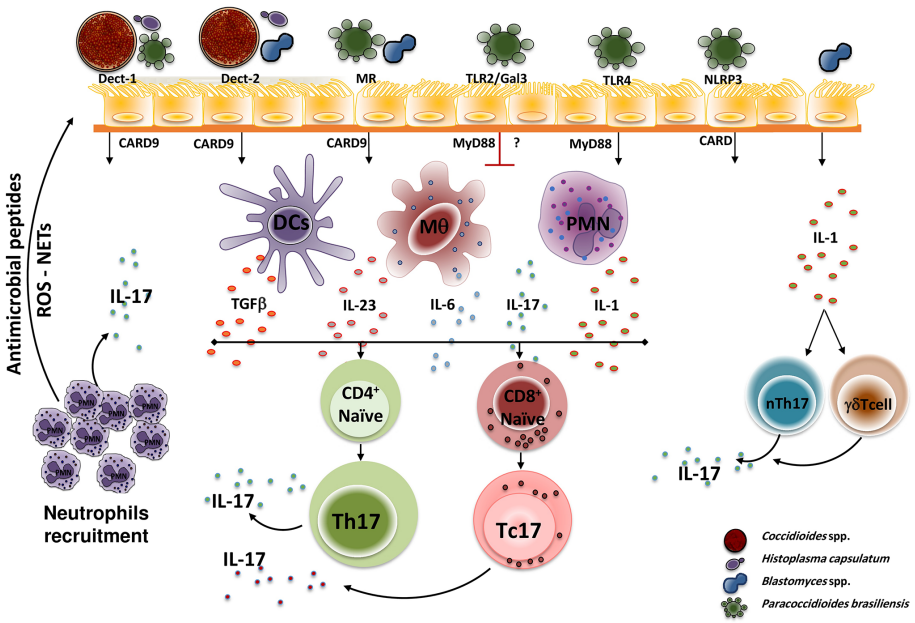

FIGURE 1 | Dimorphic fungal pathogen recognition by PPRs. During initial infection, fungal PAPMs are recognized by different host PPRs present in antigen-presenting cells (mainly Dendritic cells, macrophages, and neutrophils), interactions that trigger a downstream signal that induces the T cell naïve ($CD4^+$ or $CD8^+$) differentiation to Th17 cells (in the presence of TGFβ, IL-1, IL-6, and IL-23) and the subsequent production of IL-17 which in turn amplified the inflammatory response by recruiting neutrophils at the site of infection. However, each PRR plays a distinctly different role for each dimorphic fungus. Thus, *H. capsulatum* and *C. posadasii* are recognized by Dectin-1 and Dectin-2, *P. brasiliensis* is recognized by Dectin-1, TLR4, MR, and NLRP3, whereas *B. dermatitidis* is only recognized by Dectin-2. After recognition, the PRRs activate downstream adaptor molecules, including MyD88 and CARD9, that finally activate transcription factors that induce the specific genes, especially this coding for IL-17. Once the IL-17 is produced, it induces the recruitment and activation of neutrophils, which in turn exhibit microbicidal mechanisms mediated by antimicrobial peptides release, reactive oxygen species (ROS) production, and NETs formation. Of note, TLR2 and Gal3 negatively regulate IL-17 production after *P. brasiliensis* recognition. Moreover, the interaction of fungal cells (i.e. *Blastomyces*) with lung epithelial cells, induces the release of IL-1 which in turn activates innate cells that then induce activation and IL-17 production by innate cells, mainly nTh17 and γδTcells. PAMP, Pathogen-associated molecular pattern; PRR, pattern recognition receptor; Th, T helper; Tc, T cytotoxic; Dect, Dectin; MR, mannose receptor; TLR, Toll-Like receptor; Gal3, Galectin-3; NLRP3, NOD-like receptor P3; CARD9, adaptor recruitment domain family member 9; MyD88, myeloid differentiation factor 88; DCs, Dendritic cells; Mq, macrophages; PMN, polymorphonuclear neutrophils; IL, interleukin; TGFβ, transforming growth factor β; ROS, reactive oxygen species; NETs, extracellular traps; nTh17, natural T helper cells (innate cells).

are the predominant sources of IL-17 (Deepe and Gibbons, 2009; Kroetz and Deepe, 2012). Moreover, the infection model for histoplasmosis showed that the development of the IL-17 protective response required IL-6 but not the participation of IL-1 receptor signaling (Nanjappa et al., 2012). More recently, it was reported that IL-22 deficiency was associated with a reduction of IFN-γ or IL-17-producing CD4+ cells in the lungs of mice infected with *H. capsulatum*, suggesting an inflammatory loop between IL-22 and a Th1/Th17 response (Prado et al., 2020).

In addition, some chemokines and their receptors also participate in the development of a Th17 response in *Histoplasma* infection; thus, the absence of CCR5 or CCL4 neutralization was associated with the impaired infiltration of the lungs of *Histoplasma*-infected mice by inflammatory cells. Those mice resolved the infection. The absence of CCR5 or CCL4 neutralization was also associated with the beneficial role of IL-17 accelerating the pathogen resolution (Kroetz and Deepe, 2010); moreover, mice lacking the CCR5 and treated with a monoclonal antibody against IL-17 showed an increase in the fungal burden and Treg cells, suggesting that this CCR5/CCL4 axis regulates the balance between Treg and Th17 cells in this fungal infection (Kroetz and Deepe, 2010). The important role of IL-17 in the *Histoplasma* infection has been clearly demonstrated, especially in immunization studies where this cytokine has been associated with the development of a protective immune response (Wüthrich et al., 2011; Deepe et al., 2018).

Coccidioidomycosis

Coccidioidomycosis, commonly known as San Joaquin Valley fever, is a systemic fungal disease caused by the inhalation of the airborne spores of *Coccidioides immitis* or *C. posadasii* (Galgiani et al., 2005). The development of a protective immune response in *Coccidioides* infection is similar to that observed in histoplasmosis. Thus, Th1 and Th17 immune patterns are pivotal in mounting an effective control of coccidioidal infection (Hung et al., 2011; Wüthrich et al., 2011). Several studies employing different coccidioidal antigens and adjuvants for immunization protocols have been reported; these antigens include: a genetically-engineered mutant strain (Δcts2/ard1/cts3) used as a live attenuated vaccine (ΔT) (Xue et al., 2009); a ΔT

conjugated with the adjuvant EP67; a peptide agonist of the biologically active C-terminal region of human complement component C5a (Hung et al., 2012); a multivalent recombinant *Coccidioides* polypeptide antigen (rCpa1) that consists of three previously identified antigens (Ag2/Pra, Cs-Ag, and Pmp1) and five pathogen-derived peptides with high affinity for human major histocompatibility complex class II (MHC-II) molecules (Hurtgen et al., 2012; Hung et al., 2018; Campuzano et al., 2020); and a rCpa1 encapsulated into glucan-chitin particles (GCP) or β-glucan particles (GP) (Campuzano et al., 2020). Additionally, transgenic mice expressing a human major histocompatibility complex class II (MHC II) receptor have also been employed to study the immune response to coccidioidal vaccines (Hurtgen et al., 2012; Hurtgen et al., 2016; Hung et al., 2018). All the above studies confirmed the protective effect addressed by Th1 and Th17 expansion with higher production of the signature cytokines, IFN-γ, and IL-17, respectively. Nonetheless, a higher expression of *RORc*, the hallmark transcription factor of the Th17 pathway combined with higher amounts of IL-23 and IL-6 and accompanied by a down-regulated expression of *Foxp3*, which promotes the differentiation of Treg cells, suggests the development of a biased Th17 protective immune response to coccidioidal infection (Hung et al., 2011; Wüthrich et al., 2011; Hung et al., 2012). Moreover, an additional study showed that IFN-$\gamma^{-/-}$ knock-out mice immunized with the ΔT vaccine could still be protected (100% survival), while only 40% of ΔT-vaccinated IL17 receptor A-deficient mice survived (Hung et al., 2011); again, this study shows that Th17/IL-17 axis contributes strongly to protection against *Coccidioides* infection.

More recently, a primary dendritic cell (DC)-vaccine [DC-vaccine (Ag2-DC) that was prepared by non-virally transfecting the primary bone marrow-derived DCs with a plasmid DNA encoding Ag2/PRA (protective epitope of Coccidioides)] was evaluated, and healthy mice treated with the DC-vaccine showed IL-17, IFN-γ and IL-4 cytokine-secreting cells in the lungs and lymph nodes after immunization (Awasthi et al., 2019).

Regarding PRRs that participate in the recognition of *Coccidioides* and the subsequent stimulation and development of a protective Th17 immunity response, it has been demonstrated that this mechanism is mediated by the activation of both MyD88 and Card9-associated Dectin-1 and Dectin-2 signal pathways (Wüthrich et al., 2011; Viriyakosol et al., 2013; Wang et al., 2014; Campuzano et al., 2020). Moreover, it was also demonstrated that the IL-1 receptor, but not TLR2, is essential to developing a Th17 immunity response against *Coccidioides* infection, a mechanism mediated by MyD88 (Hung et al., 2016).

Blastomycosis

Blastomycosis refers to a disease caused by the dimorphic fungi *Blastomyces dermatitidis*; this systemic disease, like endemic mycosis, has a T-cell and macrophage-mediated immune response (Chang et al., 2000). The clinical spectrum of this illness is broad, from asymptomatic patients to acute, chronic, or disseminated disease (Chapman et al., 2008). As described previously, in histoplasmosis and coccidioidomycosis, a Th1 and Th17 immune responses exert an important role in the control of infection by *Blastomyces* (Wüthrich et al., 2011; Wang et al., 2014). Thus, after the host cells recognize *Blastomyces´* fungal cell wall or its antigens by PRRs, activation and differentiation, mainly of Th17 cells, take place. Among the different PRRs that participate in *Blastomyces* recognition, Dectin-2 and Dectin-3 (also known as MCL) appear to be indispensable to developing a Th17 protective immune response and resistance to this fungal pathogen (Wüthrich et al., 2011; Wang et al., 2014; Wang et al., 2015; Wang et al., 2017). Of note, MCL regulates the development, expansion and, differentiation of Th17 through a mechanism dependent on the adaptor FcRγ (Wang et al., 2015). Furthermore, once MR recognizes a mannan-like structure on the *B. dermatitidis* cell wall, it also activates and differentiates naïve T cells into Th17 effector cells, which are pivotal to the protection of an immunized host against *Blastomyces* (Wang et al., 2016). Additional adaptor molecules, including Card9 and MyD88, are also indispensable for the development of a Th17 protective immune response against *Blastomyces* (Wüthrich et al., 2011; Wang et al., 2014; Nanjappa et al., 2015; Wang et al., 2017).

On the other hand, IL-1 and IL-6 appear also to play an important role in the development of a Th17 immune response against blastomycosis (Nanjappa et al., 2012; Wüthrich et al., 2013; Merkhofer et al., 2019). More recently, studies in animals and human beings have revealed that IL-6 had a pivotal role in the development of adaptive immunity and resistance to *B. dermatitidis* infection, through induction of a Th17 pattern. Thus, genetic analysis of an Asian population (The Hmong) that show an elevated incidence of blastomycosis in comparison with those of European ancestry (168 vs 13 per 100,000 inhabitants, respectively), demonstrated that in addition to mice that had lost IL-6 signaling, the presence of polymorphisms on the *IL-6* gene increased susceptibility to developing blastomycosis, a fact that was associated with lower levels of IL-6, IL-17, and RAR-related orphan receptor gamma t [(RORγt), the hallmark transcription factor of IL-17-producing T cells] in humans and low recruited Th17 producing cells in lungs of IL-$6^{-/-}$ mice infected with *B. dermatitidis* (Merkhofer et al., 2019). By the same token, it has been reported that the use of exogenous IL-1 enhanced the protection of weak vaccines against lethal *B. dermatitidis* infection, promoting the development of fungus-specific Th17 cells (Wüthrich et al., 2013).

Recently, it has been described that lung epithelial cells are essential for immunity against *Blastomyces*; thus, the interaction of these epithelial cells with the fungus triggers a NF-κB signaling with a subsequent increase in the number of IL-17-producing innate lymphocytes, mainly $CCR6^{+}$ natural Th17 cells (nTh17) and γδT-cells, a mechanism dependent on CCL20 chemokine production, which in turn is induced by IL-1α/IL1R signaling (Hernández-Santos et al., 2018).

Finally, vaccination against *Blastomyces* induces the development of memory Tc17 cells with different requirements for long-term persistence than Tc1 cells; thus, these anti-fungal Tc17 cells retained the expression of RORγt and showed higher proliferative renewal and lower levels of anti-apoptotic molecule Bcl-2, but required hypoxia-inducible factor 1α (HIF-1α) for their homeostasis (Nanjappa et al., 2017).

Paracoccidioidomycosis

Paracoccidioidomycosis (PCM) is a fungal infection caused by the dimorphic fungus from the genus *Paracoccidioides* and is one of the most prevalent systemic mycoses in Latin America (Restrepo et al., 2019). In PCM, cellular immunity exhibits a protective role; thus, $CD4^+$ T cells exert a protective effect through the regulation of antibody production and delayed-type hypersensitivity (DTH) reactivity, while $CD8^+$ T cells control fungal burden (Chiarella et al., 2007). Furthermore, using a PCM model, it has been demonstrated that infected *P. brasiliensis*-infected mice showed increased levels of IL-17A accompanied by the Th17 associated cytokines, IL-6 and IL-23; moreover, deficiency of these Th17-associated cytokines or IL-17RA conferred susceptibility during infection associated with reduced concentrations of TNF-α, IFN-γ, and inducible nitric oxide synthase (iNOS) expression (Tristão et al., 2017).

Regarding participation of PRRs on Th17 development in PCM, it was demonstrated that TLR2 acts as a negative regulator of Th17 cells, thus a deficiency of TLR2 was associated with a lower fungal burden, a prevalent Th17 immunity (higher levels of IL-17, IL-6, IL-23, and TGF-b), and an increased number of neutrophils; nonetheless, a exacerbated pulmonary inflammation was also observed, which was associated with a diminished expansion of regulatory T cells (Loures et al., 2009). Similarly, TLR3 also acts as a negative regulator of Tc17 cells (IL-17-$CD8^+$ producing cells); thus, in TLR3 deficient mice infected with *P. brasiliensis*, an increased number of Tc17 and Tc1 cells associated with higher levels of IL-17, IL-1β, IL-6, and IFN-γ were observed (Jannuzzi et al., 2019).

Conversely, *in vitro* studies showed that neutrophils primed with the 43kDa glycoprotein (gp43) from *P. brasiliensis* express higher levels of TLR2 and IL-17 (Gardizani et al., 2019). It is noteworthy that MyD88 (the adaptor molecule used by TLRs) is required to mount an efficient innate and adaptive immune response; thus, MyD88 deficient mice showed an association between disease severity and reduced Th17 response and IL-1β production (Loures et al., 2011).

Regarding CTL receptors, it has been reported that Dectin-1 has a critical influence in the differentiation and migration of Tc17 cells; thus, Dectin-1 deficient mice infected with *P. brasiliensis* showed a more severe infection, enhanced tissue pathology, and mortality rates, accompanied with reduced differentiation of T cells to Tc17 phenotype, increased expansion of Treg cells, impaired production of Th1, Th2, and Th17 cytokines, and migration of Tc17 and neutrophils to the site of infection (Loures et al., 2014). Moreover, monocytes from healthy individuals produced IL-17A after incubation with *P. brasiliensis* yeasts *via* activation of the Dectin-1 receptor (Romagnolo et al., 2018). Of note, dendritic cells stimulated with *P. brasiliensis* induced the differentiation of Th17/Tc17 by a mechanism mediated by TLR4, Dectin-1 and MR in a synergistic fashion (Loures et al., 2015).

Furthermore, activation of the NOD-like receptor P3 (NLRP3), which is related to the inflammasome, was associated with the development of protective immunity against *P. brasiliensis* by a mechanism mediated by Th1 and Th17 (Feriotti et al., 2017).

In another study using the experimental model of pulmonary paracoccidioidomycosis, it has been reported that IL-1α deficiency was associated with a reduction of Th17 cells and a diminished number of neutrophils in a mechanism mediated by caspase 11 (Ketelut-Carneiro et al., 2019). Moreover, the important role of IL-6 for the development of a protective Th17 immune response has been demonstrated; thus, the adoptive transfer of IL-6 competent macrophages restored the resistance in *P. brasiliensis*-infected IL-6- and IL-17RA-deficient mice (Tristão et al., 2017).

Interestingly, the results of other studies have been controversial; thus, we reported that during the early stages of infection, the depletion of neutrophils using a specific monoclonal antibody was associated with an exacerbation of the inflammatory response and high fungal burden. This neutrophil depletion was also accompanied by a decreased level of IL-17; moreover, it was confirmed that neutrophils were an essential source of IL-17 during the early stages of *P. brasiliensis* infection (Pino-Tamayo et al., 2016). Conversely, neutrophil depletion during the chronic course of paracoccidioidomycosis promotes the resolution of pulmonary inflammation and fibrosis accompanied by a reduced fungal burden. These results were associated with a decrease of proinflammatory cytokines, including IL-17, TNF-α, and TGF-β (Puerta-Arias et al., 2016). Additionally, the most severe form of PCM has been characterized by a predominant Th17/Th22 response, along with substantial participation of Th1 cells (de Castro et al., 2013). On these lines, it has been reported that *P. brasiliensis*-infected mice treated with a recombinant 60-kDa heat shock protein of this fungal pathogen increased the concentrations of proinflammatory cytokines, including IL-17, TNF-α, and IFN-γ, which lead to severe inflammation, host tissue damage, impaired granuloma formation, and fungal dissemination (Fernandes et al., 2016). The above results indicate that IL-17 plays a dual role in PCM.

Finally, in addition to CD4+Th cells, it has been demonstrated that other cell populations are important sources of IL-17, induced by dimorphic fungal pathogens; these cells include Tc17, nTh17, γδT-cells, and neutrophils (Pino-Tamayo et al., 2016; Nanjappa et al., 2017; Tristão et al., 2017; Hernández-Santos et al., 2018).

Altogether, the above findings suggest that the antifungal effect exerted by the Th17/IL-17 axis is mediated by the recruitment and activation of neutrophils and macrophages to the site of infection (Wüthrich et al., 2011; Nanjappa et al., 2012; Hernández-Santos et al., 2018).

THE ROLE OF NEUTROPHILS IN THE DIMORPHIC FUNGAL INFECTIONS

Neutrophils are the most abundant type of immune cells and constitute the first line of defense against infections by different pathogens. As multifunctional cells of the immune response, neutrophils actively participate in the development of innate and adaptative immunity (Kolaczkowska and Kubes, 2013), and exert a variety of effector functions including phagocytosis, intra and extra-cellular pathogen killing *via* oxidative and non-oxidative

cytotoxic mechanisms, extracellular release of microbicidal molecules stored in their intracellular granules, production of immune mediators including pro-inflammatory cytokines and chemokines, and formation of neutrophil extracellular traps (NETs) (Mócsai, 2013; Wang and Arase, 2014; Tecchio and Casatella, 2016; Yang et al., 2017). The latter is one of the most important microbicidal mechanisms, mainly against certain pathogens that are difficult to phagocytose due to their large size (Brinkmann et al., 2004).

The microbicidal effect of NETs has been reported in different animal and human models with infections by fungal pathogens, parasites, bacteria, and viruses. This mechanism can comprise two phases: i) the trapping and immobilization of the pathogen to prevent the spread to tissues, organs, and systems; and ii) the elimination of the pathogen by microbicidal action of the proteins present in the NETs (Brinkmann et al., 2004). Such proteins exert their effect by degrading virulence factors, damaging the cell wall, or forming a complex with metal ions important in the life cycle of some dimorphic fungi (Brinkmann et al., 2004; Urban et al., 2006; Bianchi et al., 2009; Byrd et al., 2013; Hoeksema et al., 2016). However, although NETs can prevent the pathogens' spread or directly eliminate the trapped microorganism, some studies have reported that certain peptides, as well as histones linked to the traps, trigger a high cytotoxic effect in the tissue, especially when the clearance mechanisms of the host are ineffective, thus causing a continuous inflammation as observed in several disorders or infectious diseases (Leffler et al., 2012; Cheng and Palaniyar, 2013).

Clearly, it is well known that the neutrophils are crucial in the immunity against invasive infection caused by fungal pathogens of the genus *Candida* and *Aspergillus* (Desai and Lionakis, 2018). However, in other fungal infections caused by a heterogeneous group of dimorphic fungi, including *Histoplasma capsulatum*, *Coccidioides* spp., *Paracoccidioides* spp., and *Blastomyces dermatitidis* (Hsu et al., 2010), this immune-cell apparently does not play an important role (Lionakis et al., 2017; Lionakis and Levitz, 2018). For this group of fungal infections, it has been suggested that these phagocytic cells may play a paradoxical function which depends on both the infection phase (acute or chronic) or certain conditions of the host; thus, neutrophils could exert a beneficial effect by controlling the infection, or, on the contrary, they could induce a detrimental effect with a poor prognosis of the infection/disease and worse outcomes. In **Table 1**, we summarized the role of neutrophils in the main dimorphic fungal infections.

Histoplasmosis

Although the T-cell activated macrophages play a central role in the pathogenesis of histoplasmosis, it has also been suggested that *H. capsulatum* yeasts are recognized by different phagocytic cells, including neutrophils (Deepe et al., 2008). Earlier studies in murine models of histoplasmosis have described the presence of neutrophils during the first 36 h post-infection (Procknow et al., 1960; Baughman et al., 1986). Thus, recognition of *Histoplasma* yeast cells by neutrophils is mediated by PRRs present on their surface; these PRRs include Dectin-2, NLRP3, and macrophage integrin or integrin αMβ2 (Mac-1 or CD11b/CD18) (Coxon et al., 1990; Patin et al., 2019). Notably, phagocytosis of *H. capsulatum* yeast did not induce a respiratory burst response in neutrophils; however, the production of superoxide anion was observed only when fungal cells were opsonized, indicating that the activation of this microbicidal mechanism needs the participation of either complement or Fc receptors (Schnur and Newman, 1990). Later, Newman et al. (1993) demonstrated that recognition and phagocytosis of opsonized yeast of *H. capsulatum* by neutrophils was *via* complement receptor (CR) type 1 (CR1), CR3, and FcRIII (CD16).

Additionally, Medeiros et al. (2015) demonstrated that during the acute pulmonary histoplasmosis, inflammatory mediators such as leukotriene B4 (LTB4), LTC4, platelet-activating factor (PAF), KC (murine IL-8 homolog), and TNF-α induce a strong recruitment of neutrophils into the lungs and others remote localized inflammatory sites, where these cells exhibit fungistatic activity against *H. capsulatum*. Likewise, other reports have demonstrated the limited fungicidal effect of neutrophils against *H. capsulatum* (Brummer et al., 1991; Kurita et al., 1991). Newman et al. (2000) reported that the azurophilic granules present inside neutrophils contain defensins and serprocidins, molecules that exert a fungistatic effect against *H. capsulatum* yeast. It has also been demonstrated that *H. capsulatum* inhibits apoptosis in neutrophils from both human and mouse hosts, which correlates with decreased cell-surface Mac-1 expression (Medeiros et al., 2002). Overall, it could be suggested that *H. capsulatum* can evade microbicidal mechanisms or is able to survive inside the phagocytic cells during the early phase of infection.

Moreover, a recent report has shown that NETs response promotes the loss of yeast viability and exerts a fungicidal activity, as a dependent mechanism of ROS, SyK/Src Kinase pathway, and CD18 (Thompson-Souza et al., 2020).

Although it has been described that neutrophils participate in the innate and adaptive immune response, the role of these phagocytic cells in the cell-mediated immune response against *H. capsulatum* at early times of infection is still unclear.

Coccidioidomycosis

The immunity against coccidioidomycosis is mediated mainly by macrophages and T cells, and relatively little is known about the role of neutrophils in the inflammatory response. Although the capacity of mononuclear cells to locate around parasitic-phase structures of the fungi has been shown, some studies have suggested that neutrophils may participate during the early course of the disease; thus histopathological examinations of the infected lungs of mice at the first two weeks postchallenge have shown that neutrophils are the predominant inflammatory cells located adjacent to mature spherules that have ruptured and released their endospores (Galgiani et al., 2005; Shubitz et al., 2008; Xue et al., 2009). It has been suggested that these phagocytic cells respond to the contents of spherules in a chemotaxis-like fashion, and the intense inflammatory response observed at infection sites may contribute to lung tissue damage, which could exacerbate the course of the

TABLE 1 | The role of neutrophils in dimorphic fungal infections.

Fungal infection	Findings	References
Histoplasmosis	• Fungal recognition is mediated by Dectin-2, NLRP3, and Mac-1 (CD11b/CD18)	• Coxon et al., 1990; Patin et al., 2019
	• Opsonized fungal cells are mediated by CR1, CR3, and FcRIII (CD16)	• Newman et al., 1993
	• LTB4, LTC4, PAF, KC, and TNF-α induce neutrophil recruitment	• Medeiros et al., 2015
	• Exhibited limited fungicidal activity	• Kurita et al., 1991
	• Azurophilic granules containing defensins and serprocidins exert a fungistatic effect	• Brummer et al., 1991
	• Fungus inhibit apoptosis and decreases Mac-1 expression	• Newman et al., 2000
	• NETs formation exerts fungicidal activity *via* ROS, SyK/Src kinase, and CD18	• Medeiros et al., 2002
		• Thompson-Souza et al., 2020
Coccidioidomycosis	• Neutrophils are the predominant inflammatory cells located surrounding mature spherules	• Galgiani et al., 2005; Shubitz et al., 2008; Xue et al., 2009.
	• Spherules and endospores are recognized *via* TLR-2 and Dectin-1	• Lee et al., 2015
	• Source of IL-10	• Hung et al., 2013
	• NETs and granuloma formation prevent fungal dissemination	• Shubitz et al., 2008
	• Genetic patterns and pre-exposition influence phagocytic functionality	• Hung et al., 2014
	• Presence of NOX2 limits neutrophil recruitment in coccidioidal infection	• Gonzalez et al., 2011
Blastomycosis	• Deleterious, enhance fungal replication and exacerbation of infection	• Brummer and Stevens, 1983
	• Phagocytic cells exhibit capability to kill fungus	• Brummer and Stevens, 1984; Brummer et al., 1986; Morrison et al., 1989
	• Pyogranuloma formation mediated by CXC chemokines	• Lorenzini et al., 2017
	• Neutrophil-DC hybrid exhibit a better fungicidal function, NETs formation, and ROS production	• Fites et al., 2018
Paracoccidioidomycosis	• Essential during early infection (protection) and source of IL-17	• Pino-Tamayo et al., 2016
	• Deleterious during chronic infection	• Puerta-Arias et al., 2016
	• Presence of Type I and Type II subsets	• Puerta-Arias et al., 2018
	• NETs formation and prevention of fungal dissemination	• Mejía et al., 2015; Della-Coletta et al., 2015; Bachiega et al., 2016
	• Fungal cells are recognized *via* Dectin-1, MR, TLR2, and TLR4	• Acorci-Valério et al., 2010; Balderramas et al., 2014; Gardizani et al., 2019
	• Fungal stimulation induces IL-12, IL-10, PGE2, and LTB4	• Balderramas et al., 2014
	• IL-8 production inhibits apoptosis and allows fungal replication	• Acorci et al., 2008
	• Paracoccin induces: IL-8, IL-1β, ROS production, DNA release and inhibit apoptosis	• Ricci-Azevedo et al., 2018
	• Phagocytic cells primed with IFN-γ, IL-1β, GM-CSF, TNF-α, and IL-15 exhibit antifungal activity and trigger respiratory burst	• Kurita et al., 2000; Tavian et al., 2007; Rodrigues et al., 2007
	• Host genetic background influences their immunoregulatory functions	• Pina et al., 2006; Sperandio et al., 2015

disease (Hung et al., 2005). Moreover, it has been hypothesized that neutrophils could recognize the spherules and endospores of *Coccidioides* spp. *via* TLR2 or C-type lectin receptors, including Dectin-1, and inhibit their growth through NETs or granuloma formation. In the latter structure, the neutrophils are organized to form a necrotic center accompanied by eosinophilic debris and macrophages (Shubitz et al., 2008; Gonzalez et al., 2011; Lee et al., 2015). However, it is important to mention that in a mouse model of coccidioidomycosis, it was observed that lung-infiltrated neutrophils produce high amounts of IL-10, a fact that was associated with impairment of resistance to coccidioidal infection due to a suppression of Th1, Th2, and Th17 immunity mediated by this anti-inflammatory cytokine (Hung et al., 2013).

Paradoxically, Hung et al. (2014) observed that neutrophil-depleted mice infected with spores of the virulent isolate of *C. posadasii* did not show a difference in the fungal burden or the survival rate in comparison with control mice, indicating that neutrophils are dispensable for defense against this mycosis. Nonetheless, when the mice were immunized with a live-attenuated vaccine against coccidioidomycosis, the vaccine-induced protection promoted early recruitment and elevated numbers of neutrophils to the infection site, suggesting that the role of these phagocytic cells depends on prior exposure of the host to *Coccidioides* spp. (Hung et al., 2014).

In additional studies using mice deficient of NADPH oxidase 2 (NOX2), it was reported that NOX2 deficient mice infected with *Coccidioides* showed a reduced survival accompanied by a high and sustained number of lung-infiltrated neutrophils on days 7 and 11 postchallenge compared to infected WT mice. This evidence suggests that NOX2 production plays a role in limiting neutrophil recruitment and the subsequent pathogenic inflammation in this murine model of coccidioidomycosis (Gonzalez et al., 2011).

Blastomycosis

In contrast with the other dimorphic fungal infections, immunosuppression like HIV/aids does not appear to be a risk factor in developing blastomycosis (Pappas et al., 1993; Schwartz and Kauffman, 2020); thus, neutrophils and other innate immune cells might be enough to control the infection.

Early *in vitro* studies with murine neutrophils have been controversial. Although the ability of neutrophils to kill *B.*

dermatitidis has been demonstrated (Brummer and Stevens, 1984; Brummer et al., 1986; Morrison et al., 1989), some reports have shown that neutrophils enhance and allow the replication of this fungal pathogen, a fact that was associated with an exacerbation of the infection by accumulation and death of neutrophils in the tissue lesions (Brummer and Stevens, 1983). In this sense, the presence of a fungal chemotactic factor in serum-free culture filtrated of *B. dermatitidis* has been demonstrated (Sixbey et al., 1979; Thurmond and Mitchell, 1984). Lorenzini et al. (2017) also demonstrated that *Blastomyces* produces a peptidase (DppIVA) that cleaves chemokines, specifically those belonging to the CXC family, including the CXCL-2, which is the most potent chemoattractant molecule for neutrophils, thus improving neutrophil migration and promoting a pyogranulomatous response, a typical reaction during blastomycosis infection.

The function of a subset of neutrophils has recently been described in a murine model of pulmonary blastomycosis, which shows the capability of transdifferentiation in a neutrophil-dendritic cell hybrid that was associated with a better fungicidal function, NETs formation, and a higher expression of PRRs and the production of reactive oxygen species than canonical neutrophils (Fites et al., 2018). Although the role of these cells in other fungal infections is still unknown, these cells could be expected to contribute significantly due to their ability to improve both the innate and the adaptative immunity.

Paracoccidioidomycosis

In contrast to other endemic mycoses, several studies have suggested the dual role played by neutrophils during PCM infection. The functionality of these phagocytic cells appears to depend on some factors, including the genetic pattern of the host or the stage of infection. Pina et al. (2006) observed a significant difference, in the role of neutrophils, between resistant and susceptible mice; thus, in susceptible mice, these phagocytic cells have low fungicidal activity, but in contrast, neutrophils from resistant mice are more abundant in the lesion areas and efficient to control infection. Similar results were obtained by Sperandio et al. (2015), who using resistant and susceptible mice to PCM showed that in susceptible mice, the infection was able to disseminate to their bone marrow, impairing the production and maturation of neutrophils, which is different from what was observed in resistant mice.

Similarly, it has been suggested that neutrophils are essential during the acute inflammatory phase since they represent more than 85% of inflammatory cells and could positively modulate the innate immune response through the production of pro-inflammatory cytokines and lipidic mediators in the infected lung tissue (Gonzalez and Cano, 2001; Gonzalez et al., 2003; Balderramas et al., 2014). Along these lines, using an experimental model of pulmonary PCM in mice with intermediate susceptibility to infection and treated with a monoclonal antibody specific to neutrophils, we reported that compared to control mice, infected and neutrophil-depleted mice showed decreased survival rates during the early stage of infection, accompanied by an increase in both the fungal burden and the inflammatory response with an exaggerated production of several chemokines and proinflammatory cytokines, suggesting the pivotal role of these phagocytic cells in this fungal infection during the early course of infection (Pino-Tamayo et al., 2016).

Conversely, in studies of chronic pulmonary PCM in those mice with intermediate susceptibility, it was reported that treatment with the antifungal itraconazole or the immunomodulator pentoxifylline, alone or in combination, was associated with a decreased number of neutrophils as well as with an improved outcome of the disease, suggesting that these phagocytic cells appear to play a deleterious effect during the chronic stages of PCM (Naranjo et al., 2010., Naranjo et al., 2011; Lopera et al., 2015). Subsequently, we reported that those mice treated with the monoclonal antibodies specific to neutrophils during the chronic stages of infection showed better control of infection correlated with a reduction not only on the fungal burden but also on the inflammatory response and pulmonary fibrosis, suggesting that these phagocytic cells appear to play a detrimental effect during the chronic course of pulmonary PCM (Puerta-Arias et al., 2016).

Additional studies confirmed the presence of two different subsets of murine neutrophils, the type I neutrophils associated with a pro-inflammatory response, and the type II neutrophils associated with an anti-inflammatory response. Thus, a greater number of type II neutrophils were observed, which could be related to the incapacity of the host to control *P. brasiliensis* infection without the appropriate treatment (Puerta-Arias et al., 2018).

Moreover, other reports have described the capacity of *P. brasiliensis* to survive inside neutrophils and extend the lifetime of these cells *via* IL-8 production triggered by the fungus, suggesting that *P. brasiliensis* could evade the antifungal mechanisms allowing its replication (Brummer et al., 1989; Acorci et al., 2008). Along the same lines, it has been reported that paracoccin, a lectin expressed by *P. brasiliensis*, induces IL-8, IL-1β, and ROS production. It also induces the release of DNA and inhibits apoptosis (Ricci-Azevedo et al., 2018). In contrast, it has been reported that neutrophils exhibit antifungal activity against *P. brasiliensis* yeast only when these phagocytic cells are priming with IFN-γ, GM-CSF, IL-1β, and TNF-α (Kurita et al., 2000; Rodrigues et al., 2007). Similar results were obtained when human neutrophils were activated with IL-15, which increases *P. brasiliensis* killing by a mechanism dependent on H_2O_2 and superoxide anion (Tavian et al., 2007).

On the other hand, other studies have reported that neutrophils recognize *P. brasiliensis* yeasts *via* Dectin-1, MR, TLR2, and TLR4 (Acorci-Valéro et al., 2010; Balderramas et al., 2014; Gardizani et al., 2019) and produce cytokines including IL-12, IL-10, PGE2, and LTB4 (Balderramas et al., 2014). Additionally, these interactions were able to induce NETs formation by either dependent or independent reactive oxygen species production, correlating with the fungal morphotype used for stimulation (conidia or yeast, respectively); however, the killing of the fungus by NETs was dependent on the fungal strain and previous activation by cytokines, including TNF-α, IFN-γ, and GM-CSF. In addition, NETs appear to prevent fungal

dissemination (Mejía et al., 2015; Bachiega et al., 2016). Likewise, histopathological samples of cutaneous lesions from human PCM patients have revealed the production of NETs (Della-Coletta et al., 2015).

Taken all together, the above studies clearly demonstrated the important effector and immunomodulatory roles played by neutrophils during the early stages of infection, contributing to *P. brasiliensis* host resistance. Paradoxically, these phagocytic cells could also play a detrimental role during the chronic or advanced stages of infection.

NEUTROPHILS AND IL-17 PARTICIPATION IN THE GRANULOMATOUS INFLAMMATION AND PULMONARY FIBROSIS DEVELOPMENT OF ENDEMIC MYCOSES

The lungs are the primary organs affected by the dimorphic fungal pathogens; thus, once the conidia reach the alveoli, they transform into pathogenic morphotypes (yeast cells or spherules). Initially, these fungal propagules interact with lung epithelial cells or alveolar macrophages. Such interactions trigger the activation of these host cells, which, in turn, secret soluble mediator molecules, mainly chemokines and pro-inflammatory cytokines that induce the recruitment of pro-inflammatory cells, including neutrophils and other innate cells, into the lungs (Martin and Frever, 2005). During pulmonary inflammation, neutrophils can also interact with epithelial cells, lymphocytes, macrophages, and other granulocytes inducing the activation of the adaptive immune response (Siew et al., 2017). However, neutrophils may be self-defeating; thus, they could play a protective role but could also contribute to injury and tissue damage, especially in those cases of chronic inflammation due to a continuous activation mediated by the IL-17 (Parkos, 2016; Rosales et al., 2016). Neutrophils contain a great number of proteases, inflammatory mediators, and oxidants stored in their granules that lead to the progression of pulmonary complications such as asthma, chronic obstructive pulmonary disease (COPD), granulomatous lesions, and finally fibrosis (Liu et al., 2017).

In the case of systemic and endemic mycoses, there are scant studies that link the IL-17 and/or neutrophils with the development of a chronic inflammatory process or with fibrosis development. Some studies have demonstrated the presence of neutrophils in pulmonary infiltrating cells during infections by *P. brasiliensis* (Gonzalez and Cano, 2001; Gonzalez et al., 2003), *H. capsulatum* (Baughman et al., 1986), *C. posadasii* (Hung et al., 2005), and *B. dermatitidis* (Lorenzini et al., 2017). However, as mentioned above, the role of neutrophils during these dimorphic fungal infections is not clear; moreover, their participation in the immune response appears to depend on the phase of infection (acute or chronic) (Pino-Tamayo et al., 2016; Puerta-Arias et al., 2016). Only in an experimental model of paracoccidioidomycosis, the role of neutrophils in the pulmonary fibrosis development has been studied, where it was demonstrated that these phagocytic cells are detrimental and promote granulomatous inflammation and pulmonary fibrosis during the chronic course of the mycosis, a process that was also associated with the presence of IL-17 (Pino-Tamayo et al., 2016; Puerta-Arias et al., 2016). Moreover, it was demonstrated that the Th17-associated cytokines, IL-17, IL-6, and IL-23, are crucial for granuloma formation during experimental paracoccidioidomycosis; thus, deficiency of IL-6, IL-23, or IL-17RA impaired the compact granuloma formation and conferred susceptibility to infection (Tristão et al., 2017). In an additional study conducted by Heninger et al. (2006), it was reported that the granuloma lesions induced by *Histoplasma* infection are composed mainly of $CD4^+$, $CD8^+$, Dendritic cells, and macrophages, which are the principal sources of IFN-γ and IL-17; notably, neutrophils were not evidenced. In the other fungal endemic and systemic mycosis (coccidioidomycosis and blastomycosis), the role played by neutrophils and IL-17 in the development of the fibrosis process remains to be explored.

On the other hand, pulmonary fibrosis (PF) is the final result of a chronic inflammation caused by microbial pathogens and chemical or physical agents; thus, PF is a consequence of a repetitive process of injury and reparation of the alveolar epithelium, which leads to an exacerbated wound healing process, accompanied by an excess deposition of extracellular matrix (ECM) components and a scarring process of the lung (Rydell-Tormanen et al., 2012; Chioma and Drake, 2017). Additionally, during this PF process, an increased number of myofibroblasts and fibroblasts that are known to synthesize connective tissue proteins have been observed, mainly Type III Collagen, and matrix metalloproteinases (MMP) (Baum and Duffy, 2011; Wynn and Ramalingam, 2012). In paracoccidioidomycosis, the presence of neutrophil infiltration within the granuloma is observed during the chronic form, and especially surrounding the granulomas (González et al., 2008). Additional studies have shown that treatment with a combination of Itraconazole plus an immunomodulatory agent (Pentoxifylline) during the chronic pulmonary paracoccidioidomycosis, reduced the granulomatous inflammation and neutrophils (Naranjo et al., 2011). Along the same lines, in this fungal model and using a monoclonal antibody specific to neutrophils it was demonstrated that the depletion of these phagocytic cells was associated with an attenuation of the inflammation and the fibrotic process through a down-regulation of pro-fibrotic mediators including IL-17, TGF-β1, TNF-α, MMP-8 and the tissue inhibitor of metalloproteinases (TIMP)-2 (Puerta-Arias et al., 2016). The above studies clearly suggest that both neutrophils and IL-17 are responsible, in part, for the fibrosis development, evidence that supports the idea that neutrophils and/or IL-17 can be targets of a therapeutic intervention for the treatment of fibrosis as well as mycosis.

FUTURE QUESTIONS AND CONCLUSIONS

Over the last years, it has been learned that IL17 plays an important role and appears to be indispensable in developing a protective immunity against fungal infections including systemic

and endemic mycoses, a mechanism that is mediated by the interactions between fungal PAMPs and PRRs with the subsequent activation and recruitment of neutrophils and macrophages at the site of infection. Furthermore, it has also been demonstrated that each PRR plays a distinctly different role for each dimorphic fungal pathogen. Nonetheless, both the IL17 and neutrophils play a detrimental role in inducing pathological disease, possibly due to an unrestrained inflammatory response. Future studies will need to focus on which specific fungal antigens or PAMPs are recognized by the different PRRs and confer immunity through this Th17 immune pattern or, on the contrary, which kind of interactions induce pathological disease. Additionally, it would be interesting to know if IL17 induce NETs formation as a microbicidal mechanism against these fungal dimorphic pathogens. Thus, understanding the specific interactions between fungal PAMPs and PRRs and their contributions to disease outcomes will provide potential insights for designing and developing immunotherapies to control these systemic and endemic mycoses.

AUTHOR CONTRIBUTIONS

All authors contributed to the article and approved the submitted version.

FUNDING

Supported in part by Universidad de Antioquia; Basic and Applied Microbiology Research Group (MICROBA), School of Microbiology, Universidad de Antioquia, Medellin, Colombia.

REFERENCES

Abusleme, L., and Moutsopoulos, N. M. (2017). IL-17: overview and role in oral immunity and microbiome. *Oral. Dis.* 23, 854–865. doi: 10.1111/odi.12598

Acorci, M. J., Dias-Melicio, L. A., Golim, M. A., Bordon-Graciani, A. P., Peraçoli, M. T. S., and Soares, Â.M.V. (2008). Inhibition of human neutrophil apoptosis by *Paracoccidioides brasiliensis*: role of Interleukin-8. *Basic Immunol.* 69, 73–79. doi: 10.1111/j.1365-3083.2008.02199.x

Acorci-Valério, M. J., Bordon-Graciani, A. P., Dias-Melicio, L. A., de Assis Golim, M., Nakaira-Takahagi, E., and de Campos Soares, A. M. (2010). Role of TLR2 and TLR4 in human neutrophil functions against *Paracoccidioides brasiliensis*. *Scand. J. Immunol.* 71, 99–108. doi: 10.1111/j.1365-3083.2009.02351.x

Awasthi, S., Vilekar, P., Conkleton, A., and Rahman, N. (2019). Dendritic cell-based immunization induces *Coccidioides* Ag2/PRA-specific immune response. *Vaccine* 37, 1685–1691. doi: 10.1016/j.vaccine.2019.01.034

Bachiega, T. F., Dias-Melicio, L. A., Fernandes, R. K., de Almeida Balderramas, H., Rodrigues, D. R., Ximenes, V. F., et al. (2016). Participation of dectin-1 receptor on NETs release against *Paracoccidioides brasiliensis*: Role on extracellular killing. *Immunobiology* 221, 228–235. doi: 10.1016/j.imbio.2015.09.003

Balderramas, H. A., Penitenti, M., Rodrigues, D., Bachiega, D., Fernandes, R., Ikoma, M., et al. (2014). Human neutrophils produce IL-12, IL-10, PGE2, and LTB4 in response to *Paracoccidioides brasiliensis*. Involvement of TLR2, mannose receptor and dectin-1. *Cytokine* 67, 36–43. doi: 10.1016/j.cyto.2014.02.004

Baughman, R., Kim, C., Vinegar, A., Hendricks, D., Schmidt, J., and Bullock, E. (1986). The pathogenesis of experimental pulmonary histoplasmosis. Correlative studies of histopathology, bronchoalveolar lavage, and respiratory function. *Am. Rev. Respir. Dis.* 134, 771–776. doi: 10.1164/arrd.1986.134.4.771

Baum, J., and Duffy, H. S. (2011). Fibroblasts and Myofibroblasts: what are we talking about? *J. Cardiovasc. Pharmacol.* 57, 376–379. doi: 10.1097/FJC.0b013e3182116e39

Bianchi, M., Hakkim, A., Brinkmann, V., Siler, U., Seger, R. A., Zychlinsky, A., et al. (2009). Restoration of NET formation by gene therapy in CGD controls aspergillosis. *Blood* 114, 2619–2622. doi: 10.1182/blood-2009-05-221606

Brinkmann, V., Reichard, U., Goosmann, C., Fauler, B., Uhlemann, Y., Weiss, D. S., et al. (2004). Neutrophil extracellular traps kill bacteria. *Science* 303, 1532–1535. doi: 10.1126/science.1092385

Brummer, E., and Stevens, D. A. (1983). Enhancing effect of murine polymorphonuclear neutrophils (PMN) on the multiplication of *Blastomyces dermatitidis in vitro* and *in vivo*. *Clin. Exp. Immunol.* 54, 587–594.

Brummer, E., and Stevens, D. A. (1984). Activation of murine polymorphonuclear neutrophils for fungicidal activity with supernatants from antigen-stimulated immune spleen cell cultures. *Infect. Immun.* 45, 447–452. doi: 10.1128/IAI.45.2.447-452.1984

Brummer, E., McEwen, J. G., and Stevens, D. A. (1986). Fungicidal activity of murine inflammatory polymorphonuclear neutrophils: comparison with murine peripheral blood PMN. *Clin. Exp. Immunol.* 66, 681–690.

Brummer, E., Hanson, L. H., Restrepo, A., and Stevens, D. A. (1989). Intracellular multiplication of *Paracoccidioides brasiliensis* in macrophages: killing and restriction of multiplication by activated macrophages. *Infect. Immun.* 57, 2289–2294. doi: 10.1128/IAI.57.8.2289-2294.1989

Brummer, E., Kurita, N., Yoshida, S., Nishimura, K., and Miyaji, M. (1991). Fungistatic activity of human neutrophils against *Histoplasma capsulatum*: correlation with phagocytosis. *J. Infect. Dis.* 164, 158–162. doi: 10.1093/infdis/164.1.158

Buonocore, S., Ahern, P. P., Uhlig, H. H., Ivanov, I.II, Littman, D. R., Maloy, K. J., et al. (2010). Innate lymphoid cells drive interleukin-23-dependent innate intestinal pathology. *Nature* 464, 1371–1375. doi: 10.1038/nature08949

Byrd, A. S., O'Brien, X. M., Johnson, C. M., Lavigne, L. M., and Reichner, J. S. (2013). An extracellular matrix-based mechanism of rapid neutrophil extracellular trap formation in response to *Candida albicans*. *J. Immunol.* 190, 4136–4148. doi: 10.4049/jimmunol.1202671

Campuzano, A., Zhang, H., Ostroff, G. R., Dos Santos Dias, L., Wüthrich, M., Klein, B. S., et al. (2020). CARD9-associated Dectin-1 and Dectin-2 are required for protective immunity of a multivalent vaccine against *Coccidioides posadasii* infection. *J. Immunol.* 204, 3296–3306. doi: 10.4049/jimmunol.1900793

Cao, C., Xi, L., and Chaturvedi, V. (2019). Talaromycosis (Penicilliosis) Due to *Talaromyces (Penicillium) marneffei*: Insights into the clinical trends of a major fungal disease 60 years after the discovery of the pathogen. *Mycopathologia* 184, 709–720. doi: 10.1007/s11046-019-00410-2

Cella, M., Fuchs, A., Vermi, W., Facchetti, F., Otero, K., Lennerz, J. K. M., et al. (2009). A human natural killer cell subset provides an innate source of IL-22 for mucosal immunity. *Nature* 457, 722–725. doi: 10.1038/nature0753

Chamilos, G., Ganguly, D., Lande, R., Gregorio, J., Meller, S., William, E., et al. (2010). Generation of IL-23 producing dendritic cells (DCs) by airborne fungi regulates fungal pathogenicity via the induction of th-17 responses. *PloS One* 5, e12955. doi: 10.1371/journal.pone.0012955

Chang, W., Audet, R., Aizenstein, B., Hogna, L., DeMars, R., and Klein, B. (2000). T-Cell epitopes and human leukocyte antigen restriction elements of an immunodominant antigen of *Blastomyces dermatitidis*. *Infect. Immun.* 68, 502–510. doi: 10.1128/iai.68.2.502-510.2000

Chapman, S., Dismukes, W., Proia, L., Bradsher, R., Pappas, P., Threlkeld, M., et al. (2008). Clinical practice guidelines for the management of blastomycosis: 2008 Update by the Infectious Diseases Society of America. *Clin. Infect. Dis.* 46, 1801–1812. doi: 10.1086/588300

Chen, K., and Kolls, J. K. (2017). Interluekin-17A (IL17A). *Gene* 614, 8–14. doi: 10.1016/j.gene.2017.01.016

Cheng, O. Z., and Palaniyar, N. (2013). NET balancing: a problem in inflammatory lung diseases. *Front. Immunol.* 4, 1. doi: 10.3389/fimmu.2013.00001

Chiarella, A. P., Arruda, C., Pina, A., Costa, T. A., Ferreira, R. C., and Calich, V. L. (2007). The relative importance of CD4+ and CD8+T cells in immunity to pulmonary paracoccidioidomycosis. *Microbes Infect.* 9, 1078–1088. doi: 10.1016/j.micinf.2007.04.016

Chioma, O. S., and Drake, W. P. (2017). Role of microbial agents in pulmonary fibrosis. *Yale J. Biol. Med.* 90, 219–227.

Coxon, A., Rieu, P., Barkalow, F. J., Askari, S., Sharpe, A. H., von Andrian, U. H., et al. (1990). A novel role for the beta 2 integrin CD11b/CD18 in neutrophil apoptosis: a homeostatic mechanism in inflammation. *Immunity* 5, 653–666. doi: 10.1016/s1074-7613(00)80278-2

de Castro, L. F., Ferreira, M. C., da Silva, R. M., Blotta, M. H., Longhi, L. N., and Mamoni, R. L. (2013). Characterization of the immune response in human paracoccidioidomycosis. *J. Infect.* 67, 470–485. doi: 10.1016/j.jinf.2013.07.019

Deepe, G. S.Jr., and Gibbons, R. S. (2009). Interleukins 17 and 23 influence the host response to *Histoplasma capsulatum*. *J. Infect. Dis.* 200, 142–151. doi: 10.1086/599333

Deepe, G., Gibbons, R., and Smulian, G. (2008). *Histoplasma capsulatum* manifests preferential invasion of phagocytic subpopulations in murine lungs. *J. Leukoc. Biol.* 84, 669–678. doi: 10.1189/jlb.0308154

Deepe, G. S.Jr, Buesing, W. R., Ostroff, G. R., Abraham, A., Specht, C. A., Huang, H., et al. (2018). Vaccination with an alkaline extract of *Histoplasma capsulatum* packaged in glucan particles confers protective immunity in mice. *Vaccine* 36, 3359–3367. doi: 10.1016/j.vaccine.2018.04.047

Della-Coletta, A. M., Bachiega, T. F., de Quaglia e Silva, J. C., Soares, Â.M.V., de, C., De Faveri, J., et al. (2015). Neutrophil extracellular traps identification in tegumentary lesions of patients with paracoccidioidomycosis and different patterns of NETs generation *in vitro*. *PloS Negl. Trop. Dis.* 9, e0004037. doi: 10.1371/journal.pntd.0004037

Desai, J., and Lionakis, M. (2018). The role of neutrophils in host defense against invasive fungal infections. *Curr. Clin. Microbiol. Rep.* 5, 181–189. doi: 10.1007/s40588-018-0098-6

Drummond, R. A., Saijo, S., Iwakura, Y., and Brown, G. D. (2011). The role of Syk/CARD9 coupled C-type lectins in antifungal immunity. *Eur. J. Immunol.* 41, 276–281. doi: 10.1002/eji.201041252

Feriotti, C., de Araújo, E. F., Loures, F. V., da Costa, T. A., Galdino, N. A., Zamboni, D. S., et al. (2017). NOD-Like receptor P3 inflammasome controls protective Th1/Th17 immunity against pulmonary paracoccidioidomycosis. *Front. Immunol.* 8, 786. doi: 10.3389/fimmu.2017.00786

Fernandes, F. F., Oliveira, L. L., Landgraf, T. N., Peron, G., Costa, M. V., Coelho-Castelo, A. A., et al. (2016). Detrimental effect of fungal 60-kda heat shock protein on experimental *Paracoccidioides brasiliensis* infection. *PloS One* 11, e0162486. doi: 10.1371/journal.pone.0162486

Fites, J., Gui, M., Kernien, J., Negoro, P., Dagher, Z., Sykes, D., et al. (2018). An unappreciated role for neutrophil-DC hybrids in immunity to invasive fungal infections. *PloS Pathog.* 14, e1007073. doi: 10.1371/journal.ppat.1007073

Galgiani, J., Ampel, N., Blair, J., Catanzaro, A., Johnson, R., Stevens, D., et al. (2005). Coccidioidomycosis. *Clin. Infect. Dis.* 41, 1217–1223. doi: 10.1086/496991

Gardizani, T. P., Della Coletta, A. M., Romagnoli, G. G., Puccia, R., Serezani, A. P. M., de Campos Soares, Â.M.V., et al. (2019). 43 kDa Glycoprotein (gp43) from *Paracoccidioides brasiliensis* induced IL-17A and PGE2 production by human polymorphonuclear neutrophils: Involvement of TLR2 and TLR4. *J. Immunol. Res.* 2019, 1790908. doi: 10.1155/2019/1790908

Geremia, A., Arancibia-Cárcamo, C. V., Fleming, M. P. P., Rust, N., Singh, B., Mortensen, N. J., et al. (2011). IL-23–responsive innate lymphoid cells are increased in inflammatory bowel disease. *J. Exp. Med.* 208, 1127–1133. doi: 10.1084/jem.20101712

Gonzalez, A., and Cano, L. (2001). Participation of the polymorphonuclear neutrophils in the immune response against *Paracoccidioides brasiliensis*. [Participación del polimorfonuclear neutrófilo en la respuesta inmune contra Paracoccidioides brasiliensis]. *Biomedica* 21, 264–274. doi: 10.7705/biomedica.v21i3.1117

Gonzalez, A., Sahaza, J., Ortiz, B., Restrepo, A., and Cano, L. (2003). Production of pro-inflammatory cytokines during the early stages of experimental *Paracoccidioides brasiliensis* infection. *Med. Mycol.* 41, 391–399. doi: 10.1080/13693780310001610038

González, A., Lenzi, H. L., Motta, E. M., Caputo, L., Restrepo, A., and Cano, L. E. (2008). Expression and arrangement of extracellular matrix proteins in the lungs of mice infected with *Paracoccidioides brasiliensis* conidia. *Int. J. Exp. Pathol.* 89, 106–116. doi: 10.1111/j.1365-2613.2008.00573.x

Gonzalez, A., Hung, C.-Y., and Cole, G. (2011). Absence of phagocyte NADPH oxidase 2 leads to severe inflammatory response in lungs of mice infected with *Coccidioides*. *Microb. Pathog.* 51, 432–441. doi: 10.1016/j.micpath.2011.08.003

Harrington, L. E., Mangan, P. R., and Weaver, C. T. (2006). Expanding the effector CD4 T-cell repertoire: the Th17 lineage. *Curr. Opin. Immunol.* 18, 349–356. doi: 10.1016/j.coi.2006.03.017

Hartupee, J., Liu, C., Novotny, M., Sun, D., Li, X., and Hamilton, T. A. (2009). IL-17 signaling for mRNA stabilization does not require TNF receptor-associated factor 6. *J. Immunol.* 182, 1660–1666. doi: 10.4049/jimmunol.182.3.1660

Heninger, E., Hogan, L. H., Karman, J., Macvilay, S., Hill, B., Woods, J. P., et al. (2006). Characterization of the *Histoplasma capsulatum*-induced granuloma. *J. Immunol.* 177, 3303–3313. doi: 10.4049/jimmunol.177.5.3303

Hernández-Santos, N., Wiesner, D. L., Fites, J. S., McDermott, A. J., Warner, T., Wüthrich, M., et al. (2018). Lung epithelial cells coordinate innate lymphocytes and immunity against pulmonary fungal infection. *Cell Host Microbe* 23, 511–522.e5. doi: 10.1016/j.chom.2018.02.011

Hoeksema, M., van Eijk, M., Haagsman, H. P., and Hartshorn, K. L. (2016). Histones as mediators of host defense, inflammation and thrombosis. *Future Microbiol.* 11, 441–453. doi: 10.2217/fmb.15.151

Hoshino, A., Nagao, T., Nagi-Miura, N., Ohno, N., Yasuhara, M., Yamamoto, K., et al. (2008). MPO-ANCA induces IL-17 production by activated neutrophils in vitro via its Fc region- and complement-dependent manner. *J. Autoimmun.* 31, 79–89. doi: 10.1016/j.jaut.2008.03.006

Hsu, L., Ng, E., and Koh, L. (2010). Common and emerging fungal pulmonary infections. *Infect. Dis. Clin. North Am.* 24, 557–577. doi: 10.1016/j.idc.2010.04.003

Hung, C. Y., Seshan, K. R., Yu, J. J., Schaller, R., Xue, J., Basrur, V., et al. (2005). A metalloproteinase of *Coccidioides posadasii* contributes to evasion of host detection. *Infect. Immun.* 73, 6689–6703. doi: 10.1128/IAI.73.10.6689-6703.2005

Hung, C. Y., Xue, J., and Cole, G. T. (2007). Virulence mechanisms of *Coccidioides*. *Ann. N. Y. Acad. Sci.* 1111, 225–235. doi: 10.1196/annals.1406.020

Hung, C. Y., Gonzalez, A., Wüthrich, M., Klein, B. S., and Cole, G. T. (2011). Vaccine immunity to coccidioidomycosis occurs by early activation of three signal pathways of T helper cell response (Th1, Th2, and Th17). *Infect. Immun.* 79, 4511–4522. doi: 10.1128/IAI.05726-11

Hung, C. Y., Hurtgen, B. J., Bellecourt, M., Sanderson, S. D., Morgan, E. L., and Cole, G. T. (2012). An agonist of human complement fragment C5a enhances vaccine immunity against *Coccidioides* infection. *Vaccine* 30, 4681–4690. doi: 10.1016/j.vaccine.2012.04.084

Hung, C. Y., Castro-Lopez, N., and Cole, G. T. (2013). Vaccinated C57BL/6 mice develop protective and memory t cell responses to *Coccidioides posadasii* infection in the absence of interleukin-10. *Infect. Immun.* 82, 903–913. doi: 10.1128/IAI.01148-13

Hung, Y., Jiménez-Alzate, M., del, P., Gonzalez, A., Wuthrich, M., Klein, S., et al. (2014). Interleukin-1 receptor but not Toll-like receptor 2 is essential for MyD88-dependent Th17 immunity to *Coccidioides* infection. *Infect. Immun.* 82, 2106–2114. doi: 10.1128/IAI.01579-13

Hung, C. Y., Castro-Lopez, N., and Cole, G. T. (2016). Card9- and MyD88-mediated gamma interferon and nitric oxide production is essential for resistance to subcutaneous Coccidioides posadasii infection. *Infect. Immun.* 84, 1166 –11175. doi: 10.1128/IAI.01066-15

Hung, C. Y., Zhang, H., Castro-Lopez, N., Ostroff, G. R., Khoshlenar, P., Abraham, A., et al. (2018). Glucan-chitin particles enhance Th17 response and improve protective efficacy of a multivalent antigen (rCpa1) against pulmonary *Coccidioides posadasii* infection. *Infect. Immun.* 86, e00070–e00018. doi: 10.1128/IAI.00070-18

Hurtgen, B. J., Hung, C. Y., Ostroff, G. R., Levitz, S. M., and Cole, G. T. (2012). Construction and evaluation of a novel recombinant T cell epitope-based vaccine against Coccidioidomycosis. *Infect. Immun.* 80, 3960–3974. doi: 10.1128/IAI.00566-12

Hurtgen, B. J., Castro-Lopez, N., Jiménez-Alzate, M. D. P., Cole, G. T., and Hung, C. Y. (2016). Preclinical identification of vaccine induced protective correlates in human leukocyte antigen expressing transgenic mice infected with *Coccidioides posadasii*. *Vaccine* 34, 5336–5343. doi: 10.1016/j.vaccine.2016.08.078

Isailovic, N., Daigo, K., Mantovani, A., and Selmi, C. (2015). Interleukin-17 and innate immunity in infections and chronic inflammation. *J. Autoimmun.* 60, 1–11. doi: 10.1016/j.jaut.2015.04.006

Ishikawa, T., Itoh, F., Yoshida, S., Saijo, S., Matsuzawa, T., Gonoi, T., et al. (2013). Identification of distinct ligands for the C-type lectin receptors Mincle and Dectin-2 in the pathogenic fungus *Malassezia*. *Cell Host Microbe* 13, 477–488. doi: 10.1016/j.chom.2013.03.008

Jannuzzi, G. P., de Almeida, J. R. F., Amarante-Mendes, G. P., Romera, L. M. D., Kaihami, G. H., Vasconcelos, J. R., et al. (2019). TLR3 is a negative regulator of immune responses against *Paracoccidioides brasiliensis*. *Front. Cell Infect. Microbiol.* 8, 426. doi: 10.3389/fcimb.2018.00426

Ketelut-Carneiro, N., Souza, C. O. S., Benevides, L., Gardinassi, L. G., Silva, M. C., Tavares, L. A., et al. (2019). Caspase-11-dependent IL-1α release boosts Th17 immunity against *Paracoccidioides brasiliensis*. *PloS Pathog.* 15, e1007990. doi: 10.1371/journal.ppat.1007990

Kirkland, T. N., and Fierer, J. (2018). *Coccidioides immitis* and *posadasii*; A review of their biology, genomics, pathogenesis, and host immunity. *Virulence* 9, 1426–1435. doi: 10.1080/21505594.2018.1509667

Kolaczkowska, E., and Kubes, P. (2013). Neutrophil recruitment and function in health and inflammation. *Nat. Rev. Immunol.* 13, 159–175. doi: 10.1038/nri3399

Korn, T., Bettelli, E., Oukka, M., and Kuchroo, V. K. (2009). IL-17 and Th17 Cells. *Annu. Rev. Immunol.* 27, 485–517. doi: 10.1146/annurev.immunol.021908.132710

Kroetz, D. N., and Deepe, G. S.Jr (2010). CCR5 dictates the equilibrium of proinflammatory IL-17+ and regulatory Foxp3+ T cells in fungal infection. *J. Immunol.* 184, 5224–5231. doi: 10.4049/jimmunol.1000032

Kroetz, D. N., and Deepe, G. S. (2012). The role of cytokines and chemokines in *Histoplasma capsulatum* infection. *Cytokine* 58, 112–117. doi: 10.1016/j.cyto.2011.07.430

Kurita, N., Terao, K., Brummer, E., Ito, E., Nishimura, K., and Miyaji, M. (1991). Resistance of *Histoplasma capsulatum to* killing by human neutrophils. *Mycopathologia* 115, 207–213. doi: 10.1007/BF00462229

Kurita, N., Oarada, M., Miyaji, M. , and Ito, E. (2000). Effect of cytokines on antifungal activity of human polymorphonuclear leucocytes against yeast cells of *Paracoccidioides brasiliensis*. *Med. Mycol.* 38, 177–182. doi: 10.1080/mmy.38.2.177.182

Lee, C. Y., Thompson III, G., Hastey, C., Hodge, G., Lunetta, J., Pappagianis, D., et al. (2015). *Coccidioides* endospores and spherules draw strong chemotactic, adhesive, and phagocytic responses by individual human neutrophils. *PloS One* 10, e0129522. doi: 10.1371/journal.pone.0129522

Leffler, J., Martin, M., Gullstrand, B., Tydén, H., Lood, C., Truedsson, L., et al. (2012). Neutrophil extracellular traps that are not degraded in systemic lupus erythematosus activate complement exacerbating the disease. *J. Immunol.* 188, 3522–3531. doi: 10.4049/jimmunol.1102404

Lin, A. M., Rubin, C. J., Khandpur, R., Wang, J. Y., Riblett, M., Yalavarthi, S., et al. (2011). Mast cells and neutrophils release IL-17 through extracellular trap formation in psoriasis. *J. Immunol.* 187, 490–500. doi: 10.4049/jimmunol.110012

Lionakis, M., and Levitz, S. (2018). Host control of fungal infections: Lessons from basic studies and human cohorts. *Annu. Rev. Immunol.* 36, 157–191. doi: 10.1146/annurev-immunol-042617-053318

Lionakis, M., Iliev, I., and Hohl, T. (2017). Immunity against fungi. *JCI Insights* 2, e93156. doi: 10.1172/jci.insight.93156

Liu, J., Pang, Z., Wang, G., Guan, X., Fang, K., Wang, Z., et al. (2017). Advanced role of neutrophils in common respiratory diseases. *J. Immunol. Res.* 2017:6710278. doi: 10.1155/2017/6710278

Lopera, D. E., Naranjo, T. W., Hidalgo, J. M., Echeverri, L., Patiño, J. H., Moreno, Á.R., et al. (2015). Pentoxifylline immunomodulation in the treatment of experimental chronic pulmonary paracoccidioidomycosis. *Fibrogenesis Tissue Repair* 8:10. doi: 10.1186/s13069-015-0027-8

Lorenzini, J., Fites, J. S., Nett, J., and Klein, B. (2017). *Blastomyces dermatitidis* serine protease(DppIVA) cleaves ELR$^+$CXC chemokines altering their effects on neutrophils. *Cell Microbiol.* 19:10. doi: 10.1111/cmi.12741

Loures, F. V., Pina, A., Felonato, M., and Calich, V. L. (2009). TLR2 is a negative regulator of Th17 cells and tissue pathology in a pulmonary model of fungal infection. *J. Immunol.* 183, 1279–1290. doi: 10.4049/jimmunol.0801599

Loures, F. V., Pina, A., Felonato, M., Feriotti, C., de Araujo, E. F., and Calich, V. L. (2011). MyD88 signaling is required for efficient innate and adaptive immune responses to *Paracoccidioides brasiliensis* infection. *Infect. Immun.* 79, 2470–2480. doi: 10.4049/jimmunol.0801599

Loures, F. V., Araújo, E. F., Feriotti, C., Bazan, S. B., Costa, T. A., Brown, G. D., et al. (2014). Dectin-1 induces M1 macrophages and prominent expansion of CD8+IL-17+ cells in pulmonary paracoccidioidomycosis. *J. Infect. Dis.* 210, 762–773. doi: 10.1093/infdis/jiu136

Loures, F. V., Araújo, E. F., Feriotti, C., Bazan, S. B., and Calich, V. L. G. (2015). TLR-4 cooperates with Dectin-1 and mannose receptor to expand Th17 and Tc17 cells induced by *Paracoccidioides brasiliensis* stimulated dendritic cells. *Front. Microbiol.* 6, 261. doi: 10.3389/fmicb.2015.00261

Martin, T., and Frever, C. (2005). Innate immunity in the lung. *Proc. Am. Thorac. Soc* 2, 403–411. doi: 10.1513/pats.200508-090JS

McGreal, E. P., Rosas, M., Brown, G. D., Zamze, S., Wong, S. Y., Gordon, S., et al. (2006). The carbohydrate-recognition domain of Dectin-2 is a C-type lectin with specificity for high mannose. *Glycobiology* 16, 422–430. doi: 10.1093/glycob/cwj077

Medeiros, A.II, Bonato, V. L., Malheiro, A., Dias, A. R., Silva, C. L., and Faccioli, L. H. (2002). *Histoplasma capsulatum* inhibits apoptosis and Mac-1 expression in leucocytes. *Scand. J. Immunol.* 56, 392–398. doi: 10.1046/j.1365-3083.2002.01142.x

Medeiros, A.II, Secatto, A., Bélanger, C., Sorgi, P. B., Marleau, S., and Faccioli, L. (2015). Impairment of neutrophil migration to remote inflammatory site during lung histoplasmosis. *BioMed. Res. Int.* 2015, 409309. doi: 10.1155/2015/409309

Mejía, S. P., Cano, L. E., López, J. A., Hernandez, O., and González, Á. (2015). Human neutrophils produce extracellular traps against *Paracoccidioides brasiliensis*. *Microbiology* 161, 1008–1017. doi: 10.1099/mic.0.000059

Merkhofer, R. M.Jr, O'Neill, M. B., Xiong, D., Hernandez-Santos, N., Dobson, H., Fites, J. S., et al. (2019). Investigation of genetic susceptibility to blastomycosis reveals interleukin-6 as a potential susceptibility locus. *mBio.* 10, e01224–e01219. doi: 10.1128/mBio.01224-19

Michel, M.-L., Keller, A. C., Paget, C., Fujio, M., Trottein, F., Savage, P. B., et al. (2007). Identification of an IL-17–producing NK1.1neg iNKT cell population involved in airway neutrophilia. *J. Exp. Med.* 204, 995–1001. doi: 10.1084/jem.20061551

Mócsai, A. (2013). Diverse novel functions of neutrophils in immunity, inflammation, and beyond. *J. Exp. Med.* 210, 1283–1299. doi: 10.1084/jem.20122220

Monin, L., and Gaffen, S. L. (2018). Interleukin 17 family cytokines: Signaling mechanisms, biological activities, and therapeutic implications. *Cold Spring Harb. Perspect. Biol.* 10:a028522. doi: 10.1101/cshperspecta028522

Morrison, C. J., Brummer, E., and Stevens, D. (1989). In vivo activation of peripheral blood polymorphonuclear neutrophils by gamma interferon results in enhanced fungal killing. *Infect. Immun.* 57, 2953–1958. doi: 10.1128/IAI.57.10.2953-2958.1989

Nanjappa, S. G., Heninger, E., Wüthrich, M., Gasper, D. J., and Klein, B. S. (2012). Tc17 cells mediate vaccine immunity against lethal fungal pneumonia in immune deficient hosts lacking CD4+ T cells. *PloS Pathog.* 8, e1002771. doi: 10.1371/journal.ppat.1002771

Nanjappa, S. G., Hernández-Santos, N., Galles, K., Wüthrich, M., Suresh, M., and Klein, B. S. (2015). Intrinsic MyD88-Akt1-mTOR signaling coordinates disparate Tc17 and Tc1 responses during vaccine immunity against fungal pneumonia. *PloS Pathog.* 11, e1005161. doi: 10.1371/journal.ppat.1005161

Nanjappa, S. G., McDermott, A. J., Fites, J. S., Galles, K., Wüthrich, M., Deepe, G. S.Jr, et al. (2017). Antifungal Tc17 cells are durable and stable, persisting as long-lasting vaccine memory without plasticity towards IFNγ cells. *PloS Pathog.* 13, e1006356. doi: 10.1371/journal.ppat.1006356

Naranjo, T. W., Lopera, D. E., Diaz-Granados, L. R., Duque, J. J., Restrepo, A., and Cano, L. E. (2010). Histopathologic and immunologic effects of the itraconazole treatment in a murine model of chronic pulmonary paracoccidioidomycosis. *Microbes Infect.* 12, 1153–1162. doi: 10.1016/j.micinf.2010.07.013

Naranjo, T. W., Lopera, D. E., Diaz-Granados, L. R., Duque, J. J., Restrepo, A. M., and Cano, L. E. (2011). Combined itraconazole-pentoxifylline treatment promptly reduces lung fibrosis induced by chronic pulmonary paracoccidioidomycosis in mice. *Pulm. Pharmacol. Ther.* 24, 81–91. doi: 10.1016/j.pupt.2010.09.005

Netea, M. G., Van der Meer, J. W., and Kullberg, B. J. (2006). Role of the dual interaction of fungal pathogens with pattern recognition receptors in the activation and modulation of host defence. *Clin. Microbiol. Infect.* 12, 404–409. doi: 10.1111/j.1469-0691.2006.01388.x

Netea, M. G., Brown, G. D., Kullberg, B. J., and Gow, N. A. R. (2008). An integrated model of the recognition of *Candida albicans* by the innate immune system. *Nat. Rev. Microbiol.* 6, 67–78. doi: 10.1038/nrmicro1815

Newman, S. L., Gootee, L., and Gabay, J. E. (1993). Human neutrophil-mediated fungistasis against *Histoplasma capsulatum.* Localization of fungistatic activity to the azurophil granules. *J. Clin. Invest.* 92, 624–631. doi: 10.1172/JCI116630

Newman, S., Gootee, L., Gabay, J., and Selsted, M. (2000). Identification of constituents of human neutrophil azurophil granules that mediate fungistasis against *Histoplasma capsulatum*. *Infect. Immun.* 68, 5668–5672. doi: 10.1128/iai.68.10.5668-5672.2000

Onishi, R. M., and Gaffen, S. L. (2010). Interleukin-17 and its target genes: mechanisms of interleukin-17 function in disease. *Immunology.* 129, 311–321. doi: 10.1111/j.1365-2567.2009.03240.x

Pappas, P., Threlkeld, M., Bedsole, G., Cleveland, K. O., Gelfand, M. S., and Dismukes, W. E. (1993). Blastomycosis in immunocompromised patients. *Med. (Baltimore)* 72, 311–325. doi: 10.1097/00005792-199309000-00003

Parkos, C. A. (2016). Neutrophil-epithelial interactions: A double-edged sword. *Am. J. Pathol.* 186, 1404–1416. doi: 10.1016/j.ajpath.2016.02.001

Patin, E. M., Thompson, A., and Selinda, J. O. (2019). Pattern recognition receptors in fungal immunity. *Semin. Cell Dev. Biol.* 89, 24–33. doi: 10.1016/j.semcdb.2018.03.003

Pina, A., Saldiva, P., Restrepo, L. E., and Calich, V. L. (2006). Neutrophil role in pulmonary paracoccidioidomycosis depends on the resistance pattern of hosts. *J. Leukoc. Biol.* 79, 1202–1213. doi: 10.1189/jlb.0106052

Pino-Tamayo, P., Puerta-Arias, J., Lopera, D., Urán-Jiménez, M., and Gonzalez, A. (2016). Depletion of neutrophils exacerbates the earlyi Immune response in lungs of mice infected with *Paracoccidioides brasiliensis*. *Mediators Inflamm.* 2016:3183285. doi: 10.1155/2016/3183285

Prado, M. K. B., Fontanari, C., Souza, C. O. S., Gardinassi, L. G., Zoccal, K. F., de Paula-Silva, F. W. G., et al. (2020). IL-22 promotes IFN-γ-mediated immunity against *Histoplasma capsulatum* Infection. *Biomolecules* 10, 865. doi: 10.3390/biom10060865

Procknow, J. J., Page, M.II, and Loossli, C. G. (1960). Early pathogenesis of experimental histoplasmosis. *Arch. Pathol.* 69, 420–428.

Puerta-Arias, J., Pino-Tamayo, P., Arango, J., and Gonzalez, A. (2016). Depletion of neutrophils promotes the resolution of pulmonary inflammation and fibrosis in mice infected with *Paracoccidioides brasiliensis*. *PloS One* 11, e0163985. doi: 10.1371/journal.pone.0163985

Puerta-Arias, J. D., Pino-Tamayo, P. A., Arango, J. C., Salazar-Peláez, L. M., and González, A. (2018). Itraconazole in combination with neutrophil depletion reduces the expression of genes related to pulmonary fibrosis in an experimental model of paracoccidioidomycosis. *Med. Mycol.* 56, 579–590. doi: 10.1093/mmy/myx087

Ramirez-Carrozzi, V., Sambandam, A., Luis, E., Lin, Z., Jeet, S., Lesch, J., et al. (2011). IL-17C regulates the innate immune function of epithelial cells in an autocrine manner. *Nat. Immunol.* 12, 1159–1166. doi: 10.1038/ni.2156

Reid, D. M., Gow, N. A., and Brown, G. D. (2009). Pattern recognition: recent insights from Dectin-1. *Curr. Opin. Immunol.* 21, 30–37. doi: 10.1016/j.coi.2009.01.003

Restrepo, A., Tobón, A. M., and González, A. (2019). "Paracoccidioidomycosis," in *Principles and Practice of Infectious Diseases*, *9*. Eds. G. L. Mandell, Douglas, and J. E. Bennett's (Philadelphia, PA, USA: Elsevier), 3211–3221.

Ricci-Azevedo, R., Gonçales, R. A., Roque-Barreira, M. C., and Girard, D. (2018). Human neutrophils are targets to paracoccin, a lectin expressed by *Paracoccidioides brasiliensis*. *Inflammation Res.* 67, 31–41. doi: 10.1007/s00011-017-1093-8

Rickel, E. A., Siegel, L. A., Yoon, B.-R. P., Rottman, J. B., Kugler, D. G., Swart, D. A., et al. (2008). Identification of functional roles for both IL-17RB and IL-17RA in mediating IL-25-induced activities. *J. Immunol.* 181, 4299–4310. doi: 10.4049/jimmunol.181.6.4299

Rodrigues, D. R., Dias-Melicio, L. A., Calvi, S. A., Peraçoli, M. T., and Soares, A. M. (2007). *Paracoccidioides brasiliensis* killing by IFN-gamma, TNF-alpha and GM-CSF activated human neutrophils: role for oxygen metabolites. *Med. Mycol.* 45, 27–33. doi: 10.1080/13693780600981676

Romagnolo, A. G., de Quaglia, E., Silva, J. C., Della Coletta, A. M., Gardizani, T. P., Martins, A. T. L., et al. (2018). Role of Dectin-1 receptor on cytokine production by human monocytes challenged with *Paracoccidioides brasiliensis*. *Mycoses* 6, 222–230. doi: 10.1111/myc.12725

Rosales, C., Demaurex, N., Lowell, C. A., and Uribe-Querol, E. (2016). Neutrophils: Their role in innate and adaptive immunity. *J. Immunol. Res.* 2016:1469780. doi: 10.1155/2016/1469780

Rydell-Tormanen, K., Andréasson, K., Hesselstrand, R., Risteli, J., Heinegård, T., Saxne, T., et al. (2012). Extracellular matrix alterations and acute inflammation; developing in parallel during early induction of pulmonary fibrosis. *Lab. Invest.* 92, 917–925. doi: 10.1038/labinvest.2012.57

Saijo, S., Ikeda, S., Yamabe, K., Kakuta, S., Ishigame, H., Akitsu, A., et al. (2010). Dectin-2 recognition of alphamannans and induction of Th17 cell differentiation is essential for host defense against *Candida albicans*. *Immunity* 32, 681–691. doi: 10.1016/j.immuni.2010.05.001

Schnur, R. A., and Newman, S. L. (1990). The respiratory burst response to *Histoplasma capsulatum* by human neutrophils. Evidence for intracellular trapping of superoxide anion. *J. Immunol.* 144, 765–772.

Schön, M. P., and Erpenbeck, L. (2018). The Interleukin-23/Interleukin-17 Axis Links Adaptive and Innate Immunity in Psoriasis. *Front. Immunol.* 9, 1323. doi: 10.3389/fimmu.2018.01323

Schwartz, I. S., and Kauffman, C. A. (2020). Blastomycosis. *Semin. Respir. Crit. Care Med.* 41, 31–41. doi: 10.1055/s-0039-3400281

Schwartz, I. S., Govender, N. P., Sigler, L., Jiang, Y., Maphanga, T. G., Toplis, B., et al. (2019). *Emergomyces*: The global rise of new dimorphic fungal pathogens. *PloS Pathog.* 15, e1007977. doi: 10.1371/journal.ppat.1007977

Sepúlveda, V. E., Márquez, R., Turissini, D. A., Goldman, W. E., and Matute, D. R. (2017). Genome sequences reveal cryptic speciation in the human pathogen *Histoplasma capsulatum*. *mBio* 8, e01339–e01317. doi: 10.1128/mBio.01339-17

Shubitz, L. F., Dial, S., Perrill, R., Casement, R., and Galgiani, J. (2008). Vaccine-induced cellular immune responses differ from innate responses in susceptible and resistant strains of mice infected with *Coccidioides posadasii*. *Infect. Immun.* 76, 5553–5564. doi: 10.1128/IAI.00885-08

Siew, L. Q., Wu, S. Y., Ying, S., and Corrigan, C. J. (2017). Cigarette smoking increases bronchial mucosal IL-17A expression in asthmatics, which acts in concert with environmental aeroallergens to engender neutrophilic inflammation. *Clin. Exp. Allergy* 47, 740–750. doi: 10.1111/cea.12907

Sixbey, J. W., Fields, B. T., Sun, C. N., Clark, R. A., and Nolan, C. M. (1979). Interactions between human granulocytes and *Blastomyces dermatitidis*. *Infect. Immun.* 23, 41–44. doi: 10.1128/IAI.23.1.41-44.1979

Sperandio, F. F., Fernandes, G. P., Mendes, A. C. S. C., Bani, G., de, A. C., Calich, V. L. G., et al. (2015). Resistance to *P. brasiliensis* experimental infection of inbred mice is associated with an efficient neutrophil mobilization and activation by mediators of inflammation. *Mediators Inflamm.* 2015, 430425. doi: 10.1155/2015/430525

Takatori, H., Kanno, Y., Watford, W. T., Tato, C. M., Weiss, G., Ivanov, I. I., et al. (2008). Lymphoid tissue inducer–like cells are an innate source of IL-17 and IL-22. *J. Exp. Med.* 206, 35–41. doi: 10.1084/jem.20072713

Tavian, E. G., Dias-Melicio, L. A., Acorci, M. J., Bordon-Graciani, A. P., Peraçoli, M. T. S., and Soares, A. M. V. (2007). Interleukin-15 increases *Paracoccidioides brasiliensis* killing by human neutrophils. *Cytokine* 41, 48–53. doi: 10.1016/j.cyto.2007.10.011

Tecchio, C., and Casatella, M. (2016). Neutrophil-derived chemokines on the road to immunity. *Semin. Immunol.* 28, 119–128. doi: 10.1016/j.smim.2016.04.003

Thompson-Souza, G., Santos, G., Silva, J., Muniz, V., Braga, Y., Figueiredo, R., et al. (2020). *Histoplasma capsulatum*-induced extracellular DNA trap release in human neutrophils. *Cell. Microbiol.* 22, e13195. doi: 10.1111/cmi.13195

Thurmond, L. M., and Mitchell, T. (1984). *Blastomyces dermatitidis* chemotactic factor: kinetics of production and biological characterization evaluated by a modified neutrophil chemotaxis assay. *Infect. Immunity* 46, 87–93. doi: 10.1128/IAI.46.1.87-93.1984

Toy, D., Kugler, D., Wolfson, M., Vanden Bos, T., Gurgel, J., Derry, J., et al. (2006). Cutting edge: interleukin 17 signals through a heteromeric receptor complex. *J. Immunol.* 177, 36–39. doi: 10.4049/jimmunol.177.1.36

Tristão, F. S. M., Rocha, F. A., Carlos, D., Ketelut-Carneiro, N., Souza, C. O. S., Milanezi, C. M., et al. (2017). Th17-inducing cytokines IL-6 and IL-23 are crucial for granuloma formation during experimental paracoccidioidomycosis. *Front. Immunol.* 8, 949. doi: 10.3389/fimmu.2017.00949

Turissini, D. A., Gomez, O. M., Teixeira, M. M., McEwen, J. G. , and Matute, D. R. (2017). Species boundaries in the human pathogen *Paracoccidioides*. *Fungal Genet. Biol.* 106, 9–25. doi: 10.1016/j.fgb.2017.05.007

Urban, C. F., Reichard, U., Brinkmann, V., and Zychlinsky, A. (2006). Neutrophil extracellular traps capture and kill *Candida albicans* yeast and hyphal forms. *Cell. Microbiol.* 8, 668–676. doi: 10.1111/j.1462-5822.2005.00659.x

Valeri, M., and Raffatellu, M. (2016). Cytokines IL-17 and IL-22 in the host response to infection. *Pathog. Dis.* 74, ftw111. doi: 10.1093/femspd/ftw111

van de Veerdonk, F. L., Gresnigt, M. S., Kullberg, B. J., van der Meer, J. W., Joosten, L. A., and Netea, M. G. (2009). Th17 responses and host defense against microorganisms: an overview. *BMB Rep.* 42, 776–787. doi: 10.5483/bmbrep.2009.42.12.776

Villanova, F., Flutter, B., Tosi, I., Grys, K., Sreeneebus, H., Perera, G. K., et al. (2014). Characterization of innate lymphoid cells in human skin and blood demonstrates increase of NKp44+ ILC3 in psoriasis. *J. Invest. Dermatol.* 134, 984–991. doi: 10.1038/jid.2013.477

Viriyakosol, S., Jimenez Mdel, P., Gurney, M. A., Ashbaugh, M. E., and Fierer, J. (2013). Dectin-1 is required for resistance to coccidioidomycosis in mice. *MBio* 4, e00597–e12. doi: 10.1128/mBio.00597-12

Wang, J., and Arase, H. (2014). Regulation of immune responses by neutrophils. *Ann. N. Y. Acad. Sci.* 1319, 66–81. doi: 10.1111/nyas.12445

Wang, H., LeBert, V., Hung, C. Y., Galles, K., Saijo, S., Lin, X., et al. (2014). C-type lectin receptors differentially induce th17 cells and vaccine immunity to the endemic mycosis of North America. *J. Immunol.* 192, 1107–1119. doi: 10.4049/jimmunol.1302314

Wang, H., LeBert, V., Li, M., Lerksuthirat, T., Galles, K., Klein, B., et al. (2016). Mannose receptor is required for optimal induction of vaccine-induced T-helper Type 17 cells and resistance to *Blastomyces dermatitidis* Infection. *J. Infect. Dis.* 213, 1762–1766. doi: 10.1093/infdis/jiw010

Wang, H., Li, M., Lerksuthirat, T., Klein, B., and Wüthrich, M. (2015). The C-type lectin receptor MCL mediates vaccine-induced immunity against infection with *Blastomyces dermatitidis*. *Infect. Immun.* 84, 635–642. doi: 10.1128/IAI.01263-15

Wang, H., Lee, T. J., Fites, S. J., Merkhofer, R., Zarnowski, R., Brandhorst, T., et al. (2017). Ligation of Dectin-2 with a novel microbial ligand promotes adjuvant activity for vaccination. *PloS Pathog.* 13, e1006568. doi: 10.1371/journal.ppat.1006568

Wheat, L. J., Azar, M. M., Bahr, N. C., Spec, A., Relich, R. F., and Hage, C. (2016). Histoplasmosis. *Infect. Dis. Clin. North. Am.* 30, 207–227. doi: 10.1016/j.idc.2015.10.009

Wu, S. Y., Yu, J. S., Liu, F. T., Miaw, S. C., and Wu-Hsieh, B. A. (2013). Galectin-3 negatively regulates dendritic cell production of IL-23/IL-17-axis cytokines in infection by *Histoplasma capsulatum*. *J. Immunol.* 190, 3427–3437. doi: 10.4049/jimmunol.1202122

Wüthrich, M., Gern, B., Hung, C. Y., Ersland, K., Rocco, N., Pick-Jacobs, J., et al. (2011). Vaccine-induced protection against 3 systemic mycoses endemic to North America requires Th17 cells in mice. *J. Clin. Invest.* 121, 554–568. doi: 10.1172/JCI43984

Wüthrich, M., Deepe, G., and Klein, B. (2012). Adaptive immunity to fungi. *Annu. Rev. Immunol.* 30, 115–148. doi: 10.1146/annurev-immunol-020711-074958

Wüthrich, M., LeBert, V., Galles, K., Hu-Li, J., Ben-Sasson, S. Z., Paul, W. E., et al. (2013). Interleukin 1 enhances vaccine-induced antifungal T-helper 17 cells and resistance against Blastomyces dermatitidis infection. *J. Infect. Dis.* 208, 1175–1182. doi: 10.1093/infdis/jit283

Wynn, T. A., and Ramalingam, T. R. (2012). Mechanisms of fibrosis: therapeutic translation for fibrotic disease. *Nat. Med.* 18, 1028–1040. doi: 10.1038/nm.2807

Xue, J., Chen, X., Selby, D., Hung, C. Y., Yu, J. J., and Cole, G. T. (2009). A genetically engineered live attenuated vaccine of *Coccidioides posadasii* protects BALB/c mice against coccidioidomycosis. *Infect. Immun.* 77, 3196–3208. doi: 10.1128/IAI.00459-09

Yamasaki, S., Matsumoto, M., Takeuchi, O., Matsuzawa, T., Ishikawa, E., Sakuma, M., et al. (2009). C-type lectin Mincle is an activating receptor for pathogenic fungus, *Malassezia*. *Proc. Nat. Acad. Sci. U. S. A.* 106, 1897–1902. doi: 10.1073/pnas.0805177106

Yang, F., Feng, C., Zhang, X., Lu, J., and Zhao, Y. (2017). The diverse biological functions of neutrophils, beyond the defense against infections. *Inflammation* 40, 311.23. doi: 10.1007/s10753-016-0458-4

Yao, Z., Painter, S. L., Fanslow, W. C., Ulrich, D., Macduff, B. M., Spriggs, M. K., et al. (1995). Human IL-17: a novel cytokine derived from T cells. *J. Immunol.* 155, 5483–5486.

Zhu, J., Yamane, H., and Paul, W. E. (2010). Differentiation of effector CD4 T cell populations. *Annu. Rev. Immunol.* 28, 445–489. doi: 10.1146/annurev-immunol-030409-101212

Zhu, L., Wu, Y., Wei, H., Xing, X., Zhan, N., Xiong, H., et al. (2011). IL-17R activation of human periodontal ligament fibroblasts induces IL-23 p19 production: Differential involvement of NF-κB versus JNK/AP-1 pathways. *Mol. Immunol.* 48, 647–656. doi: 10.1016/j.molimm.2010.11.008

Conflict of Interest: The authors declare that the research was conducted in the absence of any commercial or financial relationships that could be construed as a potential conflict of interest.

frontiers in Cellular and Infection Microbiology

ORIGINAL RESEARCH
published: 08 January 2021
doi: 10.3389/fcimb.2020.565571

Histoplasma capsulatum Glycans From Distinct Genotypes Share Structural and Serological Similarities to *Cryptococcus neoformans* Glucuronoxylomannan

Diego de Souza Gonçalves[1,2], Claudia Rodriguez de La Noval[1,3], Marina da Silva Ferreira[1,4], Leandro Honorato[3], Glauber Ribeiro de Sousa Araújo[5], Susana Frases[5], Claudia Vera Pizzini[6], Joshua D. Nosanchuk[7], Radames J. B. Cordero[8], Marcio L. Rodrigues[3,9], José Mauro Peralta[4], Leonardo Nimrichter[3] and Allan J. Guimarães[1]

[1] Laboratório de Bioquímica e Imunologia das Micoses, Departamento de Microbiologia e Parasitologia, Instituto Biomédico, Universidade Federal Fluminense, Niterói, Brazil, [2] Pós-Graduação em Doenças Infecciosas e Parasitárias, Faculdade de Medicina, Universidade Federal do Rio de Janeiro, Rio de Janeiro, Brazil, [3] Departamento de Microbiologia Geral, Instituto de Microbiologia Paulo de Góes, Universidade Federal do Rio de Janeiro, Rio de Janeiro, Brazil, [4] Departamento de Imunologia, Instituto de Microbiologia Paulo de Góes, Universidade Federal do Rio de Janeiro, Rio de Janeiro, Brazil, [5] Laboratório de Biofísica de Fungos, Instituto de Biofísica Carlos Chagas Filho, Universidade Federal do Rio de Janeiro, Rio de Janeiro, Brazil, [6] Laboratório de Micologia, Instituto Nacional de Infectologia Evandro Chagas, Fundação Oswaldo Cruz, Rio de Janeiro, Brazil, [7] Department of Microbiology and Immunology and Division of infectious Diseases, Albert Einstein College of Medicine of Yeshiva University, Bronx, NY, United States, [8] Department of Molecular Microbiology and Immunology, Johns Hopkins Bloomberg School of Public Health, Baltimore, MD, United States, [9] Instituto Carlos Chagas, Fundação Oswaldo Cruz (Fiocruz), Curitiba, Brazil

OPEN ACCESS

Edited by:
Yong-Sun Bahn,
Yonsei University, South Korea

Reviewed by:
Eva Pericolini,
University of Modena and Reggio Emilia, Italy
Andrew Alspaugh,
Duke University, United States

***Correspondence:**
Allan J. Guimarães
allanguimaraes@id.uff.br

Specialty section:
This article was submitted to Fungal Pathogenesis, a section of the journal Frontiers in Cellular and Infection Microbiology

Received: 25 May 2020
Accepted: 17 November 2020
Published: 08 January 2021

Citation:
Gonçalves DS, Rodriguez de La Noval C, Ferreira MS, Honorato L, Araújo GRdS, Frases S, Pizzini CV, Nosanchuk JD, Cordero RJB, Rodrigues ML, Peralta JM, Nimrichter L and Guimarães AJ (2021) Histoplasma capsulatum Glycans From Distinct Genotypes Share Structural and Serological Similarities to Cryptococcus neoformans Glucuronoxylomannan. Front. Cell. Infect. Microbiol. 10:565571. doi: 10.3389/fcimb.2020.565571

The cell wall is a ubiquitous structure in the fungal kingdom, with some features varying depending on the species. Additional external structures can be present, such as the capsule of *Cryptococcus neoformans* (*Cn*), its major virulence factor, mainly composed of glucuronoxylomannan (GXM), with anti-phagocytic and anti-inflammatory properties. The literature shows that other cryptococcal species and even more evolutionarily distant species, such as the *Trichosporon asahii, T. mucoides*, and *Paracoccidioides brasiliensis* can produce GXM-like polysaccharides displaying serological reactivity to GXM-specific monoclonal antibodies (mAbs), and these complex polysaccharides have similar composition and anti-phagocytic properties to cryptococcal GXM. Previously, we demonstrated that the fungus *Histoplasma capsulatum (Hc)* incorporates, surface/secreted GXM of *Cn* and the surface accumulation of the polysaccharide enhances *Hc* virulence *in vitro* and *in vivo*. In this work, we characterized the ability of *Hc* to produce cellular-attached (C-gly-*Hc*) and secreted (E-gly) glycans with reactivity to GXM mAbs. These C-gly-*Hc* are readily incorporated on the surface of acapsular *Cn* cap59; however, in contrast to *Cn* GXM, C-gly-*Hc* had no xylose and glucuronic acid in its composition. Mapping of recognized *Cn* GXM synthesis/export proteins confirmed the presence of orthologs in the *Hc* database. Evaluation of C-gly and E-gly of *Hc* from strains of distinct monophyletic clades showed serological reactivity to GXM mAbs, despite slight

differences in their molecular dimensions. These C-gly-*Hc* and E-gly-*Hc* also reacted with sera of cryptococcosis patients. In turn, sera from histoplasmosis patients recognized *Cn* glycans, suggesting immunogenicity and the presence of cross-reacting antibodies. Additionally, C-gly-*Hc* and E-gly-*Hc* coated *Cn* cap59 were more resistant to phagocytosis and macrophage killing. C-gly-*Hc* and E-gly-*Hc* coated *Cn* cap59 were also able to kill larvae of *Galleria mellonella*. These GXM-like *Hc* glycans, as well as those produced by other pathogenic fungi, may also be important during host-pathogen interactions, and factors associated with their regulation are potentially important targets for the management of histoplasmosis.

Keywords: cellular-attached glycans, extracellular glycans, GXM-like, *Histoplasma capsulatum*, *Cryptococcus neoformans*, pathogenesis

INTRODUCTION

Regardless of the species, all fungi possess a surrounding polysaccharide enriched cell wall that varies in composition and structural organization (Erwig and Gow, 2016; Gow et al., 2017). The main structure shared by several human pathogenic species is composed of an inner layer of chitin, a water-insoluble polymer of N-acetyl-glucosamine units linked by β-1,4-glycosidic bonds, and, just external to it, a layer of branched β-1,3- or β-1,6-glucans (Gow et al., 2017).

These fungal surface polysaccharides are pathogen-associated molecular patterns (PAMPs) that are efficiently recognized by pattern recognition receptors (PRRs) on the surface of innate immunity cells for the initiation of the immune response (Romani, 2011). Fungal β-1,3-glucan, the main content of the fungal cell wall, is recognized by Dectin-1 on the surface of macrophages and dendritic cells (Guimaraes et al., 2011; Gow et al., 2017). In turn, chitin is recognized by Toll-like receptor (TLR)- 2 (Shen et al., 2016) or indirectly mediate fungal recognition through Dectin-1 (Mora-Montes et al., 2011).

Differences in immune recognition among species are also given by specific surface components attached to these core layers, such as the pigment melanin in *Fonsecaea pedrosoi*, rodlets and galactomannans in *Aspergillus fumigatus*, glucuronoxylomannan (GXM) capsule in *Cryptococcus* sp. (Gow et al., 2017) and α-1,3-glucans in thermally dimorphic fungi, among others (Guimaraes et al., 2011; Gow et al., 2017; Ray and Rappleye, 2019). Despite mechanical protection for the fungal cells, all of these components are involved in the fungal escape of the immune response, since they all can shield cells from immune recognition (Rappleye et al., 2007; Erwig and Gow, 2016; Gow et al., 2017).

Among these, the capsular structure of *Cryptococcus* sp. has been extensively characterized and is considered one of the main virulence factors of the fungus. It is predominantly composed of two polysaccharides; GXM, the most abundant and having a wide range of dimensions and molecular weights, and glucuronoxylomannogalactan (GXMGal) fibers. These complex polysaccharides are synthesized by the incorporation of individually activated monosaccharide-nucleotides in secretory organelles, by the catalysis of multiple glycosyltransferases in the Golgi complex (Janbon, 2004; Yoneda and Doering, 2006; Zaragoza et al., 2009). Classical secretory pathways are involved in the secretion of GXM to the extracellular milieu, where they can be incorporated into the inner interface or external edge of the existing capsule at the cell surface (Yoneda and Doering, 2006). GXM attachment and correct capsule assembly are dependent on the presence of α-1,3-glucan, as mutants lacking this synthesis pathway have entirely compromised cell wall structure and display an acapsular phenotype (Reese and Doering, 2003; Reese et al., 2007).

Previous reports have characterized the capacity of fungi other than *Cryptococcus* sp. to efficiently incorporate GXM to their cell surfaces (Reese and Doering, 2003; Cordero et al., 2016). We have demonstrated that *Histoplasma capsulatum* (*Hc*) yeast cells promptly attach cellular and extracellular glycans of *Cryptococcus neoformans* (*Cn*) onto its cell wall *in vitro* and *in vivo*, which enhanced *Hc* virulence, by transferring the antiphagocytic, immune inhibitory and biofilm inducing properties of these cryptococcal polysaccharides to the newly encapsulated fungus (Cordero et al., 2016). As surface GXM anchoring by *Hc* was also dependent on α-1,3-glucan (Reese and Doering, 2003), this also raised the hypothesis that *H. capsulatum* shared similar structures on the cell surface and mechanisms for attaching carbohydrate fibers. This observation might pose an important mechanistic observation on the transfer of virulence factors among fungi and explain why patients with concomitant infections due to *Cn* and *Hc* generally have severe illnesses [reviewed in (Cordero et al., 2016)].

Besides *Cryptococcus* spp (Araujo et al., 2017), another *Basidiomycota* are also able to produce GXM-like molecules. *Trichosporon asahii* produces a functional GXM-like molecule with similar glycosyl composition to cryptococcal GXM that also manifests antiphagocytic activities (Fonseca et al., 2009). Recently, Zimbres et al. also described the production of GXM-like polysaccharides by *T. mucoides* (Zimbres et al., 2018). In the phylum *Ascomycota*, GXM-like structures have been identified in the dimorphic fungus *Paracoccidioides brasiliensis* (Albuquerque et al., 2012). These glycans are mainly composed of mannose and galactose, and traces of glucose, xylose, and rhamnose, and display a lower effective diameter relative to *Cn* GXM. Overall, as observed for *Trychosporum* sp., *P. brasiliensis* glycans react with a panel of mAbs to *Cn* GXM and are also incorporated by the cap59 acapsular mutant of *Cn*, forming a capsular-like structure and sharing the GXM-like antiphagocytic properties.

As *Hc* is able to attach *Cn* GXM to the yeast cell surface, we cannot discard the possibility that this fungus is also able to produce capsular or shed components with direct implications to fungal virulence, similar to those of *Cn, Hc* capsular material may be immunomodulatory. Notably, no comparative evaluation has been performed regarding the similarity of glycans shed by these two fungi. Herein, we aimed to molecularly characterize the cell-associated and secreted extracellular glycans of the fungus *Hc* by 1) determining the serological reactivity to mAbs raised to cryptococcal GXM to *Hc* glycans, 2) assessing glycan reactivity to serum from cryptococcosis and histoplasmosis patients, 3) defining the macromolecular structure and glycosyl composition of the glycans, and 4) determining the role of surface glycans during fungus interactions with phagocytic cells and 5) the role in pathogenesis in *Galleria mellonella* model. We found that these surface and extracellular glycans of *Hc* have similar functions to *Cn* GXM; hence, as with *Cn* and other GXM-like displaying fungi, *Hc* surface glycans may also be important for the immunomodulatory functions during the pathogenesis of histoplasmosis. Furthermore, the metabolic pathways of GXM-like production in *Hc* may also be novel targets for the development of new antifungal drugs and therapeutic strategies for the management of histoplasmosis.

METHODS

Fungal Strains and Growth Conditions

C. neoformans (*Cn*) var. *grubii* serotype A strain H99 (ATCC 208821) and the acapsular mutant *Cn* cap59 (ATCC 34873, derivative of Serotype D strain B3501) were kept on Sabouraud agar plates (Sigma-Aldrich, San Luis, MO, EUA). Colonies were inoculated in Sabouraud broth and kept at 37°C for 24 h under shaking at 150 rpm. For experimental procedures, subcultures were performed in minimal media (MM, 29.4 mM KH_2PO_4, 10 mM $MgSO_4$, 13 mM glycine, 3 μM thiamine and 15 mM D-glucose, pH 5.5) at 37°C for 48 h (Cordero et al., 2016). *H. capsulatum* (*Hc)* var. *capsulatum* strains from distinct monophyletic clades as established previously (Teixeira Mde et al., 2016; Sepulveda et al., 2017), *Hc* G217B (ATCC 26032), *Hc* G184A (ATCC 26027) and *Hc* CIB1980 (a kind gift from Corporación para Investigaciones Biológicas, Colombia) strains were cultured in HAM's F-12 (ThermoFisher Scientific) medium supplemented with glucose (18.2 g/L), glutamic acid (1 g/L), HEPES (6 g/L), and cysteine (8.4 mg/L) at 37°C for 48 h with 150 rpm shaking (Guimarães et al., 2009).

Isolation of Cellular-Attached and Extracellular Fungal Glycans

After 48 h, 1 L cultures of *Hc* G217B, *Hc* G184A and *Hc* CIB1980 or *Cn* H99 yeast cells were separately centrifuged for 10 min at 1100 x *g*. Cell pellet and cell-free culture supernatants were collected for the extraction of cellular-attached glycans (C-gly) and isolation of shed extracellular glycans (E-gly) respectively as described (Frases et al., 2008; Cordero et al., 2016). C-gly extraction was carried out by DMSO extraction. Briefly, yeast pellets obtained upon centrifugation were washed with PBS (8.0 g/L NaCl, 0.2 g/L KCl, 0.2 g/L KH_2PO_4, 1.2 g/L Na_2HPO_4, pH 7.2) and incubated in DMSO for 1 h with 150 rpm shaking and centrifuged. E-glys were obtained by ultrafiltration of the cell-free culture supernatant using an Amicon cell coupled with a nitrocellulose membrane with a nominal molecular weight limit (NMWL) of 10 KDa (Millipore, MA, USA) and N_2. Concentrated C-gly and E-gly were dialyzed against MilliQ water for 24 h, using a 3.5 KDa cut-off dialysis tube with at least 8 water exchanges performed. Glycans were lyophilized using standard protocols. Polysaccharide (PS) concentration of C-gly and E-gly were measured by phenol-sulfuric acid method as described (Masuko et al., 2005).

Binding of GXM mAbs to Cellular-Attached and Extracellular Glycans

ELISA plates were coated with 50 μl/well of a 10 μg/ml *Cn* or *Hc* glycans solution in PBS for 1 h at 37°C, followed by an overnight step at 4°C. Plates were washed 3X with TBS-T (8.0 g/L NaCl, 1.21 g/L Tris base, 0,01% Tween 20, pH 7.2) and blocked with blocking solution (1% BSA in TBS-T) for 1 h at 37°C. After washes with TBS-T, mAbs to GXM (Mukherjee et al., 1993), IgG1 18B7 or IgMs 2D10, 13F1, and 12A1 or irrelevant antibody 5C11 as a control at 25 μg/ml were serially diluted (1:2) in blocking solution across the plates and incubated at 37°C for 1 h. Wells were washed (3X) and incubated with goat anti-mouse Ig (Southern Biotech) at 1 μg/ml for 1 h at 37°C. After washes, plates were incubated with 1mg/ml of p-nitrophenylphosphate (pNPP, Sigma-Aldrich). Absorbances were recorded at 405 nm. Experiments were performed in triplicates and results shown are the average of three independent experiments.

Incorporation of *Hc* C-gly by an acapsular mutant of *Cn*

Approximately, $5x10^6$ *Cn* cap59 yeasts were suspended in 50 μg/ml of C-gly preparations from *Hc* G217B (C-gly-*Hc*) reference strain (10 μg/10^6 cells) (Cordero et al., 2016). The cell suspension was incubated for 1 h at 37°C under agitation and extensively washed with PBS to remove unbound glycans. As controls, *cap59* cells were incubated with C-gly-*Cn* H99 (positive) or PBS alone (negative) were used. Yeasts (10^6) of *Hc* G217B were also used in parallel. After three washes with PBS and centrifugations at 1100 x *g* for 10 min, yeasts were suspended in 100 μl of a solution containing 10 μg/ml mAb 18B7 (IgG1) in 1% BSA in PBS and incubated for 1 h at 37°C in an orbital shaker. Following incubation, cells were washed (3X) with PBS and collected by centrifugation. Cell pellets were suspended in 100 μl of a 5 μg/ml solution of a goat anti-mouse IgG Alexa 488-conjugated (Southern Biotech) in blocking solution and incubated for 1 h at 37°C. After three washes with PBS, yeasts were stained using 0.5 mg/ml of Uvitex 2B (stains chitin in cell wall). Cells were washed, suspended in mounting solution (Biomeda Corp, Foster City, CA), applied to a microscopy slide, and examined in a Zeiss Axiovert 200 fluorescence inverted phase and contrast microscope using a 100X/1.30 Oil Plan Neofluar objective (Carl Zeiss MicroImaging, Inc.).

Glycosyl Composition Analysis

C-gly preparations from *Hc* G217B and *Cn* H99 were lyophilized and analyzed at the Complex Carbohydrate Research Center (CCRC, Athens, GA, USA) as described (Guimaraes et al., 2010). Samples were dissolved in methanol/1M HCl, followed by incubation for 18 h at 80°C for methanolysis. Then, samples were per-O-trimethylsilylated with Tri-Sil (Pierce) for 30 min at 80°C.

Derivatives were separated on a HP5890 gas-chromatography coupled with a Supelco DB-1 silica capillary column (30 m × 0.25 mm ID). Detected peaks were fragmented and detected in tandem with a 5,970 MSD mass spectrometer. Monosaccharide standards consisted of arabinose, dulcitol, fucose, galactose, galacturonic acid, glucose, glucuronic acid, mannitol, mannose, N-acetyl gucosamine, rhamnose, sorbitol and xylose. Molecular ratios were calculated by dividing the percentage of each carbohydrate measured in the sample by its respective molecular weight. The values reported are representative of two independent analysis using different sample batches, with similar results.

Zeta Potential Analysis

Zeta potential (Z) of *Cn* H99 and acapsular mutants *Cn* cap 59 incubated with either PBS, C-gly-*Cn* H99, or C-gly-*Hc* G217B as described above, were measured in a Zeta potential analyzer (NanoBrool Omni particle, Brookhaven Instruments Corporation, Holtsville, NY) at 25°C as described (Frases et al., 2008).

Comparative Analysis of Fungal Proteins Involved in Surface Glycan Production

Several *Cn* capsule synthesis and GXM export related proteins have been described (Chang and Kwon-Chung, 1994; Chang et al., 1996; Chang and Kwon-Chung, 1998; Chang and Kwon-Chung, 1999; Levitz et al., 2001; Janbon, 2004; Moyrand et al., 2004; Zaragoza et al., 2009; Albuquerque et al., 2012). Their respective accession numbers were recorded after searches of several databases (GenBank, Swiss-Prot/TrEMBL and Uniprot) and were grouped according to their function/families: acetyltransferases, mannosyltransferases, xylosyltransferases and miscellaneous proteins, also including proteins involved in the secretion of GXM (Albuquerque et al., 2012). Each candidate was used as a query sequence in BLAST analysis (Madera and Gough, 2002), using a threshold of 1000, an automated matrix (BLOSUM 62), and a minimum of 1000 hits. Orthologs protein hits found in *Ajellomyces capsulatus* strain Nam1/WU24 (North America 1 clade) or *A. capsulatus* strain G186AR H82/ATCC MYA-2454/RMSCC 2432 (Panama clade) were utilized to construct the **Supplementary Table 1**, which included information about protein length (number of amino acids), molecular weight, percentage of identity of *Hc* protein hits to its respective *Cn* query protein, alignment score and E-value. The family, homology and domains (and their residues) of the proteins found in the database were determined using the Pfam hidden Markov models, and the databases Interpro (http://www.ebi.ac.uk/interpro) and Pfam (http://pfam.sanger.ac.uk/). Proteins were considered related when belonging to the same family and carrying out similar metabolic processes (Finn et al., 2008; Bowden et al., 2010).

Glycan Hydrodynamic Size Determination

Average hydrodynamic size and polydispersity values of glycan samples (1 mg/ml in PBS) were obtained by Dynamic Light Scattering (DLS) analysis in a 90Plus/BI-MAS NanoBrook Omni particle (Brookhaven Instruments Corporation, Holtsville, NY) as described (Frases et al., 2008; Guimaraes et al., 2010). The average diameter was considered the diameter of the imaginary cylinder coaxial with the thread. Size values are the average of 10 repeated measurements.

Sera of Patients With Histoplasmosis and Cryptococcosis Patients and Healthy Individuals

Patients (>18-years old) included in the study were residents of the Rio de Janeiro State filling the proposed requirements and criteria for the classification of histoplasmosis and cryptococcosis established by the European Organization for Research and Treatment of Cancer/Invasive Fungal Infections Cooperative Group and the National Institute of Allergy and Infectious Diseases Mycoses Study Group (EORTC/MSG) Consensus Group (De Pauw et al., 2008). These comprised diagnosis confirmation by "gold standard" fungal isolation in culture from clinical specimens of probable cases; compatible clinical (X-ray imaging), epidemiological and laboratorial records, including antibody detection against histoplasmin by immunodiffusion or *Cryptococcus* antigen detection by latex agglutination (Immuno-mycologics Inc., Norman, OK, EUA). Sera obtained from 2009 to 2018 at the Imunodiagnosis branch of the Mycology Laboratory at the National Institute of Infectious Diseases (NIID), were restricted to the first serum sample collected from patients without previous treatment for any of the diseases. Control sera were obtained from healthy subjects (27-34-years old) screened for several mycosis, including histoplasmosis, cryptococcosis, paracoccidioidomycosis and aspergillosis, who offered negative results by immunodiffusion, latex agglutination and culturing. Patients <18-years old and those without clearly accessible clinical records were excluded. The use of patient sera was approved by the ethics committee of the NIID/FIOCRUZ (Protocol number 68563017.0.0000.5262).

Indirect ELISA for Cross-Reactivity Assessment of *Hc* and *Cn* Glycans

ELISA plates were coated with 50 µl/well of a 10 µg/ml C-gly or E-gly solutions of either *Hc* or *Cn* in PBS for 1 h at 37°C, followed by an overnight incubation at 4°C. Plates were washed 3X and blocked with blocking solution (5% skin milk in TBS-T) for 1 h at 37°C. After washes, sera from healthy individuals or patients with either histoplasmosis or cryptococcosis were initially diluted at 1:100 in blocking solution. Plates were incubated at 37°C for 1 h, washed with TBS-T and incubated with goat anti-human Ig (Southern Biotech) at 1 µg/ml for 1 h at 37°C. After washes, plates were incubated with pNPP for 30 min. Absorbances were recorded at 405 nm. Experiments were performed in triplicates and results shown are the average of two independent experiments. "Cut-off value" for reactivity was defined as the average of absorbances obtained for sera of healthy individuals + 3x(standard deviation) as previously described (Guimarães et al., 2010). Histoplasmosis and cryptococcosis patient sera above the "cut-off" were considered reactive.

Association With Macrophages

Four-to-six weeks-old female C57Bl/6 mice were obtained at the Laboratory Animal Center (NAL) of the Fluminense Federal University (Niteroi, RJ, Brazil) and housed in pathogen-free facilities, with *ad libitum* access to food and water. Their use was approved by the Ethics committee for animal use of the Fluminense Federal University (protocol 5486190618), and standard protocols followed for the isolation of bone-marrow

derived macrophages (Zhang et al., 2008). Macrophages were plated at $4x10^5$ cells/well to a 24-well cell culture plate and kept in a 5% CO_2 incubator at 37°C. *Cn* cap59 yeasts were previously incubated with 40 μg/ml of NHS-Rhodamine (ThermoScientific, USA) for 30 min at 25°C and washed extensively with excess of PBS. Cells were incubated with the distinct *Cn*-gly, *Hc*-gly or control PBS at 37°C in an orbital shaker as described above. Following incubation, cells were washed, suspended in DMEM and enumerated. Yeasts were added to the macrophages in a 5:1 (yeast: macrophage) ratio and plates incubated for 1 h/5% CO_2. After three washes with PBS, macrophages were detached from the plates, washed and fixed overnight with a 4% formaldehyde solution. Samples were analyzed in a FACSCalibur (BD, USA), macrophages cells were gated and the percentage of fungi associated macrophages (% $FL2^+$) was calculated dividing the number of fungi associated macrophages ($FL2^+$ cells) over the total analyzed macrophages, as described (Cordero et al., 2016; Guimarães et al., 2019). Association experiments were performed twice, with similar results. Inhibition of interaction by each fungal glycan was calculated independently as the relative decrease of interaction levels to control *Cn cap59* for each experiment and averaged.

Yeast Killing Assay

Cn Cap59 yeasts were coated with the distinct *Hc*-gly, or incubated with *Cn*-gly or PBS as positive and negative controls, respectively. Gly-coated *Cn* cap59 yeast cells were suspended in DMEM and added in a 5:1 (yeast: macrophage) ratio to 96-well culture plates containing 10^5 macrophages/well. Plates were incubated overnight at 37°C under 5% CO_2. The wells were washed with cold sterile PBS and macrophages lysed by adding sterile water. Aliquots were plated onto Sabouraud agar plates and incubated at room temperature for 2–3 days. The number of colony forming units was enumerated and values compared among groups.

Hc-Glycans and Survival in Invertebrate Models

Larvae of *G. mellonella* (100-150 mg) in the final instar larval stage and without any signs of dark spots or melanization and pupation were selected. To test the impact of *Hc*-gly coating on fungal virulence, 10^5 yeasts of *Cn* cap59 were coated with 10 μg of each of the C-gly and E-gly from either *Hc* isolate or PBS as a control, as described above. Sham infection and PBS injections in the absence of yeasts (uninfected larvae) were used as controls to assess for the impact of injections and survival. A parallel survival experiment was also performed with 10^6 yeasts coated with 100 μg of each of glycan. After washes (3X), yeasts were suspended in 10 μl of PBS and injected in the last left pro-leg of larvae of *Galleria mellonella.* At least 10 larvae were used per group in each experiment. The numbers of living larvae were monitored twice daily and recorded. Experiments were performed twice and similar results were documented.

Statistical Analysis

All analyses were performed using GraphPad Prism version 8.00 for Windows (GraphPad Software, San Diego California USA). Ordinary One-way ANOVA test was performed for comparison among groups, with a 95% confidence interval in all experiments. Individual mean comparison to controls or between every other group was performed using Dunnett's or Tukey's post-tests. Survival results were analyzed by Kaplan-Meyer to determine the difference among groups ($p<0.05$).

RESULTS

MAbs to the Capsule of *Cn* Are Reactive to *Hc* Glycans

Serological reactivity of *H. capsulatum* (*Hc)* and *C. neoformans* (*Cn*) isolated glycans was compared using a panel of mAbs against cryptococcal GXM. Confirming previous studies (Mukherjee et al., 1993; Cordero et al., 2016), extracted C-gly-*Cn* H99 displayed a dose-dependent binding profile (**Figure 1A**) with 12A1 (IgM) displaying the highest reactivity, followed by 2D10 (IgM), 18B7 (IgG) and 13F1 (IgM). C-gly-*Hc* G217B showed only binding by the 18B7 mAb (**Figure 1B**). Binding profile of GXM mAbs to E-gly-*Hc* G217B (**Figure 1D**) was similar to that observed for E-gly-*Cn* H99 (18B7 > 2D10 > 12A1 > 13F1, **Figure 1C**), besides lower values of maximum binding. Overall, mAbs to GXM reacted to both cellular-attached C-gly-*Hc* G217B and extracellular E-gly-*Hc* G217B glycans, with the highest binding of the mAb 18B7, suggesting the presence of GXM-like epitopes in *Hc.*

GXM mAbs React to the Yeast Phase Surface Polysaccharides of *Hc*

Cross-reactivity of GXM-mAb 18B7 to *Hc* glycans led us to evaluate the C-gly distribution and reactivity pattern over the *H. capsulatum* surface by immunofluorescence. This mAb reacts with yeast of *Cn* H99 by immunofluorescence showing a bright ring pattern (Guimaraes et al., 2010; Cordero et al., 2016). For *Hc* G217B yeast, some displayed a ring pattern, with regions showing more concentrated labeling (**Figure 2A**), although the majority of yeasts had a discrete dotted pattern of labeling along with the entire cell wall extension (**Figure 2B**).

Incorporation of C-gly-Hc by Acapsular Mutants of *Cn*

We previously reported that *Hc* incorporates *Cn* glycans *in vitro* and *in vivo* (Cordero et al., 2016). In turn, we now examined whether *Hc* glycans could be incorporated by an acapsular mutant of *Cn* (*cap59*). The PS production by *Cn cap59* is defective and, subsequently, is not able to form a capsular network, as indicated by the absence of binding by the 18B7 mAb (**Figure 2C**). However, this strain retains the ability to incorporate exogenously added cryptococcal PS (Reese and Doering, 2003; Garcia-Rivera et al., 2004), as confirmed by C-gly-*Cn* H99 incorporation resulting in the appearance of a ring-like (e.g. circumferential) labeling, with some punctate enriched regions on *Cn cap59* yeasts after sequential incubation with mAb 18B7 (**Figure 2D**). We found that *Cn cap59* incorporates the heterologous C-gly-*Hc* G217B into its cell wall, displaying a similar pattern to the C-gly-*Cn* H99 incorporation, suggesting the presence of conserved anchoring mechanisms for glycans of distinct fungal origin (**Figure 2E**).

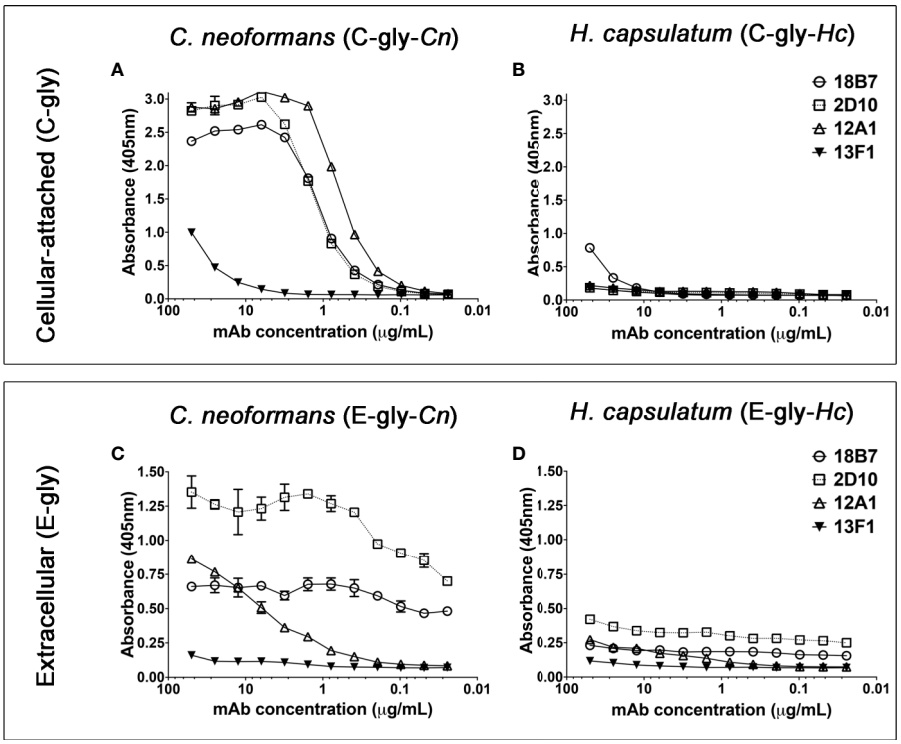

FIGURE 1 | Monoclonal antibodies (MAbs) to *C. neoformans* glucuronoxylomannan (GXM) are able to bind cellular-attached (C-gly) and extracellular (E-gly) glycans of *H. capsulatum*. **(A, B)** The most widely used mAbs against CTAB-purified GXM from *C. neoformans* (12A1, 2D10, 13F1, and 18B7) were tested against DMSO extracted cellular-attached glycans of **(A)** *C. neoformans* H99 (C-gly-*Cn* H99) and **(B)** *H. capsulatum* G217B (C-gly-*Hc* G217B); the last displayed reactivity only to the 18B7 mAb, but in lower magnitude compared to control C-gly-*Cn* H99 ($p<0.05$). **(C, D)** GXM specific mAbs also reacted more efficiently with extracellular glycans of *C. neoformans* (E-gly-*Cn* H99) than **(D)** *H. capsulatum* (E-gly-*Hc* G217B; $p<0.05$), despite the similar relative reactivity ranking of the mAbs.

Cn and *Hc* C-glys Analysis Reveals Distinct Glycosyl Composition and Charge

Cn and *Hc* C-gly were extracted, and their relative glycosyl composition compared (**Supplementary Figures 1A, B**). C-gly-*Cn* H99 was mostly composed of glucose (54.7%), followed by mannose (23.4%) and xylose (14.4%); glucuronic acid represented 4.7% of total composition (**Figure 3A**). C-gly-*Cn* H99 also displayed small amounts of galactose (2.8%), which may be from traces of GXMGal composing these fractions. However, C-gly-*Hc* G217B displayed a significantly different composition than C-gly-*Cn* H99 being mostly composed of mannose (64.8%; $p<0.001$), followed by glucose (17.9%; $p<0.0001$; **Figure 3A**). Galactose was also detected at 12.7% ($p<0.001$) and N-acetyl glucosamine in 4.6% of total carbohydrate composition, with the later being absent in C-gly-*Cn* H99 ($p<0.05$). As opposed to C-gly-*Cn* H99, *x*ylose and glucuronic acid were not detected in the C-gly-*Hc* G217B fractions ($p<0.0001$ and $p<0.05$, respectively).

The absence of negative charge residues of glucuronic acid in the C-gly-*Hc* G217B, led us to evaluate the overall surface charge change upon incorporation by *Cn* cap59 mutants (**Figure 3B**). *Cn* H99 controls had a zeta potential of −52.5±7.0 mV, which was much greater in magnitude than the charge of the acapsular *Cn* cap59, −13.7±2.6 mV ($p<0.0001$). Incorporation of C-gly-*Cn* H99 restored the values to −42.9±10.0 mV relative to *Cn* H99 ($p>0.05$). In contrast, C-gly-*Hc* G217B incorporation by *Cn* cap59 did not significantly affect surface charge (−21.9±5.0 mV, $p>0.05$).

Cryptococcal Capsular Protein Orthologs in *Hc*

Given the unexpected serological reactivity of *Hc* glycans to cryptococcal GXM-specific mAbs, we performed a high BLAST probability analysis of *Cn* capsular protein orthologs in the *Hc* genome (strains NAm1/WU24 and G186AR/H82/ATCC MYA-2454/RMSCC 2432, belonging to the NAm1 and Panama clades, respectively (Sepulveda et al., 2017) and a comparison of the relationship between the nearest orthologs allowed us to predict protein functions. A total of 39 *Cn* proteins recognized in the participation of capsule synthesis and assembly (Zaragoza et al., 2009) were organized in four main groups (acetyltransferases, mannosyltransferases, xylosyltransferases and miscellaneous) and used in a general BLAST search (**Supplementary Table 1**). In the acetyltransferase group, 4 out of 13 cryptococcal proteins (Cas4p, Cas8, Cas41p, Cas41p, and Cas42p; 31%) had orthologs in both Nam 1 and Panama strains (**Figure 4A**). Orthologs of the Cas91 and Cas92 proteins were also found specifically in the Panama strain. Regarding the three *Cn* mannosyltransferases (Cap59, Cap60, and

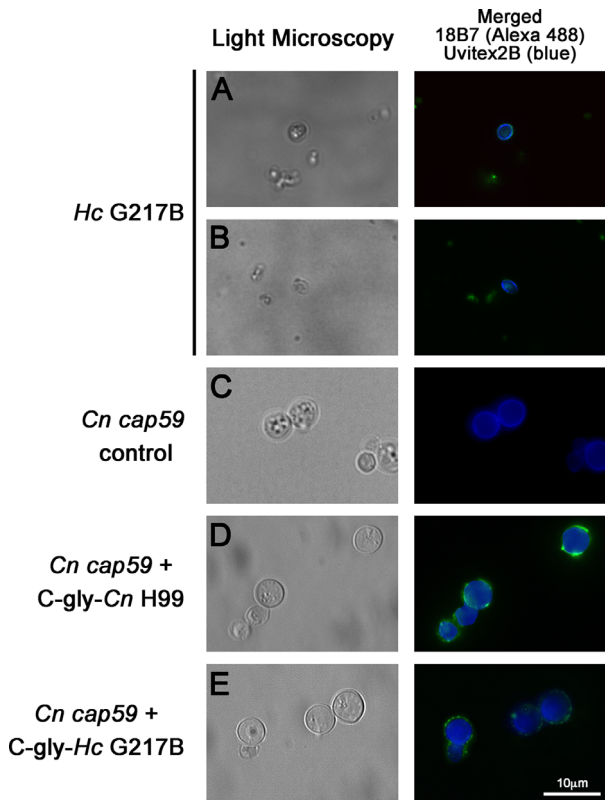

FIGURE 2 | Glucuronoxylomannan (GXM) monoclonal antibodies (mAbs) bound to the C-gly on the *H. capsulatum* yeast surface, and these extracted glycans are promptly incorporated by acapsular mutants of *C. neoformans*. **(A, B)** The 18B7 mAb to *C. neoformans* GXM bound C-gly-*Hc* on the surface of the *H. capsulatum* (*Hc*) yeast, with labeling ranging from a **(A)** punctuated to a **(B)** ring pattern. **(C–E)** Acapsular *C. neoformans cap59* (*Cn cap59*) mutants were used in glycans incorporation. **(C)** *Cn cap59* incubated with PBS as negative control did not display binding by 18B7 mAb. **(D)** Incubations of *Cn* cap59 with C-gly-*Cn* H99 used as a positive control did not result in capsular structure visible by light microscopy, but surface incorporation was detected by binding of the 18B7 mAb through immunofluorescence. **(E)** *Cn* cap59 incubation with C-gly-*Hc* resulted in a similar pattern to C-gly-*Cn*, suggesting conserved anchoring mechanisms of glycans from distinct origin. Pictures were taken with an 100X objective magnification. Scale bar = 10 μm.

CMT1, **Figure 4B**) and the two mannosyltransferases (Cap10 and CXT1, **Figure 4C**) all the proteins evaluated had orthologs in both *Hc* strains. Lastly, from the miscellaneous class, 15 out of 21 cryptococcal proteins (71.4%) evaluated had orthologs in both Nam1 and Panama (**Figure 4D** and **Supplementary Table 1**). Importantly, absence of orthologs to *UGD1 Cn* UDP-glucose 6 dehydrogenase, which converts UDP-glucose into UDP-glucuronic acid, nor *UUT1 Cn* UDP-glucuronic acid transporter in *Hc* genome could explain the lack of glucuronic acid in the in the C-gly-*Hc* fractions, whereas the lack of its downstream derivative xylose is directly associated to the missing ortholog to UXS1 *Cn* UDP-glucuronic acid decarboxylase, which catalyzes the conversion of UDP-glucuronic acid into UDP-xylose. Overall, from all the *Cn* proteins, 61.5% (24 out of 39) had orthologs in the *Hc* Nam1 genotype, whereas 69.2% (25/35) had orthologs in the *Hc* Panama genotype, with a high correlation of similarities to *Cn* orthologs between these two strains (**Supplementary Figure 2**). The presence of cryptococcal capsular-related proteins orthologs in the *Hc* genome is consistent with the development of similar phenotypic traits to *Cn* under certain growth conditions, particularly in presenting exposed glycan structures that are ultimately sensed and processed by host immune components.

Cryptococcal GXM mAb 18B7 Binds Cellular-Attached and Extracellular Fractions of *Hc* From Three Distinct Clades

To evaluate the distribution of GXM-like epitopes on C-gly-*Hc* and E-gly-*Hc*, we have extracted these fractions from three distinct monophyletic species of *Hc* and performed an ELISA with the cross-reactive mAb 18B7 (**Figure 5**). Controls of C-gly-*Cn* H99 confirmed higher binding of mAb 18B7 in comparison to C-gly-*Hc* (**Figure 5A**). However, comparison of mAb 18B7 reactivity among C-gly-*Hc* demonstrated higher binding to C-gly-*Hc* G184A and C-gly-*Hc* CIB1980, and slightly less binding to C-gly-*Hc* G217B from the reference strain. Evaluation of mAb 18B7 binding to E-gly also revealed the highest binding to E-gly-*Cn* H99 as expected (**Figure 5B**). All three E-gly-*Hc* evaluated (*Hc* G217B, *Hc* G184A, and *Hc* CIB1980), however, displayed similar low reactivity to mAb 18B7 ($p>0.05$).

Size of *Hc* Glycans From Three Distinct Clades

The slight differences in reactivity of *Cn* GXM mAb to C-gly-*Hc and* E-gly-*Hc* led us to examine the *Hc* surface glycans in more refined detail. We have compared the average hydrodynamic sizes of cellular-attached glycans (C-gly) isolated from *Cn* H99 (C-gly-*Cn* H99) and the three distinct isolates of *Hc* (C-gly-*Hc*) yeast cells (**Figure 6**). As our reference, C-gly-*Cn* H99 exhibited two main populations, with a small group ranging from 1,230 to 1,421 nm and a larger fraction from 6030 to 8654 nm (effective diameter= 7,212 nm, **Figure 6A**). The C-gly-*Hc* diameter had slight variations depending on the clade the strain belonged to. C-gly-*Hc* G217B displayed a small population ranging from 72 to 778 nm and a larger population from 1,800 to 3,600 nm (effective diameter= 1,802 nm, **Figure 6B**). The C-gly-*Hc* G184A in turn, overall displayed two populations of smaller sizes than the C-gly-*Hc* G217B, with a small population ranging from 83 to 282 nm and a larger population from 1,085 to 1,770 nm (effective diameter 487 nm, **Figure 6C**). The C-gly-*Hc* CIB 1980 displayed the shortest fibers, with a small population ranging from 129 to 165 nm and a larger population from 350 to 450 nm (effective diameter 254 nm, **Figure 6D**).

Regarding the extracellular glycans, the E-gly-*Cn* control displayed two populations, a small from 139 to 286 nm and a larger ranging from 2,312 to 4,040 nm (effective diameter= 1,930 nm, **Figure 6E**). *Hc* yeasts secreted smaller fibers, with the E-gly-*Hc* G217B displaying a small population from 118 to 185 nm and a larger from 995 to 1743 nm (effective diameter= 808 nm, **Figure 6F**). The E-gly-*Hc* G184A displayed a small from 101 to 152 nm and a larger from 528 to 799 nm (effective diameter=

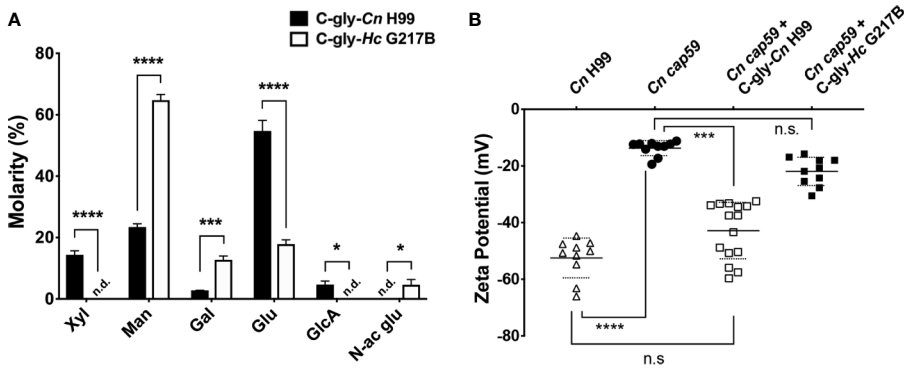

FIGURE 3 | Cellular-attached glycans of *C. neoformans (Cn)* and *H. capsulatum (Hc)* had distinct glycosyl composition. **(A)** Molarity percentage of the monosaccharide blocks detected by GC-MS analysis, displaying a distinct composition with comparing the C-gly-*Cn* H99 and C-gly-*Hc* G217B. Notably, no glucuronic acid was found in C-gly-*Hc* G217B, which could influence charge. Xyl, xylose; Man, mannose; Gal, Galactose; Glu, glucose; GlcA, Glucuronic acid; N-ac glu, N-acetyl glucosamine. n.d., not detected (*p < 0.05, ***p < 0.001, and ****p < 0.0001). **(B)** Zeta potential experiments were used to measure the overall charge of cap59 *C. neoformans* yeast. Incorporation of C-gly-*Cn* H99 to *Cn cap59* significantly increased the magnitude of the negative charge, whereas the addition of C-gly-*Hc* G217B had a limited effect on the charge (***p = 0.007; ****p < 0.0001).

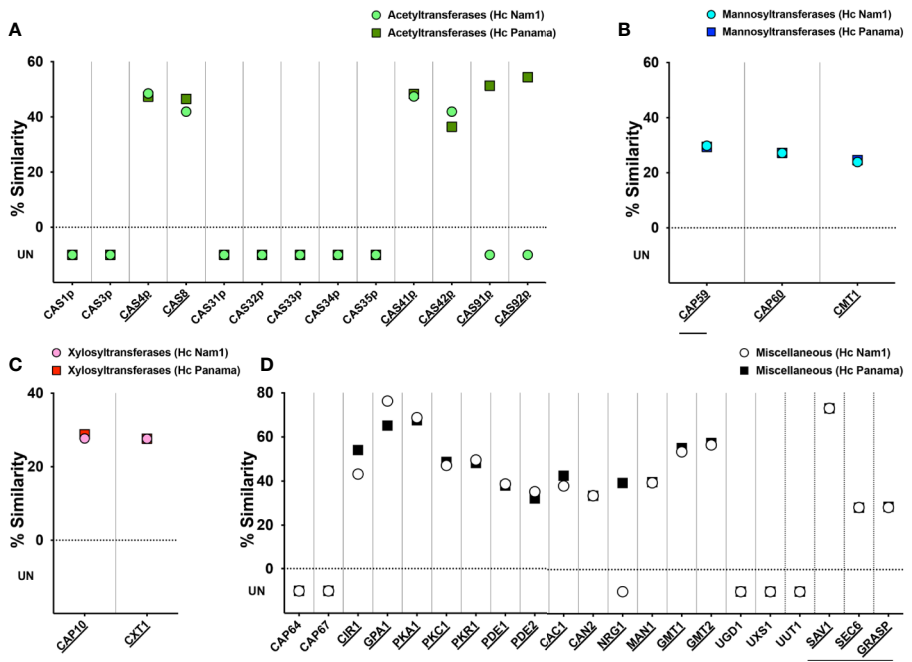

FIGURE 4 | Similarity of glucuronoxylomannan synthesis and capsular production-related proteins of *C. neoformans (Cn)* and *H. capsulatum (Hc)*. *Cn* var. *grubii* serotype A (strain H99/ATCC 208821) proteins were clustered into four groups: **(A)** acetyltransferases (green), **(B)** mannosyltransferases (blue), **(C)** xylosyltransferases (pink), and **(D)** miscellaneous (white) and sequences blasted un Uniprot in a search for orthologs from *Hc* Nam1/WU24 (light color) and the Panama/G186AR strain/H82 strains (dark colors). Similarities were recorded and used to construct the graphs of each specific protein class. Underlined protein names indicate those *C. neoformans* proteins with orthologs in *Hc*, with identical protein domains/families as annotated by Interpro/Pfam. Horizontal lines indicate proteins involved in glucuronoxylomannan (GXM) export.

445 nm, **Figure 6G**). In the other hand, the E-gly-*Hc* CIB 1980 displayed the largest fibers with a small population from 5 to 244 nm and a larger from 694 to 1,054 nm (effective diameter of 290 nm, **Figure 6H**). Overall, the small differences observed for the C-gly-*Hc* were also similarly observed for the E-gly-*Hc* (*Hc* G217B> *Hc* G184A > *Hc* CIB 1980) from distinct strains.

Serological Cross-Reactivity of Sera From Cryptococcosis Patients to *Hc* Glycans

The reactivity of 18B7 mAb to *Hc*-gly led us to evaluate whether antibodies naturally generated during cryptococcosis that react with *Cn*-gly were also able to bind to *Hc*-gly. Sera of five patients with cryptococcosis were initially screened against C-gly-*Cn* H99 and

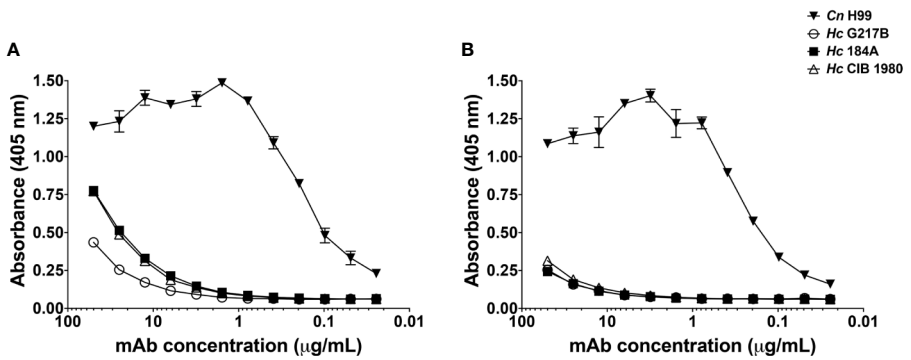

FIGURE 5 | MAb 18B7 to capsular antigens of *C. neoformans (Cn)* reacted similarly to cellular-attached (C-gly) and extracellular (E-gly) polysaccharides of distinct strains of *H. capsulatum (Hc)* belonging to three different monophyletic branches. Reactivity of 18B7 mAb to **(A)** C-gly and **(B)** E-gly was compared among the *Cn* H99 control and *Hc* strains from three distinct monophyletic branches: *Hc* G217B, *Hc* G184A, and *Hc* CIB1980.

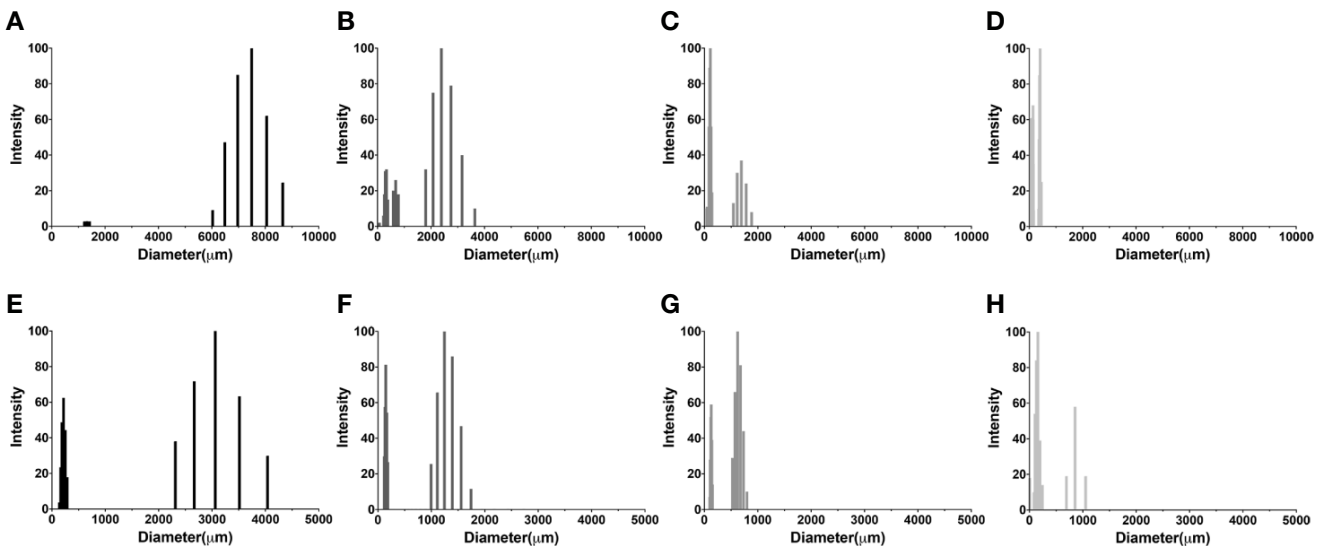

FIGURE 6 | Comparison of C-gly and E-gly dimensions of *C. neoformans (Cn)* and strains of *H. capsulatum (Hc)* from three different monophyletic branches (Nam 2 *Hc* G217B, Panama *Hc* G186, and LAm CIB 1980) reveals structural differences and distinct architecture. Dynamic light Scattering (DLS) was used to measure the fiber dimensions of cellular-attached and extracellular glucans of both fungi. Cellular-attached glycans of: **(A)** C-gly-*Cn* H99, **(B)** C-gly-*Hc* of *Hc* G217B, **(C)** C-gly-*Hc* of *Hc* G184A and **(D)** C-gly-*Hc* of Hc CIB1980 strains. Extracellular glycans of: **(E)** E-gly-*Cn* H99, **(F)** E-gly-*Hc* of *Hc* G217B, **(G)** E-gly-*Hc* of *Hc* G184A, and **(H)** E-gly-*Hc* of *Hc* CIB1980 strains.

E-gly-*Cn* H99 to confirm the presence of reacting antibodies to these fractions (as controls for serum from patients with cryptococcosis and their reactivity, shown in **Figures 8A, B**, respectively). Then, their reactivity against C-gly-*Hc* and E-gly-*Hc* of distinct clades was compared to sera from patients with histoplasmosis. Overall, average absorbances for sera from patients with cryptococcosis reacting to either C-gly-*Hc* G217B or C-gly-*Hc* G184A had similar values to "cut off", as 3 out of 5 sera from cryptococcosis patients (sera 1, 4 and 5) displayed good reactivity to both (**Figure 7A**). When sera from cryptococcosis patients were tested against C-gly-*Hc* CIB1980, average absorbances were about 3 times higher than "cut off" values, with all five sera demonstrating good reactivity (*p<0.05). Therefore, reactivity comparison of sera from cryptococcosis patients among the three C-gly-*Hc* indeed revealed that the best reactivity was to C-gly-*Hc* CIB1980 (###p<0.001).

Regarding the reactivity of sera from cryptococcosis patients to E-gly-*Hc*, only one serum (serum 2) had good reactivity to E-gly-*Hc* G217B, with average values below the "cut-off" (**Figure 7B**). Reactivity to E-gly-*Hc* G184A was observed with three out of five sera (sera 2, 3, and 5), with average of absorbance above the "cut off". Lastly, all sera from cryptococcosis patients displayed reactivity to E-gly-*Hc* CIB1980, with average of absorbances about three times than "cut off" (*p<0.05), configuring the best reactivity among the E-gly-*Hc* (###p<0.001).

Cross-Reactivity of Antibodies From Histoplasmosis Patients to *Cn*-Glycans

To also evaluate the humoral immunogenicity of *Hc*-gly, we tested the cross-reactivity of sera from patients with histoplasmosis against *Hc*-gly, and verified whether raised antibodies also recognized epitopes in *Cn*-gly (**Figure 8**). Their reactivity to C-gly-*Hc* and E-gly-*Hc* from distinct *Hc* strains are found on **Figures 7A, B**, respectively. These sera displayed average absorbances for C-gly-*Hc* G217B and C-gly-*Hc* G184A of 2.4 and 3.2 times higher than "cut-off" values (*p<0.05 and **p<0.01, respectively; **Figure 7A**), with three out of five sera demonstrating reactivity (sera 2, 3, and 4). However, average absorbance was 4.5 times higher to C-gly-*Hc* CIB1980 (**p<0.01; **Figure 7A**), with all sera reacting against this fraction, demonstrating best reactivity among the C-gly-*Hc* (###p<0.001). Reactivity to E-gly-*Hc* of distinct origin followed a similar behavior, but with fairly higher values of absorbances (**Figure 7B**).

Antibodies raised against *Hc*-gly and present in the sera of patients with histoplasmosis also cross-reacted with epitopes present in *Cn*-gly. Average absorbance for sera from patients with histoplasmosis was 1.5 higher than "cut-off" values (*p<0.05), with 4 out of 5 sera (sera 2,3,4 and 5) reacting to C-gly-*Cn* H99 (**Figure 8A**). Regarding reactivity to E-gly-*Cn* H99 average absorbance was three times higher than "cut-off" (**p<0.01), as 4 out of 5 sera (sera 1, 2, 3, and 5) demonstrating high reactivity (**Figure 8B**). Overall, cross-reacting antibodies in sera from patients with histoplasmosis better recognized epitopes present in E-gly-*Cn* H99 fractions,

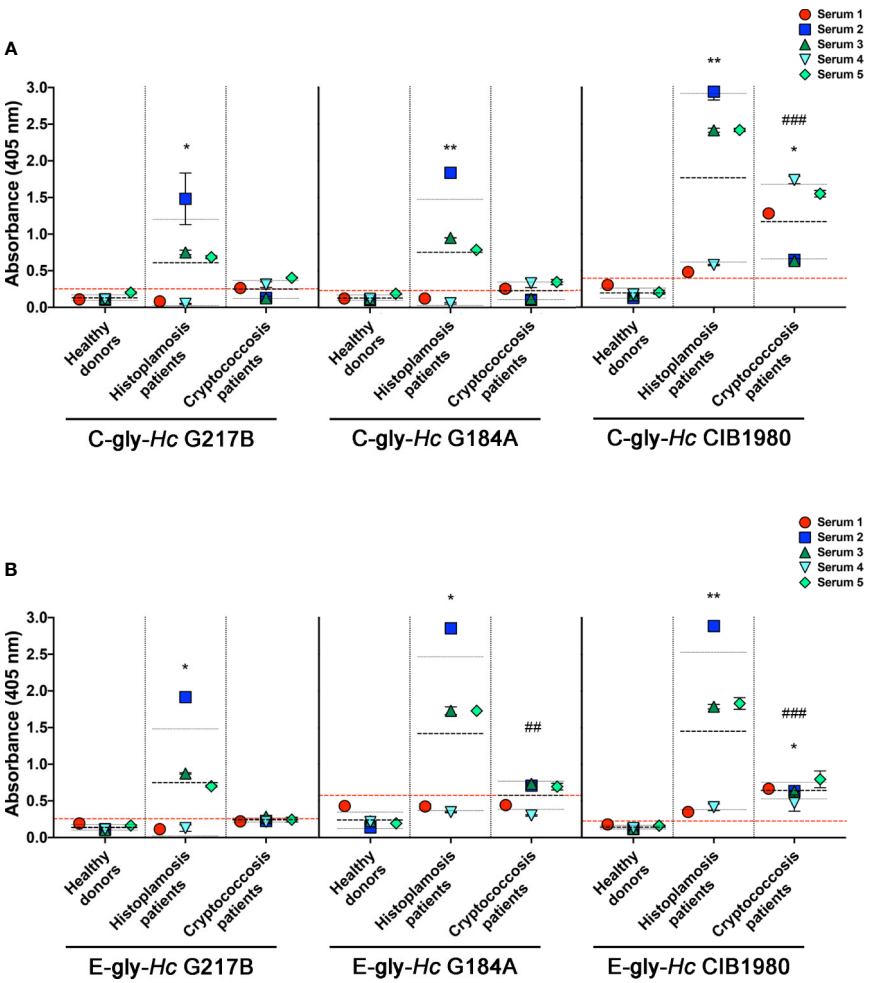

FIGURE 7 | Serological cross-reactivity of sera from patients with cryptococcosis to *H. capsulatum* cellular-attached (C-gly-*Hc*) and extracellular (E-gly-*Hc*) polysaccharides from strains from three distinct monophyletic groups, *Hc* glycans were attached to ELISA plate and the reactivity of sera from patients with cryptococcosis against *Hc*-gly was compared to reactivity of negative control sera from heathy subjects and controls of sera from patients with histoplasmosis. **(A)** Reactivity of the cellular-attached glycans C-gly *Hc* G217B, C-gly *Hc* G184A, and C-gly C-gly-*Hc* of *Hc* CIB1980 strains. **(B)** Reactivity of the Extracellular glycans E-gly-*Hc* of *Hc* G217B, E-gly-*Hc* of *Hc* G184A, and E-gly-*Hc* of *Hc* CIB1980 strains. *P ≤ 0.05 and **p ≤ 0.01; comparison of histoplasmosis or cryptococcosis patient's sera reactivity to *Hc* glycans versus healthy subjects control; $^{\#\#}$p ≤ 0.01, $^{\#\#\#}$p ≤ 0.001; comparison among the distinct Hc glycans demonstrated higher reactivity of cryptococcosis patient's sera to *Hc* CIB 1980 glycans versus the respective glycan from either *Hc* G217B or *Hc* G184A.

H. capsulatum Glycans Inhibited Phagocytosis and Antifungal Activity by Peritoneal Macrophages.

The antiphagocytic properties of C-gly and E-gly from *Hc* were evaluated and compared to the established antiphagocytic C-gly-*Cn* and E-gly-*Cn* (**Figures 9A, B**). Relative to untreated yeasts, *Cn cap59* yeasts coated with C-gly from the distinct *Hc* strains equally displayed enhanced resistance to phagocytosis by peritoneal macrophages (*Hc* G217B, 41% inhibition; *Hc* G184A, 46% and *Hc* CIB 1980, 42%), which were at levels similar to that achieved following incubation of *Cn cap59* with C-gly-*Cn* H99 (54% inhibition; **Figures 9A, C**). E-gly-*Hc* also inhibited phagocytosis of *Cn cap 59* coated yeasts (*Hc* G217B, 52% inhibition; *Hc* G184A, 56%, and *Hc* CIB 1980, 54%), similarly to E-gly-*Cn* (56% inhibition; **Figures 9B, C**). Additionally, resistance to killing by macrophages was also enhanced when cap59 *C. neoformans* were coated with either C-gly or E-gly from the three *Hc* strains (**Figure 9D**).

Hc Glycans Enhance the Virulence of Acapsular Mutants of *Cn* in Invertebrate Models of *Galleria mellonella*

We used *G. mellonella* larvae as a model to investigate the impact of *Hc* glycans in fungal virulence. *Cn cap59* yeasts were coated with *Hc* glycans and used to infect the larvae, Infections with uncoated *Cn cap59* or coated with *Cn* H99 glycans were used as controls. As expected, controls of C-gly-*Cn* H99 and E-gly-*Cn* H99 coated *Cn* cap59 infected larvae of *G. mellonella* died faster than those infected with uncoated *Cn cap59* control ($p<0.05$). From the groups of *Hc*-glycans coated *Cn cap59*, only the C-gly-*Hc* G217B coated *Cn cap59* killed the larvae faster than uncoated *Cn cap59* control ($p=0.035$; **Figure 10A**), whereas the C-gly-*Hc* G184A displayed a trend for higher killing capacity ($p=0.076$). From the E-gly-*Hc* coated *Cn* cap59 yeasts, only those coated with E-gly-*Hc* G184A were able to reduce larvae survival ($p<0.05$; **Figure 10B**).

Increasing the inoculum (10^6 yeasts/larvae) resulted in faster killing of the larvae by *Cn* cap59 controls and no difference was observed among groups (**Figures 10C, D**), despite of a trend for accelerated death with the E-gly-*Hc* G217B coated *Cn cap59* infected larvae in comparison to *Cn cap59* control ($p=0.067$).

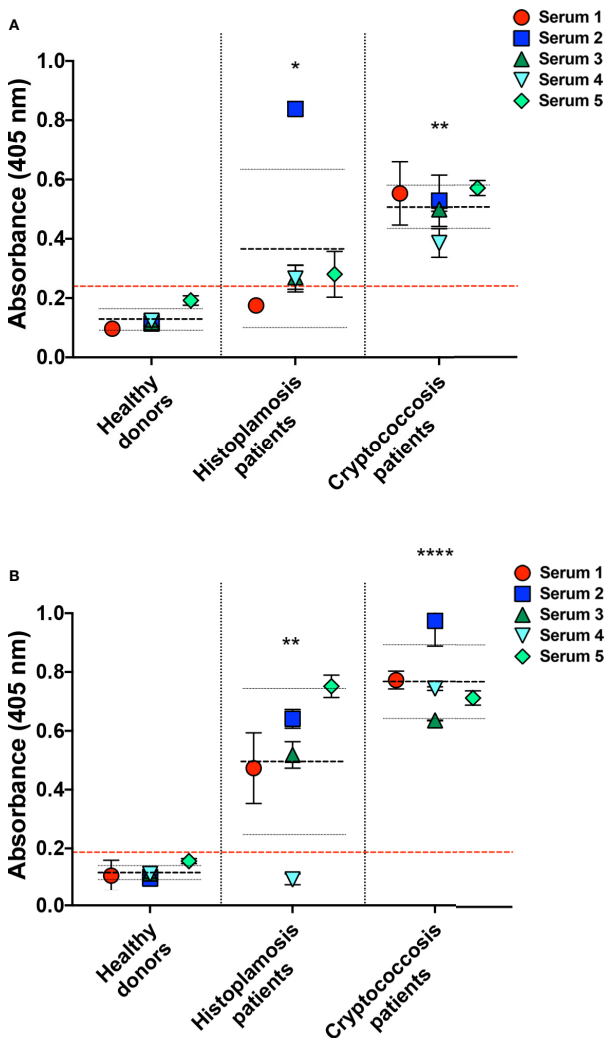

FIGURE 8 | Serological cross-reactivity of sera from patients with histoplasmosis to *C. neoformans* capsular (C-gly-*Cn*) and extracellular (E-gly-*Cn*) polysaccharides confirmed the presence of immunogenic epitopes in *Hc* glycans. Reactivity of antibodies from histoplasmosis patient sera was evaluated against *C. neoformans (Cn)* glycans **(A)** C-gly-*Cn* H99 and **(B)** E-gly-*Cn* H99, confirming the presence of antibodies raised by *Hc* glycans that are able to recognize similar epitopes in *Cn* glycans. As a controls, reactivity was compared to negative control sera from healthy individuals and positive control sera of cryptococcosis. *$P \leq 0.05$, **$p \leq 0.01$, ***$p \leq 0.0001$; comparison of histoplasmosis or cryptococcosis patient's sera reactivity to *Cn* glycans versus healthy subjects control.

DISCUSSION

Polysaccharides compose up to 80% of the fungal cell wall (Erwig and Gow, 2016; Gow et al., 2017), displaying several functions related to immune recognition and playing a central role in fungal pathogenesis (Gow et al., 2017). The fungal cell wall is a dynamic and metamorphic structure. In *Candida albicans*, for example, adaptation to environmental stress, including changes in carbon sources, involves a complex regulatory network by switching its metabolism and morphogenesis, including cell wall remodeling and, altogether, alterations in the cell wall result in changes in virulence (Brown et al., 2014). Simpler direct mechanisms also are involved in the regulation of the cell wall thickness and composition, such as the secretion of Eng1 β-glucanase by *H. capsulatum* (*Hc*) (Garfoot et al., 2016), which trims the β-1,3-glucans off the cell wall, reducing its exposure and subsequent immune recognition through Dectin-1 to contribute to the immune escape and enhanced the virulence of this fungus (Brown, 2016).

Ascomycete dimorphic fungi, such as *Hc* (Klimpel and Goldman, 1988), *P. brasiliensis* (San-Blas and Vernet, 1977; Tomazett et al., 2005) and *Blastomyces dermatitidis* (Hogan and Klein, 1994) are able to modify the recognition of β-1,3-glucan by

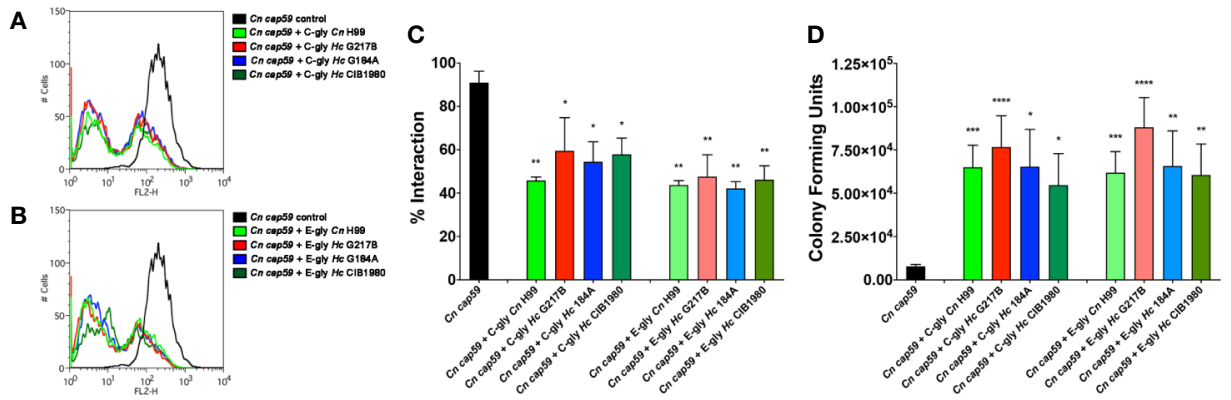

FIGURE 9 | *H. capsulatum* glycans (*Hc*-gly) incorporation by a cap59 acapsular mutant of *C. neoformans (Cn)* confers resistance to phagocytosis by macrophages. **(A, B)** Representative histograms demonstrating the interactions of uncoated or coated *Cn cap59* with **(A)** C-gly-*Hc* or **(B)** E-gly-*Hc* from *H. capsulatum (Hc)* strains from distinct monophyletic branches. **(C)** Incorporation of either C-gly-*Hc* or E-gly-*Hc* by the acapsular mutant *Cn cap59* significantly inhibited the fungal association with murine peritoneal macrophages, as values similar to *Cn* gly controls**. (D)** Co-culture of macrophages with *Cn cap59* coated with C-gly-*Hc* or E-gly-*Hc* from distinct strains also inhibited the killing of yeasts by murine peritoneal macrophages. Bars represent mean ± standard error of quadruplicates. *P ≤ 0.05; **p ≤ 0.01; ***p ≤ 0.001; ****p ≤ 0.0001.

innate immune cells by altering the production and display of α-1,3-glucan during morphogenic transformation from hyphal forms to yeast cells. In contrast, loss of this polysaccharide is linked to a reduction of virulence *in vivo* (San-Blas and Vernet, 1977; Rappleye et al., 2004).

In *C. neoformans* (*Cn*), α-1,3-glucan is responsible for GXM fibers attachment to the cell surface, as the absence of this polysaccharide results in acapsular phenotypes despite normal GXM shedding mechanisms (Reese and Doering, 2003; Reese et al., 2007). Previous observations by Reese and Doering demonstrated that α-1,3-glucan expressing *Hc* is also able to anchor cryptococcal GXM and form a capsule-like structure (Reese and Doering, 2003). Further observations by our group (Cordero et al., 2016) mechanistically demonstrated that cryptococcal GXM incorporation by *Hc* had implications on biofilm formation and fungal resistance to phagocytosis, resulting in enhanced fungal virulence and worst prognosis of the co-infection. However, the fact that *Hc* incorporated cryptococcal GXM and cross-reactivity of some mAbs generated against cryptococcal GXM to *Hc* filamentous and yeast cell surface, suggested the production and expression of GXM-like fibers by this fungus.

To address this hypothesis, in the present study, we carried out the characterization of cellular-attached and secreted extracellular pools of glycans (C-gly and E-gly, respectively) obtained from *Hc* and initially tested their serological reactivity against a panel of mAbs to *Cn* GXM. We decided to keep the term glycans as a general denomination for fibers composed by glycosidic-bound monosaccharides, as no structural determination was carried out. C-gly and E-gly extracted from the reference *Hc* G217B strain reacted only with the 18B7 mAb, but at lower levels when compared to *Cn* fractions. Lower affinity of *Hc* glycans to GXM antibodies might be dictated by structural differences and/or relative abundance of the target epitopes. It is well documented that the mAb 13F1 differs in specificity to others in the panel, and usually labels the *Cn* yeast in a punctate pattern throughout the capsule (Nussbaum et al., 1997; Cleare et al., 1999). This mAb also shows a discrete reactivity to *P. brasiliensis* C-gly by ELISA, and a punctuated labeling pattern on the yeast surface by immunofluorescence (Albuquerque et al., 2012). Nevertheless, it is clear that the absence of reactivity of the 13F1 mAb to either *Hc* C-gly and E-gly indicates that its target epitope might be absent in this glycan pool.

The reactivity of the 18B7 mAb, which is by far the most used in studies of cryptococcal capsule characterization, to *Hc* glycans by ELISA led us to evaluate its binding profile and target epitope distribution on *Hc*. MAb 18B7 labeling ranged from a dotted to a ring pattern, confirming previous indications by our group (Cordero et al., 2016). This same binding pattern was originally reported for *Cn* (Casadevall et al., 1998) and other GXM-like polysaccharide producing fungi, such as *C. liquefaciens* (Araujo et al., 2017), *T. asahii* (Fonseca et al., 2009), *T. mucoides* (Zimbres et al., 2018) and *P. brasiliensis* (Albuquerque et al., 2012).

As a GXM-like component, C-gly-*Hc* could be promptly incorporated by the *Cn cap59* acapsular mutant, forming a capsule-like structure, with some dotted regions, resembling the capsule formed when C-gly-*Cn* was used. A similar profile was also observed for the incorporation of other GXM-like components of the most diverse origin, likely indicating a shared property among them (Fonseca et al., 2009; Albuquerque et al., 2012; Araujo et al., 2017; Zimbres et al., 2018). As for *Cn* GXM, C-gly-*Hc* incorporation could occur *via* α-1,3-glucan (Reese and Doering, 2003) or attachment to cell wall chitin (Ramos et al., 2012).

An intriguing point is the structural characterization of these GXM-like molecules. For *Cn*, GXM is composed of a backbone of mannan with substitutions of xylose and glucuronic acid, creating a high diversity of motifs and possible combinations (Cherniak et al., 1998; McFadden et al., 2006). *T. asahii* GXM-like, in turn, displays a relatively higher number of mannosyl units and distinct positions of xylosyl substitutions per motif (Fonseca et al., 2009). The closely

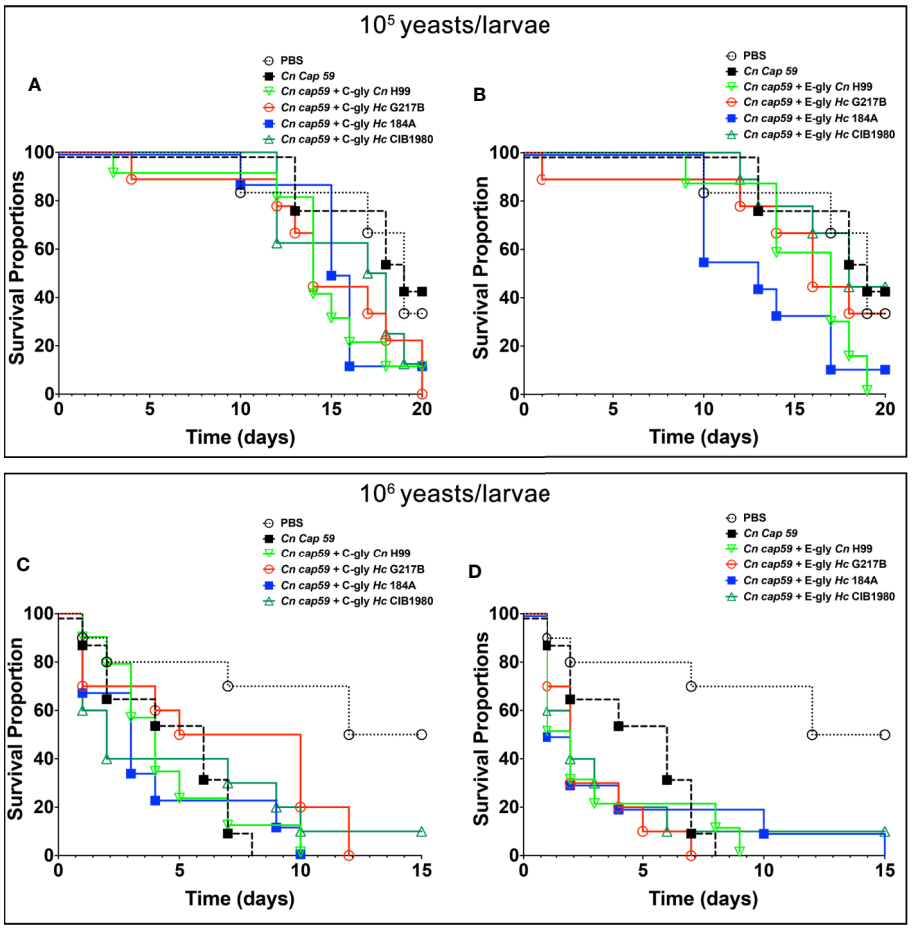

FIGURE 10 | *H. capsulatum* glycans (*Hc*-gly) are able to turn the avirulent *C. neoformans (Cn) cap59* into virulent yeasts. **(A, B)** *Cn cap59* were coated with **(A)** C-gly or **(B)** E-gly from distinct strains of *Hc* or controls yeast *Cn* H99 and used to infect (10^5 yeast/larvae) of *Galleria mellonela*. **(C, D)** *Cn cap59* were coated with **(C)** C-gly or **(D)** E-gly from distinct strains of *Hc* or controls yeast *Cn* H99 and 10^6 yeast/larvae used for infections.

related *T. mucoides* displays a very similar composition to *T. asahii*, except for the higher number of glucuronic acid substitutions (Zimbres et al., 2018). The *P. brasiliensis* GXM-like polysaccharide is mainly composed of mannose and galactose, and traces of glucose, xylose, and rhamnose, with an absence of glucuronic acid (Albuquerque et al., 2012). Similarly, in surface glycans of *Hc*, mannose and glucose were detected, in addition to small amounts of galactose and N-acetyl glucosamine; however, the main observation in our analyses was the absence of xylose and glucuronic acid. However, we cannot rule out the possibility that these identified *Hc* glycans could have similar compositions to polysaccharides antigens previously described (Zancope-Oliveira et al., 1994), or to the cross-reacting galactomannans of *P. brasiliensis* (San-Blas and San-Blas, 1982).

As expected, due to the absence of both residues, incorporation of C-gly-*Hc* G217 by *Cn cap59* had no effect on surface charge. In contrast, the incorporation of C-gly-*Cn* H99 bearing glucuronic acid and xylose clearly resulted in a more negative charge, similar to *Cn* H99 controls. Xylose seems not to alter the overall charge of polysaccharide fibers in a wide range of pH (Barbosa et al., 2019), including physiological pH 7.2 used in our experiments, Therefore, pKa of glucuronic acid in the range of ~3.0 confers a more negative charge to GXM.

Cn mutants deficient in the production of glucuronic acid and xylose have been described in the literature both with defective capsule production. A *Cn* mutant deficient in UDP-glucose 6 dehydrogenase (*UGD1*), lacks UDP-glucuronic acid and its downstream product UDP-xylose, displaying an acapsular avirulent phenotype and are highly sensitive to temperature and environmental stress (Moyrand et al., 2002; Moyrand and Janbon, 2004; Griffith et al., 2004). A mutant deficient in UDP-xylose synthase (*UXS1* or also called UDP-glucuronic acid decarboxylase), lacks UDP-xylose and displays a hypocapsular, hypovirulent phenotype, and are not recognized by some mAbs to GXM (Moyrand et al., 2002; Griffith et al., 2004). Intriguingly, these mutants displayed accumulated UDP-glucuronic acid to levels 64 times higher than WT *Cn*.

A comparative protein database search for the presence of homologous proteins in two distinct genotypes of *Hc* (NAm1/WU24 and G186AR/H82) to those involved in the GXM

synthesis and capsule architecture assembly in *Cn*, also revealed the absence of *UUT*1, *UGD1* and *UXS1*, orthologs in both *Hc* genomes, in agreement with the lack of these residues in C-gly-*Hc* and supporting the aforementioned glycosyl composition results. Overall, these would effectively correlate to small fibers observed for C-gly-*Hc* and capsule absence on *Hc* yeasts, as opposed to C-gly-*Cn*, cationic bridges with glucuronic acid residues result in the formation of larger fiber composing the cryptococcal capsular network (Nimrichter et al., 2007).

However, the suggestive presence of GXM-like molecules on the surface of *Hc* led us to perform additional searches that included acetyltransferases, mannosyltransferases, xylosyltransferases and miscellaneous (Chang and Kwon-Chung, 1994; Chang et al., 1996; Chang and Kwon-Chung, 1998; Chang and Kwon-Chung, 1999; Levitz et al., 2001; Janbon, 2004; Moyrand et al., 2004; Zaragoza et al., 2009; Albuquerque et al., 2012). BLAST displayed high similarity to *Cn* and *Hc* proteins, indicating both species share metabolic pathways required for the synthesis of molecules that resemble *Cn* GXM, and a possible evolutionary relationship between these two species. All the *Cn* protein groups evaluated had orthologs in *Hc*, supporting the presence of a GXM-like structure in the last. In addition, it must be stressed that one important gene, cap67 that encodes a cryptococcal chitin deacetylase, had no orthologs in neither *Hc* strains evaluated. The absence of this gene in *Cryptococcus* sp. is related to a capsular deficiency phenotype, despite a regular secretion of GXM (Jacobson et al., 1982; Reiss et al., 1986); however, *Hc* might express other genes that could function similarly and compensate for the absence of these orthologs.

Supporting these results, the 18B7 mAb raised against cryptococcal GXM reacted with C-gly and E-gly of three distinct strains of *Hc*, suggesting the presence of similar GXM epitopes across distinct clades of this fungus. Slight differences in reactivity among strains might be explained by differences in molecular dimensions and epitope diversity (Nimrichter et al., 2007; Albuquerque et al., 2014). On the other hand, distinct reactivity by ELISA using sera of cryptococcosis patients might also suggest that these C-gly and E-gly from distinct *Hc* strains might have a distinct set of epitopes, also found in cryptococcal GXM, with best cross-reactivity to glycans of *Hc* CIB1980. Further evaluation by ELISA also demonstrated that serum of histoplasmosis patients also have antibodies able to recognize cryptococcal C-gly and E-gly, suggesting once more a similarity between these two species and that the similar epitopes found in *Hc* are sufficiently immunogenic to induce a measurable humoral response.

Regardless of the relative composition of the GXM-like polysaccharides and the serological reactivity to *Cn* GMX mAbs, C-gly-*Hc* and E-gly-*Hc* were effectively incorporated onto the surface of *Cn* cap59 acapsular mutants impaired phagocytosis by macrophages and enhancing yeast intracellular survival in these phagocytes. These results provide additional evidence for the similarity among the GXM-like polysaccharides and further support their protective activity to other fungi against phagocytes, suggesting that they might be involved in fungal pathogenesis in distinct models (Fonseca et al., 2009; Albuquerque et al., 2012; Araujo et al., 2017; Zimbres et al., 2018).

Overall, together with previous studies showing incorporation of *Cn* GXM by *Hc* and virulence enhancement *in vitro* and *in vivo* (Cordero et al., 2016), here we also show the capacity of *Hc* to produce a GXM-like molecule. Therefore, the presence of the GXM-like polysaccharides across the fungal kingdom, in both Ascomycetes and Basidiomycetes, and their role as a crucial component for the pathogenesis process as well as their capacity for eliciting humoral responses offers additional support that they could be targeted for the treatment of mycosis. As such, certain distinct scenarios could be developed to improve the portfolio of strategies: (i) drug design of new antifungal molecules that block the pathways involved in the GXM synthesis, which would have a wide antifungal spectrum and (ii) the use of cross-reactive mAbs, as for example, the 18B7 mAb, which offered protection in infection models of *Cn*, in further passive immunization studies involving other models or for use in pan-fungal radioimmunotherapy (Nosanchuk and Dadachova, 2011), and (iii) targeted modulation of the immune response to polysaccharides to speed the resolution of infection and benefit the host. These examples focused on approaches to surface GXM-like compounds provide a strong foundation for a very promising path forward to the design of new antifungal strategies (Rappleye et al., 2007; Amarsaikhan and Templeton, 2015).

DATA AVAILABILITY STATEMENT

The raw data supporting the conclusions of this article will be made available by the authors, without undue reservation.

ETHICS STATEMENT

The animal study was reviewed and approved by animal institute committee of the Fluminense Federal University (protocol 5486190618).

AUTHOR CONTRIBUTIONS

All authors contributed to conception and design of the study. DG, CR, MF, LH, GA, RC, and AG performed the experiments. DG, CN, MF, RC and AG organized the database. DG, CN, MF and AG performed the statistical analysis. All authors designed experiments and participated in scientific discussions. DG, CN, MF, JN, RC and AG wrote the first draft of the manuscript. All authors contributed to the article and approved the submitted version.

FUNDING

AG was supported by grants from the Brazilian agencies Conselho Nacional de Desenvolvimento Científico e Tecnológico (CNPq, grants 311470/2018-1) and Fundação Carlos Chagas de Amparo à Pesquisa no Estado do Rio de Janeiro (E-26/202.696/2018).

SUPPLEMENTARY MATERIAL

The Supplementary Material for this article can be found online at: https://www.frontiersin.org/articles/10.3389/fcimb.2020.565571/full#supplementary-material

SUPPLEMENTARY FIGURE 1 | Chromatograms of the glycosyl composition of *C. neoformans* and *H. capsulatum* C-glycans. **(A)** C-gly-*Cn* H99 and **(B)** C-gly-*Hc* G217B displayed a distinct composition.

SUPPLEMENTARY FIGURE 2 | Correlation the *H. capsulatum* Nam1/WU24 and the Panama/G186AR strain/H82 strain regarding their similarities to the *C neoformans* var. grubii serotype A (strain H99/ATCC 208821) strain. Circle filling colors denote the acetyltransferases (green), mannosyltransferases (blue), acetyltransferases (pink), and miscellaneous (white) groups. Similarity values of proteins from the two strains displayed a correlation (R2 = 0.70, ****p<0.0001; UN – unidentified in the database).

SUPPLEMENTARY TABLE 1 | Glucuronoxylomannan synthesis and capsular production-related proteins of *C. neoformans* and their respective orthologs in *H. capsulatum* Nam1/WU24 and the Panama/G186AR strain/H82 strains. Cryptococcal proteins were classified as acatyltransferases, mannosyltransferases, xylosyltransferases, and miscellaneous, including polysaccharide transport and GXM export proteins. Underlined protein names indicate those *C. neoformans* proteins with orthologs in *H. capsulatum*, with identical protein domains/families as annotated by Interpro/Pfam.

REFERENCES

Albuquerque, P. C., Cordero, R. J., Fonseca, F. L., Peres da Silva, R., Ramos, C. L., Miranda, K. R., et al. (2012). A Paracoccidioides brasiliensis glycan shares serologic and functional properties with cryptococcal glucuronoxylomannan. *Fungal Genet. Biol.* 49 (11), 943–954. doi: 10.1016/j.fgb.2012.09.002

Albuquerque, P. C., Fonseca, F. L., Dutra, F. F., Bozza, M. T., Frases, S., Casadevall, A., et al. (2014). *Cryptococcus neoformans* glucuronoxylomannan fractions of different molecular masses are functionally distinct. *Future Microbiol* 9 (2), 147–161. doi: 10.2217/fmb.13.163

Amarsaikhan, N., and Templeton, S. P. (2015). Co-recognition of beta-glucan and chitin and programming of adaptive immunity to *Aspergillus fumigatus*. *Front. Microbiol* 6, 344. doi: 10.3389/fmicb.2015.00344

Araujo, G. R. S., Freitas, G. J. C., Fonseca, F. L., Leite, P. E. C., Rocha, G. M., de Souza, W. S., et al. (2017). The environmental yeast Cryptococcus liquefaciens produces capsular and secreted polysaccharides with similar pathogenic properties to those of *C. neoformans*. *Sci. Rep.* 7, 46768. doi: 10.1038/srep46768

Barbosa, J. A. C., Abdelsadig, M. S. E., Conway, B. R., and Merchant, H. A. (2019). Using zeta potential to study the ionisation behaviour of polymers employed in modified-release dosage forms and estimating their pK(a). *Int. J. Pharm. X* 1, 100024. doi: 10.1016/j.ijpx.2019.100024

Bowden, P., Pendrak, V., Zhu, P., and Marshall, J. G. (2010). Meta sequence analysis of human blood peptides and their parent proteins. *J. Proteomics* 73 (6), 1163–1175. doi: 10.1016/j.jprot.2010.02.007

Brown, A. J., Brown, G. D., Netea, M. G., and Gow, N. A. (2014). Metabolism impacts upon Candida immunogenicity and pathogenicity at multiple levels. *Trends Microbiol* 22 (11), 614–622. doi: 10.1016/j.tim.2014.07.001

Brown, G. D. (2016). Trimming Surface Sugars Protects Histoplasma from Immune Attack. *mBio* 7 (2), e00553–e00516. doi: 10.1128/mBio.00553-16

Casadevall, A., Cleare, W., Feldmesser, M., Glatman-Freedman, A., Goldman, D. L., Kozel, T. R., et al. (1998). Characterization of a murine monoclonal antibody to *Cryptococcus neoformans* polysaccharide that is a candidate for human therapeutic studies. *Antimicrob. Agents Chemother.* 42 (6), 1437–1446. doi: 10.1128/AAC.42.6.1437

Chang, Y. C., and Kwon-Chung, K. J. (1994). Complementation of a capsule-deficient mutation of *Cryptococcus neoformans* restores its virulence. *Mol. Cell Biol.* 14 (7), 4912–4919. doi: 10.1128/MCB.14.7.4912

Chang, Y. C., and Kwon-Chung, K. J. (1998). Isolation of the third capsule-associated gene, CAP60, required for virulence in *Cryptococcus neoformans*. *Infect. Immun.* 66 (5), 2230–2236. doi: 10.1128/IAI.66.5.2230-2236.1998

Chang, Y. C., and Kwon-Chung, K. J. (1999). Isolation, characterization, and localization of a capsule-associated gene, CAP10, of *Cryptococcus neoformans*. *J. Bacteriol.* 181 (18), 5636–5643. doi: 10.1128/JB.181.18.5636-5643.1999

Chang, Y. C., Penoyer, L. A., and Kwon-Chung, K. J. (1996). The second capsule gene of *Cryptococcus neoformans*, CAP64, is essential for virulence. *Infect. Immun.* 64 (6), 1977–1983. doi: 10.1128/IAI.64.6.1977-1983.1996

Cherniak, R., O'Neill, E. B., and Sheng, S. (1998). Assimilation of xylose, mannose, and mannitol for synthesis of glucuronoxylomannan of *Cryptococcus neoformans* determined by 13C nuclear magnetic resonance spectroscopy. *Infect. Immun.* 66 (6), 2996–2998. doi: 10.1128/IAI.66.6.2996-2998.1998

Cleare, W., Brandt, M. E., and Casadevall, A. (1999). Monoclonal antibody 13F1 produces annular immunofluorescence patterns on *Cryptococcus neoformans* serotype AD isolates. *J. Clin. Microbiol.* 37 (9), 3080. doi: 10.1128/JCM.37.9.3080-3080.1999

Cordero, R. J., Liedke, S. C., Araujo, G. R. S., Martinez, L. R., Nimrichter, L., Frases, S., et al. (2016). Enhanced virulence of *Histoplasma capsulatum* through transfer and surface incorporation of glycans from *Cryptococcus neoformans* during co-infection. *Sci. Rep.* 6, 21765. doi: 10.1038/srep21765

De Pauw, B., Walsh, T. J., Donnelly, J. P., Stevens, D. A., Edwards, J. E, Calandra, T., et al. (2008). Revised definitions of invasive fungal disease from the European Organization for Research and Treatment of Cancer/Invasive Fungal Infections Cooperative Group and the National Institute of Allergy and Infectious Diseases Mycoses Study Group (EORTC/MSG) Consensus Group. *Clin. Infect. Dis.* 46 (12), 1813–1821. doi: 10.1086/588660

Erwig, L. P., and Gow, N. A. (2016). Interactions of fungal pathogens with phagocytes. *Nat. Rev. Microbiol* 14 (3), 163–176. doi: 10.1038/nrmicro.2015.21

Finn, R. D., Tate, J., Mistry, J., Coggill, P. C., Sammut, S. J, Hotz, H. R., et al. (2008). The Pfam protein families database. *Nucleic Acids Res.* 36 (Database issue), D281–D288. doi: 10.1093/nar/gkm960

Fonseca, F. L., Frases, S., Casadevall, A., Fischman-Gompertz, O., Nimrichter, L, and Rodrigues, M. L. (2009). Structural and functional properties of the Trichosporon asahii glucuronoxylomannan. *Fungal Genet. Biol.* 46 (6-7), 496–505. doi: 10.1016/j.fgb.2009.03.003

Frases, S., Nimrichter, L., Viana, N. B., Nakouzi, A., and Casadevall, A. (2008). *Cryptococcus neoformans* capsular polysaccharide and exopolysaccharide fractions manifest physical, chemical, and antigenic differences. *Eukaryot Cell* 7 (2), 319–327. doi: 10.1128/EC.00378-07

Garcia-Rivera, J., Chang, Y. C., Kwon-Chung, K. J., and Casadevall, A. (2004). *Cryptococcus neoformans* CAP59 (or Cap59p) is involved in the extracellular trafficking of capsular glucuronoxylomannan. *Eukaryot Cell* 3 (2), 385–392. doi: 10.1128/EC.3.2.385-392.2004

Garfoot, A. L., Shen, Q., Wuthrich, M., Klein, B. S., and Rappleye, C. A. (2016). The Eng1 beta-Glucanase Enhances Histoplasma Virulence by Reducing beta-Glucan Exposure. *mBio* 7 (2), e01388–e01315. doi: 10.1128/mBio.01388-15

Gow, N. A. R., Latge, J. P., and Munro, C. A. (2017). The Fungal Cell Wall: Structure, Biosynthesis, and Function. *Microbiol Spectr.* 5 (3), 1–25. doi: 10.1128/9781555819583.ch12

Griffith, C. L., Klutts, J. S., Zhang, L., Levery, S. B., and Doering, T. L. (2004). UDP-glucose dehydrogenase plays multiple roles in the biology of the pathogenic fungus *Cryptococcus neoformans*. *J. Biol. Chem.* 279 (49), 51669–51676. doi: 10.1074/jbc.M408889200

Guimarães, A. J., Frases, S., Gomez, F. J., Zancopé-Oliveira, R. M., and Nosanchuk, J. D. (2009). Monoclonal antibodies to heat shock protein 60 alter the pathogenesis of *Histoplasma capsulatum*. *Infect. Immun.* 77 (4), 1357–1367. doi: 10.1128/IAI.01443-08

Guimaraes, A. J., Frases, S., Cordero, R. J., Nimrichter, L., Casadevall, A., and Nosanchuk, J. D. (2010). *Cryptococcus neoformans* responds to mannitol by increasing capsule size in vitro and in vivo. *Cell Microbiol* 12 (6), 740–753. doi: 10.1111/j.1462-5822.2010.01430.x

Guimarães, A. J., Pizzini, C. V., De Abreu Almeida, M., Peralta, J. M., Nosanchuk, J. D., and Zancopé-Oliveira, R. M. (2010). Evaluation of an enzyme-linked immunosorbent assay using purified, deglycosylated histoplasmin for different clinical manifestations of histoplasmosis. *Microbiol Res. (Pavia)* 1 (1), 1–21. doi: 10.4081/mr.2010.e2

Guimaraes, A. J., de Cerqueira, M. D., and Nosanchuk, J. D. (2011). Surface architecture of *histoplasma capsulatum*. *Front. Microbiol.* 2, 225. doi: 10.3389/fmicb.2011.00225

Guimarães, A. J., de Cerqueira, M. D., Zamith-Miranda, D., Lopez, P. H., Rodrigues, M. L., Pontes, B., et al. (2019). Host membrane glycosphingolipids and lipid microdomains facilitate *Histoplasma capsulatum* internalisation by macrophages. *Cell Microbiol* 21 (3), e12976. doi: 10.1111/cmi.12976

Hogan, L. H., and Klein, B. S. (1994). Altered expression of surface alpha-1,3-glucan in genetically related strains of Blastomyces dermatitidis that differ in virulence. *Infect. Immun.* 62 (8), 3543–3546. doi: 10.1128/IAI.62.8.3543-3546.1994

Jacobson, E. S., Ayers, D. J., Harrell, A. C., and Nicholas, C. C. (1982). Genetic and phenotypic characterization of capsule mutants of *Cryptococcus neoformans*. *J. Bacteriol* 150 (3), 1292–1296. doi: 10.1128/JB.150.3.1292-1296.1982

Janbon, G. (2004). *Cryptococcus neoformans* capsule biosynthesis and regulation. *FEMS Yeast Res.* 4 (8), 765–771. doi: 10.1016/j.femsyr.2004.04.003

Klimpel, K. R., and Goldman, W. E. (1988). Cell walls from avirulent variants of *Histoplasma capsulatum* lack alpha-(1,3)-glucan. *Infect. Immun.* 56 (11), 2997–3000. doi: 10.1128/IAI.56.11.2997-3000.1988

Levitz, S. M., Nong, S., Mansour, M. K., Huang, C., and Specht, C. A. (2001). Molecular characterization of a mannoprotein with homology to chitin deacetylases that stimulates T cell responses to *Cryptococcus neoformans*. *Proc. Natl. Acad. Sci. U.S.A.* 98 (18), 10422–10427. doi: 10.1073/pnas.181331398

Madera, M., and Gough, J. (2002). A comparison of profile hidden Markov model procedures for remote homology detection. *Nucleic Acids Res.* 30 (19), 4321–4328. doi: 10.1093/nar/gkf544

Masuko, T., Minami, A., Iwasaki, N., Majima, T., Nishimura, S., and Lee, Y. C. (2005). Carbohydrate analysis by a phenol-sulfuric acid method in microplate format. *Anal. Biochem.* 339 (1), 69–72. doi: 10.1016/j.ab.2004.12.001

McFadden, D. C., De Jesus, M., and Casadevall, A. (2006). The physical properties of the capsular polysaccharides from *Cryptococcus neoformans* suggest features for capsule construction. *J. Biol. Chem.* 281 (4), 1868–1875. doi: 10.1074/jbc.M509465200

Mora-Montes, H. M., Netea, M. G., Ferwerda, G., Lenardon, M. D., Brown, G. D., Mistry, A. R., et al. (2011). Recognition and blocking of innate immunity cells by Candida albicans chitin. *Infect. Immun.* 79 (5), 1961–1970. doi: 10.1128/IAI.01282-10

Moyrand, F., and Janbon, G. (2004). UGD1, encoding the *Cryptococcus neoformans* UDP-glucose dehydrogenase, is essential for growth at 37 degrees C and for capsule biosynthesis. *Eukaryot Cell* 3 (6), 1601–1608. doi: 10.1128/EC.3.6.1601-1608.2004

Moyrand, F., Klaproth, B., Himmelreich, U., Dromer, F., and Janbon, G. (2002). Isolation and characterization of capsule structure mutant strains of *Cryptococcus neoformans*. *Mol. Microbiol.* 45 (3), 837–849. doi: 10.1046/j.1365-2958.2002.03059.x

Moyrand, F., Chang, Y. C., Himmelreich, U., Kwon-Chung, K. J., and Janbon, G. (2004). Cas3p belongs to a seven-member family of capsule structure designer proteins. *Eukaryot Cell* 3 (6), 1513–1524. doi: 10.1128/EC.3.6.1513-1524.2004

Mukherjee, J., Casadevall, A., and Scharff, M. D. (1993). Molecular characterization of the humoral responses to *Cryptococcus neoformans* infection and glucuronoxylomannan-tetanus toxoid conjugate immunization. *J. Exp. Med.* 177 (4), 1105–1116. doi: 10.1084/jem.177.4.1105

Nimrichter, L., Frases, S., Cinelli, L. P., Viana, N. B., Nakouzi, A., Travassos, L. R., et al. (2007). Self-aggregation of *Cryptococcus neoformans* capsular glucuronoxylomannan is dependent on divalent cations. *Eukaryot Cell* 6 (8), 1400–1410. doi: 10.1128/EC.00122-07

Nosanchuk, J. D., and Dadachova, E. (2011). Radioimmunotherapy of fungal diseases: the therapeutic potential of cytocidal radiation delivered by antibody targeting fungal cell surface antigens. *Front. Microbiol.* 2, 283. doi: 10.3389/fmicb.2011.00283

Nussbaum, G., Cleare, W., Casadevall, A., Scharff, M. D., and Valadon, P. (1997). Epitope location in the *Cryptococcus neoformans* capsule is a determinant of antibody efficacy. *J. Exp. Med.* 185 (4), 685–694. doi: 10.1084/jem.185.4.685

Ramos, C. L., Fonseca, F. L., Rodrigues, J., Guimaraes, A. J., Cinelli, L. P., Miranda, K., et al. (2012). Chitin-like molecules associate with *Cryptococcus neoformans* glucuronoxylomannan to form a glycan complex with previously unknown properties. *Eukaryot Cell* 11 (9), 1086–1094. doi: 10.1128/EC.00001-12

Rappleye, C. A., Engle, J. T., and Goldman, W. E. (2004). RNA interference in Histoplasma capsulatum demonstrates a role for alpha-(1,3)-glucan in virulence. *Mol. Microbiol.* 53 (1), 153–165. doi: 10.1111/j.1365-2958.2004.04131.x

Rappleye, C. A., Eissenberg, L. G., and Goldman, W. E. (2007). *Histoplasma capsulatum* alpha-(1,3)-glucan blocks innate immune recognition by the beta-glucan receptor. *Proc. Natl. Acad. Sci. U.S.A.* 104 (4), 1366–1370. doi: 10.1073/pnas.0609848104

Ray, S. C., and Rappleye, C. A. (2019). Flying under the radar: *Histoplasma capsulatum* avoidance of innate immune recognition. *Semin. Cell Dev. Biol.* 89, 91–98. doi: 10.1016/j.semcdb.2018.03.009

Reese, A. J., and Doering, T. L. (2003). Cell wall alpha-1,3-glucan is required to anchor the *Cryptococcus neoformans* capsule. *Mol. Microbiol.* 50 (4), 1401–1409. doi: 10.1046/j.1365-2958.2003.03780.x

Reese, A. J., Yoneda, A., Breger, J. A., Beauvais, A., Liu, H., Griffith, C. L., et al. (2007). Loss of cell wall alpha(1-3) glucan affects *Cryptococcus neoformans* from ultrastructure to virulence. *Mol. Microbiol.* 63 (5), 1385–1398. doi: 10.1111/j.1365-2958.2006.05551.x

Reiss, E., White, E. H., Cherniak, R., and Dix, J. E. (1986). Ultrastructure of acapsular mutant *Cryptococcus neoformans* cap 67 and monosaccharide composition of cell extracts. *Mycopathologia* 93 (1), 45–54. doi: 10.1007/BF00437014

Romani, L. (2011). Immunity to fungal infections. *Nat. Rev. Immunol.* 11 (4), 275–288. doi: 10.1038/nri2939

San-Blas, G., and San-Blas, F. (1982). Variability of cell wall composition in Paracoccidioides brasiliensis: a study of two strains. *Sabouraudia* 20 (1), 31–40. doi: 10.1080/00362178285380061

San-Blas, G., and Vernet, D. (1977). Induction of the synthesis of cell wall alpha-1,3-glucan in the yeastlike form of *Paracoccidioides brasiliensis* strain IVIC Pb9 by fetal calf serum. *Infect. Immun.* 15 (3), 897–902. doi: 10.1128/IAI.15.3.897-902.1977

Sepulveda, V. E., Marquez, R., Turissini, D. A., Goldman, W. E., and Matute, D. R. (2017). Genome Sequences Reveal Cryptic Speciation in the Human Pathogen *Histoplasma capsulatum*. *mBio*. 8 (6), 1–23. doi: 10.1128/mBio.01339-17

Shen, P., Li, W., Wang, Y., He, X., and He, L. (2016). Binding mode of chitin and TLR2 via molecular docking and dynamics simulation. *Mol. Simulation* 42 (11), 936–941. doi: 10.1080/08927022.2015.1124102

Teixeira Mde, M., Patané, J. S., Taylor, M. L., Gómez, B. L., Theodoro, R. C., de Hoog, S., et al. (2016). Worldwide Phylogenetic Distributions and Population Dynamics of the Genus Histoplasma. *PloS Negl. Trop. Dis.* 10 (6), e0004732. doi: 10.1371/journal.pntd.0004732

Tomazett, P. K., Cruz, A. H., Bonfim, S. M., Soares, C. M., and Pereira, M. (2005). The cell wall of Paracoccidioides brasiliensis: insights from its transcriptome. *Genet. Mol. Res.* 4 (2), 309–325.

Yoneda, A., and Doering, T. L. (2006). A eukaryotic capsular polysaccharide is synthesized intracellularly and secreted via exocytosis. *Mol. Biol. Cell* 17 (12), 5131–5140. doi: 10.1091/mbc.e06-08-0701

Zancope-Oliveira, R. M., Bragg, S. L., Reiss, E., and Peralta, J. M. (1994). Immunochemical analysis of the H and M glycoproteins from *Histoplasma capsulatum*. *Clin. Diagn. Lab. Immunol.* 1 (5), 563–568. doi: 10.1128/CDLI.1.5.563-568.1994

Zaragoza, O., Rodrigues, M. L., De Jesus, M., Frases, S., Dadachova, E., and Casadevall, A. (2009). The capsule of the fungal pathogen *Cryptococcus neoformans*. *Adv. Appl. Microbiol.* 68, 133–216. doi: 10.1016/S0065-2164(09)01204-0

Zhang, X., Goncalves, R., and Mosser, D. M. (2008). The isolation and characterization of murine macrophages. *Curr. Protoc. Immunol.* Chapter 14: Unit 14 1, 1–18. doi: 10.1002/0471142735.im1401s83

Zimbres, A. C. G., Albuquerque, P. C., Joffe, L. S., Souza, T. N., Nimrichter, L., Frazao, S. O., et al. (2018). A glucuronoxylomannan-like glycan produced by Trichosporon mucoides. *Fungal Genet. Biol.* 121, 46–55. doi: 10.1016/j.fgb.2018.09.009

Conflict of Interest: The authors declare that the research was conducted in the absence of any commercial or financial relationships that could be construed as a potential conflict of interest.

frontiers in Cellular and Infection Microbiology

ORIGINAL RESEARCH
published: 22 January 2021
doi: 10.3389/fcimb.2020.591950

Heat Shock Protein 60, Insights to Its Importance in *Histoplasma capsulatum*: From Biofilm Formation to Host-Interaction

Nathália Ferreira Fregonezi[1], *Lariane Teodoro Oliveira*[1], *Junya de Lacorte Singulani*[1], *Caroline Maria Marcos*[1], *Claudia Tavares dos Santos*[1], *Maria Lucia Taylor*[2], *Maria José Soares Mendes-Giannini*[1], *Haroldo Cesar de Oliveira*[1*†] *and Ana Marisa Fusco-Almeida*[1*]

[1] Department of Clinical Analysis, School of Pharmaceutical Sciences, São Paulo State University-UNESP, Araraquara, Brazil, [2] Unidad de Micología, Departamento de Microbiología y Parasitología, Facultad de Medicina, UNAM—Universidad Nacional Autónoma de México, Mexico City, Mexico

OPEN ACCESS

Edited by:
Angel Gonzalez,
University of Antioquia, Colombia

Reviewed by:
Ernesto Satoshi Nakayasu,
Pacific Northwest National Laboratory (DOE), United States
Jeniel E. Nett,
University of Wisconsin-Madison, United States

***Correspondence:**
Ana Marisa Fusco-Almeida
ana.marisa@uol.com.br
Haroldo Cesar de Oliveira
haroldocdoliveira@gmail.com

†Present address:
Haroldo Cesar de Oliveira,
Instituto Carlos Chagas,
Fundação Oswaldo Cruz (Fiocruz),
Curitiba, Brazil

Specialty section:
This article was submitted to Fungal Pathogenesis, a section of the journal Frontiers in Cellular and Infection Microbiology

Received: 05 August 2020
Accepted: 04 December 2020
Published: 22 January 2021

Citation:
Fregonezi NF, Oliveira LT, Singulani JL, Marcos CM, dos Santos CT, Taylor ML, Mendes-Giannini MJS, de Oliveira HC and Fusco-Almeida AM (2021) Heat Shock Protein 60, Insights to Its Importance in Histoplasma capsulatum: From Biofilm Formation to Host-Interaction. Front. Cell. Infect. Microbiol. 10:591950. doi: 10.3389/fcimb.2020.591950

Heat shock proteins (Hsps) are among the most widely distributed and evolutionary conserved proteins, acting as essential regulators of diverse constitutive metabolic processes. The Hsp60 of the dimorphic fungal *Histoplasma capsulatum* is the major surface adhesin to mammalian macrophages and studies of antibody-mediated protection against *H. capsulatum* have provided insight into the complexity involving Hsp60. However, nothing is known about the role of Hsp60 regarding biofilms, a mechanism of virulence exhibited by *H. capsulatum*. Considering this, the present study aimed to investigate the influence of the Hsp60 on biofilm features of *H. capsulatum*. Also, the non-conventional model *Galleria mellonella* was used to verify the effect of this protein during *in vivo* interaction. The use of invertebrate models such as *G. mellonella* is highly proposed for the evaluation of pathogenesis, immune response, virulence mechanisms, and antimicrobial compounds. For that purpose, we used a monoclonal antibody (7B6) against Hsp60 and characterized the biofilm of two *H. capsulatum* strains by metabolic activity, biomass content, and images from scanning electron microscopy (SEM) and confocal laser scanning microscopy (CLSM). We also evaluated the survival rate of *G. mellonella* infected with both strains under blockage of Hsp60. The results showed that mAb 7B6 was effective to reduce the metabolic activity and biomass of both *H. capsulatum* strains. Furthermore, the biofilms of cells treated with the antibody were thinner as well as presented a lower amount of cells and extracellular polymeric matrix compared to its non-treated controls. The blockage of Hsp60 before fungal infection of *G. mellonella* larvae also resulted in a significant increase of the larvae survival compared to controls. Our results highlight for the first time the importance of the Hsp60 protein to the establishment of the *H. capsulatum* biofilms and the *G. mellonella* larvae infection. Interestingly, the results with Hsp60 mAb 7B6 in this invertebrate model suggest a pattern of fungus-host interaction different from those previously found in a

murine model, which can be due to the different features between insect and mammalian immune cells such as the absence of Fc receptors in hemocytes. However further studies are needed to support this hypothesis

Keywords: histoplasmosis, biofilm, Hsp60, adhesins, *Galleria mellonella*

INTRODUCTION

Histoplasma capsulatum is a dimorphic pathogenic fungus that causes histoplasmosis, one of the most common pulmonary mycosis in the United States (US) (Armstrong et al., 2018; Maiga et al., 2018; Salzer et al., 2018). Despite endemic in certain areas of the US (e.g. Ohio and Mississippi river valleys), histoplasmosis has a worldwide distribution and is also one of the top AIDS-defining conditions and AIDS-related causes of death in Latin America (Adenis et al., 2018; Papalini et al., 2019).

The histoplasmosis infection occurs *via* inhalation of conidial spores that transform into yeasts within the mammalian host (Mittal et al., 2019). As a facultative intracellular fungus, *H. capsulatum* yeasts are readily phagocytosed by resident macrophages, where they survive and replicate. During the early phases of infection, alveolar macrophages (Mφ) recognize unopsonized *H. capsulatum* yeasts and microconidia *via* the CD18 family of adhesion-promoting glycoproteins, LFA-1 (CD11a/CD18), complement receptor 3 (CR3; CD11b/CD18), and CR4 (CD11c/CD18) (Bullock and Wright, 1987; Newman et al., 1990).

The adhesion capacity to host tissue is important to several microorganisms, and a relevant mechanism of virulence is described to dimorphic fungi (McMahon et al., 1995; Brandhorst and Klein, 2000; Marcos et al., 2016; Portuondo et al., 2016). However, the interaction between host-pathogen is not the only factor involved in the infectious process, but also the cell-cell interaction/adhesion. The adhesion is also crucial for the formation of resistance structures, called biofilms (Verstrepen and Klis, 2006; Borges et al., 2018). Like many other pathogenic fungi, *H. capsulatum* yeasts can form biofilms *in vitro* (Pitangui et al., 2012; Gonçalves et al., 2020). Biofilms are defined as a dynamic community of microorganisms strongly linked with each other and attached to a biotic or abiotic surface, surrounded by a self-produced extracellular polymeric matrix (EPM) that provides protection against hostile environments and is also related to reduced antifungal activity (Costerton et al., 1995; Baillie and Douglas, 2000; Brilhante et al., 2015; Zarnowski et al., 2018). *In vivo H. capsulatum* biofilms has never been proved. However, the *H. capsulatum* yeasts can adhere to various cryopreserved bat organs, such as lung, spleen, liver, and intestine (Suarez-Alvarez et al., 2010), human epithelial cell lines (Pitangui et al., 2012) and also, to endothelium and prosthetic valves (Ledtke et al., 2012; Lorchirachonkul et al., 2013; Riddell et al., 2014).

The adhesion process could be mediated by several surface-associated proteins. In *H. capsulatum*, one of these proteins is the heat shock protein 60 (Hsp60), responsible for the adhesion and interaction with CD11b/CD18 (CR3) Mφ receptor (Long et al., 2003), therefore playing an essential role in the infection process.

Heat shock proteins (HSPs) are ubiquitously expressed, highly conserved proteins, known to act as molecular chaperones with important functions, such as the transport of proteins and promotion of folding and assembly of polypeptides in fungi (Kubota et al., 1995; Leach et al., 2012; Cleare et al., 2017). In addition to its intracellular biologic activities, Hsp60 is a prominent target of the humoral and cellular immune response to *H. capsulatum* (Gomez A. M. et al., 1991; Gomez F. J. et al., 1991). *H. capsulatum* Hsp60 was first identified as a 62-kDa protein isolated from the cell wall and membrane extract and showed antigenic (Gomez A. M. et al., 1991) and immunogenic (Gomez et al., 1995) properties.

Hsp60 is reported to be predominantly in the cytosolic fraction of cells (Kubota et al., 1995; Kalderon et al., 2015). However, to act as a ligand for the host cell, in *H. capsulatum*, Hsp60 is expressed in clusters on the cell wall (Long et al., 2003), promoting recognition, adhesion, and phagocytosis of the fungi. The Hsp60/CR3 interaction results in phagocytosis without complete activation of the phagocyte, leading to a non-inflammatory immunological response (Wolf et al., 1987; Ehlers, 2000; Lin et al., 2010; Mihu and Nosanchuk, 2012).

It is of great knowledge that *H. capsulatum* can infect mammals, and murine models are traditionally used for the study of this fungal virulence. However, it is also known that *H. capsulatum* is capable of infect *G. mellonella* larvae (Thomaz et al., 2013), making this non-conventional animal model an important tool to understand *Histoplasma*-host interaction. Invertebrate animals have emerged as alternative models to mammals because breeding is simple and inexpensive (Fuchs and Mylonakis, 2006; Binder et al., 2016). In this aspect, the study of the pathogenesis of different microorganism including dimorphic fungi such as *Paracoccidioides* spp., *Sporothrix* spp., *Talaromyces marneffei* (*Penicillium marneffei*), and *H. capsulatum* has been evaluated in *G. mellonella* larvae (Thomaz et al., 2013; Huang et al., 2015; Scorzoni et al., 2015; Clavijo-Giraldo et al., 2016). The model is especially advantageous for dimorphic fungi due to the possibility that the larvae are kept at 37°C during survival assays and they present six types of immune cells called hemocytes, which have structural and functional similarities to cells of the mammalian immune system (Singulani et al., 2018).

Our current work sought to understand the importance of Hsp60 in *H. capsulatum* biofilms formation and the fungi virulence in the alternative model *G. mellonella*, gaining new insights to a better understanding of cell biology and a future possible application of this protein as a target to therapeutic approaches to histoplasmosis management.

MATERIALS AND METHODS

Histoplasma capsulatum Strains and Growth Conditions

H. capsulatum strains used in this study included G186A (ATCC 26029), representative of chemotype II, and EH-315. EH-315 was isolated from the intestine of infected bats captured in a cave in the state of Guerrero (Mexico) and is designated by Teixeira et al. (2016) as belonging to a bat-associated species-specific clade (BAC1). EH-315 is deposited in the *H. capsulatum* Culture Collection of the Fungal Immunology Laboratory of the Department of Microbiology and Parasitology, from the School of Medicine, National Autonomous University of Mexico (UNAM) (www.histoplas-mex.unam.mx), which is registered in the database of the World Data Centre for Microorganisms (WDCM) with number LIH-UNAM WDCM817. The G186A is classified as H81 human lineage (Kasuga et al., 2003). Both strains are now deposited in the collection of strains at the Clinical Mycology Laboratory of the Faculty of Pharmaceutical Sciences, UNESP (Brazil), and maintained at 37°C in Brain Heart Infusion agar supplemented with 1% of glucose and 0.1% of L-cysteine. Before the experiments, *H. capsulatum* was cultivated in *Histoplasma*-macrophage medium (HMM), composed of HAM-F12 (Sigma) medium, supplemented with glucose (18.2 g/L), glutamic acid (1g/L), HEPES (6 g/L), and L-cysteine (8.4 mg/L) at 37°C and 150 rpm for 48 h.

H. capsulatum Viability After Treatment With Hsp60 mAb (7B6)

Yeast cells were cultured for 48 h in HMM at 37°C and 150 rpm. The cultures were centrifuged at 1000 ×*g* for 10 min, and the pellets were washed three times with phosphate-buffered saline (PBS). To evaluate the viability of *H. capsulatum* yeasts after treatment with Hsp60 mAb 7B6, 10^7 yeast cells were incubated with 10 μg/ml of Hsp60 mAb 7B6, unspecific IgG (Control IgG) in PBS or PBS alone for 1 h at 37°C. After incubation, the cells were washed with PBS and the cell viability was assessing in a hemocytometer using Trypan blue solution. The Hsp60 mAb 7B6 was gently provided by Dr. Joshua D. Nosanchuk from Albert Einstein College of Medicine. Two independent experiments were performed.

Immunofluorescence of the Hsp60

After 48 h cultivation in HMM at 37°C and 150 rpm, the *H. capsulatum* culture was centrifuged at 1,000 ×*g* for 10 min, and the pellet washed three times with phosphate-buffered saline (PBS). The yeast cells were fixed with paraformaldehyde 4% and counted with a hemacytometer. Aliquots containing 10^6 yeast cells were incubated in blocking solution [1% Bovine Serum Albumin (BSA)] for 4 h at 37°C. After washing three times with PBS-Tween 20 0.05% the yeasts were incubated with 10 μg/ml of Hsp60 mAb 7B6 or unspecific IgG (Control IgG) in blocking solution for 1 h at 37°C. Then, after three washes as previously described, yeast cells were incubated for 1 h at 37°C with Alexa Fluor 594-labeled goat anti-mouse IgG (Thermo Fisher Scientific) at a 1:1,000 dilution in blocking solution. After three washes, cells were incubated with fluorescein isothiocyanate (FITC) (Sigma) at 0.5 mg/ml for 45 min at room temperature. Then, the cells were washed and examined with a Zeiss LSM 800 confocal microscope (School of Dentistry of Araraquara, Unesp). Three independent experiments were performed.

Exploring the Involvement of Hsp60 in *H. capsulatum* Biofilm Formation

Biofilm Development

The biofilm formation was performed as described by Gonçalves et al. (2020). To test the influence of *H. capsulatum* Hsp60 in the biofilm development, the protein was blocked through the treatment with the Hsp60 mAb 7B6. To this, after 48 h growth on HMM, the cells were washed three times with PBS and 10^7 yeast cells were incubated with 10 μg/ml of Hsp60 mAb 7B6 or unspecific IgG (Control IgG) in PBS for 1 h at 37°C. After incubation, the cells were washed with PBS and the fungal suspensions were prepared in sterile PBS at 5×10^6 cells/ml. Then, 200 μl and 1,000 μl of the inoculum was added to 96-well and 24-well plates, respectively, and incubated at 37°C for 12 h for biofilm pre-adhesion. After pre-adhesion, the supernatant was removed and the wells were washed carefully to remove non-adherent cells. Then, 200 μl and 2,000 μl of HMM medium were added to 96-well and 24-well plates, respectively, and incubated until 144 h. The *H. capsulatum* biofilms were characterized by measuring the biofilm biomass (crystal violet) and metabolic activity (XTT). At the structural level, the biofilms were analyzed by Scanning Electron Microscopy (SEM) and Confocal Laser Scanning Microscopy (CLSM). Non-treated *H. capsulatum* and the yeasts treated with unspecific IgG (Control IgG) were used as controls. The tests described above were repeated three times.

Crystal Violet Assay

The biomass quantification was performed by the crystal violet assay in 96-well plates as described by Costa-Orlandi et al. (2014). After 144 h of biofilm formation, the supernatant was removed and the biofilms were washed carefully to remove non-adherent cells. Then, the biofilms were fixed with 200 μl of 100% methanol for 15 min. After removing the methanol, the wells were left to dry at room temperature. Afterward, 200 μl of 0.1% crystal violet solution was added and incubated for 20 min. The wells were then washed with distilled water three times and 200 μl of a 33% solution of acetic acid was added. Subsequently, the content of each plate was transferred to another plate for immediate spectrophotometric reading at 590 nm.

XTT Assay

Metabolic activity was evaluated by the XTT (2,3-Bis-(2-Methoxy-4-Nitro-5-Sulfophenyl)-2H-Tetrazolium-5-Carboxanilide) (Sigma) assay in 96-well plates (Martinez and Casadevall, 2007). After 144 h of biofilm formation, the supernatant was removed and the biofilms were washed carefully to remove non-adherent cells. Therefore, 50 μl of

XTT solution at 1 mg/ml and 4 µl of menadione solution at 1 mM were added. The plates were incubated at 37°C for 3 to 4 h. The content of each plate was transferred to another plate and spectrophotometric read at 490 nm. To the establishment of the kinetics curve, the XTT-menadione solution was added at 12, 24, 48, 72, 96, 120, 144, and 168 h time points, and four independent experiments were performed.

Scanning Electron Microscopy

The topography of the biofilms was assessed by SEM and samples were processed as described by Gonçalves et al. (2020). Biofilms were formed in 24-well plates as described above. After 144 h of biofilm formation, the supernatant was removed and the biofilms were washed with PBS to remove non-adherent cells. Biofilms were then fixed with 2.5% of glutaraldehyde solution (Sigma-Aldrich) for 24 h at 4°C. After fixation, the biofilms were washed with PBS and sequentially dehydrated using ethanol solutions (ranging from 20% to 100%) at room temperature. All samples were dried in a pyrex glass vacuum desiccator. Once dried, the wells were cut using a flame-heated scalpel. Subsequently, the samples were mounted on aluminum and silver cylinders and disposed of in a high vacuum evaporator for gold coating. Topographic images of biofilms were captured under the scanning electron microscope JEOL JSM- 6610LV (School of Dentistry of Araraquara, UNESP).

Confocal Laser Scanning Microscopy

Biofilms were formed in 24-well plates as described above. After 144 h of biofilm formation, the supernatant was removed and the biofilm was gently washed with PBS. Live/dead staining was performed using the LIVE/DEAD™ FungaLight™ Yeast Viability Kit (Thermo Fisher Scientific) by incubating the biofilms for 30 min at 37°C with 3.34 µM of the green-fluorescent nucleic acid stain SYTO 9 combined with 20 µM of the red-fluorescent nucleic acid stain propidium iodide (PI) in PBS. Then, the biofilms were washed with PBS, fixed with paraformaldehyde 4% for 24 h, and analyzed with a Zeiss LSM 800 confocal microscope (School of Dentistry of Araraquara, UNESP).

Survival Assay Using the Alternative Animal Model *Galleria mellonella*

Survival assay was performed according to Thomaz et al. (2013), with modifications. *G. mellonella* larvae (School of Pharmaceutical Sciences, São Paulo State University - UNESP) with a body weight ranging from 150 and 200 mg were randomly chosen for the experiments. Ten larvae per group were kept in Petri dishes at 37°C overnight before use. The inoculum of both *H. capsulatum* strains was prepared in PBS at $1x10^8$ yeasts/ml. To test the influence of Hsp60 in the interaction with the larvae, the inoculum was previously treated with 10 µg/ml of the Hsp60 mAb 7B6 for 1 h at 37°C. Then, the yeasts were washed and suspended in PBS. For each group, larvae were injected with $1x10^6$ yeasts/larvae using a 10 µl Hamilton syringe. Larvae inoculated with non-treated *H. capsulatum* strains, treated with unspecific IgG (Control IgG), and larvae inoculated with sterile PBS were used as controls. All larvae were placed in sterile Petri dishes and maintained in the dark at 37°C. Mortality was monitored for up to 10 days of infection. Larvae were considered dead when they displayed no movement in response to touch. Three independent experiments were performed.

TABLE 1 | Viability of G186A and EH-315 strains of *Histoplasma capsulatum* after incubation with Hsp60 mAb 7B6.

	G186A Mean ± SD	EH-315 Mean ± SD
Hsp60 mAb 7B6	91.34 ± 1.31	91.28 ± 1.92
Control IgG	90.58 ± 1.84	92.99 ± 0.61
PBS	92.06 ± 2.00	92.34 ± 0.40

Results are representative of two independent experiments and values expressed as mean ± SD. Cell viability after 1 h incubation with phosphate-buffered saline (PBS), unspecific IgG (Control IgG) (10 µg/ml) and Hsp60 mAb 7B6 (10 µg/ml) at 37°C and 1,500 rpm.

Statistical Analysis

All data were subjected to statistical analysis using the software GraphPad Prism 5.0 (GraphPad Software, Inc., San Diego, CA). Unless otherwise noted, results were presented as mean ± standard deviation (SD), and compared by analysis of variance (ANOVA) followed by Bonferroni or Tukey tests. Survival curves of *G. mellonella* larvae were plotted as Kaplan–Meier survival curves and compared using log-rank tests. Statistical significance was considered when $p < 0.05$.

RESULTS

H. capsulatum Viability After Treatment With Hsp60 mAb 7B6

To evaluate the influence of the Hsp60 mAb 7B6 in *H. capsulatum* viability, the yeast cells were incubated with 10µg/ml of the mAb 7B6 and also with unspecific IgG and PBS for 1 h at 37°C After the treatments, all the conditions showed viabilities higher than 90% (**Table 1**).

Hsp60 Localization by Immunofluorescence

To localize the binding of Hsp60 mAb 7B6 to G186A and EH-315 Hsp60, we assessed the interactions of the mAbs with yeast cells by fluorescence microscopy. mAb 7B6 revealed a diffusion distribution of the Hsp60 in both EH-315 and G186A (**Figure 1**) *H. capsulatum* strains, similar to the previous report of Guimaraes et al. (2009) in G217B strain. Controls with unspecific IgG and secondary antibody were added and showed no signal.

Kinetic of *H. capsulatum* Biofilm Formation

Before evaluating the influence of Hsp60 on *H. capsulatum* biofilm formation, the XTT assay and SEM analysis were

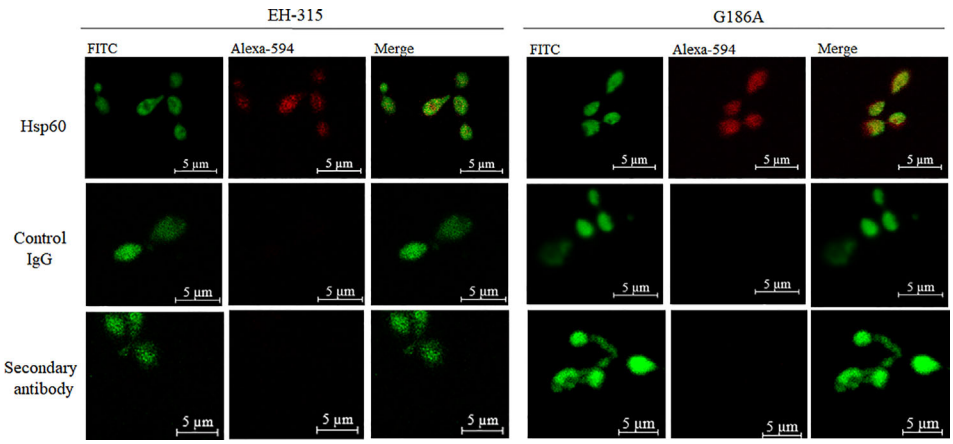

FIGURE 1 | Confocal laser scanning microscopy (CLSM) of mAb-labeled Hsp60 in *H. capsulatum*: immunofluorescence showing labeling of the *H. capsulatum* Hsp60 in EH-315 and G186A strains at 63x. Alexa 594: conjugated with Hsp60 mAb 7B6 or unspecific IgG (Control IgG).

performed with both G186A and EH-315 strains to establish a kinetic curve of the biofilm formation (**Figure 2**) and to evaluate the biofilm structure (**Figure 3**), respectively. The metabolic activity of the biofilms increased over time and the highest growth was observed in the period from 72 to 144 h. Both strains produced consistent and mature biofilms at 144 h, reaching the plateau between 144 and 168 h (**Figure 2**).

The kinetics of biofilm formation was similar for both strains during the initial steps, but after 96 h there was a statistically significant difference (P<0.005) between the strains, with EH-315 presenting higher metabolic activity (**Figure 2**). Considering that biofilm maturation occurs in 144 h (**Figure 2**), SEM analysis of G186A (**Figure 3A**) and EH-315 (**Figure 3B**) strains were performed at this time and showed numerous *H. capsulatum* yeasts firmly adhered to the plastic surface and embedded in an EPM.

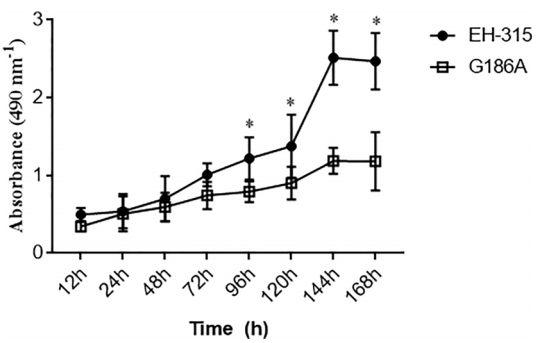

FIGURE 2 | Kinetics of *H. capsulatum* biofilm formation on polystyrene microtiter plates. The metabolic activity of EH-315 and G186A strains was evaluated by the colorimetric XTT reduction assay. Data are representative of four independent experiments and values expressed as mean ± SD. Statistically significant differences between the strains at 96, 120, 144, and 168 h. *p < 0.05.

Influence of Hsp60 on *H. capsulatum* Biofilms

Quantitative measurement of biofilms formed on polystyrene microtiter plates following incubation for 144 h was performed using crystal violet staining and XTT reduction assay, as previously described. Corroborating with the findings during XTT kinetics, the environmental *H. capsulatum* EH-315 strain presented higher metabolic activity (p<0.05) and also formed a more robust biofilm, with higher biomass content compared to the human *H. capsulatum* G186A strain.

The pre-treatment of yeasts with Hsp60 mAb 7B6 resulted in the formation of a thin biofilm, with reduced biomass to both strains (p<0.0001) (**Figure 4A**). Also, both G186A (p<0.05) and EH-315 (p<0.0001) biofilms of pre-treated yeasts presented significantly reduced metabolic activity compared to its non-treated controls (**Figure 4B**). The pre-treatment of both strains with control IgG did not alter the biomass nor the metabolic activity compared to those of untreated fungi.

To characterize the structure, density, and cell distribution of the biofilms formed after yeasts pre-treatment with Hsp60 mAb 7B6 and the control biofilms, SEM, and CLSM images were examined (**Figures 5** and **6**). The reduction of biomass content observed by the crystal violet staining could also be visually observed by SEM and CLSM.

The SEM data provided useful information on the cell morphology presented in the biofilm structure of both control and pre-treated biofilms. The biofilms of EH-315 (**Figure 5A**) presented a high amount of yeasts embedded in an EPM. The biofilms formed after pre-treatment of EH-315 with Hsp60 mAb 7B6 (**Figure 5B**) resulted in a visual reduction of the number of yeasts and the presence of the EPM.

Compared to the EH-315 strain, G186A formed a biofilm with visually less EPM (**Figure 6A**). However, the biofilms formed after the pre-treatment of G186A with Hsp60 mAb 7B6 also presented reduce in the total yeast distribution (**Figure 6B**).

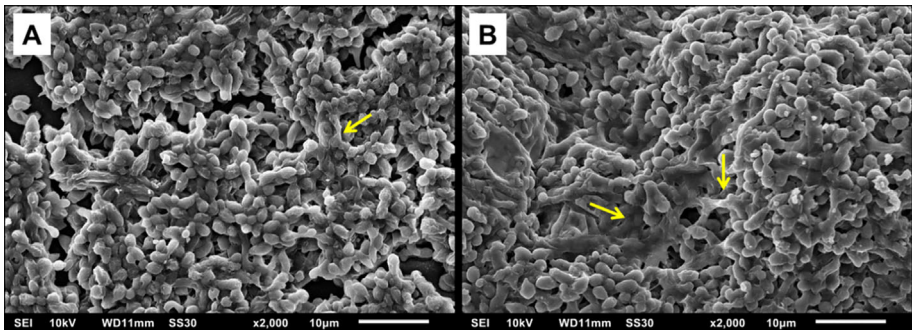

FIGURE 3 | Scanning electron microscopy (SEM) showing yeast adhered to the polystyrene plate indicating the formation of mature biofilms. **(A)** Biofilm of G186A strain at 2000x. **(B)** Biofilm of EH-315 strain at 2000x. The yellow arrows indicate the extracellular polymeric matrix (EPM).

CLSM showed that the biofilms of both EH-315 (**Figure 5D**) and G186A (**Figure 6D**) strains formed with pre-treated yeasts are thinner them their respective control (**Figures 5C** and **6C**, respectively). To the EH-315 strain, the control biofilm presented a thickness of 103.5 µm (**Figure 5C**), while the pre-treated biofilm presented 61.9 µm (**Figure 5D**). To the G186A strain, the control biofilm presented 83.6 µm of thickness (**Figure 6C**), whereas the pre-treated biofilm presented 68.0 µm (**Figure 6D**).

Blockage of *H. capsulatum* Hsp60 Impairs the Survival of Infected *G. mellonella*

An *in vivo* assay using the *G. mellonella* model was also performed to address whether Hsp60 exerted influence on larvae infected with *H. capsulatum*. First, the inoculation of both G186A and EH-315 strains led to a significant reduction in the larvae survival rate compared to the uninfected control ($p < 0.05$; **Figure 7**). We also observed that the G186A strain was slightly more virulent than the EH-315 strain since the larval survival rate on the tenth day was 22 and 26.5% after infection of each strain, respectively. Second, the blockage of Hsp60 with the Hsp60 mAb 7B6 before infection of *G. mellonella* larvae resulted in a significant increase ($p < 0.05$) of the larvae survival with rates on the tenth day of 60 and 60.7% for G186A (**Figure 7A**) and EH-315 (**Figure 7B**) strains, respectively, compared to larvae infected with untreated fungi. On the other hand, the pre-treatment of both strains with control IgG did not alter the survival curve of larvae compared to those of untreated fungi.

DISCUSSION

Heat shock proteins (Hsps), ubiquitously present in cells, are molecular chaperones conserved between microorganisms, being grouped according to their molecular mass and degree of amino acid homology. This nomenclature comes from the characteristic of being inducible through a rapid elevation in temperature. Currently, it is known that Hsps shown changes in expression profile in response to a range of stimuli, not always restricted to temperature, but also starvation, pH, pharmacological agents, and oxidative/osmotic stress (Burnie et al., 2006; Rappleye and Goldman, 2006).

A 60 kDa Hsp, known as Hsp60, is one of the most-characterized molecules on the surface of *H. capsulatum* G217B strain (Long et al., 2003; Guimaraes et al., 2009,

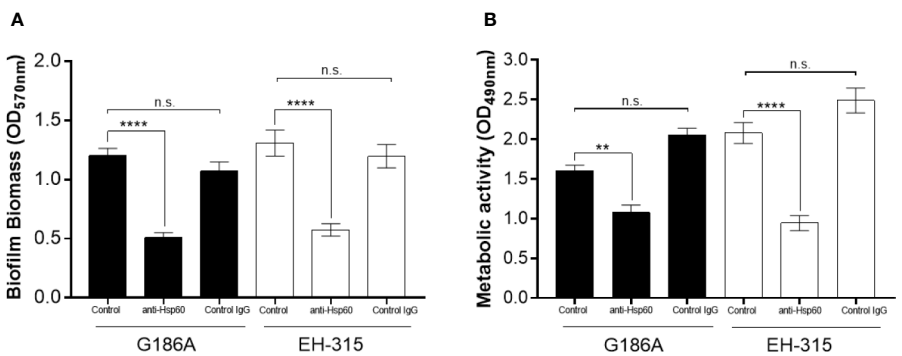

FIGURE 4 | Influence of Hsp60 in *H. capsulatum* EH-315 and G186A biofilm formation. **(A)** Quantification of total biomass by crystal violet staining and **(B)** quantification of metabolic activity by XTT reduction assay. Data are representative of three independent experiments and values expressed as mean ± SEM. $^{**}p < 0.01$; $^{****}p < 0.0001$; n.s., not significant.

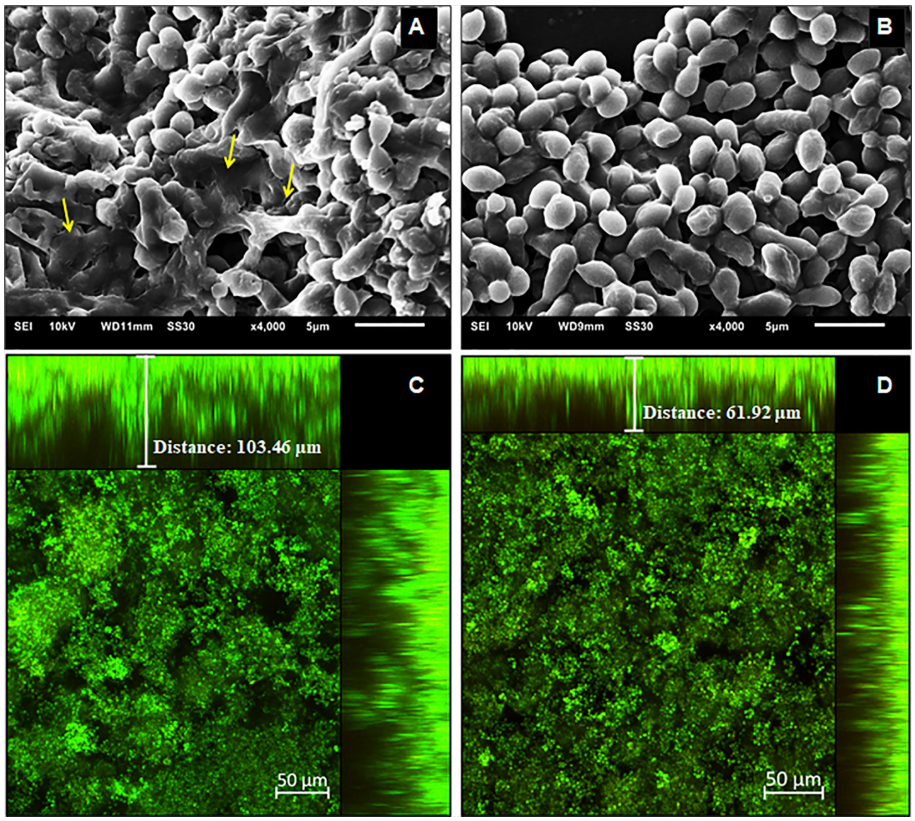

FIGURE 5 | Structural analysis of the 144 h *H. capsulatum* EH-315 biofilms. Scanning electron microscopy (SEM) of *H. capsulatum* EH-315 non-treated **(A)** and treated **(B)** with Hsp60 mAb 7B6 at 4,000x. Confocal laser scanning microscopy (CLSM) biofilm images from *H. capsulatum* EH-315 were treated with Hsp60 mAb 7B6 **(D)** and control without treatment **(C)**. CLSM images comprising an orthogonal view of Z-stacks and 3D image of Z-stacks at 20x. The yellow arrows indicate the extracellular polymeric matrix (EPM).

Guimaraes et al., 2011a). Besides being described as a molecular chaperone and enhance cellular survival under physiological stress (Kubota et al., 1995, Guimaraes et al., 2011a), Hsp60 also interacts specifically with CD11b/CD18 (CR3) on macrophages surface, facilitating the uptake of yeast cells by these phagocytes, where the yeasts can survive and replicate (Long et al., 2003; Guimaraes et al., 2009), and also possess both antigenic (Gomez F. J. et al., 1991) and immunogenic activities (Gomez A. M. et al., 1991), highlighting it's importance as a target for diagnostic and therapeutic approaches.

Moreover, the *H. capsulatum* cell surface presents several proteins that participate in host-pathogen interactions (Batanghari et al., 1998; Long et al., 2003; Bohse and Woods, 2007), sensing the environment (Isaac et al., 2013; DuBois et al., 2016) and defending the fungus against oxidative stress (Youseff et al., 2012; Holbrook et al., 2013). However, only a few have been tested for virulence roles in all strain backgrounds. Most adhesins used by *Histoplasma* to gain entry into host macrophages have only been determined for G217B strain, representative of chemotype I (Long et al., 2003; Gomez et al., 2008).

Histoplasma capsulatum strains can be divided into two chemotypes based on cell wall composition. Chemotype I lacks cell wall α-(1,3)-glucan and is represented by the G217B strain. Chemotype II, represented by G186A strain, contains a layer of α-(1,3)-glucan that masks immunostimulatory β-(1,3)-glucans from detection by the Dectin-1 receptor on host phagocytes (Rappleye et al., 2007). The α-(1,3)-glucan cell wall component is essential for chemotype II *H. capsulatum* virulence (Rappleye et al., 2004). In contrast, even without α-(1,3)-glucan, chemotype I remain fully virulent *in vivo* (Mayfield and Rine, 2007). Posteriorly Edwards et al. (2011) demonstrated that in the chemotype I the β-(1,3)-glucans are also not fully exposed and it is related to the growth phase, with more exposition during the exponential growth, and therefore allowing some interaction with Dectin-1. But in the stationary phase, the yeasts are practically undetectable, suggesting a particular mechanism to hide β-(1,3)-glucans in chemotype I.

Given the previously important roles described for Hsp60 in *H.* capsulatum, here we decided to advance and contribute to a better understanding of *H. capsulatum* Hsp60 regarding the biofilm scenario and host-pathogen interaction with the non-conventional model *G. mellonella.* For that purpose, we used a monoclonal antibody (7B6) to block the Hsp60. The biofilms of two *H. capsulatum* strains were characterized by metabolic activity, biomass content, and images from scanning electron

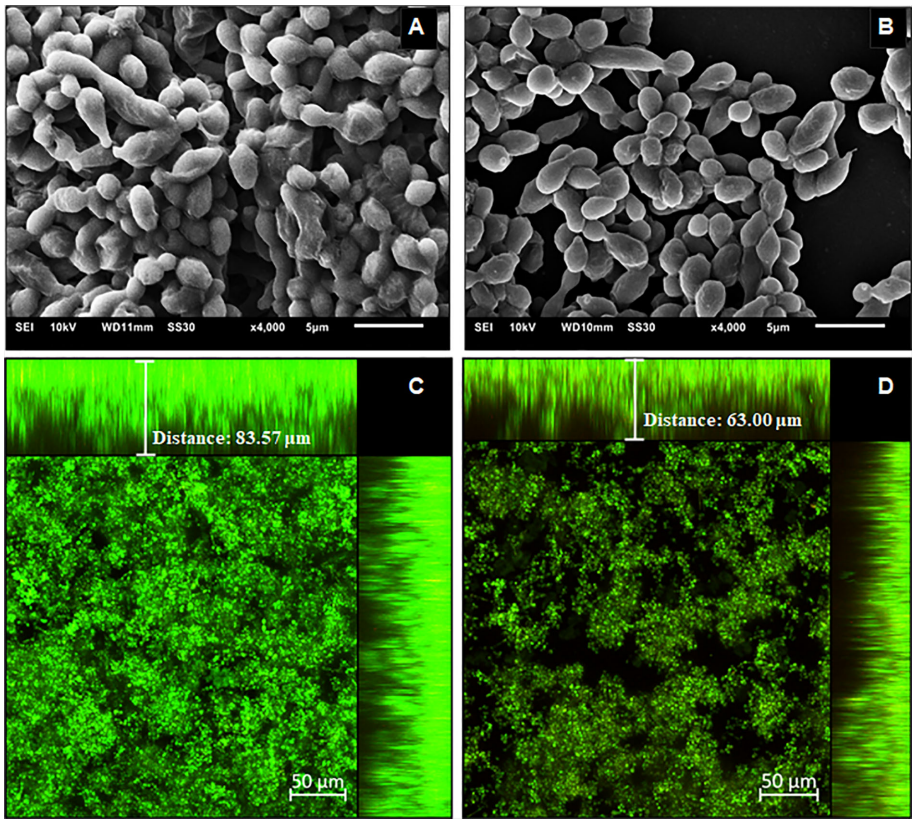

FIGURE 6 | Structural analysis of the 144 h *H. capsulatum* G186A biofilms. Scanning electron microscopy (SEM) of *H. capsulatum* EH-315 non-treated **(A)** and treated **(B)** with Hsp60 mAb 7B6 at 4,000x. Confocal laser scanning microscopy (CLSM) biofilm images from *H. capsulatum* G186A treated with Hsp60 mAb 7B6 **(D)** and control without treatment **(C)**. CLSM images comprising an orthogonal view of Z-stacks and 3D image of Z-stacks at 20x.

microscopy (SEM) and confocal laser scanning microscopy (CLSM). The *G. mellonella* infection was assessed by the establishment of the survival curve.

According to the metabolic activity, the growth stage of G186A and EH-315 biofilms comprises the period of 72 to 144 h, with an increase in metabolic activity. After 144 h, both strains produced consistent and mature biofilms, reaching the stationary phase between 144 and 168 h. Compared to other fungal pathogens, as *Candida* spp. (Sánchez-Vargas et al., 2013; Chandra and Mukherjee, 2015) and *Cryptococcus neoformans* (Martinez and Casadevall, 2007), our results showed that *H. capsulatum* exhibits a slower growth as a biofilm structure, similar to those found on *Paracoccidioides brasiliensis* (Sardi et al., 2015) and *Sporothrix schenckii* complex (Brilhante et al., 2018) biofilms. Also, EH-315 formed a more robust biofilm compared to G186A, corroborating with the findings of Gonçalves et al. (2020).

The blockage of Hsp60 was effective to reduce the metabolic activity and biomass of the biofilms from both *H. capsulatum* strains. Furthermore, the biofilms of cells treated with the antibody were thinner as well as presented a lower amount of cells and extracellular matrix compared to its non-treated controls, revealing the potential role of the Hsp60 in cell-cell or cell-surface adhesion, increasing the importance of this protein as a virulence factor of *H. capsulatum*. Guimaraes et al. (2011b) showed that the Hsp60 mAb 7B6 reduces the formation of *H. capsulatum* aggregates. This antibody has an inconsistent impact on agglutinate charge resulting in reduced cell-to-cell interaction leading to a reduced *H. capsulatum* agglutination (Guimaraes et al., 2011b). In this way, we hypothesize that a reduced cell-to-cell interaction caused in *H. capsulatum* by the treatment with the Hsp60 mAb 7B6 can contribute to the reduction of the biofilm formation observed in our study.

H. capsulatum Hsp60 has never been related to the adherence of the fungus to abiotic surfaces nor implicated in the biofilm structure. However, antibodies specific to *Histophilus somni* Hsp60, an opportunistic pathogen that causes respiratory, genitourinary, and generalized infections in cattle, also prevented biofilm formation *in vitro* (Zarankiewicz et al., 2012).

Most *H. capsulatum* studies focus on phagocytosis or immune response. However, the demonstration that *H. capsulatum* yeasts can form biofilm *in vitro* and also can adhere to pneumocytes (Pitangui et al., 2012), cryopreserved bat organs (Suarez-Alvarez et al., 2010), human endothelium (Ledtke et al., 2012), and prosthetic valves (Alexander et al., 1979; Lorchirachonkul et al., 2013), draw attention to the importance

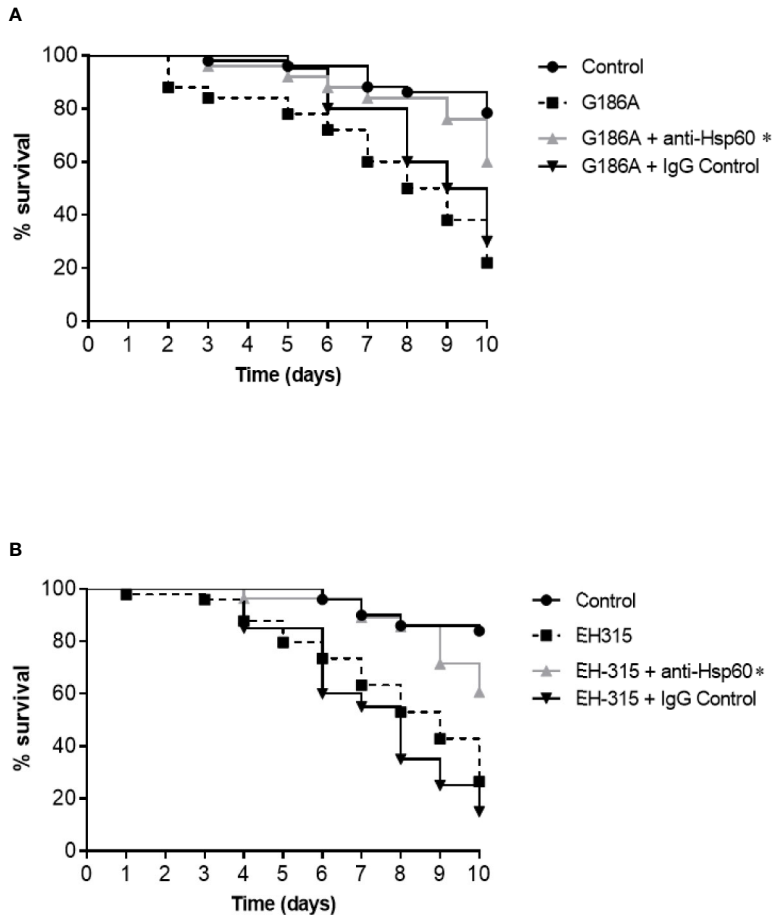

FIGURE 7 | Influence of Hsp60 in the virulence of *H. capsulatum* G186A **(A)** and EH-315 **(B)** strains using *G mellonella* as a model. Data are representative of three independent experiments. The groups of larvae infected with untreated yeasts are represented by the black dashed lines, larvae infected with yeasts treated with control IgG are represented by the black lines and the groups of larvae infected with yeasts treated with Hsp60 mAb 7B6 are represented by the gray lines. The pre-treatment of both *H. capsultaum* strains with Hsp60 mAb 7B6 significantly increased the survival of *G. mellonella* compared with non-treated yeasts and treated with unspecific IgG. *$p < 0.05$.

of *H. capsulatum* adherence to the colonization and dissemination of the fungus. Furthermore, the susceptibility of *H. capsulatum* biofilms to amphotericin B and itraconazole was reduced comparing to the planktonic growth (Brilhante et al., 2015), highlighting the importance of studying the *H. capsulatum* biofilm structure.

Nonetheless, fungal biofilms are an important clinical problem associated with significant rates of antifungal resistance, disease persistence, and an increase of mortality index (Uppuluri et al., 2010; Kollef et al., 2012; Kowalski et al., 2019).

Despite the critical role that biofilms play in the course of the disease and colonization of host tissues, many basic aspects of development and organization, such as the initial steps of adhesion to the substrate, remain inconclusive. Some families of genes have already been described as important for this adhesion process, for example, the ALS, HWP, and IFF/HYR described to *Candida albicans*, that encodes several proteins responsible to facilitate cell-cell adhesion and adhesion of *C. albicans* on abiotic surfaces (Chandra et al., 2001; Hoyer et al., 2008; Ene and Bennett, 2009; Kempf et al., 2009). A marked reduction in total biofilm biomass has been shown in adhesin knockouts *C. albicans* strains, including *Δhwp2*, *Δhyr1*, and *Δals1/Δals3* double deletion mutants (McCall et al., 2019), revealing the importance of initial adhesion for the development of biofilm biomass.

Although remarkable in *C. albicans* biofilms, in which ALS genes exhibited increased expression (O'Connor et al., 2005), there is a lack of studies regarding the presence or impact of the adhesins on biofilms among the dimorphic fungi. Sardi et al. (2015) showed the up-regulation of GP43 and GAPDH in the biofilm of *P. brasiliensis*. GP43 is an important adhesin described in *Paracoccidioides* adhesion to matrix components (Vicentini et al., 1994), while GAPDH appears to impact the adhesion processes of both *Paracoccidioides* and *Candida* spp. (Gozalbo et al., 1998; Barbosa et al., 2006).

Notably, adhesins play an important role in biofilm formation and, possibly, the reduction of biomass, concomitantly with the

reduction of metabolic activity, thickness, and presence of EPM in *H. capsulatum* biofilms formed after blocking the Hsp60 protein, suggest that this protein can also act on the adhesion to the substrate or in cell-cell adhesion, contributing to the establishment of *H. capsulatum* biofilms.

We also evaluated the role of Hsp60 of *H. capsulatum* in an invertebrate animal model, *G. mellonella*. The infection of the larvae with *H. capsulatum* was firstly tested by Thomaz et al. (2013), which used the G184ARAR (ATCC 26027) and ATCC G217B (ATCC 26032) strains to compare their virulence using different inoculum concentrations and temperatures (25 and 37 °C). Although we used other strains in this study (G186A and EH-315), the profile of the survival curve infected with $1x10^6$ yeast/larvae was similar to those, resulting in survival rates of about 20% at the end of 10 days at 37 °C in both studies. Interestingly, when the Hsp60 of G186A and EH-315 strains were blocked by 7B6 mAb before the larval infection, a significant increase in survival rate around 60% was observed.

Our findings reinforce that Hsp60, and its blocking by different antibodies, have different functions, which vary depending on the conditions and models tested. For example, Guimaraes et al. (2009) showed that the pre-treatment of mice with different antibodies anti-Hsp60 followed 2 h later by infection of *H. capsulatum* yeast cells resulted in a distinct response profile. IgG1 (11D1) and IgG2a (12D3) mAbs significantly prolonged survival and reduced the fungal load of animals, while IgG2b (7B6) mAb was not protective. Furthermore, the use of other antibodies, with different epitopes regions, promoted an increase in the phagocytosis by macrophages *in vitro*, but 7B6 and 6B7 (which both comprise the same structural cleft region of Hsp60) did not increase the phagocytosis. Specifically for 7B6, the epitope region is between 353 and 413 aa. This region represents the structural cleft on Hsp60, one of the regions responsible for CR3 interaction (Habich et al., 2006; Guimaraes et al., 2009). The presence of the Fc region itself can promote phagocytosis, however, considering that it does not occur to treatment with 7B6 and 6B7 antibodies, in addition to the presence of the Fc portion, maybe the structural cleft of the protein must be available for full interaction with CR3. Based on this, we hypothesized that this structural cleft region might not be important in the fungus-hemocyte interaction of the *G. mellonella* model. Also, although many similarities between insect and mammalian immune cells are observed, some differences such as the absence of Fc receptor in *G. mellonella* hemocyte compared to macrophage is described (Browne et al., 2013).

Another important aspect of the interaction of the Hsp60 mAb 7B6 with *H. capsulatum* was explored recently by Burnet et al. (2020). Significant changes in the plasma membrane induced when *H. capsulatum* yeast cells are treated with this and other Hsp60 mAb were shown. In all the tested mAb, but especially the 7B6, these membrane changes were characterized by an increased level of ergosterol, lead to higher sensitivity to the antifungal drug amphotericin B (Burnet et al., 2020). This higher sensitivity caused by alterations in the plasma membrane induced by the antibody can also lead to a higher sensitivity of the fungi to the immune system of the *G. mellonella*, increasing larval survival, as observed in our study.

Thus, the sum of these features can promote a different *Histoplasma*-hemocyte interaction and phagocytosis can occur normally, and consequently, lead to the death of the fungus and increasing larval survival. However further studies are needed to support this hypothesis.

Because of the importance of the different yeast ligands and host receptors on the intracellular fate of *H. capsulatum* and also the importance of the biofilms as mentioned above, the knowledge of the surface molecules repertoire that engage host infections and fungal adhesion might contribute to a better understanding of *Histoplasma* cell biology and virulence, as well as providing news targets to a more broadly applicable alternative to conventional antifungals.

DATA AVAILABILITY STATEMENT

The original contributions presented in the study are included in the article/supplementary materials. Further inquiries can be directed to the corresponding authors.

AUTHOR CONTRIBUTIONS

NF, HD, and AF-A conceived the presented idea. NF, LO, and CD designed and performed the experiments. NF, CM, HD, and JS processed the experimental data and verified the analytical methods. NF, HD, JS, CM, LO, and CD wrote the manuscript and designed the figures. MT, MM-G, HD, and AF-A supervised the findings and the writing of this manuscript. All authors discussed the results and contributed to the final manuscript.

FUNDING

This work was supported by the Fundação de Amparo à Pesquisa do Estado de São Paulo-FAPESP [16/11836-0 (AF-A), 2019/04882-4 (NF), 2015/14023-8 (HD), 2016/17048-4 (CM), 2017/06658-9 (JS), 2018/15877-9 (LO)], Programa de Apoio ao Desenvolvimento Científico da Faculdade de Ciências Farmacêuticas da UNESP-PADC, Coordenação de Aperfeiçoamento de Pessoal de Nível Superior—Brasil (CAPES), and Conselho Nacional de Desenvolvimento Científico e Tecnológico (CNPq).

ACKNOWLEDGMENTS

We are grateful to the Laboratory of Confocal Fluorescence Microscopy and to the Electron Microscopy laboratory of the Faculty of Dentistry, Campus of Araraquara for the availability of using the Confocal Fluorescence Microscope and Electron Microscopy. We also would like to thank to Joshua D. Nosanchuk from Albert Einstein College of Medicine (NY, USA) for gently provided the Hsp60 mAb (7B6).

REFERENCES

Adenis, A. A., Valdes, A., Cropet, C., McCotter, O. Z., Derado, G., Couppie, P., et al. (2018). Burden of HIV-associated histoplasmosis compared with tuberculosis in Latin America: a modelling study. *Lancet Infect. Dis.* 18, 1150–1159. doi: 10.1016/S1473-3099(18)30354-2

Alexander, W. J., Mowry, R. W., Cobbs, C. G., and Dismukes, W. E. (1979). Prosthetic valve endocarditis caused by Histoplasma capsulatum. *JAMA* 242, 1399–1400. doi: 10.1001/jama.1979.03300130043019

Armstrong, P. A., Jackson, B. R., Haselow, D., Fields, V., Ireland, M., Austin, C., et al. (2018). Multistate Epidemiology of Histoplasmosis, United States 2011-2014. *Emerg. Infect. Dis.* 24, 425–431. doi: 10.3201/eid2403.171258

Baillie, G. S., and Douglas, L. J. (2000). Matrix polymers of Candida biofilms and their possible role in biofilm resistance to antifungal agents. *J. Antimicrob. Chemother.* 46, 397–403. doi: 10.1093/jac/46.3.397

Barbosa, M. S., Báo, S. N., Andreotti, P. F., de Faria, F. P., Felipe, M. S., dos Santos Feitosa, L., et al. (2006). Glyceraldehyde-3-phosphate dehydrogenase of Paracoccidioides brasiliensis is a cell surface protein involved in fungal adhesion to extracellular matrix proteins and interaction with cells. *Infect. Immun.* 74, 382–389. doi: 10.1128/IAI.74.1.382-389.2006

Batanghari, J. W., Deepe, G. S.Jr., Di Cera, E., and Goldman, W. E. (1998). Histoplasma acquisition of calcium and expression of CBP1 during intracellular parasitism. *Mol. Microbiol.* 27, 531–539. doi: 10.1046/j.1365-2958.1998.00697.x

Binder, U., Maurer, E., and Lass-Florl, C. (2016). Galleria mellonella: An invertebrate model to study pathogenicity in correctly defined fungal species. *Fungal Biol.* 120, 288–295. doi: 10.1016/j.funbio.2015.06.002

Bohse, M. L., and Woods, J. P. (2007). RNA interference-mediated silencing of the YPS3 gene of Histoplasma capsulatum reveals virulence defects. *Infect. Immun.* 75, 2811–2817. doi: 10.1128/IAI.00304-07

Borges, K. R. A., Pimentel, I. V., Lucena, L., Silva, M., Monteiro, S. G., Monteiro, C. A., et al. (2018). Adhesion and biofilm formation of Candida parapsilosis isolated from vaginal secretions to copper intrauterine devices. *Rev. Inst. Med. Trop. Sao Paulo* 60, e59. doi: 10.1590/s1678-9946201860059

Brandhorst, T., and Klein, B. (2000). Cell wall biogenesis of Blastomyces dermatitidis. Evidence for a novel mechanism of cell surface localization of a virulence-associated adhesin via extracellular release and reassociation with cell wall chitin. *J. Biol. Chem.* 275, 7925–7934. doi: 10.1074/jbc.275.11.7925

Brilhante, R. S. N., de Lima, R. A. C., Marques, F. J. F., Silva, N. F., Caetano, E. P., Castelo-Branco, D. S. C. M., et al. (2015). Histoplasma capsulatum in planktonic and biofilm forms: in vitro susceptibility to amphotericin B, itraconazole and farnesol. *J. Med. Microbiol.* 64, 394–399. doi: 10.1099/jmm.0.000030

Brilhante, R. S. N., de Aguiar, F. R. M., da Silva, M. L. Q., de Oliveira, J. S., de Camargo, Z. P., Rodrigues, A., et al. (2018). Antifungal susceptibility of Sporothrix schenckii complex biofilms. *Med. Mycol.* 56, 297–306. doi: 10.1093/mmy/myx043

Browne, N., Heelan, M., and Kavanagh, K. (2013). An analysis of the structural and functional similarities of insect hemocytes and mammalian phagocytes. *Virulence* 4, 597–603. doi: 10.4161/viru.25906

Bullock, W. E., and Wright, S. D. (1987). Role of the adherence-promoting receptors, CR3, LFA-1, and p150,95, in binding of Histoplasma capsulatum by human macrophages. *J. Exp. Med.* 165, 195–210. doi: 10.1084/jem.165.1.195

Burnet, M. C., Zamith-Miranda, D., Heyman, H. M., Weitz, K. K., Bredeweg, E. L., Nosanchuk, J. D., et al. (2020). Remodeling of the Histoplasma Capsulatum Membrane Induced by Monoclonal Antibodies. *Vaccines (Basel)* 8 (2), 269–284. doi: 10.3390/vaccines8020269

Burnie, J. P., Carter, T. L., Hodgetts, S. J., and Matthews, R. C. (2006). Fungal heat-shock proteins in human disease. *FEMS Microbiol. Rev.* 30, 53–88. doi: 10.1111/j.1574-6976.2005.00001.x

Chandra, J., and Mukherjee, P. K. (2015). Candida Biofilms: Development, Architecture, and Resistance. *Microbiol. Spectr.* 3 (4), 1–22. doi: 10.1128/9781555817466.ch6

Chandra, J., Kuhn, D. M., Mukherjee, P. K., Hoyer, L. L., McCormick, T., and Ghannoum, M. A. (2001). Biofilm formation by the fungal pathogen Candida albicans: development, architecture, and drug resistance. *J. Bacteriol.* 183, 5385–5394. doi: 10.1128/JB.183.18.5385-5394.2001

Clavijo-Giraldo, D. M., Matinez-Alvarez, J. A., Lopes-Bezerra, L. M., Ponce-Noyola, P., Franco, B., Almeida, R. S., et al. (2016). Analysis of Sporothrix schenckii sensu stricto and Sporothrix brasiliensis virulence in Galleria mellonella. *J. Microbiol. Methods* 122, 73–77. doi: 10.1016/j.mimet.2016.01.014

Cleare, L. G., Zamith-Miranda, D., and Nosanchuk, J. D. (2017). Heat Shock Proteins in Histoplasma and Paracoccidioides. *Clin. Vaccine Immunol.* 24, 1–8. doi: 10.1128/CVI.00221-17

Costa-Orlandi, C. B., Sardi, J. C., Santos, C. T., Fusco-Almeida, A. M., and Mendes-Giannini, M. J. (2014). In vitro characterization of Trichophyton rubrum and T. mentagrophytes biofilms. *Biofouling* 30, 719–727. doi: 10.1080/08927014.2014.919282

Costerton, J. W., Lewandowski, Z., Caldwell, D. E., Korber, D. R., and Lappin-Scott, H. M. (1995). Microbial biofilms. *Annu. Rev. Microbiol.* 49, 711–745. doi: 10.1146/annurev.mi.49.100195.003431

DuBois, J. C., Pasula, R., Dade, J. E., and Smulian, A. G. (2016). Yeast Transcriptome and In Vivo Hypoxia Detection Reveals Histoplasma capsulatum Response to Low Oxygen Tension. *Med. Mycol.* 54, 40–58. doi: 10.1093/mmy/myv073

Edwards, J. A., Alore, E. A., and Rappleye, C. A. (2011). The yeast-phase virulence requirement for alpha-glucan synthase differs among Histoplasma capsulatum chemotypes. *Eukaryot. Cell* 10, 87–97. doi: 10.1128/EC.00214-10

Ehlers, M. R. (2000). CR3: a general purpose adhesion-recognition receptor essential for innate immunity. *Microbes Infect.* 2, 289–294. doi: 10.1016/S1286-4579(00)00299-9

Ene, I. V., and Bennett, R. J. (2009). Hwp1 and related adhesins contribute to both mating and biofilm formation in Candida albicans. *Eukaryot. Cell* 8, 1909–1913. doi: 10.1128/EC.00245-09

Fuchs, B. B., and Mylonakis, E. (2006). Using non-mammalian hosts to study fungal virulence and host defense. *Curr. Opin. Microbiol.* 9, 346–351. doi: 10.1016/j.mib.2006.06.004

Gomez, A. M., Rhodes, J. C., and Deepe, G. S. Jr. (1991). Antigenicity and immunogenicity of an extract from the cell wall and cell membrane of Histoplasma capsulatum yeast cells. *Infect. Immun.* 59, 330–336. doi: 10.1128/IAI.59.1.330-336.1991

Gomez, F. J., Allendoerfer, R., and Deepe, G. S. Jr. (1995). Vaccination with recombinant heat shock protein 60 from Histoplasma capsulatum protects mice against pulmonary histoplasmosis. *Infect. Immun.* 63, 2587–2595. doi: 10.1128/IAI.63.7.2587-2595.1995

Gomez, F. J., Pilcher-Roberts, R., Alborzi, A., and Newman, S. L. (2008). Histoplasma capsulatum cyclophilin A mediates attachment to dendritic cell VLA-5. *J. Immunol.* 181, 7106–7114. doi: 10.4049/jimmunol.181.10.7106

Gomez, F. J., Gomez, A. M., and Deepe, G. S.Jr. (1991). Protective efficacy of a 62-kilodalton antigen, HIS-62, from the cell wall and cell membrane of Histoplasma capsulatum yeast cells. *Infect. Immun.* 59, 4459–4464. doi: 10.1128/IAI.59.12.4459-4464.1991

Gonçalves, L. N. C., Costa-Orlandi, C. B., Bila, N. M., Vaso, C. O., Da Silva, R. A. M., Mendes-Giannini, M. J. S., et al. (2020). Biofilm Formation by Histoplasma capsulatum in Different Culture Media and Oxygen Atmospheres. *Front. Microbiol.* 11, 1455–1467. doi: 10.3389/fmicb.2020.01455

Gozalbo, D., Gil-Navarro, I., Azorin, I., Renau-Piqueras, J., Martinez, J. P., and Gil, M. L. (1998). The cell wall-associated glyceraldehyde-3-phosphate dehydrogenase of Candida albicans is also a fibronectin and laminin binding protein. *Infect. Immun.* 66, 2052–2059. doi: 10.1128/IAI.66.5.2052-2059.1998

Guimaraes, A. J., Frases, S., Gomez, F. J., Zancope-Oliveira, R. M., and Nosanchuk, J. D. (2009). Monoclonal antibodies to heat shock protein 60 alter the pathogenesis of Histoplasma capsulatum. *Infect. Immun.* 77, 1357–1367. doi: 10.1128/IAI.01443-08

Guimaraes, A. J., Nakayasu, E. S., Sobreira, T. J., Cordero, R. J., Nimrichter, L., Almeida, I. C., et al. (2011a). Histoplasma capsulatum heat-shock 60 orchestrates the adaptation of the fungus to temperature stress. *PloS One* 6, e14660. doi: 10.1371/journal.pone.0014660

Guimaraes, A. J., Frases, S., Pontes, B., de Cerqueira, M. D., Rodrigues, M. L., Viana, N. B., et al. (2011b). Agglutination of Histoplasma capsulatum by IgG monoclonal antibodies against Hsp60 impacts macrophage effector functions. *Infect. Immun.* 79, 918–927. doi: 10.1128/IAI.00673-10

Habich, C., Kempe, K., Gomez, F. J., Lillicrap, M., Gaston, H., van der Zee, R., et al. (2006). Heat shock protein 60: identification of specific epitopes for binding to primary macrophages. *FEBS Lett.* 580, 115–120. doi: 10.1016/j.febslet.2005.11.060

Holbrook, E. D., Smolnycki, K. A., Youseff, B. H., and Rappleye, C. A. (2013). Redundant catalases detoxify phagocyte reactive oxygen and facilitate

Histoplasma capsulatum pathogenesis. *Infect. Immun.* 81, 2334–2346. doi: 10.1128/IAI.00173-13

Hoyer, L. L., Green, C. B., Oh, S. H., and Zhao, X. (2008). Discovering the secrets of the Candida albicans agglutinin-like sequence (ALS) gene family–a sticky pursuit. *Med. Mycol.* 46, 1–15. doi: 10.1080/13693780701435317

Huang, X., Li, D., Xi, L., and Mylonakis, E. (2015). Galleria mellonella Larvae as an Infection Model for Penicillium marneffei. *Mycopathologia* 180, 159–164. doi: 10.1007/s11046-015-9897-y

Isaac, D. T., Coady, A., Van Prooyen, N., and Sil, A. (2013). The 3-hydroxy-methylglutaryl coenzyme A lyase HCL1 is required for macrophage colonization by human fungal pathogen Histoplasma capsulatum. *Infect. Immun.* 81, 411–420. doi: 10.1128/IAI.00833-12

Kalderon, B., Kogan, G., Bubis, E., and Pines, O. (2015). Cytosolic Hsp60 can modulate proteasome activity in yeast. *J. Biol. Chem.* 290, 3542–3551. doi: 10.1074/jbc.M114.626622

Kasuga, T., White, T. J., Koenig, G., McEwen, J., Restrepo, A., Castañeda, E., et al. (2003). Phylogeography of the fungal pathogen Histoplasma capsulatum. *Mol. Ecol.* 12, 3383–3401. doi: 10.1046/j.1365-294X.2003.01995.x

Kempf, M., Cottin, J., Licznar, P., Lefrancois, C., Robert, R., and Apaire-Marchais, V. (2009). Disruption of the GPI protein-encoding gene IFF4 of Candida albicans results in decreased adherence and virulence. *Mycopathologia* 168, 73–77. doi: 10.1007/s11046-009-9201-0

Kollef, M., Micek, S., Hampton, N., Doherty, J. A., and Kumar, A. (2012). Septic shock attributed to Candida infection: importance of empiric therapy and source control. *Clin. Infect. Dis.* 54, 1739–1746. doi: 10.1093/cid/cis305

Kowalski, C. H., Kerkaert, J. D., Liu, K. W., Bond, M. C., Hartmann, R., Nadell, C. D., et al. (2019). Fungal biofilm morphology impacts hypoxia fitness and disease progression. *Nat. Microbiol.* 4, 2430–2441. doi: 10.1038/s41564-019-0558-7

Kubota, H., Hynes, G., and Willison, K. (1995). The chaperonin containing t-complex polypeptide 1 (TCP-1). Multisubunit machinery assisting in protein folding and assembly in the eukaryotic cytosol. *Eur. J. Biochem.* 230, 3–16. doi: 10.1111/j.1432-1033.1995.tb20527.x

Leach, M. D., Budge, S., Walker, L., Munro, C., Cowen, L. E., and Brown, A. J. (2012). Hsp90 orchestrates transcriptional regulation by Hsf1 and cell wall remodelling by MAPK signalling during thermal adaptation in a pathogenic yeast. *PloS Pathog.* 8, e1003069. doi: 10.1371/journal.ppat.1003069

Ledtke, C., Rehm, S. J., Fraser, T. G., Shrestha, N. K., Tan, C. D., Rodriguez, E. R., et al. (2012). Endovascular infections caused by Histoplasma capsulatum: a case series and review of the literature. *Arch. Pathol. Lab. Med.* 136, 640–645. doi: 10.5858/arpa.2011-0050-OA

Lin, J. S., Huang, J. H., Hung, L. Y., Wu, S. Y., and Wu-Hsieh, B. A. (2010). Distinct roles of complement receptor 3, Dectin-1, and sialic acids in murine macrophage interaction with Histoplasma yeast. *J. Leukoc. Biol.* 88, 95–106. doi: 10.1189/jlb.1109717

Long, K. H., Gomez, F. J., Morris, R. E., and Newman, S. L. (2003). Identification of heat shock protein 60 as the ligand on Histoplasma capsulatum that mediates binding to CD18 receptors on human macrophages. *J. Immunol.* 170, 487–494. doi: 10.4049/jimmunol.170.1.487

Lorchirachonkul, N., Foongladda, S., Ruangchira-Urai, R., and Chayakulkeeree, M. (2013). Prosthetic valve endocarditis caused by Histoplasma capsulatum: the first case report in Thailand. *J. Med. Assoc. Thai.* 96 Suppl 2, S262–S265.

Maiga, A. W., Deppen, S., Scaffidi, B. K., Baddley, J., Aldrich, M. C., Dittus, R. S., et al. (2018). Mapping Histoplasma capsulatum Exposure, United States. *Emerg. Infect. Dis.* 24, 1835–1839. doi: 10.3201/eid2410.180032

Marcos, C. M., de Oliveira, H. C., da Silva, J. F., Assato, P. A., Yamazaki, D. S., da Silva, R. A., et al. (2016). Identification and characterisation of elongation factor Tu, a novel protein involved in Paracoccidioides brasiliensis-host interaction. *FEMS Yeast Res.* 16 (7), fow079. doi: 10.1093/femsyr/fow079

Martinez, L. R., and Casadevall, A. (2007). Cryptococcus neoformans biofilm formation depends on surface support and carbon source and reduces fungal cell susceptibility to heat, cold, and UV light. *Appl. Environ. Microbiol.* 73, 4592–4601. doi: 10.1128/AEM.02506-06

Mayfield, J. A., and Rine, J. (2007). The genetic basis of variation in susceptibility to infection with Histoplasma capsulatum in the mouse. *Genes Immun.* 8, 468–474. doi: 10.1038/sj.gene.6364411

McCall, A. D., Pathirana, R. U., Prabhakar, A., Cullen, P. J., and Edgerton, M. (2019). Candida albicans biofilm development is governed by cooperative attachment and adhesion maintenance proteins. *NPJ Biofilms Microbiomes* 5, 21. doi: 10.1038/s41522-019-0094-5

McMahon, J. P., Wheat, J., Sobel, M. E., Pasula, R., Downing, J. F., and Martin, W. J. 2. (1995). Murine laminin binds to Histoplasma capsulatum. A possible mechanism of dissemination. *J. Clin. Invest.* 96, 1010–1017. doi: 10.1172/JCI118086

Mihu, M. R., and Nosanchuk, J. D. (2012). Histoplasma virulence and host responses. *Int. J. Microbiol.* 2012, 268123. doi: 10.1155/2012/268123

Mittal, J., Ponce, M. G., Gendlina, I., and Nosanchuk, J. D. (2019). Histoplasma Capsulatum: Mechanisms for Pathogenesis. *Curr. Top. Microbiol. Immunol.* 422, 157–191. doi: 10.1007/82_2018_114

Newman, S. L., Bucher, C., Rhodes, J., and Bullock, W. E. (1990). Phagocytosis of Histoplasma capsulatum yeasts and microconidia by human cultured macrophages and alveolar macrophages. Cellular cytoskeleton requirement for attachment and ingestion. *J. Clin. Invest.* 85, 223–230. doi: 10.1172/JCI114416

O'Connor, L., Lahiff, S., Casey, F., Glennon, M., Cormican, M., and Maher, M. (2005). Quantification of ALS1 gene expression in Candida albicans biofilms by RT-PCR using hybridisation probes on the LightCycler. *Mol. Cell Probes* 19, 153–162. doi: 10.1016/j.mcp.2004.10.007

Papalini, C., Belfiori, B., Martino, G., Papili, R., Pitzurra, L., Ascani, S., et al. (2019). An Italian Case of Disseminated Histoplasmosis Associated with HIV. *Case Rep. Infect. Dis.* 2019, 7403878. doi: 10.1155/2019/7403878

Pitangui, N. S., Sardi, J. C., Silva, J. F., Benaducci, T., Moraes da Silva, R. A., Rodriguez-Arellanes, G., et al. (2012). Adhesion of Histoplasma capsulatum to pneumocytes and biofilm formation on an abiotic surface. *Biofouling* 28, 711–718. doi: 10.1080/08927014.2012.703659

Portuondo, D. L., Batista-Duharte, A., Ferreira, L. S., Martinez, D. T., Polesi, M. C., Duarte, R. A., et al. (2016). A cell wall protein-based vaccine candidate induce protective immune response against Sporothrix schenckii infection. *Immunobiology* 221, 300–309. doi: 10.1016/j.imbio.2015.10.005

Rappleye, C. A., and Goldman, W. E. (2006). Defining virulence genes in the dimorphic fungi. *Annu. Rev. Microbiol.* 60, 281–303. doi: 10.1146/annurev.micro.59.030804.121055

Rappleye, C. A., Engle, J. T., and Goldman, W. E. (2004). RNA interference in Histoplasma capsulatum demonstrates a role for alpha-(1,3)-glucan in virulence. *Mol. Microbiol.* 53, 153–165. doi: 10.1111/j.1365-2958.2004.04131.x

Rappleye, C. A., Eissenberg, L. G., and Goldman, W. E. (2007). Histoplasma capsulatum alpha-(1,3)-glucan blocks innate immune recognition by the beta-glucan receptor. *Proc. Natl. Acad. Sci. U. S. A.* 104, 1366–1370. doi: 10.1073/pnas.0609848104

Riddell, J., Kauffman, C. A., Smith, J. A., Assi, M., Blue, S., Buitrago, M. I., et al. (2014). Histoplasma capsulatum endocarditis: multicenter case series with review of current diagnostic techniques and treatment. *Medicine (Baltimore)* 93, 186–193. doi: 10.1097/MD.0000000000000034

Salzer, H. J. F., Burchard, G., Cornely, O. A., Lange, C., Rolling, T., Schmiedel, S., et al. (2018). Diagnosis and Management of Systemic Endemic Mycoses Causing Pulmonary Disease. *Respiration* 96, 283–301. doi: 10.1159/000489501

Sánchez-Vargas, L. O., Estrada-Barraza, D., Pozos-Guillen, A. J., and Rivas-Caceres, R. (2013). Biofilm formation by oral clinical isolates of Candida species. *Arch. Oral. Biol.* 58, 1318–1326. doi: 10.1016/j.archoralbio.2013.06.006

Sardi„ Pitangui, N. S., Voltan, A. R., Braz, J. D., Machado, M. P., Fusco Almeida, A. M., et al. (2015). In vitro Paracoccidioides brasiliensis biofilm and gene expression of adhesins and hydrolytic enzymes. *Virulence* 6, 642–651. doi: 10.1080/21505594.2015.1031437

Scorzoni, L., de Paula e Silva, A. C., Singulani Jde, L., Leite, F. S., de Oliveira, H. C., da Silva, R. A., et al. (2015). Comparison of virulence between Paracoccidioides brasiliensis and Paracoccidioides lutzii using Galleria mellonella as a host model. *Virulence* 6, 766–776. doi: 10.1080/21505594.2015.1085277

Singulani, J. L., Scorzoni, L., de Oliveira, H. C., Marcos, C. M., Assato, P. A., Fusco-Almeida, A. M., et al. (2018). Applications of Invertebrate Animal Models to Dimorphic Fungal Infections. *J. Fungi (Basel)* 4, 118–137. doi: 10.3390/jof4040118

Suarez-Alvarez, R. O., Perez-Torres, A., and Taylor, M. L. (2010). Adherence patterns of Histoplasma capsulatum yeasts to bat tissue sections. *Mycopathologia* 170, 79–87. doi: 10.1007/s11046-010-9302-9

Teixeira, M., Patane, J. S., Taylor, M. L., Gomez, B. L., Theodoro, R. C., de Hoog, S., et al. (2016). Worldwide Phylogenetic Distributions and Population Dynamics

of the Genus Histoplasma. *PloS Negl. Trop. Dis.* 10, e0004732. doi: 10.1371/journal.pntd.0004732

Thomaz, L., Garcia-Rodas, R., Guimaraes, A. J., Taborda, C. P., Zaragoza, O., and Nosanchuk, J. D. (2013). Galleria mellonella as a model host to study Paracoccidioides lutzii and Histoplasma capsulatum. *Virulence* 4, 139–146. doi: 10.4161/viru.23047

Uppuluri, P., Chaturvedi, A. K., Srinivasan, A., Banerjee, M., Ramasubramaniam, A. K., Kohler, J. R., et al. (2010). Dispersion as an important step in the Candida albicans biofilm developmental cycle. *PloS Pathog.* 6, e1000828. doi: 10.1371/journal.ppat.1000828

Verstrepen, K. J., and Klis, F. M. (2006). Flocculation, adhesion and biofilm formation in yeasts. *Mol. Microbiol.* 60, 5–15. doi: 10.1111/j.1365-2958.2006.05072.x

Vicentini, A. P., Gesztesi, J. L., Franco, M. F., de Souza, W., de Moraes, J. Z., Travassos, L. R., et al. (1994). Binding of Paracoccidioides brasiliensis to laminin through surface glycoprotein gp43 leads to enhancement of fungal pathogenesis. *Infect. Immun.* 62, 1465–1469. doi: 10.1128/IAI.62.4.1465-1469.1994

Wolf, J. E., Kerchberger, V., Kobayashi, G. S., and Little, J. R. (1987). Modulation of the macrophage oxidative burst by Histoplasma capsulatum. *J. Immunol.* 138, 582–586.

Youseff, B. H., Holbrook, E. D., Smolnycki, K. A., and Rappleye, C. A. (2012). Extracellular superoxide dismutase protects Histoplasma yeast cells from host-derived oxidative stress. *PloS Pathog.* 8, e1002713. doi: 10.1371/journal.ppat.1002713

Zarankiewicz, T., Madej, J., Galli, J., Bajzert, J., and Stefaniak, T. (2012). Inhibition of in vitro Histophilus somni biofilm production by recombinant Hsp60 antibodies. *Pol. J. Vet. Sci.* 15, 373–378. doi: 10.2478/v10181-012-0056-9

Zarnowski, R., Sanchez, H., Covelli, A. S., Dominguez, E., Jaromin, A., Bernhardt, J., et al. (2018). Candida albicans biofilm-induced vesicles confer drug resistance through matrix biogenesis. *PloS Biol.* 16, e2006872. doi: 10.1371/journal.pbio.2006872

Conflict of Interest: The authors declare that the research was conducted in the absence of any commercial or financial relationships that could be construed as a potential conflict of interest.

frontiers in Cellular and Infection Microbiology

REVIEW
published: 25 January 2021
doi: 10.3389/fcimb.2020.594973

Role of Cell Surface Hydrophobicity in the Pathogenesis of Medically-Significant Fungi

Carina Danchik and Arturo Casadevall*

Department of Molecular Microbiology and Immunology, Bloomberg School of Public Health, Johns Hopkins University, Baltimore, MD, United States

Cell surface hydrophobicity (CSH) is an important cellular biophysical parameter which affects both cell-cell and cell-surface interactions. In dimorphic fungi, multiple factors including the temperature-induced shift between mold and yeast forms have strong effects on CSH with higher hydrophobicity more common at the lower temperatures conducive to filamentous cell growth. Some strains of *Cryptococcus neoformans* exhibit high CSH despite the presence of the hydrophilic capsule. Among individual yeast colonies from the same isolate, distinct morphologies can correspond to differences in CSH. These differences in CSH are frequently associated with altered virulence in medically-significant fungi and can impact the efficacy of antifungal therapies. The mechanisms for the maintenance of CSH in pathogenic fungi remain poorly understood, but an appreciation of this fundamental cellular parameter is important for understanding its contributions to such phenomena as biofilm formation and virulence.

Keywords: fungi, cell surface hydrophobicity, virulence, drug resistance, cell wall

OPEN ACCESS

Edited by:
Carlos Pelleschi Taborda, University of São Paulo, Brazil

Reviewed by:
Michael S. Price, Liberty University, United States
Daniel Santos, Federal University of Minas Gerais, Brazil
Marcelo Afonso Vallim, Federal University of São Paulo, Brazil

****Correspondence:***
Carina Danchik
cdanchi1@jhmi.edu

Specialty section:
This article was submitted to Fungal Pathogenesis, a section of the journal Frontiers in Cellular and Infection Microbiology

Received: *14 August 2020*
Accepted: *09 December 2020*
Published: *25 January 2021*

Citation:
Danchik C and Casadevall A (2021) Role of Cell Surface Hydrophobicity in the Pathogenesis of Medically-Significant Fungi. Front. Cell. Infect. Microbiol. 10:594973. doi: 10.3389/fcimb.2020.594973

INTRODUCTION

Cell surface hydrophobicity (CSH) is a biophysical measurement of a cell's affinity for a hydrophobic versus hydrophilic environment. Cells with higher CSH prefer a hydrophobic environment while those with lower CSH will preferentially remain in an aqueous environment (Krasowska and Sigler, 2014). This property can impact fungal virulence and biofilm formation (Galán-Ladero et al., 2013; Muadcheingka and Tantivitayakul, 2015; Dabiri et al., 2018) and is targeted by numerous antifungal drugs (Sivasankar et al., 2015; Kurakado et al., 2017; Suchodolski et al., 2020).

Despite the broad contributions of CSH to the biology and virulence of pathogenic dimorphic fungal species, data on this topic remains limited with most of the literature focusing on *Candida* species. A previous review of cell surface hydrophobicity in microbes (Krasowska and Sigler, 2014) also contained limited information on CSH in dimorphic fungal species, possibly because this area has not received as much interest in fungi as CSH in bacteria. However, given that CSH is a cellular property that has widespread effects on many aspects of microbial physiology, a more thorough understanding of fungal CSH is important, particularly as this virulence factor is altered by the switch between the yeast and hyphal forms of dimorphic fungi, which is essential for the virulence of certain pathogenic fungi (McBride et al., 2019; Sil, 2019; Staniszewska, 2020).

MOLECULAR MECHANISMS OF HYDROPHOBICITY

CSH is a macroscopic property and extrapolating the molecular structures that determine it is difficult across the size scales. Nevertheless, the level of CSH must reflect the properties of the molecules on the surface of microbes that determine their interaction with water. Treatment of hydrophobic *Candida albicans* cells with proteases decreased CSH suggesting that this property was conferred by surface proteins (Hazen et al., 1990). However, these proteins are not always exposed. Depending on the growth condition they can be masked by hydrophilic fibrils (K. C. Hazen and Hazen, 1992) and the level of glycosylation (Hazen and Glee, 1994). Similarly, proteins appear to be responsible for CSH in *Aspergillus fumigatus* (Peñalver et al., 1996). In *Aspergillus* spp. these proteins include hydrophobins, small proteins with hydrophobic domains that allow interactions with hydrophobic surfaces (Wosten et al., 1993; Thau et al., 1994; Ohtaki et al., 2006). For *Cryptococcus neoformans* no information is currently available on the mechanisms responsible for CSH differences between strains or for the high CSH of some strains despite their surrounding hydrophilic polysaccharide capsule. The multifactorial nature of hydrophobicity presents a challenge in studying and understanding the impact of this property, especially in dimorphic fungi.

METHODS FOR MEASUREMENT OF CSH

The microbial adhesion to hydrocarbons (MATH) assay is a common method for determining CSH in fungi (Borecká-Melkusová and Bujdáková, 2008; Ellepola et al., 2013a; Galán-Ladero et al., 2013; Rajkowska et al., 2015; Sivasankar et al., 2015; Ichikawa et al., 2017; Kurakado et al., 2017; Souza et al., 2018; Angiolella et al., 2020; Ramos et al., 2020; Suchodolski et al., 2020). This assay measures the decrease in culture density of an aqueous solution after thorough mixing with, and separation of, a hydrocarbon layer. Cells with low CSH will preferentially remain in the aqueous layer while cells with higher CSH will move into the hydrocarbon layer, decreasing culture density in the aqueous layer. Thus, a large decrease in aqueous culture density will occur in a sample with high CSH, and there will be minimal change in a sample with low CSH (Rosenberg, 1984). However, differences in protocols, settling cultures, and the inherent background noise of the assay can lead to variable results. This issue can be ameliorated by performing additional replicates (Ma et al., 2015) or using multiple methods to measure CSH in parallel (Ichikawa et al., 2017; Vij et al., 2020).

Another frequently used method quantifies the adherence of polystyrene microspheres to yeast cells (Antley and Hazen, 1988; San Millan et al., 1996; Hazen et al., 2000; Singleton et al., 2001; Ichikawa et al., 2017; Vij et al., 2020). Due to their hydrophobicity, the microspheres will attach selectively to hydrophobic cells. A cutoff of >3 beads per cell is widely used to designate hydrophobic versus non-hydrophobic yeasts, and individual cells can be counted and binned into these categories to determine the %CSH (Hazen and Hazen, 1987). Flow cytometry can also be used to separate these two populations when fluorescent microspheres are used (Colling et al., 2005).

For filamentous fungi, contact angle measurement can be used to determine the hydrophobicity of a mycelial mat although this technique is seldom used for human pathogens (Smits et al., 2003). In this method, drops of water are placed on top of the filamentous fungi mat and the contact angle between the water droplet and the mycelial mat is measured. A hydrophilic mycelial mat will have a low contact angle (cutoff of <30°) while a hydrophobic mat will have a higher contact angle (cutoff of >60°) (Smits et al., 2003).

FACTORS AFFECTING CSH

Microbial CSH can be affected by multiple variables, including by altered cell wall composition, genetic modification, changes in temperature, and altered nutrient availability.

Among colonies of *Trichosporon asahii*, different yeast cell morphologies were indicative of differences in hydrophobicity (Ichikawa et al., 2017). Morphology is believed to affect virulence for this pathogen through an unknown mechanism. Colonies of several morphologies isolated from a single clinical sample had distinct morphologies that aligned with different levels of CSH. Heat-killing led to a slight but insignificant decrease in CSH for all strains, but when periodate was used to degrade cell wall polysaccharides, CSH dramatically decreased in all three strains tested. This suggests that the variance in cell wall composition and extracellular polysaccharides between strains of different morphologies may have directly contributed to the differences in CSH (Ichikawa et al., 2017).

Other components of the cell wall can also contribute to CSH in *C. albicans*, including mannoproteins, glucans, lipids, and chitin (Masuoka and Hazen, 1997; Pitarch et al., 2002). The sterol profile and lipid content also impact CSH in *C. albicans*, and differences in the expression of *ERG11* which encodes CYP51A1 alters both of these plasma membrane characteristics (Suchodolski et al., 2020). Additionally, knockout of *CSH1* which encodes a hydrophobic 38-kDa protein Csh1p decreased both CSH and adhesion to fibronectin in C. *albicans* (Singleton et al., 2001). Although a large portion of expressed Csh1p is localized to the cytoplasm, it is also associated with the cell wall and is upregulated upon increased temperature (Singleton and Hazen, 2004). Clearly a complicated property of the cell surface, CSH can be altered by manipulation of multiple components.

Nutrient availability, fungal growth phase, and temperature also affect CSH. Stationary phase cultures of *C. albicans* at 37°C diluted into fresh media can rapidly decrease their CSH in response to the newly accessible nutrients (Hazen and Hazen, 1988). Stationary phase cultures at either room temperature or 37˚C had an initial drop in CSH regardless of previous or current growth temperature, but CSH several hours after dilution was dependent on the growth temperature of the subculture with

room temperature cultures having higher CSH (Hazen and Hazen, 1988).

In dimorphic fungi, the shift between hyphal and yeast forms is partially controlled by temperature and is associated with dramatic morphological, gene regulation, and cell surface composition changes. Most CSH studies in dimorphic fungi have focused on the organisms grown at 37°C (Muadcheingka and Tantivitayakul, 2015; Ichikawa et al., 2017; Llopis-Torregrosa et al., 2019; Angiolella et al., 2020; Ramos et al., 2020) although several studies have compared cultures grown at 37°C versus room temperature, identifying a general trend of higher CSH at lower temperatures and in the hyphal form (Antley and Hazen, 1988; Hazen and Hazen, 1988; Hazen et al., 1988; Singleton et al., 2001; Borecká-Melkusová and Bujdáková, 2008; Galán-Ladero et al., 2013).

Although most *Cryptococcus neoformans* are yeasts that usually do not have a filamentous form, they can expand from 5–7 μm to up to 100 μm and take on a distinct morphology known as titan or giant cells during infection (Zaragoza and Nielsen, 2013). In the context of *Galleria mellonella* infection, giant cells (>30 μm diameter) had similar infection outcomes to regularly sized *C. neoformans* despite being phagocytosed at a lower rate, demonstrating the importance of multiple virulence factors during infection. These giant cells had large cell bodies and thick polysaccharide capsules, both of which contributed to their increased size. The enlarged polysaccharide capsules additionally had decreased permeability. Although the study did not look at hydrophobicity, the reduction in capsule permeability suggests a structural change in the capsule which likely also alters the CSH (García-Rodas et al., 2011).

RELATIONSHIP TO BIOFILM FORMATION AND VIRULENCE

High CSH is generally considered to be a virulence factor for numerous dimorphic fungal species (Hazen et al., 1991). For the purposes of this discussion we will use the definitions of pathogenicity and virulence proposed by the damage-response framework of microbial pathogenesis whereby these refer to the inherent and relative capacities of microbes to cause damage in hosts, respectively, such that disease occurs if the damage is sufficient to affect homeostasis (Casadevall and Pirofski, 1999). Since the relationship between these properties and CSH involves a measurement of relative abilities, the term virulence is used. There are numerous studies in dimorphic fungi, especially on clinical isolates of *C. albicans* and non-*Candida albicans Candida* species, which demonstrate that high CSH is a common feature of these disease-causing isolates (Galán-Ladero et al., 2013; Muadcheingka and Tantivitayakul, 2015; Dabiri et al., 2018). Despite this, few studies have found any correlation between high CSH and biofilm formation, an important step in the establishment of infection, *in vitro*.

Adhesion is the process of cells attaching to another surface and is the first step of biofilm formation. CSH was directly correlated with adhesion across 12 clinical isolates of *Candida haemulonii* species complex. This correlation makes sense as CSH is a property of the cell surface which affects the way cells interact with their environment. Despite the substantial differences in CSH for these isolates and the correlation with adhesion for fungal cultures alone, no differences were seen between strains in a phagocytosis assay. Only one condition and time were tested, however, so it is possible that the kinetics would have varied at other time points or conditions and were simply not picked up in this assay. In a *Galleria melonella* infection model, only two strains had significantly more virulence, and both of these, surprisingly, had very low CSH (Ramos et al., 2020). In this instance, although CSH and adhesion were positively correlated, this did not translate to similar associations between CSH and phagocytosis or virulence in *Galleria melonella*.

Likely due to the many dynamics at play during the complex process of biofilm formation, high CSH does not have a consistent and direct association with biofilm formation ability. A comparison of CSH, adhesion to polystyrene, and biofilm formation ability for *Malassezia sympodialis* identified no significant correlation between CSH or adhesion and biofilm ability (Angiolella et al., 2020). This also held true for cells of several different morphology types from a clinical isolate of *Trichosporon asahii* which had no correlation between hydrophobicity and biofilm formation. In fact, the morphology associated with the highest CSH actually had the lowest ability to form biofilm (Ichikawa et al., 2017). An analysis of a hundred clinical isolates found a weak positive correlation was identified between CSH and biofilm formation ability for *C. albicans*, and a moderate correlation between these two factors was identified for *non-Candida albicans Candida* species (Muadcheingka and Tantivitayakul, 2015). Another study looked at CSH and biofilm formation ability across multiple *Candida* species and only found positive correlations between the two virulence factors for two of these species, *C. parapsilosis* and *C. tropicalis* while another found that adhesion and biofilm formation ability were moderately correlated with each other but neither was correlated with CSH (Dabiri et al., 2018; Souza et al., 2018).

The presence or absence of a relationship between CSH and biofilm formation may be temperature dependent. For *C. tropicalis* grown at 37°C, high CSH and filamentation, a transition from the yeast to hyphal state required for successful biofilm formation, were significantly correlated; however, no relationship was found between these two variables for the same strains grown at 22°C. Despite this association between CSH and filamentation at 37°C, neither CSH or adhesion correlated with biofilm formation, re-enforcing the understanding that these virulence factors are related but distinct (Galán-Ladero et al., 2013).

Additionally, higher CSH is not always correlated with higher virulence, as demonstrated by the *trk1Δ* mutant of *C. glabrata* (Llopis-Torregrosa et al., 2019). *TRK1* encodes for a high affinity potassium transporter which is the only potassium uptake system in this organism. Deletion of this gene impaired the cells' ability to take up potassium and decreased cell fitness. The *trk1Δ* mutant also manifested altered the cell wall composition

which, in turn, increased the CSH, regardless of potassium availability. The *trk1Δ* mutant formed significant biofilms at a wider range of potassium concentrations than the parental strain *in vitro*. Despite these *in vitro* results, in each of the three infection models tested (*Drosophila melanogaster*, *Galleria mellonella*, and THP-1 macrophage-like cells), the *trk1Δ* mutant was less virulent than the parental strain. In animal hosts, extracellular potassium is generally in the low mM range, and the mutant cells grew poorly under that condition. This overwhelmed the benefit of increased CSH, adherence, and biofilm formation in these pathogens because they were not able to grow well in the host environment and demonstrates that not only CSH itself, but also the mechanism of CSH, is important for virulence (Llopis-Torregrosa et al., 2019).

The host response to pathogen exposure can also alter CSH. During infection, pathogens may be bound by antibodies that coat their surfaces. Three mAbs (21E6, B9E, and 3D9) targeting cell wall fibrillar adhesins important for the adhesion of *C. albicans* germ tubes were tested for their effects on adhesion to polystyrene and filamentation (San Millan et al., 1996). mAb 21E6 enhanced adhesion but reduced filamentation, and mAb B9E decreased both adhesion and filamentation. mAb 21E6 decreased the CSH of C. albicans while B9E increased it. 3D9 had no reactivity against the tested adhesins, did not alter CSH, and had no effect on either process (San Millan et al., 1996). These effects were antibody-specific and may have different mechanisms. In *C. neoformans*, binding of the protective capsular mAb 18B7 increased CSH in a dose-dependent manner while two non-protective capsular mAb 12A1 and 13F1 had no effect on CSH (Vij et al., 2020). This increase in CSH will presumably facilitate engulfment by macrophages. Thus, antibody binding as a component of the immune response to infection may act in part through exogenous manipulation of CSH to promote pathogen clearance.

Biofilm formation and virulence are multifactorial processes, and CSH has a much more direct relationship with adhesion than with the more complex process of biofilm formation. Biofilm formation is often a key step in fungal pathogenesis and establishment of infection. Although CSH is not often directly correlated with biofilm formation, it may promote virulence through more complex and currently unexplored mechanisms which are not recapitulated under the *in vitro* conditions tested, resulting in higher CSH being associated stronger virulence.

RESPONSE TO ANTIFUNGAL TREATMENTS

An understanding of CSH is also critical when developing new antifungal strategies as differences in CSH can cause variable responses to antifungal treatment. In addition, many therapeutics reduce CSH. This emphasizes the importance of considering CSH when determining the best treatment option.

Fluconazole is a major antifungal drug, which inhibits ergosterol metabolism by blocking the activity of CYP51A1. One recent study found that fluconazole had much lower efficacy against a more hydrophobic strain of *C. albicans* (Suchodolski et al., 2020). Fluconazole was tested, alone or in combination with gentamicin, against two strains of *C. albicans*: CAF2-1 and CAF4-2. CAF4-2 had higher CSH as well as higher expression of *ERG11*, the gene which encodes for CYP51A1, and promotes ergosterol production and *CDR1* which encodes Cdr1, a drug efflux pump. Fluconazole treatment increased the CSH of the more hydrophilic CAF2-1 strain but not that of CAF4-2. It also increased *ERG11* expression much more in the hydrophilic than the hydrophobic strain, demonstrating that CYP51A1 overexpression is protective against fluconazole treatment (Suchodolski et al., 2020). This mechanism of resistance holds true across numerous studies and was previously reviewed (Berkow and Lockhart, 2017). *ERG11* overexpression can have multiple causes, including gain of function mutations in the transcription factor Upc2p which is induced upon ergosterol depletion, altered sterol biosynthesis, and mutations in *ERG11* itself (Heilmann et al., 2010; Berkow and Lockhart, 2017).

Differences in *ERG11* expression alter the surface sterol profile and presumably the CSH through this mechanism. Therefore, the difference in treatment response between the CAF2-1 and CAF4-2 strains may be due to changes in lipid homeostasis and metabolism (Suchodolski et al., 2020). Another older study, however, found that a subinhibitory concentration of fluconazole did not affect CSH in *C. albicans* although it did sensitize the fungi to killing by murine polymorphonuclear leukocytes (Hazen et al., 2000). This difference is likely due to the specific strains used in each study as, in the more recent study, fluconazole only affected CSH in one of the two strains tested.

Subinhibitory doses of four antifungals, including fluconazole, were tested for their effects on CSH and biofilm formation ability in both *C. albicans* and *C. dubliniensis* (Borecká-Melkusová and Bujdáková, 2008). The 50 isolates were classified into four genotypes based on the details of the presence or absence of a group I intron at a specific location on the 25S rRNA gene, three genotypes for *C. albicans* (A, B, and C) and one for *C. dubliniensis* (D). The *C. dubliniensis* isolates were generally more hydrophobic than the *C. albicans* ones. In the tested range of concentrations, fluconazole did not affect CSH of *C. albicans* but did effectively reduce biofilm formation. Conversely, it decreased CSH in *C. dubliniensis* but did not decrease biofilm formation. Voriconazole reduced both biofilm formation and CSH for all four genotypes tested. Amphotericin B decreased CSH in all genotypes but only reduced biofilm formation for genotypes A, B, and D. Itraconazole decreased CSH in genotypes A, B, and D and decreased biofilm formation for all three genotypes of *C. albicans*. Because the comparisons were made among aggregates of data for all four genotypes, some information may have been lost as each genotype contained a wide range of CSH values, but decreased CSH and biofilm formation were both common outcomes of low dose antifungal exposure, and the two appear to be independent of each other (Borecká-Melkusová and Bujdáková, 2008).

Chlorhexidine gluconate is a common active ingredient in mouthwash with broad antimicrobial activity. Even at

subtherapeutic doses, it has been shown to decrease CSH in *C. dubliniensis* and *C. albicans* (Ellepola et al., 2013a; Ellepola et al., 2013b). As CSH helps to mediate adhesion which is necessary for the establishment of infection, chlorhexidine gluconate, even at low doses, may help to reduce oral fungal infection.

Minocycline, a tetracycline derivative, was active against the budded-to-hyphal-form transition of *C. albicans* at sub-growth inhibitory concentrations (Kurakado et al., 2017). This transition is necessary for full virulence and for biofilm formation. Minocycline significantly decreased CSH at the concentration necessary for decreased biofilm formation. In addition, it downregulated the expression of several hyphal and biofilm formation-related genes. These included the hypha-specific genes *HWP1* and *ECE1*, the hypha-related transcription factor genes *EFG1*, *CPH1*, and *TEC1*, the adhesion-related gene *ALS3*, and the biofilm-related gene *BCR1* (Kurakado et al., 2017).

Malassezia spp. have a high percentage of lipids in their cell wall (~15%–20% w/w) which contributes to their high CSH. L-glutathione, an antioxidant with antifungal activity, decreased CSH by 85%–95% in four species of *Malassezia* without affecting viability (Sivasankar et al., 2015). It increased the time to cell aggregation specifically through its reduction of CSH without altering cell surface charge as measured by zeta-potential. It also decreased fungal virulence in a blood sensitivity assay by 64%–73% for the same four species, suggesting that CSH is a major virulence factor for this genus of dimorphic fungi (Sivasankar et al., 2015).

The effects of numerous non-clinically approved agents on CSH have also been assessed in various dimorphic fungal species. The extract of the plant *Eugenia uniflora* which has antioxidant and antimicrobial activity was tested against *Candida* spp. and was able to decrease CSH, adhesion to human buccal epithelial cells, and biofilm formation to different extents (Souza et al., 2018). Several essential oils, specifically tea tree, thyme, and clove, have also been examined for their effects on CSH in several *Candida* species. The results were essential oil and strain-dependent, but, particularly when used in combination, the essential oils tested often significantly decreased CSH (Rajkowska et al., 2015). A bacteriocin isolated from *Streptococcus sanguinis* culture media was also effective against *C. albicans* and *C. tropicalis*. Although its activity was multifactorial, it decreased CSH (Ma et al., 2015). Reducing CSH appears to be a common activity for many antifungal agents, both clinically approved and investigational.

As may be anticipated, higher CSH is associated with higher phagocytic efficiency. Increasing CSH in *C. neoformans* was positively correlated with phagocytosis by the natural predator *Acanthamoeba castellani* (Vij et al., 2020). Additionally, in *C. albicans*, murine polymorphonuclear leukocytes (PMNs) were more effective at engulfing more hydrophobic cells cultured at room temperature than they were for cells grown at 37°C (Antley and Hazen, 1988). The opposite trend was seen for cell killing, however, with PMNs being more effective at killing the less hydrophobic cells grown at 37°C. This is due to the enhanced ability of the room temperature cultured cells to form germ tubes. Germ tube formation is correlated with CSH. In line with this, *C. albicans* grown at room temperature had higher CSH and led to more rapid death in a mouse model than *C. albicans* cells grown at 37°C (Antley and Hazen, 1988; Hazen et al., 2000). Therefore, the impact of CSH on phagocytosis and killing appears to be two-fold. Higher hydrophobicity makes the cells initially easier to engulf, but also makes them more prone to germ tube formation and resistance to phagocytic killing.

CSH is clearly an important virulence factor to consider in relation to both treatment options and drug development. As CSH can alter the efficacy of antifungal therapies, it could be helpful in informing treatment selection. CSH is also frequently reduced by antifungal therapies as part of their activity and provides a good, easily quantifiable phenotypic readout which can be used to measure this virulence factor *in vitro*. In addition, further exploration of the mechanisms through which these drugs reduce CSH and subsequently virulence could elucidate additional pathways involved in pathogenesis and lead to the development of novel strategies to target fungal infections.

SYNTHESIS

Our review of the CSH information available for medically-important fungi revealed disparate observations obtained from different organisms and variable experimental settings. This makes it difficult to propose a coherent perspective that includes all of these observations into on cohesive theory, especially given that some studies report conflicting results. Although this complicates a clear, mechanistic understanding of the impact of CSH on pathogenesis and drug resistance across organisms and studies, CSH is a property of the cell wall, which provides a protective barrier between the cell and its environment and as such, is indisputably a key factor in these processes. More work on this topic, particularly in other medically-significant dimorphic fungi such as *Coccidiodes immitis*, *Paracoccidioides brasiliensis*, *Blastomyces dermatitis*, *Histoplasma capsulatum*, and *Sporothrix schenckii* is needed because the literature on the CSH species is limited or non-existent. In this regard, comparative studies across diverse species could provide additional important insights on the specific effects of high or low CSH, which might help clarify the current, conflicting results. We are hopeful that our delineation of the variable effects of CSH on virulence, biofilm formation and drug resistance stimulates additional studies to explore how this critical cell parameter affects these processes.

CONCLUSIONS

The body of work available on CSH in dimorphic fungi, mostly in *Candida* species, demonstrates that this biophysical parameter plays important and complex roles in the processes of virulence, biofilm formation, and response to treatment. High CSH frequently but not universally corresponds to stronger

virulence. Although related, CSH is distinct from biofilm formation, and there is often no direct correlation between the two properties, although both are important for virulence. Much of the existing literature on CSH in dimorphic fungi focuses on *Candida* species, and similar experiments for other pathogenic dimorphic fungi could provide a better understanding of these organisms from both a basic science and clinical perspective. In general, CSH is a relatively understudied cellular property in fungi that merits more attention given its fundamental nature for microbial physiology, cellular attachment, virulence, and as a drug target.

AUTHOR CONTRIBUTIONS

CD wrote the manuscript. AC edited and wrote parts of the manuscript. All authors contributed to the article and approved the submitted version.

FUNDING

AC was supported in part by NIH grants AI052733, AI15207, and HL059842. CD was supported by NIH grant GM008752.

REFERENCES

Angiolella, L., Rojas, F., Mussin, J., Greco, R., Sosa, M., de los, A., et al. (2020). Biofilm formation, adherence, and hydrophobicity of M. sympodialis, M. globosa, and M. slooffiae from clinical isolates and normal skinVirulence factors of M. sympodialis, M. globosa and M. slooffiae. *Med. Mycol* 0, 1–7. doi: 10.1093/MMY/MYAA017

Antley, P. P., and Hazen, K. C. (1988). Role of Yeast Cell Growth Temperature on Candida albicans Virulence in Mice. *Infect Immun.* 56 (11), 2884–2890. doi: 10.1128/IAI.56.11.2884-2890.1988

Berkow, E. L., and Lockhart, S. R. (2017). Fluconazole resistance in Candida species: A current perspective. *In Infect Drug Resistance* 10, 237–245). doi: 10.2147/IDR.S118892

Borecká-Melkusová, S., and Bujdáková, H. (2008). Variation of cell surface hydrophobicity and biofilm formation among genotypes of Candida albicans and Candida dubliniensis under antifungal treatment. *Can. J. Microbiol.* 54 (9), 718–724. doi: 10.1139/W08-060

Casadevall, A., and Pirofski, L. A. (1999). Host-pathogen interactions: Redefining the basic concepts of virulence and pathogenicity. *In Infect Immun.* 67 (8), 3703–3713). doi: 10.1128/iai.67.8.3703-3713.1999

Colling, L., Carter, R. N., Essmann, M., and Larsen, B. (2005). Evaluation of relative yeast cell surface hydrophobicity measured by flow cytometry. *Infect. Dis. Obstetr Gynecol* 13 (1), 43–48. doi: 10.1155/2005/739101

Dabiri, S., Shams-Ghahfarokhi, M., and Razzaghi-Abyaneh, M. (2018). Comparative analysis of proteinase, phospholipase, hydrophobicity and biofilm forming ability in Candida species isolated from clinical specimens. *J. Mycol Med* 28 (3), 437–442. doi: 10.1016/j.mycmed.2018.04.009

Ellepola, A. N. B., Joseph, B. K., and Khan, Z. U. (2013a). Changes in the Cell Surface Hydrophobicity of Oral ***Candida albicans*** from Smokers, Diabetics, Asthmatics, and Healthy Individuals following Limited Exposure to Chlorhexidine Gluconate. *Med. Principles Pract.* 22 (3), 250–254. doi: 10.1159/000345641

Ellepola, A. N. B., Joseph, B. K., and Khan, Z. U. (2013b). Cell surface hydrophobicity of oral Candida dubliniensis isolates following limited exposure to sub-therapeutic concentrations of chlorhexidine gluconate. *Mycoses* 56 (1), 82–88. doi: 10.1111/j.1439-0507.2012.02203.x

Galán-Ladero, M. A., Blanco-Blanco, M. T., Hurtado, C., Pérez-Giraldo, C., Blanco, M. T., and Gómez-García, A. C. (2013). Determination of biofilm production by *Candida tropicalis* isolated from hospitalized patients and its relation to cellular surface hydrophobicity, plastic adherence and filamentation ability. *Yeast* 30 (9), 331–339. doi: 10.1002/yea.2965

García-Rodas, R., Casadevall, A., Rodríguez-Tudela, J. L., Cuenca-Estrella, M., and Zaragoza, O. (2011). Cryptococcus neoformans capsular enlargement and cellular gigantism during Galleria mellonella infection. *PloS One* 6 (9), e24485. doi: 10.1371/journal.pone.0024485

Hazen, K. C., and Glee, P. M. (1994). Hydrophobic cell wall protein glycosylation by the pathogenic fungus Candida albicans. *Can. J. Microbiol.* 40 (4), 266–272. doi: 10.1139/m94-043

Hazen, K. C., and Hazen, B. W. (1987). A polystyrene microsphere assay for detecting surface hydrophobicity variations within Candida albicans populations. *J. Microbiol Methods* 6 (5), 289–299. doi: 10.1016/0167-7012(87)90066-2

Hazen, B. W., and Hazen, K. C. (1988). Dynamic expression of cell surface hydrophobicity during initial yeast cell growth and before germ tube formation of Candida albicans. *Infect Immun.* 56 (9), 2521–2525. doi: 10.1128/IAI.56.9.2521-2525.1988

Hazen, K. C., and Hazen, B. W. (1992). Hydrophobic surface protein masking by the opportunistic fungal pathogen Candida albicans. *Infect Immun.* 60 (4), 1499–1508. doi: 10.1128/iai.60.4.1499-1508.1992

Hazen, B. W., Liebert, R. E., and Hazen, K. C. (1988). Relationship of Cell Surface Hydrophobicity to Morphology of Monomorphic and Dimorphic Fungi. *Mycologia* 80 (3), 348. doi: 10.2307/3807632

Hazen, K. C., Lay, J. G., Hazen, B. W., Fu, R. C., and Murthy, S. (1990). Partial biochemical characterization of cell surface hydrophobicity and hydrophilicity of Candida albicans. *Infect Immun.* 58 (11), 3469–3476. doi: 10.1128/iai.58.11.3469-3476.1990

Hazen, K. C., Brawner, D. L., Riesselman, M. H., Jutila, M. A., and Cutler, J. E. (1991). Differential adherence of hydrophobic and hydrophilic Candida albicans yeast cells to mouse tissues. *Infect Immun.* 59 (3), 907–912. doi: 10.1128/iai.59.3.907-912.1991

Hazen, K. C., Mandell, G., Coleman, E., and Wu, G. (2000). Influence of fluconazole at subinhibitory concentrations on cell surface hydrophobicity and phagocytosis of Candida albicans. *FEMS Microbiol. Lett.* 183 (1), 89–94. doi: 10.1111/j.1574-6968.2000.tb08938.x

Heilmann, C. J., Schneider, S., Barker, K. S., Rogers, P. D., and Morschhäuser, J. (2010). An A643T mutation in the transcription factor Upc2p causes constitutive ERG11 upregulation and increased fluconazole resistance in Candida albicans. *Antimicrobial Agents Chemother* 54 (1), 353–359. doi: 10.1128/AAC.01102-09

Ichikawa, T., Hirata, C., Takei, M., Tagami, N., Murasawa, H., and Ikeda, R. (2017). Cell surface hydrophobicity and colony morphology of *Trichosporon asahii* clinical isolates. *Yeast* 34 (3), 129–137. doi: 10.1002/yea.3220

Krasowska, A., and Sigler, K. (2014). How microorganisms use hydrophobicity and what does this mean for human needs? *Front. Cell. Infect Microbiol.* 4:2014.00112 (112), 112. doi: 10.3389/fcimb.2014.00112

Kurakado, S., Takatori, K., and Sugita, T. (2017). Minocycline Inhibits Candida albicans Budded-to-Hyphal-Form Transition and Biofilm Formation. *Jpn. J. Infect. Dis.* 70, 490–494. doi: 10.7883/yoken.JJID.2016.369

Llopis-Torregrosa, V., Vaz, C., Monteoliva, L., Ryman, K., Engstrom, Y., Gacser, A., et al. (2019). Trk1-mediated potassium uptake contributes to cell-surface properties and virulence of Candida glabrata. *Sci. Rep.* 9 (1), 7529. doi: 10.1038/s41598-019-43912-1

Ma, S., Zhao, Y., Xia, X., Dong, X., Ge, W., and Li, H. (2015). Effects of Streptococcus sanguinis Bacteriocin on Cell Surface Hydrophobicity, Membrane PermeabilitMa, S., Zhao, Y., Xia, X., Dong, X., Ge, W., & Li, H. (2015). Effects of Streptococcus sanguinis Bacteriocin on Cell Surface Hydrophobicity, Membrane Permea. BioMed Research International, 2015. https://doi.org/10.1155/2015/514152.

Masuoka, J., and Hazen, K. C. (1997). Cell wall protein mannosylation determines Candida albicans cell surface hydrophobicity. *Microbiology* 143 (9), 3015–3021. doi: 10.1099/00221287-143-9-3015

McBride, J. A., Gauthier, G. M., and Klein, B. S. (2019). Turning on virulence: Mechanisms that underpin the morphologic transition and pathogenicity of Blastomyces. *In Virulence* 10 (1), 801–809). doi: 10.1080/21505594.2018.1449506

Muadcheingka, T., and Tantivitayakul, P. (2015). Distribution of Candida albicans and non-albicans Candida species in oral candidiasis patients: Correlation between cell surface hydrophobicity and biofilm forming activities. *Arch. Oral. Biol.* 60 (6), 894–901. doi: 10.1016/j.archoralbio.2015.03.002

Ohtaki, S., Maeda, H., Takahashi, T., Yamagata, Y., Hasegawa, F., Gomi, K., et al. (2006). Novel hydrophobic surface binding protein, HsbA, produced by Aspergillus oryzae. *Appl. Environ. Microbiol.* 72 (4), 2407–2413. doi: 10.1128/AEM.72.4.2407-2413.2006

Peñalver, M. C., Casanova, M., Martínez, J. P., and Gil, M. L. (1996). Cell wall protein and glycoprotein constituents of Aspergillus fumigatus that bind to polystyrene may be responsible for the cell surface hydrophobicity of the mycelium. *Microbiology* 142 (7), 1597–1604. doi: 10.1099/13500872-142-7-1597

Pitarch, A., Sánchez, M., Nombela, C., and Gil, C. (2002). Sequential fractionation and two-dimensional gel analysis unravels the complexity of the dimorphic fungus Candida albicans cell wall proteome. *Mol. Cell. Proteomics: MCP* 1 (12), 967–982. doi: 10.1074/mcp.M200062-MCP200

Rajkowska, K., Kunicka-Styczyńska, A., and Pęczek, M. (2015). Hydrophobic properties of Candida spp. under the influence of selected essential oils*. *Acta Biochim. Pol.* 62 (4), 663–668. doi: 10.18388/abp.2015_1096

Ramos, L. S., Oliveira, S. S. C., Silva, L. N., Granato, M. Q., Gonçalves, D. S., Frases, S., et al. (2020). Surface, adhesiveness and virulence aspects of Candida haemulonii species complex. *Med. Mycol* 0, 1–14. doi: 10.1093/MMY/MYZ139

Rosenberg, M. (1984). Bacterial adherence to hydrocarbons: a useful technique Bacterial adherence to hydrocarbons: a useful technique for studying cell surface hydrophobicity). . *FEMS Microbiol. Lett.* 22 (3), 289–295. doi: 10.1111/j.1574-6968.1984.tb00743.x

San Millan, R., Ezkurra, P. A., Quindós, G., Robert, R., Senet, J. M., and Pontón, J. (1996). Effect of monoclonal antibodies directed against Candida albicans cell wall antigens on the adhesion of the fungus to polystyrene. *Microbiology* 142 (8), 2271–2277. doi: 10.1099/13500872-142-8-2271

Sil, A. (2019). Molecular regulation of Histoplasma dimorphism. *In Curr. Opin. Microbiol.* 52, 151–157). doi: 10.1016/j.mib.2019.10.011

Singleton, D. R., and Hazen, K. C. (2004). Differential surface localization and temperature-dependent expression of the Candida albicans CSH1 protein. *Microbiology* 150 (2), 285–292. doi: 10.1099/mic.0.26656-0

Singleton, D. R., Masuoka, J., and Hazen, K. C. (2001). Cloning and analysis of a Candida albicans gene that affects cell surface hydrophobicity. *J. Bacteriol.* 183 (12), 3582–3588. doi: 10.1128/JB.183.12.3582-3588.2001

Sivasankar, C., Ponmalar, A., Bhaskar, J. P., and Pandian, S. K. (2015). Glutathione as a promising anti-hydrophobicity agent against *Malassezia* spp. *Mycoses* 58 (10), 620–631. doi: 10.1111/myc.12370

Smits, T. H. M., Wick, L. Y., Harms, H., and Keel, C. (2003). Characterization of the surface hydrophobicity of filamentous fungi. *Environ. Microbiol.* 5 (2), 85–91. doi: 10.1046/j.1462-2920.2003.00389.x

Souza, L. B. F. C., Silva-Rocha, W. P., Ferreira, M. R. A., Soares, L. A. L., Svidzinski, T.II, Milan, E. P., et al. (2018). Influence of eugenia uniflora extract on adhesion to human buccal epithelial cells, biofilm formation, and cell surface hydrophobicity of candida spp. from the oral cavity of kidney transplant recipients. *Molecules* 23 (10), 2418. doi: 10.3390/molecules23102418

Staniszewska, M. (2020). Virulence Factors in Candida species. *Curr. Protein Pept. Sci.* 21 (3), 313–323. doi: 10.2174/1389203720666190722152415

Suchodolski, J., Muraszko, J., Korba, A., Bernat, P., and Krasowska, A. (2020). Lipid composition and cell surface hydrophobicity of Candida albicans influence the efficacy of fluconazole–gentamicin treatment. *Yeast* 37 (1), 117–129. doi: 10.1002/yea.3455

Thau, N., Monod, M., Crestani, B., Rolland, C., Tronchin, G., Latge, J. P., et al. (1994). rodletless mutants of Aspergillus fumigatus. *Infect Immun.* 62 (10), 4380–4388. doi: 10.1128/iai.62.10.4380-4388.1994

Vij, R., Danchik, C., Crawford, C., Dragotakes, Q., and Casadevall, A. (2020). Variation in Cell Surface Hydrophobicity among Cryptococcus neoformans Strains Influences Interactions with Amoebas. *MSphere* 5 (2), e00310–e00320. doi: 10.1128/mSphere.00310-20

Wosten, H. A. B., de Vries, O. M. H., and Wessels, J. G. H. (1993). Interfacial self-assembly of a fungal hydrophobin into a hydrophobic rodlet layer. *Plant Cell* 5 (11), 1567–1574. doi: 10.1105/tpc.5.11.1567

Zaragoza, O., and Nielsen, K. (2013). Titan cells in Cryptococcus neoformans: Cells with a giant impact. *In Curr. Opin. Microbiol.* 16 (4), 409–413). doi: 10.1016/j.mib.2013.03.006

Conflict of Interest: The authors declare that the research was conducted in the absence of any commercial or financial relationships that could be construed as a potential conflict of interest.

frontiers in Cellular and Infection Microbiology

ORIGINAL RESEARCH
published: 08 February 2021
doi: 10.3389/fcimb.2020.598701

Reduced Severity in Patients With HIV-Associated Disseminated Histoplasmosis With Deep Lymphadenopathies: A Trench War Remains Within the Lymph Nodes?

Mathieu Nacher[1,2], Kinan Drak Alsibai[3], Antoine Adenis[1,2], Romain Blaizot[2,4], Philippe Abboud[5], Magalie Demar[6,7], Félix Djossou[5], Loïc Epelboin[5], Caroline Misslin[8], Balthazar Ntab[9], Audrey Valdes[10] and Pierre Couppié[2,4]*

[1] CIC INSERM 1424, Centre hospitalier Andree Rosemon Cayenne, Cayenne, French Guiana, [2] DFR Santé, Université de Guyane, Cayenne, French Guiana, [3] Department of Pathology, Centre hospitalier Andrée Rosemon, Cayenne, French Guiana, [4] Department of Dermatology, Centre hospitalier Andrée Rosemon, Cayenne, French Guiana, [5] Service des Maladies Infectieuses et Tropicales, Centre hospitalier Andrée Rosemon Cayenne, Cayenne, French Guiana, [6] Laboratory, Centre hospitalier Andrée Rosemon Cayenne, Cayenne, French Guiana, [7] UMR Tropical Biome and Immunopathology, Université de Guyane, Cayenne, French Guiana, [8] Service de Médecine, Centre hospitalier de l'Ouest Guyanais, Saint Laurent du Maroni, French Guiana, [9] Département d'Information Médicale, Centre hospitalier de l'Ouest Guyanais, Saint Laurent du Maroni, French Guiana, [10] Equipe Opérationnelle d'hygiène hospitalière, Centre hospitalier Andrée Rosemon Cayenne, Cayenne, French Guiana

OPEN ACCESS

Edited by:
Carlos Pelleschi Taborda, University of São Paulo, Brazil

Reviewed by:
Alexandre Alanio, Université Paris Diderot, France
Aylin Döğen, Mersin University, Turkey
Beatriz L. Gómez, Rosario University, Colombia

***Correspondence:**
Mathieu Nacher
mathieu.nacher66@gmail.com

Specialty section:
This article was submitted to Fungal Pathogenesis, a section of the journal Frontiers in Cellular and Infection Microbiology

Received: *25 August 2020*
Accepted: *09 December 2020*
Published: *08 February 2021*

Citation:
Nacher M, Alsibai KD, Adenis A, Blaizot R, Abboud P, Demar M, Djossou F, Epelboin L, Misslin C, Ntab B, Valdes A and Couppié P (2021) Reduced Severity in Patients With HIV-Associated Disseminated Histoplasmosis With Deep Lymphadenopathies: A Trench War Remains Within the Lymph Nodes? Front. Cell. Infect. Microbiol. 10:598701. doi: 10.3389/fcimb.2020.598701

Background: Disseminated histoplasmosis is a major killer of patients with advanced HIV. It is proteiform and often hard to diagnose in the absence of diagnostic tests. We aimed to describe disseminated histoplasmosis with lymphadenopathies in French Guiana and to compare survival and severity of those patients to patients without lymphadenopathies.

Methods: A retrospective cohort study was performed on data records collected between January 1, 1981 and October 1, 2014.

Results: Among 349 cases of disseminated histoplasmosis 168 (48.3%) had superficial lymphadenopathies and 133(38.1%) had deep lymphadenopathies. The median LDH concentration, ferritin concentration, TGO concentration, and WHO performance status were lower among patients with deep lymphadenopathies than those without deep lymphadenopathies. There was a significant decrease in the risk of early death (<1 month) among those with deep lymphadenopathies relative to those without (OR=0.26 (95% CI=0.10–0.60), P=0.0006) and in the overall risk of death (OR=0.33 (95%CI=0.20-0.55), P<0.0001). These associations remained strongly significant after adjusting for time period, CD4 counts, age, delay between beginning of symptoms and hospital admission, antifungal and antiretroviral treatment.

Conclusions: The present data show that in patients with advanced HIV and disseminated histoplasmosis, the presence of deep lymphadenopathies is associated with fewer markers of severity and a lower risk of death. To our knowledge it is the first study to show this. The presence of deep lymphadenopathies is hypothesized to reflect the patient's partially effective defense against *H. capsulatum*.

Keywords: HIV, disseminated histoplasmosis, liposomal amphotericin B, French Guiana, lymph node

INTRODUCTION

Histoplasma capsulatum is a dimorphic ascomycete that grows in soil and bird and bat guano. After spores are inhaled, it transforms into a pathogenic yeast and replicates within macrophages which can transport the yeast from the lungs to any organ (Horwath et al., 2015). The efficient clearance of *Histoplasma* yeasts requires the activation of macrophages through the Th1 response. The recognition of *H. capsulatum* by dendritic cells and macrophages promotes the differentiation and recruitment of Th1 cells. However, this process fails in immunocompromised individuals who therefore are at risk for disseminated infection. Antigen presenting cells migrate to the nearest lymph node where the antigen they express along with MHCII molecules can be presented to a variety of circulating naïve lymphocytes that can eventually become activated and proliferate. Humans usually have about 500 lymph nodes, which are divided into groups and are more concentrated near the trunk (Standring, 2016). As secondary lymphoid organs, lymph nodes have a central role in the development of adaptive immunity against pathogens. During infections, they may become enlarged and palpable. Ever since the beginning of the HIV epidemic, lymph node pathology has been known to be an important consequence of human immunodeficiency virus (HIV) infection. The central role that lymphoid tissues play in HIV pathogenesis has been suggested by the structural and functional alterations induced by HIV. (Dimopoulos et al., 2017) Enlarged lymph nodes are common among HIV-infected patients and there may be several causes, infections by *Mycobacterium tuberculosis*, Lymphoma, Castelman syndrome, Kaposi syndrome, or HIV itself. Hence, before being called HIV, the virus responsible for AIDS was called Lymphadenopathy Associated Virus. Another infecting pathogen that can cause lymphadenopathies is *Histoplasma capsulatum*.

Since the 1980s, HIV has spread in French Guiana, a French overseas territory between Brazil and Suriname. A distinct feature of patients with advanced HIV in French Guiana is that disseminated histoplasmosis is the most frequent AIDS-defining infection and cause of death. This epidemiological fact has been known by dermatologists since the 1980s, and then spread in the medical community further accelerated by fungal culture from a variety of tissue samples, which increasingly allowed identifying the fungal pathogen (Nacher et al., 2019; Morote et al., 2020). Lymphadenopathies are common and easily accessible sites to sample tissue to diagnose histoplasmosis (Huber et al., 2008).

In this context, we aimed to describe our experience regarding disseminated histoplasmosis with lymphadenopathies in French Guiana and to compare survival and severity of those patients to patients without lymphadenopathies.

METHODS

Study Design

A retrospective multicentric study was performed on patients with confirmed disseminated histoplasmosis included between January 1st, 1981 and October 1st, 2014. The cohort is not funded and its updating it will require the availability of staff sufficiently trained to collect all these data until 2020.

Study Population

Co-infections with HIV and histoplasmosis were enrolled in the Histoplasmosis and HIV database of French Guiana. The inclusion criteria were as follows: confirmed HIV infection; first proven episode of histoplasmosis [EORTC/MSG criteria (De Pauw et al., 2008)]; and age >18 years.

Study Design

This database was created in 1992. It included incident cases of HIV-associated histoplasmosis in the three hospitals of French Guiana. Epidemiological, clinical, paraclinical, immunovirological and therapeutic data were collected on a standardized case record form until October 2014. Hospitalized incident cases of HIV-associated histoplasmosis were included. Sex, age, place of birth, symptoms on admission, clinical entrance examination, immunovirological status, standard biological examinations, medical imaging, mycology, pathology, treatment received, and survival data during the study period were collected. Lymphadenopathies were classified according to size (<=2 cm, between 2 and 5 cm, and > 5 cm) and superficial (palpable) or deep lymphadenopathies, which were not palpable but visible in patients having benefitted from medical imagery (ultrasound, CT-scanner).

Statistical Analysis

STATA© (College Station, Texas, USA) was used. Quantitative variables were described using medians and interquartile ranges, they were compared between groups with or without superficial lymphadenopathies, or between groups with or without deep lymphadenopathies using ranksum non-parametric tests or Student's t-test, where appropriate. For qualitative variables, Chi2 or Fisher tests were computed comparing the proportions between those with and without lymphadenopathies. We also compared those with lymphadenopathies >2 cm to those without lymphadenopathies >2 cm. Multivariate logistic regression was used to adjust for potential confounders. Modeling included variables that significantly differed between those with and without lymphadenopathies. Model fit was verified using the Hosmer Lemeshow goodness of fit test. Kaplan Meier curves were computed and the Log Rank test was used to compare patients with and without lymphadenopathies. Patients lost to follow-up were right-censored at the date of last visit. Statistical significance was set at $P<0.05$.

Ethical and Regulatory Aspects

The research was approved by the Comité Consultatif pour le Traitement de l'Information pour la Recherche en Santé (CCTIRS) (number 10.175 bis, 10/06/2010), the French National Institute of Health and Medical Research institutional review board (CEEI INSERM) (IRB0000388, FWA00005831 18/05/2010), and the Commission Nationale Informatique et Libertés (CNIL) (number JZU0061856X, 07/16/2010).

RESULTS

Among 349 cases of disseminated histoplasmosis between January 1, 1981 and October 1, 2014, 168 (48.3%) had superficial lymphadenopathies and 133 had deep lymphadenopathies (38.1% if considering all patients, but 133/294 (45.2%) when only considering patients having had CT-scans or ultrasonography). **Figure 1** shows a flowchart breaking down the types and sizes of lymphadenopathies, and the persons with concomitant tuberculosis, atypical mycobacteriosis, and chronic herpes.

Superficial Lymphadenopathies

Among the 168 patients with superficial lymphadenopathies, 108 (64.3%) had lymphadenopathies <2 cm, 63 (37%) between 2 and 5 cm, and 4 (2.4%) >5 cm (**Table 1**). Patients with lymphadenopathies >2 cm were less likely to have pulmonary signs than those without lymphadenopathies >2 cm (**Table 2**). Patients with lymphadenopathies >2cm were also less likely to have had thoracic or abdominopelvic CT-scans, digestive endoscopy and bone marrow aspiration than those without lymphadenopathies >2 cm (**Table 2**). The median neutrophil count was higher among patients with lymphadenopathies >2cm than those without lymphadenopathies >2 cm (**Table 2**). The median platelet count was higher among patients with lymphadenopathies >2cm than those without lymphadenopathies >2 cm (**Table 2**). There were no significant differences between those with or without superficial lymphadenopathies for hemoglobin, ferritin, C-reactive protein, or LDH (data not shown).

Patients with superficial lymphadenopathies were less likely to receive presumptive antifungal treatment than those without superficial lymphadenopathies, 80.9% vs 88.8%, P=0.04. There was no significant difference in median CD4 count (32 (IQR=12-73) vs 31 (IQR=14-65), P=0.7) between those with and without superficial lymphadenopathies, respectively. The delay between diagnosis of histoplasmosis and the beginning of symptoms was longer among patients with superficial lymphadenopathies >2 cm than in those without. However, these patients had greater CD4 counts than those without superficial lymphadenopathies >2 cm (**Table 2**). There was no difference in the proportion of patients receiving amphotericin b (liposomal or deoxycholate) whether they had superficial lymphadenopathies or not (45.4%, vs. 41.8, P=0.5). However, those with superficial lymphadenopathies >2 cm were less likely to receive amphotericin B induction therapy than those without (**Table 2**).

Although there seemed to be a lower proportion of deaths within 1 month after antifungal therapy among those with superficial lymphadenopathies than those without, the difference was not significant (11.3% vs 17.2%, P=0.11). Similarly, for all deaths, there was a non-significant trend for fewer deaths in the superficial lymphadenopathies (36.9% vs 45.5%, P=0.1).

Among persons explored with medical imagery, persons with superficial lymphadenopathies were more likely to also have deep lymphadenopathies (OR=1.87 (95%CI=1.18-2.97), P=0.004.

Deep Lymphadenopathies

Regarding deep lymphadenopathies, the median LDH concentration was lower among patients with deep lymphadenopathies than those without deep lymphadenopathies (**Table 2**). The median ferritin concentration was lower among patients with deep lymphadenopathies than those without deep lymphadenopathies (**Table 2**). The median TGO concentration was lower among patients with deep lymphadenopathies than those without deep lymphadenopathies (**Table 2**). Ultrasonographic measurement of hepatomegaly showed that the proportion of patients with hepatomegaly was lower among patients with deep lymphadenopathies than in those without deep lymphadenopathies (**Table 2**).

When looking at the WHO performance status there was less general condition alteration among those with deep lymphadenopathies (**Table 2**).

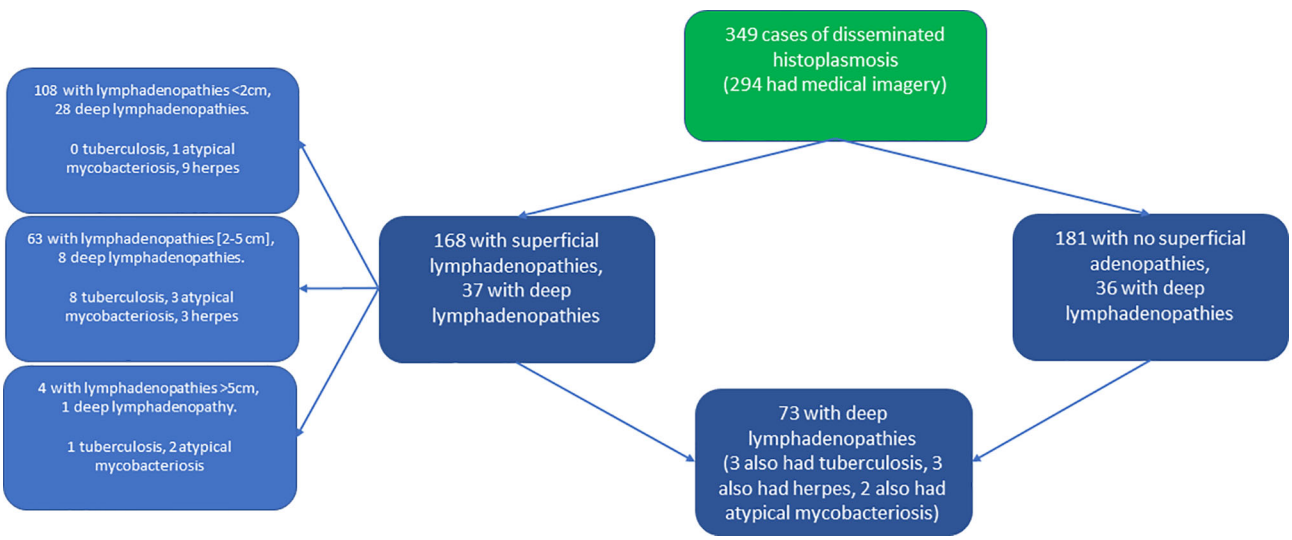

FIGURE 1 | Flowchart stratifying patient counts by presence of superficial or deep lymphadenopathies.

TABLE 1 | Superficial and deep lymphadenopathies in human immunodeficiency virus (HIV)-infected patients with disseminated histoplasmosis.

Variable	n/N	Percentage
Presence of superficial† lymphadenopathies	168/349	48
Superficial lymphadenopathies<2 cm	108/168	64
cervical lymphadenopathies<2 cm	60/100	60
supraclavicular lymphadenopathies <2 cm	11/100	11
axilary lymphadenopathies <2 cm	38/100	38
inguinal lymphadenopathies<2 cm	49/100	49
Medium size superficial lymphadenopathies (2–5 cm)	63/168	37
cervical lymphadenopathies (2–5 cm)	23/35	65
supraclavicular lymphadenopathies (2–5 cm)	6/35	17
axilary lymphadenopathies (3–5 cm)	19/35	54
inguinal lymphadenopathies (3–5 cm)	8/35	23
Large superficial lymphadenopathies (>5 cm)	4/168	2
cervical lymphadenopathies>5 cm	2/4	50
supraclavicular lymphadenopathies >5 cm	0/4	0
axilary lymphadenopathies >5 cm	2/4	50
inguinal lymphadenopathies>5 cm	1/4	25
Deep‡ lymphadenopathies	133/349	38
Mediastinal lymphadenopathies on chest Xray	4/132	3
Deep lymphadenopathies on abdominopelvic ultrasonography	82/234*	35
Abdominal	76/83	91
Celiomesenteric	32/83	38
interaortico-caval	18/83	21
Lombo-aortic	14/83	16
hepatic hilus	12/83	14
Illiac	6/83	7
Latero-caval	5/83	6
Deep lymphadenopathies on abdominal-pelvic CT-scanner	60/98*	61
Abdominal	40/61	65
Celiomesenteric	32/61	52
Retroperitoneal	24/61	39
Lombo-aortic	13/61	21
interaortico-caval	12/61	19
Illiac	12/61	19
Hepatic hilus	5/61	8
Latero-caval	3/61	4
Deep lymphadenopathies on thoracic CT-scanner	37/100*	37
Mediastinal	31/37	83
Axillary and supraclavicular	9/37	24
Hilar	7/37	18
Sub carinal	2/37	5
Barety's space	1/37	2

**Number of procedures performed; †superficial lymphadenopathies are palpable during clinical examination; ‡deep lymphadenopathies are not palpable and only visible through medical imagery.*

Time and Lymphadenopathies

When comparing the proportion of patients with lymphadenopathies between four time-periods (<1998, 1998-2003, 2004-2009, 2010-2014) there was no significant difference between the proportion of patients with superficial lymphadenopathies during different time periods. However, **Figure 2** shows that over time the proportion of lymphadenopathies >2 cm decreased whereas those < 2 cm increased (P for linear trend <0.0001), and among those having benefitted from medical imagery the proportion of deep lymphadenopathies increased (P<0.0001). There was a strong negative correlation between time period and the duration between symptoms' onset and hospital admission (Spearman's rho –0.57, P<0.0001).

There was a significant decrease in the risk of early death (<1 month) among those with deep lymphadenopathies relative to those without (OR=0.26 (95%CI=0.10–0.60), P=0.0006) and in the overall risk of death (OR=0.33 (95%CI=0.20–0.55), P<0.0001). These associations remained strongly significant after adjusting for time period, CD4 counts, age, delay between beginning of symptoms and hospital admission, antifungal and antiretroviral treatment. **Figures 3** and **4** show the Kaplan Meier curves for survival by deep lymphadenopathies and superficial lymphadenopathies considering the onset of symptoms as origin, the date of death, and censoring at the date when the patient was last seen. This amounted to 850 person-years of follow up. Both curves suggest that survival was greater among those with lymphadenopathies but the log Rank was not significant for superficial lymphadenopathies. The incidence rate of death among patients without superficial lymphadenopathies was 17.5 per 100 person-years, and for those with superficial lymphadenopathies it was 12.3 per 100 person-years. The incidence rate of death among patients without deep lymphadenopathies was 19.5 per 100 person-years, and for those with deep lymphadenopathies it was 8.4 per 100 person-years.

Overall, there were no differences between those with or without lymphadenopathies and transmission modes, history of opportunistic infections, antiretroviral treatment, nationality, sex (data not shown). There were 9 (12.3%) concomitant tuberculosis cases in those with lymphadenopathies and 9(14.3%) concomitant tuberculosis cases in those without lymphadenopathies, P=0.7. There were 6 (8.2%) concomitant cases of atypical mycobacterial infection in those with lymphadenopathies and 1(1.6%) concomitant case of atypical mycobacterial infection in those without lymphadenopathies, P=0.08. There were 12 (16.4%) concomitant chronic herpes cases in those with lymphadenopathies and 8(12.7%) concomitant chronic herpes cases in those without lymphadenopathies, P=0.5. Performing the above comparisons between patients with and without superficial or deep lymphadenopathies after excluding persons with concomitant tuberculosis, mycobacteriosis and chronic herpes did not change the observed differences (data not shown). There were 23/55 positive direct examinations of lymph node samples and 43/53 positive cultures of lymph node samples, and 39/63 positive pathological examinations of lymph node biopsies.

DISCUSSION

Superficial lymphadenopathies were very common among patients with disseminated histoplasmosis and 19% of all patients had lymphadenopathies >2 cm. Among patients having benefitted from ultrasonography or CT-scanner, 45% had deep lymphadenopathies. Patients with superficial lymphadenopathies seemed less severe that those without superficial lymphadenopathies but this failed to reach statistical significance. However, patients with deep lymphadenopathies were definitely less severe than patients without deep lymphadenopathies. After adjusting for several potential confounders, they were less likely to die, at one month and at any temporal horizon than patients without deep

TABLE 2 | Comparisons between patients with and without large superficial lymphadenopathies (>2 cm), and with and without deep lymphadenopathies.

	Superficial† lymphadenopathies>=2cm N=67	No superficial† lymphadenopathies>2cm N=282	P*
Delay between symptoms onset and diagnosis (median [IQR]) days	143 [51–261]	42 [20–188]	0.0004
Pulmonary symptoms and signs	36.5	60.9	0.002
Thoracic CT Scan (%)	14.3	44.7	<0.0001
Abdominopelvic CT Scan (%)	11.1	40	<0.0001
Bone marrow aspiration (%)	6.3	26.7	0.001
Endoscopy (%)	28.5	44.7	0.03
Neutrophils (median [IQR]) per mm3	2,240 [1,380–3,050]	1,525 [6–2,726]	0.001
Platelets (median [IQR]) per mm3	194,500 [101,000–262,500]	106,000 [384–213,500]	0.001
CD4 count (median [IQR]) per mm3	46 [19–112]	26 [60–103]	0.003
Proportion receiving liposomal amphotericin B induction (%)	34.9	52	0.03
	Deep lymphadenopathies‡ N=133	**No deep lymphadenopathies‡ N=216**	**P***
LDH (median [IQR]) U/L	349 [261–540]	538 [320–1,309]	<0.0001
Ferritin (median [IQR]) ng/ml	1082 [388–1,908]	1347 [641-5,449]	0.01
TGO (median [IQR]) IU	50 [31–75]	60 [35–119]	0.01
WHO performance status>2 (%)	41.5	51.8	<0.001
Proportion with ultrasonographic hepatomegaly (%)	56.2	75.5	0.02

**chi square test for proportions, rank sum test for medians; †superficial lymphadenopathies are palpable during clinical examination; ‡deep lymphadenopathies are not palpable and only visible through medical imagery.*

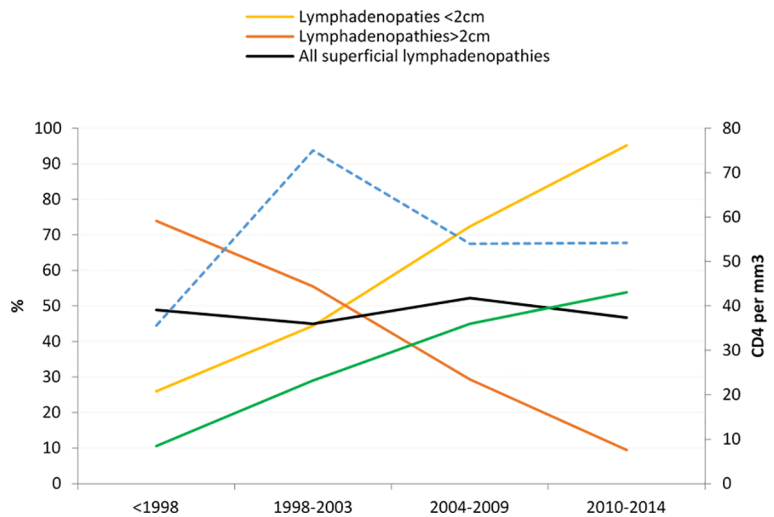

FIGURE 2 | Evolution of the proportion of patients with lymphadenopathies by size.

lymphadenopathies. Consistently with this finding, markers that can serve as a proxy for severity (Couppie et al., 2004) were more favorable than those of patients without deep lymphadenopathies. Hence, LDH, Ferritin, and TGO levels were significantly lower, and platelet counts were higher in those with deep lymphadenopathies. They were also less likely to have ultrasonographic hepatomegaly than those without deep lymphadenopathy, and the WHO performance status score was lower (indicating less alteration of the patient's general condition) among patients with deep lymphadenopathies than among those without deep lymphadenopathies.

Patients with superficial lymphadenopathies >2 cm were less likely to have further explorations than those without, presumably because they were less likely to have respiratory problems, to have leukocyte or platelets cytopenias than patients without lymphadenopathies >2 cm. In addition, the attending physicians may also have focused on the tangible anomaly at hand and thus, they were less intensively explored. Patients with superficial lymphadenopathies were less likely to receive presumptive antifungal treatment than those without superficial lymphadenopathies. The delay between diagnosis of histoplasmosis and the beginning of symptoms was longer among patients with superficial lymphadenopathies>2cm than in those without such lesions. These patients had greater CD4 counts than those without superficial lymphadenopathies >2 cm. Patients with superficial lymphadenopathies >2 cm were less

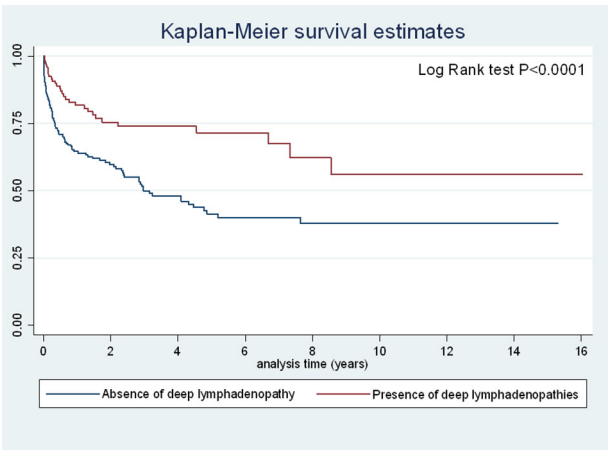

FIGURE 3 | Incidence of death among patients with disseminated histoplasmosis stratified by the presence of deep lymphadenopathies.

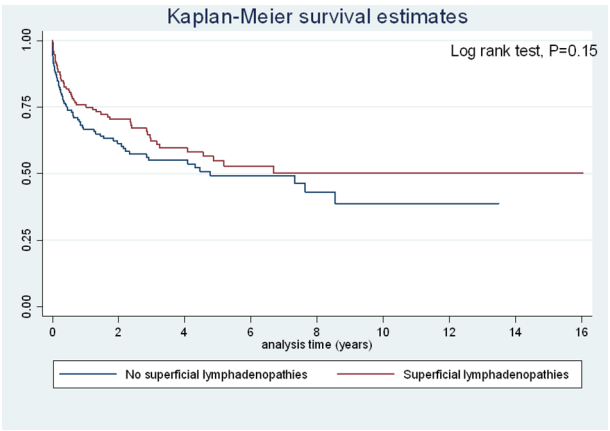

FIGURE 4 | Incidence of death among patients with disseminated histoplasmosis stratified by the presence of superficial lymphadenopathies.

likely to receive amphotericin B induction therapy than those without, which is also an indication they were less severe.

There were a number of potential limitations. Lymphadenopathies are frequent in HIV-infection, a frequency that may vary depending on the proportion of advanced immunosuppression or the pathogen ecosystem (Cortez et al., Sep-Oct; Kamana et al., 2010; Hadadi et al., 2014). Among patients with concomitant opportunistic infections that can cause lymphadenopathy we did not observe any significant differences between those with or without superficial lymphadenopathies, but the total numbers of coinfections were relatively small. It was hence often not possible to determine for sure the cause of enlarged lymphadenopathies when there was no aspiration or biopsy for fungal diagnosis. Diagnosis was reached in different ways and the fungal load was not known. It is possible to suspect a bias where those with superficial lymphadenopathies would be diagnosed earlier because of the externality of lymph nodes. However, the fact that the delay between symptoms' onset and diagnosis was longer in those with superficial lymphadenopathies >2 cm than in those without, and that their CD4 count was higher was consistent with the observation that deep lymphadenopathies were associated with less mortality. Finding deep lymphadenopathies depended on actually looking for them using medical imagery. This raises the question of considering that those who did not get an ultrasound or a CT-scan could wrongly be considered as not having deep lymphadenopathies. However, when excluding those who did not have ultrasonographic or CT-scanographic explorations, the findings did not change at all. Over 34 years many things have changed, HIV testing, histoplasmosis diagnostic capacity and awareness, antifungal treatment, and HIV treatment (Nacher et al., 2020). All this may introduce biases, but our observations of reduced death remained very significant after taking into account confounders such as age, the duration of symptoms before admission, antifungal and antiretroviral treatment, and CD4 count. Therefore, we are confident in the conclusion that disseminated histoplasmosis with deep lymphadenopathies is statistically less severe that when there are no deep lymphadenopathies. An intriguing finding was the fact that superficial lymphadenopathies >2 cm became significantly less frequent over time, whereas lymphadenopathies <2 cm became more frequent, while median CD4 count remain stable all along. This was perhaps linked to the gradual decline of delays between the onset of symptoms and hospitalization and treatment, which left less time for lymphadenopathies to grow.

The corpus of knowledge of pathologists also brings an interesting way to consider our results. Histopathological lesions in histoplasmosis reflect the host reaction against *H. capsulatum* and are usually classified into four categories including tuberculoid, anergic, mixed, and sequelae types. The tuberculoid form generally corresponds to a low inoculation and effective tissue response of the host. In this form, *H. capsulatum* are usually few in number and are located in the cytoplasm of macrophages (intracellular). The anergic form is usually seen in HIV patients and shows little or no tissue response but abundant intracellular and extracellular yeast. In anergic forms the local macrophages remain inactive. The mixed form represents an intermediate form between the tuberculoid and the anergic type. Finally, in the sequelae type, scarring fibrosis is predominant and inflammation is mild. In this form, *H. capsulatum* yeasts are rare and may correspond to a relapse case or possible reactivation.

In our Histoplasmosis pathology experience, 31 patients had histological confirmation of lymph node histoplasmosis by the presence of *H. capsulatum* yeasts on lymph node biopsies or surgical specimens. Interestingly and consistently with the clinical outcome of this study the granulomatous inflammatory reaction of tuberculoid type was the most frequent (24/31, 77.4%) which usually corresponds to effective tissue response (Drak Alsibai et al., 2020). Among these 24 granulomatous cases, histological variants perfectly mimicking tuberculosis with epithelioid granulomas, multinucleated giant cells and caseous necrosis were found in 10 cases, followed by less typical epithelioid granulomatous variants where giant cells and necrosis

were absent in eight cases, then by forms with predominant macrophage infiltration in six cases. The remaining seven lymph nodes showed non-specific hyperplastic lymphadenitis.

Lymph nodes function as an active innate barrier that can help improve patients' defenses against the spread of infection. Furthermore, they can be actively modulated to rapidly recruit additional cells in response to a response default. In the normal lymph node, the macrophages reside in the subcapsular sinus and medullary sinus. Lymphatic fluid brings pathogens and antigen-presenting cells to lymph nodes macrophages (Bogoslowski and Kubes, 2018). In infectious diseases, the granuloma is the result of a complex interaction between the infectious agent and a wide range of inflammatory cells (macrophages, lymphocytes T and B, etc…) and biological mediators (cytokines, interleukins, chemokines, growth factors, etc…).

Granuloma formation is promoted by a close relationship between activated macrophages that strongly express major histocompatibility complex (MHC) class II molecules and CD4+ T helper cells 1 (Th1) (James, 2000). Macrophages may develop into epithelioid cells and can also fuse to form multinucleated giant cells. Th1 recognize protein peptides presented to them by antigen presenting cells carrying MHC II molecules. Th1 subsequently induces interleukin-1 on macrophages that promote granuloma formation. The overstimulation of Th1 cells compared to T helper cells 2 (Th2) leads to cell hyperactivity, tissue destruction and granuloma reaction. Instead, when the Th2 is over-stimulated, it causes an anergy and apoptosis. The activation of Th1 and Th2 lymphocytes is controlled by B7-CD28/CTLA-4 stimulation pathways (James, 2000).

Our convergent findings strongly suggest that patients who have significantly enlarged superficial and deep lymphadenopathies are less severe. An enlarged lymph node is a sign that there is a battle going on in the lympnode, where circulating lymphocytes are confronted with antigen presenting cells. For the proliferation to take place the immunocompromised host must still have some capacity to mount part of a response. An analogy could be immune reconstitution syndromes, for which one of the common presentations are rapidly growing and at times compressive lymphadenopathies where the reconstitution of the immune system is "visible" in the lymphnodes (Nacher et al., 2006; Melzani et al., 2020). Even though the patient has low CD4 counts, the enlarged lymphadenopathies in patients with disseminated histoplasmosis may thus testify than an active "front line" is remaining. This lower severity is of course relative, and disseminated histoplasmosis is still a very serious disease even with deep lymphadenopathies as shown by the incidence rate of 8.4 deaths per 100 person-years. The patterns of dissemination of this proteiform disease are still obscure, in some disseminating to certain organs and in others in different organs (Couppié et al., 2019). The interplay between inoculum, immunity, personal factors, random factors results in a great variety of clinical presentations, requiring different microbiologic diagnostic approaches; all this lead to the difficulty of this diagnosis in the absence of antigen detection tests (Wheat, 1994).

In conclusion, the present data showed that in patients with advanced HIV and disseminated histoplasmosis, the presence of deep lymphadenopathies- and perhaps of superficial lymphadenopathies- was associated with fewer markers of severity and a lower risk of death. To our knowledge it is the first study to show this.

DATA AVAILABILITY STATEMENT

The raw data supporting the conclusions of this article will be made available by the authors after permission from the commission nationale informatique et libertés, without undue reservation.

ETHICS STATEMENT

Written informed consent was obtained from the individual(s) for the publication of any potentially identifiable images or data included in this article.

AUTHOR CONTRIBUTIONS

Conceptualization, MN. Methodology, MN. Formal analysis, MN. Investigation, LE, RB, AV, AA, PA, FD, MD, CM, BN, KA, PC. Data curation, AA, PC. Writing—original draft preparation, MN. Review and editing, LE, RB, AV, AA, PA, FD, MD, CM, BN, KA, PC. All authors contributed to the article and approved the submitted version.

ACKNOWLEDGMENTS

Thank you to many ward physicians who contributed over the years to systematic data collection.

REFERENCES

Bogoslowski, A., and Kubes, P. (2018). Lymph Nodes: The Unrecognized Barrier against Pathogens. *ACS Infect. Dis.* 4, 1158–1161. doi: 10.1021/acsinfecdis.8b00111

Cortez, M. V., Oliveira, C. M., Monte, R. L., Araujo, J. R., Braga, B. B., Reis, D. Z., et al. (Sep-Octc). HIV-associated tuberculous lymphadenitis: the importance of polymerase chain reaction (PCR) as a complementary tool for the diagnosis of tuberculosis - a study of 104 patients. *Bras. Dermatol.* 86, 925–931. doi: 10.1590/S0365-05962011000500010

Couppie, P., Sobesky, M., Aznar, C., Bichat, S., Clyti, E., Bissuel, F., et al. (2004). Histoplasmosis and acquired immunodeficiency syndrome: a study of prognostic factors. *Clin. Infect. Dis.* 38, 134–138. doi: 10.1086/379770

Couppié, P., Herceg, K., Bourne-Watrin, M., Thomas, V., Blanchet, D., Alsibai, K. D., et al. (2019). The Broad Clinical Spectrum of Disseminated Histoplasmosis in HIV-Infected Patients: A 30 Years' Experience in French Guiana. *J. Fungi* 5, 115. doi: 10.3390/jof5040115

De Pauw, B., Walsh, T. J., Donnelly, J. P., Stevens, D. A., Edwards, J. E., Calandra, T., et al. (2008). Revised definitions of invasive fungal disease from the European Organization for Research and Treatment of Cancer/Invasive Fungal Infections Cooperative Group and the National Institute of Allergy and Infectious Diseases Mycoses Study Group (EORTC/MSG) Consensus Group. *Clin. Infect. Dis.* 46, 1813–1821. doi: 10.1086/588660

Dimopoulos, Y., Moysi, E., and Petrovas, C. (2017). The Lymph Node in HIV Pathogenesis. *Curr. HIV/AIDS Rep.* 14, 133–140. doi: 10.1007/s11904-017-0359-7

Drak Alsibai, K., Couppié, P., Blanchet, D., Adenis, A., Epelboin, L., Blaizot, R., et al. (2020). Cytological and Histopathological Spectrum of Histoplasmosis: 15 Years of Experience in French Guiana. *Front. Cell. Infect. Microbiol.* 10, 591974. doi: 10.3389/fcimb.2020.591974

Hadadi, A., Jafari, S., Jebeli, Z. H., and Hamidian, R. (2014). Frequncy and etiology of lymphadenopathy in Iranian HIV/AIDS patients. *Asian Pacific J. Trop. Biomed.* 4, S171–S176. doi: 10.12980/APJTB.4.2014C1253

Horwath, M. C., Fecher, R. A., and Deepe, G. S. (2015). Histoplasma capsulatum, lung infection and immunity. *Future Microbiol.* 10, 967–975. doi: 10.2217/fmb.15.25

Huber, F., Nacher, M., Aznar, C., Pierre-Demar, M., El Guedj, M., Vaz, T., et al. (2008). AIDS-related Histoplasma capsulatum var. capsulatum infection: 25 years experience of French Guiana. *AIDS* 22, 1047–1053. doi: 10.1097/QAD.0b013e3282ffde6700002030-200805310-00006[pii

James, D. G. (2000). A clinicopathological classification of granulomatous disorders. *Postgrad. Med. J.* 76, 457–465. doi: 10.1136/pmj.76.898.457

Kamana, N. K., Wanchu, A., Sachdeva, R. K., Kalra, N., and Rajawanshi, A. (2010). Tuberculosis is the leading cause of lymphadenopathy in HIV-infected persons in India: Results of a fine-needle aspiration analysis. *Scandinavian J. Infect. Dis.* 42, 827–830. doi: 10.3109/00365548.2010.498016

Melzani, A., de Reynal de Saint Michel, R., Ntab, B., Djossou, F., Epelboin, L., Nacher, M., et al. (2020). Incidence and Trends in Immune Reconstitution Inflammatory Syndrome Associated With Histoplasma capsulatum Among People Living With Human Immunodeficiency Virus: A 20-Year Case Series and Literature Review. *Clin. Infect. Dis.* 70, 643–652. doi: 10.1093/cid/ciz247

Morote, S., Nacher, M., Blaizot, R., Ntab, B., Blanchet, D., Drak Alsibai, K., et al. (2020). Temporal trends of cutaneo-mucous histoplasmosis in persons living with HIV in French Guiana: early diagnosis defuses South American strain dermotropism. *PLoS Negl. Trop. Dis.* 14 (10), e0008663. doi: 10.1371/journal.pntd.0008663

Nacher, M., Sarazin, F., El Guedj, M., Vaz, T., Alvarez, F., Nasser, V., et al. (2006). Increased incidence of disseminated histoplasmosis following highly active antiretroviral therapy initiation. *J. Acquir. Immune Defic. Syndr.* 41, 468–470. doi: 10.1097/01.qai.0000209927.49656.8d

Nacher, M., Leitao, T. S., Gómez, B. L., Couppié, P., Adenis, A., Damasceno, L., et al. (2019). The Fight against HIV-Associated Disseminated Histoplasmosis in the Americas: Unfolding the Different Stories of Four Centers. *J. Fungi (Basel)* 5 (2), 51. doi: 10.3390/jof5020051

Nacher, M., Adenis, A., Guarmit, B., Lucarelli, A., Blanchet, D., Demar, M., et al. (2020). What is AIDS in the Amazon and the Guianas in the 90-90-90 era? *PloS One* 15, e0236368. doi: 10.1371/journal.pone.0236368

Standring, S. (2016). *Gray's anatomy: the anatomical basis of clinical practice*. Elsevier Limited 41st edition

Wheat, J. (1994). Histoplasmosis: Recognition and Treatment. *Clin. Infect. Dis.* 19, S19–S27. doi: 10.1093/clinids/19.Supplement_1.S19

Conflict of Interest: The authors declare that the research was conducted in the absence of any commercial or financial relationships that could be construed as a potential conflict of interest.

frontiers in Cellular and Infection Microbiology

ORIGINAL RESEARCH
published: 10 February 2021
doi: 10.3389/fcimb.2020.592022

Paracoccidioides brasiliensis Releases a DNase-Like Protein That Degrades NETs and Allows for Fungal Escape

*Yohan Ricci Zonta[1], Ana Laura Ortega Dezen[1], Amanda Manoel Della Coletta[1], Kaio Shu Tsyr Yu[1], Larissa Carvalho[1], Leandro Alves dos Santos[2], Igor de Carvalho Deprá[3], Rachel M. Kratofil[4,5,6], Michelle Elizabeth Willson[4,5,6], Lori Zbytnuik[4,5,6], Paul Kubes[4,5,6], Valdecir Farias Ximenes[7] and Luciane Alarcão Dias-Melicio[1,2,8]**

[1] Laboratory of Immunopathology and Infectious Agents - LIAI, UNIPEX - Experimental Research Unity, Sector 5, Medical School of Botucatu, São Paulo State University (UNESP), Botucatu, Brazil, [2] Confocal Microscopy Laboratory, UNIPEX - Experimental Research Unity, Medical School of Botucatu, São Paulo State University (UNESP), Botucatu, Brazil, [3] Laboratory of Genetic Basis of Endocrinological Diseases, Experimental Research Unity (UNIPEX), Sector 5, São Paulo State University (UNESP), Botucatu, Brazil, [4] Calvin, Phoebe, and Joan Snyder Institute for Chronic Diseases, University of Calgary, Calgary, AB, Canada, [5] Department of Physiology and Pharmacology, Cumming School of Medicine, University of Calgary, Calgary, AB, Canada, [6] Department of Microbiology, Immunology and Infectious Diseases, Cumming School of Medicine, University of Calgary, Calgary, AB, Canada, [7] Department of Chemistry, Sciences School, São Paulo State University (UNESP), Bauru, Brazil, [8] Department of Pathology, Medical School of Botucatu, São Paulo State University (UNESP), Botucatu, Brazil

OPEN ACCESS

Edited by:
Angel Gonzalez,
University of Antioquia, Colombia

Reviewed by:
Zhengkai Wei,
Foshan University, China
Patricia Xander,
Federal University of São Paulo, Brazil

***Correspondence:**
Luciane Alarcão Dias-Melicio
dias.melicio@unesp.br

Specialty section:
This article was submitted to Fungal Pathogenesis, a section of the journal Frontiers in Cellular and Infection Microbiology

Received: *06 August 2020*
Accepted: *28 December 2020*
Published: *10 February 2021*

Citation:
Zonta YR, Dezen ALO, Della Coletta AM, Yu KST, Carvalho L, Santos LAd, Deprá IdC, Kratofil RM, Willson ME, Zbytnuik L, Kubes P, Ximenes VF and Dias-Melicio LA (2021) Paracoccidioides brasiliensis Releases a DNase-Like Protein That Degrades NETs and Allows for Fungal Escape. Front. Cell. Infect. Microbiol. 10:592022. doi: 10.3389/fcimb.2020.592022

Paracoccidioidomycosis is a systemic fungal disease, considered endemic in Latin America. Its etiological agents, fungi of the *Paracoccidioides* complex, have restricted geographic habitat, conidia as infecting form, and thermo-dimorphic characteristics. Polymorphonuclear neutrophils (PMNs) are responsible for an important defense response against fungus, releasing Neutrophil Extracellular Traps (NETs), which can wrap and destroy the yeasts. However, it has been described that some pathogens are able to evade from these DNA structures by releasing DNase as an escape mechanism. As different NETs patterns have been identified in PMNs cultures challenged with different isolates of *Paracoccidioides brasiliensis*, the general objective of this study was to identify if different patterns of NETs released by human PMNs challenged with Pb18 (virulent) and Pb265 (avirulent) isolates would be correlated with fungal ability to produce a DNase-like protein. To this end, PMNs from healthy subjects were isolated and challenged *in vitro* with both fungal isolates. The production, release, and conformation of NETs in response to the fungi were evaluated by Confocal Microscopy, Scanning Microscopy, and NETs Quantification. The identification of fungal DNase production was assessed by DNase TEST Agar, and the relative gene expression for hypothetical proteins was investigated by RT-qPCR, whose genes had been identified in the fungal genome in the GenBank (PADG_11161 and PADG_08285). It was possible to verify the NETs release by PMNs, showing different NETs formation when in contact with different isolates of the fungus.

The Pb18 isolate induced the release of looser, larger, and more looking like degraded NETs compared to the Pb265 isolate, which induced the release of denser and more compact NETs. DNase TEST Agar identified the production of a DNase-like protein, showing that only Pb18 showed the capacity to degrade DNA in these plates. Besides that, we were able to identify that both PADG_08528 and PADG_11161 genes were more expressed during interaction with neutrophil by the virulent isolate, being PADG_08528 highly expressed in these cultures, demonstrating that this gene could have a greater contribution to the production of the protein. Thus, we identified that the virulent isolate is inducing more scattered and loose NETs, probably by releasing a DNase-like protein. This factor could be an important escape mechanism used by the fungus to escape the NETs action.

Keywords: paracoccidioidomycosis, neutrophils, neutrophil extracellular traps (NETs), DNase, escape mechanism

INTRODUCTION

Paracoccidioidomycosis (PCM) is a systemic fungal disease, considered a neglected disease endemic to Latin America, occurring from Mexico to Argentina with its main foci of infection in countries such as Brazil, Venezuela, and Colombia, usually affecting agricultural workers, gardeners, and transporters (Coutinho et al., 2002; Restrepo and Tobón, 2005; Colombo et al., 2011; Marques, 2013). Some cases have been reported outside the endemic areas, such as Europe and North America, but in these cases, the infected individuals moved to these regions after infection occurred (Wagner et al., 2016). Its etiological agents are fungi from the *Paracoccidioides* complex, composed of five species that are restricted geographically (Matute et al., 2006). The infectious form is conidia with thermo-dimorphic characteristics, which means that it alters its morphology according to the temperature to which it is exposed, taking the form of mycelium at room temperature, and upon entering the body (37°C), it turns into yeast form (Colombo et al., 2011). The fungus *Paracoccidioides* spp. belongs to the same family as other etiological agents that cause deep fungal mycoses, such as *Histoplasma capsulatum* and *Coccidioides immitis*, that are also onygenalean human pathogenic fungi (Matute et al., 2006). A recent study used molecular polymorphism, phylogenetic reconstruction, genetic and morphological population analysis of yeasts and conidia of different species demonstrated that the *Paracoccidioides* complex (previously known as four cryptic species of the *P. brasiliensis* and *P. lutzii*) can actually be divided in different species, and with that, proposed a new nomenclature for these different agents: *P. americana* for PS2, *P. restrepiensis* for PS3, and *P. venezuelensis* for PS4, while *P. brasiliensis* would be restricted to species S1 (Matute et al., 2006; Teixeira et al., 2009; Teixeira et al., 2014; Turissini et al., 2017).

After inhalation, the infectious conidia are lodged in the lower airways (bronchioles and alveoli) (Marques, 2013; Shikanai-Yasuda et al., 2018) where they germinate into yeast forming the Primary Pulmonary Complex (Severo et al., 1979). The fungus can be destroyed or become latent, characterizing PCM-infection (Shikanai-Yasuda et al., 2018), or spread to other organs such as the liver, spleen, adrenal *via* the lymphohematogenous pathway, characterizing PCM-disease (Shikanai-Yasuda et al., 2018), which can be presented in two different forms, the acute/subacute and the chronic forms (Bocca et al., 2013; Shikanai-Yasuda et al., 2018). In the specific case of PCM, the massive infiltration of neutrophils was found in the inflammatory tissues of patients (Franco, 1987), as well as in the lesions of different experimental models of the disease (Defaveri et al., 1989; Defaveri et al., 1992; Calich et al., 1994). Human neutrophils are associated with resistance to *P. brasiliensis* infection *in vitro*, as polymorphonuclear cells can ingest the fungal yeast through the phagocytosis process (Dias et al., 2004). However, when the yeasts are larger than the supported size by the cell, the cells generate a kind of extracellular vacuole before attacking the fungus (Dias et al., 2004). However, although sometimes neutrophils are successful in the phagocytosis process, this does not seem to be sufficient to kill the fungus (Kurita et al., 1999). Some studies have shown that human neutrophils have no fungicidal or fungistatic activity against *P. brasiliensis* (Kurita et al., 1999; Kurita et al., 2005). This activity, however, is increased when cells are activated by IFN-γ, TNF-α, GM-CSF, or Reactive Oxygen Species (ROS), which initiates an offensive mechanism against the fungus dependent on reactive oxygen species (Rodrigues et al., 2007). However, studies indicate that specific cytokines, such as IL-10, also act as suppressors of polymorphonuclear mediated response (Costa et al., 2007).

A key defense mechanism of neutrophils is the ability to expel nuclear contents into the surrounding environment in the form of neutrophil extracellular traps (NETs). NETs are composed of large amounts of DNA decorated with granule proteins such as enzymes, histones, and antimicrobial peptides (Brinkmann et al., 2004; Brinkmann and Zychlinsky, 2012; Ravindran et al., 2019). The high concentration of these proteins within NETs, associated with the physical structure created around the microorganism, are directly associated with the antimicrobial activity of these structures (Brinkmann et al., 2004; Pilsczek et al., 2010; Papayannopoulos et al., 2010; McDonald et al., 2012;

Ravindran et al., 2019; Thanabalasuriar et al., 2019; Castanheira and Kubes, 2019; Liew and Kubes, 2019).

Recently, it was demonstrated that *P. brasiliensis* could induce the release of NETs (Mejía et al., 2015; Della Coletta et al., 2015; Bachiega et al., 2016). Our research group identified that the virulent fungal isolate (Pb18) is able to induce NETs release by human neutrophils from healthy individuals *via* dectin-1 signaling, and that NET release resulted in extracellular fungicidal activity (Bachiega et al., 2016). Additionally, we have also identified the presence of NETs in cutaneous lesions of patients with paracoccidioidomycosis, and after challenging neutrophils from these patients with Pb18 (more virulent) and Pb265 (less virulent) isolates, we identified different patterns of NET formation induced by the different fungal isolates (Della Coletta et al., 2015). In the more virulent Pb18 isolate, the NET pattern was loose and scattered covering a large surface area, whereas in the less virulent Pb265 isolate, NETs were smaller, more dense and compacted (Della Coletta et al., 2015). We previously hypothesized that the different patterns of NETs could be due to the production of a DNase or an enzyme with DNase-like activity by the Pb 18 isolate as a mechanism of fungal escape from host defenses, leading to degradation of NETs during fungal infection (Della Coletta et al., 2015). It was shown that some pathogens such as *Staphylococcus aureus* (Berends et al., 2010; Thammavongsa et al., 2013; Hoppenbrouwers et al., 2018), *Pseudomonas aeruginosa* (Wilton et al., 2018), *Mycoplasma bovis* (Zhang et al., 2016; Gondaira et al., 2017; Mitiku et al., 2018), *Streptococcus spp* (Buchanan et al., 2006; de Buhr et al., 2014; Morita et al., 2014; Liu et al., 2017), *Vibrio cholerae* (Seper et al., 2013), *Ehrlichia chaffeensis* (Teymournejad et al., 2017), other bacterias (Sharma et al., 2019), and beyond, *Leishmania spp* (Freitas-Mesquita et al., 2019), *Candida albicans* (Riceto et al., 2015; Zhang et al., 2017), *Cryptococcus spp* (Sánchez and Colom, 2010), *Trichosporon spp* (Bentubo and Gompertz, 2014), are able to produce DNase or exonucleases as an escape mechanism from NETs.

Thus, the objective of this work was to identify whether the fungal isolates Pb18 and Pb265 produce a DNase or DNase-like enzyme that could degrade NETs from human neutrophils *in vitro*, and correlate this enzymatic activity with the NETs patterns observed by the different fungal isolates. Ultimately, this study is fundamental to better understand the fungal mechanisms involved in the escape of host defenses.

MATERIALS AND METHODS

Casuistics

Neutrophils were obtained from 40 ml of peripheral blood after venipuncture of 10 healthy volunteers. All subjects were informed of the research goals and signed a consent form. The study was conducted according to the National Health Guidelines 196/96, and it was approved by the Research Ethics Committee of Medical School of Botucatu, UNESP – São Paulo State University (CAAE: 85654018.9.0000.5411; protocol: 2.577.243/2018).

Neutrophil Isolation

After the venous puncture, neutrophils were isolated by a density gradient centrifugation (Histopaque® 1,119 g/ml and Histopaque® 1,083 g/ml - Sigma-Aldrich - St. Louis, Missouri, USA) at 1,500 rpm for 30 min (room temperature). Erythrocytes were lysed with a hypotonic solution (NaCl 0.1%), and the neutrophil viability was assessed with trypan blue dye exclusion (95% viability). Cell cultures were then resuspended in RPMI-1640 medium (Cultilab – Campinas, São Paulo, BRA) supplemented with 10% of calf serum (Sigma-Aldrich) and 1% Gentamicin (Schering- Plough, New Jersey, EUA) and adjusted for $2x10^6$ cells/ml before all procedures.

Fungal Isolates and Culture Conditions

Two isolates of *P. brasiliensis* were used during the experiments: Pb18, a virulent isolate, and Pb265, a non-virulent isolate. Isolates were cultivated in GPY agar (BD - Franklin Lakes, New Jersey, USA) and incubated at 37°C for six days. After the growing period, a sample was collected and diluted in RPMI-1640 (Cultilab) medium in a tube containing glass beads. The tubes were vortexed to separate de bud cells from the mother cells, and after sedimentation for 5 min, the supernatant with smaller yeasts was collected. After that, the fungi were counted in a Neubauer chamber to verify the cell concentration and viability by the phase-contrast method (Acorci et al., 2009). The fungus concentration was adjusted to $4x10^4$ cells (1:50 ratio).

Immunofluorescence for Neutrophil Extracellular Traps Visualization and Quantification

Isolated neutrophils (500 µl/well) from healthy volunteers adhered to coverslips treated with Poly-L-Lysine 0, 01% (Sigma-Aldrich) in 24-well bottom for adherence. Cells were then challenged with 500 µl/well from *P. brasiliensis* (Pb18 and Pb265) for 2 h at 37°C in 5% of CO2. Some cultures were treated with PMA (Sigma Aldrich, 100 ng/ml) as a positive control, and some wells were treated with DNase (100 U/ml– Thermo Fisher Scientific - Waltham, Massachusetts, USA), as a negative control. Cocultures were then fixed with PBS+BSA (bovine serum albumin)+PFA (paraformaldehyde) 2% and incubated with PBS+BSA 5% (for nonspecific binding block) for 30 min. Anti-neutrophil elastase at 0,1% (Calbiochem – Merck Millipore - Burlington, Massachusetts, USA) and anti-histone H1 at 0,9% (Merck Millipore) primary antibodies were diluted in blocking buffer and added to the coverslips for 1 h a 37°C. Cultures were washed three times with PBS and incubated with anti-rabbit-FITC at 1% (Millipore) and anti-mouse-Texas red at 0,5% (Calbiochem – Merck Millipore) secondary antibodies for elastase and histone visualization. Mounting medium for fluorescence with DAPI was used to mount the slides (Vectashield-Vector Labs, Burlingame, California, USA). Confocal images were taken in a Leica TCS SP8 from Confocal Microscopy Laboratory, UNIPEX - Experimental Research Unity, FMB-UNESP, Botucatu. The images were further analyzed using IMARIS® software

(Oxford Instruments) at Calvin, Phoebe, and Joan Snyder Institute for Chronic Diseases, University of Calgary/CA. The total area and intensity of the NETs were analyzed using the images of cultures challenged with Pb18 and Pb265, with the analysis of the elastase staining.

Neutrophil Extracellular Traps by Scanning Electron Microscopy

Neutrophils cultures underwent 2 h of adherence on coverslips treated with Poly-L-Lysine 0, 01% (Sigma-Aldrich) in 24-well bottom plates before fungal challenge or activation with PMA (Sigma Aldrich, 100 ng/ml). Some cultures were treated with DNase (Thermo-Fisher, 100 U/ml) as a negative control. After 2 h of challenge, supernatants were removed, and cultures were fixed with 2.5% of glutaraldehyde for scanning electron microscopy analysis at CME (Electron Microscopy Center – Institute of Bioscience — UNESP— Botucatu). The analyses were performed under a scanning microscope FEI Quanta 200 model from the same lab above.

Neutrophil Extracellular Trap Quantification

Supernatants of neutrophils cultures challenged with Pb18, and Pb265 isolates were collected for NETs quantification by an immunoassay using anti-elastase (Calbiochem – Merck Millipore) and Quant-iT™ PicoGreen® kit (Invitrogen - Carlsbad, Califórnia, USA) according to the manufacturer's instructions, with some adaptations (Czaikoski et al., 2016; Colón et al., 2019). Some cultures were treated with PMA or DNase, as positive and negative controls, respectively. Briefly, anti-elastase (5 μg/ml) antibody (Calbiochem – Merck Millipore) was used to coat a 96-well clear-bottom black plate (Corning - Corning, Nova York, EUA) overnight at 4°C. Supernatants were then settled to the plate, and the extracellular DNA bounded to the elastase, a NET constituent, was measured with Quant-iT™ PicoGreen® kit to evaluate and to quantify these complexes. Samples were analyzed by fluorescence intensity (excitation at 488 nm and emission at 525 nm wavelength) by a FlexStation 3 Microplate Reader (Molecular Devices, CA, USA), and concentrations were calculated comparing to a standard curve using known levels of DNA concentrations.

DNase Test Agar

To identify the possible DNase-like production, with an extracellular deoxyribonuclease activity, we utilized a DNase Test Agar (Acumedia, Neogen Culture Media) supplemented with 0,5% gentamicin sulfate (Novafarma) and 5% fungal aqueous extract (obtained from our Pb192 isolate). Petri plates (90x15 mm) were filled with 25 ml of medium and were incubated for one day before the experiment to exclude any contaminated plate. Each of the $4x10^4$ cells/ml fungal suspension was diluted until $4x10^3$ cells/ml and had 100 μl plated using an L-shaped glass rod. The plates were flooded with HCl 1N to precipitate the DNA, after 14 days of incubation, then a halo around the colonies with some deoxyribonuclease activity was revealed. As a positive and negative control, *Staphylococcus aureus and Saccharomyces cerevisiae*, respectively, were also plated in the DNase Test Agar medium, showing the effectiveness of the method in identifying positive DNase colonies.

Real-Time RT-PCR

To verify the gene expression related to a possible DNase-like production, we performed a Real-Time RT-PCR to verify the mRNA expression of two potential genes related, PADG_11161 and PADG_08285, according to GenBank. At first, neutrophil cultures were challenged with both isolates of *P. brasiliensis*, as previously mentioned, in the periods of 0 and 2 h in the incubator at 37°C in 5% CO2. The cells were lysed with TRI Reagent® RNA Isolation Reagent (Sigma-Aldrich, San Luis, Missouri, EUA), and the mRNA was extracted utilizing the Invitrogen™ PureLink™ RNA Mini Kit according to the manufacturer´s instruction (Invitrogen, Carlsbad, Califórnia, EUA). The mRNA samples were treated with DNase I, RNAse free (Thermo Fisher ScientificTM Waltham, Massachusetts, EUA) and a ribonuclease inhibitor (Thermo Fisher Scientific) and then transformed into cDNA by reverse transcription using the High-Capacity RNA-to-cDNA™ Kit (Applied Biosystems™, Foster City, Califórnia, EUA). The Real-Time RT-PCR was performed on the StepOnePlus™ Real-Time PCR System (Applied Biosystems™) with LUNA™ Universal qPCR Master Mix (New England Biolabs Inc., Ipswich, Massachusetts, EUA). The hypothetical sequences responsible for the deoxyribonuclease production were obtained from GenBank (https://www.ncbi.nlm.nih.gov/genbank/) and the primers, designed on Primer-BLAST (Ye et al., 2012) – see **Table 1**. Reactions were prepared with Luna Universal qPCR Master Mix (New England Biolabs) at 1× final concentration, 400 nM of each primer and 4 μl of the RT reaction, for a total volume of 10 μl. Real-time PCR was performed on a StepOnePlus instrument (Applied Biosystems), the amplification protocol consisting of a 10min step at 95°C for polymerase activation, followed by 40 cycles of 15s at 95°C and 60s at 60°C, and the melting curve step using instrument default settings. Results were analyzed by the ΔΔCT method (Pfaffl, 2001), using the rRNA subunit as normalizer. There were two hypothetical sequences on *P. brasiliensis* genome (ABKI00000000.2) (Desjardins et al., 2011), that could be responsible for DNase release: PADG_11161 (Gene

TABLE 1 | Sequences of the primers used and their specificities.

Primer sequences	Product length	Target species
rRNA 5,8S	93 pb	Both
F: TGAAGAACGCAGCGAAATGC		
R: GGAATACCAGAGGGCGCAAT		
NW_011371358.1	146 pb	*P. brasiliensis*
F: CCGGCAACAGCATTAGCATC		
R: TGATCCGCTCTGATCTTCGC		
NW_011371372.1	127 pb	*P. brasiliensis*
F: ACGACCGTCTCTTCCTCTCA		
R: CGTTCAAAATCCTCGCTCGC		
XM_015847918.1	111 pb	*P. lutzii*
F: TGCAGTTGAGATCCAATTACCCT		
R: TGAACAAGGCCTCCCTTTGG		
XM_002790819.1	140 pb	*P. lutzii*
F: TTCTTCAGGAGCTGCTACGC		
R: TATCCGGCAGCAGTAAGACG		

ID: 22587058) and PADG_08285 (Gene ID: 22586608) (Access codes NW_011371358.1 and NW_011371372.1)33,38. The positive control was a fungal rRNA region (rRNA 5,8S). The primers were synthesized by Thermo Fisher Scientific – Brazil. The Real-Time RT-PCR from isolated neutrophil cultures was not performed as the presence of fungal primer sequences in the human genome was verified by GenBank, and no match was found. P. lutzii hypothetical regions for DNase expression PAAG_12429 and PAAG_07101 (Access code XM_015847918.1 and XM_002790819.1) were also tested in Pb18 and Pb265 samples, but no expression was detected (data not shown).

Statistics

All data were firstly tested by the Shapiro-Wilk normality test. Extracellular DNA quantification was analyzed by the Friedmann test, followed by the posttest of the multiple Dunn comparisons. Imaris analysis was tested by the Mann-Whitney test for fluorescence Intensity and paired T-test for Area. PCR analysis was performed by the Kruskal-Wallis test, followed by Dunn's Test. Data were analyzed using GraphPad Prism 5.01 Software (GraphPad Software INC., CA, USA) with a significance value set at p<0,05%.

RESULTS

Scanning Electron Microscopy of Neutrophil Cultures Challenged With Pb18 and Pb265 Isolates

PMN cultures were performed and challenged over 2 h, with two different isolates of *P. brasiliensis*, Pb18 and Pb265, and were analyzed by scanning electron microscopy. The images demonstrated that there were two different patterns of NETs for the two different isolates of the fungus, as showed in the previous study (Della Coletta et al., 2015). The neutrophil culture was incubated just with a culture medium for 2 h, a control culture (**Figure 1A**).

Neutrophil cocultures challenged with the Pb18 showed larger, looser, delicate, diffuse networks than NETs induced by Pb265, which covered most of the analysis area, consistent with a less effective structure in fungal entrapment (**Figure 1C**).

Unlike NETs released in response to the virulent isolate (Pb18), the NETs found in cultures challenged with the avirulent isolate (Pb265) were much more compact and denser, more localized, promoting higher yeast entrapment, as can be seen in the image (**Figure 1D**).

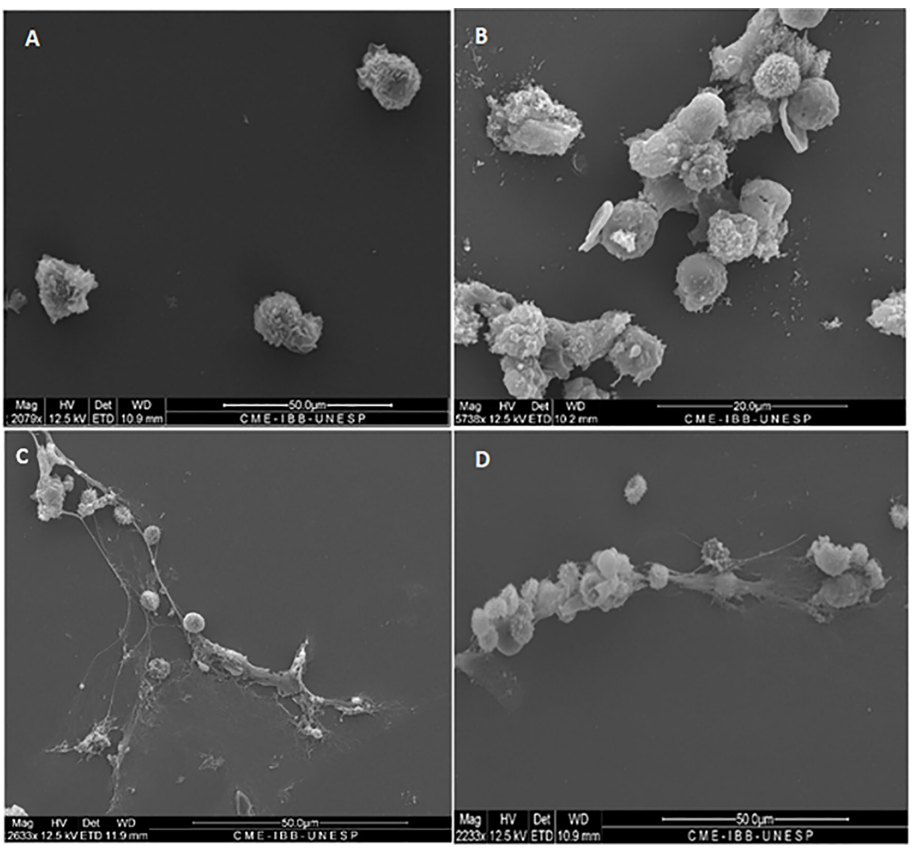

FIGURE 1 | Scanning electron microscopy of neutrophils challenged or not with *P. brasiliensis* (50:1 ratio), showing different patterns of neutrophil extracellular traps (NETs) release **(C, D)**. All cultures were incubated during 2 h at 37°C at 5% CO2, with or not PMA+DNase (control cultures). **(A)** normal neutrophils; **(B)** neutrophils treated with PMA plus DNase, showing absence of NETs; **(C)** neutrophils challenged with Pb18 showing looser, dispersed and bigger aspect of NETs; **(D)** neutrophils challenged with Pb265 showing denser, more condensed and compacter aspect of NETs. The images are reprentative of 10 individuals tested.

Figure 1B shows the absence of NETs, which were degraded by the action of DNase added in the cultures stimulated by PMA. It can also be observed some residues present in the slides, possibly from components present in the NETs, other than DNA, due to the degradation (**Figure 1B**).

Confocal Microscopy of Neutrophil Cultures Challenged With Pb18 and Pb265 Isolates

The presence of NETs and their components were evaluated by confocal microscopy, characterizing the presence of NETs in neutrophil cultures challenged with the avirulent fungal isolate (Pb265). Nuclear DNA and extracellular deconcentrated DNA were labeled with DAPI (**Figure 2A** and **Figure S1A**). Elastase and histones, other major components of NETs were also identified after immunostaining with specific primary and secondary antibodies (**Figures 2B, C** and **Figure S1B, C**) and, as expected, the overlap of the three stainings, showing the colocalization of three components (**Figure 2D** and **Figure S1D**). **Figure 2** and **Figure S1** show a dense, localized structures with very intense elastase immunostaining. It also caught our attention, the presence of fungi staining with anti-histone, allowing the identification of several fungi trapped in the formed NETs (**Figure 2C** and **Figure S1C**).

By analyzing the slides of cultures challenged with Pb18, it was possible to see differences regarding the spatial arrangement and fluorescence intensity of these Pb18-induced NETs compared to Pb265-induced NETs. The virulent isolate Pb18 (**Figure 3** and **Figure S2**) induced the formation of a visually bigger, more dispersed, looking more discondensed and delicate structures with lower fluorescence intensity compared to the isolate Pb265 (**Figure 2** and **Figure S1**), whose induced denser, more compact, and with higher fluorescence intensity of NETs, as seen by electron scanning microscopy. Interestingly, it´s seems that histone staining (Texas RED) also marked the yeasts, although no specific fungal labeling was used (**Figure 3C** and **Figure S2C**), although the number of yeasts evidenced was lower. This fact makes apparent that in cultures challenged

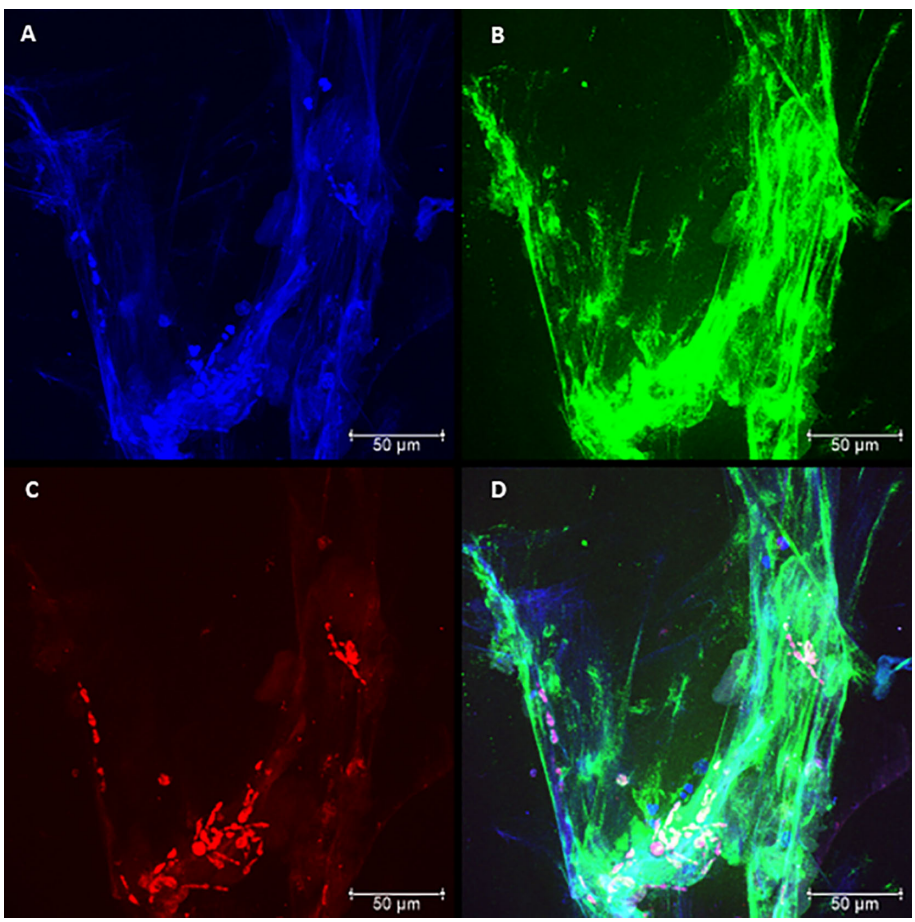

FIGURE 2 | Confocal microscopy of neutrophils challenged with *P. brasiliensis* - Pb265 (50:1 ratio), showing the pattern of neutrophil extracellular traps (NETs) release. Cocultures were stained with DAPI **(A)**, labeled with anti-elastase antibody followed by FITC-conjugated secondary antibody **(B)**, and anti-histone H1 secondary antibody followed by Texas Red **(C)**. In the last frame, the overlapping images showing the three components of NETs **(D)**. (Bar size 50 µm). The images are reprentative of 10 individuals tested.

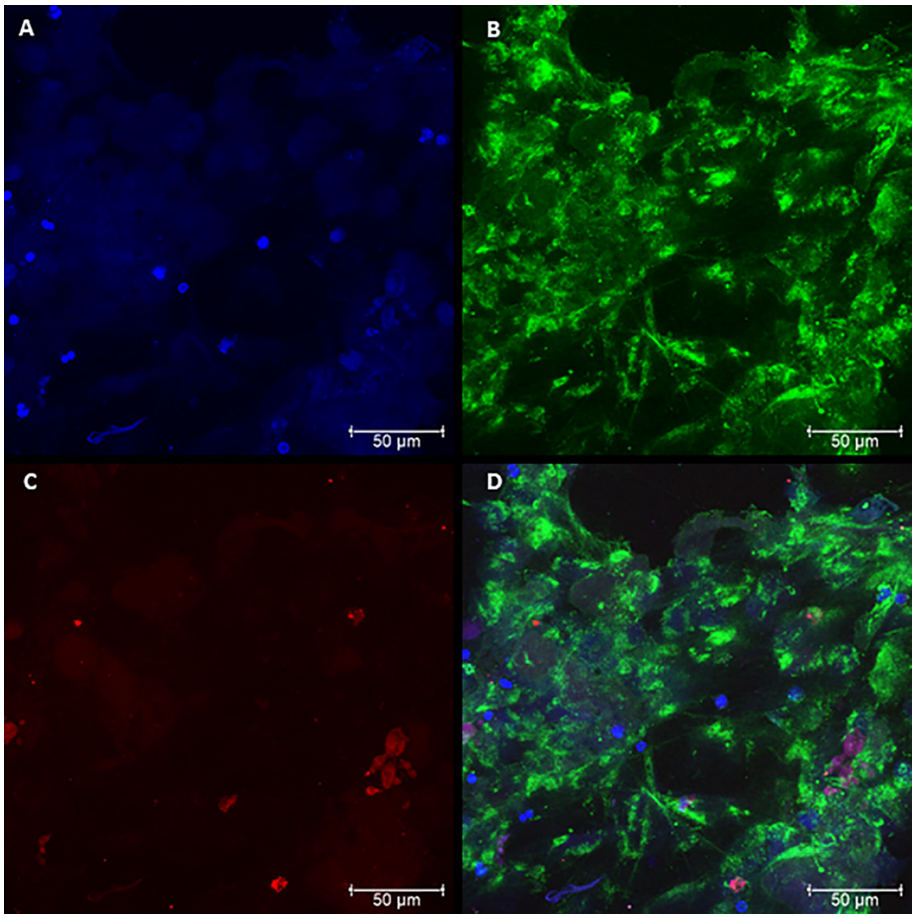

FIGURE 3 | Confocal microscopy of neutrophils challenged with *P. brasiliensis* - Pb18 (50:1 ratio), showing the pattern of neutrophil extracellular traps (NETs) release. Cocultures were stained with DAPI **(A)**, labeled with anti-elastase antibody followed by FITC-conjugated secondary antibody **(B)**, and anti-histone H1 secondary antibody followed by Texas Red **(C)**. In the last frame, the overlapping images showing the three components of NETs **(D)**. (Bar size 50µm). The images are reprentative of 10 individuals tested.

with Pb265 the number of yeasts trapped in NETs is much higher than in cultures challenged with Pb18.

Neutrophil Extracellular Trap Quantification in Neutrophil Cultures Challenged With Pb18 and Pb265

The results shown that PMA-treated cultures showed a significant increase in the concentrations of NETs present in the cultures compared to normal neutrophils (**Figure 4A**). These values were significantly decreased when cultures were stimulated with PMA and treated with DNase, demonstrating that quantification was useful in identifying the increase in induction of NETs by PMA, and also decreased structures when stimulated cultures were treated with DNase, which promoted the degradation of the NETs.

The results regarding the quantifications of cultures challenged with Pb265 and Pb18 corroborate the data presented so far, demonstrating that the Pb265 induced a large amount of NETs compared to neutrophil-only or Pb18-challenged cultures (**Figure 4B**). The levels of NETs in cultures challenged with Pb18 demonstrate lower levels than Pb265-challenged cultures and could indicate a low capacity of this isolate to induce NETs or the action of a fungal DNase that would act on virulent isolate-induced NETs.

Neutrophil Extracellular Trap Fluorescence Intensity and Area Quantification

The fluorescence intensity and area of NETs induced by the virulent and avirulent isolates of the fungus (Pb18 and Pb265, respectively), were evaluated using the confocal images acquired and the IMARIS® software at Calvin, Phoebe, and Joan Snyder Institute for Chronic Diseases, University of Calgary/CA (**Figure 5**). Analysis showed that NETs released in response to the avirulent Pb265 were much more intense (fluorescence intensity) than those released in response to the virulent isolate (**Figure 5A**). However, the area of NETs was larger in virulent isolate images (**Figure 5B**), although the results did not show statistical differences between the two isolates.

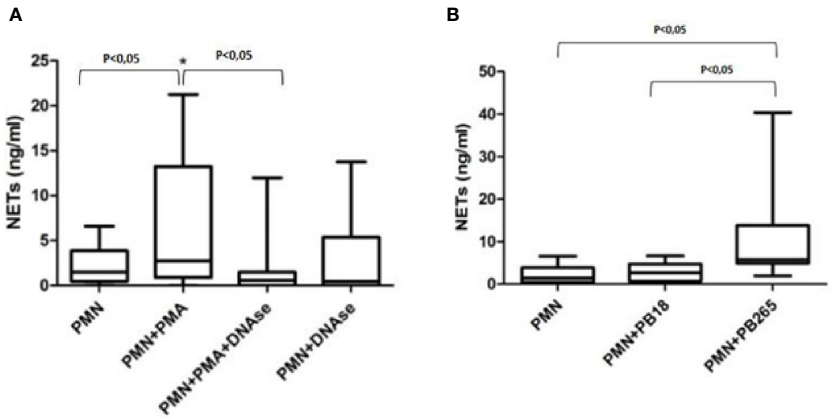

FIGURE 4 | Quantification of neutrophil extracellular traps (NETs) in neutrophil culture supernatants treated or not with PMA (100 ng/ml) and/or DNase (100 U/ml) **(A)**; or in neutrophil culture supernatants challenged or not with Pb18 or Pb265 **(B)**. Representative box plots of 10 individuals tested.

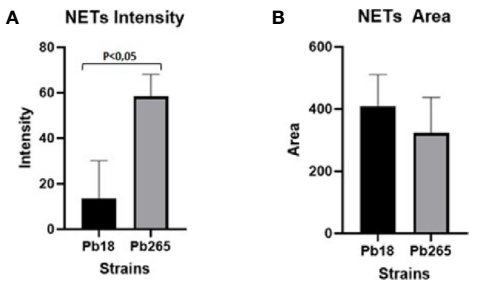

FIGURE 5 | Analysis of neutrophil extracellular traps (NETs) fluorescence intensity **(A)** and area **(B)** by IMARIS software. The total area and intensity of the NETs were analyzed using the images acquired from cultures challenged with Pb18 and Pb265, using the elastase staining. The results are representative of aquired images of 10 individuals analysed.

DNase Production by Fungi Evaluated by DNase Test Agar

To assess the production and release of a possible DNase by the virulent and avirulent isolates of the fungus (Pb18 and Pb265, respectively), DNase Test Agar was used. The images made with the virulent isolate Pb18 demonstrated the degradation of the DNA present in the medium, leading to the formation of a halo around the fungal colonies. Because of the halos coalesced, we can spot a big translucent area (**Figure 6A**).

Cultivating the avirulent isolate in the DNase test agar medium, the images showed that the Pb265 isolate (**Figure 6B**) was not able to produce a halo as consistent and intense as the virulent isolate (Pb18). This fact corroborates our results regarding the previous analyzes. We conducted control experiments using a positive and negative control with *S. aureus* and *S. cerevisiae*, known as a DNase producer and non-DNase producer, respectively, to validate our analyses (**Figure S3**).

DNase Expression Evaluation by RT-qPCR

To evaluate the gene expression over time for each isolate, we performed RT- qPCR. Pb18 and Pb265 were analyzed for both genes (PADG_11161 and PADG_08285) in isolated cultures and in PMN-fungus challenged cultures for 2 h.

The Pb18 demonstrated a much higher relative expression of the PADG_08285 gene after 2 h of a challenge with neutrophil, when compared to the expression of the gene in the culture of isolated yeasts (**Figure 7A**). The Pb265 isolate also showed an increase in the relative expression of this gene after 2 h of challenge, higher than the isolated yeasts cultures. Therefore, the virulent isolate demonstrated a much higher expression of this gene than the avirulent isolate (**Figure 7A**).

The PADG_11161 gene also demonstrated higher relative expression in cultures of neutrophils challenged with both isolates than in isolated fungi cultures, whereas in cultures challenged with the virulent isolate, the expression was much higher than controls and cultures challenged with the avirulent isolate (**Figure 7B**).

DISCUSSION

The actions of NETs are studied in all sorts of inflammatory diseases - infection, sterile injury, cancer (Yipp and Kubes, 2013; Castanheira and Kubes, 2019; Liew and Kubes, 2019; Phillipson and Kubes, 2019; Snoderly et al., 2019; Mutua and Gershwin, 2020). Studies have shown that when the pathogen is too large to be phagocytized, neutrophils respond to releasing NETs by the process known as NETosis (Branzk et al., 2014). Other studies have already presented several microorganisms as NETs inducers, such as *S. aureus, Shigella flexneri, Streptococcus pneumoniae, Leishmania amazonensis, Aspergillus fumigatus, C. albicans, Aspergillus nidulans, and P. brasiliensis* itself, some of these studies even showing microbicidal activity (Brinkmann

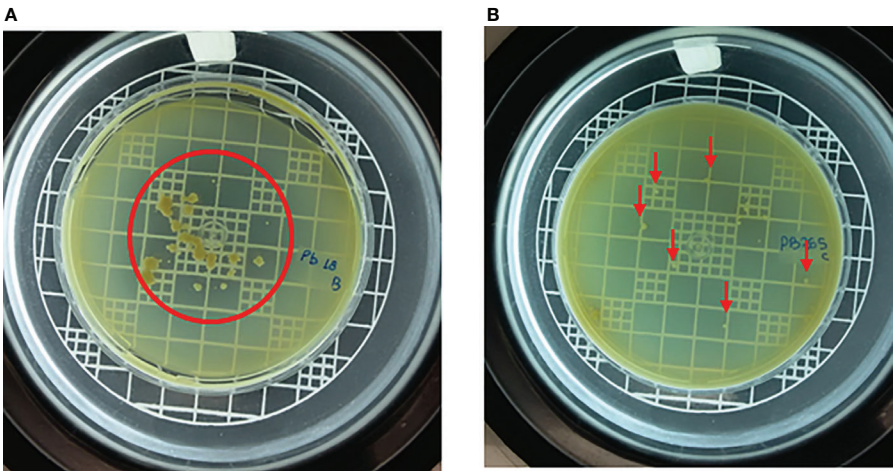

FIGURE 6 | Virulent isolate (Pb18) **(A)** and avirulent isolate (Pb265) **(B)** grown on DNase test agar medium for 14 days, demonstrating degradation of DNA from medium by fungus. The red line marks the translucid halo boundaries in Pb18 plate, and the red arrow idicates the colonies of Pb265 without halo formation. Images representative of three experiments.

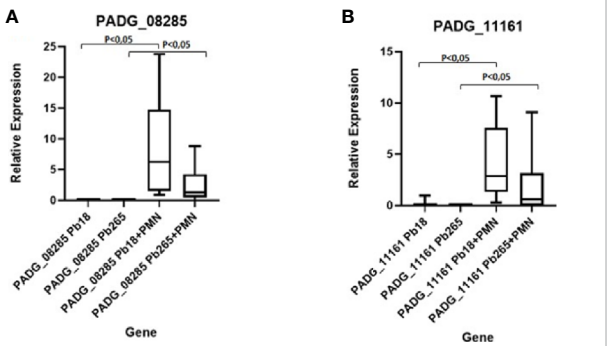

FIGURE 7 | Relative Gene Expression of PADG_08285 and PADG_11161 Genes in neutrophil cultures challenged with Pb18 and Pb265. **(A)** Gene PADG_08285 and **(B)** Gene PADG_11161. Representative Box Plot from 10 individuals tested.

et al., 2004; Urban et al., 2006; Wartha et al., 2007; Bianchi et al., 2009; Bruns et al., 2010; Brinkmann and Zychlinsky, 2012; Mejía et al., 2015; Della Coletta et al., 2015; Bachiega et al., 2016; Thanabalasuriar et al., 2019; Castanheira and Kubes, 2019; Liew and Kubes, 2019).

The interaction between *P. brasiliensis* and NETs is still being investigated, but a study has already shown the production of NETs in contact with *P. brasiliensis* yeast and how these structures are involved in extracellular fungal death, also showing that the dectin-1 receptor mainly mediates the NETs released in response to the *P. brasiliensis* isolates (Bachiega et al., 2016). The NETs release against *P. brasiliensis* have also been demonstrated in cutaneous lesions in patients with paracoccidioidomycosis (Della Coletta et al., 2015), corroborating with the previous studies. The same study that raised the hypothesis that distinct NETs patterns induced by different isolates of the fungus (Pb18 and Pb265), could be related to a fungal DNase-like activity, once the enzyme (DNase) is an endonuclease that catalyzes the hydrolysis of extracellular DNA (Lazarus and Wagener, 2019).

In this study, the Scanning Electron Microscopy assays demonstrated similar structures to those shown in the previous studies (Della Coletta et al., 2015; Bachiega et al., 2016). In the current results, the release of NETs was evidenced and confirmed by confocal microscopy, where it was observed the presence and colocalization of extracellular DNA, histones, and elastase. However, the patterns of the NETs differed from each other according to the fungal isolate tested. When the most virulent isolate (Pb18) was evaluated, the NETs aspect was looser, dispersed, covering most area of the coverslips. When the less virulent isolate (Pb265) was tested, the NETs were denser, more condensed and compacter, covering smaller areas of the coverslips, closer to the fungus. These results directly resemble previous studies (Della Coletta et al., 2015). The difference between NETs was also demonstrated by the analysis of intensity using IMARIS software and by quantification method. The results showed that the fluorescence intensity of NETs released in response to Pb265 was greater than that released in response to Pb18. These results suggest a possible degradation of the DNA present in the NETs by the virulent isolate, corroborating the hypothesis mentioned by Della Coletta et al. (2015), that Pb18 isolate could be producing some protein with DNase-like activity and that this protein could be degrading the NETs, acting as an escape mechanism (Della Coletta et al., 2015), or even a lower induction capacity of NETs by this isolate. Some studies have already shown the release of endonucleases by different microorganisms as an escape mechanism from NETs, as already indicated (Buchanan et al., 2006; Berends et al., 2010;

Sánchez and Colom, 2010; Thammavongsa et al., 2013; Seper et al., 2013; de Buhr et al., 2014; Morita et al., 2014; Bentubo and Gompertz, 2014; Riceto et al., 2015; Zhang et al., 2016; Gondaira et al., 2017; Liu et al., 2017; Teymournejad et al., 2017; Zhang et al., 2017; Hoppenbrouwers et al., 2018; Wilton et al., 2018; Mitiku et al., 2018; Sharma et al., 2019; Freitas-Mesquita et al., 2019), and such as some pathogenic fungi such as *C. albicans* (Riceto et al., 2015; Zhang et al., 2017), *Cryptococcus spp* (Sánchez and Colom, 2010) and, *Trichosporon spp* (Bentubo and Gompertz, 2014). These microorgansms use these nucleases as a way of cleaving NETs, enhancing their survival within their hosts.

Interestingly, although no specific labeling was used for the fungus yeast, we noted that the histone labeling was able to label *P. brasiliensis* yeasts, enabling the identification of yeasts trapped in the formed NETs. This fact, although not expected, allowed very interesting observations, demonstrating that in the images related to cultures challenged with Pb265, there were a much larger number of yeasts that were trapped in the formed NETs, a fact that was not observed in cultures challenged with isolate Pb18, that is, the presence of trapped fungus was much smaller when compared to cultures challenged with avirulent isolate, a phenomenon that could be explained by our results. And another observation is that if the yeasts were labeled with anti-histone, allowing the visualization of the fungus in the images, probably was due to an effect of yeast coverage by histones present on the NETs, that could be a factor involved in fungicidal activity of NETs against fungi, once it was demonstrated previously by our research group, that NETs can act against *P. brasiliensis*, causing yeast morphological changes and fungus killing (Bachiega et al., 2016). Besides histones activities on binding and regulating DNA expression, they also exert defensive functions and promote the inflammatory response, being the major components of NETs, contributing both to the killing of pathogens and to tissue injury (Hoeksema et al., 2016). Ballard et al. (2020) (Ballard et al., 2020) demonstrated that lysozyme and histones inhibited hyphal metabolic activity in *A. fumigatus* isolates in a dose-dependent manner, and imaging flow cytometry revealed that histones inhibited the germination of *A. fumigatus* conidia. Recently, it was demonstrated that histone H2A enters *Escherichia coli and S. aureus* through membrane pores formed by the AMPs LL-37 and magainin-2, depolarizing the bacterial membrane potential, and impairing membrane recovery (Doolin et al., 2020). Once inside cell, H2A reorganizes bacterial chromosomal DNA, inhibiting global transcription, acting directly on killing of bacteria (Doolin et al., 2020).

The presence of NETs was also evaluated and quantified by an immunoassay using anti-elastase and Quant-IT Picogreen Kit, and this methodology has already been used in other studies (Czaikoski et al., 2016; Colón et al., 2019). The extracellular DNA quantification was used to assess the NETs release in response to *Mycobacterium tuberculosis*, *L. amazonensis* and other microorganisms as well (Ramos-Kichik et al., 2009; Guimarães-Costa et al., 2009; Della Coletta et al., 2015; Bachiega et al., 2016). However, the use of the Picogreen Kit alone, with only extracellular DNA labeling, has been widely criticized, since extracellular DNA could come from both the NETosis process and other cellular phenomena. Thus, we chose to quantify the elastase-extracellular DNA complex, giving us the quantification of NETs. Our results showed that the culture challenged with the virulent isolate presented a smaller amount of NETs when compared to the avirulent isolate, corroborating the confocal and scanning microscopy results, and the above results.

As said before, some organisms are capable of releasing DNase to escape from the immune system (Buchanan et al., 2006; Berends et al., 2010; Sánchez and Colom, 2010; Thammavongsa et al., 2013; Seper et al., 2013; de Buhr et al., 2014; Morita et al., 2014; Bentubo and Gompertz, 2014; Riceto et al., 2015; Zhang et al., 2016; Gondaira et al., 2017; Liu et al., 2017; Teymournejad et al., 2017; Zhang et al., 2017; Hoppenbrouwers et al., 2018; Wilton et al., 2018; Mitiku et al., 2018; Sharma et al., 2019; Freitas-Mesquita et al., 2019) and the DNase Test Agar is commonly used in tests to identify this production, mainly by *S. aureus*, since this microorganism is a known producer of DNase (Kateete et al., 2010). In the present study, using this methodology, it was possible to identify the production of a DNase-like protein by the virulent isolate of *P. brasiliensis* (Pb18), demonstrating DNA degradation in the cultures plaques, while the avirulent isolate did not demonstrate any significant production nor DNase activity. This result prove the hypothesis raised in our previous studies, which showed that the NETs released in response to the virulent isolate were looser and had a more degraded appearance when compared to the NETs released in response to the avirulent isolate (Della Coletta et al., 2015). This leads us to believe that this pattern of NETs occurs due to a release of a protein with DNase-like activity by the virulent isolate, as shown by our results, that Pb18 could produce a DNase-like protein, suggesting an action on NETs degradation, which would explain the observed results.

With the identification of a DNase-like protein action by Pb18 isolate using DNase Test Agar, it was tested different genes (PADG_08528 and PADG_11161) that was found in the fungus genome as hypothetical proteins (Desjardins et al., 2011), and it was demonstrated that the PADG_08528 gene showed much higher expression than the PADG_11161 gene when yeast cells were challenged with human neutrophils. Interestingly, both genes showed higher expression in Pb18 yeast challenged cultures. This demonstrates that both genes may be associated with the production and release of a DNase-like, however when these yeasts were placed in contact with human neutrophils, the PADG_08528 gene had a much larger expression, thus, probably, indicating that this gene could be involved in the release of the DNase-like protein and consequent degradation of NETs. These results also confirm the raised hypothesis, that the virulent isolate (Pb18) would be releasing a DNase-like protein as a way to degrade NETs and survive the neutrophils attack (Della Coletta et al., 2015).

Thus, given the observed results we can conclude that the NETs pattern induced by the virulent isolate (Pb18) with looser, dispersed and bigger aspect is due the release of a DNase-like

protein by Pb18. This factor could be an important escape mechanism of the fungus to circumvent the action of NETs, thus subverting this important neutrophil effector mechanism. Our lab is conducting other studies to better identify and characterize this protein by these isolates and other species of *Paracoccidioides*.

DATA AVAILABILITY STATEMENT

The raw data supporting the conclusions of this article will be made available by the authors, without undue reservation.

ETHICS STATEMENT

The studies involving human participants were reviewed and approved by the Research Ethics Committee of Medical School of Botucatu, UNESP – São Paulo State University (CAAE: 85654018.9.0000.5411; protocol: 2.577.243/2018). The patients/participants provided their written informed consent to participate in this study.

AUTHOR CONTRIBUTIONS

LADM conceptualized the study. YRZ, ALOD, AMDC, LC, KSTY, LAS, ICD, RMK, MEW, and VFX developed the methodology. YRZ, ALOD, AMDC, LC, KSTY, LAS, ICD, and RMK validated the study. YRZ, ALOD, AMDC, LC, KSTY, LAS, ICD, and RMK conducted the investigation. LADM, YRZ, LAS, ICD, and RMK performed the formal analysis. LADM provided the resources. LADM and YRZ wrote the original draft. LADM, RMK, LZ, and PK wrote, reviewed, and edited the manuscript. LM supervised the study. LM conducted the project administration. All authors contributed to the article and approved the submitted version.

FUNDING

This study was supported by São Paulo Research Foundation (FAPESP 2018/09706-7) and FAPESP MS fellowship (YRZ—FAPESP 2017/26230-3). This study was financed in part by the Coordenação de Aperfeiçoamento de Pessoal de Nível Superior—Brasil (CAPES)—Finance Code 001, master student in the Post-Graduate Program in Pathology, Botucatu Medical School, UNESP—São Paulo State University, Botucatu, São Paulo, Brazil. It was also supported by CAPES PrInt: Program for Institutional Internationalization granted to LAS, and by Programa de Apoio para a realização de Estágio no Exterior (PAREex)—PROPG UNESP—Edital 03/2018 PROPG, granted to LADM, head of the Department of Pathology, Botucatu Medical School, UNESP—São Paulo State University, Botucatu, São Paulo, Brazil. The funders had no role in study design, data collection, and analysis, decision to publish, or preparation of the manuscript.

ACKNOWLEDGMENTS

We thank the CME (Electron Microscopy Center–Biosciences Institute—UNESP– Botucatu) for acquiring the images by Scanning Electron Microscopy and Confocal Microscopy Laboratory from UNIPEX—Medical School of Botucatu—UNESP) for acquiring the images by Confocal Laser Scanning Microscopy. We acknowledge P. Colarusso and the support staff of the Snyder Institute Live Cell Imaging Facility at the University of Calgary for assisting in the image capturing and analysis.

SUPPLEMENTARY MATERIAL

The Supplementary Material for this article can be found online at: https://www.frontiersin.org/articles/10.3389/fcimb.2020.592022/full#supplementary-material

REFERENCES

Acorci, M. J., Dias-Melicio, L. A., Golim, M. A., Bordon-Graciani, A. P., and Soares, A. M. V. C. (2009). Inhibition of human neutrophil apoptosis by *Paracoccidioides brasiliensis*: Role of Interleukin-8. *Scand. J. Immunol.* 69, 73–79. doi: 10.1111/j.1365-3083.2008.02199.x

Bachiega, T. F., Dias-Melicio, L. A., Fernandes, R. K., Balderramas, H., Rodrigues, D. R., Ximenes, V. F., et al. (2016). Participation of dectin-1 receptor on NETs release against *Paracoccidioides brasiliensis*: Role on extracellular killing. *Immunobiology* 221 (2), 228–235. doi: 10.1016/j.imbio.2015.09.003

Ballard, E., Yucel, R., Melchers, W. J. G., Brown, A. J. P., Verweij, P. E., and Warris, A. (2020). Antifungal activity of antimicrobial peptides and proteins against *Aspergillus fumigatus*. *J. Fungi* 6 (2), 65. doi: 10.3390/jof6020065

Bentubo, H. D. L., and Gompertz, O. F. (2014). Effects of temperature and incubation time on the *in vitro* expression of proteases, phospholipases, lipases and DNases by different species of *Trichosporon*. *Springerplus* 3, 377. doi: 10.1186/2193-1801-3-377

Berends, E. T., Horswill, A. R., Haste, N. M., Monestier, M., Nizet, V., and von Köckritz-Blickwede, M. (2010). Nuclease expression by *Staphylococcus aureus* facilitates escape from neutrophil extracellular traps. *J. Innate Immun.* 2, 576–586. doi: 10.1159/000319909

Bianchi, M., Hakkim, A., Brinkmann, V., Siler, U., Seger, R. A., Zychlinsky, A., et al. (2009). Restoration of NET formation by gene therapy in CGD controls aspergillosis. *Blood* 114 (13), 2619–2622. doi: 10.1182/blood-2009-05-221606

Bocca, A. L., Amaral, A. C., Teixeira, M. M., Sato, P. K., Shikanai-Yasuda, M. A., and Soares Felipe, M. S. (2013). Paracoccidioidomycosis: eco-epidemiology, taxonomy and clinical and therapeutic issues. *Future Microbiol.* 8 (9), 1177–1191. doi: 10.2217/fmb.13.68

Branzk, N., Lubojemska, A., Hardison, S. E., Wang, Q., Gutierrez, M. G., Brown, G. D., et al. (2014). Neutrophils sense microbe size and selectively release neutrophil extracellular traps in response to large pathogens. *Nat. Immunol.* 15 (11), 1017–1025. doi: 10.1038/ni.2987

Brinkmann, V., and Zychlinsky, A. (2012). Neutrophil extracellular traps: is immunity the second function of chromatin? *J. Cell Biol.* 198, 773–783. doi: 10.1083/jcb.201203170

Brinkmann, V., Reichard, U., Goosmann, C., Fauler, B., Uhlemann, Y., Weiss, D. S., et al. (2004). Neutrophil extracellular traps kill bacteria. *Science* 303, 1532–1535. doi: 10.1126/science.1092385

Bruns, S., Kniemeyer, O., Hasenberg, M., Aimanianda, V., Nietzsche, S., Thywissen, A., et al. (2010). Production of extracellular traps against

Aspergillus fumigatus in vitro and in infected lung tissue is dependent on invading neutrophils and influenced by hydrophobin RodA. *PloS Pathog.* 6 (4), e1000873. doi: 10.1371/journal.ppat.1000873

Buchanan, J. T., Simpson, A. J., Aziz, R. K., Liu, G. Y., Kristian, S. A., Kotb, M., et al. (2006). DNAse expression allows the pathogen group A *Streptococcus* to escape killing in neutrophil extracellular traps. *Curr. Biol.* 16 (4), 396–400. doi: 10.1016/j.cub.2005.12.039

Calich, V. L. G., Russo, M., Vaz, C. A. C., Burger, E., and Singer-Vermes, L. M. (1994). Resistance mechanism to experimental *Paracoccidioides brasiliensis* infection. *Cienc. Cult. (São Paulo)* 46, 455–461.

Castanheira, F. V. S., and Kubes, P. (2019). Neutrophils and NETs in modulating acute and chronic inflammation. *Blood* 133 (20), 2178–2185. doi: 10.1182/blood-2018-11-844530

Colombo, A. L., Tobón, A., Restrepo, A., Queiroz-Telles, F., and Nucci, M. (2011). Epidemiology of endemic systemic fungal infections in Latin America. *Med. Mycol.* 49, 785–798. doi: 10.3109/13693786.2011.577821

Colón, D. F., Wanderley, C. W., Franchin, M., Silva, C. M., Hiroki, C. H., Castanheira, F. V. S., et al. (2019). Neutrophil extracellular traps (NETs) exacerbate severity of infant sepsis. *Crit. Care* 23 (1), 113. doi: 10.1186/s13054-019-2407-8

Costa, D. L., Dias-Melicio, L. A., Acorci, M. J., Bordon, A. P., Tavian, E. G., Peracoli, M. T. S., et al. (2007). Effect of interleukin-10 on the *Paracoccidioides brasiliensis* killing by gamma-interferon activated human neutrophils. *Microbiol. Immunol.* 51 (1), 73–80. doi: 10.1111/j.1348-0421.2007.tb03892.x

Coutinho, Z. F., Silva, D., Lazera, M., Petri, V., Oliveira, R. M., Sabroza, P. C., et al. (2002). Paracoccidioidomycosis mortality in Brazil (1980-1995). *Cad. Saude Publica* 18 (5), 1441–1454. doi: 10.1590/S0102-311X2002000500037

Czaikoski, P. G., Mota, J. M., Nascimento, D. C., Sônego, F., Castanheira, F. V., Melo, P. H., et al. (2016). Neutrophil extracellular traps induce organ damage during experimental and clinical sepsis. *PloS One* 11 (2), e0148142. doi: 10.1371/journal.pone.0148142

de Buhr, N., Neumann, A., Jerjomiceva, N., von Köckritz-Blickwede, M., and Baums, C. G. (2014). *Streptococcus suis* DNase SsnA contributes to degradation of neutrophil extracellular traps (NETs) and evasion of NET-mediated antimicrobial activity. *Microbiology* 160, 385–395. doi: 10.1099/mic.0.072199-0

Defaveri, J., Coelho, K. I. R., Rezkallah-Iwasso, M. T., and Franco, M. F. (1989). Hypersensitivity pneumonitis to *Paracoccidioides brasilensis* antigens in mice. *J. Med. Vet. Mycol.* 27, 93–104. doi: 10.1080/02681218980000131

Defaveri, J., Rezkallah-Iwasso, M. T., and Franco, M. F. (1992). Pulmonary paracoccidioidomycosis in immunized mice. *Mycopathologia* 119, 1–9.

Della Coletta, A. M., Bachiega, T. F., Silva, J. C. Q., Soares, A. M. V. C., De Faveri, J., Marques, S. A., et al. (2015). Neutrophil extracellular traps identification in tegumentar lesions of patients with paracoccidioidomycosis and different patterns of NETs generation *in vitro*. *PloS Negl. Trop. Dis.* 9 (9), e0004037. doi: 10.1371/journal.pntd.0004037

Desjardins, C. A., Champion, M. D., Holder, J. W., Muszewska, A., Goldberg, J., Bailão, A. M., et al. (2011). Comparative genomic analysis of human fungal pathogens causing paracoccidioidomycosis. *PloS Genet.* 7 (10), e1002345. doi: 10.1371/journal.pgen.1002345

Dias, M. F., Figueira, A. L., and de Souza, W. (2004). A morphological and cytochemical study of the interaction between *Paracoccidiodes brasiliensis and* neutrophils. *Microsc. Microanal.* 10, 215–223. doi: 10.1017/S1431927604040061

Doolin, T., Amir, H. M., Duong, L., Rosenzweig, R., Urban, L. A., and Bosch, M. (2020). Mammalian histones facilitate antimicrobial synergy by disrupting the bacterial proton gradient and chromosome organization. *Nat. Commun.* 11, 3888. doi: 10.1038/s41467-020-17699-z

Franco, M. (1987). Host–parasite relationship in paracoccidioidomycosis. *J. Med. Vet. Mycol.* 25, 5–18. doi: 10.1080/02681218780000021

Freitas-Mesquita, A. L., Dick, C. F., dos Santos, A. L. A., Nascimento, M. T. C., Rochael, N. C., Saraiva, E. M., et al. (2019). Cloning, expression and purification of 3'-nucleotidase/nuclease, an enzyme responsible for the *Leishmania* escape from neutrophil extracellular traps. *Mol. Biochem. Parasitol.* 229, 6–14. doi: 10.1016/j.molbiopara.2019.02.004

Gondaira, S., Higuchi, H., Nishi, K., Iwano, H., and Nagahata, H. (2017). *Mycoplasma bovis* escapes bovine neutrophil extracellular traps. *Vet. Microbiol.* 199, 68–73. doi: 10.1016/j.vetmic.2016.12.022

Guimarães-Costa, A. B., Nascimento, M. T. C., Froment, G. S., Soares, R. P., Morgado, F. N., Conceição-Silva, S., et al. (2009). *Leishmania amazonensis* promastigotes induce and are killed by neutrophil extracellular traps. *Proc. Natl. Acad. Sci. U. S. A.* 106 (16), 6748–6753. doi: 10.1073/pnas.0900226106

Hoeksema, M., van Eijk, M., Haagsman, H. P., and Hartshorn, K. L. (2016). Histones as mediators of host defense, inflammation and thrombosis. *Future Microbiol.* 11 (3), 441–453. doi: 10.2217/fmb.15.151

Hoppenbrouwers, T., Sultan, A. R., Abraham, T. E., Lemmens-den-Toom, N. A., Manásková, S. H., van Cappellen, W. A., et al. (2018). Staphylococcal protein A is a key factor in neutrophil extracellular traps formation. *Front. Immunol.* 9, 165. doi: 10.3389/fimmu.2018.00165

Kateete, D. P., Kimani, C. N., Katabazi, F. A., Okeng, A., Okee, M. S., Nanteza, A., et al. (2010). Identification of *Staphylococcus aureus*: DNase and manitol salt agar improve the efficiency of the tube coagulase test. *Ann. Clin Microbiol. Antimicrob.* 9, 23. doi: 10.1186/1476-0711-9-23

Kurita, N., Oarada, M., Ito, E., and Miyaji, M. (1999). Antifungal activity of human polymorphonuclear leucocytes against yeast cells of *Paracoccidioides brasiliensis*. *Med. Mycol.* 37, 261– 267. doi: 10.1080/j.1365-280X.1999.00229.x

Kurita, N., Oarada, M., and Brummer, E. (2005). Fungicidal activity of human peripheral blood leukocytes against *Paracoccidioides brasiliensis* yeast cells. *Med. Mycol.* 43, 417–422. doi: 10.1080/13693780400011088

Lazarus, R. A., and Wagener, J. S. (2019). Recombinant Human Deoxyribonuclease I. *Pharm. Biotechnol.* 14, 471–488. doi: 10.1007/978-3-030-00710-2_22

Liew, P. X., and Kubes, P. (2019). The neutrophil's role during health and Disease. *Physiol. Rev.* 99, 1223–1248. doi: 10.1152/physrev.00012.2018

Liu, J., Sun, L., Liu, W., Guo, L., Liu, Z., Wei, X., et al. (2017). A nuclease from *Streptococcus mutans* facilitates biofilm dispersal and escape from killing by neutrophil extracellular traps. *Front. Cell. Infect. Microbiol.* 7, 97. doi: 10.3389/fcimb.2017.00097

Marques, S. A. (2013). Paracoccidioidomycosis: epidemiological, clinical, diagnostic and treatment up-dating. *An. Bras. Dermatol.* 88 (5), 700–711. doi: 10.1590/abd1806-4841.20132463

Matute, D. R., McEwen, J. G., Puccia, R., Montes, B. A., San-Blas, G., Bagagli, E., et al. (2006). Cryptic speciation and recombination in the fungus *Paracoccidioides brasiliensis* as revealed by gene genealogies. *Mol. Biol. Evol.* 23, 65–73. doi: 10.1093/molbev/msj008

McDonald, B., Urrutia, R., Yipp, B. G., Jenne, C. N., and Kubes, P. (2012). Intravascular neutrophil extracellular traps capture bacteria from the bloodstream during sepsis. *Cell Host Microbe* 12, 324–333. doi: 10.1016/j.chom.2012.06.011

Mejía, S. P., Cano, L. E., Lopez, J. A., Hernandez, O., and Gonzalez, A. (2015). Human neutrophils produce extracellular traps against *Paracoccidioides brasiliensis*. *Microbiology* 161, 1008– 1017. doi: 10.1099/mic.0.000059

Mitiku, F., Hartley, C. A., Sansom, F. M., Coombe, J. E., Mansell, P. D., Beggs, D. S., et al. (2018). The major membrane nuclease MnuA degrades neutrophil extracellular traps induced by *Mycoplasma bovis*. *Vet. Microbiol.* 218, 13–19. doi: 10.1016/j.vetmic.2018.03.002

Morita, C., Sumioka, R., Nakata, M., Okahashi, N., Wada, S., Yamashiro, T., et al. (2014). Cell- wall anchored nuclease of *Streptococcus sanguinis* contributes to escape from neutrophil extracellular trap-mediated bactericidal activity. *PloS One* 9 (8), e103125. doi: 10.1371/journal.pone.0103125

Mutua, V., and Gershwin, L. J. (2020). A review of neutrophil extracellular traps (NETs) in disease: potential anti-NETs therapeutics. *Clin. Rev. Allergy Immunol.* 1, 1–18. doi: 10.1007/s12016-020-08804-7

Papayannopoulos, V., Metzler, K. D., Hakkim, A., and Zychlinsky, A. (2010). Neutrophil elastase and myeloperoxidase regulate the formation of neutrophil extracellular traps. *J. Cell. Biol.* 191, 677–691. doi: 10.1083/jcb.201006052

Pfaffl, M. W. (2001). A new mathematical model for relative quantification in real-time RT-PCR. *Nucleic Acids Res.* 29 (9), e45. doi: 10.1093/nar/29.9.e45

Phillipson, M., and Kubes, P. (2019). The healing power of neutrophils. *Trends Immunol.* 40 (7), 635–647. doi: 10.1016/j.it.2019.05.001

Pilsczek, F. H., Salina, D., Poon, K. K., Fahey, C., Yipp, B. G., Sibley, C. D., et al. (2010). A novel mechanism of rapid nuclear neutrophil extracellular trap formation in response to *Staphylococcus aureus*. *J. Immunol.* 185, 7413–7425. doi: 10.4049/jimmunol.1000675

Ramos-Kichik, V., Mondragon-Flores, R., Mondragon-Castelan, M., Gonzalez-Pozos, S., Muñiz-Hernandez, S., Rojas-Espinosa, O., et al. (2009). Neutrophil

extracellular traps are induced by *Mycobacterium tuberculosis*. *Tuberculosis (Edinb).* 89 (1), 29–37. doi: 10.1016/j.tube.2008.09.009

Ravindran, M., Khan, M. A., and Palaniyar, N. (2019). Neutrophil Extracellular Trap Formation: Physiology, Pathology, and Pharmacology. *Biomolecules* 9 (8), 365. doi: 10.3390/biom9080365

Restrepo, A., and Tobón, A. M. (2005). "Paracoccidioides brasiliensis," in *Principles and practice of Infectious Diseases*. Eds. G. L. Mandell, J. E. Bennett and R. Dollin (Elsevier: Philadelphia), 3062–3068.

Riceto, E. B., Menezes, R. P., Penatti, M. P., and Pedroso, R. S. (2015). Enzymatic and hemolytic activity in different *Candida* species. *Rev. Iberoam. Micol.* 72 (2), 79–82. doi: 10.1016/j.riam.2013.11.003

Rodrigues, D. R., Dias-Melicio, L. A., Calvi, S. A., Peracoli, M. T. S., and Soares, A. M. V. C. (2007). *Paracoccidioides brasiliensis* killing by IFN-gamma, TNF-alpha and GM-CSF activated human neutrophils: role for oxygen metabolites. *Med. Mycol.* 45, 27–33. doi: 10.1080/13693780600981676

Sánchez, M., and Colom, F. (2010). Extracellular DNase activity of *Cryptococcus neoformans* and *Cryptococcus gattii*. *Rev. Iberoam. Micol.* 27, 10–13. doi: 10.1016/j.riam.2009.11.004

Seper, A., Hosseinzadeh, A., Gorkievickz, G., Lichtenegger, S., Roier, S., Leitner, D. R., et al. (2013). *Vibrio cholerae* evades neutrophil extracellular traps by the activity of two extracellular nucleases. *PloS Pathog.* 9 (9), e1003614. doi: 10.1371/journal.ppat.1003614

Severo, L. C., Geyer, G. R., Londero, A. T., Porto, N. S., and Rizzon, C. F. (1979). The primary pulmonary lymph node complex in Paracoccidioidomycosis. *Mycopathologia* 67 (2), 115–118.

Sharma, P., Garg, N., Sharma, A., Capalash, N., and Singh, R. (2019). Nucleases of bacterial pathogens as virulence factors, therapeutic targets and diagnostic markers. *Int. J. Med. Microbiol.* 309, 151354. doi: 10.1016/j.ijmm.2019.151354

Shikanai-Yasuda, M. A., Telles Filho, F. Q., Mendes, R. P., Colombo, A. R., and Moretti, M. A. (2018). II Consenso de paracoccidioidomicose. *Epidemiol. Serv. Saúde* 27, e0500001. doi: 10.5123/S1679-49742018000500001

Snoderly, H. T., Boone, B. A., and Bennewitz, M. F. (2019). Neutrophil extracellular traps in breast cancer and beyond: current perspectives on NET stimuli, thrombosis and metastasis, and clinical utility for diagnosis and treatment. *Breast Cancer Res.* 21, 145. doi: 10.1186/s13058-019-1237-6

Teixeira, M. M., Theodoro, R. C., de Carvalho, M. J., Fernandes, L., Paes, H. C., Hahn, R. C., et al. (2009). Phylogenetic analysis reveals a high level of speciation in the *Paracoccidioides* genus. *Mol. Phylogenet. Evol.* 52, 273–283. doi: 10.1016/j.ympev.2009.04.005

Teixeira, M. M., Theodoro, R. C., Nino-Vega, G., Bagagli, E., and Felipe, M. S. (2014). *Paracoccidioides* species complex: ecology, phylogeny, sexual reproduction, and virulence. *PloS Pathog.* 10, e1004397. doi: 10.1371/journal.ppat.1004397

Teymournejad, O., Lin, M., and Rikihisa, Y. (2017). *Ehrlichia chaffeensis and* its invasin EtpE block reactive oxygen species generation by macrophages in a DNase X-dependent manner. *mBio* 8, e01551–e01517. doi: 10.1128/mBio.01551-17

Thammavongsa, V., Missiakas, D. M., and Schneewind, O. (2013). *Staphylococcus aureus* degrades neutrophil extracellular traps to promote immune cell death. *Science* 342 (6160), 863–866. doi: 10.1126/science.1242255

Thanabalasuriar, A., Scott, B. N. V., Peiseler, M., Willson, M. E., Zeng, Z., Warrener, P., et al. (2019). Neutrophil extracellular traps confine *Pseudomonas aeruginosa* ocular biofilms and restrict brain invasion. *Cell Host Microbe* 25, 526–536.e4. doi: 10.1016/j.chom.2019.02.007

Turissini, D. A., Gomez, O. M., Teixeira, M. M., McEwen, J. G., and Matute, D. R. (2017). Species boundaries in the human pathogen *Paracoccidioides*. *Fungal Genet. Biol.* 106, 9–25. doi: 10.1016/j.fgb.2017.05.007

Urban, C. F., Reichard, U., Brinkmann, V., and Zychlinsky, A. (2006). Neutrophil extracellular traps capture and kill *Candida albicans* yeast and hyphal forms. *Cell Microbiol.* 8 (4), 668–676. doi: 10.1111/j.1462-5822.2005.00659.x

Wagner, G., Moertl, D., Eckhardt, A., Sagel, U., Wrba, F., Dam, K., et al. (2016). Chronic Paracoccidioidomycosis with adrenal involvement mimicking tuberculosis – A case report from Austria. *Med. Mycol. Case Rep.* 14, 12–16. doi: 10.1016/j.mmcr.2016.12.002

Wartha, F., Beiter, K., Albiger, B., Fernebro, J., Zychlinsky, A., Normark, S., et al. (2007). Capsule and D- alanylated lipoteichoic acids protects *Streptococcus pneumoniae* against neutrophil extracellular traps. *Cell Microbiol.* 9 (5), 1162–1171. doi: 10.1111/j.1462-5822.2006.00857.x

Wilton, M., Halverson, T. W. R., Charron-Mazenod, L., Parkins, M. D., and Lewenza, S. (2018). Secreted phosphatase and deoxyribonuclease are required by *Pseudomonas aeruginosa* to defend against neutrophil extracellular traps. *Infect. Immun.* 86 (9), e00403–e00418. doi: 10.1128/IAI.00403-18

Ye, J., Coulouris, G., Zaretskaya, I., Cutcutache, I., Rozen, S., and Madden, T. (2012). Primer-BLAST: A tool to design target-specific primers for polymerase chain reaction. *BMC Bioinform.* 13, 134. doi: 10.1186/1471-2105-13-134

Yipp, B. G., and Kubes, P. (2013). NETosis: how vital is it? *Blood* 122 (16), 2784–2794. doi: 10.1182/blood-2013-04-457671

Zhang, H., Zhao, G., Guo, Y., Menghwar, H., Chen, Y., Chen, H., et al. (2016). *Mycoplasma bovis* MBOV_RS02825 encodes a secretory nuclease associated with cytotoxicity. *Int. J. Mol. Sci.* 17 (5), 628. doi: 10.3390/ijms17050628

Zhang, X., Zhao, S., Sun, L., Li, W., Wei, Q., Ashman, R. B., et al. (2017). Different virulence of *Candida Albicans* is attributed to the ability of escape from neutrophil extracellular traps by secretion of DNAse. *Am. J. Trans. Res.* 9 (1), 50–62.

Conflict of Interest: The authors declare that the research was conducted in the absence of any commercial or financial relationships that could be construed as a potential conflict of interest.

frontiers in Cellular and Infection Microbiology

MINI REVIEW
published: 11 February 2021
doi: 10.3389/fcimb.2020.605679

The Trojan Horse Model in *Paracoccidioides*: A Fantastic Pathway to Survive Infecting Human Cells

Gustavo Giusiano *

Mycology Department, Instituto de Medicina Regional, Universidad Nacional del Nordeste, Consejo Nacional de Investigaciones Científicas y Técnicas (CONICET), Resistencia, Argentina

Paracoccidioidomycosis (PCM) is the most relevant systemic endemic mycosis limited to Latin American countries. The etiological agents are thermally dimorphic species of the genus *Paracoccidioides*. Infection occurs *via* respiratory tract by inhalation of propagules from the environmental (saprophytic) phase. In the lung alveoli the fungus converts to the characteristic yeast phase (parasitic) where interact with extracellular matrix proteins, epithelial cells, and the host cellular immunity. The response involves phagocytic cells recognition but intracellular *Paracoccidioides* have demonstrated the ability to survive and also multiply inside the neutrophils, macrophages, giant cells, and dendritic cells. Persistence of *Paracoccidioides* as facultative intracellular pathogen is important in terms of the fungal load but also regarding to the possibility to disseminate penetrating other tissues even protected by the phagocytes. This strategy to invade other organs *via* transmigration of infected phagocytes is called Trojan horse mechanism and it was also described for other fungi and considered a factor of pathogenicity. This mini review comprises a literature revision of the spectrum of tools and mechanisms displayed by *Paracoccidioides* to overcame phagocytosis, discusses the Trojan horse model and the immunological context in proven models or the possibility that *Paracoccidioides* apply this tool for dissemination to other tissues.

Keywords: dissemination, transmigration, internalized parasitic cells, Paracoccidioidomycosis, immune response evasion

OPEN ACCESS

Edited by:
Carlos Pelleschi Taborda, University of São Paulo, Brazil

Reviewed by:
Gil Benard, University of São Paulo, Brazil
Juan G. McEwen, University of Antioquia, Colombia

***Correspondence:**
Gustavo Giusiano
gustavogiusiano@yahoo.com.ar

Specialty section:
This article was submitted to Fungal Pathogenesis, a section of the journal Frontiers in Cellular and Infection Microbiology

Received: *12 September 2020*
Accepted: *30 December 2020*
Published: *11 February 2021*

Citation:
Giusiano G (2021) The Trojan Horse Model in Paracoccidioides: A Fantastic Pathway to Survive Infecting Human Cells. Front. Cell. Infect. Microbiol. 10:605679. doi: 10.3389/fcimb.2020.605679

INTRODUCTION

Onygenalean (Ascomycota) organisms including *Paracoccidioides*, have typically adapted to saprobic conditions in soil but also to the live tissues of animal hosts. This biotrophic lifestyle is possible thanks to genomics adaptations allowing them the capability to degrade animal substrates suggesting a duality in lifestyle that could enable pathogenic species of Onygenales to transfer from soil to animal hosts (Desjardins et al., 2011). The potential of this thermodimorphic fungi to become a pathogen and to invade a host it's based on numerous fungal strategies to escape and to bypass the host defense mechanisms (Teixeira et al., 2014; De Oliveira et al., 2015; Camacho and Niño-Vega, 2017).

Paracoccidioides species complex is widely distributed on Latin American soils with high incidence in South America (Negroni, 1993; Restrepo et al., 2012). Paracoccidioidomycosis (PCM) process start after inhalation of the environmental morphotype, when reaches the lung alveoli. At this point, the dimorphic transition to the yeast form and the interaction with the extracellular matrix (ECM) proteins, epithelial cells, and the host cellular immunity mediated by the phagocytic cells of the innate immune and adaptive systems, they are the first steps in a complex relationship between *Paracoccidioides* and the host that can lead to a granulomatous disease. This multi-factorial host–pathogen interactions involves fungal virulence factors, adaptation, adhesion and invasion depending on the host immune status and its response (Negroni, 1993; González et al., 2005; González et al., 2008a; De Oliveira et al., 2015; Hernández-Chávez et al., 2017).

In this damage-response framework, the host attempt to kill the infecting microbe causing none or the minimum possible damage. On the other hand, *Paracoccidioides* spp. develops several tools as strategies to evade the host immune response (González and Hernández, 2016; Camacho and Niño-Vega, 2017). One of the most interesting mechanism is the ability to survive inside the phagocytes as a facultative intracellular pathogen (Brummer et al., 1989; Moscardi-Bacchi et al., 1994). This strategy could allow *Paracoccidioides* to leave the lung and to penetrate other tissues protected by the phagocytic cells (Silvana dos Santos et al., 2011). This important mechanism of pathogenesis, involving carriage inside the infected macrophage or dendritic cell, allowing extrapulmonary dissemination phagocytes associated, is named Trojan horse model.

Phagocytes Activation

Phagocytosis followed by degradation of the fungal particles internalized by phagocytic cells is an essential innate immune response to prevent the dissemination. Initially, the response involves neutrophils, alveolar macrophages, and dendritic cells (DCs) recognition. Their digestive and killing capabilities will be decisive to the destiny of the infectious process, then they will stimulate the adaptive immune system through their cytokines and chemokines. All phagocytes exist in degrees of readiness. During an infection, they receive chemical signals which prepares for its specific function. Resistance against *Paracoccidioides* infection depends mainly on the phagocytes being activated, which exhibit an increased capacity to ingest and fungicidal functions. Such events are modulated by fungal components and host factors. Therefore, activation of these cells is essential (Cano et al., 1998; Rodrigues et al., 2007; Thind et al., 2015; González and Hernández, 2016; Marcos et al., 2016; Camacho and Niño-Vega, 2017).

The recognition of fungal wall components named pathogen-associated molecular patterns (PAMPs) by pathogen recognition receptors (PRRs) initiates the complex host innate immune response. These conserved transmembrane or intracytoplasmatic PRRs include the Toll-like receptors (TLRs), mannose receptors (MR), complement receptors (CR), and the family of C-type lectin receptors (CLRs) such as CRL dectin-1, 2, and 3, among others. This interaction drive to the activation of the innate immune system cells and the succeeding production of mediators involved into the removal of the agent and to the control of the adaptative immune responses (Calich et al., 2008; Loures et al., 2014; Loures et al., 2015; Preite et al., 2018).

Knowledge about the immunopathogenesis of PCM is based on *in vivo* and *in vitro* experimental studies (González et al., 2008b; González and Hernández, 2016). Human and murine models showed de crucial role of TLRs inducing the production of inflammatory cytokines that drives naive T cells to Th and Treg cells. Patients with T cell deficiencies are more susceptible to fungal infections such as PCM. T cells are the major source of cytokines and lead to generate Th1 cytokines in order to activate macrophages and DCs in a next step. Th1 cells secrete interferon gamma (IFN-γ) and tumor necrosis factor (TNF-α), both cytokines activates macrophages and DCs enhancing their ability to kill or inhibit intracellular fungi and to present antigens to T lymphocytes (Cano et al., 1998; González et al., 2003; Silvana dos Santos et al., 2011; Thind et al., 2015; Marcos et al., 2016; Camacho and Niño-Vega, 2017).

The cytokine balance limited by the mutual regulation between Th1, Th2, Th17, and Treg polarization is necessary in order to optimize clearance and minimize inflammatory damage to the infected tissues. There are two possible outcomes of this balance that can result in control and removal of the fungal infection or lead to persistence of the infection and progress to a severe pathology (Olszewski et al., 2010; de Castro et al., 2013). Th1 and Th2 patterns of cytokine expression have been associated with PCM resistance and susceptibility, respectively (Cano et al., 1998; Mamoni et al., 2002; Benard, 2008; de Castro et al., 2013).

How to Survive and Even Multiply Into the Phagocytes

The phagosome has a powerful antimicrobial effect. A combination of factors gives this organelle sufficient capability to eliminate pathogens, from inducing nutrients and trace elements deficiencies to producing different antimicrobial compounds that stress the internalized microbe (González and Hernández, 2016). Several studies trying to elucidate how the parasitic yeast-like form of *Paracoccidioides* manage to survive inside phagocytic cells. The strategy to evade the hostile host conditions includes a multiplex approach (**Figure 1**).

Polymorphonuclear Neutrophils

They are the most abundant leukocytes and the main effector cells in the prevention of fungal infections. Polymorphonuclear neutrophils (PMNs), the primary phagocytic cells of the innate immune system, when activated *via* TLRs initiate the inflammatory response against *Paracoccidioides*. Chemokines produced by neutrophils are involved in the chemotaxis for the rapid migration of immune cells to the infection site. Neutrophils granules contain antimicrobial peptides, nucleolytic enzymes, and also oxygen metabolites acting in the removal process disrupting the cell membrane of fungus (Traynor and Huffnagle, 2001; Rodrigues et al., 2007; González et al., 2008b; Pathakumari et al., 2020). In addition, PMNs are able to produce extracellular traps (NETs), these structures are able to capture microbials, degrade their virulence factors, and eliminate the pathogens (Mejía et al., 2015; Restrepo et al., 2015).

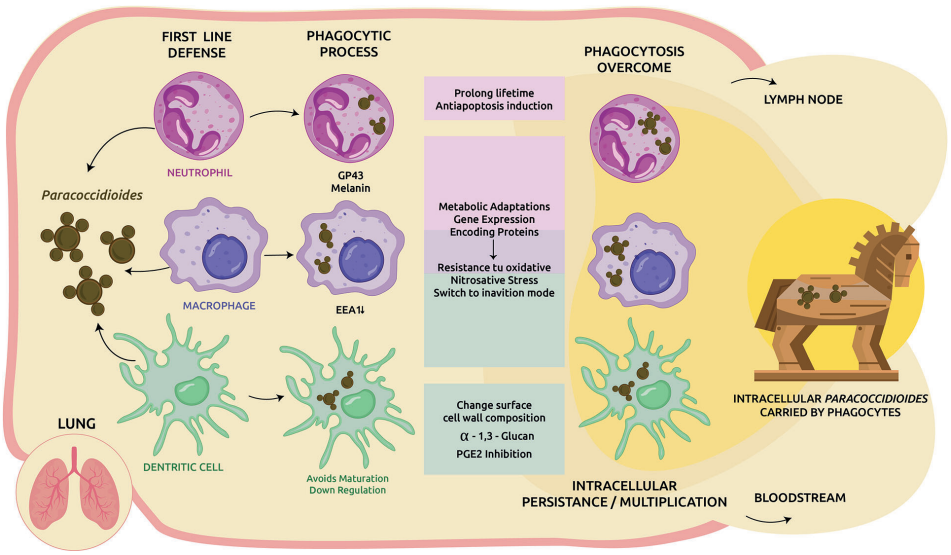

FIGURE 1 | Cellular response to *Paracoccidioides* infection in the lung and immune-evasion mechanisms. Upon inhalation the saprophytic form converts to the yeast-like parasitic and trigger the host cellular immune response. Phagocytes are motivated to clear the invasive fungi. In addition to its own structural virulence determinants such as gp43, melanin, among others, *Paracoccidioides* spp. applies several strategies to overcome the host harsh environment, including: modulate host apoptosis, metabolic adaptations, and expression of genes to achieve an inanition mode and also resistance to the host oxidative burst. When intracellular survival is possible, part of the phagocytosed fungi could be transported by DCs/macrophages to lymphoid tissues or other organs *via* circulation as facultative intracellular pathogens but protected by phagocytes (Trojan horse mechanism).

The balance between pro-inflammatory and anti-inflammatory cytokines is a prerequisite for a successful host/fungal interaction. Participation of TLR2, TLR-4, and dectin-1 receptors in recognition, internalization, and consequent activation of neutrophils was demonstrated in human neutrophils stimulated by *Paracoccidioides brasiliensis*. In this study, the more virulent strain induced production of only TNF-α. The less virulent, in contrast, triggers a controlled immune response with balanced production of TNF-α and IL-10, preferentially recognized by TLR2 and dectin-1 (Bonfim et al., 2009).

Non activated cells failing to exhibit an antifungal activity was demonstrated. Due to the capability of human PMNs to release higher oxygen metabolites, an activation process by IFN-γ, TNF-α, and GM-CSF cytokines is required for killing *P. brasiliensis* (Rodrigues et al., 2007). This fact is important to understand one of the mechanisms through which *Paracoccidioides* could adapt to the host environment and survive. Transcriptome analysis of *P. brasiliensis* reveals many resources of this fungus as antioxidant defense system to combat reactive species. The parasite's abilities to overcame the oxidative and nitrosative stress by genes coding proteins involved in this response were described and include catalase and superoxide dismutase isoenzymes, peroxiredoxin, cytochrome c peroxidase, among others (Campos et al., 2005).

At this point, the cytokine balance is also critical. The lack of an adequate *in vivo* activation of PMNs as a consequence of a depressed Th1 response releasing low levels of cytokines, leads to the possible inability of PMNs to successfully kill *Paracoccidioides* (Kurita et al., 1999; Rodrigues et al., 2007).

PMNs ingest yeast cells of *P. brasiliensis* through a typical phagocytic process. These phagocytes are shortlived cells, after few hours they undergo spontaneous apoptosis. Intracellular microorganisms may block or delay this process to create an environmental for their survival and replication. *In vitro* studies showed that *P. brasiliensis* can prolong the lifetime of normal PMNs and also induce an anti-apoptotic process associated with an increase in PMNs IL-8 production as an strategy to facilitate intracellular persistence (Acorci et al., 2009).

For decades, the role of PMNs in some granulomatous diseases they have been studied showing an abnormal function with a significantly lower ability to digest *P. brasiliensis in vitro* than PMNs from normal individuals or from patients with unrelated diseases (Goihman-Yahr et al., 1980).

This mechanism is another pathway that contribute to understand the PCM pathogenesis. Inhibition of phagocytic cells apoptosis allow *P. brasiliensis* to survive within the PMNs, gain time for multiplication and also dissemination.

Macrophages

Lung macrophages participate as one of the main mechanisms of cellular immunity trying to prevent the parasitic invasion of host tissues and its dissemination through phagocytosis or granuloma formation (González et al., 2008b). Studies using murine macrophages and also proteomic analysis showed the activations process as a requirement to obtain a more vigorous defense with significantly more capability to kill the yeast-like phase of *P. brasiliensis*. Otherwise, the ingested *P. brasiliensis* can multiply inside non-activated cells (Brummer et al., 1989; Cano et al., 1992; Moscardi-Bacchi et al., 1994; Parise-Fortes et al., 2000; Chaves et al., 2019).

T cells are mandatory for antifungal host defense. Th1 cells are involved in cell-mediated immunity supporting classical activation of macrophages for fungal clearance and are associated with strong proinflammatory responses. In contrast to the protective role of Th1, a Th2 humoral with insufficient production or deficient IFN-γ, TNF-α, and IL-12 response, is non-protective and was related with fungal persistence and pathology. Th1 pattern is associated to asymptomatic and mild PCM forms while an Th2 pattern has been related with progressive juvenile and multifocal forms (Cano et al., 1998; Mamoni et al., 2002; González et al., 2003; González et al., 2008b; Olszewski et al., 2010; de Castro et al., 2013). A strong Th2 response suppresses the Th1 and Th17 response and triggers the alternative macrophage activation mediated by IL-4 and IL-13. The imbalance of Th2 responses, is inadequate to control the infection and lead to an uncontrolled inflammatory host response. This pathway do not express the fungicidal effect of the nitric oxide and other intermediates and has been associated with intracellular *Paracoccidioides* survival since it is not affected by the nitrosative stress (González et al., 2008b; Olszewski et al., 2010; Borghi et al., 2014). Th2 response is also characterized by IgG4 and IgE, low macrophages activation, granulomas, and eosinophilic inflammation (Mamoni et al., 2002).

TLRs shows their important participation in the effector and regulatory mechanisms of innate and adaptative immunity against fungal infections. Even if TLRs receptors promote an immune response against infectious agents, experimental models demonstrated that parasitic phase of *Paracoccidioides* could use not conventional phagocytic receptors such as TLR2 and TLR4 to penetrate into macrophages and infect mammalian hosts. Although this process should generate a phagocytic process, the killing activity was demonstrated not able to reduce the fungal burden. *P. brasiliensis* seems to use TLRs as a virulence mechanism, which facilitates its access into murine macrophages *in vitro* and *in vivo*. Despite their TLR-mediated activation, macrophages are not able to control fungal growth. However, the interaction between TLR and other PRRs can result in different effector (Th1, Th2, and Th17) and regulatory responses (Treg), which ultimately determine disease outcome. The recognition of *P. brasiliensis via* host TLR2 and TLR4 receptors of innate immunity is considered an escape mechanism that allows the fungus to survive and replicate inside macrophages (Calich et al., 2008).

Microbicidal activity of macrophages include the induction of a low availability of nutrients but also, they activate an oxidative burst. At this point, *Paracoccidioides* display a spectrum of tools to adapt into in the intracellular environment, requiring metabolic adaptations.

A decisive success is based on its resistance to oxidative and nitrosative stresses and glucose deprivation. Reactive oxygen species (ROS) and reactive nitrogen species (RNS) are generated inside the phagolysosome, such us nitric oxide, peroxynitrite, superoxide anion radical, and hydroxyl radical. In the face of the oxidative and nitrosative stress, *Paracoccidioides* triggers a powerful antioxidant defense system expressing several enzymes including catalases, superoxide dismutases, thioredoxin, and particularly cytochrome c peroxidase (González et al., 2000; de Arruda Grossklaus et al., 2013; Parente-Rocha et al., 2015; Marcos et al., 2016; Bueno et al., 2016; Chaves et al., 2019). The central role of the alternative oxidase (PbAOX) in the intracellular redox balancing and in the resistance of *P. brasiliensis* to the oxidative burst created by alveolar macrophages was also demonstrated (Hernández Ruiz et al., 2011).

Adaptation, in order to survive under this stress, also includes metabolic changes such us an alternative metabolic pathway during carbon starvation. Several studies including proteomic and transcriptomic analysis showed the shift of *P. brasiliensis* to an "inanition mode," including an increase in the synthesis of glucose by gluconeogenesis and ethanol production, amino acid degradation and utilization of fatty acids by beta-oxidation (Lima et al., 2014; Parente-Rocha et al., 2015; Chaves et al., 2019). Metabolic alterations also include the activation of the pentose phosphate pathway to provide NADPH, a reducer substrate used to reduce the oxidative effects when exposed to peroxide hydrogen (de Arruda Grossklaus et al., 2013).

Many fungal genes have been studied as probably involved in the survival of *P. brasiliensis* in the host. Genes encoding proteins essential to the life and those indispensable for the interaction with the host were reported. Using murine macrophages transcriptional plasticity of *P. brasiliensis* in response to the hostile macrophage intracellular environment was reported. To adapt and consequent survive, *P. brasiliensis* expresses genes associated with glucose and amino acid limitation, cell wall construction and oxidative stress (Popi et al., 2002). It has also been demonstrated that *Paracoccidioides* could develop a fermentation process to obtain energy enabling its adaptation to glucose-poor microenvironments. Even more, can also produce ATP under low oxygen conditions, in turn reducing the reactive oxygen species levels produced by the host (Tavares et al., 2015).

In addition, lung murine infection models showed that *Paracoccidioides* increased the expression of serine proteinase. This protein is involved in cell rescue, defense, and as a virulence factor that favors survival upon nitrogen deprivation, as well as tissue invasion (Parente et al., 2010; Lacerda Pigosso et al., 2017). Increased expression of heat shock proteins and proteins involved in detoxification and stress response were observed using proteomic analysis in *P. brasiliensis* recovered of primed and non-primed macrophages (Chaves et al., 2019).

On the other hand, host cells try to prevent intracellular survival and multiplication sequestering essential fungal nutrients such as iron and zinc using high-affinity proteins, transferrin, and ferritin. Iron is required for the saprophytic phase-to-yeast transition, necessary for the pathogenic process development, as well as yeast replication inside macrophages and monocytes (González et al., 2007). In order to persist inside this environmental condition, *Paracoccidioides* activate effectives iron and zinc uptake pathways, adjusting their energy metabolism to an iron-independent mode by increasing glycolytic activity and also expression of genes involved in the production of siderophores (Parente et al., 2011; Silva-Bailão et al., 2014). Even more, develops a non-traditional reductive iron assimilation pathway, transporting zinc and iron inside the fungal cell *via* iron reduction and zinc-regulated transporter homologs (Zrt1 and Zrt2) (Camacho and Niño-Vega, 2017). Another iron

acquisition mechanism mediate by the putative hemoglobin receptor Rbt5 was demonstrated. *Paracoccidioides* Rbt5 was able to bind to hemin, protoporphyrin, and hemoglobin *in vitro* and could function as a heme group receptor, which could help in the acquisition of iron from host sources (Bailão et al., 2014).

Gp43 is the *Paracoccidioides* surface main antigen. This high mannose glycoprotein of 43 kDa is an adhesin, important as one of the mediators of fungus adhesion to host epithelial cells and macrophages internalization. In peritoneal macrophages from resistant and susceptible mice, gp43 acts an inhibitor of phagocytosis and the intracellular fungal killing, even induce protection. Therefore, is considered as one of the evasion mechanisms of the primary infection in susceptible hosts and to establish the fungal infection in distant niches favoring the dissemination (Popi et al., 2002; Konno et al., 2012; De Oliveira et al., 2015; Camacho and Niño-Vega, 2017). Gp43 also prevents the release of nitric oxide from macrophages reducing the nitrosative stress and stimulates IL-10 liberation, reducing the inducible nitric oxide synthase expression and its enzymatic activity. The suppressor effect of IL-10 blocks the IFN-γ and TNF-α-induced activation of phagocytic cells, by inhibiting their fungicidal activity and ability to produce the oxidative metabolites (oxide nitric and oxygen peroxide) involved in fungus killing. Gp43 mediates another escape mechanism of *Paracoccidioides*, impairing the ingestion process and the interaction macrophage–fungus, inducing the deactivation of the phagocytic cell (Popi et al., 2002; Moreira et al., 2010). In addition, the early monocyte/macrophage secretion of IL-10, particularly when these cells were challenged with gp43 was observed. In patients with both the acute/subacute and chronic forms of PCM, the imbalance in cytokine production was involved in the gp43-hyporesponsiveness and a marked (non-protective) antibody production. (Benard et al., 2001).

Paracoccidioides produce cell wall-associated melanin-like components *in vivo* and during infection. Melanin is another virulence factor that has been shown to interfere with host defense mechanisms enhancing the resistance to immune effector cells attacks (Taborda et al., 2008). In macrophage-like cell lines, the phagocytic index for melanized *P. brasiliensis* yeast cells was half that for the non-melanized cells. Yeast melanization interfere the binding of macrophages lectin receptors to cell wall components, consequently they are poorly phagocytized and more resistant to the antifungal activity of murine macrophages (da Silva et al., 2006).

One more survival strategy used when infected macrophages are established consists in the inhibition of the phagosome-endosome fusion. *Paracoccidioides* decrease the expression of the endocytic protein EEA1 (early endosome antigen 1) that has a critical function as organelle-tethering molecule responsible for traffic endosomal. Therefore, cellular nutrition is impaired and also the traffic of *Paracoccidioides* yeast for it final destruction in the lysosome (Voltan et al., 2013).

Dendritic Cells

Lung cells such as DCs are part of the first line of defense against *Paracoccidioides*. DCs, as antigen-presenting cells, also plays a crucial role as sentinels in peripheral tissues inducing cell-mediated immune responses. PAMP-dependent or independent activation is also required. They capture antigens, processed, and converted these proteins to peptides that are immediately presented on major histocompatibility complex molecules recognized by T lymphocytes. DCs migrates to the lymph nodes, present antigens and initiate T cell activation/responses. These phagocytic are involved in detection, binding, phagocytosis, processing, antigen presentation, T cell activation and killing of the organism (Cano et al., 1998; Silvana dos Santos et al., 2011; Thind et al., 2015; Marcos et al., 2016; Camacho and Niño-Vega, 2017).

To adapt for survival in adverse conditions or stress, fungus has the ability to modify its cell wall structure and also composition. Polysaccharides of the cell wall are the main fungal PAMPs and trigger the immune response when are recognized by PRRs. Nevertheless, *Paracoccidioides* display strategies to evade recognition by phagocytic cells, changing the amount of certain surface cell wall components (Hernández-Chávez et al., 2017). During the morphologic change, cell wall composition of dimorphic fungi is altered as well as the carbohydrate polymer structure. Filamentous phase contains both β- and α-(1,3)-glucans, but conversion to the parasitic yeast form produce an increase of the much less immunogenic α-(1,3)-glucan (Marcos et al., 2016). Several studies demonstrated that DCs maturation is altered by the parasitic form, influencing the susceptibility to this fungus. When monocytes migrate to the infection site, they interact with components of *Paracoccidioides* cell wall. In this sense, the critical role of its cell wall in the host immune response during PCM was postulated. Two cell wall fractions, one constituted mainly by α-glucan and other by β-(1,3)-glucans, chitin, and proteins and the alkali-soluble were investigated, demonstrating the induction of a dysregulation in DCs differentiation. *Paracoccidioides* cell wall α-glucan, presented as the mayor neutral polysaccharide in the yeast phase, also influences favoring Th2 polarization and contributes to pathogen persistence (Puccia et al., 2011; Souza et al., 2019). On the other hand, the lower efficiency of DCs from mice susceptible to *P. brasiliensis* in inducing a Th1 response was observed, an effect that could be related to the progression of the disease *in vivo* (Almeida and Lopes, 2001).

Other *in vitro* studies using human immature DCs also demonstrated that *P. brasiliensis* inhibit prostaglandin E2 production by DCs, impairing its maturation in response to this fungus and showing another evasion mechanism. These authors suggest opposite mechanisms applied by *P. brasiliensis* to scape DCs and monocytes responses, since increased production of PGE2 by monocytes inhibits their killing mechanism, while inhibited production by DCs avoid their maturation (Fernandes et al., 2015).

The main immunodominant glycoprotein gp43 was reported affecting many functions of the host phagocytic cells and might be used by *Paracoccidioides* to reduce the effectiveness of the immune response. Studies with *P. brasiliensis* infection in mice and purified gp43 lead to down-regulate properties of immature DCs (Ferreira et al., 2004).

Spread *via* Transmigration of Infected Phagocytes

The Trojan horse-like mechanism was described for other fungal infections and well-studied in *Cryptococcus*, explaining the

mechanism of cryptococcal brain invasion (Shi and Mody, 2016). As well as *Paracoccidioides*, cryptococcal infection begins in the lung and experimental evidence showed that host phagocytes play a role in subsequent dissemination. This transmigration model contributes significantly to fungal barrier crossing and *Cryptococcus*-containing phagocytes can cross the blood-brain barrier *via* transendothelial pores (Santiago-Tirado et al., 2017; Casadevall et al., 2018). Three mechanisms have been proposed for pathogens to cross the blood-brain barrier: transcellular migration, paracellular migration and/or by means of infected phagocytes (Trojan horse model), proliferating and causing grave illness (Shi and Mody, 2016). Evidence for this model were showed using mice infected with macrophages containing ingested cryptococcal cells (Charlier et al., 2009). Although Trojan horse-like mechanism has been more studied in *Cryptococcus*, and its glucuronoxylomannan capsule plays an important role in the inhibition of phagocytosis, *Paracoccidioides* deploys numerous effectives abilities to persist and also multiply inside phagocytes as a facultative intracellular pathogen (**Figure 1**). Therefore, access to this mechanism is feasible by *Paracoccidioides*, and dissemination to other organs/systems could occur (Brummer et al., 1989; Moscardi-Bacchi et al., 1994).

Although alveolar macrophages have well-defined immunoregulatory functions, these cells are generally considered as restricted to the alveoli. It was demonstrated that murine alveolar macrophages constitutively migrate from lung to the lung draining lymph nodes and that following exposure to bacteria, they rapidly transport bacteria to this site. Alveolar macrophages, such as DC, appear responsible for the earliest delivery of these bacteria to secondary lymphoid tissue. The identification of this transport suggests an important role for macrophages in the transport of invading pathogens to lymphoid organs (Kirby et al., 2009).

Non-lytic exocytosis for yeast infecting phagocytes where demonstrated. Viable yeast cells can come out of the macrophages without phagocytes lysis (Alvarez and Casadevall, 2006). Like other yeasts, *Paracoccidioides* could escape from intracellular confines of mammalian macrophages to continue propagation and, possibly, dissemination. Also *Candida albicans* spread *via* phagocyte-dependent mechanism. Using *in vitro* and zebrafish disease models, how neutrophils and macrophages can be vehicles for dissemination have been demonstrated. *Candida albicans* survive within macrophages and can be released far from the site of infection through non-lytic exocytosis. The intracellular viable yeast is able to get into the bloodstream and use blood flow to transmigrate to other tissues (Scherer et al., 2020).

In *Paracoccidioides* little is known about which pathways this fungus activates to escape from the monocyte-phagocyte system. Murine animal models are considered the gold standard for *in vivo* studies to simulate the fungal infection (De Oliveira et al., 2015). The migration of lung DCs to the lymph nodes and also lung DCs phagocyting *P. brasiliensis* yeast *in vivo* were demonstrated (Ferreira et al., 2007).

After *P. brasiliensis* infection, an increase in DCs expression of the chemokine receptors CCR7, CD103, and MHC-II occurs, enabling DCs migration from the infection site to the secondary lymphoid after interacting with the fungus. This fact indicate that *Paracoccidioides* induce migration of DCs. Animal model showed bone marrow-derived DCs stimulated by *P. brasiliensis* can migrate to the lymph nodes and activate a T-cell response. Even more, it was demonstrated *in vivo* that DCs migrate and transport the yeast parasitic form of the fungus to lymph nodes (Silvana dos Santos et al., 2011). This strategy allows *Paracoccidioides* to leave the lung and to penetrate other tissues protected by the phagocytic cells. Lung DCs could act as Trojan horses for this fungus.

DISCUSSION

Paracoccidioides-phagocytic cells interaction comprise a complex transcriptional and translational plan including a powerful antioxidant defense system. The host is under pressure to develop resistance while the parasite tries to tolerate, adapt to this new biotrophic lifestyle and overcome host environmental stressors and reach to subsist.

The recognition of the fungal cells by the capable host immune system trigger a large number of processes to control these organisms, but not only the immune responses pattern determines the progression of the disease and the clinical outcome. Despite the efficient host fighting and even when it has already been engulfed by phagocytes, we reviewed in this article the amazing set of tools and strategies exposed by *Paracoccidioides* to stay alive.

These pathogenic abilities allow not only their survival but the possibility of gain access to other tissues *via* transmigration of infected phagocytes. In this process, *Paracoccidioides* also causes phagocytes to play a dual role, they can contain the PCM or be instrumental to disseminate the infection. This mechanism, which actually includes a spectrum of strategies increases the virulence of this dimorphic fungus.

The Trojan horse mechanism represents a striking demonstration of the admirable adaptability of the yeast-like pathogenic form of *Paracoccidioides* to adverse conditions, as an accidental fact in the life cycle of this environmental fungi trying to survive after inhalation.

Nowadays, we understand better about how this fungus spreads throughout a host. However, although PCM poses a significant clinical risk, we still understand little about what roles plays the host in limiting or enabling its dissemination. The possibility of occurrence probably is not only related to the patient's immune status, but on a multiplicity of factors including sex, age, lifestyle, its genetic background, and also the inhaled fungal load depending on the environmental context, among others.

AUTHOR CONTRIBUTIONS

The author confirms being the sole contributor of this work and has approved it for publication.

REFERENCES

Acorci, M. J., Dias-Melicio, L. A., Golim, M. A., Bordon-Graciani, A. P., Peraçoli, M. T. S., and Soares, A. M. V. C. (2009). Inhibition of human neutrophil apoptosis by *Paracoccidioides brasiliensis*: Role of interleukin-8. *Scand. J. Immunol.* 69 (2), 73–79. doi: 10.1111/j.1365-3083.2008.02199.x

Almeida, S. R., and Lopes, J. D. (2001). The low efficiency of dendritic cells and macrophages from mice susceptible to *Paracoccidioides brasiliensis* in inducing a Th1 response. *Braz. J. Med. Biol. Res.* 34 (4), 529–537. doi: 10.1590/S0100-879X2001000400014

Alvarez, M., and Casadevall, A. (2006). Phagosome extrusion and host-cell survival after *Cryptococcus neoformans* phagocytosis by macrophages. *Curr. Biol.* 16 (21), 2161–2165. doi: 10.1016/j.cub.2006.09.061

Bailão, E. F., Cardoso, L., Alves Parente, J., Lacerda Pigosso, L., Pacheco de Castro, K., Lopes Fonseca, F., et al. (2014). Hemoglobin uptake by *Paracoccidioides* spp. is receptor-mediated. *PloS Neg. Trop. Dis.* 8 (5), e2856. doi: 10.1371/journal.pntd.0002856

Benard, G., Romano, C. C., Cacere, C. R., Juvenale, M., Mendes-Giannini, M. J. S., and Duarte, A. J. S. (2001). Imbalance of IL-2, IFN-γ and IL-10 secretion in the immunosuppression associated with human paracoccidioidomycosis. *Cytokine* 13 (4), 248–252. doi: 10.1006/cyto.2000.0824

Benard, G. (2008). An overview of the immunopathology of human paracoccidioidomycosis. *Mycopathol* 165 (4–5), 209–221. doi: 10.1007/s11046-007-9065-0

Bonfim, C. V., Mamoni, R. L., and Souza Lima Blotta, M. H. (2009). TLR-2, TLR-4 and Dectin-1 expression in human monocytes and neutrophils stimulated by *Paracoccidioides brasiliensis*. *Med. Mycol.* 47 (7), 722–733. doi: 10.3109/13693780802641425

Borghi, M., Renga, G., Puccetti, M., Oikonomou, V., Palmieri, M., Galosi, C., et al. (2014). Antifungal Th immunity: growing up in family. *Front. Immunol.* 5, 506. doi: 10.3389/fimmu.2014.00506

Brummer, E., Hanson, L. H., Restrepo, A., and Stevens, D. A. (1989). Intracellular multiplication of *Paracoccidioides brasiliensis* in macrophages: killing and restriction of multiplication by activated macrophages. *Infect. Immun.* 57 (8), 2289–2294. doi: 10.1128/iai.57.8.2289-2294.1989

Bueno, R. A., Thomaz, L., Muñoz, J. E., Da Silva, C. J., Nosanchuk, J. D., Pinto, M. R., et al. (2016). Antibodies against glycolipids enhance antifungal activity of macrophages and reduce fungal burden after infection with *Paracoccidioides brasiliensis*. *Front. Microbiol.* 7, 74. doi: 10.3389/fmicb.2016.00074

Calich, V. L. G., Pina, A., Felonato, M., Bernardino, S., Costa, T. A., and Loures, F. V. (2008). Toll-like receptors and fungal infections: the role of TLR2, TLR4 and MyD88 in paracoccidioidomycosis. *FEMS Immunol. Med. Microbiol.* 53 (1), 1–7. doi: 10.1111/j.1574-695X.2008.00378.x

Camacho, E., and Niño-Vega, G. A. (2017). *Paracoccidioides* spp.: virulence factors and immune-evasion strategies. *Mediators Inflamm.* 2017, 5313691. doi: 10.1155/2017/5313691

Campos, E. G., Santos Amorim Jesuino, R., da Silva Dantas, A., de Macedo Brígido, M., and Felipe, M. S. S. (2005). Oxidative stress response in *Paracoccidioides brasiliensis*. *Genet. Mol. Res.* 4 (2), 409–429.

Cano, L. E., Arango, R., Salazar, M. E., Brummer, E., Stevens, D. A., and Restrepo, A. (1992). Killing of *Paracoccidioides brasiliensis* conidia by pulmonary macrophages and the effect of cytokines. *Med. Mycol.* 30 (2), 161–168. doi: 10.1080/02681219280000211

Cano, L. E., Kashino, S. S., Arruda, C., André, D., Xidieh, C. F., Vermes, L. M., et al. (1998). Protective role of gamma interferon in experimental pulmonary paracoccidioidomycosis. *Infect. Immun.* 66 (2), 800–806. doi: 10.1128/IAI.66.2.800-806.1998

Casadevall, A., Coelho, C., and Alanio, A. (2018). Mechanisms of *Cryptococcus neoformans*-mediated host damage. *Front. Immunol.* 9:855. doi: 10.3389/fimmu.2018.00855

Castro, L. F., Ferreira, M. C., da Silva, R. M., de Souza Lima Blotta, M. H., Alegrini Longhi, L. N., and Mamoni, R.,. L. (2013). Characterization of the immune response in human paracoccidioidomycosis. *J. Infect.* 67 (5), 470–855. doi: 10.1016/j.jinf.2013.07.019

Charlier, C., Nielsen, K., Daou, S., Brigitte, M., Chretien, F., and Dromer, F. (2009). Evidence of a role for monocytes in dissemination and brain invasion by *Cryptococcus neoformans*. *Infect. Immun.* 77 (1), 120–127. doi: 10.1128/IAI.01065-08

Chaves, E. G. A., Alves Parente-Rocha, J., Baeza, L. C., Silva Araújo, D., Borges, C. L., Pelli de Oliveira, M. A., et al. (2019). Proteomic analysis of *Paracoccidioides brasiliensis* during infection of alveolar macrophages primed or not by interferon-gamma. *Front. Microbiol.* 10, 96. doi: 10.3389/fmicb.2019.00096

da Silva, M. B., Marques, A. F., Nosanchuk, J. D., Casadevall, A., Travassos, L. R., and Taborda, C. P. (2006). Melanin in the Dimorphic Fungal Pathogen *Paracoccidioides brasiliensis*: Effects on Phagocytosis, Intracellular Resistance and Drug Susceptibility. *Microb. Infect.* 8 (1), 197–205. doi: 10.1016/j.micinf.2005.06.018

de Arruda Grossklaus, D., Melo Bailão, A., Vieira Rezende, T. C., Borges, C. L., Pelli de Oliveira, M. L., Alves Parente, J., et al. (2013). Response to oxidative stress in *Paracoccidioides* yeast cells as determined by proteomic analysis. *Microb. Infect.* 15 (5), 347–364. doi: 10.1016/j.micinf.2012.12.002

De Oliveira, H. C., Assato, P. A., Marcos, C. M., Scorzoni, L., Silva, A. C. A. A., de, P. E., et al. (2015). *Paracoccidioides*-Host Interaction: An Overview on Recent Advances in the Paracoccidioidomycosis. *Front. Microbiol.* 6, 1319. doi: 10.3389/fmicb.2015.01319

Desjardins, C., Champion, M. D., Holder, J. W., Muszewska, A., Goldberg, J., Bailão, A. M., et al. (2011). Comparative genomic analysis of human fungal pathogens causing paracoccidioidomycosis. *PloS Genet.* 7 (10), e1002345. doi: 10.1371/journal.pgen.1002345

Fernandes, R. K., Bachiega, T. F., Rodrigues, D. R., Golim, M., de, A., Dias-Melicio, L. A., et al. (2015). *Paracoccidioides brasiliensis* interferes on dendritic cells maturation by inhibiting PGE2 production. *PloS One* 10 (3), 1–17. doi: 10.1371/journal.pone.0120948

Ferreira, K. S., Lopes, J. D., and Almeida, S. R. (2004). Down-regulation of dendritic cell activation induced by *Paracoccidioides brasiliensis*. *Immunol. Lett.* 94 (1–2), 107–114. doi: 10.1016/j.imlet.2004.04.005

Ferreira, K. S., Ramalho Bastos, K., Russo, M., and Almeida, S. R. (2007). Interaction between *Paracoccidioides brasiliensis* and pulmonary dendritic cells induces Interleukin-10 production and Toll-Like Receptor–2 expression: possible mechanisms of susceptibility. *J. Infect. Dis.* 196 (7), 1108–1115. doi: 10.1086/521369

Goihman-Yahr, M., Essenfeld-Yahr, E., de Albornoz, M. C., Yarzábal, L., de Gómez, M. H., San Martín, B., et al. (1980). Defect of *in vitro* digestive ability of polymorphonuclear leukocytes in paracoccidioidomycosis. *Infect. Immun.* 28 (2), 557–566.

González, A., de Gregori, W., Velez, D., Restrepo, A., and Cano, L. E. (2000). Nitric oxide participation in the fungicidal mechanism of gamma interferon-activated murine macrophages against *Paracoccidioides brasiliensis* conidia. *Infect. Immun.* 68 (5), 2546–2552. doi: 10.1128/IAI.68.5.2546-2552.2000

González, A., Sahaza, J. H., Ortiz, B. L., Restrepo, A., and Cano, L. E. (2003). Production of pro-inflammatory cytokines during the early stages of experimental *Paracoccidioides brasiliensis* Infection. *Med. Mycol.* 41 (5), 391–399. doi: 10.1080/13693780310001610038

González, A., Gómez, B. L., Diez, S., Hernández, H., Restrepo, A., Hamilton, A. J., et al. (2005). Purification and partial characterization of a *Paracoccidioides brasiliensis* protein with capacity to bind to extracellular matrix proteins. *Infect. Immun.* 73 (4), 2486–2495. doi: 10.1128/IAI.73.4.2486-2495.2005

González, A., Restrepo, A., and Cano, L. E. (2007). Role of iron in the nitric oxide-mediated fungicidal mechanism of IFN-gamma-activated murine macrophages against *Paracoccidioides brasiliensis* conidia. *Rev. Inst. Med. Trop. São Paulo* 49 (1), 11–16. doi: 10.1590/S0036-46652007000100003

González, A., Lenzi, H. L., Motta, E. M., Caputo, L., Restrepo, A., and Cano, L. E. (2008a). Expression and arrangement of extracellular matrix proteins in the lungs of mice infected with *Paracoccidioides brasiliensis* conidia. *Int. J. Exper. Pathol.* 89 (2), 106–116. doi: 10.1111/j.1365-2613.2008.00573.x

González, A., Restrepo, A., and Cano, L. E. (2008b). Pulmonary Immune Responses Induced in BALB/c Mice by *Paracoccidioides brasiliensis* Conidia. *Mycopathol* 165 (4–5), 313–330. doi: 10.1007/s11046-007-9072-1

González, A., and Hernández, O. (2016). New insights into a complex fungal pathogen: the case of *Paracoccidioides* spp. *Yeast* 33 (4), 113–128. doi: 10.1002/yea.3147

Hernández Ruiz, O., Gonzalez, A., Almeida, A. J., Tamayo, D., Garcia, A. M., Restrepo, A., et al. (2011). Alternative Oxidase Mediates Pathogen Resistance in *Paracoccidioides brasiliensis* Infection. *PloS Neg. Trop. Dis.* 5 (10), e1353. doi: 10.1371/journal.pntd.0001353

Hernández-Chávez, M., Pérez-García, L., Niño-Vega, G., and Mora-Montes, H. (2017). Fungal strategies to evade the host immune recognition. *J. Fungi.* 3 (4), 51. doi: 10.3390/jof3040051

Kirby, A. C., Coles, M. C., and Kaye, P. M. (2009). Alveolar macrophages transport pathogens to lung draining lymph nodes. *J. Immunol.* 183 (3), 1983–1989. doi: 10.4049/jimmunol.0901089

Konno, F. T. C., Maricato, J., Konno, A. Y. C., Guereschi, M. G., Vivanco, B. C., dos Santos Feitosa, L., et al. (2012). *Paracoccidioides brasiliensis* GP43-derived peptides are potent modulators of local and systemic inflammatory response. *Microb. Infect.* 14 (6), 517–527. doi: 10.1016/j.micinf.2011.12.012

Kurita, N., Oarada, M., Ito, E., and Miyaji, M. (1999). Antifungal activity of human polymorphonuclear leucocytes against yeast cells of *Paracoccidioides brasiliensis*. *Med. Mycol.* 37 (4), 261–267. doi: 10.1046/j.1365-280X.1999.00229.x

Lacerda Pigosso, L., Baeza, L. C., Vieira Tomazett, M., Rodrigues Faleiro, M. B., Brianezi Dignani de Moura, V. M., Melo Bailão, A., et al. (2017). *Paracoccidioides brasiliensis* presents metabolic reprogramming and secretes a serine proteinase during murine infection. *Virulence* 8 (7), 1417–1434. doi: 10.1080/21505594.2017.1355660

Lima, P., de, S., Casaletti, L., Melo Bailão, A., Ribeiro de Vasconcelos, A. T., da Rocha Fernandes, G., et al. (2014). Transcriptional and proteomic responses to carbon starvation in *Paracoccidioides*. *PloS Neg. Trop. Dis.* 8 (5), e2855. doi: 10.1371/journal.pntd.0002855

Loures, F. V., Araújo, E. F., Feriotti, C., Bazan, S. B., Costa, T. A., Brown, G. D., et al. (2014). Dectin-1 induces M1 macrophages and prominent expansion of CD8+IL-17+ cells in pulmonary paracoccidioidomycosis. *J. Infect. Dis.* 210 (5), 762–773. doi: 10.1093/infdis/jiu136

Loures, F. V., Araujo, E. F., Feriotti, C., Bazan, S. B., and Calich, V. L. G. (2015). TLR-4 cooperates with Dectin-1 and Mannose receptor to expand Th17 and Tc17 cells induced by *Paracoccidioides brasiliensis* stimulated dendritic cells. *Front. Microbiol.* 6, 261. doi: 10.3389/fmicb.2015.00261

Mamoni, R. L., Nouér, S. A., Oliveira, S. J., Musatti, C. C., Rossi, C. L., Camargo, Z. P., et al. (2002). Enhanced production of specific IgG4, IgE, IgA and TGF-ß in sera from patients with the juvenile form of paracoccidioidomycosis. *Med. Mycol.* 40 (2), 153–159. doi: 10.1080/mmy.40.2.153.159

Marcos, C. M., Oliveira, H. C., de, Antunes de Melo, W., de Cassia, M., da Silva, J. de F., Assato, P. A., et al. (2016). Anti-immune strategies of pathogenic fungi. *Front. Cell. Infect. Microbiol.* 6, 142. doi: 10.3389/fcimb.2016.00142

Mejía, S. P., Cano, L. E., López, J. A., Hernández, O., and González, A. (2015). Human neutrophils produce extracellular traps against *Paracoccidioides brasiliensis*. *Microbiol* 161 (5), 1008–1017. doi: 10.1099/mic.0.000059

Moreira, A. P., Dias-Melicio, L. A., and Campos Soares, A. M. V. (2010). Interleukin-10 but not transforming growth factor beta inhibits murine activated macrophages *Paracoccidioides brasiliensis* killing: Effect on H2O2 and NO production. *Cell. Immunol.* 263 (2), 196–203. doi: 10.1016/j.cellimm.2010.03.016

Moscardi-Bacchi, M., Brummer, E., and Stevens, D. A. (1994). Support of *Paracoccidioides brasiliensis* multiplication by human monocytes or macrophages: Inhibition by activated phagocytes. *J. Med. Microbiol.* 40 (3), 159–164. doi: 10.1099/00222615-40-3-159

Negroni, R. (1993). Paracoccidioidomycosis (South american blastomycosis, Lutz's Mycosis). *Internat. J. Dermatol.* 32 (12), 847–859. doi: 10.1111/j.1365-4362.1993.tb01396.x

Olszewski, M., Zhang, Y., and Zeltzer, S. (2010). Th1, Th2, and Beyond: What We Know About Adaptive Immunity for Fungal Infections. *Internat. J. Clin. Rev.* 4 (3), 96–103. doi: 10.5275/ijcr.2010.12.05

Parente, J. A., Salem-Izacc, S. M., Santana, J. M., Pereira, M., Borges, C. L., Bailão, A. M., et al. (2010). A Secreted Serine Protease of *Paracoccidioides brasiliensis* and Its Interactions with Fungal Proteins. *BMC Microbiol.* 10 (1), 292. doi: 10.1186/1471-2180-10-292

Parente, A. F. A., Bailão, A. M., Borges, C. L., Parente, J. A., Magalhães, A. D., Ricart, C. A. O., et al. (2011). Proteomic Analysis Reveals That Iron Availability Alters the Metabolic Status of the Pathogenic Fungus *Paracoccidioides brasiliensis*. *PloS One* 6 (7), e22810. doi: 10.1371/journal.pone.0022810

Parente-Rocha, J. A., Parente, A. F. A., Baeza, L. C., Bonfim, S. M. R. C., Hernandez, O., McEwen, J. G., et al. (2015). Macrophage Interaction with *Paracoccidioides brasiliensis* Yeast Cells Modulates Fungal Metabolism and Generates a Response to Oxidative Stress. *PloS One* 10 (9), e0137619. doi: 10.1371/journal.pone.0137619

Parise-Fortes, M. R., Pereira Da Silva, M. F., Sugizaki, M. F., Defaveri, J., Montenegro, M. R., Soares, A. M. V., et al. (2000). Experimental Paracoccidioidomycosis of the Syrian Hamster: Fungicidal Activity and Production of Inflammatory Cytokines by Macrophages. *Med. Mycol.* 38 (1), 51–60. doi: 10.1080/mmy.38.1.51.60

Pathakumari, B., Liang, G., and Liu, W. (2020). Immune Defence to Invasive Fungal Infections: A Comprehensive Review. *Biomed. Pharmacother.* 130, 110550. doi: 10.1016/j.biopha.2020.110550

Popi, F. A., Lopes, J. D., and Mariano, M. (2002). GP43 from *Paracoccidioides brasiliensis* Inhibits Macrophage Functions. An Evasion Mechanism of the Fungus. *Cell. Immunol.* 218 (1–2), 87–94. doi: 10.1016/S0008-8749(02)00576-2

Preite, N. W., Feriotti, C., Souza De Lima, D., Borges Da Silva, B., Condino-Neto, A., Pontillo, A., et al. (2018). The Syk-Coupled C-Type Lectin Receptors Dectin-2 and Dectin-3 Are Involved in *Paracoccidioides brasiliensis* Recognition by Human Plasmacytoid Dendritic Cells. *Front. Immunol.* 9, 464. doi: 10.3389/fimmu.2018.00464

Puccia, R., Vallejo, M. C., Matsuo, A. L., and Guilhen Longo, L. V. (2011). The *Paracoccidioides* Cell Wall: Past and Present Layers Toward Understanding Interaction with the Host. *Front. Microbiol.* 2, 257. doi: 10.3389/fmicb.2011.00257

Restrepo, A., Gómez, B. L., and Tobón, A. (2012). Paracoccidioidomycosis: Latin America's Own Fungal Disorder. *Curr. Fungal Infect. Rep.* 6 (4), 303–311. doi: 10.1007/s12281-012-0114-x

Restrepo, A., Cano, L. E., and González, A. (2015). The power of the small: the example of *Paracoccidioides brasiliensis* conidia. *Rev. Inst. Med. Trop. São Paulo* 57 (suppl 19), 5–10. doi: 10.1590/s0036-46652015000700003

Rodrigues, D. R., Dias-Melicio, L. A., Calvi, S. A., Peraçoli, M. T. S., and Soares, A. M. V. C. (2007). *Paracoccidioides brasiliensis* Killing by IFN-γ, TNF-α and GM-CSF Activated Human Neutrophils: Role for Oxygen Metabolites. *Med. Mycol.* 45 (1), 27–33. doi: 10.1080/13693780600981676

Santiago-Tirado, F. H., Onken, M. D., Cooper, J. A., Klein, R. S., and Doering, T. L. (2017). Trojan Horse Transit Contributes to Blood-Brain Barrier Crossing of a Eukaryotic Pathogen. *MBio* 8 (1), 1–16. doi: 10.1128/mBio.02183-16

Scherer, A. K., Blair, B. A., Park, J., Seman, B. G., Kelley, J. B., and Wheeler, R. T. (2020). Redundant Trojan Horse and Endothelial-Circulatory Mechanisms for Host-Mediated Spread of *Candida albicans* Yeast. *PloS Path.* 16 (8), e1008414. doi: 10.1371/journal.ppat.1008414

Shi, M., and Mody, C. H. (2016). Fungal Infection in the Brain: What We Learned from Intravital Imaging. *Front. Immunol.* 7, 292. doi: 10.3389/fimmu.2016.00292

Silva-Bailão, M. G., Cardoso Bailão, E. F. L., Lechner, B. E., Gauthier, G. M., Lindner, H., Melo Bailão, A. M., et al. (2014). Hydroxamate Production as a High Affinity Iron Acquisition Mechanism in *Paracoccidioides* spp. *PloS One* 9 (8), e105805. doi: 10.1371/journal.pone.0105805

Silvana dos Santos, S., Spadari Ferreira, K., and Almeida, S. R. (2011). *Paracoccidioides brasilinsis*-Induced Migration of Dendritic Cells and Subsequent T-Cell Activation in the Lung-Draining Lymph Nodes. *PloS One* 6 (5), e19690. doi: 10.1371/journal.pone.0019690

Souza, A. C. O., Favali, C., Soares, N. C., Machado Tavares, N., Sousa Jerônimo, M., Veloso, P. H., J., et al. (2019). New Role of *P. brasiliensis* α-Glucan: Differentiation of Non-Conventional Dendritic Cells. *Front. Microbiol.* 10, 2445. doi: 10.3389/fmicb.2019.02445

Taborda, C. P., da Silva, M. B., Nosanchuk, J. D., and Travassos, L. R. (2008). Melanin as a Virulence Factor of *Paracoccidioides brasiliensis* and Other Dimorphic Pathogenic Fungi: A Minireview. *Mycopathol* 165 (4–5), 331–339. doi: 10.1007/s11046-007-9061-4

Tavares, A. H., Fernandes, L., Lorenzetti Bocca, A., Silva-Pereira, I., and Felipe, M. S. (2015). Transcriptomic Reprogramming of Genus Paracoccidioides in Dimorphism and Host Niches. *Fungal Genet. Biol.* 81, 98–109. doi: 10.1016/j.fgb.2014.01.008

Teixeira, M. M., Theodoro, R. C., Nino-Vega, G., Bagagli, E., and Felipe, M. S. (2014). *Paracoccidioides* Species Complex: Ecology, Phylogeny, Sexual Reproduction, and Virulence. *PloS Path.* 10 (10), e1004397. doi: 10.1371/journal.ppat.1004397

Thind, S. K., Taborda, C. P., and Nosanchuk, J. D. (2015). Dendritic Cell Interactions with *Histoplasma* and *Paracoccidioides*. *Virulence* 6 (5), 424–432. doi: 10.4161/21505594.2014.965586

Traynor, T. R., and Huffnagle, G. B. (2001). Role of Chemokines in Fungal Infections. *Med. Mycol.* 39 (1), 41–50. doi: 10.1080/mmy.39.1.41.50

Voltan, A. R., De Cassia Orlandi Sardi, J., Pienna Soares, C., Pelajo Machado, M., Fusco Almeida, A. M., and Mendes-Giannini, M. J. S. (2013). Early Endosome

Antigen 1 (EEA1) Decreases in Macrophages Infected with *Paracoccidioides brasiliensis*.. *Med. Mycol.* 51 (7), 759–764. doi: 10.3109/13693786.2013.777859

Conflict of Interest: The author declares that the research was conducted in the absence of any commercial or financial relationships that could be construed as a potential conflict of interest.

frontiers in Cellular and Infection Microbiology

PERSPECTIVE
published: 15 March 2021
doi: 10.3389/fcimb.2021.619459

HIV-Associated Disseminated Histoplasmosis and Rare Adrenal Involvement: Evidence of Absence or Absence of Evidence

Mathieu Nacher[1,2], Kinan Drak Alsibai[3], Audrey Valdes[4], Philippe Abboud[5], Antoine Adenis[1,2], Romain Blaizot[2,6], Denis Blanchet[7], Magalie Demar[7,8], Félix Djossou[5], Loïc Epelboin[5], Caroline Misslin[9], Balthazar Ntab[10], Nadia Sabbah[11] and Pierre Couppié[2,6]*

[1] Centre d'Investigation Clinique (CIC) INSERM 1424, Centre hospitalier Andree Rosemon Cayenne, Cayenne, French Guiana, [2] Département Formation Recherche (DFR) Santé, Université de Guyane, Cayenne, French Guiana, [3] Service d'Anatomopathologie, Centre Hospitalier Andrée Rosemon, Cayenne, French Guiana, [4] Equipe Opérationnelle d'hygiène hospitalière, Centre hospitalier Andree Rosemon Cayenne, Cayenne, French Guiana, [5] Department of Dermatology, Centre hospitalier Andree Rosemon Cayenne, Cayenne, French Guiana, [6] Service des Maladies Infectieuses et Tropicales, Centre hospitalier Andree Rosemon Cayenne, Cayenne, French Guiana, [7] Laboratory, Centre hospitalier Andree Rosemon Cayenne, Cayenne, French Guiana, [8] Unité Mixte de Recherche (UMR) Tropical Biome and Immunopathology, Université de Guyane, Cayenne, French Guiana, [9] Service de Médecine, Centre hospitalier de l'Ouest Guyanais, Saint Laurent du Maroni, French Guiana, [10] Département d'Information Médicale, Centre hospitalier de l'Ouest Guyanais, Saint Laurent du Maroni, French Guiana, [11] Service d'endocrinologie diabétologie, Gastroentérologie, Centre Hospitalier Andrée Rosemon, Cayenne, French Guiana

OPEN ACCESS

Edited by:
Angel Gonzalez, University of Antioquia, Colombia

Reviewed by:
Blanca Samayoa, Universidad de San Carlos de Guatemala, Guatemala
Julio Zuniga Moya, University of Michigan, United States

***Correspondence:**
Mathieu Nacher
mathieu.nacher66@gmail.com

Specialty section:
This article was submitted to Fungal Pathogenesis, a section of the journal Frontiers in Cellular and Infection Microbiology

Received: *20 October 2020*
Accepted: *16 February 2021*
Published: *15 March 2021*

Citation:
Nacher M, Alsibai KD, Valdes A, Abboud P, Adenis A, Blaizot R, Blanchet D, Demar M, Djossou F, Epelboin L, Misslin C, Ntab B, Sabbah N and Couppié P (2021) HIV-Associated Disseminated Histoplasmosis and Rare Adrenal Involvement: Evidence of Absence or Absence of Evidence. Front. Cell. Infect. Microbiol. 11:619459. doi: 10.3389/fcimb.2021.619459

Adrenal histoplasmosis and primary adrenal insufficiency are mostly described in immunocompetent patients. This particular tropism is attributed to the presence of cortisol within the adrenal gland, a privileged niche for *Histoplasma* growth. In French Guiana, disseminated histoplasmosis is the main opportunistic infection in HIV patients. Our objective was to search in our HIV-histoplasmosis cohorts to determine how frequent adrenal insufficiency was among these patients. Between January 1, 1981 and October 1, 2014, a multicentric retrospective, observational study of histoplasmosis was conducted. Patients co-infected by HIV and histoplasmosis were enrolled in French Guiana's histoplasmosis and HIV database. Among 349 cases of disseminated histoplasmosis between 1981 and 2014, only 3 had adrenal insufficiency (0.85%). Their respective CD4 counts were 10, 14 and 43 per mm3. All patients had regular electrolyte measurements and 234/349 (67%) had abdominal ultrasonography and 98/349 (28%) had abdominopelvic CT scans. None of these explorations reported adrenal enlargement. Overall, these numbers are far from the 10% reports among living patients and 80-90% among histoplasmosis autopsy series. This suggests 2 conflicting hypotheses: First, apart from acute adrenal failure with high potassium and low sodium, less advanced functional deficiencies, which require specific explorations, may have remained undiagnosed. The second hypothesis is that immunosuppression leads to different tissular responses that are less likely to incapacitate the adrenal function. Furthermore, given the general immunosuppression, the adrenal glands no longer represent a particular niche for *Histoplasma* proliferation.

Keywords: Histoplasmosis, Advanced HIV, adrenal gland, French Guiana, Immunosuppression, AIDS-related opportunistic infections

INTRODUCTION

Histoplasmosis was discovered over a century ago. Its severity varies with the intensity of exposure and host immunity. In immunocompetent individuals, presentations hence range from asymptomatic infections or mild pulmonary disease for low-intensity exposures, to severe pulmonary infections for heavy exposures. A chronic lung infection may develop with gradual loss of pulmonary function among patients with underlying lung disease, and if untreated, it will result in death. Among immunosuppressed patients the infection progressively disseminates to other organs causing non-specific syndromes. Various organs such as the lungs, gastrointestinal tract, bone marrow, central nervous system, liver or lymph nodes may thus be involved in the same patient. Histoplasmosis has been an AIDS defining infection since 1987. It is estimated to be one of the main opportunistic infections and cause of death among patients with advanced HIV in Latin America (Adenis et al., 2018). The literature reviews on histoplasmosis often mention adrenal histoplasmosis and primary adrenal insufficiency (Wheat, 1989; Larbcharoensub et al., 2011; Koene et al., 2013). Most cases are described in immunocompetent patients, and the explanation of this particular tropism is that the presence of cortisol within the *zona reticularis* and *zona fasciculata* of the adrenal gland constitutes a privileged niche for the unhampered growth of *Histoplasma*. Studies in immunocompromised patients with disseminated histoplasmosis suggest 10% of patients have adrenal involvement but, autopsy studies report that 80-90% of patients have adrenal involvement (Goodwin et al., 1980; Wheat, 1989). The adrenal gland is a richly vascularized organ that contains cortex and medulla. The cortex produces several steroid hormones and the medulla produces catecholamines. The early adrenal response to infection is an increase in the functioning of the hypothalamic-pituitary-adrenal axis leading to increased local and systemic corticosteroid levels and adrenocorticotrophin (ACTH). ACTH causes increased blood flow to the adrenal gland, which is a predisposing condition for hemorrhage (Salim et al., 1988). The hypercortisolism deregulates the normal immune response in the sites of inflammation, by altering the cytokine production and function, and decreasing the migration of effector cells. Moreover, the local production and release of glucocorticoids by the cortex and a relative lack of phagocytic reticuloendothelial cells facilitate the tropism of *H. capsulatum* for the adrenal gland. The destruction of the adrenal gland may later occur *via* the direct effect of *H. capsulatum* leading to vasculitis resulting in local ischemia and caseation necrosis (Roubsanthisuk et al., 2002). In advanced HIV disease, adrenal exhaustion, infection with opportunistic pathogens, and development of anti-corticosteroid and anti-adrenal gland cells antibodies (Salim et al., 1988; Sinha et al., 2011) often low level of ACTH are considered as potential mechanisms for progression to overt adrenal insufficiency even when no apparent lesion with medical imagery.

In French Guiana, disseminated histoplasmosis has been the main opportunistic infection and cause of death in HIV patients for decades. The impression of clinicians regarding adrenal failure is that it is seldom observed. Our objective was to search in our HIV-histoplasmosis cohorts to determine how frequent adrenal insufficiency was among these patients.

THE FRENCH GUIANA HIV/ DISSEMINATED HISTOPLASMOSIS COHORT EXPERIENCE

Between January 1, 1981 and October 1, 2014, a multicentric retrospective, observational study of histoplasmosis was conducted. Patients co-infected by HIV and histoplasmosis were enrolled in French Guiana's histoplasmosis and HIV database. The inclusion criteria were: age >18 years, HIV infection; first proven episode of histoplasmosis following the EORTC/MSG criteria (De Pauw et al., 2008). Suspected but unproven histoplasmosis (patients cured by successful empirical antifungal therapy), diagnosis solely based on positive PCR, or histoplasmosis recurrence were not included. French Guiana is a French territory and as such hospitalized patients benefit from free explorations, treatments. Imagery such as ultrasonography, CT scanner, MRI are routinely prescribed for hospitalized patients in search of a diagnosis. Blood samples routinely measure electrolytes, notably sodium and potassium levels, which are markers of acute adrenal deficiency. The database was created in 1992. Incident HIV-associated histoplasmosis cases were included in the three hospitals of French Guiana. Sociodemographic, clinical, biological, immunovirological and therapeutic data were collected on a standardized paper form until October 2014: sex, age, place of birth, symptoms on admission, clinical entrance examination, immunovirological assessment, medical imaging, mycology, pathology, treatment received, duration, dosage, route of administration. Survival data was collected for the study period. STATA© (College Station, Texas, USA) was used for the statistical analysis. The analysis was descriptive with frequencies and percentages for qualitative variables and median and interquartile range for quantitative variable.

The 1992 Histoplasmosis and HIV anonymized database has been approved by the French National Institute of Health and Medical Research institutional review board (CEEI INSERM) (IRB0000388, FWA00005831 18/05/2010), by the Comité Consultatif pour le Traitement de l'Information pour la Recherche en Santé(CCTIRS) (N° 10.175bis, 10/06/2010), and the Commission Nationale Informatique et Libertés (CNIL) (n ° JZU0048856X, 07/16/2010).

The median age was 39 years (interquartile range (IQR)=34-46), the median CD4 count was 31 per mm3 (IQR=12-70). Among 349 cases of disseminated histoplasmosis between January 1, 1981 and October 1, 2014, only 3 had adrenal insufficiency (0.85%). Their respective CD4 counts were 10, 14 and 43 per mm3. The first patient, a 30-year-old male from Suriname, died 34 days after the diagnosis of acute adrenal failure the reported cause of death was disseminated histoplasmosis. Among all patients with disseminated histoplasmosis all had regular electrolyte measurements and

234/349 (67%) had abdominal ultrasonography and 98/349 (28%) had abdominopelvic CT scans. CT scans became increasingly frequent over time (Chi2 for trend, P<0.001). Before 2006, 13/50(26%) were explored with a CT scan whereas after 2005 81/150 patients (53%) were explored with an abdominal-pelvic CT scan. None of these explorations reported adrenal enlargement.

DISCUSSION

Here in a hospital cohort of 349 cases of disseminated histoplasmosis in patients with advanced HIV disease the proportion of patients with adrenal deficiency was 0.85%, and among patients having benefitted from abdominal imaging, none had reports of adrenal enlargement. Overall, these numbers are far from the 10% reports among living patients and 80-90% among histoplasmosis autopsy series. Our retrospective analysis was a significant limitation, and all patients were not explored in the same manner depending on their clinical presentation (for example, cases with diarrhea benefitted from colonoscopy whereas those with enlarged superficial lymphadenopathies were more likely to have lymph node aspiration or biopsy) or the availability of different diagnostic tools at the time of their diagnosis, possible sources of information bias (Nacher et al., 2020). In French Guiana, fungal culture was first implemented in 1998, liposomal amphotericin B became available in 2003, and, perhaps more importantly for the capacity to detect adrenal enlargement, over time the use of thoraco-abdomino-pelvic CT-scan became increasingly frequent. These factors could therefore lead to a cohort effect but given the relative frequency of blood electrolyte measurements and decades of CT-scans, it seems likely that patent adrenal failure and adrenal enlargement are indeed rare.

Adrenal involvement is not necessarily associated with functional adrenal insufficiency. A literature review of 242 patients with adrenal histoplasmosis spanning 41 years found that 41.3% had adrenal hypofunction (Koene et al., 2013). It was often diagnosed incidentally. During active tuberculosis the adrenal glands are one of the 5 main organs involved (Lam and Lo, 2001). A large autopsy study in Hong Kong found 52/871 (5.9%) patients with adrenal involvement. Of the 52, 7(13.4%) had Addison's disease due to bilateral involvement. Caseous necrosis and granulomatous inflammation with Langhan's giant cells were seen in 71% and 40% of patients, respectively (Lam and Lo, 2001). Histoplasmosis lesions in immunocompetent hosts also leads to granulomatous inflammation and proliferation which explains the frequently enlarged adrenal glands.

Histopathological lesions reflect host reactions against *H. capsulatum*. They are classified into 4 categories: (i) tuberculoid, (ii) anergic, (iii) mixed and (iv), *sequelae*. Tuberculoid lesions usually correspond to a low inoculum and effective host tissular response. Anergic responses are observed in HIV patients and there is scarce or no tissue response. Local macrophages are inactive. Typically, there is an abundance of intracellular and extracellular yeast. The mixed form is intermediate between tuberculoid and anergic. One interpretation of our results is that given the intense immune suppression in our cohort the tissular response does not lead to adrenal enlargement, which would explain why imagery (ultrasonography or CT scan) remained negative. However, functionally, in hospitalized patients that can benefit from any exploration in a European hospital, in a hot tropical country, (Hahner et al., 2010; Hahner et al., 2015) conditions which would be predicted to precipitate acute adrenal failure, we only found 3 cases. This suggests 2 conflicting hypotheses: First, apart from acute adrenal failure with high potassium and low sodium, less advanced functional deficiencies, which require specific explorations may have remained undiagnosed. This suggests that systematic testing –instead of clinically oriented explorations— of the adrenal response would have unmasked more cases and that there may be a need for systematizing screening protocols. The second hypothesis, is that immunosuppression leads to different tissular responses that are less likely to incapacitate the adrenal gland function. Furthermore, given the general immunosuppression, the adrenal glands no longer represent a particular niche for *Histoplasma* proliferation. While the second hypothesis is hardly testable, the first one seems quite feasible and systematically testing the adrenal function would allow to determine whether the rarity of diagnoses of adrenal involvement in patients with advanced HIV is evidence of absence of adrenal insufficiency or whether the lack of systematic explorations is simply absence of evidence.

DATA AVAILABILITY STATEMENT

Upon approval by the Commission Nationale Informatique et Libertés, the raw data supporting the conclusions of this article will be made available by the authors, without undue reservation.

ETHICS STATEMENT

The studies involving human participants were reviewed and approved by French National Institute of Health and Medical Research institutional review board (CEEI INSERM) (IRB0000388, FWA00005831 18/05/2010). The patients/participants provided their written informed consent to participate in this study.

AUTHOR CONTRIBUTIONS

MN-conception, first draft writing and final draft approval; KDA PC-validation and and editing; PA, AA, DB, RB, FD, MD, LE, CM, BN, NS, AV-review, investigation. All authors contributed to the article and approved the submitted version.

REFERENCES

Adenis, A. A., Valdes, A., Cropet, C., McCotter, O. Z., Derado, G., Couppie, P., et al. (2018). Burden of HIV-associated histoplasmosis compared with tuberculosis in Latin America: a modelling study. *Lancet Infect. Dis.* 18, 1150–1159. doi: 10.1016/S1473-3099(18)30354-2

De Pauw, B., Walsh, T. J., Donnelly, J. P., Stevens, D. A., Edwards, J. E., Calandra, T., et al. (2008). Revised definitions of invasive fungal disease from the European Organization for Research and Treatment of Cancer/Invasive Fungal Infections Cooperative Group and the National Institute of Allergy and Infectious Diseases Mycoses Study Group (EORTC/MSG) Consensus Group. *Clin. Infect. Dis.* 46, 1813–1821. doi: 10.1086/588660

Goodwin, R. A. Jr., Shapiro, J. L., Thurman, G. H., Thurman, S. S., and DES PREZ, R. M. (1980). Disseminated histoplasmosis: clinical and pathologic correlations. *Medicine* 59, 1–33. doi: 10.1097/00005792-198001000-00001

Hahner, S., Loeffler, M., Bleicken, B., Drechsler, C., Milovanovic, D., Fassnacht, M., et al. (2010). Epidemiology of adrenal crisis in chronic adrenal insufficiency: the need for new prevention strategies. *Eur. J. Endocrinol.* 162, 597–602. doi: 10.1530/EJE-09-0884

Hahner, S., Spinnler, C., Fassnacht, M., Burger-Stritt, S., Lang, K., Milovanovic, D., et al. (2015). High Incidence of Adrenal Crisis in Educated Patients With Chronic Adrenal Insufficiency: A Prospective Study. *J. Clin. Endocrinol. Metab.* 100, 407–416. doi: 10.1210/jc.2014-3191

Koene, R. J., Catanese, J., and Sarosi, G. A. (2013). Adrenal hypofunction from histoplasmosis: a literature review from 1971 to 2012. *Infection* 41, 757–759. doi: 10.1007/s15010-013-0486-z

Lam, K. Y., and Lo, C. Y. (2001). A critical examination of adrenal tuberculosis and a 28-year autopsy experience of active tuberculosis. *Clin. Endocrinol.* 54, 633–639. doi: 10.1046/j.1365-2265.2001.01266.x

Larbcharoensub, N., Boonsakan, P., Aroonroch, R., Rochanawutanon, M., Nitiyanant, P., Phongkitkarun, S., et al. (2011). Adrenal histoplasmosis: a case series and review of the literature. *Southeast Asian J. Trop. Medicineand Public Health* 42, 920.

Nacher, M., Valdes, A., Adenis, A., Blaizot, R., Abboud, P., Demar, M., et al. (2020). Heterogeneity of Clinical Presentations and Paraclinical Explorations to Diagnose Disseminated Histoplasmosis in Patients with Advanced HIV: 34 Years of Experience in French Guiana. *J. Fungi (Basel Switzerland)* 6. doi: 10.3390/jof6030165

Roubsanthisuk, W., Sriussadaporn, S., Phoojaroenchanachai, M., Peerapatdit, T., Nitiyanant, W., Vannasaeng, S., et al. (2002). Primary adrenal insufficiency caused by disseminated histoplasmosis: report of two cases. *Endocrine Pract.* 8, 237–241. doi: 10.4158/EP.8.3.237

Salim, Y. S., Faber, V., Wiik, A., Andersen, P. L., HØIer-Madsen, M., and Mouritsen, S. (1988). Anti-corticosteroid antibodies in AIDS patients. *Apmis* 96, 889–894.

Sinha, U., Sengupta, N., Mukhopadhyay, P., and Roy, K. S. (2011). Human immunodeficiency virus endocrinopathy. *Indian J. Endocrinol. Metab.* 15, 251–260. doi: 10.4103/2230-8210.85574

Wheat, L. J. (1989). Diagnosis and management of histoplasmosis. *Eur. J. Clin. Microbiol. Infect. Dis.* 8, 480–490. doi: 10.1007/BF01964063

Conflict of Interest: The authors declare that the research was conducted in the absence of any commercial or financial relationships that could be construed as a potential conflict of interest.

frontiers in Cellular and Infection Microbiology

ORIGINAL RESEARCH
published: 16 March 2021
doi: 10.3389/fcimb.2021.622899

β2 Integrin-Mediated Susceptibility to *Paracoccidioides brasiliensis* Experimental Infection in Mice

Stephan Alberto Machado de Oliveira[1,2‡], Janayna Nunes Reis[1‡], Elisa Catão[2], Andre Correa Amaral[3], Ana Camila Oliveira Souza[1†], Alice Melo Ribeiro[2], Lúcia Helena Faccioli[4], Fabiana Pirani Carneiro[5], Clara Luna Freitas Marina[6], Pedro Henrique Bürgel[6], Larissa Fernandes[7], Aldo Henrique Tavares[7] and Anamelia Lorenzetti Bocca[1,2,6]*

[1] Molecular Pathology Graduation Course, Faculty of Medicine, University of Brasilia, Brasilia, Brazil, [2] Department of Cell Biology, Institute of Biological Sciences, University of Brasilia, Brasilia, Brazil, [3] Institute of Tropical Pathology and Public Health, Federal University of Goiás, Goiania, Brazil, [4] Faculty of Pharmaceutical Sciences of Ribeirão Preto, University of São Paulo, Ribeirão Preto, Brazil, [5] Area of Pathology, Faculty of Medicine, University of Brasilia, Brasilia, Brazil, [6] Molecular Biology Graduation Course, Institute of Biological Sciences, University of Brasilia, Brasilia, Brazil, [7] Faculty of Ceilândia, University of Brasília, Brasília, Brazil

The earliest interaction between macrophages and *Paracoccidioides brasiliensis* is particularly important in paracoccidioidomycosis (PCM) progression, and surface proteins play a central role in this process. The present study investigated the contribution of β2 integrin in *P. brasiliensis*-macrophage interaction and PCM progression. We infected β2-low expression ($CD18^{low}$) and wild type (WT) mice with *P. brasiliensis* 18. Disease progression was evaluated for fungal burden, lung granulomatous lesions, nitrate levels, and serum antibody production. Besides, the *in vitro* capacity of macrophages to internalize and kill fungal yeasts was investigated. Our results revealed that $CD18^{low}$ mice infected with Pb18 survived during the time analyzed; their lungs showed fewer granulomas, a lower fungal load, lower levels of nitrate, and production of high levels of IgG1 in comparison to WT animals. Our results revealed that *in vitro* macrophages from $CD18^{low}$ mice slowly internalized yeast cells, showing a lower fungal burden compared to WT cells. The migration capacity of macrophages was compromised and showed a higher intensity in the lysosome signal when compared with WT mice. Our data suggest that β2 integrins play an important role in fungal survival inside macrophages, and once phagocytosed, the macrophage may serve as a protective environment for *P. brasiliensis*.

Keywords: $CD18^{low}$ mice, nitric oxide, β2 integrin, *Paracoccoidioides brasiliensis*, susceptibility

OPEN ACCESS

Edited by:
Angel Gonzalez, University of Antioquia, Colombia

Reviewed by:
Flavio Vieira Loures, Federal University of São Paulo, Brazil
Claudia Feriotti, Queen's University Belfast, United Kingdom
Sandro Rogerio Almeida, University of São Paulo, Brazil

***Correspondence:**
Anamelia Lorenzetti Bocca
albocca@unb.br

***Present address:**
Ana Camila Oliveira Souza, Department of Pharmaceutical Sciences, St Jude Children's Research Hospital, Memphis, TN, United States

These authors have contributed equally to this work

Specialty section:
This article was submitted to Fungal Pathogenesis, a section of the journal Frontiers in Cellular and Infection Microbiology

Received: *29 October 2020*
Accepted: *25 January 2021*
Published: *16 March 2021*

Citation:
de Oliveira SAM, Reis JN, Catão E, Amaral AC, Souza ACO, Ribeiro AM, Faccioli LH, Carneiro FP, Marina CLF, Bürgel PH, Fernandes L, Tavares AH and Bocca AL (2021) β2 Integrin-Mediated Susceptibility to Paracoccidioides brasiliensis Experimental Infection in Mice. Front. Cell. Infect. Microbiol. 11:622899. doi: 10.3389/fcimb.2021.622899

INTRODUCTION

Paracoccidioides brasiliensis (Pb) is a facultative intracellular fungus that causes paracoccidioidomycosis (PCM), a deep, chronic, and granulomatous disease prevalent in Latin America (Bocca et al., 2013). The disease manifests in multiple forms that range from benign and localized lesions to severe and disseminated infection, depending on the extent of the lowering of

cellular immunity (Restrepo et al., 2008; Mendes et al., 2017). As described for other systemic mycoses, cellular immune response, mediated mainly by IFN-γ activated macrophages, is the host's major defense mechanism against PCM (Bocca et al., 1999; Souto et al., 2000; Souto et al., 2003; Schimke et al., 2017). Activated macrophages show a fundamental role during all the disease outcomes, along with granuloma formation, to protect the host against the dissemination of the infection (Bocca et al., 1999; Souto et al., 2000; Pagliari et al., 2019). Granuloma formation relies on the secretion of cytokines such as IFN-γ and TNF-α, which confer resistance against Pb by macrophage activation, fungal contention, and nitric oxide (NO) production, resulting in the killing of the pathogen (Pagliari et al., 2019). Furthermore, IFN-γ modulates chemokines and chemokine receptors' macrophage expression and the lung cellular infiltration pattern in mice experimentally infected with Pb (Souto et al., 2000). During PCM development, all antibody isotypes are increased in the highest amounts. They are reflected in the immune response's polarization, since they are closely associated with Th1 and Th2 immune responses (Mamoni et al., 2002; Pinto et al., 2006; Tristão et al., 2013).

Although the host cellular immune response shows an essential role against infection, the interaction mechanisms involved in macrophage activation have not yet been thoroughly described. Due to the complexity of the interaction between the host and Pb, various studies have attempted to unveil the fungus' innate host defense mechanisms (Calich et al., 2008; Pagliari et al., 2019). The interaction of host macrophages and Pb is mediated by cell surface receptors on the outer membrane of the macrophage, including mannose receptor, C-type lectin receptors (CTLR), such as dectin-1, Toll-like receptor 2 (TLR-2), TLR-4, surfactant protein, scavenger receptor, and complement receptor types 3 (CR3) and 4 (CR4) (Jimenez Mdel et al., 2006; Calich et al., 2008; Tan, 2012; Feriotti et al., 2013). Pb yeasts opsonized with fresh serum are more efficiently internalized than when opsonized with inactivated serum; therefore, CR3 shows particular importance in fungal internalization (Jimenez Mdel et al., 2006). The Pb yeast form can activate both the classical and alternative complement pathways *in vitro*, resulting in opsonization and phagocytosis by macrophages (Calich et al., 2008). CR3 is a receptor related to the fungal internalization by macrophages from both susceptible and resistant mice to fungus infection, while mannose receptors are associated only with phagocytes from resistant mice. This difference could influence the host's susceptibility mechanisms during fungal infection (Jimenez Mdel et al., 2006). CR3 (CD11b/CD18) and CR4 (CD11c/CD18) share the beta subunit CD18, which is a heterodimer that belongs to the leukocyte β2-integrin family (Tan, 2012).

Integrin is a cell adhesion molecule that shows an important role in immunity, wound healing, and hemostasis (Tan, 2012). The β2 integrins comprise four members: LFA-1 (CD11a/CD18), Mac-1 or CR3 (CD11b/CD18), p150,95 or CR4 (CD11c/CD18), and αDβ2 (CD11d/CD18). CR3 and CR4 are mainly expressed in myeloid origin cells and mediate phagocytosis *via* iC3b-opsonized particles; they are also involved in monocytes' adhesion to endothelial cells. Moreover, CR3 can mediate microorganism phagocytosis by recognizing the β 1-3 glucan component present on the cell wall of some fungi (Ross et al., 1987). The CR3 role in recognition and phagocytosis of different microbes has been described, including *Mycobacterium tuberculosis*, *Candida albicans*, *Francisella tularensis*, and *Cryptococcus neoformans* (Fukazawa and Kagaya, 1997; Velasco-Velasquez et al., 2003; Luo et al., 2006; Dai et al., 2013). Besides their phagocytosis role, during *Streptococcus pneumonie*, pulmonary infection, CR3 showed another important role in disease prevention: regulating neutrophil and T cell recruitment into the lung (Kadioglu et al., 2011). However, CR3 has also been related to a harmful role in the immune response to *Leishmania major* infection (Polando et al., 2013; Ricardo-Carter et al., 2013). The engagement of CR3 by various *Leishmania* ligands inhibits IL-12 and NO production by a mechanism independent of NFκB, MAPK, IRF, and ETS in an experimental model using CD11b-deficient mice (Ricardo-Carter et al., 2013). Furthermore, using the same experimental model, *Leishmania* opsonization with fresh serum influences phagosome trafficking and delays the maturation process (Polando et al., 2013).

Previous studies have linked an important role for CR3 in macrophage-Pb interaction and fungal phagocytosis. However, the CR3 role in the outcome of different experimental infection models is not a consensus. Here, we investigated the role of β2 integrins, low expression macrophages, during the *in vivo* and *ex-vivo P. brasiliensis* infection to better understand the importance of high internalization of fungal yeasts for fungal survival in macrophages.

MATERIALS AND METHODS

Fungal Strain

The yeast form of a high virulent strain of *P. brasiliensis* (Pb18) was obtained from the fungal collection of the Laboratory of Applied Immunology's fungal library. It was previously kindly provided by Dr. Peraçoli, from Unesp/Botucatu. It was maintained in mice, and to perform the experiments, fungal cells were recovered and grown in YPD culture medium at 36°C for five days. The yeast cells were then washed in phosphate-buffered saline (PBS) and adjusted to $1x10^7$ yeast/ml.

Mice

Eight-week-old (n=24) C57BL/6 (WT) and homozygous *CD18low* mice of the C57BL/6 background were obtained from the animal facilities of the Pharmaceutical Science Faculty of Ribeirão Preto – University of São Paulo (FCFRP-USP), Brazil. The *CD18low* (B6.129S7-Itgb2^{tm1bay}) mice were purchased at the Jackson Laboratory and serve as a model for the moderate form of human CD18 deficiency. Mice were placed in propylene cages in a controlled temperature room, fed with a standard diet, and given water *ad libitum*. The Animal Ethics Committee of the University of Brasilia approved all experiments using animal subjects (UnBDOC n°. 33798/2007).

In vivo experiments, mice were infected *via* intravenous (iv) route with 10^6 yeast forms of Pb 18 to mimic a disseminated infection (n= 12 animal/group). At 15-, 30-, and 60-days post-infection, four animals per point were euthanized, and blood, lung, and spleen samples were aseptically collected for later analysis. For representative survival curves, we used the Kaplan-Meier estimator of an experimental intravenous infection carried out in WT and $CD18^{low}$ mice with a suspension of 1×10^6 Pb18, as previously described (Goel et al., 2010). Data were expressed as a percentage of live animals observed for 120 days (Granger et al., 1996). For *ex-vivo* analysis, mice were intraperitoneally inoculated with 3 ml of thioglycolate 3% and euthanized after four days for peritoneal macrophage collection.

Fungal Burden Assay

Infection was assessed by counting the number of Colony Forming Units (CFUs) of *P. brasiliensis* recovered from infected mice's lungs. Four animals from each group were euthanized by CO_2 chamber at indicated time points, and the lungs were aseptically collected. One longitudinal section of each lung was weighed and macerated within sterilized PBS. One hundred μl from the homogenized lung tissues was plated into BHI agar supplemented with 4% horse serum; 5% *P. brasiliensis* 192 isolate yeast culture filtrated supernatant, and 40 mg/L of gentamicin (Gentamicin Sulfate, Schering-Plough, Rio de Janeiro, Brazil). Plates were incubated for seven days at 37°C, and CFUs were counted.

Histopathologic and Histocytometry Analysis

Liver and lung fragments were removed from the two experimental groups and fixed in 10% phosphate-buffered formalin for 6 h, followed by 70% ethanol until embedding in paraffin. Several 5-μm sections were stained with H&E for light microscopic analysis. The diameters of the granulomatous lesions in the lung were quantified by histocytometry using an image analyzer (Image Pro-Plus Version 5.1.0.20 Copyright 1993-2004- Media Cybernectics, Inc.). and a computer and compared to the size of the fragment. The mean size of the lesions and the mean percentage of the lesioned area of the lung were also determined. The data were obtained by triplicate analysis of the sections performed by two observers.

NO Production

The concentration of nitric oxide (NO) in the serum was determined by enzymatically reducing nitrate to nitrite with nitrate reductase, as previously described (Pina et al., 2008). The total amount of nitrite was then quantified by the Griess method. A microplate reader measured the absorbance at 540 nm.

Lysosome Staining

To perform the staining of acid organelles, 1×10^5 intraperitoneal macrophages were seeded in chamber slides and incubated at 37° C and 5% CO2. Next, the cells were co-incubated with *P. brasiliensis* (MOI 1:0.5) previously stained with Calcofluor (Sigma-Aldrich, St. Louis, MO, USA). After 24 h, extracellular fungi were washed with RPMI medium, and the cells were stained with Lysotracker® Red DND-99 (Thermo Scientific, Waltham, MA, USA) (1:1,000) for 15 min at 37°C and directly used for microscopy using the Live Cell Imaging approach. Lysotracker Mean Fluorescent Intensity (MFI) was measured using ImageJ software.

Antibody Isotypes Analysis

The specific IgG1 and IgG2a isotypes were measured in the serum by Enzyme-Linked ImmunoSorbent Assay (ELISA) (Sigma-Aldrich, St. Louis, MO, USA) as per the manufacturer's instructions. Briefly, 96-well plates were coated overnight at 4°C with protein extract of the fungal cell wall (100 μl/well). The plates were blocked with mouse serum (1:100) for 2h at 37°C. The serum samples were added to the plates and incubated for 2 h at room temperature. After washing with PBS 0.05% Tween 20, peroxidase-labeled antibodies specific for mouse IgG1 or IgG2a isotypes were added (1:5,000), and plates were incubated for 2h at 37°C. Next, the plates were washed seven times with PBS 0.05% Tween 20 and incubated with H_2O_2 and o-phenylenediamine for the reaction. After the addition of 20 μl of H_2SO_4, 2N (stop solution), the reactions were read at 490 nm in an ELISA plate reader (BioRad, model 2550, Hercules, CA, USA).

Cytokine Secretion

The cytokines interleukin-10 (IL-10), interferon-gamma (IFN-γ), and TNF-α were measured using a commercial ELISA kit (according to the guidelines established by BD Biosciences, San Diego, CA, USA). The cytokine levels present in the lung homogenates or cell culture supernatant were calculated based on a standard curve provided by the commercial kit.

Cellular Migration

The percentages of migrating cells were determined at 72 h after Pb18 heat killed (HKPb18, $1x10^6$ cells) or thioglycolate (1.5 ml of 3% solution) inoculation into mice peritoneum. At four days post-inoculation, WT, and $CD18^{low}$ mice were euthanized using 80 mg/kg of ketamine and 16 mg/kg of xylazine, and the peritoneal contents were washed with 5 ml of Hank's solution for leukocyte collection. The total cell suspension was centrifuged, and the pellet was resuspended in RPMI-1640 with 5% of fetal bovine serum (Sigma-Aldrich, St. Louis, MO, USA). The cells were counted in a hemocytometer chamber in the presence of trypan blue. For differential counting, cytospins were stained with a Panótico® kit (Laborclin, Brasília, DF, Brazil) to identify specific leukocytes (neutrophils, macrophages, and lymphocytes). The flow cytometry approach is used to analyze the pulmonary cell migration profile. Mice were infected with 1x105 heat-killed *P. brasiliensis* yeast (HKPb18) in the intranasal route. After three days, a collection of bronchoalveolar lavage (BAL) fluid was performed, and the mice were euthanized by CO2 overdose. Cold PBS and a 1-inch 22G catheter without a needle into the trachea were used to perform the lavage. Moreover, 5x105 cells were blocked with PBS, supplemented

with 10% FBS for 1 h. After washing, cells were stained with anti-CD3 APC and anti-F4/80 FITC (Invitrogen, Carlsbad, Califórnia, USA) for 30 min, in ice, in the dark. Next, cells were washed two times and analyzed by Flow Cytometry.

Ex-Vivo Phagocytosis Index

The kinetics of Pb18 internalization by the phagocytosis index was also investigated. At 6, 24, and 48 h after co-culture, the supernatant was removed, and the cells were stained with Panotico® (Laborclin, Brasília, DF, Brazil). Phagocytosis was measured under the optic microscope (100×) in approximately one hundred cells. Phagocytosis index was determined by calculating the number of internalized cells in the phagocytosis and the yeasts' average phagocytosed by the macrophages. A similar experiment was performed with fluorescent microscopy to identify and differentiate intra- and extracellular Pb18. Before co-incubation with macrophages, fungi were stained with 3 mg/ml of Fluorescein isothiocyanate (FITC) (Sigma-Aldrich, St. Louis, MO, USA) for 2 h in the dark at room temperature. Next, Pb18 was washed and incubated with macrophages for 24 h. After washing extracellular fungi, Calcofluor staining (Sigma-Aldrich, St. Louis, MO, USA) (10 ug/ml) was performed for 20 min at 37°C in the dark. After washing, phagocytosis index was measured by fluorescent microscopyA similar experiment was performed with fluorescent microscopy to identify and differentiate intra- and extracellular Pb18. Before co-incubation with macrophages, fungi were stained with 3 mg/ml of Fluorescein isothiocyanate (FITC) (Sigma-Aldrich, St. Louis, MO, USA) for 2 h in the dark at room temperature. Next, Pb18 was washed and incubated with macrophages for 24 h. After washing extracellular fungi, Calcofluor staining (Sigma-Aldrich, St. Louis, MO, USA) (10 ug/ml) was performed for 20 min at 37°C in the dark. After washing, phagocytosis index was measured by fluorescent microscopy. Data are expressed as mean ± SEM of three independent experiments.

Statistical Analysis

Differences between the two experimental groups were analyzed by using ANOVA followed by the Bonferroni t-test. The p-value of <0.05 was considered significant

RESULTS

β2 Integrin Influences Host Survival in *P. brasiliensis* Infection

To evaluate the course of the chronic model of PCM in the β2 integrin low expression model, WT, and CD18^{low} mice were infected with a virulent strain of *P. brasiliensis* (Pb18) *via* i.v. route and monitored for survival for 120 days (**Figure 1**). Mice from both groups displayed clinical evidence of disease, and WT mice survived, on average, approximately 90 days. However, all infected CD18^{low} mice survived during the entire time course. At this point of infection, CD18^{low} mice were euthanized to perform the lung analysis, in which we observed lung granulomatous lesions and viable fungal cells within granuloma (data not shown). Nevertheless, CD18^{low} mice showed higher resistance to Pb18 infection in comparison to WT mice.

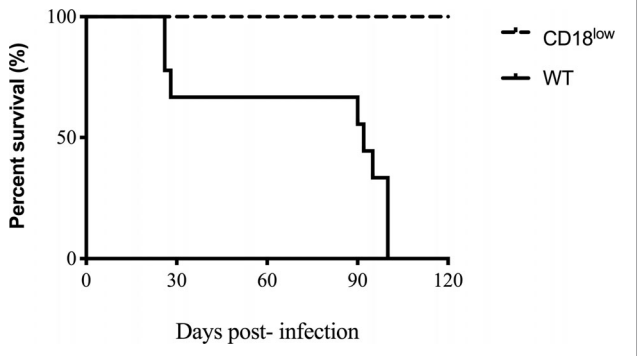

FIGURE 1 | Survival curve of WT and CD18^{low}. Mice were infected *via* i.v. with 10^6 yeast forms of *P. brasiliensis* (Pb18) to mimic a chronic infection. Kaplan-Meier estimator was used to represent WT representative survival curves (solid line) and CD18^{low} (dashed line). For both groups, n=12. Data are expressed as the percentage of live animals observed for 120 days.

Positive Outcome in CD18^{low} Mice After *P. brasiliensis* Infection

To investigate Pb infection kinetics in WT and CD18^{low} expression mice, lungs were aseptically removed and macerated to recover fungal burden. According to survive curve days related to mice mortality, the mice were euthanized at 15, 30, and 60 days post-infection. Sine *P. brasiliensis* is a facultative intracellular fungus and can grow outside macrophages, is option to use the whole tissue is to evaluate the total fungal population viability. A higher number of CFUs was observed in tissue recovered from CD18^{low} mice at 15 days post-infection when compared to WT animals. However, at 60 days post-infection, the CFU and the granuloma structures were higher in WT than CD18^{low} (**Figure 2A**). The fungal cells can also be observed in the granuloma (**Figures 2B–E**).

The histopathological analyses depict granuloma in both WT (**Figures 2B, C**) and CD18^{low} mice lung tissue (**Figures 2B, D**) at 15 days post-infection. WT mice lung granulomas were well organized, composed of epithelioid cells, lymphocytes, and a few multinuclear giant cells characterizing epithelioid granulomas. The CD18^{low} mice lungs showed granulomas with a reduction of the alveolar spaces, with lymphocyte infiltration and significant yeast levels at 15 days post-infection (**Figure 2D**). However, at 60 days post-infection, the granulomas in WT mice were less organized, showing an incipient pattern of granulomatous structures, with multinuclear giant cells within yeast forms fungus (**Figure 2E**). Besides, at 60 days post-infection, in the disease's disseminated phase, the granulomas were more organized in CD18^{low} mice, with an increase in lymphocyte migration (**Figure 2F**). Comparing the granuloma lesion sizes between the groups, CD18^{low} mice granulomas impaired a lower area of lung (**Figure 2B**), so the lung was less compromised.

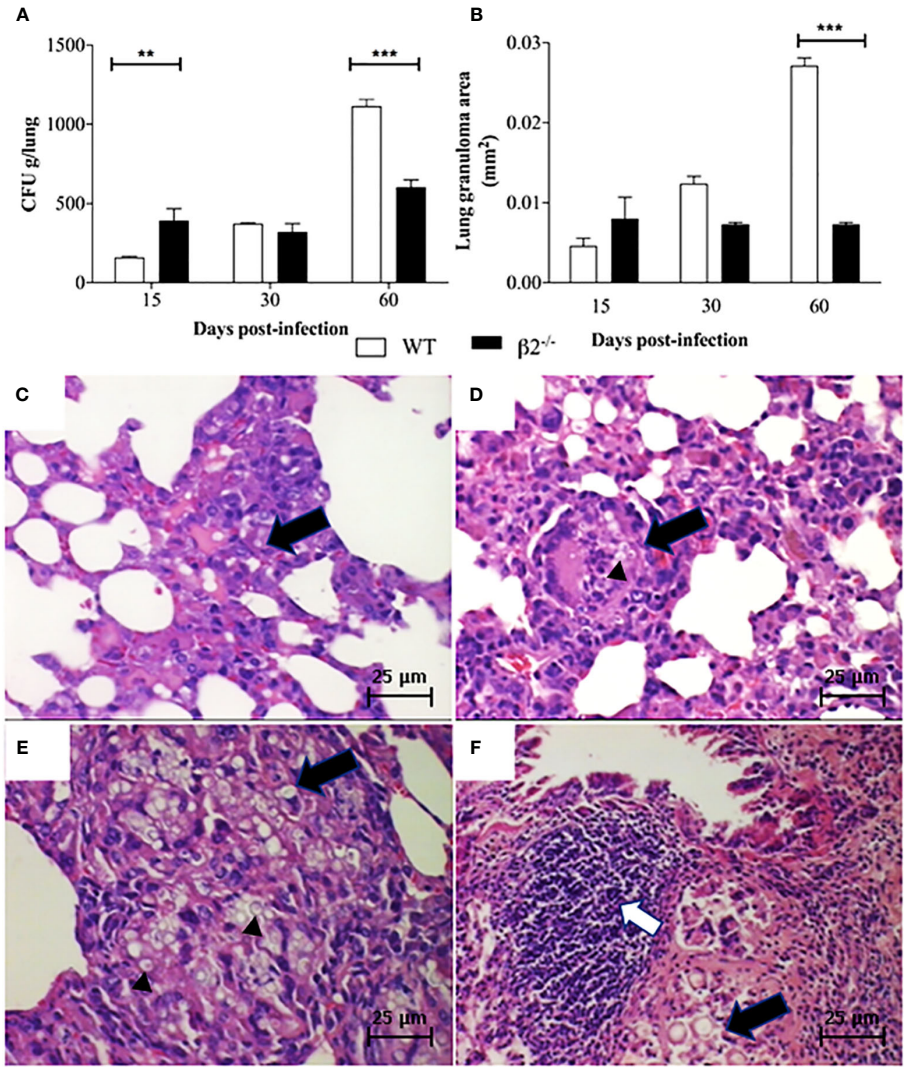

FIGURE 2 | Fungal burden and granuloma in lung tissue. Mice were infected *via* i.v. with 10^6 yeast forms of *P. brasiliensis* (Pb18) to mimic a disseminated infection. **(A)** Analysis of fungal burden of lung CFUs *in vivo*. **(B)** Measurement of the granuloma size in the lung tissue of infected animals. **(C, D)** Histological images of the granuloma formation (black arrows) and presence of yeast (black arrow head in Figure D) in WT and $CD18^{low}$ mice at 15 days post-infection – 100x. **(E, F)** histological images represented granuloma formation (black arrows), and presence of yeast (black arrow head in Figure E) and lymphocytic infiltrate (white arrow) in WT and $CD18^{low}$ mice 60 days post-infection – 100x. Data are presented as the mean ± SEM of three independent experiments (**significant difference $p<0.01$, ***significant difference $p<0.001$).

Nitric Oxide and Cytokine Secretion Are Altered in the Course of $CD18^{low}$ or WT Mice Infection

The serums nitrate levels were measured in the WT and $CD18^{low}$ *P. brasiliensis* infected mice to evaluate the nitric oxide production. At 15 and 60 days, post-infection, higher levels of nitrate were found in WT serum compared to $CD18^{low}$ mice. At 60 days post-infection, the NO production was higher in WT mice (**Figure 3A**). No differences were observed at 30 days post-infection. Regarding the levels of IgG1 and IgG2a, antibody production was not observed in the serum of WT non-infected mice (data not shown). On the other hand, IgG1 levels were significantly higher in the serum of $CD18^{low}$ infected mice compared with WT infected mice at all evaluated time points (**Figure 3B**). Nevertheless, levels of anti-*P. brasiliensis* IgG2a increased significantly in the serum of $CD18^{low}$ mice only at day 60 post-infection.

Concerning cytokine secretion, IL-10, IL-12, TNF-α, and IFN-γ were quantified in lung cell homogenates. A significantly higher level of IL-10 in $CD18^{low}$ mice was observed at 15 days post-infection in comparison to WT mice (**Figure 3C**). No significant differences were found when analyzing the presence

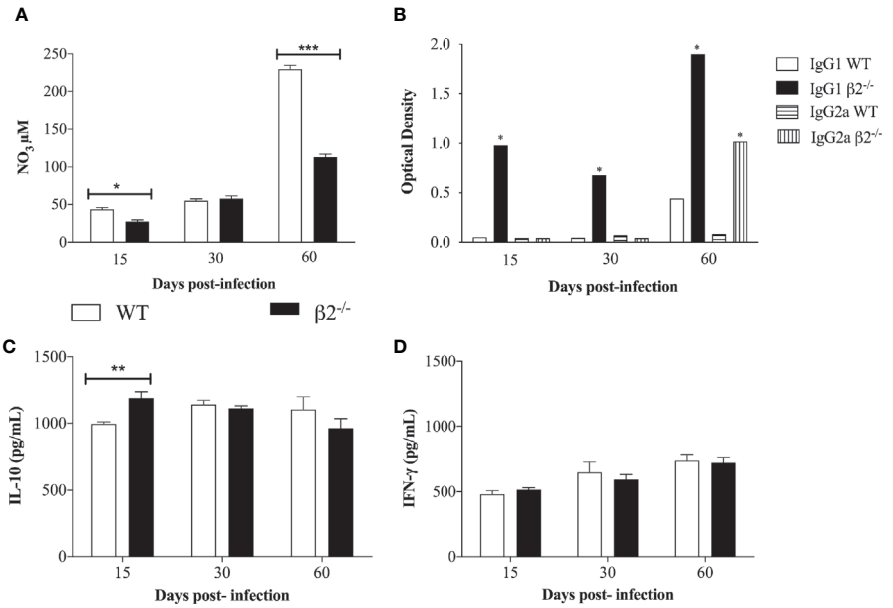

FIGURE 3 | Quantification of nitric oxide, IgG1, and IgG2 and cytokine secretion in a *P. brasiliensis* infection systemic model. Mice were infected *via* i.v. with 10^6 yeast forms of *P. brasiliensis* (Pb18) to mimic a chronic infection. **(A)** NO3 production was determined at 15-, 30-, and 60- days post-infection by Griess reagent. **(B)** IgG1 and IgG2a isotype levels in serum of WT and $CD18^{low}$ mice were detected after 15-, 30- and 60- days post-infection by ELISA. The antibody titers were expressed in optic density (O.D). **(C, D)** IL-10 and IFN-γ secretion analyzed by ELISA from lung cell homogenates. Data are expressed as the mean ± SEM. (*Indicates significant difference $p<0.05$; **significant difference $p<0.01$, ***significant difference $p<0.001$).

of IFN-γ (**Figure 3D**). There were no statistical differences in TNF- α and IL-12 levels between the groups (**Supplementary Figure 1**). It is possible to correlate the higher CFU in $CD18^{low}$ mice at 15 days post-infection with the low NO_3 secretion at this time point. Among other functions, IL-10 is also stimulatory toward TCD8+ cells, and this can be associated with the decrease in the CFU at 60 days post-infection in $CD18^{low}$ mice.

Cellular Migration After *P. brasiliensis* Stimulus

To analyze whether the differences between granuloma formation could be associated with cellular migration to the inflammatory site, since the molecules that depend on β2 integrin expression to promote the cell migration were decreased, we checked the leukocyte migration into the peritoneum after stimulation with heat-killed *P. brasiliensis* yeast (HKPb18) or thioglycolate. No difference in the percentage of total migrating leukocytes was detected between WT and $CD18^{low}$ mice, although the thioglycolate treatment induced higher cellular migration (**Figure 4A**). Considering the differential migration into the WT peritoneum, thioglycolate stimulus caused more significant macrophage migration than neutrophils and lymphocytes (**Figure 4B**). The migration into the $CD18^{low}$ mice peritoneum showed significantly higher lymphocyte migration levels after both treatments (**Figure 4B**). To compare the lung's migration profile, we carried out the cell migration using heat-killed *P. brasiliensis* yeast (HKPb18) in the intranasal route (**Supplementary Figure 2**). The CD18low BAL confirmed the higher levels of lymphocyte migration to the tissue.

The *In Vitro* Macrophage Activity

To evaluate the phagocytic activity of macrophages in WT and $CD18^{low}$ mice, peritoneal macrophages from both groups of mice were co-cultivated *in vitro* with the yeast of Pb18. The fungal cells' internalization and viability were assessed by phagocytic index, considering the colony-forming units (CFU) counting after 6 h, 24 h, 48 h, and 72 h of co-incubation.

It was found that macrophages from both WT and $CD18^{low}$ mice were able to internalize Pb 18. Yeast phagocytosis increased more when the cells were opsonized with fresh serum compared to inactivated serum (data not shown). The phagocytosis index was significantly higher in WT macrophages than $CD18^{low}$ cells at six and 24 h of co-culture (**Figure 4C**). There was a time-dependent increment in fungal burden in both macrophage groups during the kinetics. Considering the technical limitation to separate the adhered and internalized yeast, we carried out the phagocytosis index determination using fluorescent staining (**Supplementary Figure 3**). The results are similar to the **Figure 4C**, confirming a lower internalization of $CD18^{low}$ macrophages. Nonetheless, we observed a higher number of viable *P. brasiliensis* recovered from WT when compared to $CD18^{low}$ macrophages (**Figure 4D**).

Furthermore, macrophage activation through the acidification of the phagolysosome was also measured using Lysotracker staining and microscopy analysis (**Figure 5**). We

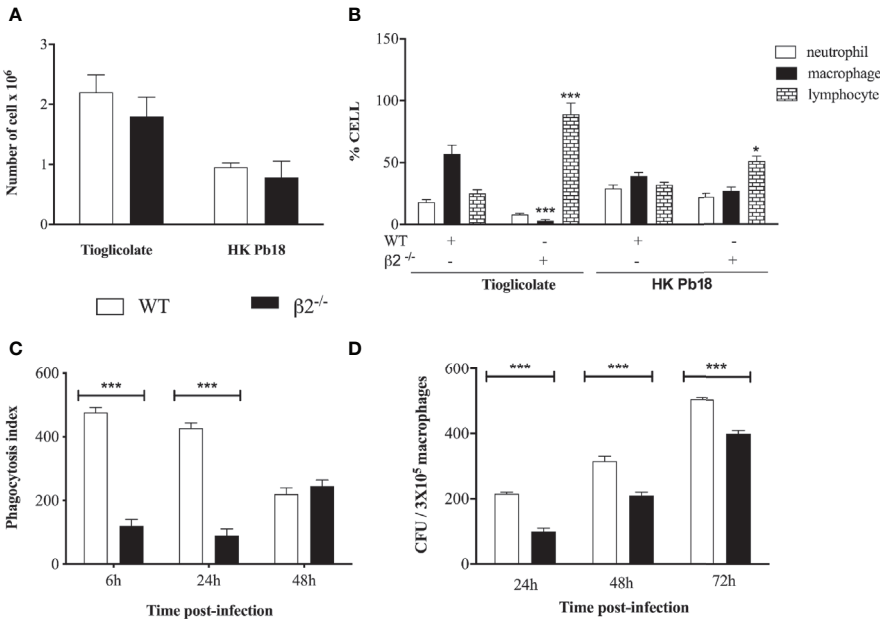

FIGURE 4 | In vivo mobilization of cells in WT and CD18 low mice after i.p. inoculation of thioglycolate and heat-killed P. brasiliensis. **(A)** Total of cells migrating to the peritoneal cavity of WT and CD18^{low} mice at 4 days post-treatment with HKPb18 and thioglycolate. **(B)** Percentage of specific cell type counted in WT and CD18^{low} mice's peritoneal cavity after treatment with HKPb18 and thioglycolate. **(C)** *In vitro* analysis of the phagocytosis index in WT and CD18^{low} mice derived macrophages at 6, 24, 48 h post-co-incubation with Pb18 (MOI 1:1). **(D)** Viable yeast recovered from WT and CD18^{low} macrophage-infected *in vitro* with Pb18 and plated at 24, 48, and 72 h post-co-incubation. Data are expressed as the mean ± SEM. (*Indicates significant difference $p<0.05$; ***significant difference $p<0.001$).

also analyzed the mean fluorescence intensity (MFI) of lysosome staining. A lower intensity in the lysosome signal is observed in WT mice infected with fresh serum-opsonized *P. brasiliensis*. We did not observe differences in CD18^{low} macrophages' lysosomal activities in relation to yeast opsonization.

DISCUSSION

The PCM outcome depends on several factors, among which fungal interaction with macrophages is a critical one. The interactions between resident fungi and macrophages determine the subsequent mechanisms of innate and adaptive immune activation. These processes are different when comparing the reactions of susceptible and resistant mice to experimental PCM (Pina et al., 2008). At the beginning of the infection, the susceptible mice developed better fungal growth control, with high NO and IL-12 production levels and increased expression of CD40, but with disseminated disease and low mice survival rate. On the other hand, the resistant mice showed a low production of NO, high levels of IL-10 and GM-CSF, and increased expression of Class II MHC molecules, with a well-controlled adaptive immune response. Other authors have suggested that the disease outcome is a consequence of initial pathogen recognition, followed by an exacerbated immune response associated with low fungal killing and CD4+ T-cells anergy (Pina et al., 2008). However, the juvenile form of PCM shows eosinophilia and high TGF-b levels and a T helper 2 cytokines patter (Mamoni et al., 2002), indicating that several cytokines are associated with the initial immune response, capable of modulating the disease outcomes.

There are some receptors associated with *P. brasiliensis* recognition, such as TLRs, CTLRs, and CRs. TLR-4 and TLR-2 are associated with a robust initial response and a non-controlled disease compared with deficient mice for these receptors (Calich et al., 2008; Loures et al., 2009; Loures et al., 2010). Contrarily, the Dectin-1 receptor is associated with increased response in resistant mice through inflammasome activation and IL-1β production (Feriotti et al., 2015). The role of a complement system has been previously described (Calich et al., 2008). However, the role of its receptors has not yet been fully elucidated. To verify the role of b2-integrin, we carried out *in vivo* experimental infections using CD18^{low} mice. The CD18^{low} Pb infected mice showed a higher fungal burden and lower NO_3 levels at 15 days post-infection; however, the animal controlled the infection at 30 days post-infection. The resistance of these mice was confirmed by the survival curve, in which we detected a small number of CFUs in the lung compared to CFUs recovered from WT mice at 60 days post-infection. Our *in vivo* data corroborate reports on TLR-4 and TLR-2 KO infected mice (Pinto et al., 2006; Loures et al., 2009; Loures et al., 2010). It is possible to correlate the higher CFUs in CD18^{low} mice at 15 days post-infection with the low NO_3 secretion at this time point. However, the levels of NO should also be analyzed in the lung. However, already at 15 dpi, we observed high levels of IL-10.

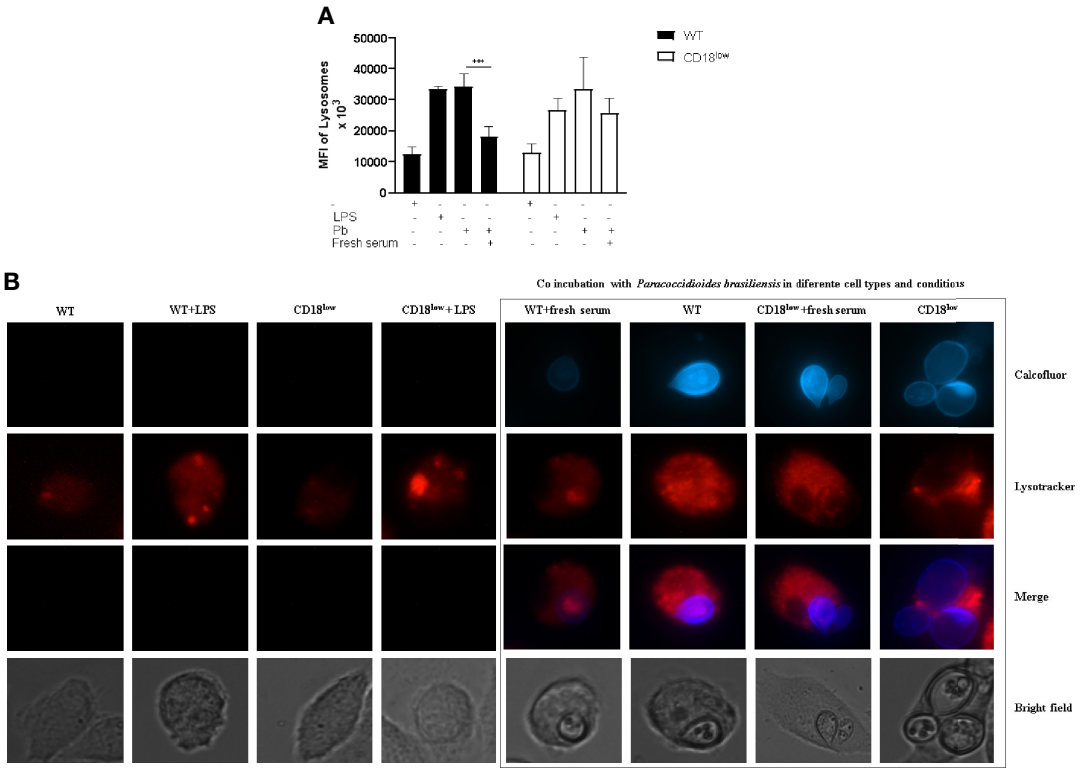

FIGURE 5 | Lysosomal recruitment and acidification to evaluate macrophage activation. Detection of lysosomal acidification/recruitment in infected WT and CD18^{low} macrophages was performed using LysoTracker® Red DND-99. **(A)** Representative pictures depicting calcofluor white stained fungi (blue) and Lysotracker staining (red). **(B)** Quantification of Mean Fluorescence Intensity (MFI) after Lysotracker staining of both WT and CD18^{low} macrophages after *P. brasiliensis* interactions *in vitro*. Images were taken using the Live Cell Imaging platform, and ImageJ analyzed MFI. Data are presented as mean ± SEM of at least three independent experiments (***indicates significant difference p<0.001).

Among other functions, IL-10 is also stimulatory towards TCD8+ cells, and this can be associated with the decrease in the CFUs at 60 days post-infection in CD18^{low} mice.

The histopathological and histocytometry analysis confirmed a progressive inflammatory response with extensive areas of granulomas in Pb infected mice. There are differences between granuloma structure between the two groups, and our results corroborate the granuloma formations described in susceptible (B10.A) and resistant (A/Sn) mice exposed to *P. brasiliensis* (Calich et al., 2008; Loures et al., 2009; Loures et al., 2010). To better understand if the smaller granulomatous lesions were associated with a low cellular migration to the lung, we carried out a migration assay. The lower expression of LFA-1 (CD11a/CD18) has no influence on total leukocyte migration. However, CD18^{low} mice showed more migration of lymphocytes than macrophages for both stimuli, explaining the increase of lymphocyte infiltration in the CD18^{low} lung. Another explanation for the higher levels of lymphocytes in the lung is that CD18 is also part of αDβ2, an adhesive and multiligand receptor, which is moderately expressed in circulating leukocytes, but it is upregulated in inflammatory macrophages. This adhesive property is microenvironment-dependent, and the b2-integrin density is important for migration to the inflammatory focus through extravascular space (Palecek et al., 1997). This receptor is also crucial to macrophage retention on tissue, promoting chronic inflammation (Yakubenko et al., 2008). Our results showed significantly lower macrophage migration into the peritoneum after thioglycolate stimulus, which can be explained by a low expression of αDβ2. The microenvironment with macrophage depletion and a rise in lymphocytes can modulate granuloma formation, fungal viability, and resistance to the infection, as observed in our results.

Furthermore, the granulomas can be modulated by NO production. The treatment of susceptible mice with an inhibitor of NOS2 (inducible nitric oxide synthase 2) induces a considerable increase in the number and the size of liver granulomas. Simultaneously, in animals with the regular expression of NO, there were smaller granulomas, despite the worse immunological parameters during infection. These results suggest that NO levels are closely correlated with the extension of granulomatous lesions. The cessation of NO production during the initial phase may cause more severe disease. In contrast, the overproduction of this mediator is associated with susceptibility (Yakubenko et al., 2008).

In our work, the NO_3 serum levels of CD18^{low} mice in response to *P. brasiliensis* infection were higher only at 15 days

post-infection. However, this production did not increase during infection progression, as observed in WT mice levels. The correlation between the activation of NO production and fungal lung infections and immunosuppressant mechanisms has been previously reported during a *P. brasiliensis* mouse infection. These studies revealed that, although NO is an essential microbicidal mechanism for macrophages infected with *P. brasiliensis*, the overproduction of NO in PCM contributes to immunosuppression during the disease (Nascimento et al., 2002; Yakubenko et al., 2008). One of the NO immunosuppressive pathways reduces class II MHC expression, with antigen-presentation for T-cells, decreased IFN-γ levels, and inhibition of IFN-γ-dependent production of NO synthase, which prevents excessive NO formation and tissue injury (Sicher et al., 1994; Bocca et al., 1998; Bocca et al., 1999). The physiological role of NO in host immunity suppression to avoid tissue injury can also modulate granuloma formation. In some cases, it can increase host susceptibility, as described in the PCM model, and confirmed in this work.

In several infection models, including PCM, macrophages' fungicidal activity against fungi has been associated with IFN−γ-macrophage activation and, consequently, NO production induced by NO synthase. Therefore, NO induction depends on the synergy between Th1 cytokines, TNF-α and IFN-γ, and/or cellular constituents of the pathogen (Brummer et al., 1988; Xie et al., 1991; Bocca et al., 1998; Bogdan et al., 2000). The phagocyte's fungicidal activity seems to be dependent on the equilibrium between stimulating and suppressing cytokines during interaction with the fungus to regulate the NO levels. The early production of IL-10 by $CD18^{low}$ mice is probably associated with a reduction in NO production at a later time point and the prevention of its immunosuppressive role.

Th1 lymphocytes are essential for an effective cellular immune response against intracellular pathogens because of IFN-γ secretion, which activates macrophages and stimulates T $CD8^+$ cells. In murine models, IFN-γ also induces the production of both IgG2a and IgG3, which contribute to antimicrobial immunity through their complementary and opsonization activities. Our data revealed that $CD18^{low}$ mice underwent a significant increase in IgG1 produced during the time analyzed and in IgG2a levels at 60 days post-infection compared to WT mice. The phagocytosis efficacy of *Cryptococcus neoformans* by macrophages is mediated by opsonization of IgM and IgA antibodies and is correlated with CR3 expression (Taborda and Casadevall, 2002). However, it was demonstrated that when blocking CR3, the phagocytosis mediated by IgG1 was partially inhibited, suggesting that phagocytosis mediated by IgG1 is not entirely dependent on β integrins and that $CD18^{low}$ macrophages used a similar pathway to internalize the yeast cells. The pattern of IgG production in $CD18^{low}$ mice in experimental PCM needs to be better explored; however, we can presume that the levels of IgG1 correlate with a non-inflammatory response at the beginning of the infection and the IgG2a with a Th1 response at the end of the infection.

Macrophages can play different roles in the lung, as shown in pulmonary infection caused by *C. neoformans* or *A. fumigatus*. The populations associated with tolerance and tissue homeostasis have produced low levels of CXCL2 and high levels of IL-10 and complement component 1q (C1q) (Xu-Vanpala et al., 2020). Activation of the complement system by *P. brasiliensis*, either by the classical or alternative pathways, results in yeast cell opsonization, promoting phagocytosis and fungicidal killing (Calich et al., 2008). We analyzed the kinetics of the *in vitro* phagocytosis of *P. brasiliensis* yeast opsonized with fresh serum by macrophages from WT and $CD18^{low}$ mice, and WT macrophages internalized more yeast cells.

Several works have demonstrated that the phagocytosis of microorganisms such as *C. neoformans* (Kelly et al., 2005; Luo et al., 2006), *C. albicans* (Triebel et al., 2003; Gruber et al., 1998), *M. tuberculosis* (Velasco-Velasquez et al., 2003), and *L. monocytogenes* (Drevets et al., 1996) in the presence of fresh human serum is more efficient than in the presence of inactivated serum. The low phagocytosis rate of yeasts by $CD18^{low}$ macrophages emphasizes the importance of complement receptors in internalization. Nevertheless, the phagocytosis of *P. brasiliensis* yeast cells can occur by other receptors, which may explain why the phagocytic activity increased progressively after 24 h, although at 48 h post-infection, we observed no differences in the phagocytosis index between the groups. The fungal load in macrophages increased during the kinetic analyses for both groups; however, despite showing the same number of internalized yeast cells at 48 h, we observed a reduction in the viability of Pb in $CD18^{low}$ macrophages. These results are consistent with more efficient macrophage killing of fungal cells in this group. The complement receptors (CR1, CR3, and CR4) expressed in macrophages are important for recognition and adhesion of *M. tuberculosis*. As observed in our results, similar studies using *M. tuberculosis* have demonstrated that bacteria also exploit receptors to enter macrophages' cytoplasm (Hirsch et al., 1994; Velasco-Velasquez et al., 2003) and modulate phagocyte activation and disease outcome.

The ability of microorganisms to be destroyed has been related to phagocyte intracellular acidification. When this mechanism fails, improper phagosome acidification is positively associated with the intracellular survival of *C. neoformans* and *Leishmania* (Hirsch et al., 1994; Xu-Vanpala et al., 2020). The β2 integrin receptor has been well described using a *Leishmania* model, corroborating several studies that have associated the presence of CR3 with a delay in lysosome recruitment and phagolysosome maturation (Carter et al., 2009; Polando et al., 2013; Ricardo-Carter et al., 2013). Our results showed increased lysosomal recruitment on both WT and β2-/-infected macrophages with non-opsonized fungal cells. The opsonization of yeast cells with fresh serum produced reduced lysosome recruitment in WT macrophages, suggesting low phagocyte activation. β2 integrin is one of two chains in CR3 conformation, and other components can be related to the lysosomal recruitment pathway in *P. brasiliensis* infection, such as CR1, related to early phagolysosome maturation.

Nevertheless, the relationship between CD18 and PCM in an early phase of infection must be evaluated. Regarding the role of CR3 in diverse species of intracellular pathogens, this receptor

can crosstalk with TLRs and interfere in several diseases' pathogenesis. The role of CR3/TLR2 or CR3/TLR4 has not been studied in PCM, and the understanding of *P. brasiliensis* survival in macrophages should be better explored.

In the present manuscript, we focused on active antifungal macrophages after infections with *P. brasiliensis*. Our data suggest that the presence of β2 integrin is associated with an initial inflammatory response and intracellular fungal survival. The beta chain protein could serve as a "safe passage" for the fungus, supporting its proliferation, and its default would lead the fungus to enter the macrophages *via* a less "friendly" receptor, able to activate this phagocytic cell more efficiently.

DATA AVAILABILITY STATEMENT

The raw data supporting the conclusions of this article will be made available by the authors, without undue reservation.

ETHICS STATEMENT

The animal study was reviewed and approved by The Animal Ethics Committee of then University of Brasilia (UnBDOC n°. 33798/2007).

AUTHOR CONTRIBUTIONS

AB and AA- conceived, and designed research. SM, JN, EC, PHB, and AS - conducted experiments. AB, AT, LM, and LF - contributed with reagents and analytical tools. SM, JN, FC, PHB, and AR - analyzed data. AB, SM, AA, and LM - wrote the manuscript. All authors contributed to the article and approved the submitted version.

FUNDING

We would like to thank Dr. Magda Verçosa Carvalho Branco from UNICEUB for providing isogenic C57Bl/6 mice. This research was funded by a grant from CNPq (Conselho Nacional de Pesquisa - 306515/2019-9), FAPDF (Fundação de apoio à Pesquisa do Distrito Federal –193.000496/2009 and 193.000417/2016), and CAPES.

SUPPLEMENTARY MATERIAL

The Supplementary Material for this article can be found online at: https://www.frontiersin.org/articles/10.3389/fcimb.2021.622899/full#supplementary-material

Supplementary Figure 1 | Quantification TNF-α and IL-12 secretion in a *P. brasiliensis* infection systemic model. Mice were infected *via* i.v. with 10^6 yeast forms of *P. brasiliensis* (Pb18) to mimic a chronic infection. **(A)** TNF-α and **(B)** IL-12 secretion analyzed by ELISA from lung cell homogenates. Data are expressed as the mean ± SEM. (* Indicates significant difference $p<0.05$; **significant difference $p<0.01$, *** significant difference $p<0.001$).

Supplementary Figure 2 | Cell migration in BAL of WT and KO animals. Wild Type and CD18 low mice were infected with heat killed Pb18 in the intranasal route. After euthanasia, BAL cells were collected and stained with anti CD3 and anti- F4/80 before Flow Cytometry analyses. **(A)** Dot plot of WT cells depicting lymphocytes and macrophages after specific staining. **(B)** Dot plot of CD18low cells depicting lymphocytes and macrophages after specific staining. **(C)** Quantification of anti-CD3 and anti-F4/80 fluorescence in both cell populations of WT and CD18low BAL. Data are expressed as the mean ± SEM. (*Indicates significant difference $p<0.05$; **significant difference $p<0.01$, ***significant difference $p<0.001$).

Supplementary Figure 3 | Phagocytosis index of Pb18 by WT and CD18low cells. Pb18 was stained with Fluorescein isothiocyanate (FITC) before co-incubation with macrophages. Next, extracellular fungi were stained with Calcofluor. Phagocytosis index was analyzed by fluorescent microscopy. **(A)** Picture panel depicting intracellular Pb18 (green) and extracellular Pb18 (blue). **(B)** Quantification of phagocytosis index of both WT and KO cells. Data are expressed as the mean ± SEM. (*Indicates significant difference $p<0.05$; **significant difference $p<0.01$, ***significant difference $p<0.001$).

REFERENCES

Bocca, A. L., Hayashi, E. E., Pinheiro, A. G., Furlanetto, A. B., Campanelli, A. P., Cunha, F. Q., et al. (1998). Treatment of *Paracoccidioides brasiliensis* – infected mice with a nitric oxide inhibitor prevents the failure of cell-mediated immune response. *J. Immunol.* 161, 3056–3063.

Bocca, A. L., Silva, M. F., Silva, C. L., Cunha, F. Q., and Figueiredo, F. (1999). Macrophage Expression of Class II Major Histocompatibility Complex Gene Products in *Paracoccidioides brasiliensis*-infected Mice. *Am. J. Trop. Med. Hyg.* 61, 280–287. doi: 10.4269/ajtmh.199.61.280

Bocca, A. L., Amaral, A. C., Teixeira, M. M., Sato, P. K., Shikanai-Yasuda, M. A., and Soares-Felipe, M. S. (2013). Paracoccidioidomycosis: eco-epidemiology, taxonomy, and clinical and therapeutic issues. *Future Microbiol.* 8 (9), 1177–1191. doi: 10.2217/fmb.13.68

Bogdan, C., Rollinghoff, M., and Diefenbach, A. (2000). Reactive oxygen and reactive nitrogen intermediates in innate and specific immunity. *Curr. Opin. Immunol.* 12, 64–76. doi: 10.1016/S0952-7915(99)00052-7

Brummer, E., Hanson, L. H., Restrepo, A., and Stevens, D. A. (1988). In vivo and in vitro activation of pulmonary macrophages by IFN-gamma for enhanced killing of *Paracoccidioides brasiliensis* or *Blastomyces dermatitidis*. *J. Immunol.* 40, 2786–2789.

Calich, V. L., da Costa, T. A., Felonato, M., Arruda, C., Bernardino, S., Loures, F. V., et al. (2008). Innate immunity to *Paracoccidioides brasiliensis* infection. *Mycopathologia* 165 (4-5), 223–236. doi: 10.1007/s11046-007-9048-1

Carter, C. R., Whitcomb, J. P., Campbell, J. A., Mukbel, R. M., and McDowell, M. A. (2009). Complement Receptor 3 Deficiency Influences Lesion Progression during *Leishmania major* Infection in BALB/c Mice. *Infect. Immun.* 77 (12), 5668–5675. doi: 10.1128/IAI.00802-08

Dai, S., Rajaram, M. V., Curry, H. M., Leander, R., and Schlesinger, L. S. (2013). Fine tuning inflammation at the front door: macrophage complement receptor 3-mediates phagocytosis and immune suppression for Francisella tularensis. *PloS Pathog.* 9 (1), e1003114. doi: 10.1371/journal.ppat.1003114

Drevets, D. A., Leenen, P. J., and Campbell, P. A. (1996). Complement receptor type 3 mediates phagocytosis and killing of *Listeria monocytogenes* by a TNF-alpha- and IFN-gammastimulated macrophage precursor hybrid. *Cel Immunol.* 169, 1–6. doi: 10.1006/cimm.1996.0083

Feriotti, C., Loures, F. V., Frank de Araújo, E., da Costa, T. A., and Calich, V. L. (2013). Mannosyl-recognizing receptors induce an M1-like phenotype in macrophages of susceptible mice but an M2-like phenotype in mice resistant to a fungal infection. *PloS One* 8 (1), e54845. doi: 10.1371/journal.pone.0054845

Feriotti, C., Bazan, S. B., Loures, F. V., Araújo, E. F., Costa, T. A., and Calich, V. L. (2015). Expression of dectin-1 and enhanced activation of NALP3 inflammasome are associated with resistance to paracoccidioidomycosis. *Front. Microbiol.* 6, 913. doi: 10.3389/fmicb.2015.00913

Fukazawa, Y., and Kagaya, K. (1997). Molecular bases of adhesion of Candida albicans. *J. Med. Vet. Mycol.* 35 (2), 87–99. doi: 10.1080/02681219780000971

Goel, M. K., Khanna, P., and Kishore, J. (2010). Understanding survival analysis: Kaplan-Meier estimate. *Int. J. Ayurveda Res.* 1 (4), 274–278. doi: 10.4103/0974-7788.76794

Granger, D. L., Taintor, R. R., Boockvar, K. S., and Hibbs, J. B. Jr. (1996). Measurement of nitrate and nitrite in biological samples using nitrate reductase and Griess reaction. *Methods Enzymol.* 268, 142–151. doi: 10.1016/S0076-6879(96)68016-1

Gruber, A., Lukasser-Vogl, E., Von Zepelin, M. B., Dierich, M. P., and Wurzner, R. (1998). Human immunodeficiency virus type1 gp160 and gp41 binding to *Candida albicans* selectively enhances candidal virulence in vitro. *J. Infect. Dis.* 177, 1057–1063. doi: 10.1086/515231

Hirsch, C. S., Ellner, J. J., Russell, D. G., and Rich, E. A. (1994). Complement receptor-mediated uptake and tumor necrosis factor-alpha-mediated growth inhibition of *Mycobacterium tuberculosis* by human alveolar macrophages. *J. Immunol.* 152, 743–753.

Jimenez Mdel, P., Restrepo, A., Radzioch, D., Cano, L. E., and Garcia, L. F. (2006). Importance of complement 3 and mannose receptors in phagocytosis of *Paracoccidioides brasiliensis* conidia by Nramp1 congenic macrophages lines. *FEMS Immunol. Med. Microbiol.* 47 (1), 56–66. doi: 10.1111/j.1574-695X.2006.00059.x

Kadioglu, A., De Filippo, K., Bangert, M., Fernandes, V. E., Richards, L., Jones, K., et al. (2011). The integrins Mac-1 and alpha4beta1 perform crucial roles in neutrophil and T cell recruitment to lungs during Streptococcus pneumoniae infection. *J. Immunol.* 15186 (10), 5907–5915. doi: 10.4049/jimmunol.1001533

Kelly, R. M., Chen, J., Yauch, L., and Levitz, S. M. (2005). Opsonic requirements for dendritic cell-mediated responses to *Cryptococcus neoformans*. *Infect. Immun.* 73, 592–598. doi: 10.1128/IAI.73.1.592-598.2005

Loures, F. V., Pina, A., Felonato, M., and Calich, V. L. G. (2009). TLR2 is a negative regulator of Th17 cells and tissue pathology in a pulmonary model of fungal infection. *J. Immunol.* 183, 1279–1290. doi: 10.4049/jimmunol.0801599

Loures, F. V., Pina, A., Fenonato, M., Araujo, E. F., Leite, K. R. M., and Calich, V. L. C. (2010). Toll-like receptor 4 signaling leads to severe fungal infection associated with enhanced proinflammatory immunity and impaired expansion of regulatory T cell. *Infect. Immun.* 78 (3), 1078–1088. doi: 10.1128/IAI.01198-09

Luo, Y., Cook, E., Fries, B. C., and Casadevall, A. (2006). Phagocytic efficacy of macrophage-like cells as a function of cell cycle and Fcgamma receptors (FcgammaR) and complement receptor (CR)3 expression. *Clin. Exp. Immunol.* 145 (2), 380–387. doi: 10.1111/j.1365-2249.2006.03132.x

Mamoni, R. L., Neuer, S. A., Oliveira, S. J., Musatti, C. C., Rossi, C. L., Camargo, Z. P., et al. (2002). Enhanced production of specific IgG4, IgE, IgA and TGF-beta in sera from patients with the juvenile form of paracoccidioidomycosis. *Med. Mycol.* 40 (2), 153–159. doi: 10.1080/mmy.40.2.153.159

Mendes, R. P., Cavalcante, R. S., Marques, S. A., Marques, M. E. A., Venturini, J., Sylvestre, T. F., et al. (2017). Paracoccidioidomycosis: Current Perspectives from Brazil. *Open Microbiol. J.* 11, 224–282. doi: 10.2174/1874285801711010224

Nascimento, F. R., Calich, V. L., Rodríguez, D., and Russo, M. (2002). Dual role for nitric oxide in paracoccidioidomycosis: essential for resistance, but overproduction associated with susceptibility. *J. Immunol.* 168 (9), 4593–4600. doi: 10.4049/jimmunol.168.9.4593

Pagliari, C., Kanashiro-Galo, L., Jesus, A. C. C., Saldanha, M. G., and Sotto, M. N. (2019). Paracoccidioidomycosis: characterization of subpopulations of macrophages and cytokines in human mucosal lesions. *Med. Mycol.* 57 (6), 757–763. doi: 10.1093/mmy/myy120

Palecek, S. P., Loftus, J. C., M. Ginsberg, G., Lauffenburger, D. A., and Horwitz, A. F. (1997). Integrin-ligand binding properties govern cell migration speed through cell-substratum adhesiveness. *Nature* 385, 537–554. doi: 10.1038/385537a0

Pina, A., Bernardino, S., and Calich, V. L. G. (2008). Alveolar macrophages from susceptible mice are more competent than those of resistant mice to control initial *Paracoccidioides brasiliensis* infection. *J. Leukoc. Biol.* 83, 1088–1099. doi: 10.1189/jib.1107738

Pinto, J. G., Martins, L. A., Cavalheiro, J. S., Accorsi, M. J., Pedrini, S. C., Soares, A. M., et al. (2006). Cytokine production in lungs and adrenal glands of high and low antibody-producing mice infected with *Paracoccidioides brasiliensis*. *Med. Mycol.* 44 (6), 505–514. doi: 10.1080/13693780600760781

Polando, R., Dixit, U. G., Carter, C. R., Jones, B., Whitcomb, J. P., Ballhorn, W., et al. (2013). The roles of complement receptor 3 and Fcγ receptors during Leishmania phagosome maturation. *J. Leukoc. Biol.* 93 (6), 921–932. doi: 10.1189/jlb.0212086

Restrepo, A., Benard, G., de Castro, C. C., Agudelo, C. A., and Tobón, A. M. (2008). Pulmonary paracoccidioidomycosis. *Semin. Respir. Crit. Care Med.* 29 (2), 182–197. doi: 10.1055/s-2008-1063857

Ricardo-Carter, C., Favila, M., Polando, R. E., Cotton, R. N., Bogard Horner, K., Condon, D., et al. (2013). *Leishmania major* inhibits IL-12 in macrophages by signaling through CR3 (CD11b/CD18) and down-regulation of ETS-mediated transcription. *Parasite Immunol.* 35 (12), 409–420. doi: 10.1111/pim.12049

Ross, G. D., Cain, J. A., Myones, B. L., Newman, S. L., and Lachmann, P. J. (1987). Specificity of membrane complement receptor type three (CR3) for beta-glucans. *Complement* 4, 61–74. doi: 10.1159/000463010

Schimke, L. F., Hibbard, J., Martinez-Barricarte, R., Khan, T. A., de Souza Cavalcante, R., Borges de Oliveira Junior, E., et al. (2017). Paracoccidioidomycosis Associated With a Heterozygous STAT4 Mutation and Impaired IFN-γ Immunity. *J. Infect. Dis.* 216 (12), 1623–1634. doi: 10.1093/infdis/jix522

Sicher, S. C., Vazques, M. A., and Lu, C. Y. (1994). Inhibition of macrophage Ia expression by nitric oxide. *J. Immunol.* 153, 1293–1300.

Souto, J. T., Figueiredo, F., Furlanetto, A., Pfeffer, K., Rossi, M. A., and Silva, J. S. (2000). Interferon-gamma and tumor necrosis factor-alpha determine resistance to *Paracoccidioides brasiliensis* infection in mice. *Am. J. Pathol.* 156 (5), 1811–1820. doi: 10.1016/s0002-9440(10)65053-5

Souto, J. T., Aliberti, J. C., Campanelli, A. P., Livonesi, M. C., Maffei, C. M., Ferreira, B. R., et al. (2003). Chemokine production and leukocyte recruitment to the lungs of *Paracoccidioides brasiliensis*-infected mice is modulated by interferon-gamma. *Am. J. Pathol.* 2003. 163 (2), 583–590. doi: 10.1016/s0002-9440(10)63686-3

Taborda, C. P., and Casadevall, A. (2002). CR3 (CD11b/CD18) and CR4 (CD11c/CD18) are involved in complement-independent antibody-mediated phagocytosis of. *Cryptococcus Neoformans Immun* 16 (6), 791–802. doi: 10.1016/s1074-7613(02)00328-x

Tan, S. M. (2012). The leucocyte β2 (CD18) integrins: the structure, functional regulation, and signaling properties. *Biosci. Rep.* 32 (3), 241–269. doi: 10.1042/BSR20110101

Triebel, T., Grillhosl, B., Kacani, L., Lell, C. P., Fuchs, A., Speth, C., et al. (2003). Importance of the terminal complement components for immune defence against *Candida*. *Int. J. Med. Microbiol.* 292, 527–536. doi: 10.1078/1438-4221-00211

Tristão, F. S., Panagio, L. A., Rocha, F. A., Cavassani, K. A., Moreira, A. P., Rossi, M. A., et al. (2013). cell-deficient mice display enhanced susceptibility to *Paracoccidioides brasiliensis* infection. *Mycopathologia* 176 (1-2), 1–10. doi: 10.1007/s11046-013-9671-y

Velasco-Velasquez, M. A., Barrera, D., Gonzalez-Arenas, A., Rosales, C., and Agramonte-Hevia, J. (2003). Macrophage-*Mycobacterium tuberculosis* interactions: role of complement receptor 3. *Microbial Pathog.* 35, 125–131. doi: 10.1016/s0882-4010(03)00099-8

Xie, Q. W., Cho, H. J., Calaycay, J., Mumford, R. A., Swiderek, K. M., Lee, T. D., et al. (1991). Cloning and characterization of inducible nitric oxide synthase from mouse macrophages. *Science* 256, 225–228. doi: 10.1126/science.1373522

Xu-Vanpala, S., Deerhake, M. E., Wheaton, J. D., Parker, M. E., Juvvadi, P. R., MacIver, N., et al. (2020). Functional heterogeneity of alveolar macrophage population based on expression of CXCL2. *Sci. Immunol.* 5 (50), eaba7350. doi: 10.1126/sciimmunol.aba7350

Yakubenko, V. P., Belevych, N., Mishchuk, D., Schurin, A., Lam, S. C., and Ugarova, T. P. (2008). The role of integrin $\alpha_D\beta_2$ (CD11d/CD18) in monocyte/macrophage migration. *Exp. Cell Res.* 314, 2569–2578. doi: 10.1016/j.yexcr.2008.05.016

Conflict of Interest: The authors declare that the research was conducted in the absence of any commercial or financial relationships that could be construed as a potential conflict of interest.

frontiers in Cellular and Infection Microbiology

ORIGINAL RESEARCH
published: 13 May 2021
doi: 10.3389/fcimb.2021.592826

Lipid Secretion by Parasitic Cells of *Coccidioides* Contributes to Disseminated Disease

Carlos Alberto Peláez-Jaramillo[1,2,3], *Maria Del Pilar Jiménez-Alzate*[1,2*], *Pedronel Araque-Marin*[4], *Chiung-Yu Hung*[1], *Natalia Castro-Lopez*[1] *and Garry T. Cole*[1]

[1] The Biology Department and South Texas Center for Emerging Infectious Diseases, University of Texas at San Antonio, San Antonio, TX, United States, [2] Grupo Interdisciplinario de Estudios Moleculares, Chemistry Institute, Faculty of Natural and Exact Sciencess, Medellín, Antioquia, Colombia, [3] Grupo Micología Médica, Microbiology and Parasitology Department, School of Medicine, Universidad de Antioquia, Medellín, Antioquia, Colombia, [4] School of Life Sciences, EIA University (Universidad Escuela de Ingenieros de Antioquia), Envigado, Antioquia, Colombia

OPEN ACCESS

Edited by:
Carlos Pelleschi Taborda, University of São Paulo, Brazil

Reviewed by:
Marcus De Melo Teixeira, University of Brasilia, Brazil
Maurizio Del Poeta, Stony Brook University, United States

***Correspondence:**
Maria Del Pilar Jiménez-Alzate
delpilar.jimenez@udea.edu.co

Specialty section:
This article was submitted to Fungal Pathogenesis, a section of the journal Frontiers in Cellular and Infection Microbiology

Received: *08 August 2020*
Accepted: *14 April 2021*
Published: *13 May 2021*

Citation:
Peláez-Jaramillo CA, Jiménez-Alzate MDP, Araque-Marin P, Hung C-Y, Castro-Lopez N and Cole GT (2021) Lipid Secretion by Parasitic Cells of Coccidioides Contributes to Disseminated Disease. Front. Cell. Infect. Microbiol. 11:592826. doi: 10.3389/fcimb.2021.592826

Coccidioides is a soil-borne fungal pathogen and causative agent of a human respiratory disease (coccidioidomycosis) endemic to semi-desert regions of southwestern United States, Mexico, Central and South America. Aerosolized arthroconidia inhaled by the mammalian host first undergo conversion to large parasitic cells (spherules, 80–100 μm diameter) followed by endosporulation, a process by which the contents of spherules give rise to multiple endospores. The latter are released upon rupture of the maternal spherules and establish new foci of lung infection. A novel feature of spherule maturation prior to endosporulation is the secretion of a lipid-rich, membranous cell surface layer shed *in vivo* during growth of the parasitic cells and secretion into liquid culture medium during *in vitro* growth. Chemical analysis of the culture derived spherule outer wall (SOW) fraction showed that it is composed largely of phospholipids and is enriched with saturated fatty acids, including myristic, palmitic, elaidic, oleic, and stearic acid. NMR revealed the presence of monosaccharide- and disaccharide-linked acylglycerols and sphingolipids. The major sphingolipid components are sphingosine and ceramide. Primary neutrophils derived from healthy C57BL/6 and DBA/2 mice incubated with SOW lipids revealed a significant reduction in fungicidal activity against viable *Coccidioides* arthroconidia compared to incubation of neutrophils with arthroconidia alone. Host cell exposure to SOW lipids had no effect on neutrophil viability. Furthermore, C57BL/6 mice that were challenged subcutaneously with *Coccidioides* arthroconidia in the presence of the isolated SOW fraction developed disseminated disease, while control mice challenged with arthroconidia alone by the same route showed no dissemination of infection. We hypothesize that SOW lipids contribute to suppression of inflammatory response to *Coccidioides* infection. Studies are underway to characterize the immunosuppressive mechanism(s) of SOW lipids.

Keywords: *Coccidioides*, spherule outer wall, phospholipids, sphingolipids, immunomodulation, fungal lipids, SOW-lipid extract

INTRODUCTION

Coccidioides posadasii and *Coccidioides immitis* are dimorphic fungal pathogens, the etiologic agents of coccidioidomycosis, a mild to potentially life-threatening respiratory disease. *Coccidioides* spp. is a desert soil-inhabiting fungal pathogen that is found in the southwestern United States and in certain regions of Mexico, Central America, and South America. Despite the genetic diversity between the two species of *Coccidioides* revealed by comparative genomic sequence analyses (Fisher et al., 2001; Sharpton et al., 2009), laboratory studies have shown that they have comparable virulence in mice. *Coccidioides* spp. is a primary pathogen that can cause diseases in both immunocompetent and immunocompromised individuals (Galgiani et al., 2005). Disease onset typically results from inhalation of dry, air-dispersed arthroconidia released by the soilborne saprobic phase of the pathogen. Inhaled arthroconidia of *Coccidioides* spp become hydrated and undergo isotropic growth to form spherule initials (10 to 30 μm diameter) (Cole et al., 2006). These parasitic cells presumably first come in contact with epithelial cells and macrophages in the respiratory tract of the host. These spherules grow isotropically to produce large parasitic cells (60 to >100 μm in diameter) and once the spherule is developed, a surface outer wall (SOW) is produced (Cole et al., 1988). The spherules undergo an elaborate process of endogenous wall growth and cytoplasmic compartmentalization, which culminates in production and the release of a multitude of endospores (each of them 4 to 10 μm in diameter). Endospores are small enough to be disseminated hematogenously, grow and differentiate into a second generation of spherules (Cole et al., 1988). It is suggested that SOW produced is around the endospores released in order to protect them from phagocytosis or killing by the cells of the innate immune response.

Tarbet and Breslau (1953) in their founding studies reported that the walls of mature spherules are rich in "lipid complexes", which they identified as phospholipids. These authors suggested that the lipid layer of the spherule wall may "resist the diffusion of large molecules", but "retain certain chemotactic substances within the cell and block or alter chemical interchange between parasite and tissues" of the host. The lipid-rich SOW layer may be a protective barrier that contributes to the survival of the pathogen in host tissue. Frey and Drutz (1986) presented evidence that an extracellular matrix produced by the spherule may partly account for its survival in the presence of leukocytes from healthy donors. The authors suggested that the matrix might impede contact between polymorphonuclear neutrophils and the fungus and somehow reduce the efficiency of host attack against spherules. Release of some of these immunoreactive macromolecules *in vivo* may be attributed to digestive activity by host cells (e.g. polymorphonuclear neutrophils) adjacent to the spherule envelope (Drutz and Huppert, 1983).

The physical properties of membrane lipids in pathogenic fungi have received significant attention in recent years. Studies have shown that lipid microdomains consisting of glycosphingolipids and sterols might serve to concentrate virulence factors (Siafakas et al., 2006; Farnoud et al., 2014), infectivity (Tagliari et al., 2012), and pathogenicity (Singh et al., 2012). Thus, the physical properties of the plasma membrane appear to affect the outcome of the infection (Rella et al., 2016. Certain glycosphingolipids, such as glucosylceramide (GlcCer), have been shown to be involved in the regulation of virulence in fungi affecting plants (Thevissen et al., 2004; Ramamoorthy et al., 2007) and humans (Rittershaus et al., 2006; Singh and Del Poeta, 2011).

The synthesis of GlcCer has been demonstrated in fungi that are pathogenic to humans, such as *Cryptococcus neoformans* (*C. neoformans)* (Hogan et al., 1996), *Candida albicans* (*C. albicans*) (Leipelt et al., 2001), *Aspergillus fumigatus* (*A. fumigatus*) (Levery et al., 2002), *Histoplasma capsulatum* (*H. capsulatum*) (Klimpel and Goldman, 1988), *Paracoccidioides brasiliensis* (*P. brasiliensis*) (San-Blas and San-Blas, 1977), and *Sporotrix schenckii* (*S. schenckii*) (Toledo et al., 2000). Other studies have suggested a role for GlcCer in the regulation of fungal growth and pathogenesis. For instance, in *C. neoformans* GlcCer is mainly localized in the cell wall and mostly accumulates at the budding site of dividing cells (Rittershaus et al., 2006). Interestingly, antibodies against *C. neoformans* GlcCer produced by patients affected with cryptococcosis inhibit budding and division of *C. neoformans* cells grown *in vitro* (Rodrigues et al., 2000) as well as differentiation and germ-tube formation of *Pseudallescheria boydii* (*P. boydii*) and *C. albicans* (Shimamura, 2012). Additionally, production of antibodies against fungal glycolipids has been demonstrated in patients with paracoccidioidomycosis (Bertini et al., 2007). In other fungi, disruption of the GlcCer biosynthetic pathway altered spore germination, hyphal development, and fungal growth (Levery et al., 2002). Monoclonal antibodies against fungal GlcCer have been produced, and interestingly, these antibodies protected mice against lethal cryptococosis (Rodrigues et al., 2007), and also the treatment with anti-GlcCer antibody enhanced macrophage function against the fungus *Fonsecaea pedrosoi* (*F. pedrosoi*) (Nimrichter et al., 2004). Taken together, these studies suggest an important role of GlcCer in fungal cell growth and differentiation. Furthermore, GlcCer might also be implicated in the regulation of fungal virulence.

Lipid composition of fungal cell wall has been characterized for several species. Studies of the parasitic phase (yeast) of the dimorphic fungus *P. brasiliensis* have identified 49 phospholipid including phosphatidylcholine, phosphatidylethanolamine, phosphatidylserine, phosphatidylglycerol, phosphatidylinositol, and phosphatidic acid (Longo et al., 2013). Among the fatty acids, C18:1 and C18:2 were the most abundant. The prevalent glycolipid species was Hex-C18:0-OH/d19:2-Cer, although other minor glycolipid species were also detected. The most abundant sterol was brassicasterol (Longo et al., 2013).

In the present study, the chemical analysis of the lipids extracted from the spherule outer wall (SOW) fraction of *Coccidioides posadasii* showed that they are composed largely of phospholipids, enriched with saturated fatty acids and the major sphingolipid components are sphingosine and ceramide.

A neutrophil killing assay and a murine model of coccidioidomycosis were also explored to characterize the biological effect of SOW lipids in immune function.

MATERIALS AND METHODS

Coccidioides Cultures and Spherule Staining

Coccidioides posadasii isolate C735 is a virulent clinical isolate. Hyphal growth of *Coccidioides* spp were cultured on glucose-yeast extract (GYE) agar plates at 25°C for 4 weeks to produce arthroconidia that were used to produce spherules in Converse medium using 250 ml Erlenmeyer flasks with rubber stoppers. Each culture flask contained $1–5 \times 10^7$ arthroconidia in 100 ml of Converse medium that was purged with a medical grade gas mixture (20% CO_2 and 80% air) for 3 min and incubated in a CO_2 incubator for 5–14 days at 39°C, 10% CO_2 with shaking (Cole et al., 1985). The flasks were purged with $C0_2$-air every 2 days after inoculation. Production of the sloughing, membranous SOW was monitored by phase-contrast microscopy. All steps of the inoculation and subsequent isolation procedure were performed in a Biosafety level 3 laboratory at University of Texas at San Antonio.

Fungal cells were labeled with a florescent dye cocktail containing 0.4 mg/ml Calcofluor White (CFW; Sigma, St. Louis, MO) and 5% FM™4-64FX (Thermo-Fisher Scientific, Waltham, MA), which bind to cell wall and lipophilic membrane, respectively. Spherules were washed twice with PBS and resuspended in 2% PFA. Cell images were acquired with an Amines ImageStream MKII cytometer and analyzed using IDEAS® software.

SOW Isolation and Lipid Extraction

SOW was isolated from parasitic culture of *Coccidioides* in Converse medium as previously reported (Cole et al., 1988). Hexane was added to SOW, and an aliquot of the SOW fraction was subjected to sterility tests on GYE culture plates. Sterile SOW fractions were then taken to BSL2 laboratory for lipid extraction.

Two extraction methods were performed, a one-step method with hexane alone and a sequential extract method using three solvents (hexane, chloroform, and methanol) with increased polarity (JT Baker. ThermoFisher Scientific Inc.). The extraction procedures were conducted with a percolating Soxhlet extractor. The extracts were concentrated by rotary evaporation and then further dried under a nitrogen gas stream. The absence of the glycoprotein in the SOW lipid fraction was confirmed by immunoblot analysis with anti-SOWgp glycoprotein serum (Hung et al., 2002) and the Bradford method to estimate the protein content (Bradford, 1976).

Characterization of Lipid Extracts of SOW by Thin Layer Chromatography

The qualitative characterization of lipids extracted from SOW was performed by one- and two-dimensional thin layer chromatography (TLC) using silica gel 60 F254 (Merck®, USA) plates. The lipid bands/spots on silica plates were revealed with iodine and visualized under an UV-light. The retention factor (Rf) was used to compare and identify the SOW lipids. The Rf value is equal to the distance traveled by the lipid divided by the distance traveled by the solvent front, both measured from the origin.

Gas Chromatography Analysis of SOW Fatty Acids

Fatty acids were extracted from the lipid fractions with 0.5 N NaOH and then methylated with 20% boron trifluoride (BF3) using a standard protocol (Ackman, 1998; Ichihara and Fukubayashi, 2010). The methylated fatty acids were purified in n-Heptane and dehydrated using anhydrous sodium sulfate. Finally, the sample was filtered and injected into a gas chromatograph (Agilent 6890N) that is equipped with a flame ionization detector (FID). The samples were separated using a capillary column (DB23). Data was acquired and analyzed using Chemstation software.

UPHPLC-MS/MS Analysis

Phospholipids and glycolipids were characterized by electrospray ionization tandem mass spectrometry (ESI-MS/MS) on a linear ion-trap mass spectrometer system using a ACQUITY UPLC® BEH C18 column (Xevo G2-XS QTOF Quadrupole Time-of-Flight Mass Spectrometry; Waters Corporation, Milford, MA. EEUU). The mobile phase contained a mixture of formic acid and acetonitrile solution, at a flow rate of 0.300 ml/min and ionization source ESI positive detector was used to acquire the data. Samples were dissolved in 10 mM LiOH/methanol with 2.5 mM phosphatidylcholine (C11:0/C11:0-PC) as an internal standard. Full-scan spectra were collected at the 500–1,000 m/z range, and samples were subjected to total-ion mapping (TIM) [2 a.m.u. isolation width; pulsed-Q dissociation (PQD) to 29% normalized collision energy; activation Q of 0.7; and activation time of 0.1 ms]. Methylated glycolipids were dissolved in methanol and analyzed as described for phospholipids with some modifications (acquisition at the 500–2000 m/z range; PQD to 32% normalized collision energy). Spectra from both phospholipids and glycolipids were analyzed manually according to Pulfer and Murphy, 2003.

Chemical Structure Analysis of SOW Lipids Using FTIR and NMR

Methanol lipid extracts of SOW were suspended in 20 mM HEPES buffer (pH 7.4) at molar ratios from 1:0.0 to 1:1.0 for infrared spectroscopic measurements using an IFS-55 spectrometer (Bruker, Karlsruhe, Germany). Samples were placed in a CaF2 cuvette with a 12.5 μm Teflon spacer. Consecutive heating scans were performed automatically from 10 to 70°C with a heating rate of 0.6°C min^{-1}. Every 3°C, 200 interferograms were accumulated, apodized, Fourier transformed, and converted to absorbance spectra. The peak position of the asymmetric stretching vibration of the methylene band versus (CH_2) sensitive marker lipid order was plotted versus temperature. Phase transition temperatures were derived

by determination of the maximum of the first derivative of the heating scans. For measurement of hydrated lipids, samples were spread on an attenuated total reflectance (ATR) ZnSe crystal and free water was evaporated under a stream of N_2. Vibrational bands from the interface region (1,700–1,750 cm^{-1}), amide I (1,600–1,700 cm^{-1}), and head groups (1,000–1,300 cm^{-1}) were analyzed. The instrumental wave number resolution was better than 0.02 cm^{-1}; the wave number reproducibility in repeated scans was better than 0.1 cm^{-1}.

The ^{1}H- and ^{13}C-NMR and two-dimensional spectra were obtained in an AMX300 spectrometer (Bruker BioSpin GmbH, Rheinstetten, Germany) operating at 300 MHz for ^{1}H and 75.0 for ^{13}C using CDC^{l3} or dimethyl sulfoxide d6. Shifts are reported in δ units (ppm) and coupling constants (J) in Hz.

Polymorphonuclear Neutrophil Isolation and Killing Assay

Inbred C56BL/6 and DBA/2J mice were obtained from the National Cancer Institute/Charles River Laboratories. Mice were housed in a specific-pathogen free animal facility at UTSA and handled according to guidelines approved by the IACUC at UTSA. At 8 to 12 weeks of age, sex-matched mice were relocated into an ABSL3 laboratory before experimentation.

Polymorphonuclear neutrophils (PMNΦs) were harvested from peritoneal exudates of C57BL/6 and DBA/2J mice that were intraperitoneally injected with 4% thioglycollate at 4 h post injection. PMNΦs were further enriched using a Ficoll-Paque density gradient and incubated with *C. posadasii* arthroconidia (MOI: 5:1) plus an indicated concentration of the SOW lipid methanol extracts for 4 h at 35°C, 5% CO_2. PMNΦs incubated with arthroconidia alone were used as a control. Percentages of killing were determined by serial dilution on GYE agar plates of the mixtures as previously described (Gonzalez et al., 2011). Assays of killing efficiency were repeated in three separate experiments.

Subcutaneous Challenge and Treatment With SOW Lipids

Hair on an area of the posterior quadrant of the abdomen (approximately 2 by 2 cm) was removed and swabbed with 70% ethanol. Mice were challenged subcutaneously (s.c.) with 5×10^4 viable arthroconidia of *C. posadasii* isolate C735 suspended in 100 µl PBS on the posterior border of the hairless abdominal region as previously described (Hung et al., 2016). Arthroconidia inoculation resulted in a small raised skin inflammation (≈2 mm), which dissipated within 24 h post-challenge. The subcutaneous injection of 5,000 µg/ml of SOW lipids was done at days 0, 4, 8, 12, and 16 after *Coccidioides* infection. The fungal burden in infected hypodermal tissue, which included visible abscesses and adjacent draining lymph nodes, was determined at the indicated days post-challenge by plating serial dilutions of the tissue homogenates on GYE agar containing 50 µg/ml chloramphenicol as described previously (Xue et al., 2009). The skin abscesses and adjacent draining lymph nodes were radically enlarged and fused together in most of the infected mice at 9 and 20 days post-challenge (dpc). Thus, both tissues were combined for CFU determination. The fungal burdens in skin, lung and spleen homogenates were determined in the same manner. The number of CFU of *Coccidioides* was expressed on a log scale and reported for individual mice of each group as previously described (Xue et al., 2009).

Statistical Analysis

The Mann–Whitney U test was used to analyze CFUs and cell numbers as previously described (Xue et al., 2009). A P-value of <0.05 was considered statistically significant. The killing percentage of arthroconidia by PMNΦs treated with SOW lipids was analyzed with one-way ANOVA. The GraphPad software version 6.0a was used for the statistical analysis.

RESULTS

Coccidioides SOW Mainly Contains Lipids

C. posadasii consistently produces and sheds membranous SOW that is accumulated in the Converse medium *in vitro*. Image analysis of spherules revealed that there is a lipid layer labeled with a lipophilic dye, FM™4-64FX between the spherule outer and the inner wall (SOW & SIW; the greenish yellow layer in **Figure 1**). Notably, the peeling SOW also bound well to FM™4-64FX. Cross examination of the lyophilized SOW extracts showed light-weighted and fiber-like powder appearance (Cole et al., 1988). Approximately, 67% of SOW dry weight was soluble in organic solvents including 53.2% in methanol, 9.9% in chloroform, and 3.9% in hexane, respectively. These fractions did not contain SOWgp protein, a major GPI-anchored antigen located on SOW, as it was not detected in any of the solvent extracts by Western blot analysis with a SOWgp-specific serum (**Supplemental Figure S1**). TLC separation of the lipid extracts revealed that the major compounds were lipids with Rf values at 0.19–0.31, 0.77, and 1.0 in the methanol extract; Rf values at 0.16, 0.73, and 0.94 in the chloroform extract, and 0.34, 0.41, 0.77, and

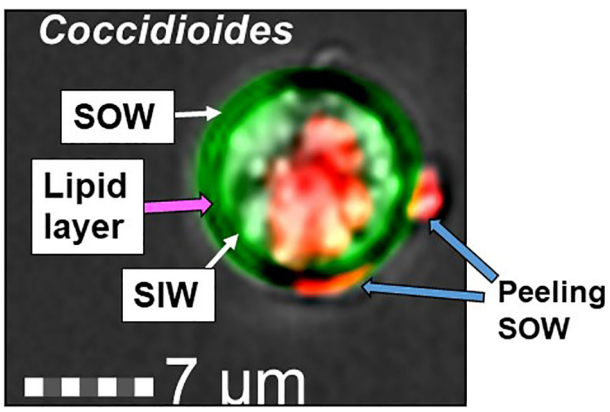

FIGURE 1 | Image of a *Coccidioides* spherule labeled with Calcofluor White (green) and FM™4-64FX (red). A thin greenish yellow layer visible between the spherule outer and inner wall represents colocation of SOW lipids and fungal cell wall chitin/glucan component. The lipophilic probe, FM™4-64FX bound to a central vacuole (V) and peeling SOW.

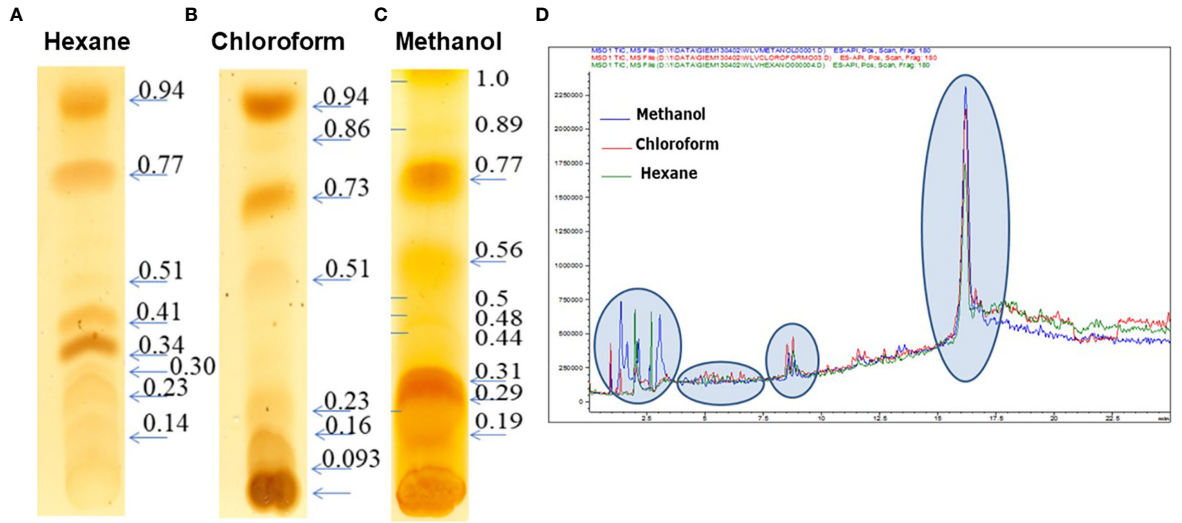

FIGURE 2 | TLC analysis of extracts of SOW lipids with hexane **(A)**, chloroform **(B)** and methanol **(C)** and UPHPLC chromatography of the SOW lipid extracts separated with hexane, chloroform, and methanol **(D)**. TLC separation was carried out with a mixture solvent containing eluent phase as hexane: chloroform 1:2.

0.94 in hexane, respectively (**Figures 2A–C**). Despite lipid compositions varied in these three extracts, the major lipids were apparently present in all three extracts with most abundant in the methanol extract. Further analysis of lipid extracts using Ultra High Performance Liquid Chromatography (UHPLC) revealed that the spectra of these three solvent extracts were almost overplayed (**Figure 2D**), suggests the methanol extract contained representative SOW lipid species. Hence, we focused on chemical and biological analysis of the methanol extract.

Coccidioides SOW Lipids Consist of Both Phospholipids and Sphingolipids

The major lipid peak (circled in **Figure 2D**; ~17 min) in the methanol extract was subjected to mass spectroscopy analysis (UHPLC-MS/MS). A total of seven phospholipids and six sphingolipids were identified (**Table 1**). GCxGC-TOF analysis of FAMES derived from the methanol extract revealed that the SOW lipids contained mainly saturated fatty acids (30.7%) and only

TABLE 1 | Major lipids identified in the methanol extract of SOW.

Lipids	Fatty acids	Observed mass (*m/z*)	Predicated Mass (+modification)
Phosphatidylethanolamine (PE)	C18:2	493.5	494.6 ($M + NH4^+$)
	C14:0	486.1	484.6 ($M + NH4^+$)
	C18:0	479.0	481.6 (M^+)
	C18:1	484.4	480.6 ($M + H^+$)
Phosphatidic acid (PA)	C20:0	480.4	482.6 ($M + NH4^+$)
	C12:0	375.1	375.3 ($M + Na^+$)
Phosphatidylglycerol (PG)	C12:0	486.1	487.6 ($M + NH4^+$)
Sphingosine (C_{18}-α-OH-Δ8)		323.4	333.5 ($M + NH4^+$)
Sphingosine-phosphate (C_{18}-α-OH-Δ8)		437.3	432.5 ($M + Na^+$)
Sphingomyelin-phosphocholine (C_{18}-α-OH-Δ4, Δ8, C9-methyl)	C14:0	675.7	673.7 ($M + H^+$)
Sphingomyelin-phosphoethanolamine (C_{18}-α-OH-Δ4, Δ8, C9-methyl)	C14:0	437.4	435.6 ($M + H^+$)
Dihexosylceramide (C_{18}-s-OH-Δ4)	C14:0	900.7	904.2 (M^+)
	C16:0	868.3	875.2.3 (M^+)

TABLE 2 | Fatty acid composition of SOW lipids.

Saturated fatty acids	**%**
Decanoic acid, (C10:0)	0.2
Dodecanoic acid (C12:0)	2.1
Myristic acid (C14:0)	1.4
Pentadecanoic acid (C15:0)	0.2
Palmitic acid (C16:0)	21.2
Heptadecanoic acid (C17:0)	0.5
Stearic acid (C18:0)	3.6
Arachidic acid (C20:0)	0.3
Heneicosanoic acid (C21:0)	0.1
Behenic acid (C22:0)	0.7
Tricosanoic acid (C23:0)	0.2
Lignoceric acid (C24:0)	0.3
Subtotal	**30.7**
Unsaturated fatty acids	**%**
Elaidic acid (C18:1n9t)	0.12
Oleic acid (C18:1n9c)	
Heneicosanoic acid	0.1
Linolelaidic acid (C18:2n6t)	0.04
Linoleic acid (C18:2n6c)	
Subtotal	**0.17**
Ratio of Unsaturated/Saturated	**0.0055**

The bold font was used to highlight the values of subtotals of saturated, unsaturated and the ratio between them.

trace amounts of unsaturated molecules (0.17%; **Table 2**). The major fatty acids were palmitic acid (C16:0) and stearic acid (18:0).

Infrared (FTIR) analysis of the methanol extract allowed confirmation of the signals of substituents more representatives (**Figure 3**). The signals at 3,364, 2,900, 1,711, 1,641, 1,464, and 1,378 indicate the presence of -OH group linked to alcohols, -CH2 group in aliphatic compounds, -C=O group in fatty acids or esterified compounds, -NH amine group in sphingolipids and phosphate groups in phospholipids. These results were in agreement with the TLC and UHLPC/MS studies (**Figure 2** and **Table 1**). These data suggest that SOW lipids consist of phospholipids and sphingolipids.

Sphingolipids of SOW lipids were further confirmed using both ^{1}H- and ^{13}C-NMR analyses. ^{1}H-NMR analysis showed the presence of protons adjacent at phosphate groups (-CH2-O-P), protons adjacent to oxygens (-CH2-O), methylene adjacent to double- bonds (R=CH2-CH2) or carbon α (**Figure 4A**). Additionally, ^{13}C-NMR analysis showed the presence of both glycerol and sphingosine (**Figure 4B**). Taken together, SOW lipids consist of fatty acids, triacylclycerols, phospholipids (PA, PE and PG), and sphingolipids including sphingosine chain without a fatty acid and ceramides with a fatty acid side chain.

SOW Lipids Suppress Neutrophil Killing of *Coccidioides* Arthroconidia *In Vitro*

Peritoneal neutrophils were isolated from C57BL/6 and DBA/2J mice after eliciting with 4% thioglycolate. Viability and purity of the isolated were assessed as shown in **Table S2**. The purified PMNΦs were capable of killing 60–80% of *Coccidioides* arthroconidia after 4 h incubation. The PMNΦs incubated with an indicated concentration of SOW lipids at 1,000, 5,000, and 10,000 μg/ml significantly decrease the killing activity of *Coccidioides* arthroconidia from ~20 to 50% for B6 and DBA/2J mice, respectively (**Figures 5A, B**).

The difference between different treatments was not statistically significative. The viability of SOW lipids treated PMNΦs were evaluated by flow cytometry analysis after staining with carboxyfluorescein diacetate (CFDA) and Annexin V for detecting apoptotic cells. The results confirmed that PMNΦs were viable after incubating with SOW lipids even at the highest concentration (these results are presented in **Supplemental Figure S3** and **Table S3**). These results suggest that SOW lipids suppress PMNΦs killing functions without impacting viability of these phagocytes.

SOW Lipids Suppress Protective Immunity Against *Coccidioides* Infection

In vivo impact of SOW lipids was evaluated using a murine model of subcutaneous coccidioidomycosis (Hung et al., 2016). A group of mice was treated with 5,000 μg/ml of SOW lipids by the same subcutaneous route at 0, 4, 8, 12, and 16 days post-challenge. Mice were injected with PBS as controls. Both groups of mice were sacrificed at 9 and 20 days post-challenge for evaluating fungal burden (CFUs). The CFU´s recovered from the injection site (skin) at 9 and 20 days post-challenge are shown in **Figures 6A**, **D**, respectively. At 9 days post-challenge, there was a trend of increased fungal burden in the lungs and spleen of the mice that were treated with SOW lipids, albeit that was not statistically significant (**Figures 6B, C**). Interestingly, the mice treated with a total dose of 25,000 μg/ml of SOW lipids and euthanized 20 days post-challenge showed significantly increased amounts of CFUs in their lungs compared to the mice injected with PBS alone (**Figure 6E**; 5.5 Log_{10} versus 4.0 Log_{10}; Mann–Whitney U test p = 0.0306). Furthermore, the SOW lipid-treated mice also significantly increased fungal dissemination to the spleen (**Figure 6F**; p = 0.0012), while only one mouse of the lipid non-treated group had detectable fungal burden in the spleen. These results suggested that SOW lipids suppress protective immunity of mice against subcutaneous *Coccidioides* infection.

DISCUSSION

Coccidioidal SOW is a unique structure of fungal cell surface among medically important fungal pathogens. In 1953, Tarbet

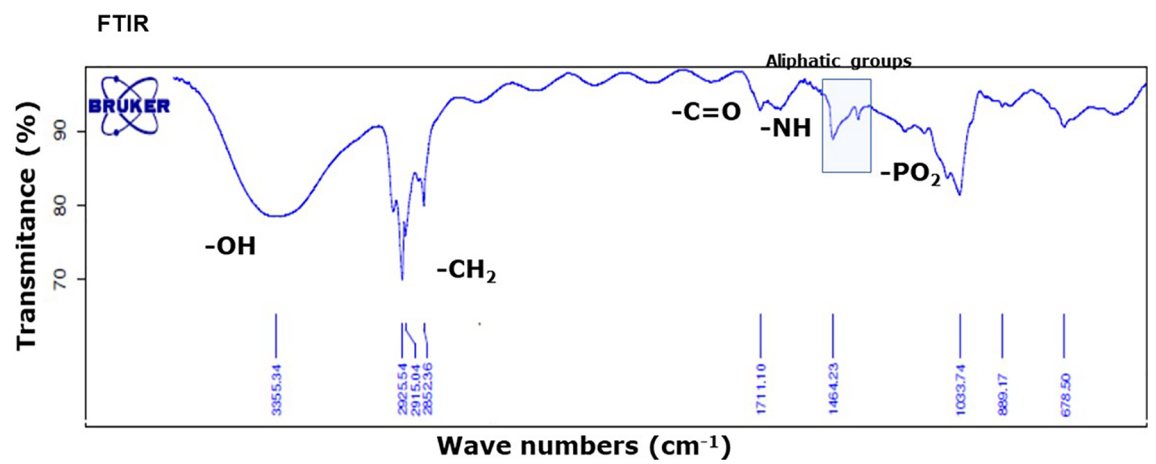

FIGURE 3 | FTIR absorption spectrum of SOW lipids in the methanol extract shows the presence of contribution functional groups (OH, CH_2, CO, NH, and PO_2) that are labeled at the corresponding spectral positions.

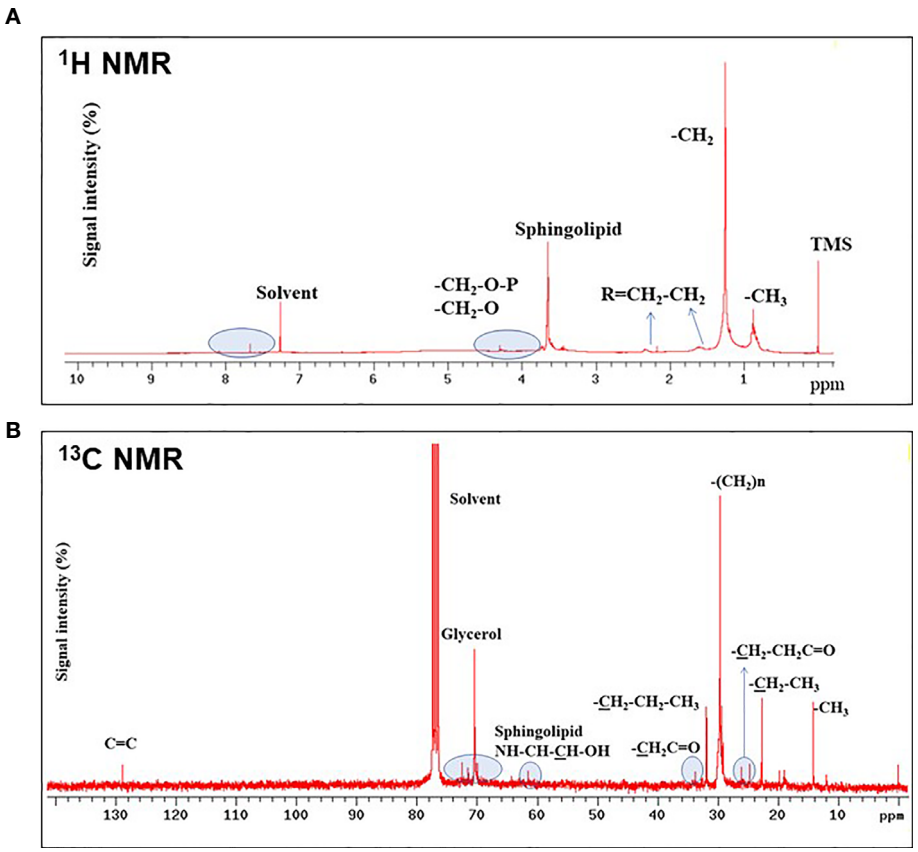

FIGURE 4 | ^{1}H- **(A)** and ^{13}C-NMR **(B)** analyses of SOW lipids in the methanol extract. Contributions from specific functional groups are labeled at the corresponding spectral positions.

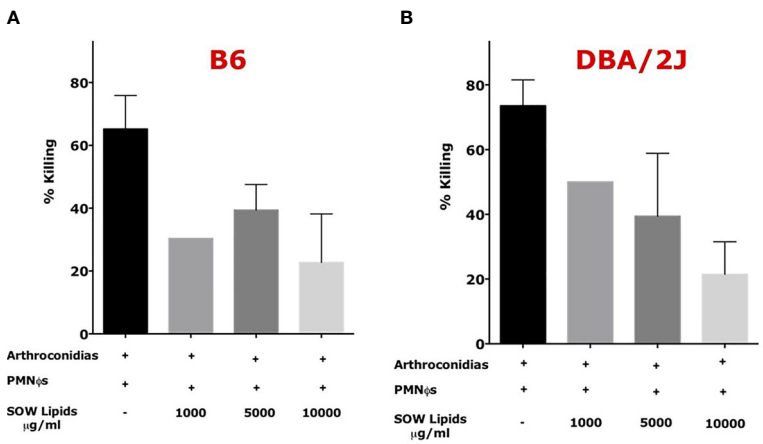

FIGURE 5 | SOW lipid treatment of murine neutrophils (PMN*Φ*s) resulted in loss of killing efficiency of *Coccidioides* arthroconidia. PMN*Φ*s were incubated with *Coccidioides* arthroconidia for 4 h in the presence of SOW lipids at an indicated concentration from 1,000 to 10,000 µg/ml. Bar data show the mean percentage of *Coccidioides* arthroconidia killed for PMN*Φ*s isolated from both C57BL/6 **(A)** and DBA/J mice **(B)**. Representative results (mean ± SD for $n = 3$ technical replicates) per treatment from one of three independent experiments are shown. Killing percentage is presented as mean killing relative to vehicle-treated cells (normalized to 100%). Statistical analysis was done with one-way ANOVA.

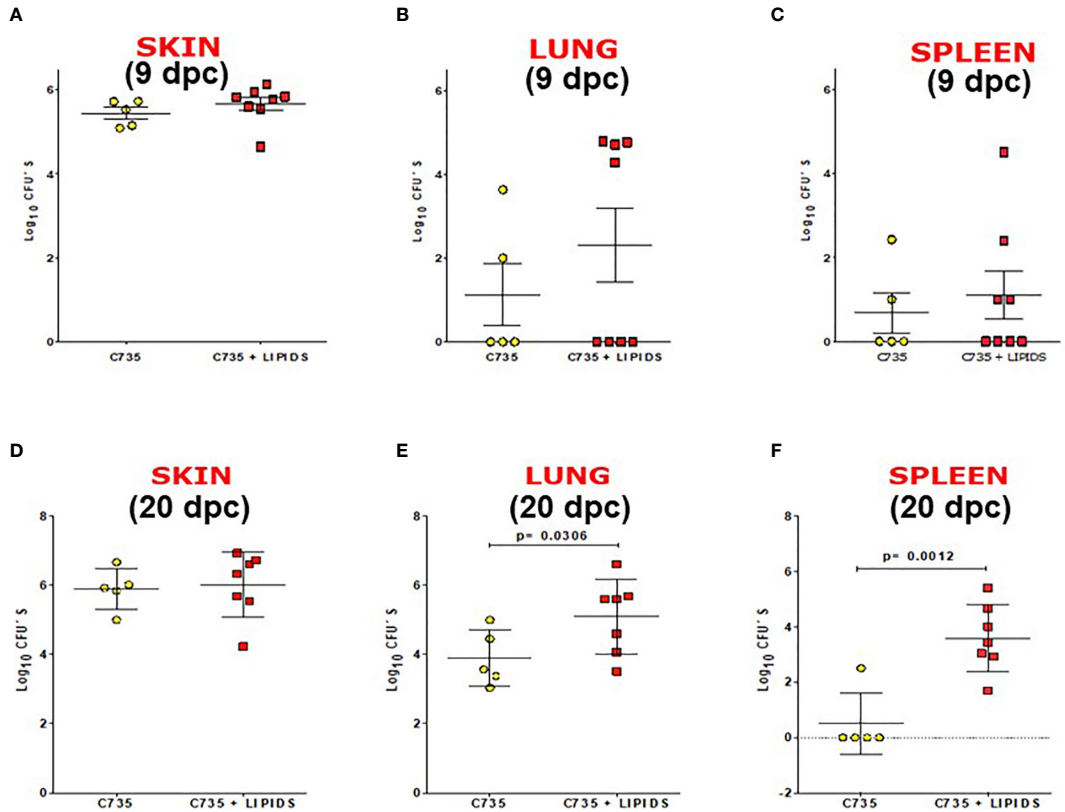

FIGURE 6 | SOW lipids suppress protective immunity against a subcutaneous infection with *Coccidioides*. Comparison of fungal burden in the subcutaneous infection site **(A, D)** lungs **(B, E)** and spleen **(C, F)** of SOW lipid-treated and mock mice at 9 and 20 days post-challenge. The median CFUs (log10) are indicated by horizontal lines inside each group. A statistically significant difference was revealed between the fungal burden in the lungs and spleen of treated and mock mice at 20 dpc.

and Breslau demonstrated that *Coccidioides* spherules were positive for the Baker acid-hematin test, a technique to detect phospholipids (Tarbet and Breslau, 1953). Spherules from all stages of parasitic growth are tested positive for surface phospholipids, except endospores. The thickness of the phospholipid layer was seen to be proportional to the size of spherules. The lipid bilayer (tripartite) structure was also shown in electron microscopy examination of SOW that was labeled with osmium tetroxide (OsO4) to enhance the visibility of lipoids (Figure 1 in Cole et al., 1988; Figure 8B in Hung et al., 2002). SOW consists of multiple layers of the bilayer tripartite structures interwoven together with OsO4-negative layers that presumably are made of polysaccharides. Lipids are enriched in the inner leaflets of SOW. When SOW is peeled away from the spherule surface the lipids are exposed and readily bound to lipophilic FM^{TM}4-64FX dye (**Figure 1A**). Qualitative and quantitative differences in lipid contents are found between fungal species, culture conditions and specific cell structure components including fungal cell wall, whole cells, mycelial wall, spore wall and yeast wall (Longo et al., 2013; Feofilova et al, 2015). Fungal cell wall is thought to mainly compose of glycoproteins and polysaccharides such as α- and β-linked glucan, chitin, and other sugar polymers. Surprisingly, we found that lipids constitute over 67% of SOW dry weight and they are the major chemical components of spherule outer wall.

SOW is shed into culture media in large quantities once the fungus has undergone a transformation process to spherules in the parasitic phase growth of *Coccidioides* (Cole et al., 1988). SOW is accumulated in the parasitic cultures using a chemically defined Converse medium that only contains glucose as carbon source, N-Z amine and ammonia acetate as nitrogen source, phosphate salts and trace amounts of metals (Converse, 1956 and 1957; Levine, 1962). Spherules in the murine lungs also shed SOW which can be engulfed by adjacent host phagocytic cells. Studies of the chemical compositions and biogenesis of SOW are fundamental steps to learn the biological functions.

SOW is harvested using a stepwise, differential centrifugation method that produces over 50 mg of SOW per litter of spherule cultures at day 7 post inoculation (Cole et al., 1988). We have tested three solvents with increased polarity (hexane, chloroform and methanol) to extract neutral lipids, phospholipids and glycolipids of SOW, respectively. The yield of SOW lipids has been improved by using a percolation Soxhlet system compared

to regular sonication method. TLC analysis reveals that there are relatively high portions of non-polar lipids (Rf valve > 0.7) compared to chloroform and methanol extracts, while all lipid types are apparently present in all three solvents. For chemical structure characterization, we have decided to analyze the methanol extract that had the highest lipid yield among the three extracts.

Composition and chemical structures of *Coccidioides* SOW lipids were analyzed using UHPLC-MS/MS, GC-FID, GCxGC-MS, FT-IR and NMR (both ^{1}H and ^{13}C spectra). SOW lipids include free fatty acids, triacylglycerides, steroids, phospholipids, and sphingolipids. Although these lipid molecules are common for many fungal pathogens and mammalian bilayer membrane, they constitute a specific profile in SOW lipids. SOW lipids are enriched in phospholipids including phosphatidylethanolamine (PE), phosphatidic acid (PA) and phosphatidylglycerol (PG) (**Table 1**). Surprisingly, phosphatidylcholine (PC), an abundant phospholipid of the cell wall of *Paracoccidioides brasiliensis* and other filamentous fungi is not detected (Dembitsky and Pechenkina, 1991; Longo et al., 2013). Interestingly, sphingomyelin-phosphocholine with a myristic acid (C14:0) linking to a ceramide is detected. Both PC and sphingomyelin share a phophocholine functional group, yet it is not determined whether this sphingomyelin-phosphocoline can replace PC to be an important part of SOW structure. Additional sphingolipids are detected in relatively high amounts that include sphingosine, sphingosine-phosphate, sphingomyelin-phosphoethanolamine and dihexosylceramide. The latter is the predominant SOW glycosphingolipid that contains mainly saturated fatty acids (C14:0 and C16:0). Likewise, the prevalent glycolipid of *Paracoccidioides brasiliensis* is also a hexosylceramide (Hex-C18:0-OH/d19:2-Cer) that is linked to a longer C18:0 fatty acid (Longo et al., 2013). Further fatty acid composition analysis of SOW lipids reveals that palmitic acid (C16:0) and stearic acid (C18:0) are the two major components. These two fatty acids are commonly present in bilayer membrane. Notably, fatty acid composition of whole SOW lipids is different from the major glycosphingolipid. Taken together, these results suggest that the biosynthesis and metabolic enzymes in the SOW glycolipid synthesis pathways have a preference of shorter fatty acids (C14:0 and C16:0 compared to C18:0). Only few amounts of unsaturated fatty acids are detected in SOW lipids (**Table 2**). Biological membrane fluidity is highly regulated for cells to acclimate growth at different temperature conditions (Thompson and Nozawa, 1984). Temperature-induced alteration of fatty acid compositions for microbes has been reported (Hung et al, 1995). Cells grown at higher temperature tend to contain higher amounts of long chain and saturated fatty acids that have higher melting points compared to short chain and unsaturated fatty acids (Hung et al., 1995; Knothe and Dun, 2009). High content of saturated fatty acids may be beneficent for *Coccidioides* to grow at 39°C of the culture condition of the parasitic phase.

Fungal cell wall is an excellent reservoir of antigenic components that can contribute to the interactions between fungi and their hosts. The host attempts to recognize the microbial pathogen and inhibit its growth and dissemination, whereas the pathogen tries to subvert recognition and suppress host responses. SOWgp is predicted to be a GPI-anchored protein that is identified as a major antigenic glycoprotein located on SOW (Cole et al., 1988, Hung et al., 2000 and 2002). SOWgp elicits both humoral and cell-mediated immune responses in *Coccidioides* patients and mice that are vaccinated with formalin-killed spherules (Cole et al., 1988 and Hung et al., 2000). Mice vaccinated with bacterial-expressed recombinant SOWgp protein combined with the complete Freud's adjuvant and other adjuvant systems gave non-consistent protective efficacy from 0 to 50% survival in a murine model of pulmonary coccidioidomycosis, depending on vaccine doses, adjuvants and mouse strains (Hung et al., 2000; Cox and Magee, 2004; data not shown). The protective capacity and immune regulation role of SOWgp is still elusive. Notably, the *sowgp* mutant strain created by targeted gene replacement shows partial loss of virulence (Hung et al., 2002). These findings suggest that beside the SOWgp, other components in the SOW may play an important role in modulation of the immune response to *Coccidioides* infection.

Coccidioides SOW lipids can modulate immune response is an appealing idea. PMNΦs are the main cells recruited to the infection sites after C*occidioides* challenge. PMNΦs are thought to play double-edged swords against many microbial infections. Early infiltration of PMNΦs may facilitate microbial killing. On the other hand, mass infiltration of PMNΦs may contribute to tissue damage (Kaplan and Radic, 2012). Endospores released from mature spherules trigger an influx of neutrophils to the *Coccidioides* infection sites. It has been showed *in vitro* that neutrophils can inhibit the growth of spherules initials and endospores (<10 μm) (Drutz and Huppert, 1983; Lee et al., 2015). Apparently, PMNΦs are also essential in the early stage of vaccine-induced immunity, as depletion of PMNΦs using a specific anti-Ly6G mAb renders the protective efficacy of the live, attenuated vaccine against pulmonary *Coccidioides* infection in mice (Hung et al, 2014). Interestingly, our data show that SOW lipids suppress PMNΦs killing of *Coccidioides* arthroconidia. For the *in vivo* evaluation of the immune suppressive activity of SOW lipids, we used a murine model of subcutaneous *Coccidioides* spp infection. The subcutaneous infection route is not a common portal of entry for coccidioidomycosis, but it allows the delivery of a larger and more consistent dose of arthroconidia and results in significant fungal burden in the hypodermis but not dissemination of the pathogen to multiple vital organs (Hung et al., 2016). In this model, SOW lipid-treated mice develop disseminated disease to both the lungs and spleen after 20 days post-challenge while the mock treated mice mainly had fungal burden in the skin. These data confirm that SOW lipids suppress protective immunity and promote fungal dissemination. We early have reported that *Coccidioides* parasitic cells can release a soluble molecule(s) in culture medium to suppress nitric oxide production in bone marrow derived macrophages (Gonzalez et al., 2011). The work to explore whether SOW lipids can suppress NO production and other immune mechanisms is under way.

DATA AVAILABILITY STATEMENT

The raw data supporting the conclusions of this article will be made available by the authors, without undue reservation.

ETHICS STATEMENT

The animal study was reviewed and approved by UTSA and handled according to guidelines approved by IACUC.

AUTHOR CONTRIBUTIONS

CP-J did all the lipid extraction procedures and the chemical characterization. MdP-JA designed and did the biological activity evaluation experiments. PA-M helped in the HPL/MS analysis and with CP-J did the compound identification. C-YH designed and analyzed the experiments. NC-L helped with the mice experiments. GC designed and analyzed the experiments. All the authors contributed to the article and approved the submitted version.

FUNDING

This work was supported by the National Institutes of Health Grants R01-AI071118A (to GC and to MJ-A) and R01AI135005 (to C-YH) and Universidad de Antioquia to CP-J. and MJ-A).

SUPPLEMENTARY MATERIAL

The Supplementary Material for this article can be found online at: https://www.frontiersin.org/articles/10.3389/fcimb.2021.592826/full#supplementary-material

Supplementary Figure 1 | Western blot showing the lack of the SOWgp protein.

Supplementary Table 2 | CD11+Ly6G+ positive cells after the Ficoll-Paque density gradient.

Supplementary Figure 3 | *Coccidioides* SOW lipids did not affect the viability of C57BL/6 and DBA/2J neutrophils.

Supplementary Table 3 | Annexin V and CFDA staining of neutrophils treated with different concentrations of SOW lipids.

REFERENCES

Ackman, R. G. (1998). Remarks on Official Methods Employing Boron Trifluoride in the Preparation of Methyl Esters of the Fatty Acids of Fish Oils. *J. Am. Oil Chem Soci.* 75, 541–545. doi: 10.1007/s11746-998-0263-9

Bertini, S., Colombo, A. L., Takahashi, H. K., and Straus, A. H. (2007). Expression of Antibodies Directed to *Paracoccidioides Brasiliensis* Glycosphingolipids During the Course of Paracoccidioidomycosis Treatment. *Clin. Vaccine Immunol.* 14 (2), 150–156. doi: 10.1128/CVI.00285-06

Bradford, M. M. (1976). A Rapid and Sensitive Method for the Quantitation of Microgram Quantities of Protein Utilizing the Principle of Protein-Dye Binding. *Analyt Biochem.* 72, 248–254. doi: 10.1016/0003-2697(76)90527-3

Cole, G. T., Xue, J., Seshan, K., Borra, P., Borra, R., Tarcha, E., et al. (2006). "Virulence Mechanisms of Coccidioides," in *Molecular Principles of Fungal Pathogens*. Eds. J. Heitman, S. G. Filler, J. E. Edwards and A. P. Mitchell (Washington, DC: ASM Press), 363–391.

Cole, G. T., Seshan, R., Franco, M., Bukownik, E., Sun, S. H., and Hearn, V. M. (1988). Isolation and Morphology of an Immunoreactive Outer Wall Fraction, Produced by Spherules of Coccidioides Immitis. *Infect. Immun.* 56, 2686–2694. doi: 10.1128/IAI.56.10.2686-2694.1988

Cole, G. T., Sun, S. H., and Huppert, M. (1985). "Morphogenesis of Coccidioides Immitis," in *Filamentous Microorganisms: Biomedical Aspects*. Ed. T. Arai (Tokyo: Japan Scientific Societies Press), 279–294.

Converse, J. L. (1956). Effect of Physico-Chemical Environment on Spherulation of *Coccidioides Immitis* in a Chemically Defined Medium. *J.Bacteriol.* 72 (6), 784–792. doi: 10.1128/JB.72.6.784-792.1956

Converse, J. L. (1957). Effect of Surface Active Agents on Endosporulation of *Coccidioides Immitis* in a Chemically Defined Medium. *J. Bacteriol.* 74, 106–107. doi: 10.1128/JB.74.1.106-107.1957

Cox, R. A., and Magee, M. (2004). Coccidioidomycosis: Host Response and Vaccine Development. *Clin. Microbiol. Rev.* 17 (4), 804–839. doi: 10.1128/CMR.17.4.804-839.2004

Dembitsky, V., and Pechenkina, E. E. (1991). Phospholipid and Fatty-Acid Compositions of Higher Fungi. *Chem. Natural Compd* 27 (2), 155–156. doi: 10.1128/cmr.17.4.804–839.2004

Drutz, D. J., and Huppert, M. (1983). Coccidioidomycosis: Factors Affecting the Host Parasite Interaction. *J. Infect. Dis.* 147, 372–390. doi: 10.1093/infdis/147.3.372

Farnoud, A. M., Mor, V., Singh, A., and Del Poeta, M. (2014). Inositol Phosphosphingolipid Phospholipase C1 Regulates Plasma Membrane ATPase (Pma1) Stability in Cryptococcus Neoformans. *FEBS Lett.* 588, 3932–3938. doi: 10.1016/j.febslet.2014.09.005

Feofilova, E. P., Sergeeva, Y., Mysyakina, I. S., and Bokareva, D. A. (2015). Lipid Composition in Cell Walls and in Mycelial and Spore Cells of Mycelial Fungi. *Microbiology* 84 (2), 170–176. doi: 10.1134/s0026261715020046

Fisher, M. C., Koenig, G. L., White, T. J., San-Blas, G., Negroni, R., Gutiérrez-Alvarez, I., et al. (2001). Biogeographic Range Expansion Into South America by *Coccidioides Immitis* Mirrors New World Patterns of Human Migration. *PNAS* 98 (4), 4558 –44562. doi: 10.1073/pnas.071406098

Frey, C. L., and Drutz, D. J. (1986). Influence of Fungal Surface Components on the Interaction of *Coccidioides Immitis* With Polymorphonuclear Neutrophils. *J. Infect. Dis.* 153, 933–943. doi: 10.1093/infdis/153.5.933

Galgiani, J. N., Ampel, N. M., Blair, J. E., Catanzaro, A., Johnson, R. H., Stevens, D. A., et al. (2005). Coccidioidomycosis. *Clin. Infect. Dis.* 41, 1217–1223. doi: 10.1086/496991

Gonzalez, A., Hung, C. Y., and Cole, G. T. (2011a). Nitric Oxide Synthase Activity has Limited Influence on the Control of Coccidioides Infection in Mice. *Microb. Pathog.* 51 (3), 161–168. doi: 10.1016/j.micpath.2011.03.013

Gonzalez, A., Hung, C. Y., and Cole, G. T. (2011b). Absence of Phagocyte Nadph Oxidase 2 Leads to Severe Inflammatory Response in Lungs of Mice Infected With Coccidioides. *Microb. Pathog.* 51, 6, 432–441. doi: 10.1016/j.micpath.2011.08.003

Hogan, L. H., Klein, B. S., and Levitz, S. M. (1996). Virulence Factors of Medically Important Fungi. *Clin. Microbiol. Rev.* 9, 469–488. doi: 10.1128/CMR.9.4.469

Hung, C.-Y., Castro-Lopez, N., and Cole, G. T. (2016). Card9- and MyD88-mediated Gamma Interferon and Nitric Oxide Production is Essential for Resistance to Subcutaneous *Coccidioides Posadasii* Infection. *Infect. Immun.* 84 (4), 1166 –11175. doi: 10.1128/IAI.01066-15

Hung, C. Y., Jiménez-Alzate, Maríad. P., Gonzalez, A., Wüthrich, M., Klein, B. S., and Cole, G. T. (2014). Interleukin-1 Receptor But Not Toll-Like Receptor 2 Is Essential for MyD88-Dependent Th17 Immunity to *Coccidioides* Infection. *Infect. Immun.* 82 (5), 2106–2114. doi: 10.1128/iai.01579-13

Hung, C. Y., NEIL , M., Ampel, N. H., Christian, L., Seshan, K. R., and Cole, G. T. (2000). A Major Cell Surface Antigen of Coccidioides immitis Which Elicits Both Humoral and Cellular Immune Responses. *Inf. Immun.* 68 (2), 584–593.

Hung, C. Y., Ko, Y.-G., and Thompson, J. G. A. (1995). Temperature-Induced Alteration of Inositolphosphorylceramides in the Putative Glycosylated Lipid Precursors of Tetrahymena Mimbres Glycosylphosphatidylinositol-Anchored Proteins. *Biochem. J.* 307, 107–113. doi: 10.1042/bj3070107

Hung, C. Y., Yu, J. J., Seshan, K. R., Reichard, U., and Cole, G. T. (2002). A Parasitic Phase-Specific Adhesin of *Coccidioides Immitis* Contributes to the Virulence of This Respiratory Fungal Pathogen. *Infect. Immun.* 70 (7), 3443–3456. doi: 10.1128/IAI.70.7.3443-3456.2002

Ichihara, K., and Fukubayashi, Y. (2010). Preparation of Fatty Acid Methyl Esters for Gas-Liquid Chromatography. *J. Lipid Res.* 51, 635–640. doi: 10.1194/jlr.d001065

Kaplan, M. J., and Radic, M. (2012). Neutrophil Extracellular Traps: Double-Edged Swords of Innate Immunity. *J. Immunol.* 189, 2689–2695. doi: 10.4049/jimmunol.1201719

Klimpel, K. R., and Goldman, W. E. (1988). Cell Walls From Avirulent Variants of *Histoplasma Capsulatum* Lack Alpha-(1,3)-Glucan. *Infect. Immun.* 56, 2997–3000. doi: 10.1128/IAI.56.11.2997-3000.1988

Knothe, G., and Dun, R. O. (2009). A Comprehensive Evaluation of the Melting Points of Fatty Acids and Esters Determined by Differential Scanning Calorimetry. *J. Am. Oil Chem. Soc.* 86, 843–856. doi: 10.1007/s11746-009-1423-2

Lee, C.-Y., Thompson, G. R.II, Hastey, C. J., Hodge, G. C., Lunetta, J. M., Pappagianis, D., et al. (2015). *Coccidioides* Endospores and Spherules Draw Strong Chemotactic, Adhesive, and Phagocytic Responses by Individual Human Neutrophils. *PLoS One* 10 (6), e0129522. doi: 10.1371/journal.pone.0129522

Leipelt, M., Warnecke, D., Za¨hringer, U., Ott, C., Müller, F., Hube, B., et al. (2001). Glucosylceramide Synthases, a Gene Family Responsible for the Biosynthesis of Glucosphingolipids in Animals, Plants, and Fungi. *J. Biol. Chem.* 276 (36), 33621–33629. doi: 10.1074/jbc.M104952200

Levery, S. B., Momany, M., Lindsey, R., Toledo, M. S., Shayman, J. A., Fullere, M., et al. (2002). Disruption of the Glucosylceramide Biosynthetic Pathway in *Aspergillus Nidulans* and *Aspergillus Fumigatus* by Inhibitors of UDP-Glc: ceramide Glucosyltransferase Strongly Affects Spore Germination, Cell Cycle, and Hyphal Growth. *FEBS Lett.* 525, 59–64. doi: 10.1016/S0014-5793(02)03067-3

Levine, H. B. (1962). Purification of the Spherule-Endospore Phase Of Coccidioides Immitis. *Sabouraudia* 1 (2), 112–115. doi: 10.1080/00362176285190231

Longo, L. V. G., Nakayasu, E. S., Gazos-Lopes, F., Vallejo, M. C., Matsuo, A. L., Almeida, I. C., et al. (2013). Characterization of Cell Wall Lipids From the Pathogenic Phase of *Paracoccidioides Brasiliensis* Cultivated in the Presence or Absence of Human Plasma. *PLoS One* 8 (5), e63372. doi: 10.1371/journal.pone.0063372

Nimrichter, L., Barreto-Bergter, E., Mendonça-Filho, R. R., Kneipp, L. F., Mazzi, M. T., Salve, P., et al. (2004). A Monoclonal Antibody to Glucosylceramide Inhibits the Growth of *Fonsecaea Pedrosoi* and Enhances the Antifungal Action of Mouse Macrophages. *Microbes Infect* 6, 657–665. doi: 10.1016/j.micinf.2004.03.004

Pulfer, M., and Murphy, R. C. (2003). Electrospray Mass Spectrometry of Phospholipids. *Mass Spectrom Rev.* 22, 332– 364. doi: 10.1002/mas.10061

Ramamoorthy, V., Cahoon, E. B., Li, J., Thokala, M., Minto, R. E., and Shah, D. M.. (2007). Glucosylceramide Synthase is Essential for Alfalfa Defensin-Mediated Growth Inhibition But Not for Pathogenicity of Fusarium Graminearum. *Mol. Microbiol.* 66, 771–786. doi: 10.1111/j.1365-2958.2007.05955.x

Rella, A., Farnoud, A. M., and Del Poeta, M. (2016). Plasma Membrane Lipids and Their Role in Fungal Virulence. *Prog. Lipid Res.* 61, 63–72. doi: 10.1016/j.plipres.2015.11.003

Rittershaus, P. C., Kechichian, T. B., Allegood, J. C., Merrill, A. H.Jr., Hennig, M., Luberto, Ch., et al. (2006). Glucosylceramide Synthase is an Essential Regulator of Pathogenicity of *Cryptococcus Neoformans*. *J. Clin. Invest.* 116, 1651–1659. doi: 10.1172/JCI27890

Rodrigues, M. L., Shi, L., Barreto-Bergter, E., Nimrichter, L., Farias, S. E., Rodrigues, E. G., et al. (2007). Monoclonal Antibody to Fungal Glucosylceramide Protects Mice Against Lethal *Cryptococcus Neoformans* Infection. *Clin. Vaccine Immunol.* 14 (10), 1372–1376. doi: 10.1128/CVI.00202-07

Rodrigues, M. L., Travassos, L. R., Miranda, K. R., Franzen, A. J., Rozental, S., de Souza, W., et al. (2000). Human Antibodies Against a Purified Glucosylceramide From *Cryptococcus Neoformans* Inhibit Cell Budding and Fungal Growth. *Infect. Immun.* 68 (12), 7049–7060. doi: 10.1128/iai.68.12.7049-7060.2000

San-Blas, G., and San-Blas, F. (1977). *Paracoccidioides Brasiliensis*: Cell Wall Structure and Virulence. *A Rev Mycopathol* 62, 77–86. doi: 10.1007/BF01259396

Sharpton, T. J., Stajich, J. E., Rounsley, S. D., Gardner, M. J., Wortman, J. R., Jordar, V. S., et al. (2009). Comparative Genomic Analyses of the Human Fungal Pathogens *Coccidioides* and Their Relatives. *Genome Res.* 19, 1722–1731. doi: 10.1101/gr.087551.108

Shimamura, M. (2012). Immunological Functions of Steryl Glycosides. *Arch. Immunol. Ther. Exp. (Warsz)* 60, 351–359. doi: 10.1007/s00005-012-0190-1

Siafakas, A. R., Wright, L. C., Sorrell, T. C., and Djordjevic, J. T. (2006). Lipid Rafts in *Cryptococcus Neoformans* Concentrate the Virulence Determinants Phospholipase B1 and Cu/Zn Superoxide Dismutase. *Eukaryot Cell* 5, 488–498. doi: 10.1128/EC.5.3.488-498.2006

Singh, A., Wang, H., Silva, L. C., Na, C., Prieto, M., Futerman, A. H., et al (2012). Methylation of Glycosylated Sphingolipid Modulates Membrane Lipid Topography and Pathogenicity of Cryptococcus Neoformans. *Cell Microbiol.* 14 (4), 500–516. doi: 10.1111/j.1462-5822.2011.01735.x

Singh, A., and Del Poeta, M. (2011). Lipid Signalling in Pathogenic Fungi. *Cell Microbiol.* 13, 177–185. doi: 10.1111/j.1462-5822.2010.01550.x

Tagliari, L., Toledo, M. S., Lacerda, T. G., Suzuki, E., Straus, A. H., and Takahashi, H. K.. (2012). Membrane Microdomain Components of *Histoplasma Capsulatum* Yeast Forms, and Their Role in Alveolar Macrophage Infectivity. *Biochim. Biophys. Acta* 1818, 458–466. doi: 10.1016/j.bbamem.2011.12.008

Tarbet, J. E., and Breslau, A. M. (1953). Histochemical Investigation of the Spherule of *Coccidioides Immitis* in Relation to Host Reaction. *J. Infect. Dis.* 72, 183–190. doi: 10.1093/infdis/92.2.183

Thevissen, K., Warnecke, D. C., Francois, I. E., Leipelt, M., Heinz, E., Ott, C., et al. (2004). Defensins From Insects and Plants Interact With Fungal Glucosylceramides. *J. Biol. Chem.* 279, 3900–3905. doi: 10.1074/jbc.M311165200

Thompson, G. A., and Nozawa, Y. (1984). "The Regulation of Membrane Fluidity in Tetrahymena," in *Membrane Fluidity. Biomembranes*, vol. 12 . Eds. M. Kates and L. A. Manson (Boston, MA: Springer). doi: 10.1007/978-1-4684-4667-8_13

Toledo, M. S., Levery, S. B., Straus, A. H., and Takahashi, H. K. (2000). Dimorphic Expression of Cerebrosides in the Mycopathogen *Sporothrix Schenckii*. *J. Lipid Res.* 41, 797–806. doi: 10.1016/S0022-2275(20)32388-9

Xue, J., Chen, X., Selby, D., Hung, C. Y., Yu, J. J., and Cole, G. T. (2009). A Genetically Engineered Live Attenuated Vaccine of *Coccidioides Posadasii* Protects BALB/C Mice Against Coccidioidomycosis. *Infect. Immun.* 77, 3196–33208. doi: 10.1128/IAI.00459-09

Conflict of Interest: The authors declare that the research was conducted in the absence of any commercial or financial relationships that could be construed as a potential conflict of interest.

frontiers in Cellular and Infection Microbiology

REVIEW
published: 15 October 2021
doi: 10.3389/fcimb.2021.751947

Caenorhabditis elegans as an Infection Model for Pathogenic Mold and Dimorphic Fungi: Applications and Challenges

Chukwuemeka Samson Ahamefule[1,2,3], *Blessing C. Ezeuduji*[4], *James C. Ogbonna*[3], *Anene N. Moneke*[3], *Anthony C. Ike*[3], *Cheng Jin*[1,2], *Bin Wang*[1,5*] and *Wenxia Fang*[1,5*]

[1] National Engineering Research Center for Non-Food Biorefinery, Guangxi Academy of Sciences, Nanning, China, [2] College of Life Science and Technology, Guangxi University, Nanning, China, [3] Department of Microbiology, University of Nigeria, Nsukka, Nigeria, [4] Department of Microbiology, University of Jos, Jos, Nigeria, [5] State Key Laboratory of Non-Food Biomass and Enzyme Technology, Guangxi Academy of Sciences, Nanning, China

OPEN ACCESS

Edited by:
Carlos Pelleschi Taborda,
University of São Paulo, Brazil

Reviewed by:
Yen-Ping Hsueh,
Academia Sinica, Taiwan
Helen Fuchs,
Rhode Island Hospital, United States

***Correspondence:**
Bin Wang
bwang@gxas.cn
Wenxia Fang
wfang@gxas.cn

Specialty section:
This article was submitted to Fungal Pathogenesis, a section of the journal Frontiers in Cellular and Infection Microbiology

Received: 02 August 2021
Accepted: 28 September 2021
Published: 15 October 2021

Citation:
Ahamefule CS, Ezeuduji BC, Ogbonna JC, Moneke AN, Ike AC, Jin C, Wang B and Fang W (2021) Caenorhabditis elegans as an Infection Model for Pathogenic Mold and Dimorphic Fungi: Applications and Challenges. Front. Cell. Infect. Microbiol. 11:751947. doi: 10.3389/fcimb.2021.751947

The threat burden from pathogenic fungi is universal and increasing with alarming high mortality and morbidity rates from invasive fungal infections. Understanding the virulence factors of these fungi, screening effective antifungal agents and exploring appropriate treatment approaches in *in vivo* modeling organisms are vital research projects for controlling mycoses. *Caenorhabditis elegans* has been proven to be a valuable tool in studies of most clinically relevant dimorphic fungi, helping to identify a number of virulence factors and immune-regulators and screen effective antifungal agents without cytotoxic effects. However, little has been achieved and reported with regard to pathogenic filamentous fungi (molds) in the nematode model. In this review, we have summarized the enormous breakthrough of applying a *C. elegans* infection model for dimorphic fungi studies and the very few reports for filamentous fungi. We have also identified and discussed the challenges in *C. elegans*-mold modeling applications as well as the possible approaches to conquer these challenges from our practical knowledge in *C. elegans*-*Aspergillus fumigatus* model.

Keywords: *Caenorhabditis elegans*, dimorphic fungi, filamentous fungi, *in vivo* model, pathogenicity, high-throughput screening

INTRODUCTION

Pathogenic fungi pose an enormous global threat to humanity, leading to millions of deaths and substantial financial losses annually (Fisher et al., 2012; Rhodes, 2019). Morbidity and mortality rates from opportunistic fungal pathogens, such as *Candida albicans*, *Aspergillus fumigatus*, and *Cryptococcus neoformans*, have been increasing for some years, especially in immunocompromised patients (Pal, 2017; Linder et al., 2019; de Sousa-Neto et al., 2020). Addressing the pathogenesis of these fungal pathogens and finding controllable strategies are crucial and urgent. To tackle this threat, model organisms are required to conduct research focusing on the identification of virulence factors, screening of effective antifungal agents, and exploring appropriate treatment approaches.

Several model organisms have been adopted for studying of dimorphic and filamentous pathogenic fungi, including invertebrate models such as *Drosophila melanogaster* (Lamaris et al., 2008; Regulin and Kempken, 2018; Sampaio et al., 2018; Wurster et al., 2019), *Galleria mellonella* (Gomez-Lopez et al., 2014; Long et al., 2018; Silva et al., 2018; Staniszewska et al., 2020), *Bombyx mori* (Matsumoto et al., 2013; Uchida et al., 2016; Nakamura et al., 2017; Matsumoto and Sekimizu, 2019), *Caenorhabditis elegans* (Okoli and Bignell, 2015; Song et al., 2019; Wong et al., 2019; Ahamefule et al., 2020a), and vertebrate models such as mice (Fakhim et al., 2018; Skalski et al., 2018; Wang et al., 2018; Mueller et al., 2019), guinea pigs (Vallor et al., 2008; Nadăş et al., 2013; Garvey et al., 2015), and zebrafish (Chen et al., 2015; Knox et al., 2017; Koch et al., 2019; Kulatunga et al., 2019).

C. elegans is a microscopic multicellular nematode that lives freely in soil (Muhammed et al., 2012; Kim et al., 2017). Advantages, such as short life cycle, physiological simplicity, transparent body, complete sequenced genome, mature genetic manipulation system, and no requirement for ethical license, have greatly encouraged the wide adoption of this nematode as a model organism in scientific research with assorted applications across several research fields (Okoli et al., 2009; Ballestriero et al., 2010; Huang et al., 2014; Jiang and Wang, 2018). Some of these applications have been established for decades now whereas others are still in their nascent stages undergoing several studies. Nematode infection by the natural nematophagous obligate filamentous fungus *Drechmeria coniospora* is a common incidence in nature. *C. elegans* is usually applied for studying the innate immunity of nematodes to this fungus (Engelmann et al., 2011; Couillault et al., 2012; Zugasti et al., 2016). This nematode model has also been explored as an *in vivo* model for studying infections of human pathogenic filamentous fungi (Okoli and Bignell, 2015; Ahamefule et al., 2020a).

Application of the nematode model for dimorphic pathogenic fungi studies has resulted in numerous publications whereas only a few publications thus far have been recorded for human filamentous pathogenic fungi studies, such as *A. fumigatus* (Okoli and Bignell, 2015; Ahamefule et al., 2020a; Eldesouky et al., 2020a). Here, we have extensively portrayed *C. elegans*-dimorphic fungi (in particular *Candida* spp.) infection models for determining virulence factors (reported within the last decade) and evaluated the effectiveness of anticandidal agents, including drugs, bioactive compounds, and live biotherapeutic products (reported within the last 5 years). The practical challenges constraining the applications of the *C. elegans* model for filamentous fungi are elaborated, and possible solutions are raised for future improvement.

APPLICATION OF *C. elegans* FOR DIMORPHIC FUNGI STUDIES

C. elegans has been extensively used for studying several dimorphic fungi of clinical relevance. The most devastating and pathogenic dimorphic fungus that has been adequately explored with this nematode model is *Candida albicans* (Hans et al., 2019a; Hans et al., 2019b; Song et al., 2019; Venkata et al., 2020) and a few other non-*albicans* species such as *C. tropicalis* (Brilhante et al., 2016; Feistel et al., 2019; Pedroso et al., 2019), *C. krusei* (De Aguiar Cordeiro et al., 2018; Kunyeit et al., 2019), and *C. auris* (Eldesouky et al., 2018a; Mohammad et al., 2019). Another important clinical dimorphic fungus, *Talaromyces* (*Penicillium*) *marneffei*, has also been studied in a *C. elegans* model for both virulence tests and antifungal agent efficacy evaluations (Huang et al., 2014; Sangkanu et al., 2021).

Virulence factors of *C. albicans* such as genes involved in hyphal filamentation and biofilm formation (Romanowski et al., 2012; Sun et al., 2015; Holt et al., 2017), intestinal adhesion and colonization (Rane et al., 2014a; Muthamil et al., 2018; Priya and Pandian, 2020), important virulence enzymes (Ortega-Riveros et al., 2017; Song et al., 2019), transcription factors (Jain et al., 2013; Hans et al., 2019a), and environmental and nutrient factors (Hammond et al., 2013; Lopes et al., 2018; Hans et al., 2019b; Wong et al., 2019) have been identified in a *C. elegans* model to strengthen our understanding of the *in vivo* pathogenesis of this important fungal pathogen (**Table 1**). The virulence traits of some other non-*albicans* species (both dimorphic and nondimorphic) have also been investigated with this nematode model (**Table 1**). Similarly, virulence factors such as pigmentation and hyphal filamentation have been demonstrated to be critical pathogenic features of *T. marneffei* in a *C. elegans* infection model (Huang et al., 2014; Sangkanu et al., 2021). *C. elegans glp-4; sek-1* worms have mostly been used in these studies (aside from the wild-type strain, N2) because of their inability to produce progeny at 25°C due to the *glp-4* mutation and their susceptibility to pathogens due to *sek-1* mutation, thus making the worms immunocompromised for infection by opportunistic human fungi (Huang et al., 2014; Okoli and Bignell, 2015; Ahamefule et al., 2020a)

Moreover, the adoption of a *C. elegans* model for searching and screening of effective bioactive compounds against several species of *Candida* has also received much attention. Effective bioactive compounds from marine habitats (Subramenium et al., 2017; Ganesh Kumar et al., 2019), plant parts (Shu et al., 2016; Pedroso et al., 2019), and other sources (**Table 2**) have been discovered because of their *in vivo* efficacies against several *Candida* species and were simultaneously evaluated for their cytotoxicity in a *C. elegans* model. Compounds such as alizarin, chrysazin, sesquiterpene, and purpurin were discovered to be quite effective in *in vivo* assays with effective doses ranging from 1 to 10 μg/ml (**Table 2**), indicating potential future prospects for antifungal drug research and discovery. Other compounds such as thymol (Shu et al., 2016), coumarin (Xu et al., 2019), and theophylline (Singh et al., 2020), were only effective at high concentrations of 64, 2, and 1.6 mg/ml, respectively (**Table 2**). Most of these compounds were certified as nontoxic at such effective concentrations as they were able to rescue infected nematodes and significantly elongated their lifespan (**Table 2**).

TABLE 1 | Application of *C. elegans* in determining/confirming *in vivo* virulence of *Candida* spp.

***Candida* spp.**	***C. elegans* strain used**	**Identified virulence factors/conditions**	**Effect on host**	**References**
C. albicans	N2 Bristol (wild type) and *sek-1Δ* worms	Transcription factor *CAS5* Kinase *CEK1* Transcription factor *RIM101*	Avirulence or attenuated virulence of pathogen in host.	Feistel et al. (2019)
C. albicans, *C. dubliniensis*, *C. tropicalis*, *C. parapsilosis*	N2 Bristol (wild type) and *sek-1Δ* worms	Screen diverse pathogen strain backgrounds and species	*C. albicans*, *C. tropicalis*, and *C. dubliniensis* gave the most virulent effect on healthy nematode populations while *C. parapsillosis*, *C. tropicalis*, and *C. albicans* were the most virulent on immunocompromised worms	Feistel et al. (2019)
C. albicans	*glp-4; sek-1* adult worms	Alcohol dehydrogenase 1 (*ADH1*)	Significant ($p < 0.05$) increase in survival time of worms infected by *ADHI* mutant strain (adh1Δ/Δ) compared with the wild-type and reconstituted strains	Song et al., 2019
C. albicans	N2 L4-young adult worms	Filamentation and virulence induced by phosphate conditions	Strain ICU1 caused mortality in worms in a phosphate-dependent manner while ICU12 caused mortality both in low and high phosphate conditions albeit consistent with degree of filamentation. Worms generally displayed an avoidance behavior on *C. albicans* grown in low phosphate medium	Romanowski et al. (2012)
C. albicans	N2 L4 worms	Prevacuolar protein sorting gene (*VPS4*) needed for extracellular secretion of aspartyl proteases	Attenuated virulence by *vps4Δ* (66 h median survival) compared with wild type, DAY185 (42 h), and reintegrant strains (45 h)	Rane et al. (2014a)
C. albicans	N2 Bristol larval and adult worms	Effects of microgravity on virulence	Reduced virulence in both larval and adult worms in spaceflight; reduced virulence in only larval and not adult worms in clinorotation all compared with static ground controls	Hammond et al. (2013)
C. albicans	N2 Bristol L4 worms	Hypoxia (1% oxygen)	Enhanced significant virulence ($p < 0.001$) leading to more than 80% worm mortality compared with controls	Lopes et al. (2018)
C. albicans	AU37 (*glp-4; sek-1*) worms	Limiting phospholipid synthesis	Approximately 23%–38% virulence reduction in mutant strains (*LRO1*, *CHO1*, and *LPT1*) compared with control	Wong et al. (2019)
C. albicans	*glp-4; sek-1* adult worms	Transcription coactivator *SPT20*	Attenuated virulence. Absence of hyphae filamentation in worms infected by mutant strains as against visible hyphae protrusion recorded in approximately half of dead worms infected by both wild-type and reintegrated strains at 48 h	Tan et al. (2014)
C. albicans	N2 young adult worms	[helix–loop–helix/leucine zipper (bHLH/Zip)] transcription factor *CaRTG3*	Significant increased survival rate ($p < 0.05$) of worms infected with *rtg3* mutant strain (43.3%) compared with the wild-type (6.6%) and revertant (10%) strains	Hans et al. (2019a)
C. albicans + *Staphylococcus epidermidis*	*glp-4; sek-1* L3 and L4 worms	Biofilm and hyphal filamentation	Significantly reduced survival rate ($p < 0.05$) of coinfected worms (47%) compared with single infection by *C. albicans* hyphae (63%) and yeasts (81.5%) phenotypes	Holt et al. (2017)
C. albicans	*glp-4; sek-1* adult worms	Iron-sulfur subunit of succinate dehydrogenase *SDH2*	More than 85% mortality of worms infected with wild-type and reintegrated strains (all with visible hyphae) compared with 0% mortality and total absence of hyphae in worms infected with mutant (*sdh2ΔΔ*) at 120 h	Bi et al. (2018)
C. albicans	N2 L4 worms	Proton pump V-ATPase	The tetR-VMA2 mutant was avirulent	Rane et al. (2014b)
C. albicans	*glp-4; sek-1* L4 worms	Molecular chaperone Hsp104	Significant increase in survival rate ($p < 0.05$) in Hsp104 homozygous mutant strain (17.2%) relative to heterozygous mutant (12.9%), wild-type (6.0%) and reconstituted (9.3%) strains by Day 7	Fiori et al. (2012)
C. albicans	N2 Bristol and CB767 [*bli-3(e767)I*] worms from egg stage	Transcription factor Cap1 required for countering reactive oxygen species (ROS)[a] stress	Cap1 is required for virulence of *C. albicans* in nematode model. Strains lacking CAP1 induced Dar phenotype less frequently with attenuated virulence compared with the wild-type strain. Worms that could not produce ROS due to a mutation in the host oxidase showed early signs of disease and succumbed to an infection with the *cap1ΔΔ* null mutant	Jain et al. (2013)
C. albicans	N2 L4 worms	Magnesium deprivation	20% worm survival after 8 days of treatment compared with 100% mortality in control without treatment	Hans et al. (2019b)

(Continued)

TABLE 1 | Continued

Candida spp.	*C. elegans* strain used	Identified virulence factors/conditions	Effect on host	References
C. albicans, *C. dubliniensis*, *C. glabrata*, *C. krusei*, *C. metapsilosis*, *C. orthopsilosis*, and *C. parapsilosis*	*glp-4; sek-1* L4 worms	Hyphae filamentation, hydrolytic enzymes	*C. albicans* and *C. krusei* were the most virulent with survival rate of 9% by 120 h. At 72 h, *C. parapsilosis* gave a reduced virulence (with no significant difference [$p = 0.429$] from that of *C. glabrata*) with survival rate of 76% compared with 59% and 57% of *C. metapsilosis* and *C. orthopsilosis*, respectively. *C. dubliniensis* gave the least mortality (41%) by the end of the assay. *In vivo* hyphae development was observed only in infected worms with *C. albicans* and *C. krusei*	Ortega-Riveros et al. (2017)
C. glabrata, *C. nivariensis*, and *C. bracarensis*	*glp-4; sek-1* L4 worms	None	*C. glabrata* ATCC 90030, NCPF 3203; *C. nivariensis* CECT 11998, CBS 9984; and *C. bracarensis* NCYC 3133, NCYC 3397 gave varying virulence with survival rates of 40.3%/26.5%, 65.4%/45.%1; 72.9%/65.3%, 75%/73%; 89.4%/89.4%, and 97.6%/70.8% in the absence/presence of DMSO (1%), respectively at 120 h	Hernando-Ortiz et al. (2020)
C. tropicalis	*glp-4; sek-1* L4 worms	Hyphal filamentation and blastocondia	The mortality rate of the 40 strains from both humans and veterinary ranged from 31% to 98% by 98 h. No significant mortality rate difference ($p = 0.05$) between the human (86.07 ± 3.42) and veterinary (79.8 ± 14.9) strains	Brilhante et al. (2016)
C. parapsilosis (*sensu stricto*), *C. orthopsilosis*, *C. metapsilosis*	*glp-4; sek-1* worms	Develop a *C. elegans-Candida parapsilosis* infection model	The 3 *Candida* spp. caused up to 50% mortality of worms ranging from 4 to 6 days. Worms infected by the 3 *Candida* spp. in the liquid assay were susceptible to fluconazole (fluZ) and caspofungin (CAS) and could mount an immune response	Souza et al. (2018)
C. albicans	N2 young adult worms	Adhesion/colonization	Increased mortality rate (<10%) compared with the negative control fed with the *Escherichia coli* OP50 (OP50) (˜70%) by Day 9.	Priya and Pandian (2020)
C. albicans, *C. glabrata*, and *C. tropicalis*	L4 worms	Colonization and biofilm formation	Decreased survival lifespan of worms infected with *C. albicans* (156 h), *C. glabrata* (180 h), and *C. tropicalis* (252 h) compared with OP50-fed control worms (>312 h).	Muthamil et al. (2018)

[a]*Produced by host.*

The drug resistance threat of *Candida* species, similar to most other pathogens, is constantly increasing, leading to increased incidences of mortality and morbidity (Sanguinetti et al., 2015; Popp et al., 2017; Popp et al., 2019; Prasad et al., 2019). *C. elegans* has also proven to be an effective *in vivo* model for studying the infection of several azole-resistant *C. albicans* (Chang et al., 2015; Sun et al., 2018) and *C. auris* (Eldesouky et al., 2018a; Eldesouky et al., 2018b) strains. Studies have demonstrated the *in vivo* efficacy of some bioactive compounds applied singly or in combination with initially resistant antifungal drugs in the treatment of infected nematodes (**Table 3**).

Compounds such as 2-(5,7-dibromoquinolin-8-yl)oxy)-*N*′-(4-nitrobenzylidene) acetohydrazide (Elghazawy et al., 2017; Mohammad et al., 2018) and phenylthiazole small molecules (Mohammad et al., 2019) are among the recently demonstrated effective compounds with good outcomes in nematode candidiasis (with effective dose concentrations of ≥4 and ≥5 μg/ml, respectively) against fluZ-resistant *C. albicans* and/or *C. auris* (**Table 3**). The combination of caffeic acid phenethyl ester (CAPE) and fluZ (Sun et al., 2018) as well as the sulfamethoxazole and voriconazole (voZ) combination (Eldesouky et al., 2018a) effectively rescued *C. elegans* worms infected by azole-resistant *C. albicans* and *C. auris*, respectively (**Table 3**).

The search for alternative treatment drugs with new inhibition mechanisms against pathogenic fungi such as *C. albicans* is a pressing need. Obtaining effective compounds that may not necessarily have a direct effect on *Candida* planktonic cells but affect critical virulence factors has recently been made possible by evaluating the efficacy of the compounds in a *C. elegans* infection model (Graham et al., 2017; Subramenium et al., 2017; Manoharan et al., 2018) (**Table 4**).

Remarkably, some compounds such as loureirin A (Lin et al., 2019), camphor, and fenchyl alcohol (Manoharan et al., 2017b) are effective compounds protecting infected worms at concentration doses less than the *in vitro* MICs (**Table 4**). Cascarilla bark oil, α-longipinene, linalool (Manoharan et al., 2018), and *Enterococcus faecalis* bacteriocin (EntV) (Graham et al., 2017) were reported to be quite potent in rescuing infected worms at low effective concentration doses, such as ≥0.001% for cascarilla bark oil, α-longipinene and linalool and 0.1 nM for EntV (**Table 4**).

These compounds usually rescue infected nematodes through other pathways such as direct effects on cardinal virulence factors and/or by stimulating/enhancing the immune responses of the host against pathogens (Okoli et al., 2009; Peterson and Pukkila-Worley, 2018; Ahamefule et al., 2020b). Such compounds may only be screened and identified through *in vivo* assays since they usually show little or no antimicrobial activities in *in vitro* assays. The adoption of simple *in vivo* models such as *C. elegans* significantly supports the screening and identification of more such compounds, which may expand the narrative of the usual antifungal therapies that primarily address direct effects on causative pathogens.

The application of live biotherapeutic products (LBPs) consisting mainly of probiotics is another alternative approach for the treatment of nematode candidiasis. Such alternative

TABLE 2 | Evaluation of anticandidal bioactive compounds in the *C. elegans* model.

Candida spp.	*C. elegans* host	Effective antifungal compound/agent	Effective concentrations (μg/ml)	Effect	Reference
C. albicans	N2 Bristol CF512 *fer-15(b26); fem-1 (hc17)* adult worms	Alizarin, chrysazin, and purpurin	≥2	By Day 4, the survival rates of worms in the presence of 2 μg/ml alizarin, chrysazin, purpurin, and fluconazole (fluZ) control were >60%, >50%, >60%, and <50%, respectively. At 1 mg/ml, alizarin had no cytotoxic effect on nematodes whereas chrysazin, purpurin, and fluZ reduced worms survival by >60%, 35%, and >95%, respectively	Manoharan et al. (2017a)
C. albicans	N2 young adults	Magnolol and honokiol	16	Both compounds significantly ($p < 0.0001$) protected and increased the lifespan of infected worms compared with infected untreated worms by Day 5. The antifungal compounds also significantly ($p < 0.01$) reduced colonization of *C. albicans* in the nematodes	Sun et al. (2015)
C. albicans	Adult worms	Coumarin	2.0 mg/ml	Coumarin at concentrations of 0. 5–2.0 mg/ml significantly ($p < 0.05$) protected infected worms from death. However, coumarin at 2 mg/ml was significantly ($p < 0.05$) toxic to worms	Xu et al. (2019)
C. albicans	*glp-4; sek-1* L4 worms	Gallic acid, hexyl gallate, octyl gallate, and dodecyl gallate	1–60	Significant ($p < 0.05$) increased survival rates of worms (13%–33%, 18%–33%, 12%–31%, and 14%–46%) when treated with galic acid, hexyl gallate, octyl gallate, or dodecyl gallate, respectively. Dodecyl gallate was the most effective in protecting worms from *Candidal* infection. However, higher concentrations of these compounds (60 and 120 μg/ml) were toxic to worms	Singulani et al. (2017)
C. albicans	N2 worms	Kalopanaxsaponin A (KPA)	8, 16	KPA protected and increased the survival time of worms (5–6 days) compared with the untreated control (4 days). KPA also showed no cytotoxicity on worms at 64 μg/ml for 2 days	Li et al. (2019)
C. albicans	*glp-4; sek-1* worms	Chiloscyphenol A (CA)	8, 16	CA significantly ($p < 0.001$) prolonged the survival of infected worms compared with 1% DMSO control. CA at 16 μg/ml prevented hyphae filamentation and maintained worms at their usual curly growth condition. However, CA of ≥32 μg/ml was toxic to worms	Zheng et al. (2018)
C. albicans	*glp-4; sek-1* young adult worms	2,6-bis[(E)-(4-pyridyl) methylidene] cyclohexanone (PMC)	8	PMC treatment significantly ($p < 0.0015$) increased the survival rate of infected worms, similar to fluZ treatment at 4 μg/ml	de Sá et al. (2018)
C. albicans	AU37 (*sek-1*; *glp-4*) L4 worms	Ebselen	4, 8	Ebselen treatment at 4 and 8 μg/ml significantly ($p < 0.05$) reduced *C. albicans* load in infected worms when compared with the untreated control groups, same as amphotericin B (AmB), fluZ, and flucytosine (fluc) treatments	Thangamani et al. (2017)
C. albicans	N2 L4/adult worms	Vanillin (van)	125	Van protected and enhanced the survival of infected worms compared with untreated control within 4 days. Van also had no cytotoxic effects on nematodes by Day 4 of treatment	Venkata et al. (2020)
C. albicans	N2 young adults	Floricolin C (FC)	8, 16, 32	FC significantly ($p < 0.001$) enhanced the survival of infected worms at 16 μg/ml giving the highest survival rate compared with the untreated control by Day 6. FC at 64 μg/ml had only little cytotoxic effect on worms within 6 days	Zhang et al. (2018)
C. albicans	N2 L4/adult worms	Geraniol (Ger)	135	Ger enhanced the survival of infected nematodes compared to untreated control within 3 days of assay. Ger was also able to reduce persistence of *C. albicans* in worm guts. Furthermore, Ger at 135 μg/ml did not display cytotoxic effect on worms compared to control by Day 3	Singh et al. (2018)

(Continued)

TABLE 2 | Continued

Candida spp.	*C. elegans* host	Effective antifungal compound/agent	Effective concentrations (μg/ml)	Effect	Reference
C. glabrata, *C. krusei*, *C. tropicalis*, and *C. orthopsilosis*	AU37 late L4 worms	*Cupressus sempervirens* essential oil (EO), *Citrus limon* EO, gallic acid, and *Litsea cubeba* EO	Varied with pathogen and effective compounds	Among the *C. glabrata*-infected worms treated with *C. sempervirens* EO (15.62, 31.25, and 62.5 μg/ml), *C. limon* EO (125, 250, and 500 μg/ml) or gallic acid (15.62, 31.25, and 62.5 μg/ml) for 4 days, only treatment group with *C. sempervirens* EO sustained a higher survival rate of worms (˜60%). *C. krusei*-infected worms treated with *L. cubeba* EO (31.25, 62.5, and 125 μg/ml) or gallic acid (62.5, 125, and 250 μg/ml) did not witness cure from candidiasis. *C. limon* EO treatment (125 and 500 μg/ml) of *C. tropicalis*-infected worms gave 40% and 10%–15% worm survival rate, respectively. While *C. sempervirens* EO treatment (15.62–62.5 μg/ml) of *C. orthopsilosis*-infected worms increased survival rate to 80%–85% Day 4 postinfection. *C. sempervirens* and *L. cubeba* EOs (31.25–125 μg/ml) as well as gallic acid (15.62–250 μg/ml) were not toxic to worms compared with untreated control. Additionally, *C. limon* EO at 125 μg/ml was not toxic to worms but became significant toxic at higher concentrations of 250 μg/ml ($p < 0.05$) and 500 μg/ml ($p < 0.0001$) compared with untreated control	Pedroso et al. (2019)
C. albicans	N2 L4/young adult worms	Monoterpenoid perillyl alcohol (PA)	175 and 350	PA enhanced and prolonged infected nematodes with survival rates of 80% and 75% at 175 and 350 μg/ml, respectively, compared with untreated control with 16% survival by Day 7 postinfection. The persistence of *C. albicans* in the intestines of worms was reduced by PA. PA was also not toxic to *C. elegans* at 350 μg/ml after 7 days of incubation	Ansari et al. (2018)
C. albicans	*glp-4; sek-1* worms	Solasodine-3-*O*-β-D-glucopyranoside (SG)	≥8	SG significantly ($p < 0.0001$) protected and prolonged the lifespan of infected *C. elegans* compared with the 1% DMSO control, inhibiting the hyphal filamentation of *C. albicans* in infected worms by Day 6 of postinfection. Moreover, SG was not toxic to worms at 64 μg/ml in 2 days of incubation	Li et al. (2015)
C. albicans	N2 L4/young adult worms	Theophylline (THP)	1,600	THP gave over 50% more survival rate of infected worms than the untreated infected control after 6 days postinfection. THP was able to drastically lower the persistence of *C. albicans* in nematode gut. Additionally, THP did not show any toxicity at 1.6 mg/ml compared with untreated control for 6 days of treatment	Singh et al. (2020)
C. albicans	N2 and several mutant[a] worms	Thymol	64 mg/ml	Thymol significantly ($p < 0.01$) increased the survival rate and mean lifespan (10.5 ± 0.4 days) of infected *C. elegans* compared with untreated infected worms (6.1 ± 0.5 days) within 10 days postinfection. Thymol elicited important immunomodulatory response of *C. elegans* against *C. albicans* thus significantly ($p < 0.01$) reduced fungal burden in treated infected worms compared with untreated control	Shu et al. (2016)
C. albicans	Young adult worms	Sesquiterpene compound	≥10	Sesquiterpene compound prolonged the lifespan of infected worms with >70% survival rate up to 20 μg/ml treatment but became toxic at higher concentration of 50 μg/ml compared with untreated control	Ganesh Kumar et al. (2019)

[a]*KU25/pmk-1(km25) IV, AU1/sek-1(ag1) X, FK171/mek-1(ks54) X, AU3/nsy-1(ag3) II, and DA1750/adEx1750[PMK-1::GFP+rol 6(su1006)].*

TABLE 3 | Evaluation of effective agents against drug-resistant *Candida* species in a *C. elegans* model.

Candida spp.	*C. elegans* host	Kind of drug resistance and MIC	Antifungal compound/agent	Time of preinfection (min)	Effect	Reference
C. albicans	AU37 L4 worms	fluZ	2-(5,7-Dibromoquinolin-8-yl) oxy)-*N*′-(4-nitrobenzylidene) acetohydrazide (4b)	90	Compound 4b exhibited broad-spectrum antifungal activity towards species pf *Candida*, *Cryptococcus*, and *Aspergillus* at a concentration of 0.5 μg/ml, as well as enhanced survival of *C. elegans* infected with fluz-resistant *C. albicans*. This compound targets metal ion homeostasis	Elghazawy et al. (2017) and Mohammad et al. (2018)
C. albicans	N2 worms	fluZ 256 μg/ml	Caffeic acid phenethyl ester (CAPE) and fluZ	120	CAPE plus fluZ synergistically increased the survival rate of infected worms significantly compared with single treatment with either CAPE or fluZ. CAPE plus fluZ also significantly ($p < 0.01$) reduced *C. albicans* burden in nematode intestines compared with just CAPE, fluZ, or the untreated control (all at 2 μg/ml)	Sun et al. (2018)
C. albicans and *C. auris*	AU37 L4 worms	fluZ >64 μg/ml	Phenylthiazole small molecule (compound 1)	90	Compound 1 (at 5 and 10 μg/ml) enhanced the survival of *C. albicans*-infected nematodes, giving >70% survival rate (just like 5 μg/ml of 5-fluorocytosine control) by Day 3 postinfection compared with 0% of untreated infected worms. Similarly, Compound 1 (at 10 μg/ml) prolonged *C. auris*-infected worms giving ~70% survival by Day 4 compared with 0% of untreated infected worms	Mohammad et al. (2019)
C. albicans	*glp-4; sek-1* worms	fluZ >128 μg/ml	Pyridoxatin (PYR)	120	PYR rescued and prolonged infected nematodes in a dose-dependent manner with 4 μg/ml giving ~50% survival rate after 5 days of treatment	Chang et al. (2015)
C. albicans	AU37 L4 worms	fluZ >64 μg/ml; itraconazole (itZ) and voZ >16 μg/ml	Sulfa drugs[a] + fluZ	180	Sulfa (10 × MIC[b]) and fluZ (10 μg/ml) combinations gave a significant ($p < 0.05$) reduction of *C. albicans* burden in infected worms (which is comparable with 5-fluorocytosine control) after 24 h treatment compared with fluZ and the DMSO-untreated controls. There was no significant difference among the activities of the 4 sulfa with fluZ combinations	Eldesouky et al. (2018b)
C. auris	AU37 L4 worms	Azole resistant; fluZ >128 μg/ml; voZ = 16 μg/ml; itZ = 2 μg/ml	Sulfamethoxazole + voZ	30	The combination of sulfamethoxazole (128 μg/ml) with voZ (0.5 μg/ml) prolonged the life of infected worms by ~70% as against only sulfamethoxazole, voZ, or untreated control which could not keep worms alive till Day 5	Eldesouky et al. (2018a)

MIC, minimum inhibition concentration. [a]Sulfamethoxazole (SMX), sulfadoxine (SDX), sulfadimethoxine (SDM), or sulfamethoxypyridazine (SMP). [b]MICs of SMX, SDX, and SMP = 512 μg/ml, while MIC of SDM = 1,024 μg/ml.

TABLE 4 | *C. elegans* model demonstrating alternative inhibition mechanisms against *Candida* species.

***Candida* spp.**	***C. elegans* host**	**Effective antifungal agent**	**Effective concentrations (μg/ml)**	**Effect**	**Reference**
C. albicans	N2 Bristol *CF512 fer-15*; *fem-1* adult worms	7-Benzyloxyindole	0.05 mM	7-Benzyloxyindole gave nematode survival rate of >40% while the positive control (fluZ) gave >60% by Day 4, both showed significant ($p < 0.05$) increase of survival rates compared with the untreated control (8%). 7-Benzyloxyindole at 0.1 mM showed mild toxicity on worms with 22% survival rate compared with 55% survival by fluZ. 7-Benzyloxyindole protected infected worms by preventing hyphal filamentation through downregulation of important hyphae-specific and biofilm-related genes	Manoharan et al. (2018)
C. albicans	*glp-4; sek-1* young adult worms	*Enterococcus faecalis* bacteriocin (EntV)	0.1 nM	Synthetic EntV ($sEntV^{68}$) completely abrogated the virulence of *C. albicans* in infected worms, giving them lifespan similar to control worms fed with nematode food *E. coli* OP50. $sEntV^{68}$ had no effect on the viability of *C. albicans* but protected the nematode by preventing hyphal morphogenesis.	Graham et al. (2017)
C. albicans	*fer-15*; *fem-1* adult worms	Cascarilla bark oil, α-longipinene, and linalool	≥0.001%	Separate treatments with cascarilla bark oil, α-longipinene, and linalool resulted in a significant ($p < 0.05$) increase in survival rate (>90%) of infected nematodes just like fluZ treatment (all at 0.01%) compared with the negative control (<5%) by Day 4. These antifungal compounds only became toxic at >0.5% (v/v) to the worms. Cascarilla bark oil, α-longipinene, and linalool protected infected worms by preventing hyphal filamentation but no direct effect on *C. albicans* planktonic cells	Manoharan et al. (2017c)
C. albicans	*glp-4; sek-1* adult worms	Loureirin A (Lou A)	40	Lou A significantly ($p < 0.05$) protected infected nematodes compared with the DMSO control in 144 h. More so, Lou A did not display any cytotoxic activity against the worms at 160 μg/ml. At effective *in vivo* concentration of 40 μg/ml, Lou A did not inhibit the growth of *C. albicans* but suppressed virulence trait such as adhesion, colonization, and hyphal filamentation	Lin et al. (2019)
C. albicans	N2 young adult worms	Piperine	≥BIC (32)	Piperine treatment helped worms to combat infection in a dose-dependent manner leading to a significant ($p < 0.05$) reduction in *C. albicans* load. Piperine did not result in cytotoxity at sub-BIC, BIC, and 2 × BIC in worms. Piperine *in vivo* efficacy was mainly through hindering *C. albicans* colonization in nematode intestine by downregulating some important hyphae-specific genes but not affecting the growth and metabolism of the pathogen	Priya and Pandian (2020)
C. albicans, *C. glabrata*, and *C. tropicalis*	L4 worms	Quinic acid and undecanoic acid (QA-UDA)	BIC[a] (100)	QA-UDA at BIC increased the survival rates of worms infected by *C. albicans*, *C. glabrata*, and *C. tropicalis* to 216, 384, and 348 h compared with 156, 180, and 252 h of untreated infected worms, respectively. QA-UDA reduced *in vivo* biofilm formation and colonization of yeast pathogens in worms	Muthamil et al. (2018)
C. albicans	*fer-15*; *fem-1* adult worms	Camphor and fenchyl alcohol	0.01%	Treatment of infected worms with camphor and fenchyl alcohol significantly ($p < 0.05$) increased the survival rates of infected worms to >70% and >50%, respectively, compared with 5% untreated control. These compounds had no effect on worm survival and viability at concentrations of 0.05% and 0.1% in 4 days, but they became significantly toxic ($p < 0.05$) at 0.5%. Camphor and fenchyl alcohol at BIC (approximately 50 times the MIC) had effect on *C. albicans* biofilm and hyphal filamentation but not on the planktonic cells	Manoharan et al. (2017b)
C. albicans	L4 worms	5-Hydroxymethyl-2-furaldehyde (5HM2F)	MBIC (400)	Increased survival time of infected worms when treated with 5HM2F (120 h) compared with 96 h of control group. 5HM2F displayed no cytotoxic effect on worms by120 h. 5HM2F below 500 μg/ml does not have antifungal effect on *C. albicans* except on some virulence factors such as biofilm formation, morphological transition, and production of secreted hydrolases	Subramenium et al. (2017)

[a]*BICs for C. albicans, C. glabrata, and C. tropicalis in combination with QA/UDA were 100/5, 100/10, and 200/20 μg/ml, respectively. BIC, biofilm inhibition concentration; MBIC, minimum biofilm inhibitory concentration.*

therapy is an interesting and promising option since pathogenic fungi are currently developing resistance to the few clinically available antifungal drugs (Sanguinetti et al., 2015; Prasad et al., 2019). Several species of *Lactobacillus* such as *L. rhamnosus* (Poupet et al., 2019a; Poupet et al., 2019b) and *L. paracasei* (de Barros et al., 2018) as well as probiotic yeasts—*Saccharomyces cerevisiae* and *Issatchenkia occidentalis* (Kunyeit et al., 2019)—have demonstrated efficient rescue of worms infected with a number of *Candida* species. These therapeutic microorganisms drastically reduced the burden of the pathogens in the *C. elegans* intestine approximately 2 to 4 h postinfection treatment (**Table 5**).

The efficacy of these LBPs in reducing and/or eliminating fungal burden implies the future potential of LBPs in addressing the fungal menace. The demonstrated significant increase ($p < 2 \times 10^{-16}$) in worm mean lifespan (Poupet et al., 2019a; Poupet et al., 2019b) is so high that it has not been reported in any potent bioactive compounds or even established antifungal drugs. The fact that most of these LBPs are already established probiotics is yet another important parameter that would advance future research beyond nematode models.

The *in vivo* efficacy of known antifungal drugs and a number of repurposed drugs have also been applied in the treatment of nematode candidiasis. Several azoles (Souza et al., 2018; Hernando-Ortiz et al., 2020), echinocandins (Souza et al., 2018), polyenes—particularly amphotericin B (Hernando-Ortiz et al., 2020), and β-lactam antibiotics (in combination with vancomycin) (De Aguiar Cordeiro et al., 2018) have been evaluated for their *in vivo* efficacy at varying effective concentrations in rescuing worms infected with *Candida* species (**Table 6**). Synthesized azole drugs, such as 1-(4-cyclopropyl-1H-1,2,3-triazol-1-yl)-2-(2,4-difluorophenyl)-3-(1H-1,2,4-triazol-1-yl) propan-2-ol, have also been evaluated for both efficacy and cytotoxicity in a *C. elegans* model (Chen et al., 2017).

Given that decades of searching for new antifungal agents have not truly resulted in new antifungal drugs, drug repurposing is a less expensive and welcome research prospect. The *C. elegans* infection model for evaluating the efficacy of repurposed drugs on candidiasis has attracted attention (Eldesouky et al., 2020b; Singh et al., 2020) (**Table 6**) due to the advantages of saving extensive time, cumbersome labor, and enormous cost of searching and obtaining new antifungal drugs.

C. elegans and Pathogenic Molds

The deadly opportunistic mold pathogen, *A. fumigatus*, ranks as the number 1 aetiological agent for aspergilloses in immunocompromised patients (Snelders et al., 2009; Fang and Latgé, 2018; Geißel et al., 2018) with an almost 100% mortality rate in some groups of patients (Darling and Milder, 2018; Geißel et al., 2018; Linder et al., 2019). This pathogen had not been well studied in *C. elegans* until recently. Okoli and Bignell (2015) were the first to demonstrate the possibility of adopting *C. elegans* for *A. fumigatus* infection. They set up the nematode model to study the pathogenicity of the clinical strain *A. fumigatus* Af293 for 72 h postinfection after an initial preinfection of 12 h. We recently reported a breakthrough in overcoming some of the challenges usually encountered in the *C. elegans*-mold infection system, one of which is removing spores that were not ingested by worms through a hand-made filter with a membrane-attached-on-tube. We were able to develop a stable and consistent *C. elegans* model for evaluating the virulence of *A. fumigatus* mutant strains that had previously been studied in other established models, including mice and insects. We also successfully demonstrated the possibility of *in vivo* testing of antifungal agents on nematode aspergillosis using the established model (Ahamefule et al., 2020a).

The established *C. elegans-A. fumigatus* model clearly demonstrated the progression of aspergillosis infection in nematodes using the *A. fumigatus* fluorescence strain, Af293-dsRed, showing that hyphal filamentation could actually emanate from any part of the infected worms against the previously reported concept of mainly the tail region (Okoli and Bignell, 2015; Ahamefule et al., 2020a). Our worm model was able to identify important virulence factors of *A. fumigatus* such as α-(1,3)-glucan synthase, melanin pigmentation, iron transporter, Zn2Cys6-type transcription factor, and mitochondrial thiamine pyrophosphate transporter, as mutant strains without these components (triple *agsΔ*, *pksPΔ*, *ΔmrsA*, *ΔleuB*, and *ΔtptA*, respectively), all of which gave significantly attenuated virulence compared with the *A. fumigatus* parent strain KU80Δ. These reduced virulence patterns obtained by our *C. elegans* model were similar to previously reported attenuated virulence patterns of these *A. fumigatus* mutants in both vertebrate and insect models. The nematode model was also demonstrated to be an easy *in vivo* system to evaluate antifungal drug efficacy thus presenting the model as a desired platform for screening antifungal agents against *A. fumigatus* in the future (Ahamefule et al., 2020a).

CHALLENGES OF *C. elegans* APPLICATIONS IN MODELING PATHOGENIC MOLD

One of the biggest challenges usually encountered in the applications of the *C. elegans* model for filamentous fungal infection is the difficulty in infecting the worms through conidia. Worms usually avoid eating conidia unless they starve with no other option (Okoli and Bignell, 2015). This avoidance is unlike the case of dimorphic fungal and bacterial pathogens, where infection is never much of a problem as worms easily feed on the cells of these pathogens when they replace or are mixed up with nematode choice food (*E. coli* OP50 or HB101) (Breger et al., 2007; Johnson et al., 2009; Kirienko et al., 2013; Okoli and Bignell, 2015).

Giving the worms more time to starve and more access to the conidia (placed at four cardinal points) for ingestion is very important for establishing mold preinfection assays. Okoli and Bignell (2015) adopted a 12-h preinfection technique, while we modified to 16 h (Ahamefule et al., 2020a). The fact is that worms must be given such ample time to "force" them to ingest the mold conidia in a preinfection system since coinfection approach

TABLE 5 | Application of live biotherapeutic products (LBP) to nematode candidiasis.

Candida sp.	*C. elegans* host	LBP	Time of preinfection (h)	Effective concentartions/time	Effect	Reference
C. albicans	N2 L4/young adult worms	*Lactobacillus rhamnosus* Lcr35® (Lcr35)	2	2 and 4 h	High significant ($p < 2 \times 10^{-16}$) increase by Lcr35 treatment in mean lifespan (from 4 to 13 days) of worms sequentially infected with *C. albicans* compared with untreated control. However, increasing Lcr35 treatment to 6 and 24 h led to a significant decrease in mean lifespan of worms compared with 4 h treatment	Poupet et al. (2019a)
C. albicans	*glp-4; sek-1* young adult worms	*Lactobacillus paracasei* 28.4	2 and 4	2 and 4 h	*L. paracasei* significantly ($p = 0.0001$) attenuated the death rate of infected worms (with 29% increase in survival rate) compared with untreated infected worms by Day 10 of assay	de Barros et al. (2018)
C. albicans	N2 L4/young adult worms	*Lactobacillus rhamnosus* Lcr35® (Lcr35)	2	2 and 4 h	2 h Lcr35 treatment gave a significant ($p < 2 \times 10^{-16}$) increase in the mean lifespan of infected worms (from 3 to 11 days) compared with untreated infected worms. Lcr35 prevented hyphae filaments in infected worms although it could not totally eradicate pathogens from the intestine of worms. Feeding nematodes with Lcr35 alone significantly increased the mean lifespan of worms compared with *E. coli* OP50. Increasing Lcr35 treatment time beyond 4 h gave a significant drop in worm survival	Poupet et al. (2019b)
C. tropicalis, *C. krusei*, *C. parapsilosis*, and *C. glabrata*	L3 and L4 worms	Probiotic yeasts: *Saccharomyces cerevisiae* (strain KTP) and *Issatchenkia occidentalis* (strain ApC)	48	10^6 cells/20 µl	Significant increase in lifespan (by 5–6 days) of worms coinfected by any of yeast pathogens —*C. tropicalis* ($p \leq 0.0001$), *C. krusei* ($p < 0.0012$), and *C. parapsilosis* ($p < 0.0001$)— and the probiotic yeasts compared with their controls without treatments. However, such increase lifespan was not recorded for *C. glabrata* infection. The probiotics treatments significantly ($p < 0.05$) reduced pathogen colonization in the gut of nematodes with no CFU recovered at Day 5 after postinfection probiotics treatments	Kunyeit et al. (2019)

CFU, colony forming unit (in CFU/ml).

(which is usually adopted for most dimorphic fungi modeling) cannot work well for mold pathogens (Okoli et al., 2009; Okoli and Bignell, 2015; Ahamefule et al., 2020a). As conidia germinate very fast even before the worms have ingested enough spores in killing assay medium, a relatively less nutritious medium was adopted for pre-infection assay to avoid the quick growth and flooding of hyphal filaments in the rich killing assay medium (brain heart infusion medium); otherwise later experimental procedures will be severely limited (Okoli and Bignell, 2015; Ahamefule et al., 2020a).

Another challenging aspect in setting up the *C. elegans*-mold model is the separation of noningested conidia from worms after pre-infection stage. Failure at this stage leads to the germination of unseparated spores in killing or antifungal screening media thus obstructing experimental progress. Although our designed membrane-attached-on-tube filter (with a 35-µm pore diameter) was able to remove a great deal of noningested conidia, the separation was not 100% efficient. Modifying the membrane pore size to an appropriate diameter should help improve the filtration efficiency by allowing faster and better removal of conidia while keeping the preinfected L4/young adult worms (**Figure 1**). Even though the separation efficiency of noningested spores becomes 100% or close to it, hyphae growth in killing medium would still not be completely eliminated, particularly if the experiment is scheduled to go beyond 72 h postinfection. This is because we have discovered that some conidia could be egested out of the nematode intestine into the killing medium and still retain their viability of germinating to hyphae, which is a big challenge to tackle and severely affect the experiment.

Hyphal filamentation usually occurs in infected worms. Unlike most studied dimorphic fungi whose external hyphae protrude when worms were already dead (and could therefore be easily transferred), numerous worms infected with filamentous fungi such as *A. fumigatus* (Ahamefule et al., 2020a), *A. flavus*, and some strains of *Penicillium* (that we have studied in our laboratory), were discovered to still be alive with protruded hyphae. This makes these worms stuck to the killing assay plates and therefore difficult to remove (Ahamefule et al., 2020a). Such filamentation usually becomes profuse, growing and spreading very fast and may eventually obstruct visibility and affect the experimental results. Regulating the number of immunocompromised worms in killing assays, especially for highly virulent pathogenic molds, is an option to ameliorate this menace (**Figure 1**).

CONCLUSIONS

The tremendous health hazards of pathogenic fungi cannot be overemphasized. Better understanding of *in vivo* pathogeneses and identification of virulence factors are urgent and imperative to fight against these fungi. Screening, identifying and repurposing effective compounds/drugs against them as well as obtaining and optimizing effective treatment alternatives are desirable at this time. Therefore, developing, optimizing and applying better modelling organisms such as *C. elegans* is

TABLE 6 | *In vivo* activities of known and repurposed drugs against candidiasis in *C. elegans* models.

C. elegans sp.	*C. elegans* host	Antifungal compounds	Effective concentrations (μg/ml)	Effect	Reference
C. glabrata, *C. nivariensis*, and *C. bracarensis*	*glp-4; sek-1* L4 worms	Micafugin (MCF), CAS, and fluZ were prepared in water, AmB, VoZ, posaconazole (PoZ), and anidulafungin (AND) in 1% DMSO	Varying	MCF (4 μg/ml), CAS (4 μg/ml), AmB (1 μg/ml), and voZ (2 μg/ml), poZ (2 μg/ml) rescued infected worms with *C. glabrata* ATCC 90030 with survival rates of 90.6, 89.6, 82.4, 82.1, and 81.5%, respectively, by 120 h; higher similar rescues—96.8%, 94.6%, 91.8%, 85.2%, 83.8%, and 83.7%—were achieved for infected worms with *C. glabrata*	Hernando-Ortiz et al. (2020)
C. parapsilosis (*sensu stricto*), *C. rthopsilosis*, *C. etapsilosis*	*glp-4; sek-1* worms	fluZ and CAS	≥0.5 × MIC (fluZ MIC = 1.0; CAS MIC = 0.5)	Worm survival rates were dependent on the drug doses. Significant ($p < 0.001$) increase in survival of infected worms when treated with fluZ (≥57%) and CAS (69% and 74%) at 1 × MIC and 2 × MIC, respectively	Souza et al. (2018)
C. albicans, *C. parapsilosis*, *C. krusei*, and *C. tropicalis*	L4 worms	Cefepime (cef), imipenem (imi), meropenem (mer), amoxicillin (amo), and vancomycin (van)	PP and 2 × PP PP of cef, imi, mer, amo, and van = 126; 33, 33, 4, and 15, respectively	Amo treatment significantly ($p < 0.05$) increased the virulence of *C. krusei* and *C. tropicalis* on the nematodes (in separate infections) at PP and 2 × PP. However, the virulence of *C. albicans*, *C. krusei*, *C. parapsilosis*, and *C. tropicalis* were not altered by the other tested antibiotics	De Aguiar Cordeiro et al. (2018)
C. albicans	*glp-4; sek-1* adult worms	1-(4-Cyclopropyl-1H-1,2,3-triazol-1-yl)-2-(2,4-difluorophenyl)-3-(1H-1,2,4-triazol-1-yl) propan-2-ol (7l)	16	7l significantly ($p < 0.05$) prolonged and sustained infected worms, giving 70% survival rate compared with 60% recorded with 32 μg/ml of fluZ control	Chen et al. (2017)
C. albicans	N2 L4/young adult worms	Theophylline (THP)[a]	1,600	THP gave over 50% more survival rate than the untreated infected control after 6 days postinfection. THP was able to drastically lower the persistence of pathogen in nematode gut. Additionally, THP did not show any toxicity at 1.6 mg/ml compared with untreated control by Day 6	Singh et al. (2020)
C. albicans, *C. glabrata*, and *C. auris*	AU37 L4 worms	Pitavastatin (Pit)[a] plus fluZ	Varying[b]	Pit plus fluZ displayed broad spectrum activity with varying outcomes depending on fluZ concentrations, and significantly reduced *C. albicans*, *C. glabrata*, and *C. auris* burden by ~82%–96%, ~84%–93% and 14%–92% compared with 233 ± 21, 344 ± 19, and 250 ± 25 CFU/ml of untreated controls, respectively	Eldesouky et al. (2020b)

MIC, minimum inhibition concentration; PP, peak plasma concentration. [a]Repurposed drug. [b]Pit = 0.5 × MIC; fluZ = 2, 8, and 32 μg/ml.

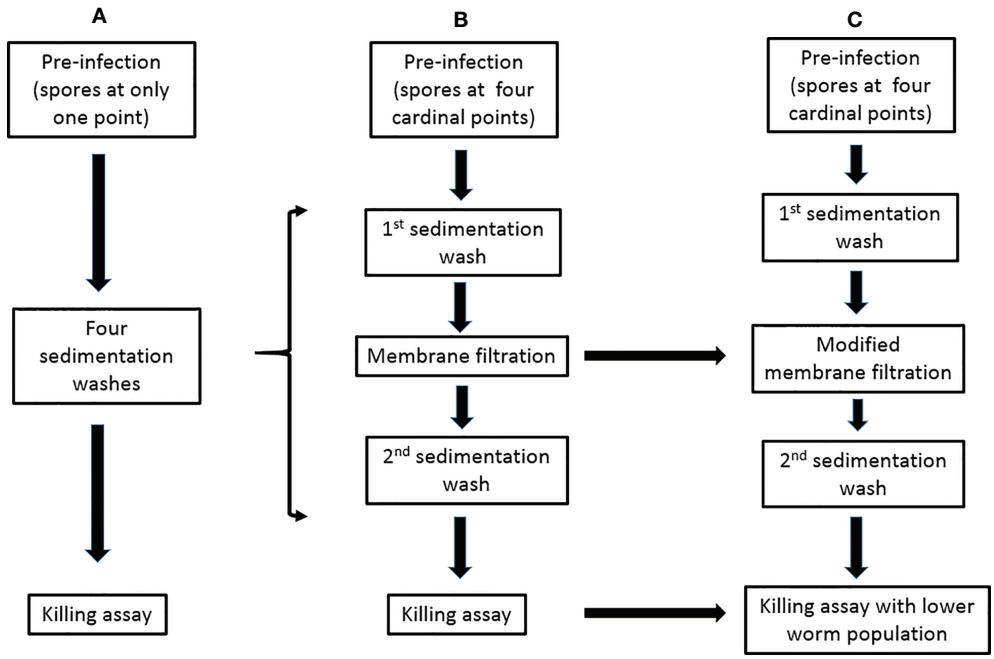

FIGURE 1 | Modifications of the preinfection to killing assays for the *C. elegans*-mold infection model. **(A)** The previously described procedure (Okoli and Bignell, 2015). **(B)** The procedure in our publication (Ahamefule et al., 2020a). **(C)** Our proposed modifications.

meaningful not only for dimorphic fungi but also for mold pathogens. Our review of the breakthrough applications of *C. elegans* for dimorphic fungi studies and progress/modifications of the *C. elegans*-mold infection model will provide a reference for studying fungal infections and developing antifungal agents.

AUTHOR CONTRIBUTIONS

CA and BE wrote the initial manuscript. JO, AM, AI, BW, CJ, and WF revised the manuscript. WF supervised the manuscript. All authors have read and agreed to the published version of the manuscript.

FUNDING

This work was supported by National Natural Science Foundation of China (31960032, 32071279), Guangxi Natural Science Foundation (2020GXNSFDA238008) to WF, Research Start-up Funding of Guangxi Academy of Sciences (2017YJJ026) to BW, and Bagui Scholar Program Fund (2016A24) of Guangxi Zhuang Autonomous Region to CJ.

REFERENCES

Ahamefule, C. S., Ezeuduji, B. C., Ogbonna, J. C., Moneke, A. N., Ike, A. C., Wang, B., et al. (2020b). Marine Bioactive Compounds Against*Aspergillus Fumigatus*: Challenges and Future Prospects. *Antibiotics* 9 (11), 813. doi: 10.3390/antibiotics9110813

Ahamefule, C. S., Qin, Q., Odiba, A. S., Li, S., Moneke, A. N., Ogbonna, J. C., et al. (2020a). *Caenorhabditis Elegans*-Based *Aspergillus Fumigatus* Infection Model for Evaluating Pathogenicity and Drug Efficacy. *Front. Cell. Infection Microbiol.* 10, 320. doi: 10.3389/fcimb.2020.00320

Ansari, M. A., Fatima, Z., Ahmad, K., and Hameed, S. (2018). Monoterpenoid Perillyl Alcohol Impairs Metabolic Flexibility of Candida Albicans by Inhibiting Glyoxylate Cycle. *Biochem. Biophys. Res. Commun.* 495 (1), 560–566. doi: 10.1016/j.bbrc.2017.11.064

Ballestriero, F., Thomas, T., Burke, C., Egan, S., and Kjelleberg, S. (2010). Identification of Compounds With Bioactivity Against the Nematode Caenorhabditis Elegans by a Screen Based on the Functional Genomics of the Marine Bacterium *Pseudoalteromonas Tunicate* D2. *Appl. Environ. Microbiol.* 76 (17), 5710–5717. doi: 10.1128/AEM.00695-10

Bi, S., Lv, Q. Z., Wang, T. T., Fuchs, B. B., Hu, D.-D., Anastassopoulou, C. G., et al. (2018). SDH2 Is Involved in Proper Hypha Formation and Virulence in Candida Albicans. *Future Microbiol.* 13 (10), 1141–1156. doi: 10.2217/fmb-2018-0033

Breger, J., Fuchs, B. B., Aperis, G., Moy, T. I., Asbel, F. M., and Mylonakis, E. (2007). Antifungal Chemical Compounds Identified Using a C. Elegans Pathogenicity Assay. *PloS Pathog.* 3 (2), e18. doi: 10.1371/journal.ppat.0030018

Brilhante, R. S. N., Oliveira, J. S., Evangelista, A. J. J., Serpa, R., Silva, A. L. D., Aguiar, F. R. M., et al. (2016). *Candida Tropicalis* From Veterinary and Human Sources Shows Similar *In Vitro* Hemolytic Activity, Antifungal Biofilm Susceptibility and Pathogenesis Against *Caenorhabditis Elegans*. *Veterinary Microbiol.* 30 (192), 213–219. doi: 10.1016/j.vetmic.2016.07.022

Chang, W., Zhang, M., Li, Y., Li, X., Gao, Y., Xie, Z., et al. (2015). Lichen Endophyte Derived Pyridoxatin Inactivates Candida Growth by Interfering With Ergosterol Biosynthesis. *Biochim. Biophys. Acta* 1850 (9), 1762–1771. doi: 10.1016/j.bbagen.2015.05.005

Chen, H.-J., Jiang, Y.-J., Zhang, Y.-Q., Jing, Q.-W., Liu, N., and Wang, Y. (2017). New Triazole Derivatives Containing Substituted 1,2,3-Triazole Side Chains:

Design, Synthesis and Antifungal Activity. *Chin. Chem. Lett.* 28, 913–918. doi: 10.1016/j.cclet.2016.11.027

Chen, Y. Z., Yang, Y. L., Chu, W. L., You, M. S., and Lo, H. J. (2015). Zebrafish Egg Infection Model for Studying Candida Albicans Adhesion Factors. *PloS One* 10 (11), e0143048. doi: 10.1371/journal.pone.0143048

Couillault, C., Fourquet, P., Pophillat, M., and Ewbank, J. J. (2012). A UPR-Independent Infection-Specific Role for a BiP/GRP78 Protein in the Control of Antimicrobial Peptide Expression in C. Elegans Epidermis. *Virulence* 3 (3), 299–308. doi: 10.4161/viru.20384

Darling, B. A., and Milder, E. A. (2018). Invasive Aspergillosis. *Pediatr. Rev.* 39 (9), 476–478. doi: 10.1542/pir.2017-0129

De Aguiar Cordeiro, R., de Jesus Evangelista, A. J., Serpa, R., Colares de Andrade, A. R., Leite Mendes, P. B., Silva Franco, J. D., et al. (2018). β-Lactam Antibiotics & Vancomycin Increase the Growth & Virulence of Candida Spp. *Future Microbiol.* 13, 869–875. doi: 10.2217/fmb-2018-0019

de Barros, P. P., Scorzoni, L., Ribeiro, F. C., Fugisaki, L. R. O., Fuchs, B. B., Mylonakis, E., et al. (2018). *Lactobacillus Paracasei* 28.4 Reduces *In Vitro* Hyphae Formation of *Candida Albicans* and Prevents the Filamentation in an Experimental Model of *Caenorhabditis Elegans*. *Microbial Pathogenesis* 117, 80–87. doi: 10.1016/j.micpath.2018.02.019

de Sá, N. P., de Paula, L. F. J., Lopes, L. F. F., Cruz, L. I. B., Matos, T. T. S., Lino, C. I., et al. (2018). *In Vivo* and *In Vitro* Activity of a Bis-Arylidenecyclo-Alkanone Against Fluconazole-Susceptible and -Resistant Isolates of *Candida Albicans*. *J. Global Antimicrobial Resistance* 14, 287–293. doi: 10.1016/j.jgar.2018.04.012

de Sousa-Neto, A., de Brito Röder, D., and Pedroso, R. (2020). Invasive Fungal Infections in People Living With HIV/AIDS. *J. Biosci. Med.* 8, 15–26. doi: 10.4236/jbm.2020.89002

Eldesouky, H. E., Li, X., Abutaleb, N. S., Mohammad, H., and Seleem, M. N. (2018a). Synergistic Interactions of Sulfamethoxazole and Azole Antifungal Drugs Against Emerging Multidrug-Resistant *Candida Auris*. *Int. J. Antimicrobial Agents* 52 (6), 754–761. doi: 10.1016/j.ijantimicag.2018.08.016

Eldesouky, H. E., Mayhoub, A., Hazbun, T. R., and Seleem, M. N. (2018b). Reversal of Azole Resistance in Candida Albicans by Sulfa Antibacterial Drugs. *Antimicrobial Agents Chemotherapy* 62 (3), e00701–e00717. doi: 10.1128/AAC.00701-17

Eldesouky, H. E., Salama, E. A., Hazbun, T. R., Mayhoub, A. S., and Seleem, M. N. (2020a). Ospemifene Displays Broad-Spectrum Synergistic Interactions With Itraconazole Through Potent Interference With Fungal Efflux Activities. *Sci. Rep.* 10 (1), 6089. doi: 10.1038/s41598-020-62976-y

Eldesouky, H. E., Salama, E. A., Li, X., Hazbun, T. R., Mayhoub, A. S., and Seleem, M. N. (2020b). Repurposing Approach Identifies Pitavastatin as a Potent Azole Chemosensitizing Agent Effective Against Azole-Resistant Candida Species. *Sci. Rep.* 10 (1), 7525. doi: 10.1038/s41598-020-64571-7

Elghazawy, N. H., Hefnawy, A., Sedky, N. K., El-Sherbiny, I. M., and Arafa, R. K. (2017). Preparation and Nanoformulation of New Quinolone Scaffold-Based Anticancer Agents: Enhancing Solubility for Better Cellular Delivery. *Eur. J. Pharm. Sci.* 105, 203–211. doi: 10.1016/j.ejps.2017.05.036

Engelmann, I., Griffon, A., Tichit, L., Montañana-Sanchis, F., Wang, G., Reinke, V., et al. (2011). A Comprehensive Analysis of Gene Expression Changes Provoked by Bacterial and Fungal Infection in C. Elegans. *PloS One* 6 (5), e19055. doi: 10.1371/journal.pone.0019055

Fakhim, H., Vaezi, A., Dannaoui, E., Chowdhary, A., Nasiry, D., Faeli, L., et al. (2018). Comparative Virulence of Candida Auris With *Candida Haemulonii*, *Candida Glabrata* and *Candida Albicans* in a Murine Model. *Mycoses* 61 (6), 377–382. doi: 10.1111/myc.12754

Fang, W., and Latgé, J. P. (2018). Microbe Profile: Aspergillus Fumigatus: A Saprotrophic and Opportunistic Fungal Pathogen. *Microbiology* 164 (8), 1009–1011. doi: 10.1099/mic.0.000651

Feistel, D. J., Elmostafa, R., Nguyen, N., Penley, M., Morran, L., Hickman, M. A., et al. (2019). A Novel Virulence Phenotype Rapidly Assesses Candida Fungal Pathogenesis in Healthy and Immunocompromised *Caenorhabditis Elegans* Hosts. *mSphere* 4 (2), e00697–e00618. doi: 10.1128/mSphere.00697-18

Fiori, A., Kucharíková, S., Govaert, G., Cammue, B. P., Thevissen, K., and Van Dijck, P. (2012). The Heat-Induced Molecular Disaggregase Hsp104 of Candida Albicans Plays a Role in Biofilm Formation and Pathogenicity in a Worm Infection Model. *Eukaryotic Cell* 11 (8), 1012–1020. doi: 10.1128/EC.00147-12

Fisher, M. C., Henk, D. A., Briggs, C. J., Brownstein, J. S., Madoff, L. C., McCraw, S. L., et al. (2012). Emerging Fungal Threats to Animal, Plant and Ecosystem Health. *Nature* 484 (7393), 186–194. doi: 10.1038/nature10947

Ganesh Kumar, A., Balamurugan, K., Vijaya Raghavan, R., Dharani, G., and Kirubagaran, R. (2019). Studies on the Antifungal and Serotonin Receptor Agonist Activities of the Secondary Metabolites From Piezotolerant Deep-Sea Fungus Ascotricha Sp. *Mycology* 10 (2), 92–108. doi: 10.1080/21501203.2018.1541934

Garvey, E. P., Hoekstra, W. J., Moore, W. R., Schotzinger, R. J., Long, L., and Ghannoum, M. A. (2015). VT-1161 Dosed Once Daily or Once Weekly Exhibits Potent Efficacy in Treatment of Dermatophytosis in a Guinea Pig Model. *Antimicrobial Agents Chemotherapy* 59 (4), 1992–1997. doi: 10.1128/AAC.04902-14

Geißel, B., Loiko, V., Klugherz, I., Zhu, Z., Wagener, N., Kurzai, O., et al. (2018). Azole-Induced Cell Wall Carbohydrate Patches Kill Aspergillus Fumigatus. *Nat. Commun.* 9 (1), 3098. doi: 10.1038/s41467-018-05497-7

Gomez-Lopez, A., Forastiero, A., Cendejas-Bueno, E., Gregson, L., Mellado, E., Howard, S. J., et al. (2014). An Invertebrate Model to Evaluate Virulence in Aspergillus Fumigatus: The Role of Azole Resistance. *Med. Mycology* 52 (3), 311–319. doi: 10.1093/mmy/myt022

Graham, C. E., Cruz, M. R., Garsin, D. A., and Lorenz, M. C. (2017). *Enterococcus Faecalis* Bacteriocin EntV Inhibits Hyphal Morphogenesis, Biofilm Formation, and Virulence of *Candida Albicans*. *Proc. Natl. Acad. Sci. United States America* 25 (114), 4507–4512. doi: 10.1073/pnas.1620432114

Hammond, T. G., Stodieck, L., Birdsall, H. H., Becker, J. L., Koenig, P., Hammond, J. S., et al. (2013). Effects of Microgravity on the Virulence of Listeria Monocytogenes, *Enterococcus Faecalis*, *Candida Albicans*, and Methicillin-Resistant *Staphylococcus Aureus*. *Astrobiology* 13 (11), 1081–1090. doi: 10.1089/ast.2013.0986

Hans, S., Fatima, Z., and Hameed, S. (2019a). Magnesium Deprivation Affects Cellular Circuitry Involved in Drug Resistance and Virulence in Candida Albicans. *J. Global Antimicrobial Resistance* 17, 263–275. doi: 10.1016/j.jgar.2019.01.011

Hans, S., Fatima, Z., and Hameed, S. (2019b). Retrograde Signaling Disruption Influences ABC Superfamily Transporter, Ergosterol and Chitin Levels Along With Biofilm Formation in Candida Albicans. *J. Mycologie Medicale* 29 (3), 210–218. doi: 10.1016/j.mycmed.2019.07.003

Hernando-Ortiz, A., Mateo, E., Ortega-Riveros, M., De-la-Pinta, I., Quindós, G., and Eraso, E. (2020). *Caenorhabditis elegans* as a Model System to Assess *Candida glabrata*, *Candida nivariensis*, and *Candida bracarensis* Virulence and Antifungal Efficacy. *Antimicrob. Agents Chemother.* 64 (10), e00824-20. doi: 10.1128/AAC.00824-20

Holt, J. E., Houston, A., Adams, C., Edwards, S., and Kjellerup, B. V. (2017). Role of Extracellular Polymeric Substances in Polymicrobial Biofilm Infections of Staphylococcus Epidermidis and *Candida Albicans* Modelled in the Nematode *Caenorhabditis Elegans*. *Pathog. Dis.* 75 (5), ftx052. doi: 10.1093/femspd/ftx052

Huang, X., Li, D., Xi, L., and Mylonakis, E. (2014). *Caenorhabditis Elegans*: A Simple Nematode Infection Model for Penicillium Marneffei. *PloS One* 9 (9), e108764. doi: 10.1371/journal.pone.0108764

Jain, C., Pastor, K., Gonzalez, A. Y., Lorenz, M. C., and Rao, R. P. (2013). The Role of Candida Albicans AP-1 Protein Against Host Derived ROS in *In Vivo* Models of Infection. *Virulence* 4 (1), 67–76. doi: 10.4161/viru.22700

Jiang, H., and Wang, D. (2018). The Microbial Zoo in the C. Elegans Intestine: Bacteria, Fungi and Viruses. *Viruses* 10 (2), 85. doi: 10.3390/v10020085

Johnson, C. H., Ayyadevara, S., McEwen, J. E., and Shmookler Reis, R. J. (2009). *Histoplasma Capsulatum* and Caenorhabditis Elegans: A Simple Nematode Model for an Innate Immune Response to Fungal Infection. *Med. Mycology* 47, 808–813. doi: 10.3109/13693780802660532

Kim, W., Hendricks, G. L., Lee, K., and Mylonakis, E. (2017). An Update on the Use of C. Elegans for Preclinical Drug Discovery: Screening and Identifying Anti-Infective Drugs. *Expert Opin. Drug Discov.* 12 (6), 625–633. doi: 10.1080/17460441.2017.1319358

Kirienko, N. V., Kirienko, D. R., Larkins-Ford, J., Wahlby, C., Ruvkun, G., and Ausubel, F. M. (2013). *Pseudomonas Aeruginosa* Disrupts Caenorhabditis Elegans Iron Homeostasis, Causing a Hypoxic Response and Death. *Cell Host Microbe* 13 (4), 406–416. doi: 10.1016/j.chom.2013.03.003

Knox, B. P., Huttenlocher, A., and Keller, N. P. (2017). Real-Time Visualization of Immune Cell Clearance of Aspergillus Fumigatus Spores and Hyphae. *Fungal Genet. Biol.* 105, 52–54. doi: 10.1016/j.fgb.2017.05.005

Koch, B. E. V., Hajdamowicz, N. H., Lagendijk, E., Ram, A. F. J., and Meijer, A. H. (2019). *Aspergillus Fumigatus* Establishes Infection in Zebrafish by Germination of Phagocytized Conidia, While Aspergillus Niger Relies on Extracellular Germination. *Sci. Rep.* 9 (1), 12791. doi: 10.1038/s41598-019-49284-w

Kulatunga, D. C. M., Dananjaya, S. H. S., Nikapitiya, C., Kim, C. H., Lee, J., and De Zoysa, M. (2019). *Candida Albicans* Infection Model in Zebrafish (*Danio Rerio*) for Screening Anticandidal Drugs. *Mycopathologia* 184 (5), 559–572. doi: 10.1007/s11046-019-00378-z

Kunyeit, L., Kurrey, N. K., Anu-Appaiah, K. A., and Rao, R. P. (2019). Probiotic Yeasts Inhibit Virulence of Non-*Albicans Candida* Species. *mBio* 10 (5), e02307–e02319. doi: 10.1128/mBio.02307-19

Lamaris, G. A., Ben-Ami, R., Lewis, R. E., and Kontoyiannis, D. P. (2008). Does Pre-Exposure of Aspergillus Fumigatus to Voriconazole or Posaconazole *In Vitro* Affect its Virulence and the *In Vivo* Activity of Subsequent Posaconazole or Voriconazole, Respectively? A Study in a Fly Model of Aspergillosis. *J. Antimicrob. Chemother.* 62 (3), 539–542. doi: 10.1093/jac/dkn224

Li, Y., Chang, W., Zhang, M., Ying, Z., and Lou, H. (2015). Natural Product Solasodine-3-O-β-D-Glucopyranoside Inhibits the Virulence Factors of Candida Albicans. *FEMS Yeast Res.* 15 (6), fov060. doi: 10.1093/femsyr/fov060

Linder, K. A., McDonald, P. J., Kauffman, C. A., Revankar, S. G., Chandrasekar, P. H., and Miceli, M. H. (2019). Invasive Aspergillosis in Patients Following Umbilical Cord Blood Transplant. *Bone Marrow Transplant.* 54, 308–311. doi: 10.1038/s41409-018-0230-5

Lin, M.-Y., Yuan, Z.-L., Hu, D.-D., Hu, G.-H., Zhang, R.-L., Zhong, H., et al. (2019). Effect of Loureirin A Against *Candida Albicans* Biofilms. *Chin. J. Natural Med.* 17 (8), 616–623. doi: 10.1016/S1875-5364(19)30064-0

Li, Y., Shan, M., Yan, M., Yao, H., Wang, Y., Gu, B., et al. (2019). Anticandidal Activity of Kalopanaxsaponin A: Effect on Proliferation, Cell Morphology, and Key Virulence Attributes of Candida Albicans. *Front. Microbiol.* 10, 2844. doi: 10.3389/fmicb.2019.02844

Long, N., Orasch, T., Zhang, S., Gao, L., Xu, X., Hortschansky, P., et al. (2018). The Zn2Cys6-Type Transcription Factor LeuB Cross-Links Regulation of Leucine Biosynthesis and Iron Acquisition in Aspergillus Fumigatus. *PloS Genet.* 14 (10), e1007762. doi: 10.1371/journal.pgen.1007762

Lopes, J. P., Stylianou, M., Backman, E., Holmberg, S., Jass, J., Claesson, R., et al. (2018). Evasion of Immune Surveillance in Low Oxygen Environments Enhances Candida Albicans Virulence. *mBio* 9, e02120–e02118. doi: 10.1128/mBio.02120-18

Manoharan, R. K., Lee, J. H., Kim, Y. G., Kim, S. I., and Lee, J. (2017c). Inhibitory Effects of the Essential Oils α-Longipinene and Linalool on Biofilm Formation and Hyphal Growth of Candida Albicans. *Biofouling* 33 (2), 143–155. doi: 10.1080/08927014.2017.1280731

Manoharan, R. K., Lee, J.-H., Kim, Y.-G., and Lee, J. (2017a). Alizarin and Chrysazin Inhibit Biofilm and Hyphal Formation by Candida Albicans. *Front. Cell. Infection Microbiol.* 7, 447. doi: 10.3389/fcimb.2017.00447

Manoharan, R. K., Lee, J. H., and Lee, J. (2017b). Antibiofilm and Antihyphal Activities of Cedar Leaf Essential Oil, Camphor, and Fenchone Derivatives Against Candida Albicans. *Front. Microbiol.* 8, 1476. doi: 10.3389/fmicb.2017.01476

Manoharan, R. K., Lee, J. H., and Lee, J. (2018). Efficacy of 7-Benzyloxyindole and Other Halogenated Indoles to Inhibit Candida Albicans Biofilm and Hyphal Formation. *Microbial Biotechnol.* 11 (6), 1060–1069. doi: 10.1111/1751-7915.13268

Matsumoto, H., Nagao, J., Cho, T., and Kodama, J. (2013). Evaluation of Pathogenicity of Candida Albicans in Germination-Ready States Using a Silkworm Infection Model. *Med. Mycology J.* 54 (2), 131–140. doi: 10.3314/mmj.54.131

Matsumoto, Y., and Sekimizu, K. (2019). Silkworm as an Experimental Animal for Research on Fungal Infections. *Microbiol. Immunol.* 63 (2), 41–50. doi: 10.1111/1348-0421.12668

Mohammad, H., Eldesouky, H. E., Hazbun, T., Mayhoub, A. S., and Seleem, M. N. (2019). Identification of a Phenylthiazole Small Molecule With Dual Antifungal and Antibiofilm Activity Against Candida Albicans and *Candida Auris*. *Sci. Rep.* 9 (1), 18941. doi: 10.1038/s41598-019-55379-1

Mohammad, H., Elghazawy, N. H., Eldesouky, H. E., Hegazy, Y. A., Younis, W., Avrimova, L., et al. (2018). Discovery of a Novel Dibromoquinoline Compound Exhibiting Potent Antifungal and Antivirulence Activity That Targets Metal Ion Homeostasis. *ACS Infect. Dis.* 4 (3), 403–414. doi: 10.1021/acsinfecdis.7b00215

Mueller, K. D., Zhang, H., Serrano, C. R., Billmyre, R. B., Huh, Y. H., Wiemann, P., et al. (2019). Gastrointestinal Microbiota Alteration Induced by Mucor Circinelloides in a Murine Model. *J. Microbiol.* 57 (6), 509–520. doi: 10.1007/s12275-019-8682-x

Muhammed, M., Coleman, J. J., and Mylonakis, E. (2012). "Caenorhabditis Elegans: A Nematode Infection Model for Pathogenic Fungi," in *Host-Fungus Interactions. Methods in Molecular Biology (Methods and Protocols)*. Eds. A. C. Brand and D. M. MacCallum (New Jersey, USA: Humana Press), 447–454. doi: 10.1007/978-1-61779-539-8_31

Muthamil, S., Balasubramaniam, B., Balamurugan, K., and Pandian, S. K. (2018). Synergistic Effect of Quinic Acid Derived From Syzygium Cumini and Undecanoic Acid Against Candida Spp. Biofilm and Virulence. *Front. Microbiol.* 9, 2835. doi: 10.3389/fmicb.2018.02835

Nadăş, G. C., Taulescu, M. A., Ciobanu, L., Fiţ, N. I., Flore, C., Răpuntean, S., et al. (2013). The Interplay Between NSAIDs and Candida Albicans on the Gastrointestinal Tract of Guinea Pigs. *Mycopathologia* 175 (3-4), 221–230. doi: 10.1007/s11046-013-9613-8

Nakamura, I., Kanasaki, R., Yoshikawa, K., Furukawa, S., Fujie, A., Hamamoto, H., et al. (2017). Discovery of a New Antifungal Agent ASP2397 Using a Silkworm Model of Aspergillus Fumigatus Infection. *J. Antibiotics* 70 (1), 41–44. doi: 10.1038/ja.2016.106

Okoli, I., and Bignell, E. M. (2015). *Caenorhabditis Elegans-Aspergillus Fumigatus* (Nematode-Mould) Model for Study of Fungal Pathogenesis. *Br. Microbiol. Res. J.* 7 (2), 93–99. doi: 10.9734/BMRJ/2015/15838

Okoli, I., Coleman, J. J., Tempakakis, E., An, W. F., Holson, E., Wagner, F., et al. (2009). Identification of Antifungal Compounds Active Against Candida Albicans Using an Improved High-Throughput *Caenorhabditis Elegans* Assay. *PloS One* 4 (9), e7025. doi: 10.1371/journal.pone.0007025

Ortega-Riveros, M., De-la-Pinta, I., Marcos-Arias, C., Ezpeleta, G., Quindós, G., and Eraso, E. (2017). Usefulness of the Non-Conventional Caenorhabditis Elegans Model to Assess *Candida* Virulence. *Mycopathologia* 182 (9-10), 785–795. doi: 10.1007/s11046-017-0142-8

Pal, M. (2018). Morbidity and Mortality due to Fungal Infections. *J. Appl. Microbiol. Biochem.* 1 (1), 1–3. doi: 10.21767/2576-1412.100002

Pedroso, R. D. S., Balbino, B. L., Andrade, G., Dias, M. C. P. S., Alvarenga, T. A., Pedroso, R. C. N., et al. (2019). *In Vitro* and *In Vivo* Anti-*Candida* Spp. Activity of Plant-Derived Products. *Plants (Basel)* 8 (11), 494. doi: 10.3390/plants8110494

Peterson, N. D., and Pukkila-Worley, R. (2018). *Caenorhabditis Elegans* in High-Throughput Screens for Anti-Infective Compounds. *Curr. Opin. Immunol.* 54, 59–65. doi: 10.1016/j.coi.2018.06.003

Popp, C., Hampe, I., Hertlein, T., Ohlsen, K., Rogers, P. D., and Morschhäuser, J. (2017). Competitive Fitness of Fluconazole-Resistant Clinical Candida Albicans Strains. *Antimicrobial Agents chemotherapy* 61 (7), e00584–e00517. doi: 10.1128/AAC.00584-17

Popp, C., Ramírez-Zavala, B., Schwanfelder, S., Krüger, I., and Morschhäuser, J. (2019). Evolution of Fluconazole-Resistant Candida Albicans Strains by Drug-Induced Mating Competence and Parasexual Recombination. *mBio* 10 (1), e02740–e02718. doi: 10.1128/mBio.02740-18

Poupet, C., Saraoui, T., Veisseire, P., Bonnet, M., Dausset, C., Gachinat, M., et al. (2019b). *Lactobacillus Rhamnosus* Lcr35 as an Effective Treatment for Preventing *Candida Albicans* Infection in the Invertebrate Model *Caenorhabditis Elegans*: First Mechanistic Insights. *PloS One* 14 (11), e0216184. doi: 10.1371/journal.pone.0216184

Poupet, C., Veisseire, P., Bonnet, M., Camarès, O., Gachinat, M., Dausset, C., et al. (2019a). Curative Treatment of Candidiasis by the Live Biotherapeutic Microorganism Lactobacillus Rhamnosus Lcr35® in the Invertebrate Model *Caenorhabditis Elegans*: First Mechanistic Insights. *Microorganisms* 8 (1), 34. doi: 10.3390/microorganisms8010034

Prasad, R., Nair, R., and Banerjee, A. (2019). Emerging Mechanisms of Drug Resistance in Candida Albicans. *Prog. Mol. Subcellular Biol.* 58, 135–153. doi: 10.1007/978-3-030-13035-0_6

Priya, A., and Pandian and, S. K. (2020). Piperine Impedes Biofilm Formation and Hyphal Morphogenesis of Candida Albicans. *Front. Microbiol.* 11, 756. doi: 10.3389/fmicb.2020.00756

Rane, H. S., Bernardo, S. M., Hayek, S. R., Binder, J. L., Parra, K. J., and Lee, S. A. (2014b). The Contribution of Candida Albicans Vacuolar ATPase Subunit V_1B, Encoded by *VMA2*, to Stress Response, Autophagy, and Virulence Is Independent of Environmental pH. *Eukaryotic Cell* 13 (9), 1207–1221. doi: 10.1128/EC.00135-14

Rane, H.,. S., Hardison, S., Botelho, C., Bernardo, S. M., Wormley, J. F., and Lee, S. A. (2014a). Candida Albicans VPS4 Contributes Differentially to Epithelial and Mucosal Pathogenesis. *Virulence* 5 (8), 810—818. doi: 10.4161/21505594.2014.956648

Regulin, A., and Kempken, F. (2018). Fungal Genotype Determines Survival of Drosophila Melanogaster When Competing With *Aspergillus Nidulans*. *PloS One* 13 (1), e0190543. doi: 10.1371/journal.pone.0190543

Rhodes, J. (2019). Rapid Worldwide Emergence of Pathogenic Fungi. *Cell Host Microbe* 26 (1), 12–14. doi: 10.1016/j.chom.2019.06.009

Romanowski, K., Zaborin, A., Valuckaite, V., Rolfes, R. J., Babrowski, T., Bethel, C., et al. (2012). *Candida Albicans* Isolates From the Gut of Critically Ill Patients Respond to Phosphate Limitation by Expressing Filaments and a Lethal Phenotype. *PloS One* 7 (1), e30119. doi: 10.1371/journal.pone.0030119

Sampaio, A. D. G., Gontijo, A. V. L., Araujo, H. M., and Koga-Ito, C. Y. (2018). *In Vivo* Efficacy of Ellagic Acid Against Candida Albicans in a Drosophila Melanogaster Infection Model. *Antimicrobial Agents Chemotherapy* 62 (12), e01716–e01718. doi: 10.1128/AAC.01716-18

Sangkanu, S., Rukachaisirikul, V., Suriyachadkun, C., and Phongpaichit, S. (2021). Antifungal Activity of Marine-Derived Actinomycetes Against Talaromyces Marneffei. *J. Appl. Microbiol.* 130, 1508–1522. doi: 10.1111/jam.14877

Sanguinetti, M., Posteraro, B., and Lass-Flörl, C. (2015). Antifungal Drug Resistance Among Candida Species: Mechanisms and Clinical Impact. *Mycoses* 58 (Suppl 2), 2–13. doi: 10.1111/myc.12330

Shu, C., Sun, L., and Zhang, W. (2016). Thymol has Antifungal Activity Against Candida Albicans During Infection and Maintains the Innate Immune Response Required for Function of the P38 MAPK Signaling Pathway in *Caenorhabditis Elegans*. *Immunologic Res.* 64 (4), 1013–1024. doi: 10.1007/s12026-016-8785-y

Silva, L. N., Campos-Silva, R., Ramos, L. S., Trentin, D. S., Macedo, A. J., Branquinha, M. H., et al. (2018). Virulence of Candida Haemulonii Complex in *Galleria Mellonella* and Efficacy of Classical Antifungal Drugs: A Comparative Study With Other Clinically Relevant Non-Albicans *Candida* Species. *FEMS Yeast Res.* 18 (7), foy082. doi: 10.1093/femsyr/foy082

Singh, S., Fatima, Z., Ahmad, K., and Hameed, S. (2018). Fungicidal Action of Geraniol Against Candida Albicans Is Potentiated by Abrogated CaCdr1p Drug Efflux and Fluconazole Synergism. *PloS One* 13 (8), e0203079. doi: 10.1371/journal.pone.0203079

Singh, S., Fatima, Z., Ahmad, K., and Hameed, S. (2020). Repurposing of Respiratory Drug Theophylline Against *Candida Albicans*: Mechanistic Insights Unveil Alterations in Membrane Properties and Metabolic Fitness. *J. Appl. Microbiol.* 129 (4), 860–875. doi: 10.1111/jam.14669

Singulani, J. L., Scorzoni, L., Gomes, P. C., Nazaré, A. C., Polaquini, C. R., Regasini, L. O., et al. (2017). Activity of Gallic Acid and Its Ester Derivatives in *Caenorhabditis Elegans* and Zebrafish (*Danio Rerio*) Models. *Future Medicinal Chem.* 9 (16), 1863–1872. doi: 10.4155/fmc-2017-0096

Skalski, J. H., Limon, J. J., Sharma, P., Gargus, M. D., Nguyen, C., Tang, J., et al. (2018). Expansion of Commensal Fungus Wallemia Mellicola in the Gastrointestinal Mycobiota Enhances the Severity of Allergic Airway Disease in Mice. *PloS Pathogen* 14 (9), e1007260. doi: 10.1371/journal.ppat.1007260

Snelders, E., Huisin't Veld, R. A. G., Rijs, A. J. M. M., Kema, G. H. J., Melchers, W. J. G., and Verweij, P. E. (2009). Possible Environmental Origin of Resistance of Aspergillus Fumigatus to Medical Triazoles. *Appl. Environ. Microbiol.* 75 (12), 4053–4057. doi: 10.1128/AEM.00231-09

Song, Y., Li, S., Zhao, Y., Zhang, Y., Lv, Y., Jiang, Y., et al. (2019). ADH1 Promotes Candida Albicans Pathogenicity by Stimulating Oxidative Phosphorylation. *Int. J. Med. Microbiol.* 309, 151330. doi: 10.1016/j.ijmm.2019.151330

Souza, A. C. R., Fuchs, B. B., Alves, V. S., Jayamani, E., Colombo, A. L., and Mylonakis, E. (2018). Pathogenesis of the Candida Parapsilosis Complex in the Model Host *Caenorhabditis Elegans*. *Genes (Basel)* 9 (8), 401. doi: 10.3390/genes9080401

Staniszewska, M., Gizińska, M., Kazek, M., de Jesús González-Hernández, R., Ochal, Z., and Mora-Montes, H. M. (2020). New Antifungal 4-Chloro-3-Itrophenyldifluoroiodomethyl Sulfone Reduces the Candida Albicans Pathogenicity in the *Galleria Mellonella* Model Organism. *Braz. J. Microbiol.* 51 (1), 5–14. doi: 10.1007/s42770-019-00140-z

Subramenium, G. A., Swetha, T. K., Iyer, P. M., Balamurugan, K., and Pandian, S. K. (2017). 5-Hydroxymethyl-2-Furaldehyde From Marine Bacterium Bacillus Subtilis Inhibits Biofilm and Virulence of *Candida Albicans*. *Microbiological Res.* 207, 19–32. doi: 10.1016/j.micres.2017.11.002

Sun, L., Liao, K., and Hang, C. (2018). Caffeic Acid Phenethyl Ester Synergistically Enhances the Antifungal Activity of Fluconazole Against Resistant Candida Albicans. *Phytomedicine* 40, 55–58. doi: 10.1016/j.phymed.2017.12.033

Sun, L., Liao, K., and Wang, D. (2015). Effects of Magnolol and Honokiol on Adhesion, Yeast-Hyphal Transition, and Formation of Biofilm by Candida Albicans. *PloS One* 10 (2), e0117695. doi: 10.1371/journal.pone.0117695

Tan, X., Fuchs, B. B., Wang, Y., Chen, W., Yuen, G. J., Chen, R. B., et al. (2014). The Role of Candida Albicans SPT20 in Filamentation, Biofilm Formation and Pathogenesis. *PloS One* 9 (4), e94468. doi: 10.1371/journal.pone.0094468

Thangamani, S., Eldesouky, H. E., Mohammad, H., Pascuzzi, P. E., Avramova, L., Hazbun, T. R., et al. (2017). Ebselen Exerts Antifungal Activity by Regulating Glutathione (GSH) and Reactive Oxygen Species (ROS) Production in Fungal Cells. *Biochim. Biophys. Acta* 1861 (1PtA), 3002–3010. doi: 10.1016/j.bbagen.2016.09.029

Uchida, R., Namiguchi, S., Ishijima, H., and Tomoda, H. (2016). Therapeutic Effects of Three Trichothecenes in the Silkworm Infection Assay With Candida Albicans. *Drug Discoveries Ther.* 10 (1), 44–48. doi: 10.5582/ddt.2016.01013

Vallor, A. C., Kirkpatrick, W. R., Najvar, L. K., Bocarnegra, R., Kinney, M. C., Fothergill, A. W., et al. (2008). Assessment of Aspergillus Fumigatus Burden in Pulmonary Tissue of Guinea Pigs by Quantitative PCR, Galactomannan Enzyme Immunoassay, and Quantitative Culture. *Antimicrobial Agents Chemotherapy* 52 (7), 2593–2598. doi: 10.1128/AAC.00276-08

Venkata, S., Zeeshan, F., Kamal, A., Luqman, A. K., and Saif, H. (2020). Efficiency of Vanillin in Impeding Metabolic Adaptability and Virulence of Candida Albicans by Inhibiting Glyoxylate Cycle, Morphogenesis, and Biofilm Formation. *Curr. Med. Mycology* 6 (1), 1–8. doi: 10.18502/cmm.6.1.2501

Wang, X., Bing, J., Zheng, Q., Zhang, F., Liu, J., Yue, H., et al. (2018). The First Isolate of Candida Auris in China: Clinical and Biological Aspects. *Emerging Microbes Infection* 187 (1), 93. doi: 10.1038/s41426-018-0095-0

Wong, D., Plumb, J., Talab, H., Kurdi, M., Pokhrel, K., and Oelkers, P. (2019). Genetically Compromising Phospholipid Metabolism Limits Candida Albicans' Virulence. *Mycopathologia* 184 (2), 213–226. doi: 10.1007/s11046-019-00320-3

Wurster, S., Bandi, A., Beyda, N. D., Albert, N. D., Raman, N. M., Raad, I. I., et al. (2019). *Drosophila Melanogaster* as a Model to Study Virulence and Azole Treatment of the Emerging Pathogen Candida Auris. *J. Antimicrobial Chemotherapy* 74 (7), 1904–1910. doi: 10.1093/jac/dkz100

Xu, K., Wang, J. L., Chu, M. P., and Jia, C. (2019). Activity of Coumarin Against Candida Albicans Biofilms. *J. Mycologie Medicale* 29 (1), 28–34. doi: 10.1016/j.mycmed.2018.12.003

Zhang, M., Chang, W., Shi, H., Li, Y., Zheng, S., Li, W., et al. (2018). Floricolin C Elicits Intracellular Reactive Oxygen Species Accumulation and Disrupts Mitochondria to Exert Fungicidal Action. *FEMS Yeast Res.* 18 (1), foy002. doi: 10.1093/femsyr/foy002

Zheng, S., Chang, W., Zhang, M., Shi, H., and Lou, H. (2018). Chiloscyphenol A Derived From Chinese Liverworts Exerts Fungicidal Action by Eliciting Both Mitochondrial Dysfunction and Plasma Membrane Destruction. *Sci. Rep.* 8 (1), 326. doi: 10.1038/s41598-017-18717-9

Zugasti, O., Thakur, N., Belougne, J., Squiban, B., Kurz, C. L., Soulé, J., et al. (2016). A Quantitative Genome-Wide RNAi Screen in C. Elegans for Antifungal Innate Immunity Genes. *BMC Biol.* 14, 35. doi: 10.1186/s12915-016-0256-3

Conflict of Interest: The authors declare that the research was conducted in the absence of any commercial or financial relationships that could be construed as a potential conflict of interest.

Publisher's Note: All claims expressed in this article are solely those of the authors and do not necessarily represent those of their affiliated organizations, or those of the publisher, the editors and the reviewers. Any product that may be evaluated in

this article, or claim that may be made by its manufacturer, is not guaranteed or endorsed by the publisher.

Advantages of publishing in Frontiers

OPEN ACCESS
Articles are free to read for greatest visibility and readership

FAST PUBLICATION
Around 90 days from submission to decision

HIGH QUALITY PEER-REVIEW
Rigorous, collaborative, and constructive peer-review

TRANSPARENT PEER-REVIEW
Editors and reviewers acknowledged by name on published articles

Frontiers
Avenue du Tribunal-Fédéral 34
1005 Lausanne | Switzerland

Visit us: www.frontiersin.org
Contact us: frontiersin.org/about/contact

REPRODUCIBILITY OF RESEARCH
Support open data and methods to enhance research reproducibility

DIGITAL PUBLISHING
Articles designed for optimal readership across devices

FOLLOW US
@frontiersin

IMPACT METRICS
Advanced article metrics track visibility across digital media

EXTENSIVE PROMOTION
Marketing and promotion of impactful research

LOOP RESEARCH NETWORK
Our network increases your article's readership